

**N-SILYLATED AMINES AS VALUABLE SYNTHONS IN METHODS DEVELOPMENT
TOWARD PHARMACEUTICALLY RELEVANT SMALL MOLECULES**

by

Ana Koperniku

B.Sc. (Pharm), National and Kapodistrian University of Athens, 2011

M.Sc. (Pharm Chem), National and Kapodistrian University of Athens, 2013

A THESIS SUBMITTED IN PARTIAL FULFILLMENT OF
THE REQUIREMENTS FOR THE DEGREE OF

DOCTOR OF PHILOSOPHY

in

The Faculty of Graduate and Postdoctoral Studies
(Pharmaceutical Sciences)

THE UNIVERSITY OF BRITISH COLUMBIA

(Vancouver)

April 2019

© Ana Koperniku, 2019

The following individuals certify that they have read, and recommend to the Faculty of Graduate and Postdoctoral Studies for acceptance, the dissertation entitled:

N-Silylated amines as valuable synthons in methods development toward pharmaceutically relevant small molecules

submitted by Ana Koperniku in partial fulfillment of the requirements

the degree of Doctor of Philosophy

in Pharmaceutical Sciences

Examining Committee:

David Grierson, Pharmaceutical Sciences

Co-supervisor

Laurel Schafer, Chemistry

Co-supervisor

Adam Frankel, Pharmaceutical Sciences

Supervisory Committee Member

Gregory Dake, Chemistry

University Examiner

Emily Cranston, Forestry

University Examiner

Additional Supervisory Committee Members:

Urs Häfeli

Supervisory Committee Member

Abstract

This thesis focuses on two distinct methods which were developed to access both a series of diheteroarylamides and a series of primary and secondary amines with a tertiary α -carbon. Crucial to the methods development for their synthesis was the use of *N*-silylated amines. The diheteroarylamides served as structural alternatives to a reference diheteroarylamide which showed potency against HIV-infected cells and the resulting primary and secondary amines were used as precursors to heterocyclic derivatives.

In Chapter 1, an introduction on the catalytic synthesis and chemistry of the *N*-silylated amines is presented. Modern catalytic reactions to access *N*-silylamines and the type of transformations the resulting *N*-silylated amines can be engaged in are discussed.

In Chapter 2, the value of *N*-silylated amines is highlighted with their use in amide bond formation of diheteroarylamides derived from electron deficient amines. The negative charge unveiled upon the desilylation of the above amines is a necessity for them to be engaged in the amidation reaction.

In Chapter 3, the focus is centered on secondary *N*-silylated α -arylated amines which are used as substrates in zirconium catalyzed hydroaminoalkylation of alkenes to access primary α -arylated amines with a tertiary center on the α to the nitrogen carbon. Efforts to cyclize the resulting primary amines with the goal to access relevant heterocycles in organic and pharmaceutical chemistry are presented.

In Chapter 4, *N*-aryl and *N*-alkylamines with a secondary α -carbon are used as substrates in zirconium catalyzed hydroaminoalkylation of alkenes to afford secondary α -arylated amines

with a tertiary α to the nitrogen carbon. In analogy with the primary amines, some of the resulting secondary amines can further be cyclized into heterocyclic derivatives.

Chapter 5 provides a summary and describes the future direction the two methods presented in Chapter 2 and 3&4 can take. For Chapter 2, the ongoing synthesis of diheteroarylamides will serve as a platform for the identification of the interactions with their target. For Chapters 3&4, there is space for the methodology improvement to control both regio- and diastereoselectivity in the resulting compounds. Further strategies on how to construct heterocycles with the resulting amines are discussed.

Lay Summary

This thesis focuses on the development of methods to access pharmaceutically relevant compounds and building blocks. In Chapter 2 a facile way to access a *library* of compounds is presented; their synthesis is done in parallel and isolation relies on simple filtration, which is a clean way of purification and ensures minimal waste generation.

Chapters 3 and 4 detail the development of a methodology to access branched amines which employs the use of catalytic amounts of zirconium. The asset of using catalytic instead of stoichiometric reagents is atom economy, the incorporation of all starting materials in the products.

Both methodologies described in Chapters 2 and 3&4 are impactful for two reasons: 1) they abide to green chemistry principles (minimal waste generation and atom economy) and 2) they open the venue for the rapid synthesis of agents which can be tested against HIV and prepare the ground for the synthesis of nicotine derivatives, candidate agents for the treatment and cure of neurological disorders, respectively.

Preface

The work presented throughout chapters 2-4 has been conducted in consultation with my supervisors, Prof. David S. Grierson and Prof. Laurel L. Schafer. All the experimental work described herein was performed by me. The published work from Chapter 2 includes contribution by Maryam Zamiri; the scheduled for publication work from Chapter 3 includes contribution by Paul J. Foth.

Chapter 2 is based on work conducted at the Faculty of Pharmaceutical Sciences at UBC and part of it has been accepted for publication in *Synthesis* published by Thieme Chemistry as: Koperniku, A.; Zamiri, M.; Grierson, D.S. “The Reaction of *N*-Trimethylsilyl Substituted Heteroarylamines with Thio- and Oxoesters: An Efficient Protocol to Access Diheteroarylamides” as a full paper.

Chapter 3 is based on work conducted at the Chemistry Department at UBC and part of it is scheduled for disclosure as: Koperniku, A.; Foth, P.J.; Sammis, G.M.; Schafer, L.L. “Zirconium Catalyzed Hydroaminoalkylation. New Disconnection for α -Arylated Primary Amines” as a communication.

Chapter 4 is based on work conducted at the Chemistry Department at UBC and part of it is scheduled for disclosure: Koperniku, A.; Schafer, L.L. “Zirconium Catalyzed Hydroaminoalkylation of Alkenes with *N*-arylated, *N*-alkylated Amines and *N*-TMS,” as an article.

In the Appendix B, I have included a review released by the European Journal of Organic Chemistry and published by Wiley VCH Verlag as: Koperniku, A.; Liu, H.; Hurley, P.B. “Mono- and Difluorination of Benzylic Carbons Atoms” *Eur. J. Org. Chem.* **2016**, 5, 871-886. This

review was written during my presence at Gilead Sciences and is *not* related to any experimental work described in this thesis.

All the publications (published and expected) from Ana Koperniku during the period of Doctor of Philosophy (2013-2018) are presented in a chronological order below:

1. Koperniku A.; Liu, H.; Hurley, P.B. “Mono- and Difluorination of Benzylic Carbon Atoms”. *Eur. J. Org. Chem.* **2016**, 5, 871-886. (Appendix B)
2. Koperniku, A.; Zamiri, M.; Grierson, D.S. “The Reaction of N-Trimethylsilyl Substituted Heteroarylamines with Thio- and Oxoesters: An Efficient Protocol to Access Diheteroarylamides”. *Synthesis.* **2019**, 51, 1779-1790. (Chapter 2)
3. Koperniku, A.; Foth, P.J.; Sammis, G.M.; Schafer, L.L. “Zirconium Catalyzed Hydroaminoalkylation. New Disconnection for α -Arylated Primary Amines”. Prepared. (Chapter 3)
4. Koperniku, A.; Schafer, L.L. “Zirconium Catalyzed Hydroaminoalkylation of Alkenes Directed toward the Synthesis of Saturated and Unsaturated *N*-Heterocycles”. Prepared. (Chapter 3 and 4)
5. Koperniku, A.; Schafer, L.L. “*N*-Silylated Amines in Catalysis: Synthesis and Chemistry”. Prepared. (Chapter 1)

Table of Contents

| | |
|---|---------------|
| Abstract..... | iii |
| Lay Summary | v |
| Preface..... | vi |
| Table of Contents | viii |
| List of Tables | xiii |
| List of Figures..... | xiv |
| List of Schemes | xv |
| List of Abbreviations | xxi |
| Acknowledgements | xxvi |
| Dedication | xxviii |
| Chapter 1: Synthesis and chemistry of <i>N</i>-silylated amines in catalysis | 1 |
| 1.1 General introduction | 1 |
| 1.2 Synthons: two sides of the same coin | 1 |
| 1.3 The silicon protecting and activating group on the nitrogen | 1 |
| 1.4 <i>N</i> -silylated amines: reactivity and synthesis | 2 |
| 1.4.1 <i>N</i> -silylated amines in stoichiometric reactions: synthesis | 2 |
| 1.4.2 <i>N</i> -silylated amines in stoichiometric reactions: reactivity | 3 |
| 1.4.3 <i>N</i> -silylated amines in catalysis: synthesis | 4 |
| 1.4.3.1 Lithium, Sodium and Potassium | 5 |
| 1.4.3.2 Magnesium, Calcium, Strontium, Barium | 7 |
| 1.4.3.3 Boron..... | 10 |

| | | |
|--|---|-----------|
| 1.4.3.4 | Aluminum | 12 |
| 1.4.3.5 | Transition metals..... | 12 |
| 1.4.3.5.1 | Titanium & Copper | 12 |
| 1.4.3.5.2 | Chromium..... | 14 |
| 1.4.3.5.3 | Ruthenium..... | 15 |
| 1.4.3.5.4 | Rhodium & Zinc..... | 18 |
| 1.4.3.5.5 | Miscellaneous transition metals | 19 |
| 1.4.3.6 | Lanthanides and Actinides | 20 |
| 1.4.3.6.1 | Ytterbium & Samarium..... | 20 |
| 1.4.3.6.2 | Uranium..... | 22 |
| 1.4.4 | <i>N</i> -silylated amines in catalysis: reactivity..... | 22 |
| 1.4.4.1 | Organo- and organoboron catalyzed reactions | 23 |
| 1.4.4.2 | Transition metal catalyzed reactions..... | 25 |
| 1.4.4.2.1 | Rhodium..... | 25 |
| 1.4.4.2.2 | Titanium & Palladium..... | 26 |
| 1.4.4.2.3 | Platinum | 27 |
| 1.4.4.2.4 | Iridium..... | 28 |
| 1.4.4.2.5 | Cobalt | 29 |
| 1.5 | Summary..... | 30 |
| 1.6 | Thesis scope | 31 |
| Chapter 2: <i>N</i>-TMS amines as amine surrogates to access diheteroarylamides | | 32 |
| 2.1 | Introduction..... | 32 |
| 2.2 | Overview of amide bond formation of aryl/heteroaryl amides..... | 35 |

| | | |
|---|--|-----------|
| 2.2.1 | Heterolytic coupling..... | 37 |
| 2.2.2 | Catalyzed coupling..... | 38 |
| 2.2.3 | Homolytic coupling | 39 |
| 2.3 | The reaction between the <i>N</i> -TMS amines and thioesters: an efficient protocol to access diheteroarylamides | 39 |
| 2.3.1 | <i>N</i> -TMS derivatives of electron deficient amines and acyl halides | 41 |
| 2.3.2 | <i>N</i> -TMS derivatives of electron deficient amines and thioesters in the amidation reaction..... | 43 |
| 2.3.3 | Efficiency of the amidation protocol and consideration of a green chemistry approach..... | 45 |
| 2.3.3.1 | Efficiency | 45 |
| 2.3.3.2 | Green chemistry | 46 |
| 2.3.4 | The amidation reaction between thioesters and <i>N</i> -TMS amines | 49 |
| 2.4 | Summary..... | 54 |
| Chapter 3: <i>N</i>-TMS amines as substrates in zirconium catalyzed hydroaminoalkylation to access primary α-arylated amines | | 55 |
| 3.1 | Introduction..... | 55 |
| 3.2 | Overview of α -arylated amines synthesis | 56 |
| 3.3 | Hydroaminoalkylation: promises and challenges | 58 |
| 3.4 | Catalyzed hydroaminoalkylation with primary amines as substrates | 60 |
| 3.5 | Catalyzed hydroaminoalkylation with protected <i>N</i> -TMS amines as substrates..... | 61 |
| 3.6 | Zirconium catalyzed hydroaminoalkylation with protected <i>N</i> -TMS amines as substrates: a promise to access primary amines with linear regioselectivity..... | 63 |

| | | |
|--|--|----|
| 3.7 | Efforts toward the synthesis of heterocycles via the zirconium catalyzed hydroaminoalkylation of alkenes with the use of <i>N</i> -TMS amines as substrates..... | 74 |
| 3.8 | Conclusions..... | 76 |
| Chapter 4: <i>N</i>-alkyl- and <i>N</i>-arylamines as substrates in zirconium catalyzed hydroaminoaminoalkylation to access secondary α-arylated amines78 | | |
| 4.1 | Introduction..... | 78 |
| 4.2 | Overview of α -arylated amine synthesis..... | 78 |
| 4.3 | Early transition metal catalyzed hydroaminoalkylation: a conscious choice for secondary α -arylated amines..... | 80 |
| 4.4 | Zirconium catalyzed hydroaminoalkylation of alkenes with <i>N</i> -phenylbenzylamine and <i>N</i> -isopropylbenzylamine as substrates..... | 83 |
| 4.5 | Zirconium catalyzed hydroaminoalkylation of alkenes: other sterically demanding secondary amine substrates..... | 90 |
| 4.6 | Application of the zirconium catalyzed hydroaminoalkylation toward the formation of saturated <i>N</i> -heterocycles..... | 92 |
| 4.7 | Conclusions..... | 94 |
| Chapter 5: Summary and future work96 | | |
| 5.1 | Summary..... | 96 |
| 5.2 | Future work..... | 97 |
| 5.2.1 | Methods refinement..... | 97 |
| 5.2.1.1 | Amidation protocol..... | 97 |
| 5.2.1.2 | Hydroaminoalkylation protocol..... | 97 |
| 5.2.2 | Applications..... | 98 |

| | | |
|-------------------------------------|---|------------|
| 5.2.2.1 | Amidation protocol | 98 |
| 5.2.2.2 | Hydroaminoalkylation protocol | 98 |
| 5.2.2.2.1 | Heterocycle syntheses | 98 |
| 5.2.2.2.2 | Unnatural amino acid synthesis..... | 103 |
| 5.3 | Conclusions..... | 104 |
| Chapter 6: Experimental..... | | 107 |
| 6.1 | General considerations and materials | 107 |
| 6.2 | Experimental data for Chapter 2 | 108 |
| 6.3 | Experimental data for Chapter 3 | 127 |
| 6.4 | Experimental data for Chapter 4 | 150 |
| Bibliography | | 1 |
| Appendix A NMR spectra | | 9 |
| A.1 | General considerations..... | 9 |
| A.2 | ¹ H, ¹³ C and ¹⁹ F NMR spectra of compounds in Chapter 2 | 10 |
| A.3 | ¹ H, ¹³ C and ¹⁹ F NMR spectra of compounds in Chapter 3 | 46 |
| A.4 | ¹ H and ¹³ C spectra and GCFID chromatograms of compounds in Chapter 4..... | 87 |
| Appendix B Microreview | | 113 |

List of Tables

| | |
|--|----|
| Table 2.1 Diheteroarylamide products 2.2 , 2.6.1-2.6.10 and 2.6.12-2.6.19 prepared <i>via</i> Schemes 2.7 and 2.10..... | 49 |
| Table 3.1 Catalyst screening for the intermolecular hydroaminoalkylation with <i>N</i> -TMS amines..... | 62 |
| Table 3.2 Zirconium catalyzed hydroaminoalkylation - alkene scope – list of alkenes..... | 64 |
| Table 3.3 Silicon substituent screening of the <i>N</i> -silylated amines for regioselectivity outcome..... | 73 |
| Table 4.1 Zirconium catalyzed hydroaminoalkylation with <i>N</i> -phenylbenzylamine - alkene scope..... | 84 |
| Table 4.2 Zirconium catalyzed hydroaminoalkylation of alkenes with <i>N</i> -isopropylbenzylamine - alkene scope..... | 87 |

List of Figures

| | |
|--|-----|
| Figure 1.1 <i>N</i> -silylated amines and a series of commercially available silylating agents..... | 2 |
| Figure 1.2 The periodic table of elements..... | 5 |
| Figure 2.1 Resonance structures of the amide bond..... | 32 |
| Figure 2.2 Amide mimics of 2.1 | 33 |
| Figure 2.3 Generic structure of structural analogs of 2.2 | 35 |
| Figure 2.4 Isomeric diheteroarylamides 2.2 and 2.2' | 52 |
| Figure 3.1 Pharmaceuticals containing a primary amine synthon..... | 55 |
| Figure 3.2 Diagnostic ¹ H NMR benzylic signals for single regioisomers (3.11.10) and mixture of regio- and diastereomers (3.11.12 , 3.12.12 and 3.13.12)..... | 67 |
| Figure 4.1 Secondary α -arylated amine motif present in pharmaceuticals/natural products..... | 78 |
| Figure 4.2 Diagnostic ¹ H NMR spectrum peaks for the different isomers 4.9.5 , 4.10.5 and 4.11.5 | 85 |
| Figure 4.3 ¹ H NMR spectrum (benzylic region) and GCFID chromatogram for the different isomers 4.12.5 , 4.13.5 and 4.14.5 | 88 |
| Figure 5.1 Nicotine derivatives to be obtained from the intramolecular cyclization of the hydroaminoalkylation product..... | 100 |
| Figure 5.2 Tetrahydroquinoline containing pharmaceuticals and natural products..... | 101 |
| Figure 5.3 Azetidine containing pharmaceuticals and natural products..... | 103 |

List of Schemes

| | |
|---|----|
| Scheme 1.1 Stoichiometric routes to synthesize <i>N</i> -silylamines..... | 3 |
| Scheme 1.2 <i>N</i> -silylamines as reagents and additives in stoichiometric reactions..... | 4 |
| Scheme 1.3 Three catalytic routes reported to deliver <i>N</i> -silylamines..... | 4 |
| Scheme 1.4 Alkali metal dehydrocoupling of hydrosilanes with amines..... | 6 |
| Scheme 1.5 Two plausible mechanisms for the alkali metal hydrosilylation with amines..... | 7 |
| Scheme 1.6 Magnesium catalyzed dehydrocoupling of hydrosilanes with ammonia and hydrazine; proposed mechanism..... | 8 |
| Scheme 1.7 Magnesium, calcium and strontium catalyzed Si-N dehydrocoupling of amines with silanes..... | 9 |
| Scheme 1.8 Alkaline earth metal catalyzed dehydrocoupling of amines with hydrosilanes..... | 9 |
| Scheme 1.9 Boron catalyzed hydrosilylation of imines..... | 10 |
| Scheme 1.10 Synthesis of indolines from indoles via the boron catalyzed Si-N dehydrocoupling..... | 11 |
| Scheme 1.11 Aluminum catalyzed dehydrocoupling of amines with silanes..... | 12 |
| Scheme 1.12 Titanium catalyzed dehydrocoupling of amines with silanes and proposed mechanism of homocoupling of silanes..... | 13 |
| Scheme 1.13 Copper (I) catalyzed dehydrogenative coupling of amines with silanes..... | 14 |
| Scheme 1.14 Chromium catalyzed Si-N dehydrocoupling..... | 15 |
| Scheme 1.15 Ruthenium catalyzed dehydrogenative Si-N coupling..... | 15 |
| Scheme 1.16 Ruthenium catalyzed dehydrocoupling for <i>N</i> -silylation of pyrroles, indoles, carbazoles, anilines, indolines..... | 16 |

| | |
|--|----|
| Scheme 1.17 Ruthenium catalyzed Si-N coupling of imines with silanes to generate <i>N</i> -silylenamines..... | 17 |
| Scheme 1.18 Ruthenium catalyzed dealkenative <i>N</i> -silylation of amines <i>via</i> silanes..... | 18 |
| Scheme 1.19 Rhodium and zinc catalyzed dehydrocoupling of amines and silanes for <i>N</i> -silylation of indoles, pyrroles and carbazoles..... | 19 |
| Scheme 1.20 Palladium catalyzed dehydrogenative coupling of amines with silanes..... | 20 |
| Scheme 1.21 Ytterbium catalyzed dehydrocoupling of amines with silanes and hydrosilylation of imines with silanes..... | 20 |
| Scheme 1.22 NHC supported ytterbium and samarium complexes for the Si-N dehydrogenative coupling of amines with silanes..... | 21 |
| Scheme 1.23 Uranium catalyzed dehydrocoupling of primary amines with silanes..... | 22 |
| Scheme 1.24 <i>N</i> -silylimines as electrophiles in the aza-Henry reaction..... | 23 |
| Scheme 1.25 <i>N</i> -silylimines as substrates for the generation of optically active secondary aziridines..... | 24 |
| Scheme 1.26 Boron catalyzed reduction of <i>N</i> -silylimines (top) and <i>E/Z</i> imines to primary amines (bottom)..... | 25 |
| Scheme 1.27 Rhodium catalyzed transfer hydrogenation of aminosilanes resulting in <i>N</i> -silylenamines..... | 26 |
| Scheme 1.28 Titanium catalyzed hydroamination of alkynes with silylated ammonia; Palladium catalyzed hydrogenation of the <i>N</i> -silylenamines..... | 26 |
| Scheme 1.29 One pot hydroamination/aldol condensation to access multisubstituted pyridines..... | 27 |

| | |
|--|----|
| Scheme 1.30 Platinum catalyzed diboration of <i>N</i> -silylimines in the aminoborylation of aldehydes to generate chiral α -amido boronic acids..... | 28 |
| Scheme 1.31 Synthesis of necessary intermediate for the synthesis of (R)-cetirizine..... | 28 |
| Scheme 1.32 Iridium-catalyzed, silyl-directed borylation of nitrogen containing <i>N</i> -heterocycles..... | 29 |
| Scheme 1.33 Cobalt catalyzed aminocarbonylation of cyclic ethers (top) and formaldehyde dialkyl acetals (bottom) using <i>N</i> -silylamines..... | 30 |
| Scheme 2.1 Possible disconnections to access diheteroarylamides..... | 36 |
| Scheme 2.2 Amide bond formation: heterolytic coupling..... | 37 |
| Scheme 2.3 Amide bond formation: catalyzed coupling..... | 39 |
| Scheme 2.4 Amide bond formation: radical initiated coupling..... | 39 |
| Scheme 2.5 Retrosynthetic analysis of diheteroarylamides 2.6 | 40 |
| Scheme 2.6 Amide bond formation with <i>N</i> -TMS amines and acyl halides..... | 42 |
| Scheme 2.7 Total synthetic route for thioester 2.33 and diheteroarylamides 2.6 | 44 |
| Scheme 2.8 Rationale for the efficiency of the protocol: precipitation of diheteroarylamides and formation of TMSF..... | 45 |
| Scheme 2.9 Synthetic route for odorless thiol 2.41 | 47 |
| Scheme 2.10 Green cycle to access diheteroarylamides 2.6 with the use of odorless thiol 2.41 | 48 |
| Scheme 2.11 Plausible mechanism for products 2.2 and 2.2' | 53 |
| Scheme 2.12 Proposed equilibrium of species 2.50 and 2.51 | 53 |

| | |
|---|----|
| Scheme 3.1 Possible disconnections to access α -arylated amines..... | 57 |
| Scheme 3.2 Benzylamines as substrates to access α -arylated amines..... | 58 |
| Scheme 3.3 Zirconium mediated α -alkenylation of <i>N</i> -silylated amines..... | 58 |
| Scheme 3.4 Early transition metal catalyzed hydroaminoalkylation..... | 59 |
| Scheme 3.5 Intramolecular zirconium catalyzed hydroaminoalkylation of alkenes with primary amines | 60 |
| Scheme 3.6 Attempted intermolecular zirconium catalyzed hydroaminoalkylation of alkenes with primary amines..... | 61 |
| Scheme 3.7 Zirconium catalyzed hydroaminoalkylation of alkenes with <i>N</i> -TMS amines as substrates..... | 63 |
| Scheme 3.8 Zirconium catalyzed hydroaminoalkylation - alkene scope – general reaction scheme..... | 64 |
| Scheme 3.9 <i>N</i> -silylation of benzylamines; reported amines in the literature: 3.5.3 , 3.14 , 3.15 | 68 |
| Scheme 3.10 Zirconium catalyzed hydroaminoalkylation - amine scope..... | 69 |
| Scheme 3.11 Proposed mechanism for the zirconium catalyzed hydroaminoalkylation of alkenes with <i>N</i> -silylamines..... | 70 |
| Scheme 3.12 Rationale for the proposed assignment of diastereomers 3.12 and 3.13 | 71 |
| Scheme 3.13 Synthesis of <i>N</i> -TIPS-amine 3.38 , <i>N</i> -TPS-amine 3.39 and <i>N</i> -TBS-amine 3.40 (top) and hydroaminoalkylation reaction with 1-octene (bottom)..... | 72 |

| | |
|--|----|
| Scheme 3.14 Intermolecular zirconium catalyzed hydroaminoalkylation (top) and intramolecular ruthenium catalyzed cyclization of aminoalcohols (bottom); reported amines in the literature: 3.42, 3.43 | 75 |
| Scheme 4.1 Possible disconnections to access secondary and tertiary α -arylated amines using catalysts..... | 79 |
| Scheme 4.2 Hydroaminoalkylation: flexibility to access both cyclic and acyclic amines..... | 80 |
| Scheme 4.3 Titanium and tantalum catalyzed hydroaminoalkylation of <i>N</i> -alkyl- and <i>N</i> -phenylbenzylamines..... | 81 |
| Scheme 4.4 Zirconium catalyzed hydroaminoalkylation of alkenes with <i>N</i> -phenylbenzylamine..... | 84 |
| Scheme 4.5 Zirconium catalyzed hydroaminoalkylation of alkenes with <i>N</i> -isopropylbenzylamine..... | 86 |
| Scheme 4.6 Zirconium catalyzed hydroaminoalkylation of vinylsilane with (<i>S</i>)- <i>N</i> -benzyl-1-phenylethan-1-amine..... | 90 |
| Scheme 4.7 Zirconium catalyzed hydroaminoalkylation of vinylsilane with heteroarylated <i>N</i> -isopropylbenzylamines..... | 91 |
| Scheme 4.8 Reductive amination conditions to access additional sterically demanding benzylamines; all amine-products are reported in the literature: 4.15, 4.17, 4.18 | 91 |
| Scheme 4.9 Intramolecular cyclization of hydroaminoalkylation products to access heterocyclic amines..... | 93 |
| Scheme 4.10 Previously reported route for the synthesis of 3'-trans methyl nicotine (route 1)... | 93 |
| Scheme 4.11 Previously reported route for the synthesis of 3'-trans methyl nicotine (route 2)... | 94 |
| Scheme 5.1 Two different cyclization routes for the formation of piperidines and pyrrolidines.. | 99 |

| | |
|---|-----|
| Scheme 5.2 Tetrahydroquinolines to be obtained from the intramolecular Buchwald-Hartwig amination of the hydroaminoalkylation products..... | 102 |
| Scheme 5.3 Proposed route to obtain 2-aryl- and 2-aryl-3-methylazetidines <i>via</i> Csp ³ -Si activation..... | 103 |
| Scheme 5.4 Proposed route for the synthesis of peptidomimetics | 104 |

List of Abbreviations

Ac acetyl

Ar aryl

ART antiretroviral therapy

B₂Pin₂ bis(pinacolato)diboron

BPinH pinacolborane

Bn benzyl

Boc tertbutoxycarbonyl

br broad

BTF₆H fluoro-*N,N,N',N'*-bis(tetramethylene)formamidinium hexafluorophosphate

calcd. calculated

C₆D₆ deuterated benzene

C₇D₈ deuterated toluene

CI chemical ionization

CDCl₃ deuterated chloroform

CD₃OD deuterated methanol

COD cyclooctadiene

CR coupling reagent

Cp cyclopentadienyl

Cy cyclohexyl

δ chemical shift

d doublet

D or **d** deuterium

DAST diethylaminosulfur trifluoride

Deoxo-fluor bis(2-methoxyethyl)aminosulfur trifluoride

dba dibenzylideneacetone

DCM dichloromethane

DFT density functional theory

DEC diethylcarbonate

DDQ 2,3-dichloro-5,6-dicyano-1,4-benzoquinone

DIPEA diisopropylethylamine

DMSO dimethylsulfoxide

DMSO-*d*₆ deuterated dimethylsulfoxide

DMIPS dimethylisopropylsilyl

DMPS dimethylphenylsilyl

DR diastereoselectivity ratio

dtbpy 4,4'-di-tert-butyl-2,2'-dipyridyl

ee enantiomeric excess

EDG electron donating group

e.g. *exempli gratia*

EI electron impact

equiv equivalent(s)

ESI electrospray ionization

Et ethyl

EWG electron withdrawing group

FmocCl fluorenylmethoxycarbonylchloride
GCFID gas chromatography – flame ionization detector
HAA hydroaminoalkylation
HIV human immunodeficiency virus
HMDS hexamethyldisilazane (N(SiMe₃)₂)
HRMS high resolution mass spectrometry
hmpa hexamethylphosphoramide
i.e. id est
Im^tBu 1,3-di-tert-butylimidazol-2-ylidene
***i*-Pr** isopropyl
IR infrared
L supporting ligand
LAH lithium aluminum hydride
m multiplet
M metal
[M] metal complex
M + H⁺ molecular ion
Me methyl
MeCN acetonitrile
MeOH methanol
MS mass spectrometry
MW molecular weight
m/z mass-to-charge ratio

$\tilde{\nu}$ wavenumber

***n*-Bu** *n*-butyl

NHC *N*-heterocycle carbene

NMR nuclear magnetic resonance

OAc acetoxy

OTf trifluoromethanesulfonate

PBAM Johnston bis(amidine) chiral proton organocatalyst

Ph phenyl

PivCl pivaloyl chloride

ppm parts per million

Py pyridine

Pyrr pyrrole

q quartet

R organic substituent

RR regioselectivity ratio

RAR rearrangement

rac racemic

rt room temperature

s singlet

SAR structure activity relationship

SN_{AR} nucleophilic aromatic substitution

t triplet

***t*-Bu** tert-butyl

TBAF tetrabutylammonium fluoride
TBA₂ tetra-*n*-butylammonium
TBAH tetrabutylammonium hydroxide
TBAI tetrabutylammonium iodide
TBDMS tert-butyldimethylsilyl
TBHP tert-butyl hydroperoxide
TBS tert-butyldimethylsilyl
tert tertiary
TES triethylsilyl
TFFH *N,N*-tetramethylfluoroformamidinium hexafluorophosphate
THF tetrahydrofuran
TIPS triisopropylsilyl
TMSF trimethylsilyl fluoride
TMS trimethylsilyl
TLC thin layer chromatography
TPS triphenylsilyl
Tol toluene
TOF turnover frequency
TON turnover number
Ts para-toluenesulfonyl (tosyl)
X halide (unless otherwise specified)
UV ultraviolet

Acknowledgements

First and foremost, I would like to thank the Universe for bringing in me the spark to apply to UBC. Secondly, I would like to thank UBC for accepting my application to pursue my graduate studies at such an Institution. I would like to thank both my supervisors, Prof. David S. Grierson and Prof. Laurel L. Schafer for two distinct reasons. I would like to thank David for accepting me into the program of PhD in Pharmaceutical Sciences. I would like to thank Laurel for her mentorship and for scientific discussions. Thank you both for the opportunity and the trust to work on these projects.

Thank you to Prof. Urs Häfeli, supervisory committee member, for editing my thesis on Jan. 1st 2019. Special thanks go to Maryam, Sonia, Safwat and Ying for their cooperation and for our discussions, scientific and not only. I am especially grateful to Dr. Sorin Rosca for his instructions on the Schlenk chemistry and his patience, support and encouragement. If the reader is currently working with Sorin, then the reader is working with a big-hearted chemist. I also thank Vani, Nirmal, Peter, and Sam for Thesis edits and all the Schafer group members.

I would like to acknowledge Prof. Marco Ciufolini and Dr. Jason Brandt for scientific discussions. Also, thank you to the Love group; I borrowed $\text{Ru}(\text{Cl})_2(\text{PPh}_3)_3$ seven times and they always welcomed me with a genuine smile.

Special thanks to Prof. Thomas Chang – Associate Dean of Graduate Studies in the Faculty of Pharmaceutical Sciences – for advising me to hold on with any remaining strength I had;

Jan 4th, 2017: “Keep your eyes to the Prize, Ana. If you step down now, you will offer the greatest of all punishments to yourself. Not you, Ana. You are the type of the person who makes things happen.”

This PhD would not have occurred without the funding provided by NSERC CREATE Sustainable Synthesis Program (2013-2015) and 4YF (2016-2018) and through my TAsip at the Faculty of Pharmaceutical Sciences.

Many thanks to Zhongxin Zhou and Jesse Wang – Senior Directors in Process Chemistry at Gilead Sciences – for assigning us the task to write a review which would summarize methods for the difluorination of the precursor to Ledipasvir – a well established medication for the *cure* of HCV – which has also received the credit for being Gilead’s biggest pride to date. I would like to thank the co-authors – Patrick Liu and Paul Hurley – for bringing together this heavy task to an end; Patrick for providing the references related to the review and Paul for advising me to combat any inconsistencies of mine (**Aug 12th, 2015**). I would like to thank Gilead Sciences for financial support (6,000\$) during my 4-months’ stay at their site; with that support I was able to pay my tuition fees in year 3 of my PhD (tuition fees: 4,500\$). Gratifyingly, our review was published. *We must* get things done. Always.

I would like to thank friends and family for listening to my misery in moments of failure and tolerating my enthusiastic voice in periods of great accomplishments. Thank you to Voula, a friend since 2000, for all the conversations throughout the years. Many thanks to Dimitris, Effie and Nikos for the Sunday lunches at their place and my landlady, Matoula, for having a tenant without precedent in her apartment. I would like to thank my parents – Albert and Mizi Koperniku – for their support to pay my tuition fees during the first two years at UBC (9,000\$). I know it was not easy for you; not because of the crisis over the past 10 years but because of your financial status throughout your life. Your moral support and encouragement throughout this PhD and my entire life to build confidence, when odds are minimal or against me, is what qualifies you to hold a very special place in my heart.

Dedication

To all those who hit rock bottom, embrace pain and get transformed into unconquerable warriors.

– Ana Koperniku

Chapter 1: Synthesis and chemistry of *N*-silylated amines in catalysis

1.1 General introduction

This thesis presents the exploitation of secondary *N*-silylated amines, derived from primary amines, as precursors in amide bond formation with electron deficient amines and as substrates in carbon-carbon bond formation to access novel α -arylated amines via the hydroaminoalkylation reaction. The *N*-silylated amines are derived from the appendage of a silicon protecting group onto the nitrogen of a starting primary or secondary amine. The facile hydrolytic Si-N cleavage and the different electronic properties of the resulting *N*-silylated amines, as compared to the parent non-silylated amines, are exploitable features which will be examined in this thesis and delineate the value of *N*-silylated amines as synthons in synthetic transformations.

1.2 Synthons: two sides of the same coin

The term synthon was introduced by E.J. Corey in 1967 and was defined as the “destructural unit within a molecule which is related to a synthetic operation”.¹ In 1988, in his Robert Robinson lecture, he updated the audience and the chemistry community that the “the term has now come to mean a synthetic building block rather than a retrosynthetic fragmentation”.² The retrosynthetic fragment and the building block are the two sides of the same coin. The inspiring synthons for the methods developed in this thesis are *N*-silylated amines. Other amines – *N*-aryl- and *N*-alkylamines – will be explored for their value as synthons in synthetic operations in Chapter 4.

1.3 The silicon protecting and activating group on the nitrogen

In Figure 1.1 the generic structure of the *N*-silylated amines is presented along with a series of commercially available silylating agents. The resulting *N*-silylated amines differ from the non-

silyl variants both sterically and electronically. The appendage of the silicon group offers steric protection to the parent amine while at the same time it renders the resulting amine less nucleophilic due to the delocalization of the lone pair of the nitrogen into the silicon orbitals via hyperconjugation.^{3, 4} Literature reports show efforts to evaluate the relative basicities among the different *N*-silylated amines, using trimethylboron as the reference acid and trimethylamine as the reference base.⁵⁻⁷

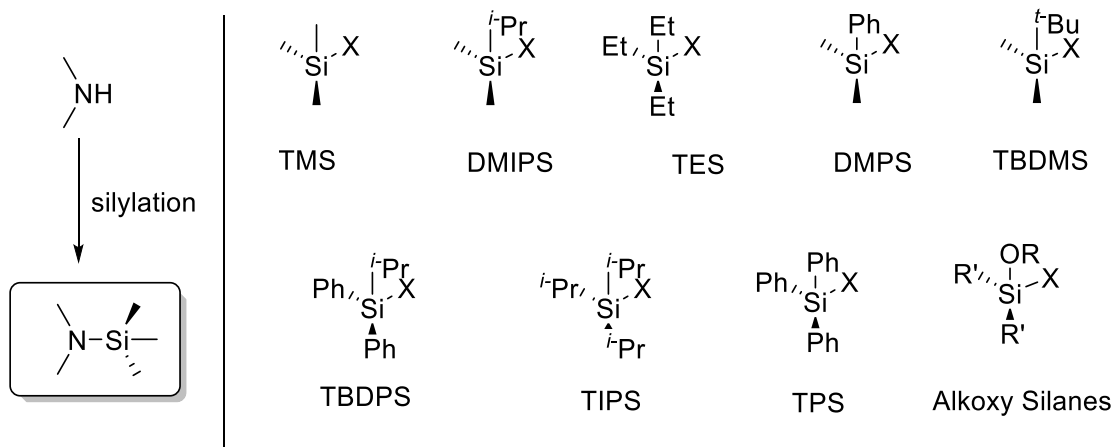


Figure 1.1 *N*-silylated amines and a series of commercially available silylating agents

1.4 *N*-silylated amines: reactivity and synthesis

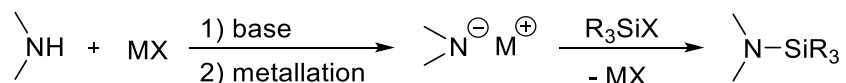
Both stoichiometric and catalytic transformations have been reported for the synthesis of *N*-silylamines. Chapters 1.4.1 and 1.4.2 include a few representative examples for their stoichiometric synthesis and reactivity, respectively. This introduction will primarily focus on the exploitation of *N*-silylated amines in catalysis, which has not been previously reviewed.

1.4.1 *N*-silylated amines in stoichiometric reactions: synthesis

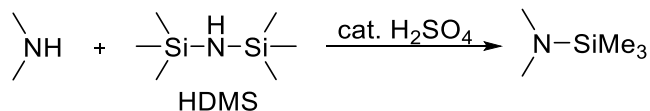
The stoichiometric synthesis of *N*-silylated amines has been described under basic, acidic and neutral conditions (Scheme 1.1). Basic conditions include the generation of the amido species of an amine *via* metallation and reaction with an halosilane.⁷ The stoichiometric production of

waste-salt is a disadvantage to this approach. Acidic conditions utilize catalytic H₂SO₄ to mediate the reaction between HDMS (hexamethyldisilazane) and an amine.^{8, 9} An example of neutral conditions involves the reaction of an amine with TMSCN under neat conditions.¹⁰ The asset of this last approach is there is no need for an ancillary base or acid, however the toxicity associated with TMSCN is a huge issue to consider when selecting a synthetic protocol.

Basic conditions



Acidic conditions



Neutral conditions

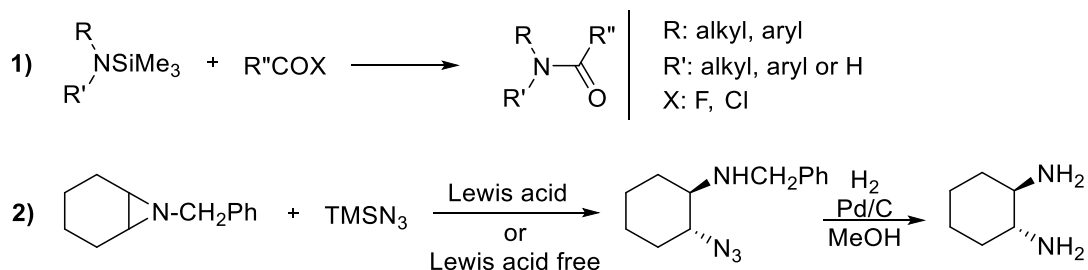


Scheme 1.1 Stoichiometric routes to synthesize *N*-silylamines

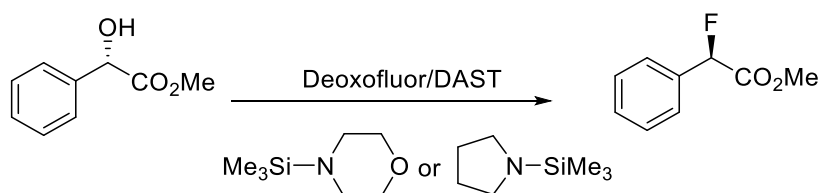
1.4.2 *N*-silylated amines in stoichiometric reactions: reactivity

N-Silylated amines have been used to activate sterically hindered and electronically suppressed amines in reactions with acyl fluorides or acyl chlorides to deliver amide products (Scheme 1.2).¹¹⁻¹³ Another example is the efficient opening of aziridines with TMSN₃, with the resulting azides serving as placeholders for primary amines.¹⁴ Moreover, there have been transformations in which *N*-silylated amines offer ancillary support for the reaction to proceed. A representative example includes the deoxyfluorination of benzylic alcohols in the presence of nucleophilic fluorinating agents and *N*-TMS amines as additives,¹⁵ and increased stereospecificity was observed in the presence of *N*-TMS amines.

N-TMS amines as reagents



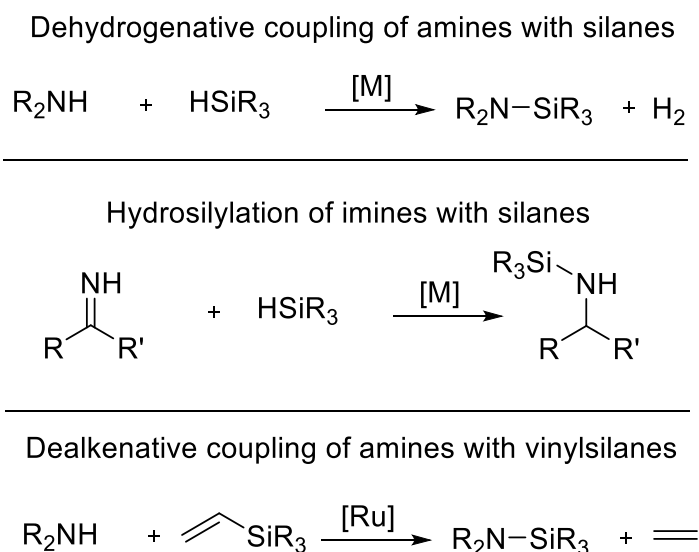
N-TMS amines as additives



Scheme 1.2 *N*-silylamines as reagents and additives in stoichiometric reactions

1.4.3 *N*-silylated amines in catalysis: synthesis

There are three methods for the catalytic synthesis of *N*-silylamines and *N*-silylenamines: dehydrogenative coupling of amines with silanes (dominant method), hydrosilylation of imines with silanes and dealkenative cross coupling of amines with silanes (Scheme 1.3).



Scheme 1.3 Three catalytic routes reported to deliver *N*-silylamines

The dehydrocoupling Si-N of amines with silanes has been reported with metals across the periodic table: alkali and alkaline earth metals, transition metals, post-transition metals, metalloids, lanthanides and actinides (Figure 1.2).^{16, 17} The hydrosilylation of imines has been reported with boron, lanthanides and actinides.¹⁸ Lastly, the dealkenative cross-coupling and Si-N dehydrocoupling leading to *N*-silylamines has been catalyzed only by ruthenium (d block).¹⁹

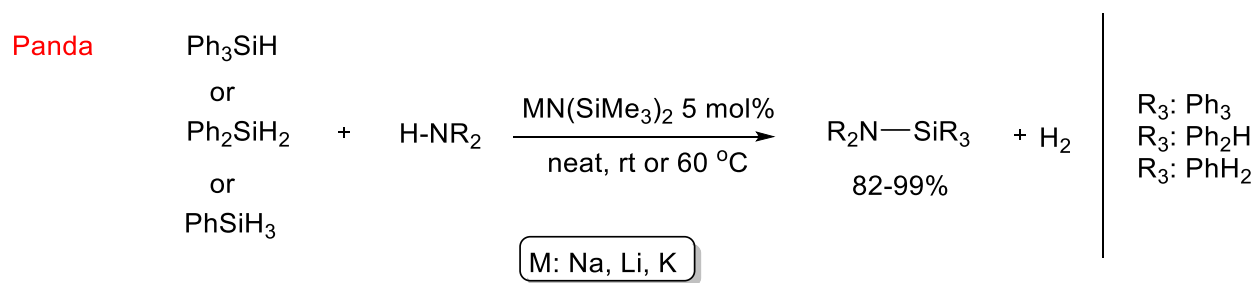
The figure shows a standard periodic table of elements, color-coded by groups. The legend at the bottom identifies the following categories: Alkali Metal (pink), Alkaline Earth (orange), Transition Metal (yellow), Basic Metal (light green), Semimetal (light blue), Nonmetal (light purple), Halogen (medium purple), Noble Gas (dark purple), Lanthanide (light pink), and Actinide (light red). The table includes element symbols, atomic numbers, and names, with atomic weights provided for many elements.

Figure 1.2 The periodic table of elements

1.4.3.1 Lithium, Sodium and Potassium

In 2016, the Panda²⁰ group reported the use of LiHMDS, NaHMDS and KHMDS as precatalysts in cross-dehydrocoupling. Potassium hexamethylsilylazide was the most active of the three precatalysts (Scheme 1.4). Amine substrates suitable for the reaction include pyrrolidine, diethylamine, tertbutylamine, benzylamine, and 2,6-diisopropylaniline. PhSiH₃, Ph₂SiH₂ and Ph₃SiH are competent in this reaction to yield products with high conversions of 82-99%. This reaction proceeds at room temperature and only when both the sterically demanding Ph₃SiH and

2,6-diisopropylaniline were used as reactants did the reaction require heating at 60 °C. The reaction of 1,2-ethylenediamine with silicon starting materials yielded a mixture of mono- and disilylated products in 1:3 ratio. For primary and secondary silanes, depending on the stoichiometry of the amine, mono-, di- and triaminated dehydrocoupling products were obtained; triaminated products in the case of primary silanes and diaminated products in the case of secondary silanes. Disilazanes were also obtained in an excess of silane.



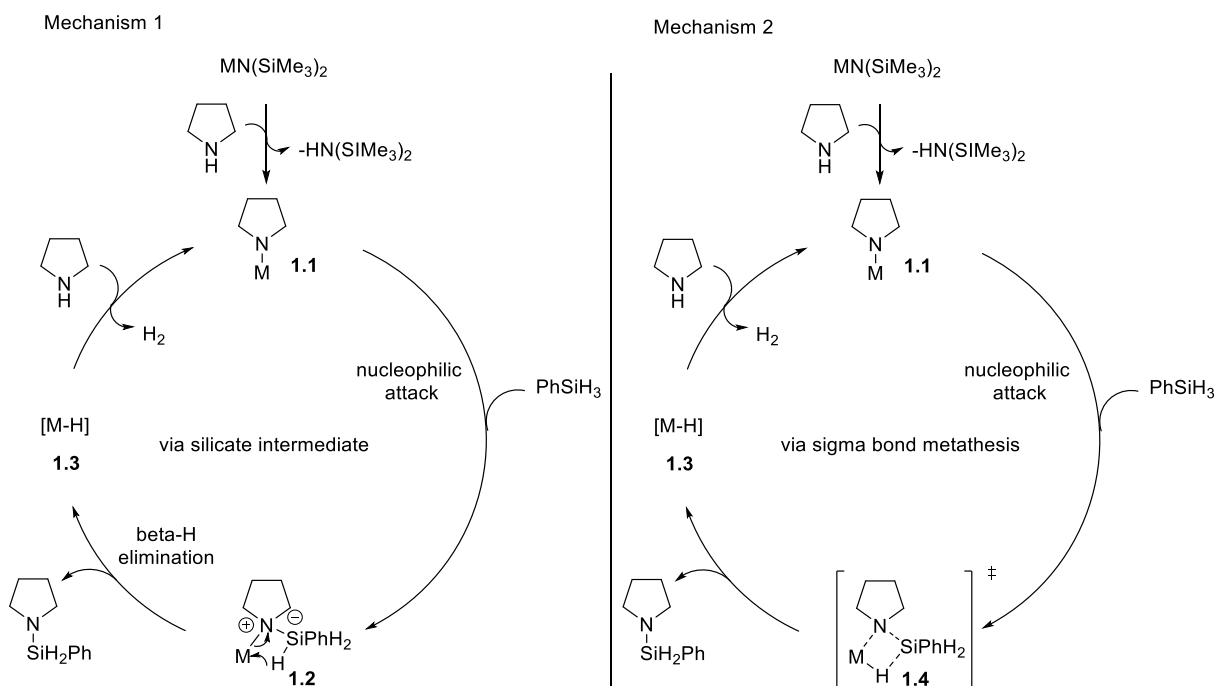
Scheme 1.4 Alkali metal dehydrocoupling of hydrosilanes with amines

There are two plausible mechanisms for the reaction, as shown in Scheme 1.5. The first mechanism features the formation of a silicate intermediate while the second one is based on σ -bond metathesis. The first mechanism proposes an initial reaction of amine substrate with the alkali amide to generate the catalytically active compound **1.1**. Compound **1.1** undergoes nucleophilic attack by the hydrosilane to give the hypervalent silicon intermediate **1.2**. β -Hydride elimination of **1.2** yields metal hydride **1.3** and concomitant release of the *N*-silylamine. The metal hydride reacts then with another pyrrolidine to generate the *N*-metallapyrrolidine **1.1**, with elimination of dihydrogen.

For mechanism 2, the cycle is the same but instead of proposing the formation of intermediate **1.2** through nucleophilic attack, σ -bond metathesis involving transition state **1.4** is proposed,

yielding *N*-silyl amine and metal hydride, which in turn will lead to the regeneration of species

1.1.

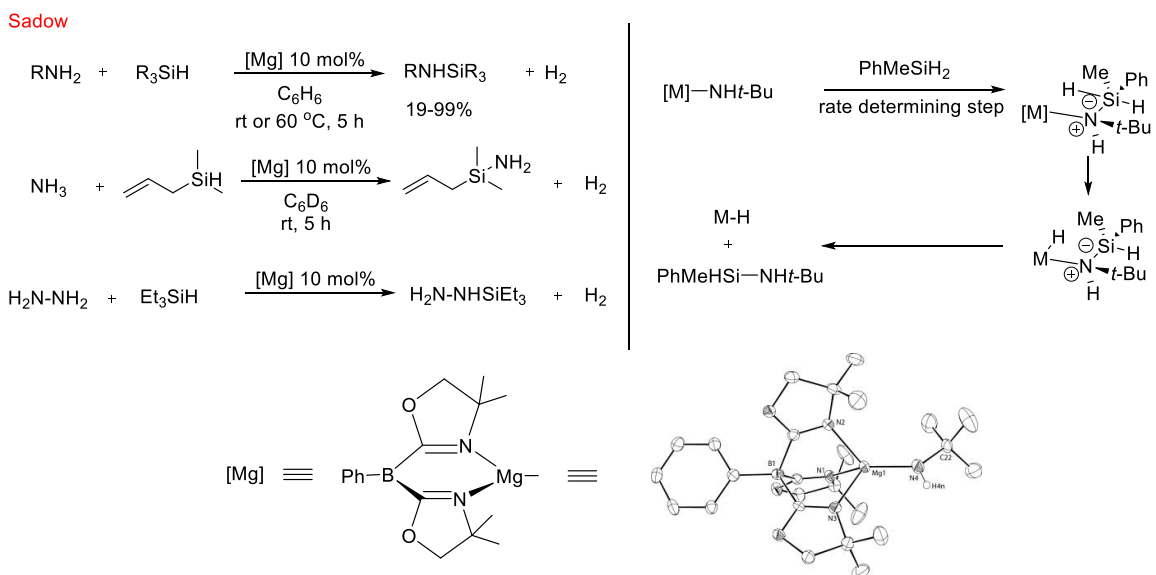


Scheme 1.5 Two plausible mechanisms for the alkali metal hydrosilylation with amines

1.4.3.2 Magnesium, Calcium, Strontium, Barium

In 2011, a tris(oxazolonyl)borato magnesium precatalyst was shown to accommodate both ammonia and hydrazine as substrates in the catalytic dehydrocoupling to form *N*-silylamines (Scheme 1.6).²¹ The amine substrate scope included *n*-propylamine, isopropylamine, tertbutylamine and aniline. Both primary and secondary silanes were reacted with amines and results showed quantitative conversion for all cases with the exception of aniline, for which heating was required to obtain an isolated yield 19%. Overall, the products were obtained in isolated yields 19-99%. Kinetic studies provided evidence for the mechanistic pathway involving the formation hypervalent silicon species (mechanism 1 in Scheme 1.5). Studies also showed that the rate determining step is the interaction of the catalyst with the silane. This is consistent with

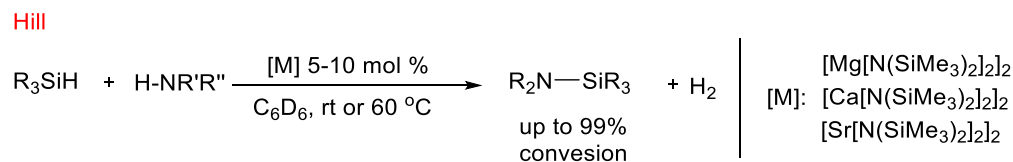
the low reaction rate observed for aniline. Considering the lower nucleophilicity/basicity of anilide as compared to the aliphatic amide, it was expected to observe lower reactivity for aniline as compared to the aliphatic amines.



Scheme 1.6 Magnesium catalyzed dehydrocoupling of hydrosilanes with ammonia and hydrazine; proposed mechanism

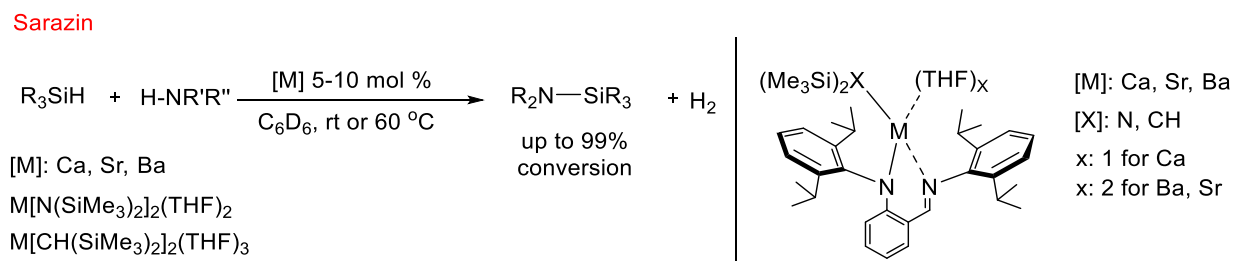
The Hill²² group has examined three alkaline earth metals (Mg, Ca, Sr) for their competency as precatalysts in the dehydrocoupling of hydrosilanes with amines (Scheme 1.7). A comparison among the three metals showed that, for the cases of calcium and magnesium, the rate consumption of the amine is first order in amine and catalyst $[\text{M}[\text{N}(\text{SiMe}_3)_2]_2]$ and zero order for the silane. When $\text{Sr}(\text{HDMS})_2$ is used the reaction rate is dependent on the amine and the silane. A broad reaction scope of both amines and silanes was examined. Results showed that both the electronic and steric properties of both the coupling partners influence the reactivity; the more limited the accessibility to the metal center, as is the case with magnesium, the greater the effect of the steric bulk of both the amine and the hydrosilane. Thus, the highest reactivity was observed with the calcium and strontium silylamides as precatalysts, as supported by the shorter

reaction times required and the milder reaction conditions applied. As is expected in cases of high reactivity, selectivity was attenuated for the cases of calcium and strontium. In contrast to the work by Sadow, aniline derivatives were shown to proceed faster than aliphatic amines.



Scheme 1.7 Magnesium, calcium and strontium catalyzed Si-N dehydrocoupling of amines with silanes

Recent work by Sarazin^{23, 24} and co-workers explored the use of Ca(HDMS)₂, Sr(HDMS)₂ and Ba(HDMS)₂ and their alkyl congeners [M[CH(SiMe₃)₂]₂ in the the Si-N dehydrocoupling of amines with silanes (Scheme 1.8). Moreover, complexes with bulky ancillary ligands attached to the metal center, bearing either *N*-silyl or *C*-silyl groups were also tested for their catalytic reactivity (Scheme 1.8).



Scheme 1.8 Alkaline earth metal catalyzed dehydrocoupling of amines with hydrosilanes

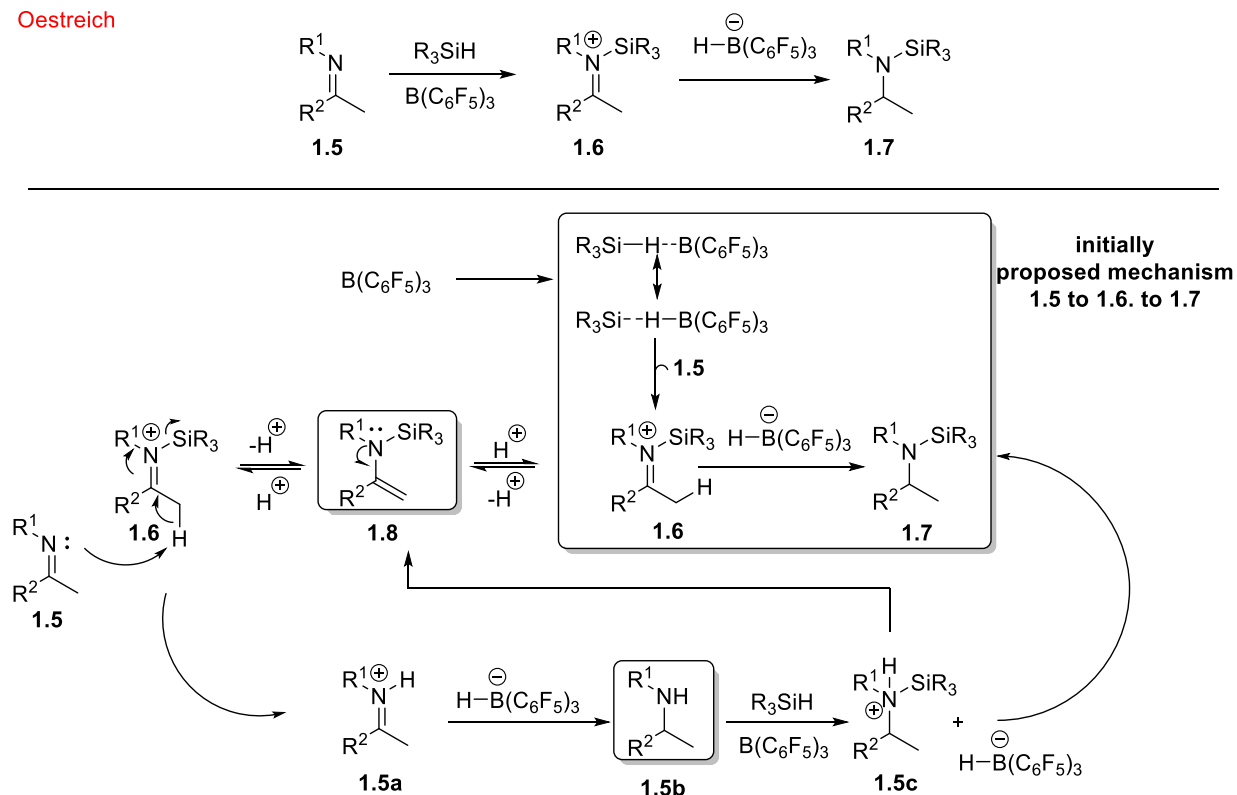
Increased reactivity was observed with barium, the largest of all three, as indicated by the high turnover frequencies (512-3600 h⁻¹), with the highest turnover frequency (3600 h⁻¹) shown with Ba[CH(SiMe₃)₂]₂(THF)₃. This is similar to the trend observed with alkali metals, where increased reactivity was observed with potassium. It has been hypothesized that larger metal allows for higher accessibility of the metal center, leading to increased reactivity. As such a scope of amines and silanes was developed based on the barium complexes (Scheme 1.8),

affording products with conversion up to 99%. Mechanistic studies, including both kinetic analysis and DFT calculations, support the hypervalent silicate mechanism (mechanism 1 in Scheme 1.5), as opposed to the σ -bond metathesis. Kinetic analysis of the reaction revealed a reaction rate that is first order with regards to barium and hydrosilane and zero order with regards to the amine. This is consistent with observations made by Harder²⁵ and Sadow²¹ and suggests that the turn-over limiting step involves the interaction of the catalyst with the silane.

1.4.3.3 Boron

Boron complexes, and particularly electron deficient complexes (frustrated Lewis acids) have been reported to catalyze the formation of Si-N bond via the hydrosilylation of imines (Scheme 1.9).

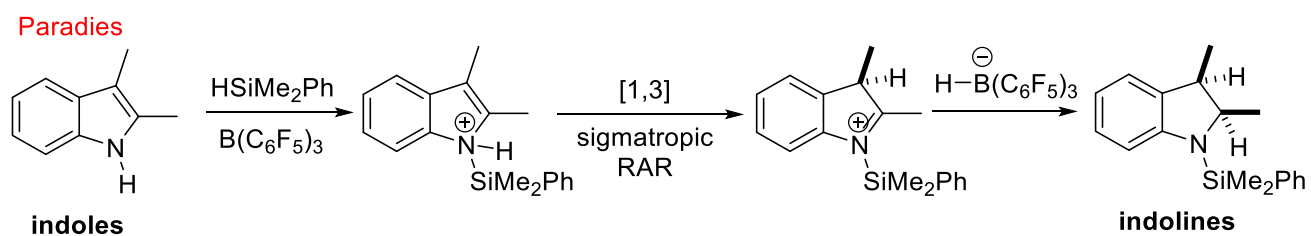
Oestreich



Scheme 1.9 Boron catalyzed hydrosilylation of imines

The Oestreich²⁶⁻²⁸ group has exhaustively investigated the mechanism for the hydrosilylation of imines, with the culminating report in 2013 in which they showed the formation of unexpected intermediates **1.8** and **1.5b** during the hydrosilylation of imines (Scheme 1.9),²⁹ and disrupted the knowledge for the borane hydrosilylation mechanism to that date which is shown in the box in Scheme 1.9. $B(C_6F_5)_3$ initially activates the Si-H bond and after nucleophilic attack of the imine **1.5**, silyliminium ion **1.6** is obtained (Scheme 1.9). The previously reported mechanism stated that, upon the formation of silyliminium ion **1.6**, a hydride transfer from the borohydride species leads to the *N*-silylated amine **1.7**. The Oestreich group showed that imine **1.6** can undergo deprotonation to give enamine **1.8**, which by reprotonation can give imine **1.6**. α -Proton abstraction by the starting imine **1.5** leads to the protonated starting imine **1.5a**, which is reduced to amine **1.5b** by the boron hydride. Amine **1.5b** upon exposure to the hydrosilane and boron complex affords the protonated amine **1.5c**. Amine **1.5c** acts, then as a Brønsted acid to protonate enamine **1.8** and deliver the final product **1.7**.

Following the work by Oestreich and co-workers, the Paradies³⁰ group reported the dehydrocoupling of aromatic amines with diphenylmethylsilane using $B(C_6F_5)_3$ as a catalyst (Scheme 1.10)



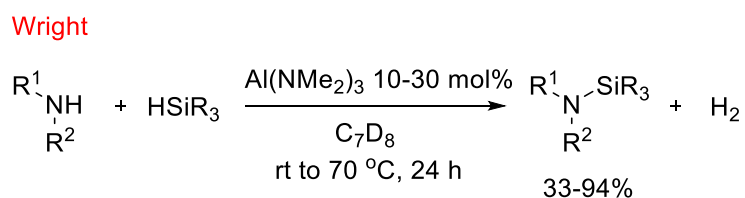
Scheme 1.10 Synthesis of indolines from indoles via the boron catalyzed Si-N dehydrocoupling

The amine scope included anilines, diarylamines, diamines and indoles, with yields ranging from 73-97%. This group reported a notable synthetic application, involving the conversion of indoles

to indolines with high diastereoselectivity for the *cis*-products (Scheme 1.10). This transformation is achieved *via* the domino Si-N dehydrocoupling/[1.3]-sigmatropic rearrangement/hydrogenation.

1.4.3.4 Aluminum

In 2015, the Wright³¹ group reported the first aluminum catalyst for the dehydrocoupling of amines with silanes (Scheme 1.11). The precatalyst used for the transformation was Al(NMe₂)₃ and both catalytic and stoichiometric reactions were conducted. The substrate scope is narrower as compared to the scope in the work by Hill²² and the precatalyst has been shown to accommodate only non-sterically demanding primary amines and silanes, with yields in the range 33-94%. Sterically demanding and electron deficient amines were not reactive.



Scheme 1.11 Aluminum catalyzed dehydrocoupling of amines with silanes

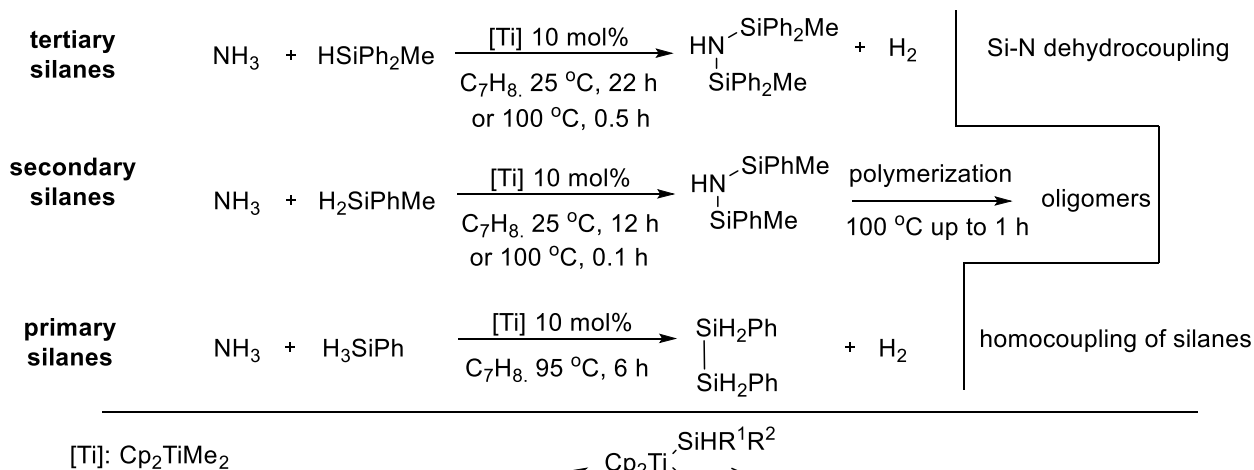
1.4.3.5 Transition metals

1.4.3.5.1 Titanium & Copper

Liu and Harrod³² reported the titanium catalyzed dehydrocoupling of ammonia with silanes to give disilazanes, with dimethyltitanocene (Cp₂TiMe₂) being the precatalyst for the transformation (Scheme 1.12). Sterically demanding tertiary silanes afforded disilazane as the only product of the reaction with a conversion of 60-70%. The reaction proceeded either in 22 h at room temperature or in 0.5 h at 100 °C. 100% conversion was observed in 12 hours at 35 °C or in 0.1 h at 100 °C. At longer reaction times, the formation of oligomers was observed. Unexpectedly, the reaction with primary silanes required 6 h at 95 °C, which can be attributed to the competition

between the homocoupling reaction of phenylsilane and the dehydrocoupling reaction of phenylsilane with ammonia (Scheme 1.12). The authors propose a mechanism for both the paths for homocoupling and dehydrocoupling (only homocoupling shown in Scheme 1.12).

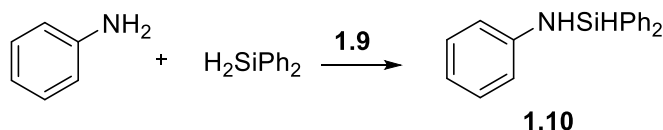
Harrod



Scheme 1.12 Titanium catalyzed dehydrocoupling of amines with silanes and proposed mechanism of homocoupling of silanes

While titanium is the early transition metal to have been reported for the synthesis of disilazanes, copper is the late transition metal to catalyze the same transformation with primary amines, such as (R)-(+)- α -methylbenzylamine, benzylamine and aniline, as substrates.³³ (R)-(+)- α -Methylbenzylamine when reacted with methylphenylsilane, in the presence of catalytic CuCl, gave two diastereomeric monosilazanes as the only products (Scheme 1.13). Benzylamine and

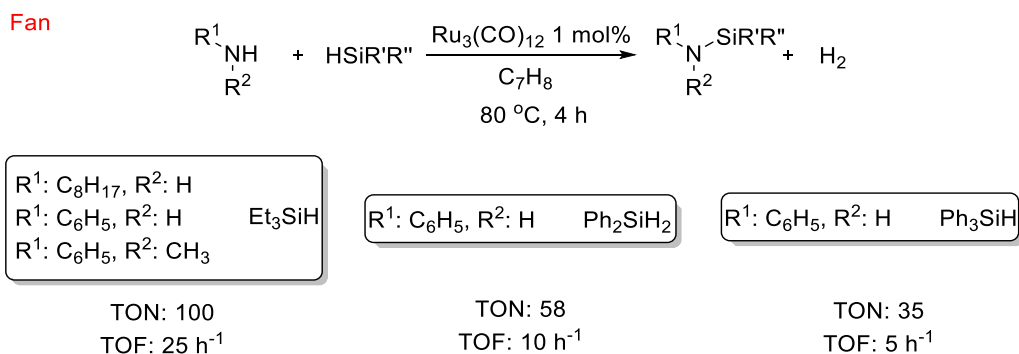
Matarasso-Tchiroukhine



Scheme 1.14 Chromium catalyzed Si-N dehydrocoupling

1.4.3.5.3 Ruthenium

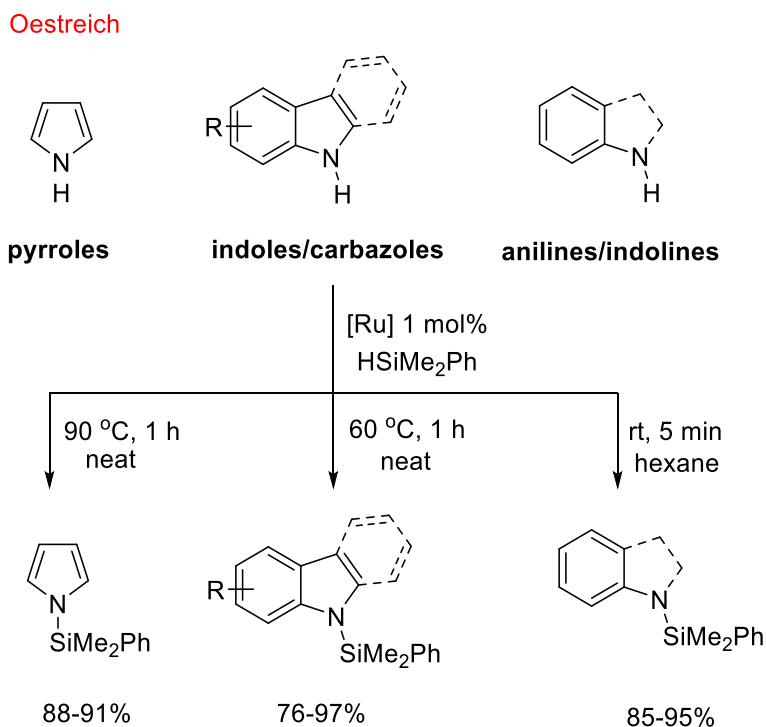
The Fan³⁵ group presented the Si-X (X = S, O, N) coupling with the use of Ru₃(CO)₁₂. For all three cases, triethylsilane (Et₃SiH), diphenylsilane (Ph₂SiH₂) and triphenylsilane (Ph₃SiH) were examined. *n*-Octylamine, aniline and *N*-methylaniline were among the substrates investigated in the amine scope (Scheme 1.15). All three types of coupling had similar TOF values under the same reaction conditions. An increase in the bulk of the silanes led to a 2-3 fold decrease of TOF and prolongation of reaction time (>4 h) to afford full conversion of all three substrates.



Scheme 1.15 Ruthenium catalyzed dehydrogenative Si-N coupling

In 2013, the Oestreich³⁶ group reported the ruthenium dehydrogenative coupling of amines and silanes for the *N*-silylation of amine containing heterocycles, such as indoles, pyrroles, carbazoles, and anilines. This work had a broader substrate scope compared to the subsequently

released work from the Paradies group which focused only on indoles and indolines.³⁰ The catalyst loading was as low as 1 mol%. As shown in Scheme 1.16, pyrroles, indoles, carbazoles, anilines, and indolines were *N*-silylated through this method, reaching conversions of >99%. Pyrroles proved to be the most demanding substrates, requiring reaction temperatures of 90 °C. This is followed by indoles and carbazoles. Notably, anilines and indolines were *N*-silylated at room temperature in 5 min, demonstrating dramatically higher reactivity than indoles and pyrroles. Due to their increased reactivity, anilines were tested for the dehydrocoupling with secondary silanes as well and, depending on the reaction time, mono- or disilylated derivatives could be obtained. Yields varied from 85% to 97% with the exception of carbazole which was obtained in 76% yield (Scheme 1.16). When excess silane was used, the reactions with indoles and pyrroles generated both C3- and *N*-silylated derivatives.

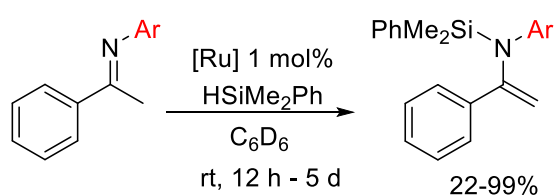


Scheme 1.16 Ruthenium catalyzed dehydrocoupling for *N*-silylation of pyrroles, indoles, carbazoles, anilines, indolines

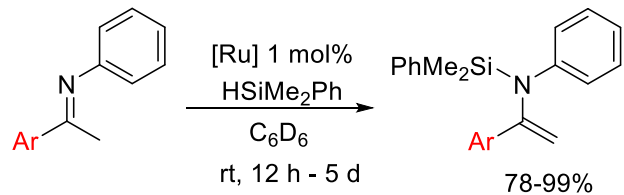
In 2014, the same group used a similar ruthenium complex for the synthesis of enamines *via* the dehydrogenative coupling of imines with silanes (Scheme 1.17).³⁷ *N*-Arylimines were used as substrates in the Si-N dehydrogenative coupling yielding the *N*-silylenamines (Scheme 1.17). Two distinct reaction scopes were developed, including the variation on the *N*-arylimine moiety and on the aryl group of the α carbon of the *N*-arylimine, leading to a mixture of *N*-silyl- and doubly *N*-silyl- & C-silylenamines in each case. In scope 1 in Scheme 1.17, the *N*-silylenamines were isolated in yields 22-99%. Ortho-substituted imines required longer reaction times to afford the corresponding *N*-silylenamines. The presence of EWG at the meta- and para-position afforded the *N*-silylenamines in shorter reaction times and in quantitative yields. When the variation on the aryl group of the α -carbon was examined, the *N*-silylenamines were obtained chemoselectively in excellent yields (78-99%). Imines with EWG on the aryl ring delivered the *N*-silylenamines within 12 h at room temperature in almost quantitative yields. The yield range for the *N*-silylamines possessing EDG on the aryl ring was 78-95%, however they required longer reaction times than their EWG-substituted congeners.

Oestreich

Scope 1



Scope 2

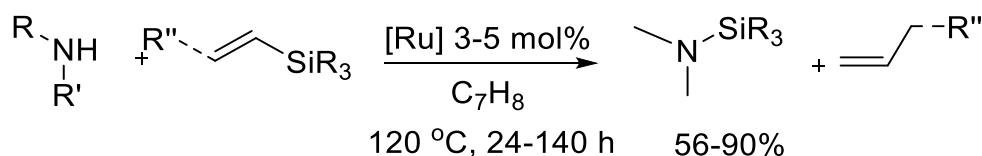


Scheme 1.17 Ruthenium catalyzed Si-N coupling of imines with silanes to generate *N*-silylenamines

For all the metals discussed to this point, the dominant transformation to catalytically yield *N*-silylated amines is the dehydrogenative coupling of amines and silanes and the closely associated hydrosilylation of imines. The Pawluć¹⁹ group developed a new method to access these products

using the ruthenium-catalyzed *N*-silylation of amines by dealkenylation of substituted vinylsilanes (Scheme 1.18). Amines employed in the transformation included dibutylamine, diethylamine, piperidine, aniline, isopropylamine, tertbutylamine, 2-ethylhexylamine, and carbazole. Electron rich amines required reaction times up to 48 h while aniline and carbazole required up to 60 and 140 h, respectively. Isolated yields of products were in the range of 56-90%.

Pawluc



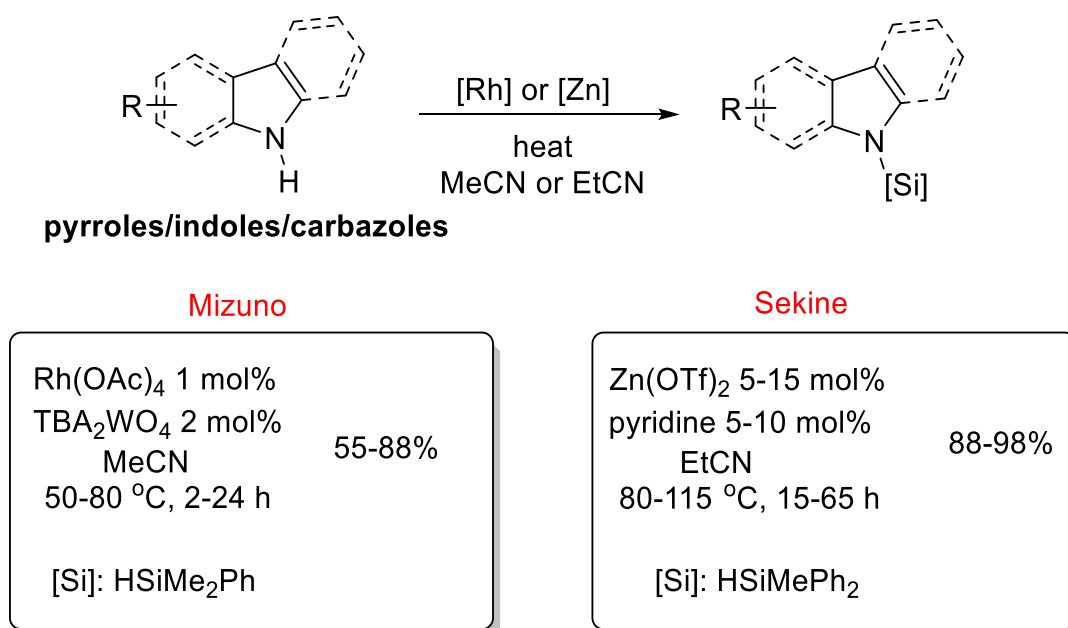
[Ru]: [RuHCl(CO)(PCy₃)₂]
 R'' = H or alkyl

Scheme 1.18 Ruthenium catalyzed dealkenative *N*-silylation of amines *via* silanes

1.4.3.5.4 Rhodium & Zinc

The Mizuno³⁸ and Sekine³⁹ groups presented the rhodium and zinc catalyzed Si-N coupling of indoles, carbazoles and pyrroles (Scheme 1.19). Unlike for the ruthenium catalysts, these two methods require the addition of a base. With the use of the zinc catalyst, the authors observed the formation of *N*-silylated indolines upon silylation of indoles, while no such products were reported to have been observed with the rhodium catalyst. The rhodium catalysis led to no product when *i*-Pr₃SiH was used as the silane; this sterically demanding group was successfully added to the indole nitrogen through the Zn(OTf)₂ catalyzed dehydrocoupling. Notably, only stoichiometric reactions allow for this transformation (metallation and *N*-silylation with

halosilanes). Both groups also reported reactivity with tertbutyldimethylsilane, a silane not tested in the ruthenium catalyzed dehydrocoupling. For the rhodium catalysis, substituents at the C2, C3, C5, and C7 positions of indole were well tolerated. However, longer reaction times were required for C2 and C7 substituted indoles. For the zinc catalysis, the indole scope was developed with the more sterically demanding Ph₂MeSiH as opposed to PhMe₂SiH, which was used for the scope development in the rhodium catalysis. Substituents including EWG and EDG at C2, C3, C5-C7 were well tolerated.



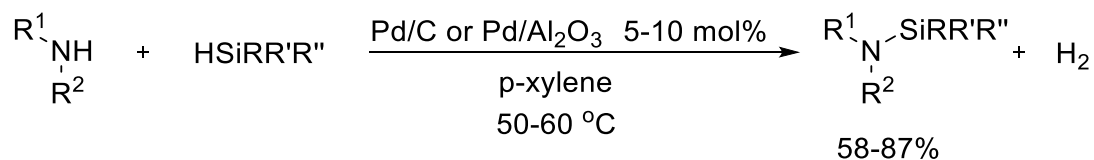
Scheme 1.19 Rhodium and zinc catalyzed dehydrocoupling of amines and silanes for *N*-silylation of indoles, pyrroles and carbazoles

1.4.3.5.5 Miscellaneous transition metals

Citron and Somer⁴⁰ disclosed a report on the utilization of Raney Ni, Pd/C, Pd/Al₂O₃ and Pt/C with a catalyst loading of 5-10% for the dehydrogenative coupling to form N-Si, S-Si and X-Si (where X is a halogen) bonds, with yields ranging from 58% to 87% for the case of N-Si coupling (Scheme 1.20). Rh/C, Rh/Al₂O₃, Ru/C, were also tested, but no reactivity was observed.

The amine scope includes pyrrolidine, isobutylamine and methylamine. For the scope of hydrosilanes, both retention and inversion of the silicon stereocenter were observed.

Somer



Scheme 1.20 Palladium catalyzed dehydrogenative coupling of amines with silanes

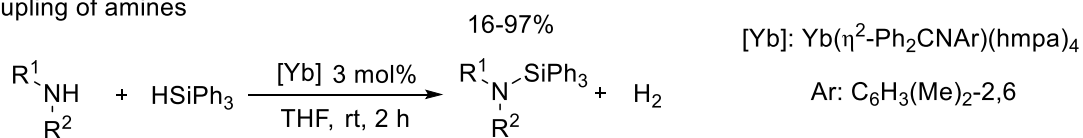
1.4.3.6 Lanthanides and Actinides

1.4.3.6.1 Ytterbium & Samarium

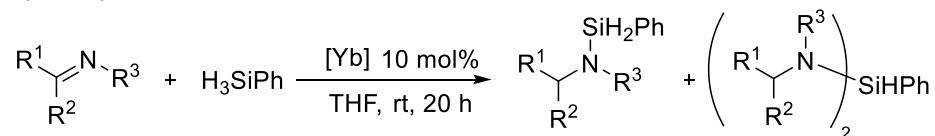
Ytterbium has been reported for both the hydrosilylation of imines and dehydrogenative coupling of amines. The Takaki group used $\text{Yb}(\eta^2\text{-Ph}_2\text{CNAr})(\text{hmpa})_n$ as the catalyst for the reaction between primary and secondary amines with triphenylsilane (Scheme 1.21).^{41, 42}

Takaki

Dehydrocoupling of amines



Hydrosilylation of imines



Scheme 1.21 Ytterbium catalyzed dehydrocoupling of amines with silanes and hydrosilylation of imines with silanes

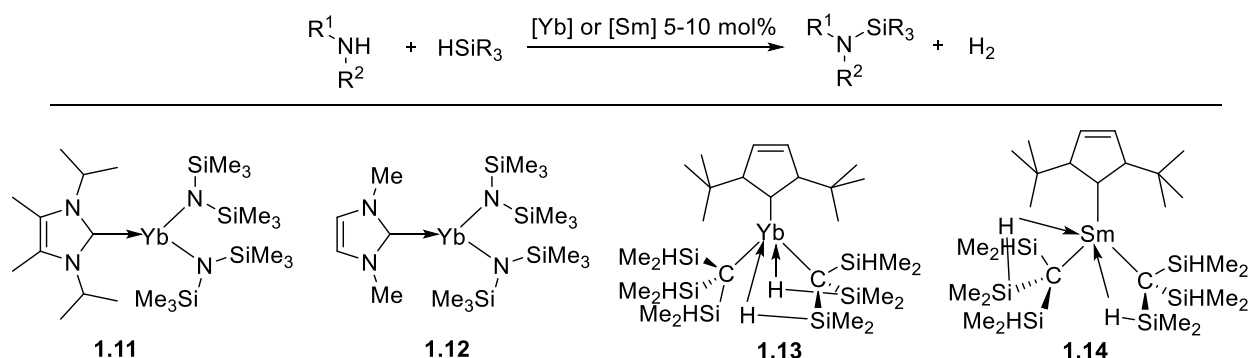
In reactions with secondary or primary silanes, diaminosilanes were the major product, with monoaminosilanes formed as a minor product. Less nucleophilic tertalkylamines and aromatic amines were less reactive (yields: 16% and 56%, respectively) as compared to more nucleophilic

primary and secondary amines (79-97%). For the hydrosilylation of imines, the scope was developed with a primary silane (PhSiH₃) and this allowed for the formation of a mixture of mono- and disilanes (Scheme 1.21).

Recently, *N*-heterocyclic carbene supported ytterbium and samarium complexes have been shown to catalyze the dehydrogenative coupling of amines with silanes. In 2012 the Cui group presented the *N*-silyl/NHC ytterbium complexes **1.11** and **1.12** and in 2016 the Sadow group presented the C-silyl/NHC ytterbium and samarium complexes **1.13** and **1.14** for the cross coupling between amines and silanes (Scheme 1.22).^{43, 44}

The Cui group tested the reactivity of **1.12** for the reaction between primary and secondary amines with PhSiH₃ and with bulky secondary silanes, showing that in the case of PhSiH₃, by altering the ratio of the amine to silane di- and trisubstituted amines could be obtained. In the work by Sadow, diethylamine and isopropylamine were the only amines tested in the transformation with primary and secondary silanes.

Cui and Sadow



Scheme 1.22 NHC supported ytterbium and samarium complexes for the Si-N dehydrogenative coupling of amines with silanes

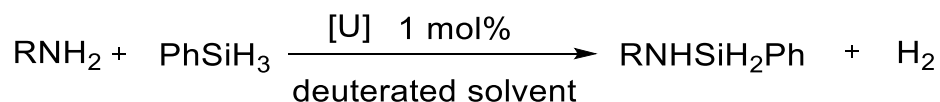
The use of tertiary silanes was not reported in either case. Notably, the C-silyl/NHC lanthanide complexes catalyze reaction of PhSiH₃ with excess isopropylamine to give the corresponding

triamine in 10 minutes. Sadow and co-workers conducted kinetic studies which suggested that the presence of other ligands such as THF and Im^tBu can inhibit their catalytic activity.

1.4.3.6.2 Uranium

Uranium has also been reported for the dehydrocoupling reaction between amines and silanes. Using PhSiH₃ and [(Et₂N)₃U][BPh₄] as a precatalyst, a series of amines were tested.⁴⁵ Primary amines are more reactive than the secondary and tertiary. Homocoupling of the silanes was not observed (Scheme 1.23).

Eisen



Scheme 1.23 Uranium catalyzed dehydrocoupling of primary amines with silanes

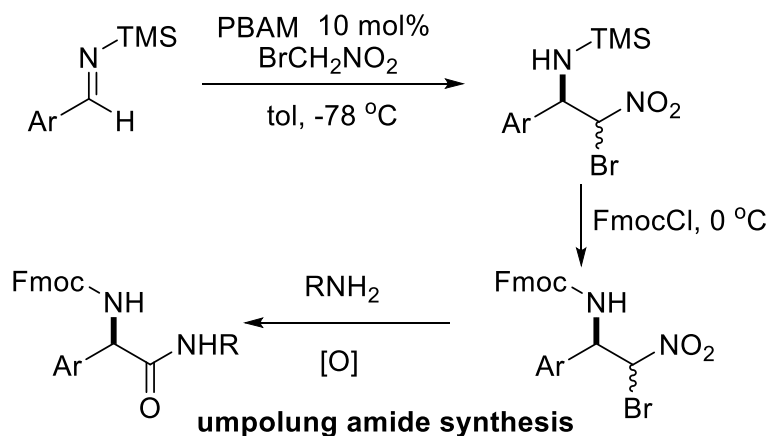
1.4.4 N-silylated amines in catalysis: reactivity

For the examination of the reactivity of *N*-silylamines (saturated: *N*-silylamines, unsaturated: *N*-silylimines and conjugated to unsaturated systems: *N*-silylenamines) in catalytic reactions, the following transformations have been reported: i) nucleophilic addition to *N*-silylimines, ii) reduction of *N*-silylimines, iii) transfer hydrogenation of vinylaminosilanes, iv) hydroamination of *N*-silylamines and reduction of resulting *N*-silylenamines, v) diboration of *N*-silylimines, vi) action of *N*-silylamines as directing groups for borylation of indoles, and vii) aminocarbonylation of *N*-silylamines. As highlighted in each example below, the *N*-silylamines are chosen as substrates in transformations due to the different electronic properties and the facile hydrolytic Si-N cleavage.

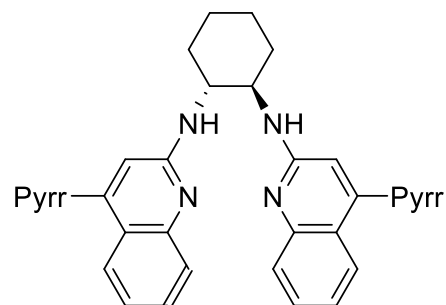
1.4.4.1 Organo- and organoboron catalyzed reactions

The *N*-(trimethylsilyl)imines have been reported as substrates in the bisamidine-catalyzed Henry reaction, the addition of a nitroalkane to a carbonyl derivative, when bromonitromethane is used as the coupling partner (Scheme 1.24).⁴⁶ Acylation of the product *N*-silyl amines to the corresponding acyl derivatives allowed for umpolung amide synthesis: utilization of an α -halonitroalkane as a carboxylic acid surrogate for direct amide synthesis (Scheme 1.24). The high demand for unnatural amino acid derivatives synthesis is one of the reasons for ongoing amide bond methods development. The authors reported high enantioselectivity in the aza-Henry reaction due to the reduced reactivity of *N*-TMS imines. When acyl imines were used as starting imines, the PBAM catalyzed aza-Henry reaction proceeded with low enantioselectivity.

Johnston



PBAM:

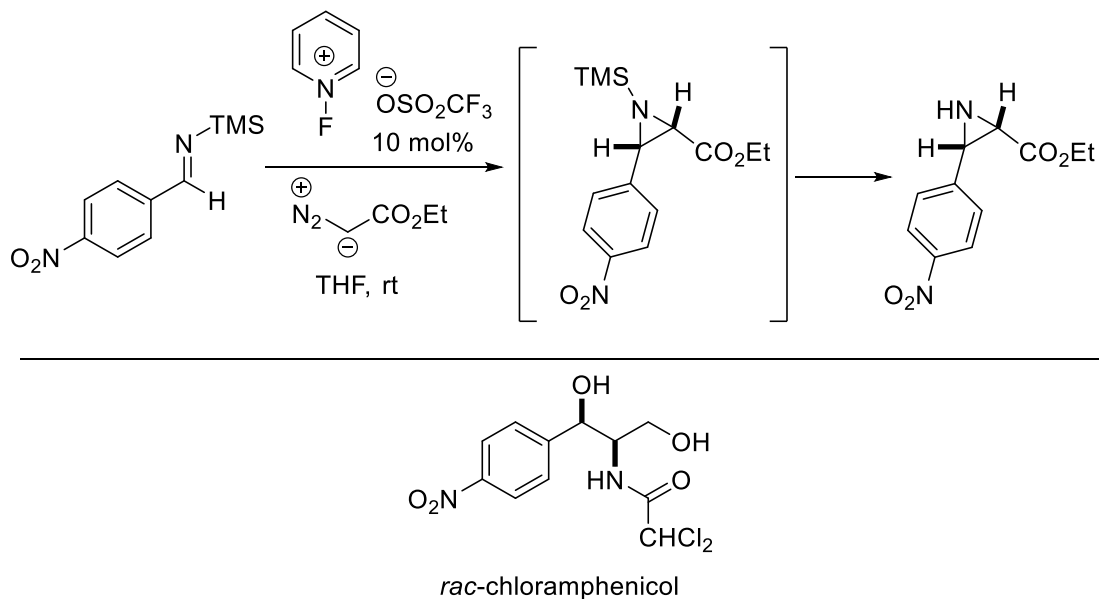


Scheme 1.24 *N*-silylimines as electrophiles in the aza-Henry reaction

N-Silylimines have also been used in fluoronium catalysis and particularly for the generation of optically active aziridines by the Bew group.⁴⁷ The authors have investigated the use of *N*-aryl imines for the synthesis of tertiary *N*-arylsubstituted aziridines. One of the steps for the synthesis of chloramphenicol utilizes the *N*-silylimine to afford the secondary aziridine shown in Scheme

1.25, due to facile hydrolytic N-Si cleavage upon workup. The aziridine moiety is not present in the final molecule, however the formation of this intermediate provides the desired stereochemistry present in chloramphenicol.

Bew

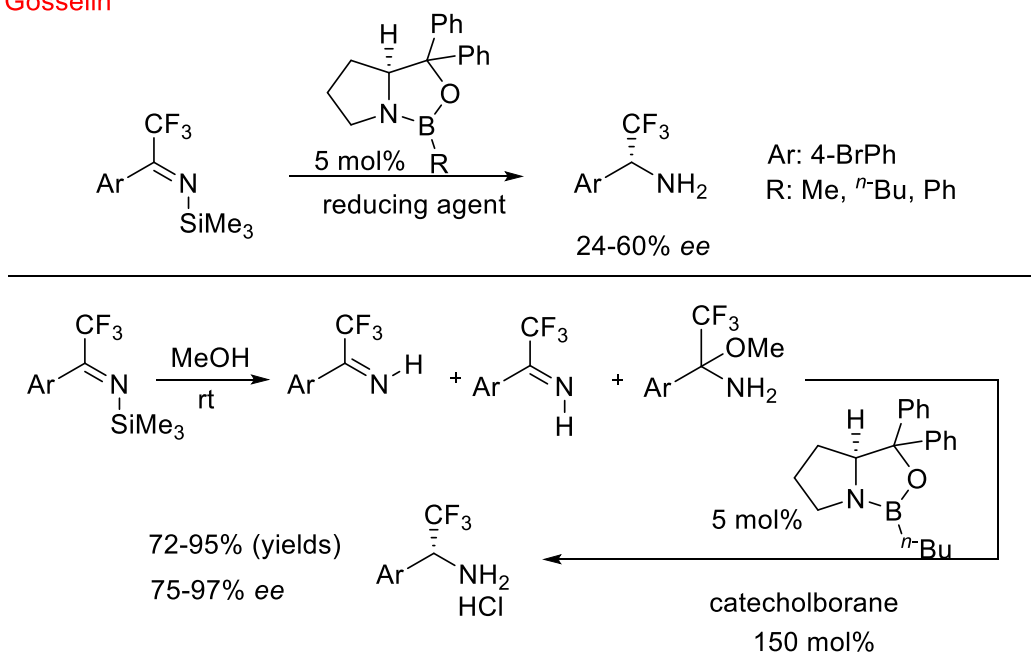


Scheme 1.25 *N*-silylimines as substrates for the generation of optically active secondary aziridines

N-Silylimines have been used as substrates in catalytic asymmetric reduction using organoboron complexes to afford chiral α -trifluoromethylated primary amines (Scheme 1.26).⁴⁸ The *N*-silylimines were generated from the corresponding perfluorinated ketones. Enantioselective reduction of the resulting *N*-silylimines produced the corresponding primary amines in high yields and moderate enantioselectivities. The low enantioselective induction was attributed to poor accessibility of the bulky *N*-silylimine to the organoboron catalyst. To increase the enantioselectivity of the reaction, the *N*-silylimines were subjected to N-Si solvolysis, giving the corresponding *E/Z* imines as well as the hemiaminal ethers (Scheme 1.26). Catalytic reduction of this mixture yielded amines with both high yields and improved enantioselectivity. It is

noteworthy to mention that direct reductive amination of the starting perfluoromethylated ketones to the primary amines is not successful due to the formation of stable hemiaminal complexes. With the generation of the *N*-silylimines this barrier is overcome and with the use of the chiral catalyst, upon solvolysis of the *N*-silylimines, access to the desired α -trifluoromethylated amines is gained.

Gosselin



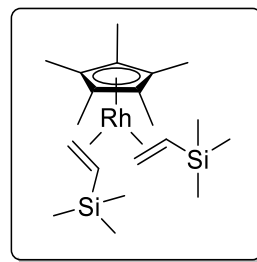
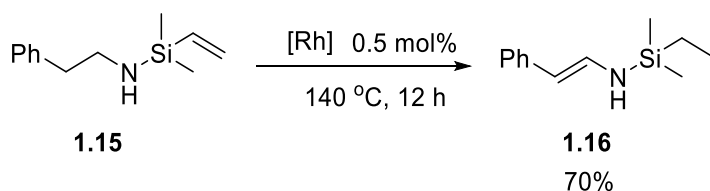
Scheme 1.26 Boron catalyzed reduction of *N*-silylimines (top) and *E/Z* imines to primary amines (bottom)

1.4.4.2 Transition metal catalyzed reactions

1.4.4.2.1 Rhodium

Rhodium catalyzed transfer hydrogenation of vinylaminosilane **1.15** to afford *N*-silylenamine **1.16** was reported by Brookhart⁴⁹ in 1999 (Scheme 1.27). The primary focus of the report was the alkoxy silane isomerization to the corresponding silyl enolates through transfer hydrogenation, however the authors also examined the amine congeners. As shown in Scheme 1.27, enamine **1.16** was obtained in 70% overall yield.

Brookhart

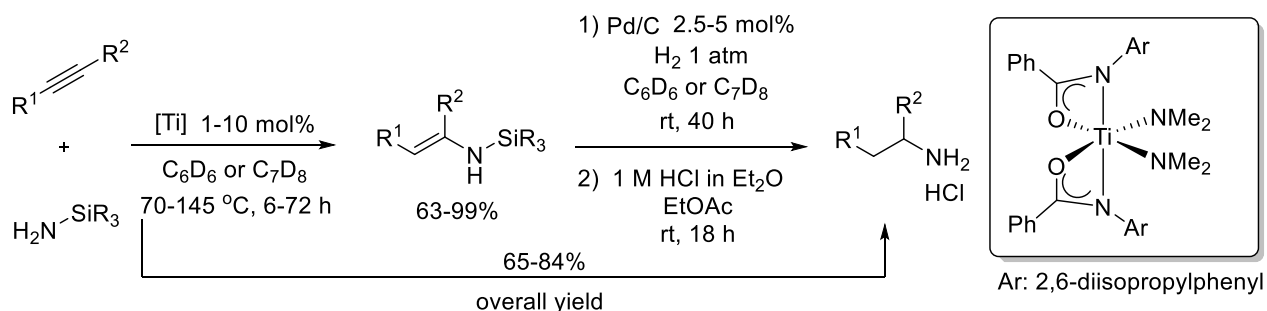


Scheme 1.27 Rhodium catalyzed transfer hydrogenation of aminosilanes resulting in *N*-silylenamines

1.4.4.2.2 Titanium & Palladium

Another transformation that utilizes *N*-silylamines is the hydroamination of alkynes using *N*-silylammonia (Scheme 1.28). The Schafer⁵⁰ group recently disclosed the anti-Markovnikov selective hydroamination of both terminal and internal alkynes with the use of a titanium bis(amidate)bis(amido) Ti (IV) complex. The resulting *N*-silylenamines were hydrogenated to the corresponding *N*-silylamines *via* palladium catalyzed hydrogenation, and due to the facility of the hydrolytic N-Si cleavage, a new method to access primary amines was realized.

Schafer



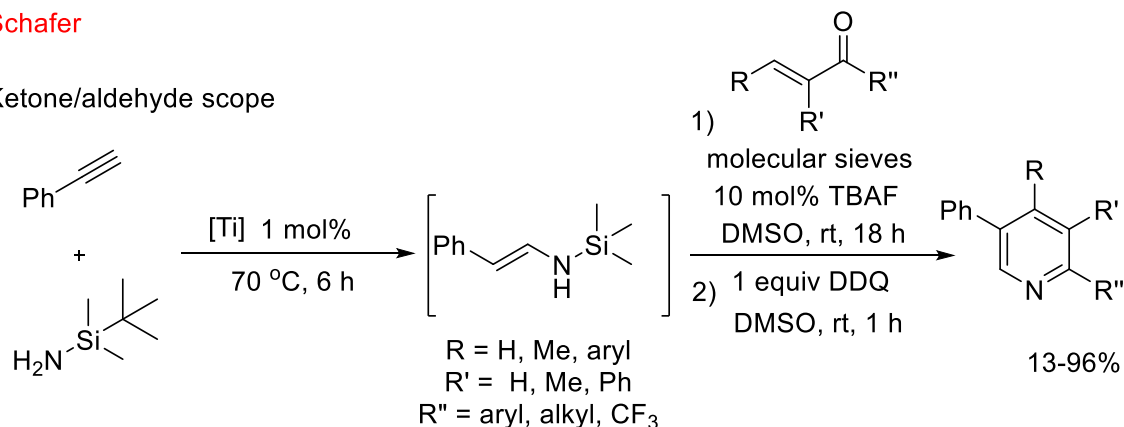
Scheme 1.28 Titanium catalyzed hydroamination of alkynes with silylated ammonia; Palladium catalyzed hydrogenation of the *N*-silylenamines

The titanium catalyzed generation of *N*-silylenamines was directed toward the formation of polysubstituted pyridines by the same group.⁵¹ The authors reported the selective synthesis of mono-, di-, tri-, tetra- and pentasubstituted pyridines. More specifically, the *in situ* generated *N*-

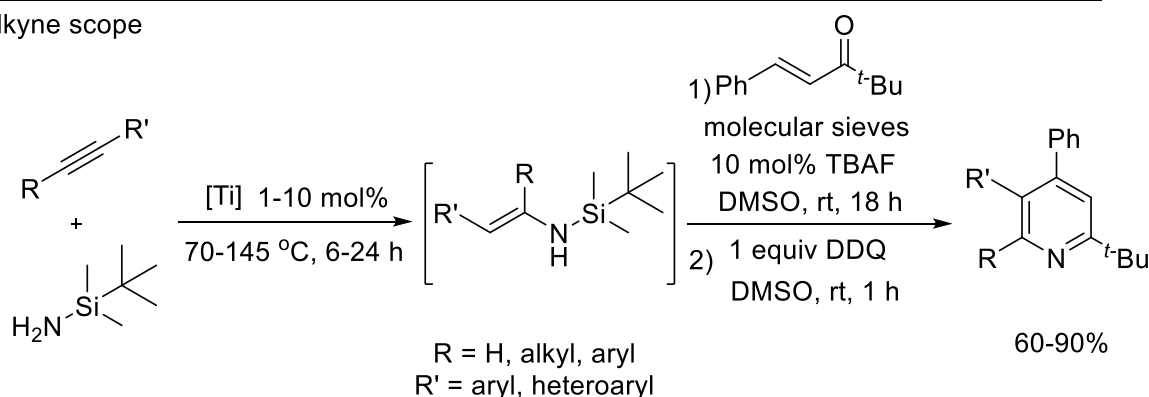
silylamines, derived from the titanium catalyzed hydroamination, were treated with α,β -unsaturated carbonyls to afford, in a one-pot reaction, a series of pyridines in yields up to 96% (Scheme 1.29).

Schafer

Ketone/aldehyde scope



Alkyne scope



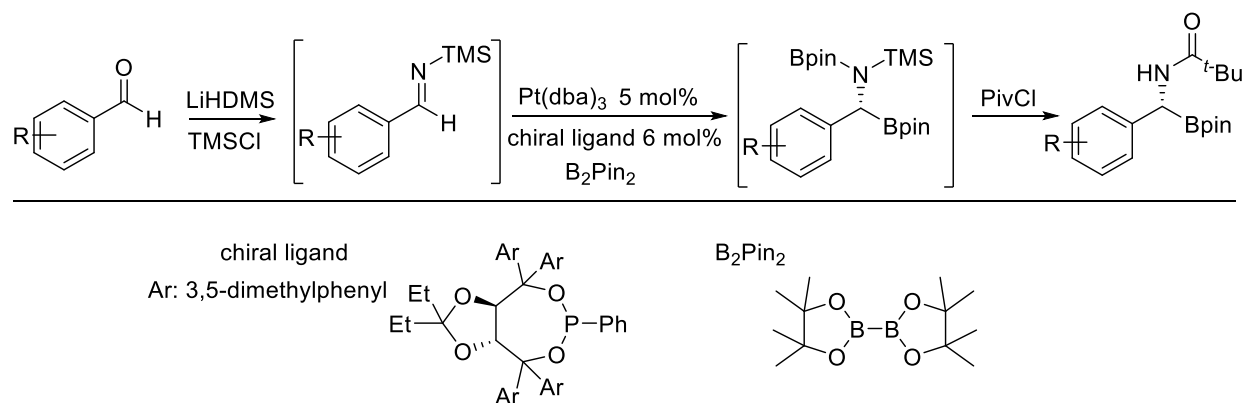
Scheme 1.29 One pot hydroamination/aldol condensation to access multisubstituted pyridines

1.4.4.2.3 Platinum

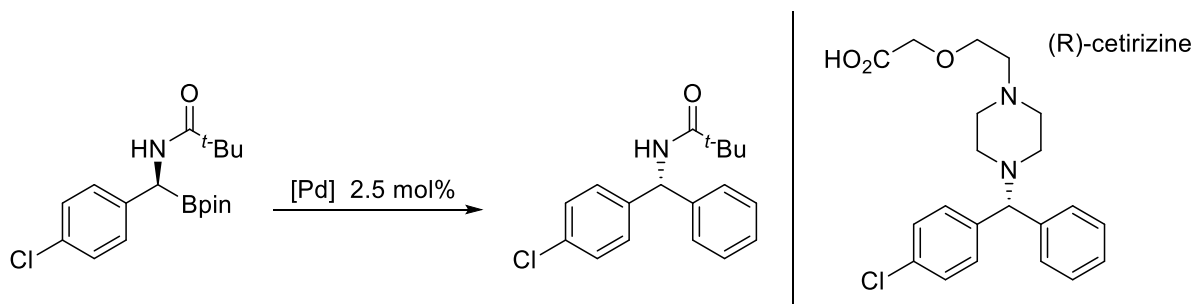
Pt(dba)₃ has been used for the transformation of *N*-silylimines to saturated diborated derivatives with the goal to synthesize chiral α -amido boronic acids.⁵² The *N*-silylimines are derived from the corresponding aldehydes and are subjected to platinum catalyzed diboration to afford chiral diborated derivatives (Scheme 1.30). The resulting chiral diborated derivatives, upon treatment with pivaloylchloride lead to chiral α -amido boronic acids. Variation on the aryl ring was examined for the reaction scope; aryl rings with both EDG and EWG were well tolerated,

affording the desired products in yields 63-87% and *ee* ratios 95:5-97:3. Tolerance was shown for heteroaryl rings, such pyridine and *N*-Boc protected indoles, too. The authors further utilized one of the derived pinacolated chiral amino acids to synthesize a necessary intermediate for the synthesis of cetirizine (Scheme 1.31).

Morken



Scheme 1.30 Platinum catalyzed diboration of *N*-silylimines in the aminoborylation of aldehydes to generate chiral α -amido boronic acids

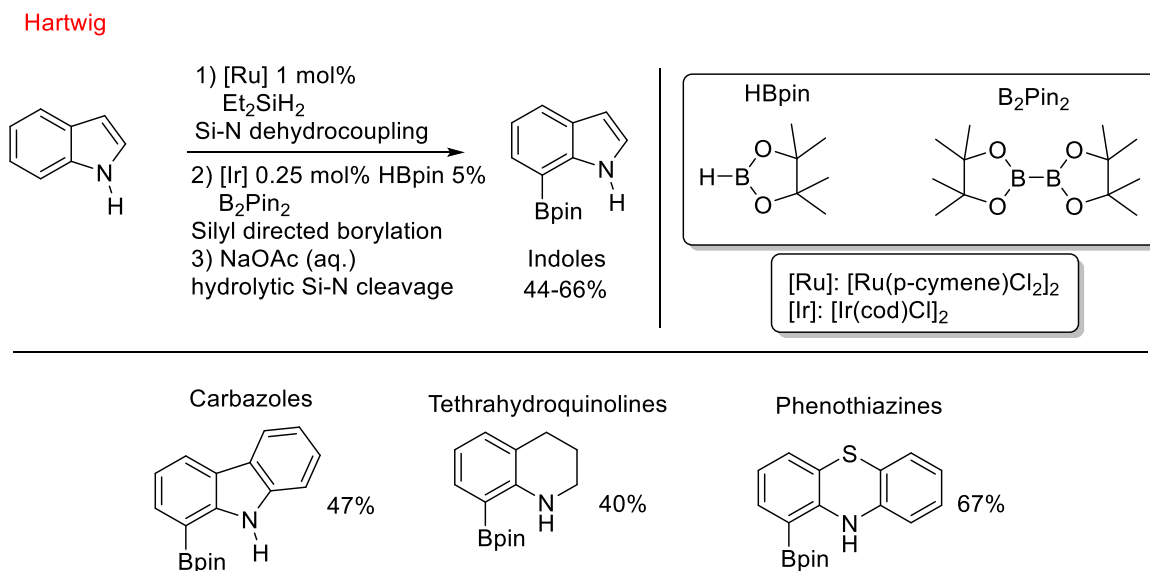


Scheme 1.31 Synthesis of necessary intermediate for the synthesis of (R)-cetirizine

1.4.4.2.4 Iridium

The Hartwig⁵³ group reported the iridium-catalyzed borylation of *N*-silylated indoles (Scheme 1.32). The *N*-silyl indoles were generated *in situ* via the ruthenium catalyzed dehydrogenative coupling of indole with silane. The borylation with B_2Pin_2 in the presence of $[Ir(cod)Cl]_2$ and 4,4'-ditertbutylbipyridine (dtbpy) occurred with a selectivity at indole position C7. Other *N*-

heterocyclic compounds, such as carbazoles, tetrahydroquinoline and phenothiazines, were also competent substrates (Scheme 1.32). The resulting borylated indoles are valuable synthons for subsequent reactions, such as the Suzuki-Miyaura coupling.



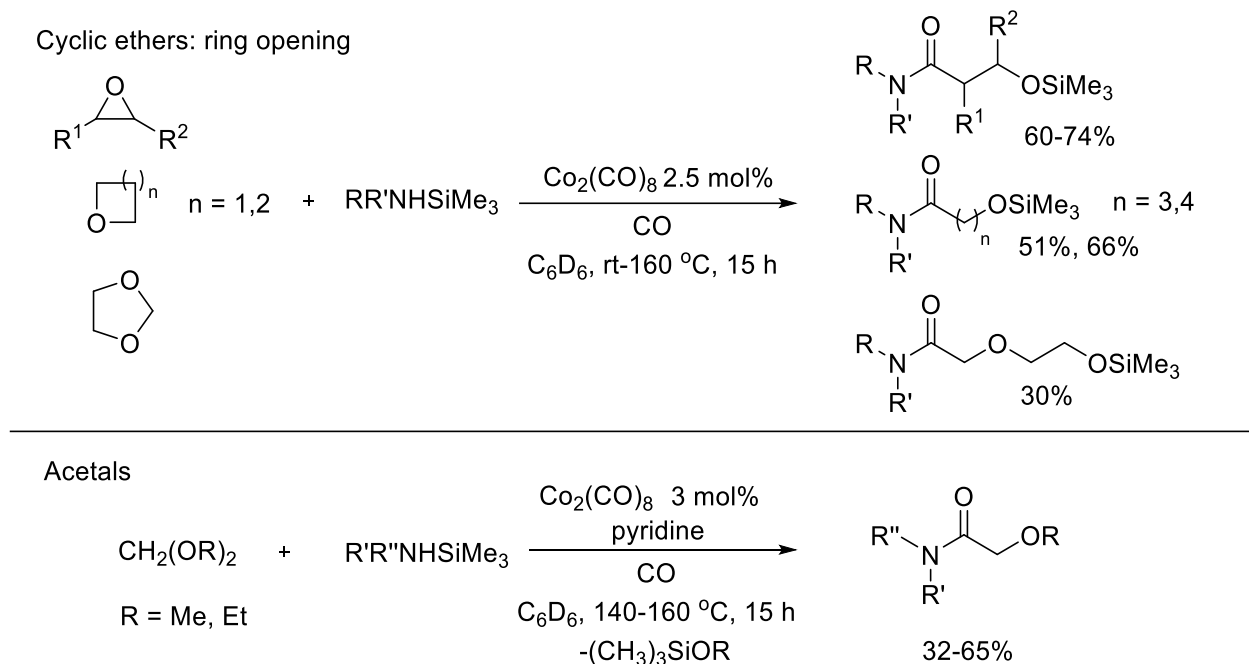
Scheme 1.32 Iridium-catalyzed, silyl-directed borylation of nitrogen containing *N*-heterocycles

1.4.4.2.5 Cobalt

Cobalt catalyzed aminocarbonylation of cyclic ethers (accompanied by ring opening) and acetals with *N*-silylamines was reported by the Watanabe group in 1989 and 1991, respectively (Scheme 1.33).^{54, 55} Cyclic ethers employed in the former transformation include epoxides, oxetane, tetrahydrofuran and 1,3-dioxolane and in the presence of catalytic dicobalt octacarbonyl they lead to silyloxyamides. Of all, epoxides demonstrated the highest reactivity, generating products at room temperature. *N*-Silylbenzylamine, *N*-silyldiethylamine and *N*-silyloctylamine were among the amines examined in the transformation. The products were obtained in yields 30-74%. Due to their reduced nucleophilicity, products resulting from ring opening from the nucleophilic attack of the *N*-silylamines were only observed in traces. The reaction between *N*-silylamines and formaldehyde acetals in the presence of Co₂(CO)₈ delivered 2-alkoxyamides

(Scheme 1.33). It was found that the addition of pyridine enhances the catalytic activity while other bases such as 2,2'-bipyridine, triethylamine inhibited the catalytic activity. Formaldehyde acetals, cyclic acetals and acetaldehyde diethyl acetals were employed in the reaction, but it was only 1,3-dioxolane, the cyclic acetal, that delivered the carboxamide in 34%. The authors reported that no reaction occurred with the free-amine in either works.

Watanabe



Scheme 1.33 Cobalt catalyzed aminocarbonylation of cyclic ethers (top) and formaldehyde dialkyl acetals (bottom) using *N*-silylamines

1.5 Summary

The catalytic dehydrogenative coupling of amines with silanes has been reviewed with various metals and also for its synthetic applications (e.g., dehydrocoupling of nitrogen containing heterocycles). The hydrosilylation of imines and dealkenative cross-coupling of amines with silanes is underdeveloped as compared to the Si-N dehydrocoupling. Expectedly, the number of

different transformations for which the *N*-silylamines (and their related unsaturated congeners) serve as synthons is greater than the corresponding number to obtain the *N*-silylamines, however, they have not received analogous attention as judged from the limited reports presented herein.

1.6 Thesis scope

This thesis aims at developing transformations in which *N*-silylamines serve as valuable synthons in both stoichiometric and catalytic transformations. In Chapter 2, the use of *N*-silylamines as precursors in stoichiometric amide bond formation will be presented. The rationale for their use is the electron deficient nature of the parent *N*-arylamines and consequent incompetence to efficiently participate in the amide bond formation with a thioester. Upon *in situ* desilylation, the derived *N*-silylamines afford activated species which render them competent to attack the electrophile and afford the amide products.

In Chapter 3, the *N*-silylamines will be examined for their reactivity as substrates in zirconium catalyzed hydroaminoalkylation reaction, a Csp^3-Csp^3 bond forming strategy. The *N*-silylamines have not been extensively employed in catalysis. The rationale for their choice is to access primary α -arylated amines branched at α to nitrogen position. The facile Si-N hydrolytic cleavage is what makes them valuable synthons in the catalytic transformation.

Chapter 4 extends the findings of Chapter 3 to investigate in hydroaminoalkylation reaction with *N*-aryl- and *N*-alkylamines- α -arylated amines. The observed reactivity of these more traditional substrates can be contrasted with the reactivity of less nucleophilic and more bulky *N*-silylamines. A greater diversity of amine substrates is explored in hydroaminoalkylation.

Chapter 2: *N*-TMS amines as amine surrogates to access diheteroarylamides

2.1 Introduction

Amide containing molecules account for approximately 25% of pharmaceuticals⁵⁶ and this reflects the continued interest of the medicinal community to optimize existing methods or identify new ways to access compounds/derivatives bearing the amide functionality. In Figure 2.1, the two resonance structures of the amide bond functionality are presented. Due to the delocalization of the lone pair on the sp^2 hybridized nitrogen over the carbon-oxygen bond, the amide function is planar, and, unlike the ester functionality, its reactivity in hydrolysis and other reactions involving addition of a nucleophile to the carbonyl carbon atom is considerably attenuated. Further, unlike typical amines, the amide nitrogen atom does not protonate (except under very strong acidic conditions). However, although neutral, both the nitrogen and oxygen atoms in amides readily participate in H-bonding interactions. This feature, plus the stability of the amide bond *in vivo*, enables the existence of proteins as essential elements and life and drug targets.

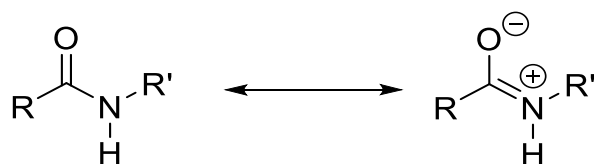


Figure 2.1 Resonance structures of the amide bond

The interest of our laboratory to access amides arises from efforts to find novel molecules that mimic the biological activity of compound **2.1 (IDC16)** (Figure 2.2). This fused tetracyclic compound is presumed to block HIV replication through perturbation of the function of the splicing factor SRSF1, a serine-arginine rich protein implicated in cellular pre-mRNA splicing and alternative splicing events carried out by the spliceosome machinery.^{57, 58} However,

compound **2.1**, like other pyridocarbazoles is inherently cytotoxic. Indeed, as a consequence of their planarity, tetracyclic indoles are known to intercalate into DNA, a property associated with their observed cytotoxic effects. Due to the absence of structural information for the SR proteins, which could provide insight as to the mode of binding of **2.1** to its putative target SRSF1, our laboratory took the initiative to design conformationally flexible mimics of **2.1**. It was hypothesized that such molecules would still interact with the SRSF1 proteins but would no longer show any affinity for DNA (Figure 2.2).

Previous research involved the synthesis of a >240 compound library of **2.1** mimics in which the two extremities of the molecule (rings A and D) were varied and the central indole moiety was replaced with different linkers (Figure 2.2). Evaluation of this library led to the identification of four diheteroarylamides (**2.2**, **2.3**, **2.4** and **2.5**), that displayed anti-HIV activity. In each of these molecules, the indole ring has been replaced by an amide linker and, and the D-ring component corresponded to a benzothiazole motif. Of the four active hits, compound **2.2** was further studied and found to block HIV replication through perturbation of the function of SRSF10⁵⁹ (and not SRSF1) at submicromolar concentrations.⁶⁰

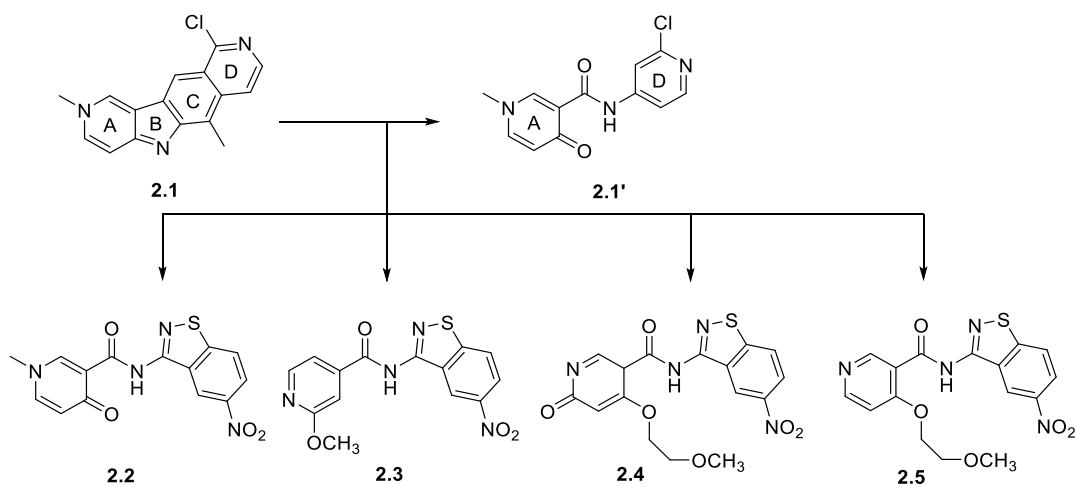


Figure 2.2 Amide mimics of **2.1**

Interestingly, when the A- and D- rings of **2.1** were retained, so as to give diheteroarylamide **2.1'**, which is the most closely related to **2.1**, no anti-HIV activity was observed. This suggests that the amide linker is not a perfect surrogate of the B/C-rings and there is need to use the parallel synthesis approach to find active compounds instead of classical SAR which would involve successive/iterative changes in **2.1**.

Further pharmacological evaluation of **2.1** and **2.2** showed that **2.2** was very significantly less cytotoxic than **2.1** and that it remained active at submicromolar concentrations against major HIV strains that confer resistance to the drugs used in ART therapy to target HIV reverse transcriptase, integrase and protease.⁵⁹ This discovery provided the impetus to explore other diheteroarylamide analogs of **2.2**, with the objective in mind of both optimizing its anti-HIV activity and exploring in detail the requirements for target binding and mechanism of action. The objective of my research was to generate a library of new **2.2** analogs in which the 4-pyridone ring as ring A is retained and diversity is introduced through variations in the structure of the D-ring (Figure 2.3).

In the earlier work in the laboratory, which led to the discovery of diheteroarylamide **2.2**, the formation of the amide bond was achieved using classical peptide coupling reagents and the acid chloride method. However, it was very quickly determined that these conditions could not be efficiently translated to the synthesis of the diheteroarylamides of interest to us. Indeed, due to the poor reactivity of the amine component in these reactions and the difficulties in separating the polar amide products from both the polar amine/acid components and the polar byproducts produced from the coupling reagents product isolation by column chromatography was rendered cumbersome and impractical. Importantly, they could not be adapted to rapid parallel synthesis of an exploratory compound library.

With the vision to improve the activity of the reference compound **2.2** a new amide bond forming methodology had to be developed which was both efficient (i.e., high yielding) and simple such that product isolation would be facilitated. In this chapter the development of an efficient protocol to access novel analogs analogs of **2.2** is described.

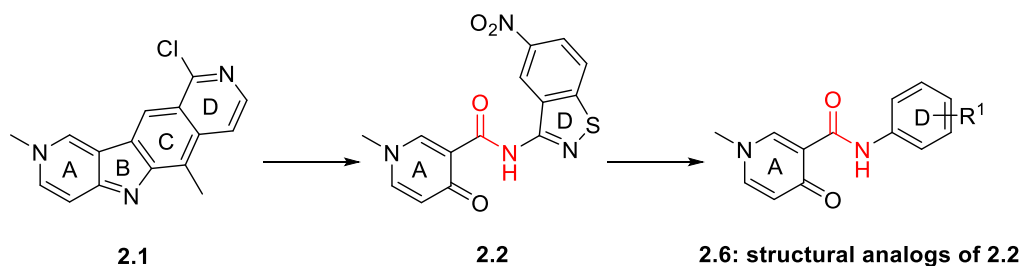


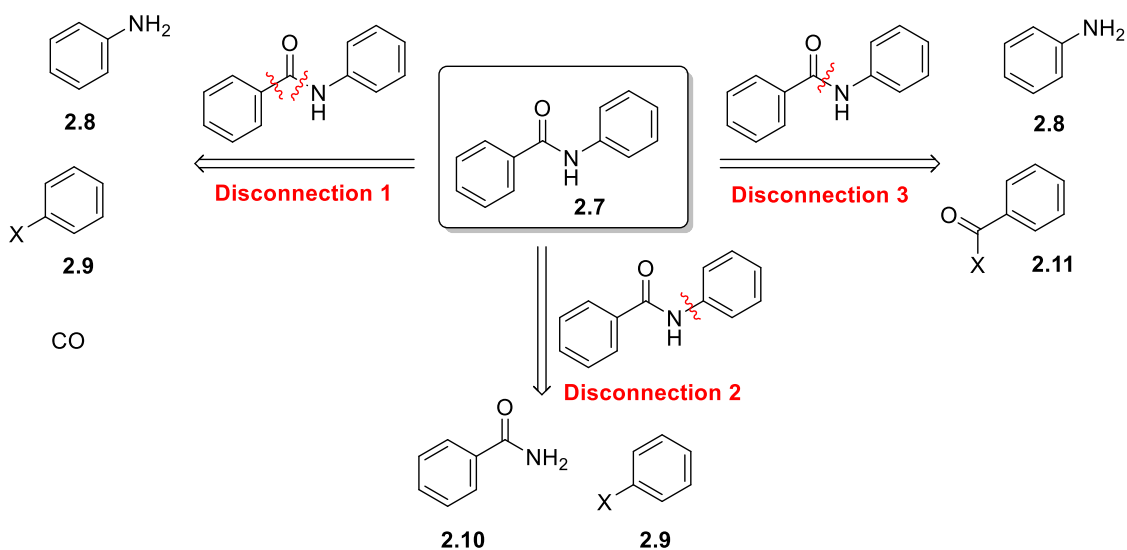
Figure 2.3 Generic structure of structural analogs of **2.2**

2.2 Overview of amide bond formation of aryl/heteroaryl amides

Before discussing our new methodology to access diheteroarylamides **2.6** (Figure 2.3), a brief overview of the formation of the amide bond between aromatic/heteroaromatic components is provided. As shown in Scheme 2.1 there are three major disconnections to access an amide bond:

- 1) disconnection 1 (the disconnection between the aryl ring and the carbonyl of the amide bond). This would imply a reaction between an arylamine **2.8**, an aryl halide **2.9** and carbon monoxide,⁶¹ with the aryl halide **2.9** and carbon monoxide establishing the heteroaryl ring from the side of the carbonyl moiety and the arylamine **2.8** is introduced last. Upon the migratory insertion of the carbonyl, treatment with sodium phenoxide follows and aminolysis of the generated ester leads to the amide product. The product of the catalytic cycle is the ester and the aminolysis takes place outside the cycle. This rationalizes the decent number of references which employ the use of electron rich amines.⁶²⁻⁶⁵ With the amidation between amines and esters occurring outside of the cycle, expectedly, the engagement of electron deficient has not received analogous attention.

- 2) disconnection 2 (the disconnection between the aryl ring and the nitrogen of the amide bond), the reaction which is reminded by the transform presented is a Buchwald type amidation (reaction between aryl halide **2.9** and arylamide **2.10**). Both palladium⁶⁶ and copper⁶⁷ have been used to affect the *N*-arylation reaction. Concerning to the use of metals in the production of polar diheteroarylamides, as is the case with the diheteroarylamides **2.6**, would be the removal of metal byproducts upon isolation of the products.
- 3) disconnection 3 (disconnection between the nitrogen and the carbonyl of the amide bond) is the most prevalent route taken to construct an amide bond. Reviews focusing on this disconnection to construct peptides cover a massive range of protocols and reagents.^{56, 68-71} The products of the transform are an arylamine **2.8** and suitable activated acid component component **2.11**.



Scheme 2.1 Possible disconnections to access diheteroarylamides

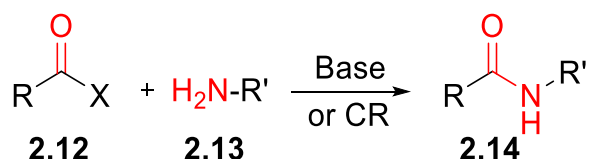
This last disconnection can serve as a platform for either an amidation or transamidation^{56, 71} reaction, depending on whether the X in Scheme 2.1 stands for any electron withdrawing group

or an amino group, respectively. As pointed at the beginning of the Chapter, amides demonstrate reduced basicity as compared to their amine counterparts, and therefore transamidation reactions are not easy to perform, let alone to use them in parallel synthesis protocols.

With disconnection 3 in our mind, and considering the discussions in Chapters 2.2.1, 2.2.2 and 2.2.3 the different reagents/reaction conditions used in amide coupling reactions can be classified as: mediators, catalysts and initiators. Examples are presented below:

2.2.1 Heterolytic coupling

In heterolytic coupling different mediators, usually a base or coupling reagent is used in the presence of super- or stoichiometric amount to activate the acid component and, therefore, allow for the amidation to occur (Scheme 2.2). The presence of a mediator is mandatory for these reactions as the reaction of an amine with a carboxylic acid (X = OH) results in the formation of the ammonium carboxylate, which is the kinetically favored product.⁷⁰ Although condensation of carboxylic acids with amines to deliver amides, in the absence of coupling reagents, can be achieved at elevated temperatures in the presence of a water absorbent,^{56, 72} it is not a general synthetic method.



X: N₃, F, Cl, OR'', SR'', NHR¹R², then base

X: OH, then coupling reagent (CR)

Scheme 2.2 Amide bond formation: heterolytic coupling

This problem can be circumvented by the conversion of the acid to the corresponding and more reactive acyl halide: acyl chlorides (Schotten-Baumann reaction), acyl fluorides,⁷³⁻⁷⁵ esters,⁷⁶ and

azides (Curtius reaction). Reviews by Montalbetti & Falque,⁷⁷ Valeur & Bradley,⁷⁸ and Campagne⁶⁹ summarize methods and strategies on heterolytic amidation couplings.

2.2.2 Catalyzed coupling

The power of the catalytic transformations lies in the use of substoichiometric amount of the mediator (catalyst up to 10%) and the freedom it gives the researchers to engage functional groups, such as alcohols as the oxygen containing precursor for the amide bond, which otherwise would not be feasible to engage. Metal, metalloid or metal-free catalysts can be engaged in the amidation reaction (Scheme 2.3). There is a plethora of methods underlining the rise of catalyst use over the past 10-15 years.^{68, 70, 79} In the review by Pattabiraman and Bode, a series of organocatalysts are presented, which are used to catalyze the amidation reaction of aldehydes, alcohols, thiols and esters with amines.⁷⁰ Recently, early transition metals such as titanium,⁸⁰⁻⁸² zirconium,⁸³⁻⁸⁵ hafnium⁸⁶ and niobium⁸⁷ have been used as catalysts in amide bond formation between carboxylic acids (group 4: titanium, zirconium and hafnium)/esters (group 4&5: zirconium and niobium) and amines. Main group metals such as sodium⁷⁶ and calcium⁸⁸ and metalloids such as boron⁸⁹⁻⁹⁴ have been shown to catalyze amidation reactions, with esters and carboxylic acids as substrates, respectively. Nickel,⁹⁵ palladium⁹⁶ and ruthenium⁹⁷ are representative examples of late transition metals which have been reported to catalyze amidation reactions, using esters as the carboxylic acid component. Carboxylic acids, for reasons which were illustrated in Chapter 2.2.1, would not undergo the amidation reaction in the absence of a catalyst. In the case of the esters, which are already activated acid components, the asset of using a catalyst underlies in improving their reactivity and reaction yielding. A notable example on the nickel cross-coupling reaction between esters and amines was presented by the Newman⁹⁵ group, affording a diverse class of amides. Arylamides were obtained, with the aryl functionality being

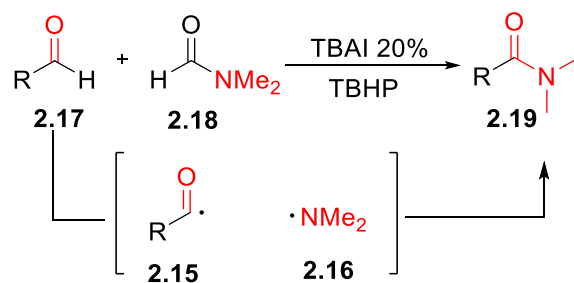
either on the side of ester or on the side of ester or the amine but no heteroarylated amines were presented in the scope of the reaction.



Scheme 2.3 Amide bond formation: catalyzed coupling

2.2.3 Homolytic coupling

A method which is characterized by uniqueness in the amide bond formation is the reaction between the acyl **2.15** and aminyl radical **2.16**, of an aldehyde **2.17** and a formamide **2.18**, respectively, which allows for the amide bond to be formed with the use of radical initiators (peroxide species as radical initiators).⁹⁸ This method, however, specifically delivers *N,N*-dimethylamido products **2.19**.



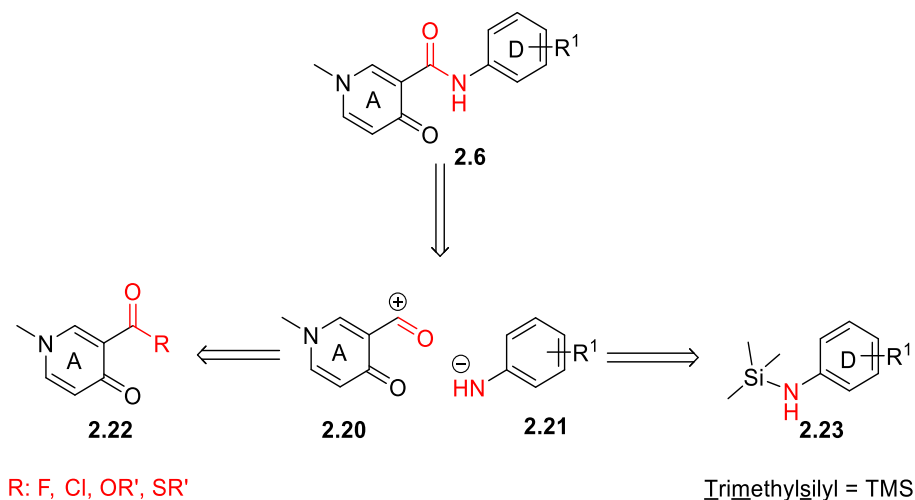
Scheme 2.4 Amide bond formation: radical initiated coupling

2.3 The reaction between the *N*-TMS amines and thioesters: an efficient protocol to access diheteroarylamides

To implement our goal to access libraries of diheteroarylamides **2.6**, we followed disconnection 3 *via* heterolytic coupling. Thus, the reaction involves an electrophile and a nucleophile in the presence or not of a base/coupling reagent. A retrosynthetic analysis of the diheteroarylamides –

structural analogs of compound **2.2** – reveals two synthons: an acyl species **2.22** and a nitrogenous species **2.23** (Scheme 2.5).

As discussed earlier in our application, the reaction of acyl chlorides with heteroaromatic amines was inefficient.⁵⁹ This is primarily due to the poor reactivity/reduced nucleophilicity of the amine component and, consequently the activated acid can alternatively degrade. The solution to this problem developed in our laboratory was to use the *N*-TMS variant **2.23** of the electron poor amines, which upon reaction with the fluoride ion would undergo desilylation to the reactive anionic species **2.21**, which nucleophilically attacks the activated acid component (Scheme 2.5).



Scheme 2.5 Retrosynthetic analysis of diheteroarylamides **2.6**

In an earlier study by Ulven,⁹⁹ non-silylated electron deficient amines have been engaged in the amidation reaction with the acid counterpart, an acyl fluoride. The methodology involves the reaction of an *in situ* generated acyl fluoride which was reacted with electron poor (hetero)arylamines at elevated temperatures. To ensure high reactivity for the amide bond protocol, we narrowed down to the use of the *N*-TMS amines, instead of the non-protected amines. The described disadvantages associated with the use of acyl chlorides led us to focus on

acyl fluorides. Inspirational work for this approach was the initial work presented by Kahn, and involves the reaction between acyl fluorides and sterically demanding amines.¹⁰⁰

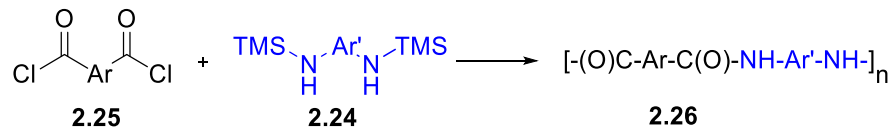
2.3.1 *N*-TMS derivatives of electron deficient amines and acyl halides

Both acyl chlorides and acyl fluorides have been reported to afford amide or *N*-acyl products with *N*-TMS amines (instead of the non-silylated variants as described in 2.3). In Scheme 2.6 all the procedures which involve the reaction of *N*-TMS amines of parent electron deficient amines and an activated acyl halide are presented.

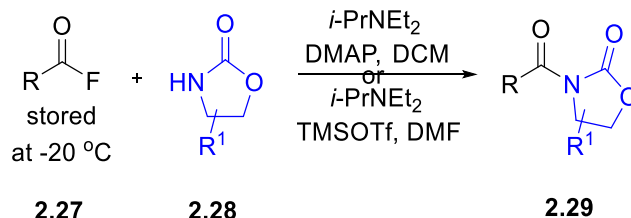
In the work described by Oishi,¹³ it is explicitly stated that the reaction between *N*-TMS variant **2.24** of electron poor arylamines demonstrated higher reactivity as compared to the non-silylated amines in the reaction with acid chlorides **2.25**, affording the polymeric products **2.26** to excellent yields. The amide bond formation via the reaction of *N*-TMS amines and acyl chlorides was first presented by Kurz in 1983.¹⁰¹

In 1987 Cava¹¹ reported the amide bond formation between *N*-TMS amines and acyl fluorides. In the work by Carreira,¹⁰² the acyl fluoride **2.27** when reacted with oxazolidinones **2.28** (not amines in their nature but they possess an electron deficient nitrogen) in the presence of TMSOTf yielded the acylated products **2.29** obtained were up to 98% (Scheme 2.6). Inspired largely by the works of Kahn and Cava, the Grierson¹² group developed the reaction of *N*-TMS aromatic/heteroaromatic amines **2.30** with the isolated and characterized acyl fluoride **2.27** as an effective strategy to circumvent the limitations encountered with the use of acyl chlorides and unreactive amines. The generation of the acyl fluorides in the latter case relied on the reaction between the precursor carboxylic acid **2.31** and TFFH (*N,N,N',N'*-tetramethylfluoroformamidinium hexafluorophosphate), a nucleophilic fluorinating agent introduced by Carpino.^{73, 74} The diheteroarylamides **2.32** were obtained in yields up to 95%.

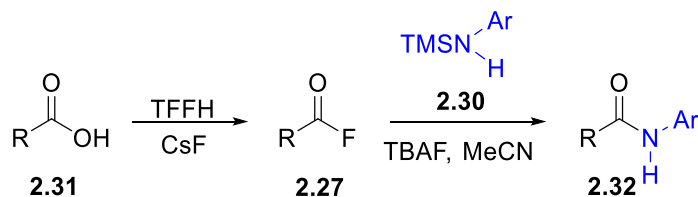
Oishi: *in situ* acid chloride - electron deficient amines



Carreira: isolated acid fluoride - oxazolidinones



Grierson (previous work): isolated acid fluoride - electron deficient amines



Scheme 2.6 Amide bond formation with *N*-TMS amines and acyl halides

Acyl halides are the most desired activated carboxylic acid components due to their high reactivity earned by the high polarizability of the bond between the electrophilic carbon and the halide. Of the two, acyl fluorides demonstrate the greater hydrolytic stability (as shown by the fact that they can undergo aqueous workup), and for that groups across the globe have engaged them in amidation reaction, exploiting various fluorinating agents^{100, 102-106} for their generation such as cyanuric fluoride, DAST, Deoxo-fluor, BTFFH, TFFH. Recent literature has also shown the use of aminodifluorosulfonium tetrafluoroborate salts¹⁰⁷ [Et₂=SF₂][BF₄] and tetrabutylammonium trifluoromethylsulfonide¹⁰⁸ (Me₄N)SCF₃. Despite their stability and relative resistance to hydrolysis to the corresponding carboxylic acids, they still require to be generated and stored under inert conditions. This feature does not pose any limitations to linear synthetic routes and total syntheses, but it becomes a limitation in the case of a developing method which

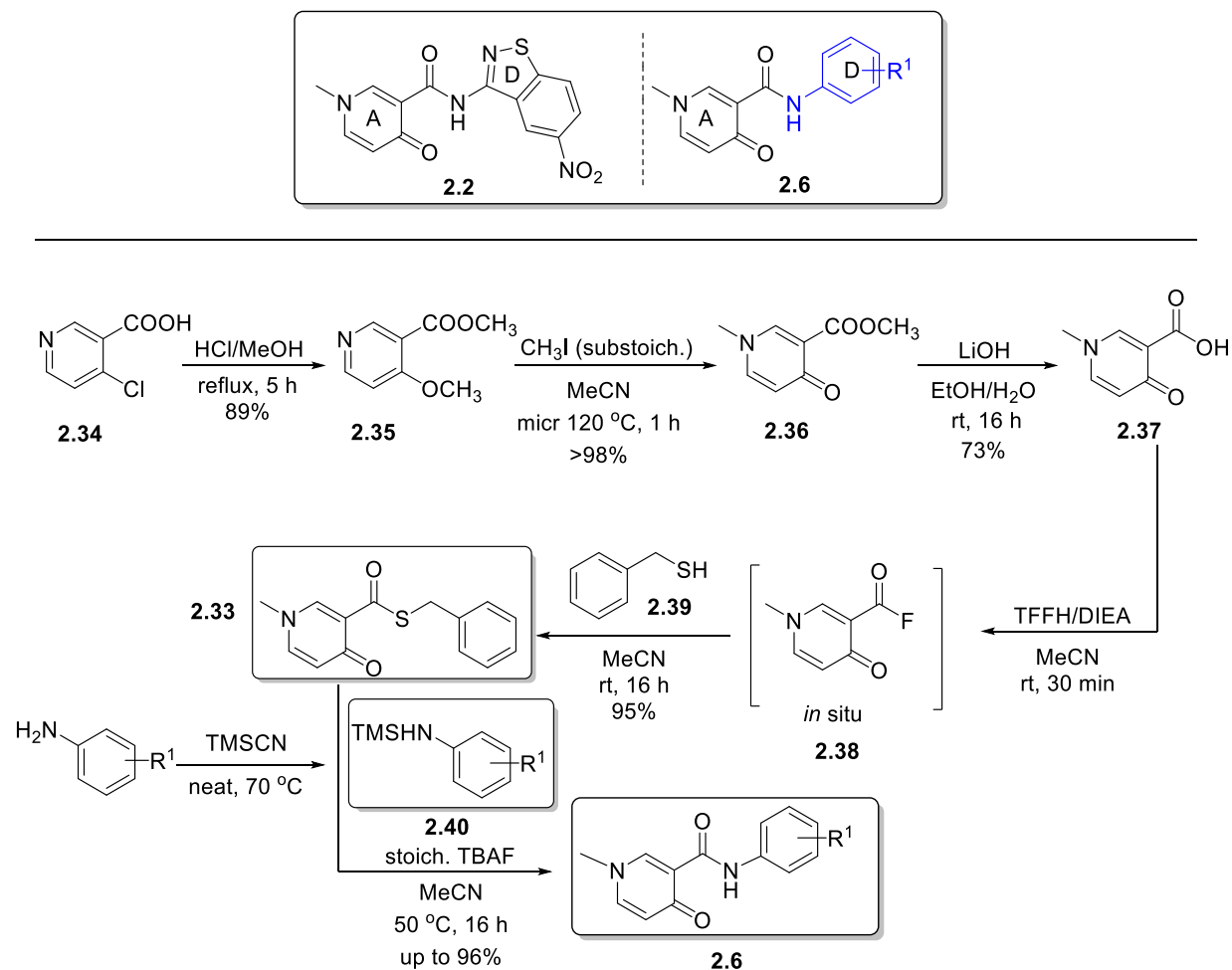
is ultimately going to be adapted in the context of parallel synthesis to afford libraries of compounds. In the work by Zamiri and Grierson,¹² the reaction was indeed adapted into the context of parallel synthesis. The downside of the acyl fluoride storage under inert conditions served as a driving force to investigate the reaction of *N*-TMS amines with thioesters, another activated acid component characterized by greater stability as compared to acyl halides.

2.3.2 *N*-TMS derivatives of electron deficient amines and thioesters in the amidation reaction

Although the aminolysis of esters to afford amides has been known since the very early ages of chemistry, it is not a general synthetic method. In fact, esters are often used as acid protecting groups in peptide synthesis. The formation of amides *in vivo* can occur through the reaction of an amine with acetyl-CoA, a thioester. Albeit the reaction of thioesters with electron rich amines and thioesters has received attention, it is not the same case with electron deficient amines.¹⁰⁹ With the goal to further develop our laboratory's methodologies to access amides from *N*-TMS amines, the objective was to identify a more stable electrophile as compared to acyl fluoride. As will be discussed in the following sections, stable thioesters proved to be ideal as the activated acid reagent. Further, the discovery that thioesters work efficiently in the coupling reaction with *N*-TMS amines motivated further investigation of oxoesters. The choice of the type of ester – at the very initial stage of this work – was based on the relative reactivity of oxoesters and thioesters; thioesters have been reported to be more reactive than oxoesters.^{110, 111} The C-O bond is more polarized than the C-S bond. However, the C-S bond is longer than the C-O bond due to the bigger size of sulfur, and therefore, more easily breakable.

As discussed in the introduction of this Chapter, due to its presence in the anti-HIV agent **2.1** the thioester derivative 4-pyridone-3-carboxylic acid, representing ring A in **2.1**, was chosen as the

activated acid component for the development of our methodology. It was reacted with a series of 19 TMS-substituted amines **2.40** of varying nucleophilicity to deliver diheteroarylamides **2.6**. In Scheme 2.7, the overall synthesis to obtain thioester **2.33** is presented.



Scheme 2.7 Total synthetic route for thioester **2.33** and diheteroarylamides **2.6**

Reaction of 4-chloro-nicotinic acid **2.34** with HCl/MeOH at reflux afforded the 4-methoxy-3-methylester pyridine derivative **2.35**.¹¹² Treatment of this intermediate **2.35** with substoichiometric amount of methyl iodide led to the corresponding *N*-methyl-4-pyridone derivative **2.36**. Saponification of ester **2.36** afforded the corresponding carboxylic acid **2.37**.

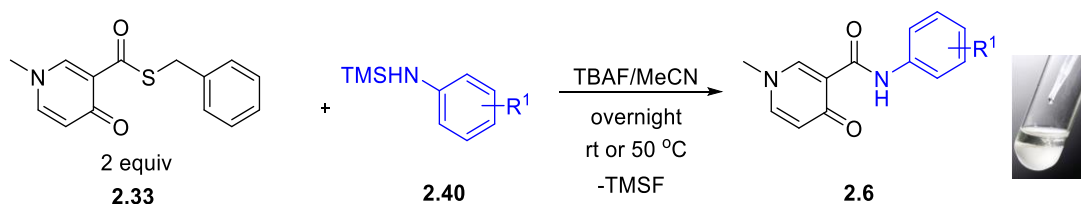
Intermediate **2.37** was then treated with TFFH and the *in situ* acyl fluoride **2.38**⁷³ was reacted with benzyl mercaptan **2.39** to afford thioester **2.33**.

Each library amine was silylated through reaction with TMSCN¹⁰ and, after the removal of the excess TMSCN, was used immediately in the amidation reaction with thioester **2.33**. The reaction between thioester **2.33** and a library amine **2.40** was carried out in MeCN, in the presence of stoichiometric amount of TBAF.

2.3.3 Efficiency of the amidation protocol and consideration of a green chemistry approach

2.3.3.1 Efficiency

The three features which render this amidation reaction, shown in Scheme 2.8, efficient are:



Scheme 2.8 Rationale for the efficiency of the protocol: precipitation of diheteroarylamides and formation of TMSF

- I. the formation of TMSF *via* the reaction of *N*-TMS amines with TBAF. The strength of the formed Si-F (582 KJ/mole) acts a thermodynamic driving force for the desilylation of the amine and the generation of the amine anion.
- II. the reactivity of anionic nitrogenous species (generated upon desilylation) toward the thioester.
- III. the precipitation of the derived amide products in MeCN. As shown in Scheme 2.8, 2 equiv of the precursor thioester were used to ensure consumption of the starting limiting *N*-TMS amine.

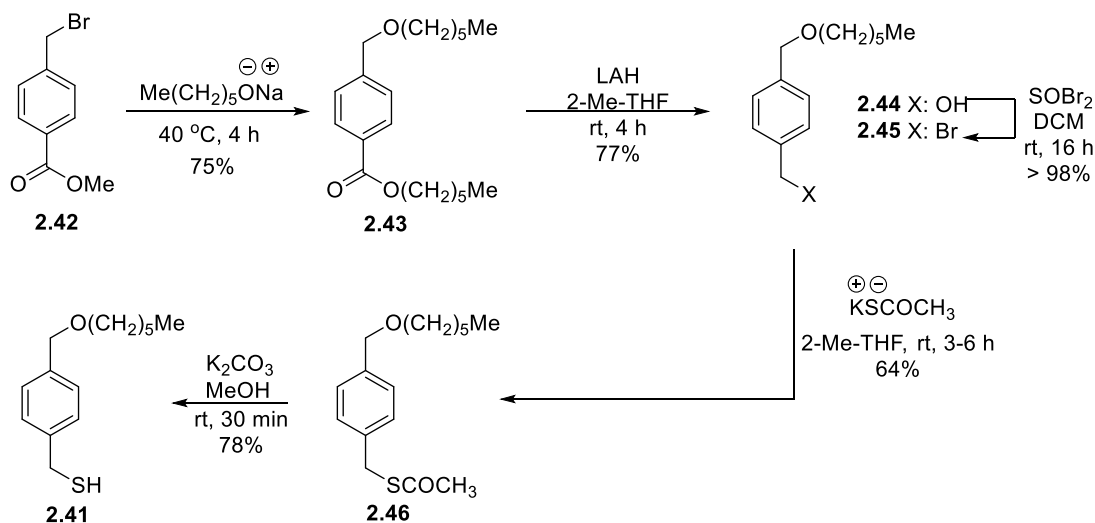
2.3.3.2 Green chemistry

As the amide products precipitated from the reaction medium, they were isolated by simple vacuum filtration and washed with MeCN or acetone ensure purification of a degree of 95%. The TBAH produced, any excess thioester **2.33** (soluble in MeCN) and the liberated thiol **2.39** (and/or its corresponding disulfide) were all completely removed in this way. The purity of the the degree of 95% was determined by ^1H NMR. It is noteworthy to mention that this purity refers to molecules possessing an active NMR nucleus, and disregards the presence of impurities with inactive NMR nuclei. By bypassing the need for column chromatography minimal waste generation is ensured (Principle 1 of Green Chemistry).

Having shown that thioester **2.33** reacts efficiently with amines, a further action to be taken to additionally improve the protocol, is to deal with the strong odor derived from the use of the commercially available benzyl mercaptan **2.39** (Scheme 2.7) to prepare the starting thioester **2.33**. This strong odor often associated with sulfur chemistry is a feature not agreeable with the principles of Green Chemistry,¹¹³ and renders the protocol unattractive as a synthetic method. To circumvent this problem we turned to the use of a higher molecular weight thioester. It is reported in the literature that the higher the ratio of carbon to sulfur atoms, the less stinky a thiol is.^{114, 115} An obvious choice for the thiol synthon could be a commercially available dodecane thiol; however we sought to synthesize an aromatic thiol which would be UV-active and, thus, trackable by TLC.

With this in mind, the long chain thiol **2.41** was prepared with *via* a five step synthetic route with an overall yield of 29% (Scheme 2.9). Initially, the 4-(bromomethyl)benzoate **2.42** was treated with sodium hexanoate to afford the etherified and esterified intermediate **2.43**. Reduction of ester **2.43** with LAH led to the corresponding alcohol **2.44**, which was then converted to the

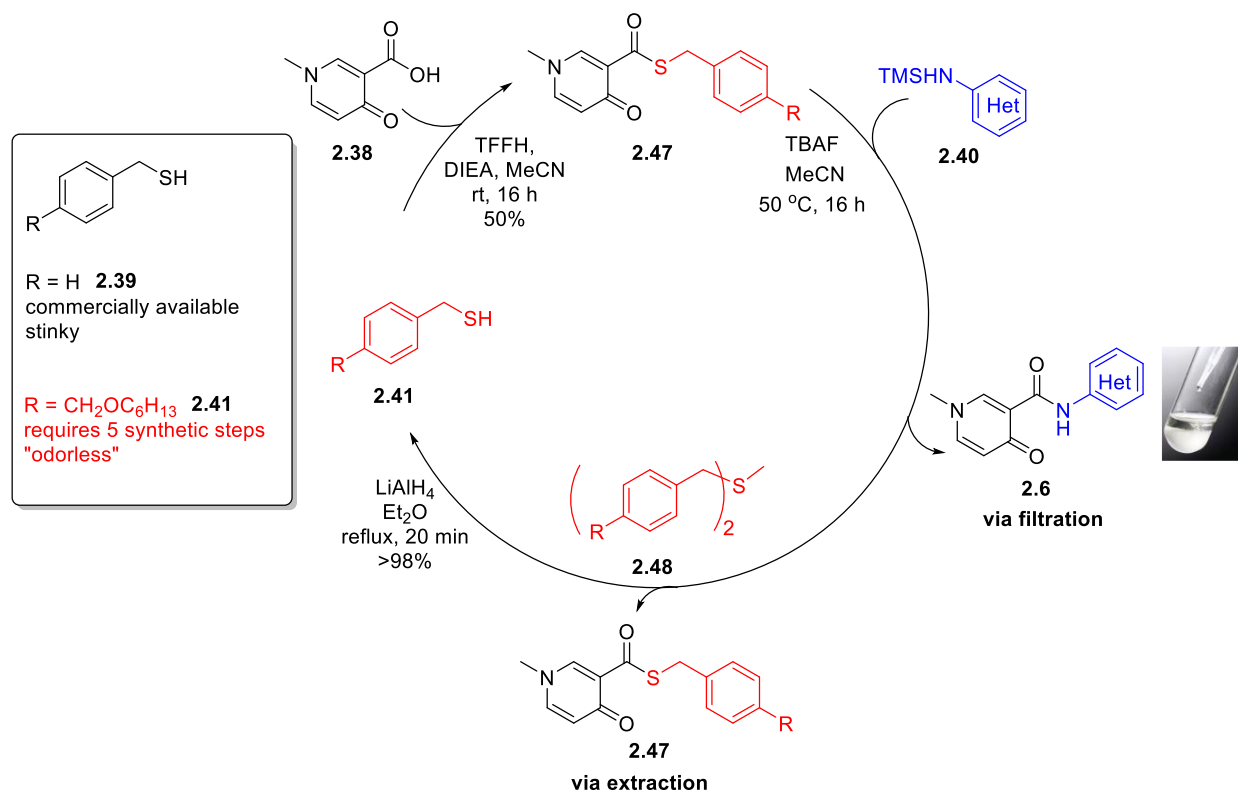
benzyl bromide **2.45** with SOBr_2 .¹¹⁶ The bromide **2.45** was converted to methyl-thioester **2.46** with KSAc , which upon hydrolysis led to the desired benzyl thiol **2.41**.¹¹⁷



Scheme 2.9 Synthetic route for odorless thiol **2.41**

Two questions which arise with the incorporation of the odorless thiol **2.41** in the process of making it greener are the following: 1) it requires five synthetic steps while the non-substituted benzyl thiol **2.39** is commercially available; therefore the use of the former will unavoidably increase the waste generation 2) the increase of the molecular weight of any reactants will unavoidably generate heavier waste. If the heavier benzyl mercaptan **2.41** is used for the formation of the thioester **2.47**, then a heavier byproduct corresponding to the liberated thiol **2.41** will be generated, as compared to thiol **2.39**, upon the reaction of thioester **2.47** with a library *N*-TMS amine **2.40**. This contradicts the principle of atom economy.¹¹⁸ To circumvent the violation of the above principles, a cycle was designed for the synthesis of diheteroarylamides through which any generated “byproducts” would be recycled and reused (Scheme 2.10). Odorless thiol **2.41** was reacted with the *in situ* generated acyl fluoride **2.38** as shown in Scheme 2.10 and the

obtained thioester **2.47** (50% yield) is then reacted with a library amine **2.40** (limiting reagent), under the same conditions used for the reaction benzyl thiol **2.39** (Scheme 2.7). Again, the derived diheteroarylamides **2.6** precipitate out from MeCN.



Scheme 2.10 Green cycle to access diheteroarylamides **2.6** with the use of odorless thiol **2.41**

As determined by ¹H NMR spectroscopy of the concentrated filtrate the liberated thiol **2.41** dimerized to the corresponding disulfide **2.48** the excess thioester **2.47**. To recycle the byproducts, the filtrates from a representative number of reactions were combined and disulfide **2.48** was extracted with heptane. Reduction of disulfide¹¹⁹ **2.48** gave back thiol **2.41** (>98%), making it available for the resynthesis of thioester **2.47** and, thus, allowing for another cycle to start. Treatment of the combined MeCN layers “as needed” allowed for recovery of 30-40% of thioester **2.47**.

2.3.4 The amidation reaction between thioesters and *N*-TMS amines

The reactivity of thioesters **2.33** and **2.47** was evaluated through the reaction with 19 amines. The *N*-TMS amines **2.40** are presented in a descending order of electron density. Based on the data in Table 2.1, the yield range for the majority of amines was 53-96%. As expected, the yields of the diheteroarylamides obtained from both thioesters **2.33** and **2.47** delivered the products **2.6** in proximal yields. It is noteworthy to mention, in the reaction of *N*-TMS amines **2.40.1-2.40.5** the yields were in the range of 11-25%. This was a consequence of the greater solubility of these relatively less polar amide products in MeCN. Indeed, it was expected that these amines, due to their higher electron density as compared to the rest of the amines, would afford the amides in higher yields.

Table 2.1 Diheteroarylamide products **2.2**, **2.6.1-2.6.10** and **2.6.12-2.6.19** prepared *via* Schemes **2.7** and **2.10**

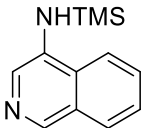
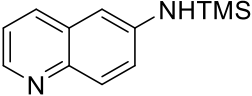
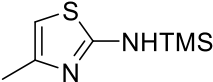
| Entry | TMS-Amine ^{12, 120} | Structure | Electron Density (eV) ^a | <i>N</i> -Silylation Time | Amide product/yield from thioesters 2.33/2.47 ^{b,c} |
|-------|------------------------------|---|------------------------------------|---------------------------|---|
| 1 | 2.40.1 ¹² |  | 120 | 30 min | 2.6.1 15% (11%) |
| 2 | 2.40.2 |  | 119.6 | 14 h | 2.6.2 16% (20%) |
| 3 | 2.40.3 ¹² |  | 119.5 | 15 min | 2.6.3 14% (25%) |

Table 2.1 cont'd on page 50

Table 2.1 cont'd from page 49

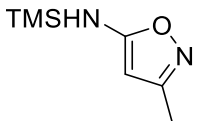
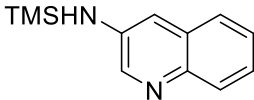
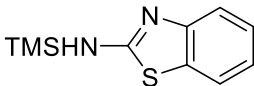
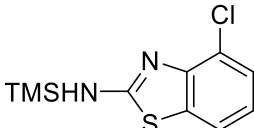
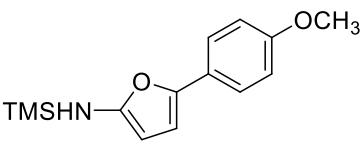
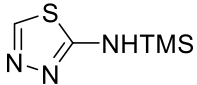
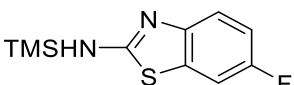
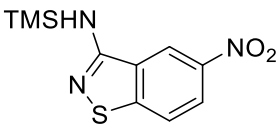
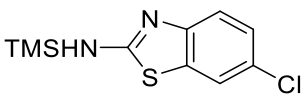
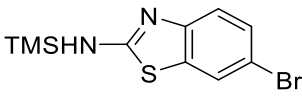
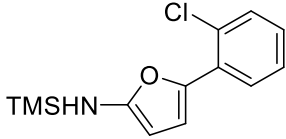
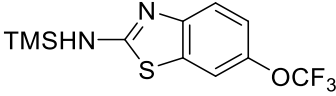
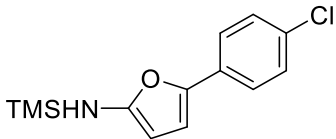
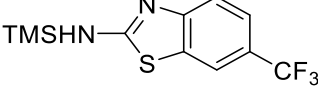
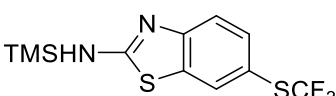
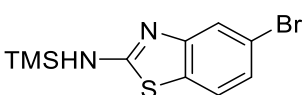
| | | | | | |
|----|-----------------------|---|------|--------|------------------|
| 4 | 2.40.4 ¹² |  | 115 | 30 min | 2.6.4 24% (17%) |
| 5 | 2.40.5 |  | 114 | 30 min | 2.6.5 17% (15%) |
| 6 | 2.40.6 ¹² |  | 97.8 | 30 min | 2.6.6 70% (70%) |
| 7 | 2.40.7 ¹² |  | 97.8 | 30 min | 2.6.7 68% (68%) |
| 8 | 2.40.8 |  | 95.7 | 30 min | 2.6.8 88% (88%) |
| 9 | 2.40.9 ¹²⁰ |  | 93.9 | 30 min | 2.6.9 92% (96%) |
| 10 | 2.40.10 |  | 93.7 | 14 h | 2.6.10 68% (68%) |
| 11 | 2.40.11 ¹² |  | 88.8 | 30 min | 2.2 33% (25%) |

Table 2.1 cont'd on page 51

Table 2.1 cont'd from page 50

| | | | | | |
|----|-----------------------|---|------|------|------------------|
| 12 | 2.40.12 |  | 81.7 | 14 h | 2.6.12 85% (84%) |
| 13 | 2.40.13 |  | 81.5 | 14 h | 2.6.13 82% (86%) |
| 14 | 2.40.14 ¹² |  | 77.3 | 1 h | 2.6.14 66% (65%) |
| 15 | 2.40.15 |  | 75.9 | 14 h | 2.6.15 67% (67%) |
| 16 | 2.40.16 |  | 75.3 | 1 h | 2.6.16 83% (82%) |
| 17 | 2.40.17 |  | 72 | 14 h | 2.6.17 69% (63%) |
| 18 | 2.40.18 |  | 70.7 | 14 h | 2.6.18 53% (53%) |
| 19 | 2.40.19 |  | 26.1 | 14 h | 2.6.19 80% (81%) |

^a Electron density calculated with *Spartan Version 6.1.7*; Wavefunction Inc: Irvine (CA, USA), 2014.

^b Reaction conditions for thioesters 2.33/2.47 (2 equiv; except for entries 8 and 16 (4 equiv) and entry 11 (1 equiv)): TBAF 1 M in THF (1 equiv), MeCN, 50 °C (rt only for 2.2), overnight. ^c Isolated yield for the amide product derived from thioester 2.47 in brackets

Interestingly the reaction of *N*-TMS-amine 2.40.11 with the thioesters led to an unexpectedly low yield of the corresponding amide 2.2 (33% and 25% with thioesters 2.33 and 2.47, respectively). When two equivalents of any of the two thioesters were employed in the amidation reaction, then the ¹H NMR spectrum showed the presence of two sets of six aromatic peaks, and two amide peaks, implying the formation of a second isomeric product 2.2' (Figure 2.4). In the lack of crystal structures of either of the two products, we suggest the amide peak at 15.58 ppm corresponds to product 2.2 and the amide peak at 14.26 ppm corresponds to product 2.2' (see experimental section in Chapter 6.2). What we can state with greater certainty is that product 2.2 is the thermodynamic product of the reaction and 2.2' is the kinetic product, as the former 2.2 possesses a tri-substituted imine while the latter 2.2' a di-substituted imine. The desired diheteroarylamide 2.2 was obtained alone when one equivalent of any of the two thioesters was employed in the amidation reaction.

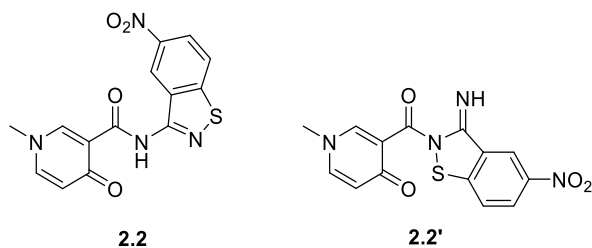
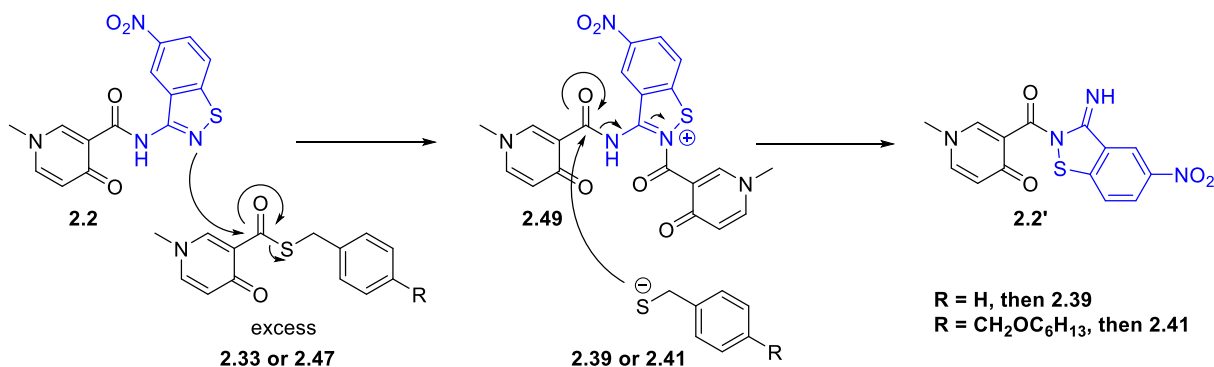


Figure 2.4 Isomeric diheteroarylamides 2.2 and 2.2'

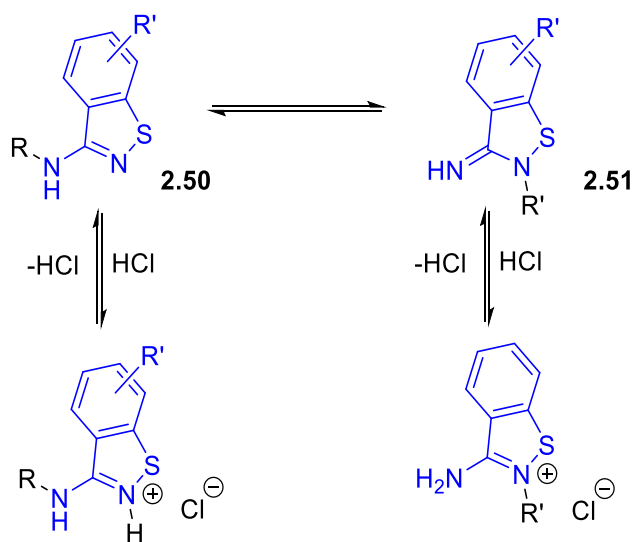
A plausible mechanism to be suggested for the presence of the isomeric compound is shown in Scheme 2.11. The initially formed amide 2.2 possesses a pyridine type nitrogen on the benzothiazole moiety whose lone pair can do a nucleophilic attack on the carbonyl of the

excess thioester **2.33** or **2.47**. The resulting intermediate **2.49** collapses to the imine derivative **2.2'** because of the attack of the liberated thiol **2.39** or **2.41** on the amide carbonyl.



Scheme 2.11 Plausible mechanism for products **2.2** and **2.2'**

What is described in the literature is an equilibrium between the two species **2.50** and **2.51** under basic conditions (Scheme 2.12). Protonation of either of two species will lead to the mixture of the corresponding protonated benzoisothiazoles with the positive charge located on the heterocyclic nitrogen.^{121, 122}



Scheme 2.12 Proposed equilibrium of species **2.50** and **2.51**

2.4 Summary

In conclusion we have developed a method for the synthesis of diheteroarylamides *via* the reaction of the *N*-TMS derivatives of weakly nucleophilic parent (hetero)arylated amines with thioesters. As compared to the use of acyl fluorides as electrophiles, the use of the more stable thioesters allows for greater amenability of the developed protocol to parallel synthesis. The efficiency of the protocol relies on the facile isolation of the amide products and removal of any byproducts by vacuum filtration. Our efforts to expand to the application of the Green Chemistry principles are reflected by the replacement of the malodorous thiol with an odorless thiol and the reuse of the byproducts (liberated thiol/disulfide) and excess thioester by recycling.

The experimental for Chapter 2 starts on page 108.

Chapter 3: *N*-TMS amines as substrates in zirconium catalyzed hydroaminoalkylation to access primary α -arylated amines

3.1 Introduction

The focus in Chapter 3 is on the Csp^3-Csp^3 bond formation using *N*-TMS amines as substrates for the hydroaminoalkylation reaction. The target structures in Chapter 3 are α -arylated amines **3.1** (Figure 3.1) which possess a branch at the carbon α to nitrogen. It is usually the abundance of a motif in pharmaceuticals that attracts the attention of the synthetic community to identify new and amended methods to complement traditional synthetic approaches. According to data presenting the top 200 pharmaceutical products by prescription – on a yearly basis – for the period 2011-2016,¹²³ there is a significant number of α -arylated amines and amine derivatives. Such an example is the antidiabetic drug, repaglinide – an amide – whose amine synthon is comprised of a primary α -arylated amine.

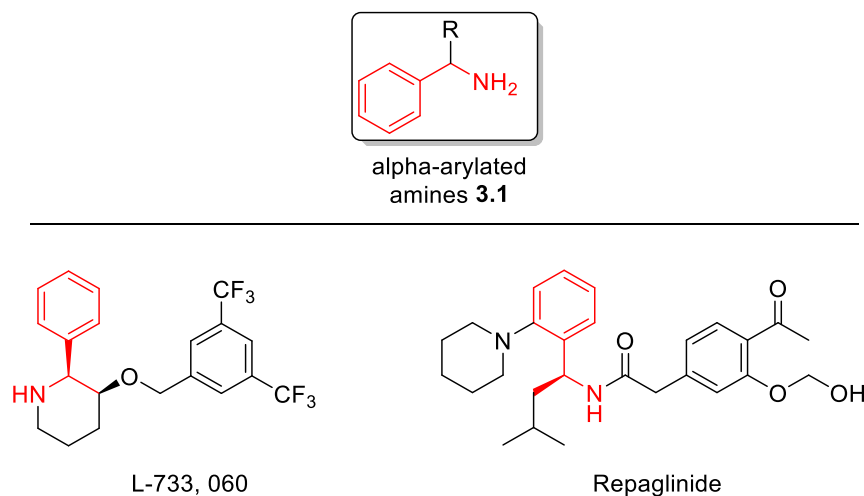


Figure 3.1 Pharmaceuticals containing a primary amine synthon

An initiative to access primary α -arylated amines was undertaken, with the goal of offering new methods to the synthetic community. Such methods can enable access to the α -arylated amine

motif of functionalized drugs which may have been rejected at the design stage due to inefficient synthetic routes. To implement this goal, the use of both selectively substituted substrates *N*-TMS amines and alkenes, and the developed technology, zirconium catalyzed hydroaminoalkylation, are exploited to realize the synthesis of primary α -arylated amines *via* Csp³-Csp³ bond formation.

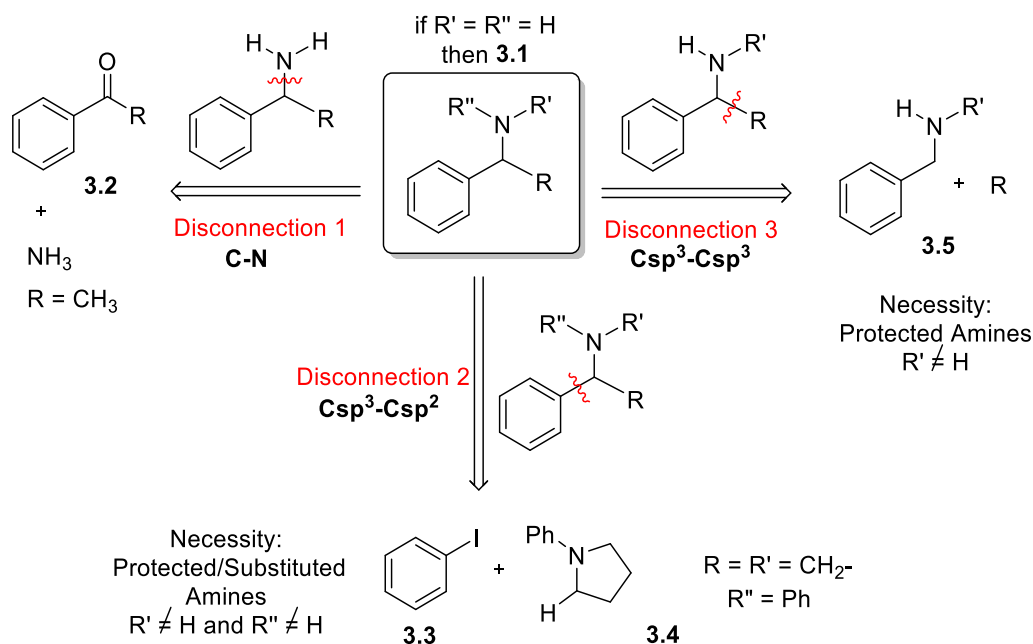
3.2 Overview of α -arylated amines synthesis

Traditional disconnections to access primary α -arylated amines are presented, with reference to both stoichiometric and catalytic variants. As this chapter presents a catalytic method to access α -arylated amines, the catalytic transformations are highlighted for each disconnection.

Of all the disconnections (Scheme 3.1), it is only disconnection 1 that allows for the utilization of ammonia without further modification to deliver primary α -arylated amines *via* C-N bond formation. Particularly, the Mignonac reaction (1921) delivers the 1-phenylethylamine ($R = \text{CH}_3$, $R' = R'' = \text{H}$, Scheme 3.1) *via* reductive amination between acetophenone **3.2**, ammonia and hydrogen, using high pressure and heating and is a catalytic example to access primary α -arylated amines. Just this year and 97 years after the introduction of the Mignonac reaction, the ruthenium catalyzed synthesis of chiral primary amines with acetophenone as a substrate was reported.¹²⁴ A stoichiometric example of reductive amination is the Leuckart reaction, in which a ketone is converted to an amine. The ammonium formate, which is used in stoichiometric amounts, acts as both the ammonia surrogate and reducing agent.

Disconnection 2 is the most prevalent disconnection in the literature and the products for this transform, in the context of catalysis, are usually an aryl halide **3.3** and a secondary or tertiary amine **3.4**. A stoichiometric example for the α -C-H arylation of secondary amines has been disclosed by the Seidel group.^{125, 126} In this case the synthons are a cyclic imine and a

nucleophile and the importance of this work lies in the use of unprotected secondary amines as substrates.

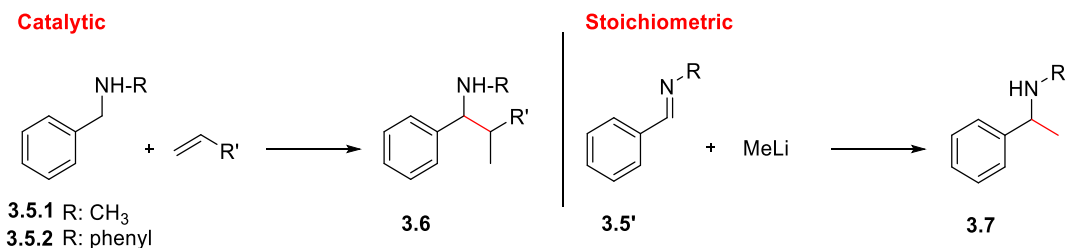


Scheme 3.1 Possible disconnections to access α -arylated amines

The Doyle^{127, 128} and Macmillan^{127, 129} groups have used photoredox catalysis with the use of nickel and iridium. Other groups have recently focused on the use of palladium¹³⁰ for such transformations, even achieving enantioselective α -arylation.¹³¹⁻¹³³ Ruthenium¹³⁴ and copper¹³⁵ have also been reported to deliver aryl substituents α to the nitrogen, however the limitation of the former is the requirement of a directing group and the latter is successful only with *N*-arylamines. This disconnection, focused on Csp³-Csp² bond formation alpha to nitrogen, though broadly used, requires secondary or tertiary amines to be used for the construction of α -arylated amines and often uses precious metals.

Disconnection 3 pertains to Csp³-Csp³ bond formation on α -arylated amines of type **3.5** (Scheme 3.1). Catalytic tantalum¹³⁶ and titanium^{137, 138} have been reported by the Schafer and Doye groups, respectively, to deliver α -arylated *N*-alkyl- and *N*-arylamines of type **3.6**, via

hydroaminoalkylation (Scheme 3.2). The development of this catalytic transformation to install tertiary centers on α to nitrogen carbon of α -arylated amines is in its infancy. A stoichiometric example for this disconnection is the addition of MeLi to arylimine **3.5'** to give the α -methylated product **3.7** (Scheme 3.2).¹³⁹ The third disconnection, which forms the Csp³-Csp³ bond *via* hydroaminoalkylation, will be discussed in detail in the below section.

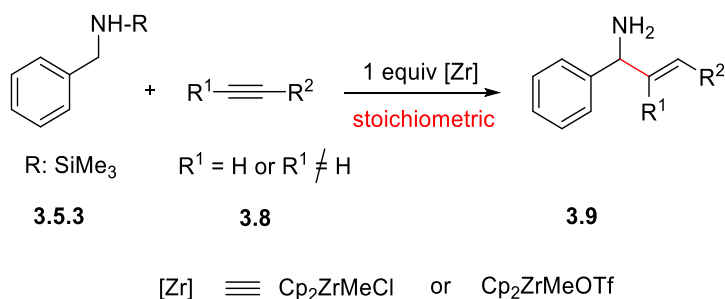


Scheme 3.2 Benzylamines as substrates to access α -arylated amines

3.3 Hydroaminoalkylation: promises and challenges

Hydroaminoalkylation is the catalytic addition of the α -C-H bond of the amine across a double bond of an alkene in the presence of a catalyst (Scheme 3.2).

Some of the first examples of this reaction were stoichiometric and were called α -alkylation or α -alkenylation of amines, depending on whether the coupling partner of the amine is an alkene or alkyne substrate, respectively (Scheme 3.3). In 1989, Buchwald presented the α -alkenylation of *N*-silylamines in the presence of stoichiometric amounts of a zirconium complex, an amine **3.5.3** and an alkyne **3.8** to form the Csp³-Csp² bond α to the nitrogen.¹⁴⁰



Scheme 3.3 Zirconium mediated α -alkenylation of *N*-silylated amines

The catalytic variant was introduced to the chemistry community by Clerici and Maspero in 1980¹⁴¹ but it was Nugent who explored and reported the mechanism of the transformation.¹⁴² In 2008 Herzon and Hartwig^{143, 144} revisited the transformation using tantalum and since then the reaction has received ongoing attention by a few groups around the globe. Early transition metals that have been employed for the catalytic reaction include scandium,^{145, 146} titanium,^{137, 138, 147-152} tantalum^{136, 143, 144, 153, 154} and niobium^{155, 156} (Scheme 3.4).



Scheme 3.4 Early transition metal catalyzed hydroaminoalkylation

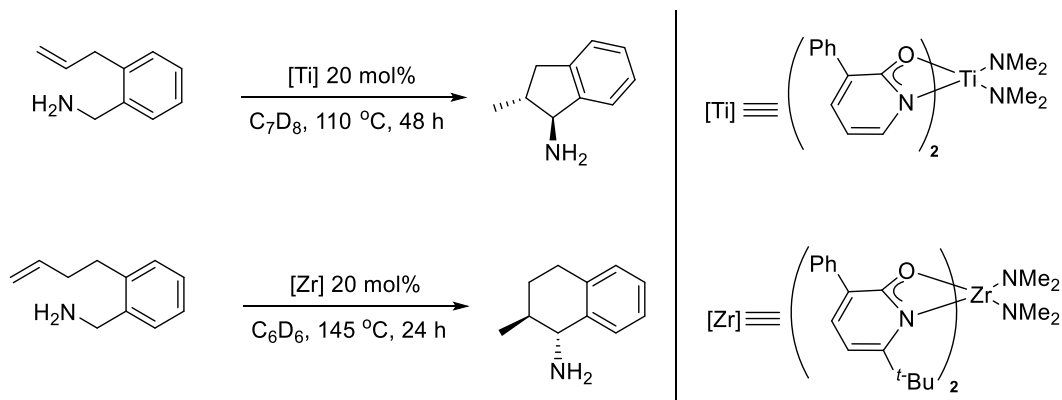
Ligand design has led to continuously improved diastereo- and enantioselectivity ratios. The regioselectivity in early transition metal catalyzed hydroaminoalkylation preferentially delivers the branched products, with scandium and titanium showing some promise for accessing linear products. The groups of Hou^{145, 146} and Doye,^{137, 138} which have employed scandium and titanium respectively, have shown that the linear products are obtained by using sterically bulky vinylsilanes and styrenes, respectively. Therefore, it is substrate controlled regioselectivity. In the case of scandium catalyzed hydroaminoalkylation complementary computational studies support that the regioselectivity outcome is due to electronics.¹⁴⁵

Exclusivity for the generation of the linear product has also been reported with late transition metals, such as ruthenium^{157, 158} and iridium.^{159, 160} These metals have been shown to achieve this via pyridyl directed C-H activation. A unified catalytic system, comprising cobalt and iridium, has been reported for the hydroaminoalkylation of conjugated dienes with a preference for the linear products in the case of terminal alkenes.¹⁶¹

For almost all literature examples of catalytic hydroaminoalkylation, the typical substrates engaged in the transformation include most often secondary amines.^{136, 137} Recent work on scandium catalyzed hydroaminoalkylation showed the utilization of tertiary amines in the reaction, too.¹⁴⁶ To date intermolecular hydroaminoalkylation with primary amines as substrates is unknown.

3.4 Catalyzed hydroaminoalkylation with primary amines as substrates

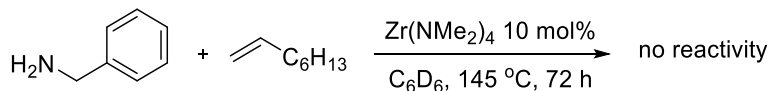
There is literature precedent on the intramolecular titanium¹⁶² and zirconium¹⁴⁷ catalyzed hydroaminoalkylation with primary amines by the Schafer group (Scheme 3.5). Using an aminoalkene substrate, both titanium and zirconium bis-pyridonate complexes were generated to catalyze hydroaminoalkylation, leading to the branched cyclic amines exclusively with a cis/trans ratio of 1:3 (only trans shown).



Scheme 3.5 Intramolecular zirconium catalyzed hydroaminoalkylation of alkenes with primary amines

With this precedent work on the intramolecular hydroaminoalkylation with primary amines, we questioned whether the intermolecular variant would be viable, using a zirconium-based catalyst. The primary α -arylated benzylamine and 1-octene were reacted in the presence of catalytic amounts of $Zr(NMe_2)_4$ with the goal to install the alkyl substituent at the α -position but no reactivity was observed (Scheme 3.6). Moreover, previous efforts in the Schafer group suggest

that neither tantalum or titanium can deliver the intermolecular hydroaminoalkylation product with primary unprotected amines. This is attributed to the two different mechanisms proposed for the intra- and intermolecular early transition metal catalyzed hydroaminoalkylation. The active catalytic species is a bridging imido species in the intramolecular variant¹⁴⁷ while in the intermolecular variant it is a metallaziridine.^{142, 144, 163}



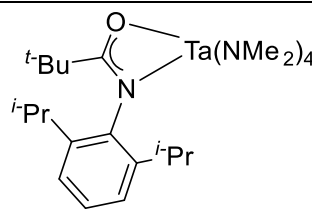
Scheme 3.6 Attempted intermolecular zirconium catalyzed hydroaminoalkylation of alkenes with primary amines

3.5 Catalyzed hydroaminoalkylation with protected *N*-TMS amines as substrates

N-Silylated amines have been used by Buchwald for the stoichiometric zirconium mediated Csp³-Csp² coupling with alkynes to deliver primary allylamines (Scheme 3.3).¹⁴⁰ This inspiring work by Buchwald served as a platform to develop a catalytic variant of this transformation. Moreover, the *N*-TMS amines were shown to be compatible catalysis substrates in the titanium catalyzed hydroamination.⁵⁰ Although secondary amines, they serve as primary amine surrogates and are easily deprotected. To date, there are no reports with *N*-TMS amines as substrates in the catalytic hydroaminoalkylation and as secondary amines as they are, they were firstly subjected to established tantalum¹³⁶ and titanium^{137, 138} hydroaminoalkylation. The results obtained (summarized in Table 3.1) suggest there is no reactivity with tantalum and titanium delivered the product in only low yield. For the catalyst screening, both homoleptic complexes Ta(NMe₂)₅ (Entry 1, Table 3.1) and Ti(NMe₂)₄ (Entry 5, Table 3.1) were tested. Particularly for tantalum, three more complexes other than the homoleptic complex, were examined for their reactivity in hydroaminoalkylation. As shown in Table 3.1, amidate ligands (Entry 2, Table 3.1),

(trimethylsilyl)methyl- (Entry 3, Table 3.1) and halogen ligands (Entries 3&4, Table 3.1) are present around the metal center. Literature precedent on the development of those complexes suggests that all of the above ligands increase the electrophilicity on metal center and, thus, enhance reactivity.^{136, 164, 165} In all cases with tantalum, the reactions were fruitless.

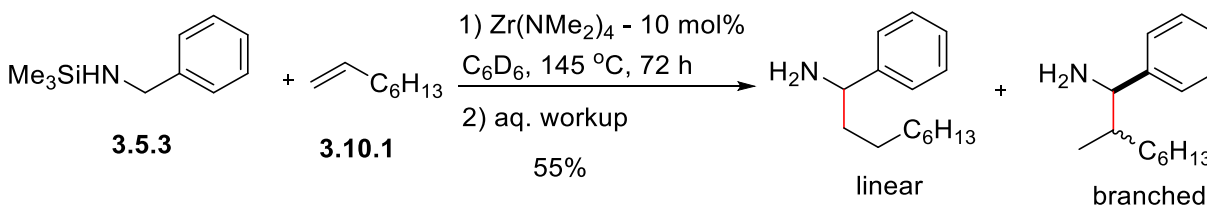
Table 3.1 Catalyst screening for the intermolecular hydroaminoalkylation with *N*-TMS amines

| Entry | Catalyst ¹ | Temp °C | Solvent | Time (h) | Yield (%) |
|-------|---|-----------|-------------------------------|----------|-----------|
| 1 | Ta(NMe ₂) ₅ | up to 160 | C ₇ D ₈ | up to 96 | - |
| 2 |  | 130 | C ₇ D ₈ | up to 96 | - |
| 3 | Ta(CH ₂ SiMe ₃) ₃ Cl ₂ | 130 | C ₇ D ₈ | up to 96 | - |
| 4 | [Ta(NMe ₂) ₃ Cl ₂] ₂ | 130 | C ₇ D ₈ | up to 96 | - |
| 5 | Ti(NMe ₂) ₄ | 145 | C ₆ D ₆ | 72 | 28 |
| 6 | Zr(NMe ₂) ₄ | 145 | C ₆ D ₆ | 72 | 55 |

¹For homoleptic complexes: 10% of catalyst loading; for non-homoleptic complexes: 5% of catalyst loading.

This data, along with the known intramolecular zirconium catalyzed hydroaminoalkylation of primary amines, shifted our focus to zirconium. Moreover, the TMS group is large and zirconium may accommodate the steric bulk better than titanium. The hydroaminoalkylation product obtained with the use of the homoleptic Zr(NMe₂)₄ (Table 3.1, Entry 6) was higher yielding as compared to the corresponding titanium complex Ti(NMe₂)₄. This suggests that the higher covalent radius of zirconium can better accommodate the sterically demanding *N*-silyl group appended to the nitrogen of the amine.¹⁶⁶ Thus, zirconium catalyzed hydroaminoalkylation for the synthesis of primary amines was targeted. The reaction scheme is presented in Scheme

3.7 and the catalyst screening is summarized in Table 3.1. *N*-TMS benzylamine **3.5.3** was used as the amine substrate and 1-octene **3.10.1** as the alkene.



Scheme 3.7 Zirconium catalyzed hydroaminoalkylation of alkenes with *N*-TMS amines as substrates

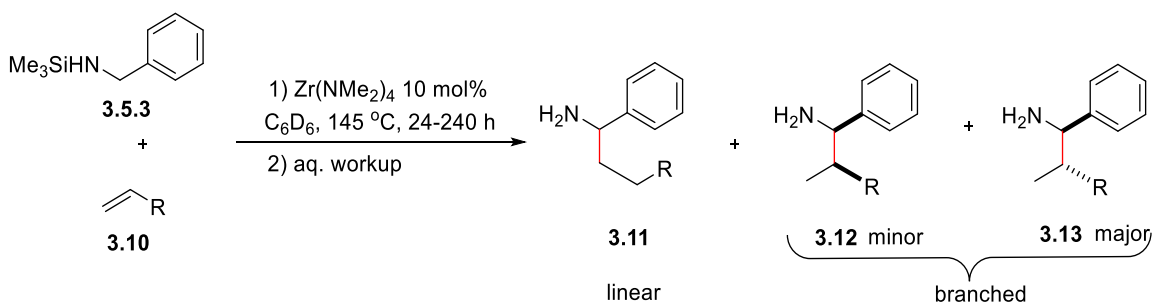
This chapter will present the development of the zirconium catalyzed hydroaminoalkylation of alkenes with *N*-TMS amines as substrates.

3.6 Zirconium catalyzed hydroaminoalkylation with protected *N*-TMS amines as substrates: a promise to access primary amines with linear regioselectivity

As shown in Scheme 3.7, the reaction between *N*-silylated benzylamine **3.5.3** and 1-octene **3.10.1** in the presence of the $\text{Zr}(\text{NMe}_2)_4$ led to a mixture of regioisomers; both the linear and the branched products were obtained. To identify the effect of the alkene substituents on the regioselectivity of the reaction, the alkene scope was tested in combination with *N*-TMS benzylamine **3.5.1** (Table 3.2). The general reaction scheme is shown in Scheme 3.8, where all three products are shown; one linear **3.11** and two diastereoisomeric branched products **3.12** (minor) and **3.13** (major) (Scheme 3.8). As shown in Scheme 3.8, the products were obtained as primary amines due to the facile Si-N hydrolytic cleavage upon aqueous workup.

Given the data presented in Table 3.2, a series of alkenes were employed in the zirconium catalyzed hydroaminolkylation of *N*-silylated benzylamines (Table 3.2). Results demonstrate the favored formation of the branched product when the steric congestion is away from the reacting site (**3.10.1-3.10.5**, Table 3.2), with the regioselectivity ratio (RR) ranging from 1:3 to 1:2 (linear:branched). For vinylcyclohexane **3.10.6** and vinylcyclohexene **3.10.7**, there is inversion in

the regioselectivity and this time the linear product is favorably formed. The RR for the resulting products is 3:1 linear:branched. The difference observed for the cyclohexane and cyclohexene derivatives lies in the DR; it is 3:1 for products **3.13.6:3.12.6** and 1:1 for products **3.13.7:3.12.7**. The equal ratio of the diastereomers observed in the latter case rendered the characterization of the mixture of the products challenging. For these three products (**3.11.7**, **3.12.7** and **3.13.7**) only indicative peaks of the benzylic signals in the ^1H NMR and ^{13}C NMR spectra are reported.



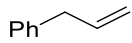
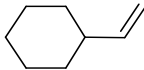
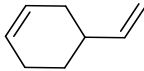
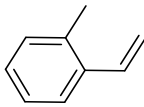
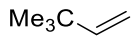
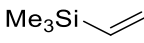
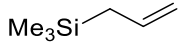
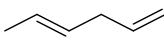
Scheme 3.8 Zirconium catalyzed hydroaminoalkylation - alkene scope – general reaction scheme

Table 3.2 Zirconium catalyzed hydroaminoalkylation - alkene scope – list of alkenes

| Alkene | Structure | Time (h) | Yield (%) ^a (3.11+3.12+3.13) | RR ^b [3.11:(3.12+3.13)] | DR ^b 3.13:3.12 |
|---------------|---------------------------|----------|--|---------------------------------------|------------------------------|
| 3.10.1 | C_6H_{13} | 72 | 55 | 1:2 | 3:1 |
| 3.10.2 | Ph | 48 | 78 | 1:3 | 3:1 |
| 3.10.3 | TBSO | 48 | 74 | 1:2 | 3:1 |
| 3.10.4 | TBSO | 72 | 51 | 1:3 | 3:1 |

Table 3.2 cont'd on page 65

Table 3.2 cont'd from page 64

| | | | | | |
|----------------|---|-----|----|------|-----|
| 3.10.5 |  | 72 | 82 | 1:2 | 3:1 |
| 3.10.6 |  | 72 | 66 | 3:1 | 3:1 |
| 3.10.7 |  | 72 | 64 | 3:1 | 1:1 |
| 3.10.8 |  | 48 | 56 | 17:1 | 7:1 |
| 3.10.9 |  | 240 | 47 | 99:1 | - |
| 3.10.10 |  | 24 | 52 | 99:1 | - |
| 3.10.11 |  | 24 | 58 | 99:1 | - |
| 3.10.12 |  | 240 | 68 | 1:7 | 3:1 |
| 3.10.13 |  | 72 | - | - | - |

^a Isolated yields of mixtures of regio- and diastereoisomers. ^b Regio- and diastereoselectivity ratios have been calculated based on the ¹H NMR spectra of the isolated mixtures of regio- and diastereoisomers.

As the steric congestion approaches the reacting site (double bond) to a greater degree as it happens for the case of 2-methylstyrene **3.10.8**, then the linear product **3.11.8** is formed with almost excellent regioselectivity (17:1 = linear:branched). Except for the branched product

derived from 4-vinylcyclohexene **3.10.7** and 2-methylstyrene **3.10.8**, in all cases the diastereoselectivity ratio (DR) of the branched product is 3:1, while for the exempted alkenes the diastereoselectivity of the product is 1:1 (**3.13.7:3.12.7**) and 7:1 (**3.13.8:3.12.8**).

3,3-Dimethylbutene **3.10.9**, trimethylvinylsilane **3.10.10** and dimethylphenylsilane **3.10.11** – also alkenes possessing the steric bulk on the 2nd position as 2-methylstyrene **3.10.8** – afforded exclusively the linear products **3.11.9**, **3.11.10** and **3.11.11**, respectively. Comparison among the reaction times for the three latter alkenes suggests when the alkyl group at the 2nd position of the alkene is replaced with a silyl group then the reactivity increases significantly, highlighting the importance of the electronic effect derived from silicon (β -silicon effect).¹⁶⁷ It is noteworthy to mention that allyltrimethylsilane **3.10.12**, which is just the next homolog of vinyltrimethylsilane **3.10.10**, afforded the product with almost the opposite regioselectivity (1:7 linear:branched) and 3:1 (**3.13.12:3.12.12**) is the diastereoselectivity ratio for the branched product. Diene **3.10.13** was reacted with *N*-TMS amine **3.5.3** and reactivity was observed only with the terminal alkene. To eliminate any doubts for the reactivity with the internal alkene, an internal alkene such as 3-hexene was tested for its reactivity and none was observed. Despite the fact that reactivity was observed with diene **3.10.13**, the isolation of the resulting products **3.11.13-3.13.13** proved to be challenging.

The regio- and diastereoselectivity ratios were calculated based on the relative integrations of the benzylic protons of the products. In Figure 3.2, linear product **3.10.10** is shown and indicative for its exclusive formation is the triplet at 3.84 ppm due to the coupling of the benzylic proton with the two neighbouring methylene protons. For the case of a mixture of regio- and diastereomers, as is the **3.11.12**, **3.12.12** and **3.13.12**, three diagnostic peaks emerge in the region where the benzylic signals are expected to resonate. For the two branched diastereoisomeric products, two

doublets are observed due to the coupling of the benzylic protons with their neighbouring methyne protons (Figure 3.2). Additionally, signals in the aliphatic region in both the ^1H and ^{13}C NMR spectra are attributable to either the linear or the two branched products and support their formation more evidently.

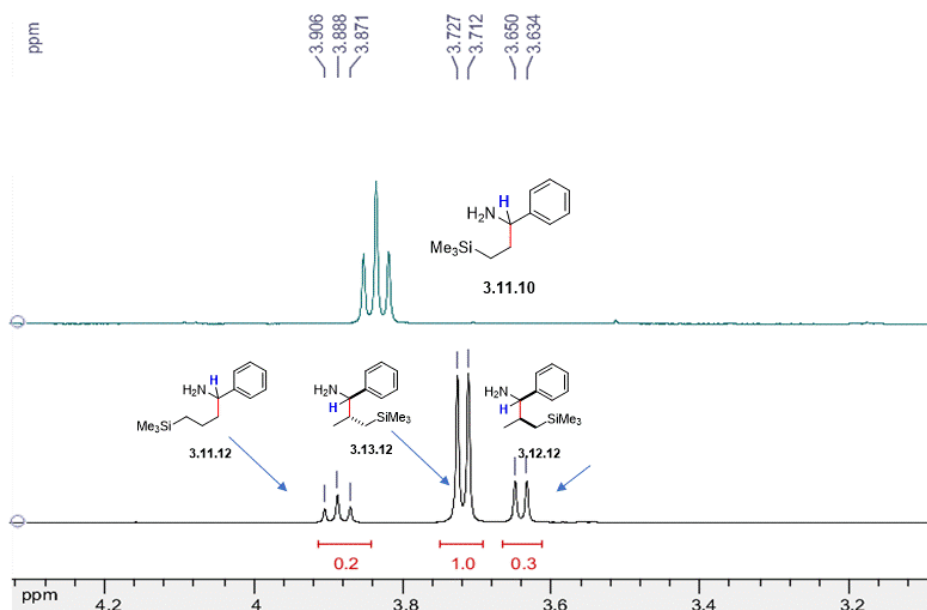
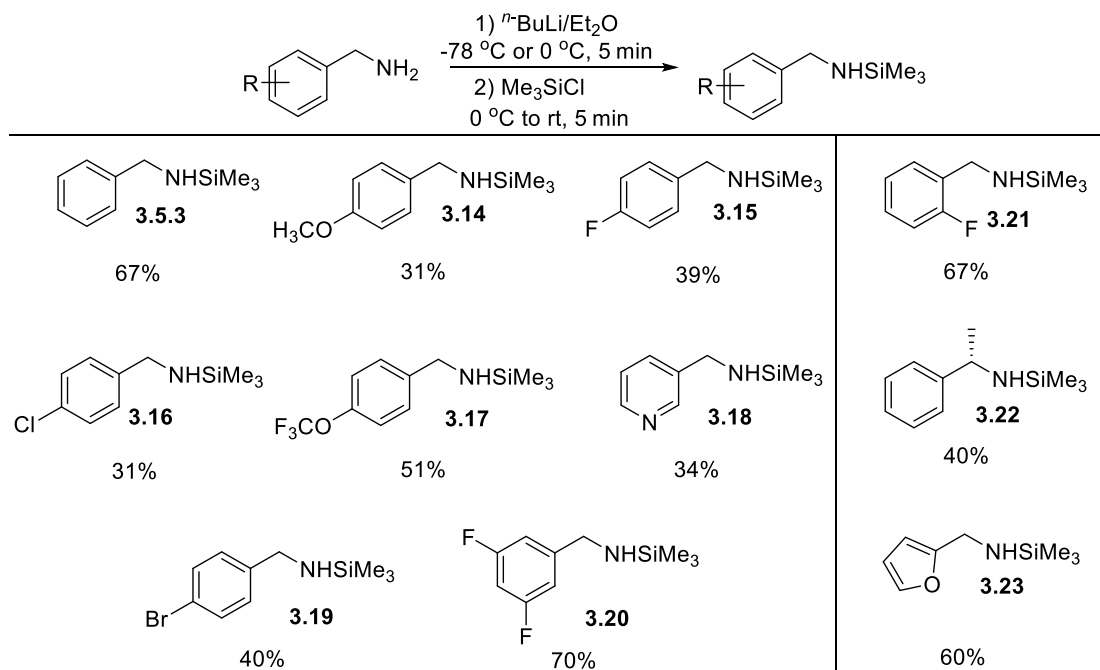


Figure 3.2 Diagnostic ^1H NMR benzylic signals for single regioisomers (3.11.10) and mixture of regio- and diastereomers (3.11.12, 3.12.12 and 3.13.12)

This data renders the $\text{Zr}(\text{NMe}_2)_4$ catalyzed hydroaminolakylation of alkenes as the first early transition metal catalyzed α -alkylation of amines to exclusively deliver linear products, a trend observed only with late transition metals to date. It is necessary to mention that this is substrate controlled regioselectivity; the linear product is exclusively obtained only in the cases of a bulky substituent on the 2nd position of the alkene (trimethylsilyl, phenyldimethylsilyl and tertbutyl).

We then developed the amine scope in which the alkene of choice was vinyltrimethylsilane **3.10.10**. For the amine scope, a series of *N*-TMS (**3.14-3.23**) amines were synthesized from the corresponding primary amines and isolated prior to their subsection to catalysis (Scheme 3.9).¹⁶⁸

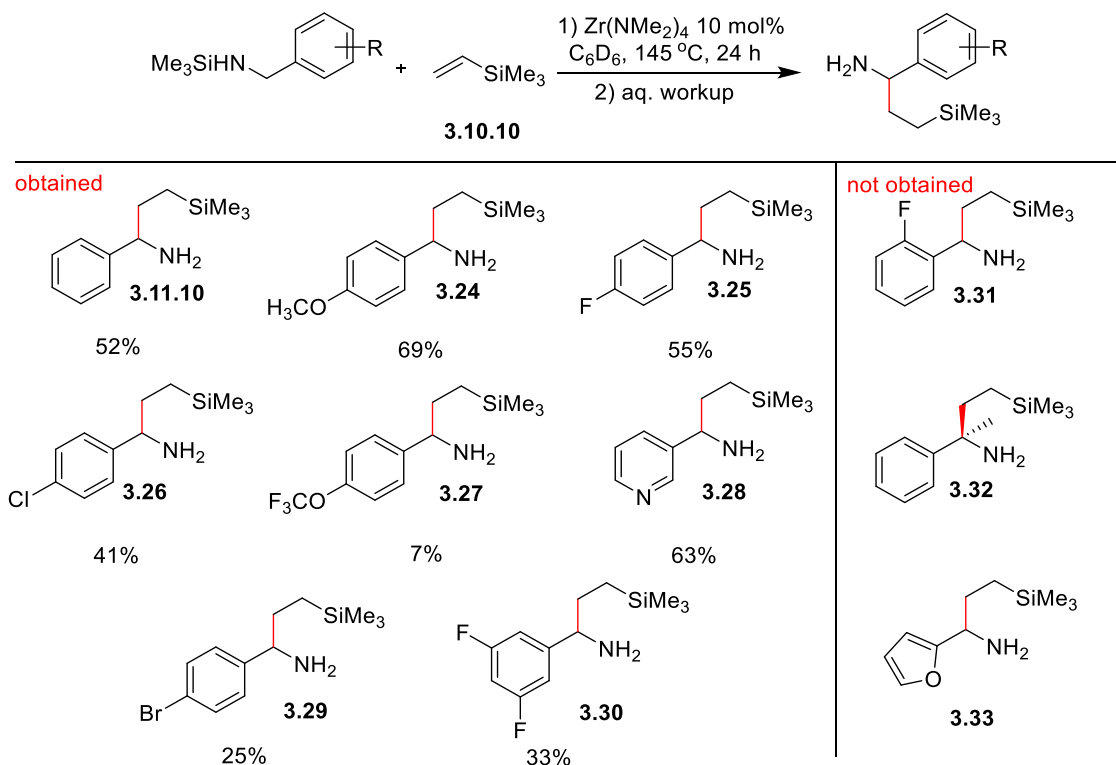


Scheme 3.9 *N*-silylation of benzylamines; reported amines in the literature: **3.5.3**,¹⁶⁸ **3.14**,¹⁶⁹ **3.15**⁸

The isolated *N*-silylated amines **3.5.3**, **3.14-3.23** were subjected to the $\text{Zr}(\text{NMe}_2)_4$ catalyzed hydroaminolactylation (Scheme 3.10). Para- and meta-substituted *N*-TMS amines possessing either EDG and EWG were well tolerated in the transformation (Scheme 3.10). For the para-trifluoromethoxy benzylamine **3.17** the yield of the product **3.27** was low, presumably due to insertion of zirconium into CF bond.^{170, 171} For the *N*-silylated-3-aminomethylpyridine **3.18** the catalyst loading was increased to 20 mol% to allow for the reaction to reach completion. This increase in catalyst loading is attributable to possible coordination of the pyridine nitrogen of the starting amine to zirconium.¹⁷²

Reactivity was not observed for *N*-silylated-2-furfurylamine **3.23** with the *N,O*-chelation to zirconium being the suggested explanation. Striking evidence for this suggestion has been the development of *N,O*-chelated tantalum,¹³⁶ titanium¹⁶² and zirconium¹⁴⁷ catalysts, derived from the coordination of amide ligands to early transition-based metal complexes in the Schafer group.

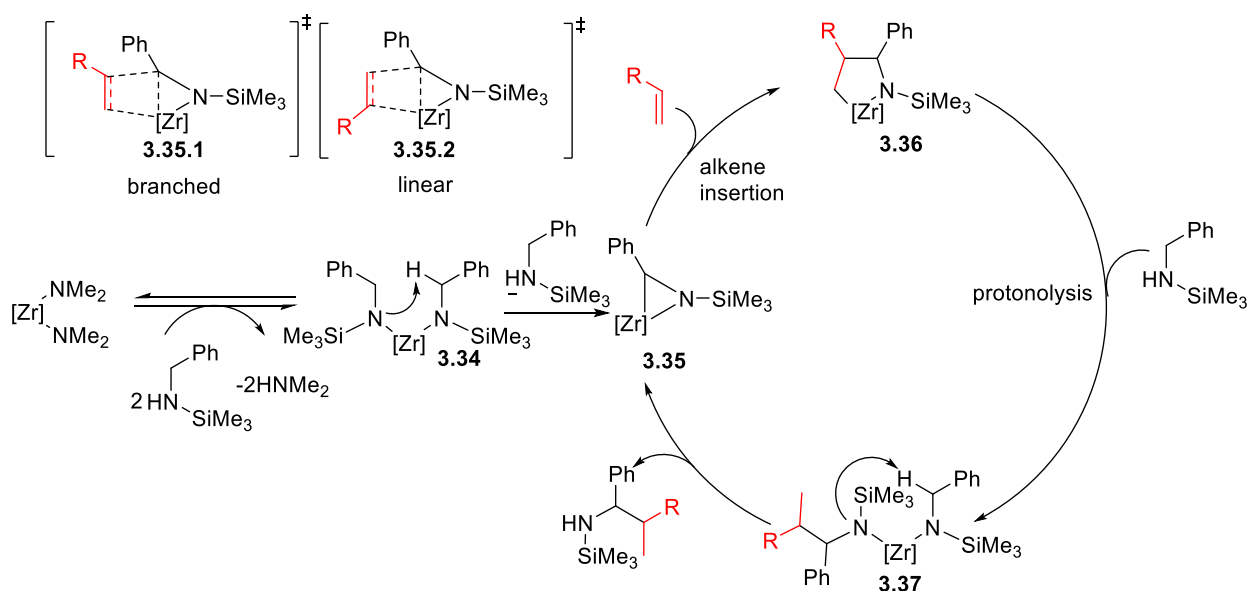
Other amines such as the 2-fluoro-*N*-silylbenzylamine **3.21** and (*S*)-1-phenyl-*N*-silylbenzylamine **3.22**, with the latter being a candidate substrate to allow for the installation of a quaternary center, did not deliver any primary amine products. The absence of the reactivity for these two latter cases fortifies the hypothesis that sterics plays an important role in the $\text{Zr}(\text{NMe}_2)_4$ hydroaminoalkylation.



Scheme 3.10 Zirconium catalyzed hydroaminoalkylation - amine scope

To rationalize the observation that the linear product is exclusively obtained in the presence of sterically bulky vinylsilanes, the proposed mechanism for the transformation is presented in Scheme 3.11.^{136, 140, 142, 144} First, the amido ligands of the starting $\text{Zr}(\text{NMe}_2)_4$ are replaced by the *N*-silylamido groups of the starting *N*-silylbenzylamine to afford complex **3.34**, which upon hydrogen abstraction leads to zirconaziridine **3.35**. What follows is the alkene insertion into the

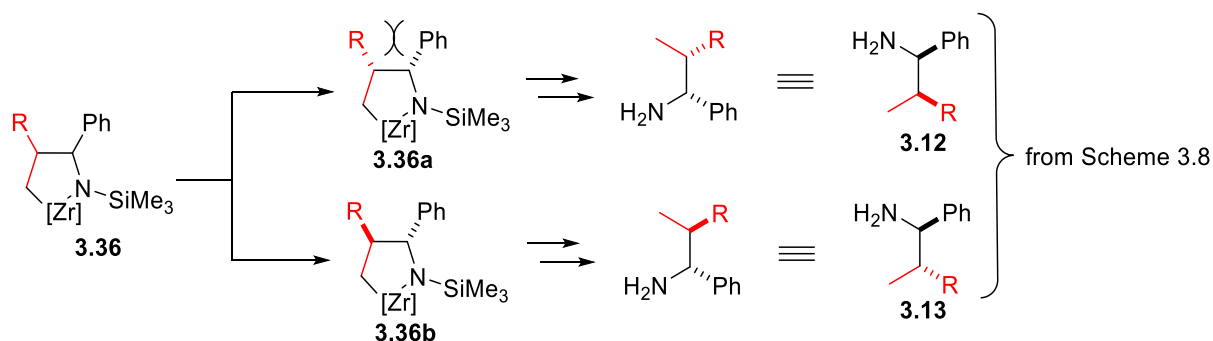
zirconaziridine **3.35** to afford zirconapyrrolidine **3.36**. Depending on the steric bulk of the alkene upon the insertion, there are two possible orientations – **3.35.1** and **3.35.2** – which determine the outcome of the regioselectivity of the hydroaminoalkylation. If the R substituent of the alkene is oriented away from the metal centre then the branched product is obtained, and if close to zirconium then the linear product is obtained. The zirconapyrrolidine intermediate **3.36** undergoes protonolysis to afford complex **3.37**, which upon hydrogen abstraction leads to the liberation of the hydroaminoalkylated alkene and the regeneration of the zirconaziridine **3.35**.



Scheme 3.11 Proposed mechanism for the zirconium catalyzed hydroaminoalkylation of alkenes with *N*-silylamines

The orientation with which the alkene inserts in the zirconaziridine **3.35** defines the regioselectivity of the reaction (Scheme 3.11). Upon alkene insertion the preferential orientation of the substituents R and Ph in the zirconapyrrolidine **3.36** is what defines the diastereoselectivity of the reaction (Scheme 3.12). It has been suggested in previous work¹⁷³ that steric repulsion is maximized in the case of syn configuration **3.36a**. Therefore substituents preferentially adopt the anti configuration **3.36b** which leads to product **3.13** (Scheme 3.8).

Based on this, we suggest that the minor branched diastereomer is **3.12** and the major is **3.13** (Scheme 3.12).

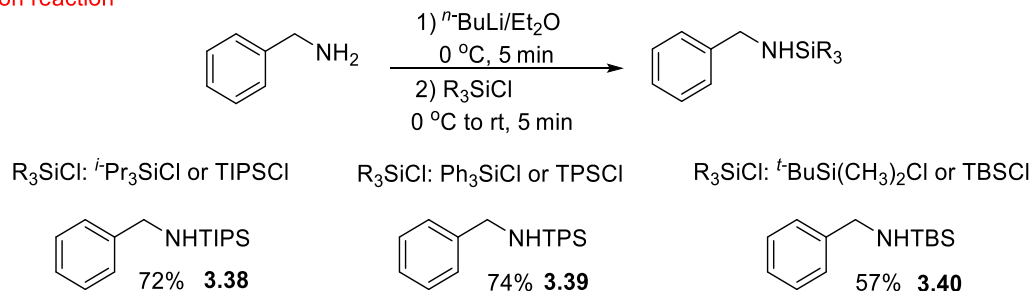


Scheme 3.12 Rationale for the proposed assignment of diastereomers **3.12** and **3.13**

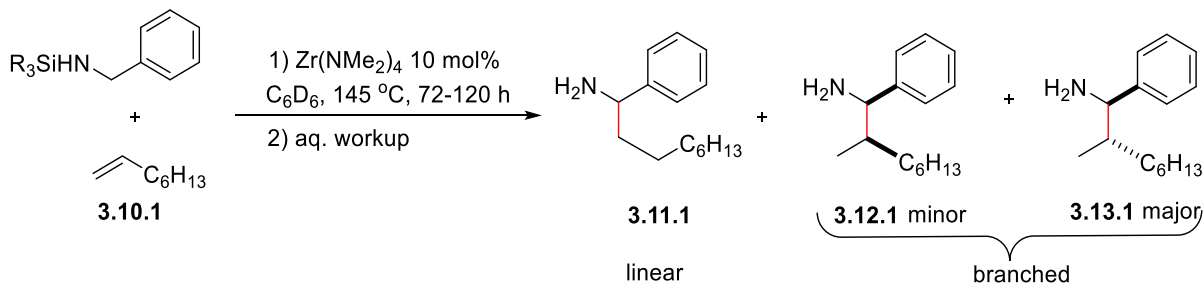
To this point, it was discussed and rationalized *via* the proposed catalytic cycle (Scheme 3.11) how the steric bulk at the 2nd position of the alkene can impact the outcome of the regioselectivity of the transformation, allowing for substrate controlled regioselectivity. The sequence of addition of the reactants in the hydroaminoalkylation reaction is: first the Zr(NMe₂)₄, second the amine and third the alkene. The question is whether the regioselectivity can be tuned *via* the amine substrate and particularly *via* the introduction of bulkier silicon substituents on the nitrogen of the amine. As steric bulk increases, it is expected that upon alkene insertion into the zirconaziridine **3.35**, the steric bulk on the nitrogen will push the phenyl ring of the benzylamine closer to the insertion site. As such, the R group of the alkene will be forced to orient itself away from the phenyl ring and closer to zirconium (orientation **3.35.2** is expected to be favored over **3.35.1**), an orientation which would ultimately lead to the linear product (Scheme 3.11).

To test this hypothesis, three more *N*-silylamines were generated: *N*-TIPS- **3.38**, *N*-TPS- **3.39** and *N*-TBS-amine **3.40** (Scheme 3.13.) These amines were then subjected to the developed catalytic hydroaminoalkylation protocol with 1-octene (Scheme 3.13).

N-silylation reaction



Hydroaminoalkylation reaction



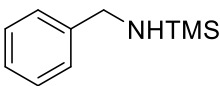
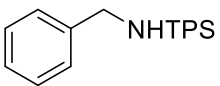
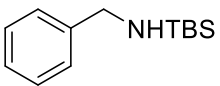
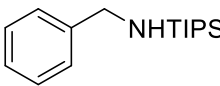
Scheme 3.13 Synthesis of *N*-TIPS-amine **3.38**, *N*-TPS-amine **3.39** and *N*-TBS-amine **3.40** (top) and hydroaminoalkylation reaction with 1-octene (bottom)

These amines were chosen based on the A-values available in literature; the A-value for the *N*-TMS group is 1.21 kcal/mol¹⁷⁴ and no data has been reported for amines **3.38-3.40**. However, there are A-values for the -OTMS (0.74 kcal/mol,¹⁷⁵ 1.31 kcal/mol,^{176, 177} 0.80 kcal/mol¹⁷⁴), -OTBS (1.06 kcal/mol),^{176, 177} -OTIPS (0.51 kcal/mol,¹⁷⁵ 0.94 kcal/mol^{176, 177}) and -OTPS (0.57 kcal/mol, 0.71 kcal/mol, 0.75 kcal/mol)¹⁷⁴ groups. From those values, the only safe comparison which can be made is that -OTBS > -OTPS, and it is hypothesized that similar trends would be observed for the *N*-silylamines.

The results for the regioselectivity and the diastereoselectivity of the reaction are summarized in Table 3.3. According to the data obtained, there was no reactivity observed with the *N*-TIPS-amine **3.38**, suggesting either inability to bind to zirconium at the beginning of the cycle or that the alkyl bulk on the silicon is such that it did not allow for any alkene insertion at all. For the *N*-TPS-amine **3.39** two different workups were conducted for the isolation of the product. Aqueous

workup of the reaction involving the formation of hydrochloric salt of the amine rendered the isolation of the product challenging as the liberated silanol partitions between the organic and aqueous layers. Its presence was not an obstacle to determine the regio- and diastereoselectivity ratios by ^1H NMR, however, no actual isolatable yield could be reported. Thus, a different strategy was pursued involving the formation of the oxalic salt (instead of hydrochloric salt as in the first place). In this case, the oxalic salt was isolated as a solid (while the hydrochloric salt was formed in solution in the first place), and the amine was liberated from it again. The amine was separated from the silanol by column chromatography. The regio- and diastereoselectivity ratios obtained are the same; 1:1 RR for linear and branched and 2:1 DR for the branched product.

Table 3.3 Silicon substituent screening of the *N*-silylated amines for regioselectivity outcome

| Amine | Structure ¹ | RR (lin/bran) ² | DR ² | Time (h) | Yield ³ (%) |
|--------------|---|----------------------------|-----------------|----------|------------------------|
| 3.5.3 |  | 1:2 | 3:1 | 72 | 55 |
| 3.39 |  | 1:1 (1:1) | 2:1 (2:1) | 120 | 32 (-) |
| 3.40 |  | 2:1 (1:1) | 1.5:1 (2:1) | 72 | 37 (19) |
| 3.38 |  | - | - | 48 | - |

¹ Structure of the starting amine ^{2a} Product of the reaction shown in Scheme 3.13 ^{2b} Regio- and diastereoselectivity ratios have been calculated based on the ¹H NMR spectra of the isolated mixtures of regio- and diastereoisomers ³ Ratios and yields outside the bracket: oxalic salt workup; ratios and yields inside the bracket: hydrochloric salt workup

For the *N*-TBS amine **3.40**, there was observed inversion in the regioselectivity as compared to *N*-TMS amine **3.5.3**, with the linear product being the dominant product of the transformation, when the oxalic salt workup was conducted, while a 1:1 ratio of the two regioisomers was obtained when the workup including the hydrochloric salt formation was followed. For both *N*-TPS and *N*-TBS amines **3.39** and **3.40**, respectively, there was a shift toward the formation of the linear product when they were used as substrates in the transformation, with the *N*-TBS amine affording a mixture of linear:branched 2:1 instead of 1:1 (*N*-TPS amine) (Table 3.3). As for the diastereoselectivity ratios, there was a sacrifice in diastereoselectivity observed in the obtained hydroaminoalkylation product for both *N*-TPS- and *N*-TBS-amines **3.39** and **3.40** as compared to the *N*-TMS-amine **3.5.3**. Specifically the ratios were 2:1 instead of 3:1, respectively.

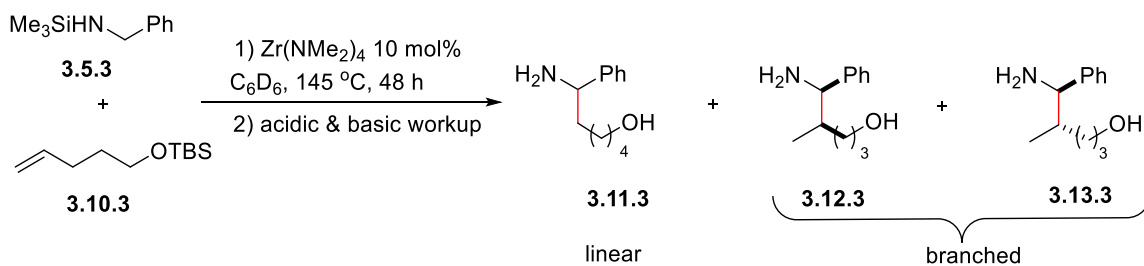
3.7 Efforts toward the synthesis of heterocycles via the zirconium catalyzed hydroaminoalkylation of alkenes with the use of *N*-TMS amines as substrates

The motif of an α -arylated amine is not as frequently encountered as other motifs (e.g., *N*-arylated amines), however, when it is found in pharmaceuticals, then it is in the form of a cyclic α -arylated amine.

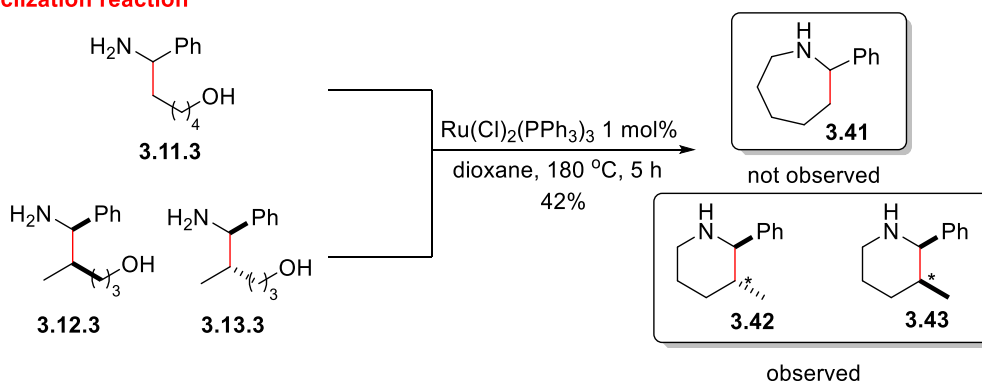
Inspired by the prevalence of the the cyclic motif, the cyclization of one of the hydroaminoalkylation products was pursued to access such an amine. The cyclization of aminoalcohols has received generous attention over the past decade,¹⁷⁸ with palladium,¹⁷⁹ iron¹⁸⁰,¹⁸¹ iridium,¹⁸² cobalt,¹⁸³ and manganese¹⁸⁴ being representative examples to catalyze the

transformation. A ruthenium complex – $\text{Ru}(\text{Cl})_2(\text{PPh}_3)_3$ – has been reported for the cyclization of aminoalcohols.^{185, 186} More specifically, the Watanabe¹⁸⁵ group used this complex for the intermolecular cyclization of both primary and secondary amines with alcohols and the Bartok¹⁸⁶ group followed to use the same complex for the intramolecular variant with the use of secondary amines as substrates. In our case we tested whether the intramolecular cyclization of primary amines with alcohols could take place in the presence of the above complex (Scheme 3.14). As shown in Scheme 3.14, the mixture of products **3.11.3**, **3.12.3** and **3.13.3** derived from the hydroaminoalkylation (branched and linear) was subjected to cyclization conditions with the use of the ruthenium complex. Expectedly, all three cyclization products **3.41**, **3.42** and **3.43** could be obtained.

Hydroaminoalkylation reaction



Cyclization reaction



Scheme 3.14 Intermolecular zirconium catalyzed hydroaminoalkylation (top) and intramolecular ruthenium catalyzed cyclization of aminoalcohols (bottom); reported amines in the literature: **3.42**,¹⁸⁷ **3.43**¹⁸⁷

Efforts to isolate the product(s) included both aqueous workup and column chromatography; however, in all cases, as well as observing the two branched diastereomers (two doublet peaks * in the aliphatic region, with the anti diastereomer **3.42** being the minor and **3.43** the major product), there was a third doublet implying presence of the starting benzylamine, precursor to the cyclized amine or unreduced imine. Suggestions to optimize the reaction efficiency include: to let the reaction proceed longer, increase the catalyst loading or use a different catalyst.

3.8 Conclusions

To summarize, we have developed the first intermolecular zirconium catalyzed hydroaminoalkylation resulting in the isolation of primary amines, with the use of *N*-TMS amines being of critical importance to their delivery. Results to date suggest that in the absence of steric bulk at the 2nd position of the alkene a mixture of regioisomers is obtained, while in the presence of bulky vinylsilanes or tertbutyl groups, the linear product is exclusively obtained. Notably, when allyltrimethylsilanes are employed the product with almost the opposite regioselectivity is obtained. The presence of a chirality center can induce diastereo- or even enantiospecificity. Moreover, electron donating substituents on the α to the silicon carbon atom have the potential to even further stabilize the α -anion effect. A corollary of this is to have a greater stabilization of the positive charge on the β to silicon carbon atom, and consequently facilitate even greater reactivity. Overall, this is the first example of an early-transition metal catalyzed α -alkylation of primary amines to exclusively afford the linear product, synchronously acknowledging it is a substrate controlled regioselectivity.

Motivated by this substrate controlled regioselectivity, the amine – and not the alkene – was tested as a substrate to selectively afford one of the two regioisomers. Particularly, a series of silicon substituents were introduced on the nitrogen of the starting benzylamine and the resulting

N-silylamines were subjected to catalytic hydroaminoalkylation. From the results obtained, no exclusive selectivity toward any of the two regioisomers – linear or branched – was observed. In the context of amine controlled regioselectivity, other options could target ortho-substituted amines. One such example, 2-fluoro-*N*-silylated benzylamine, was already tested and did not successfully deliver the hydroaminoalkylation product. Other ortho-substituted benzylamines, with non-halogenated substituents, can be considered. Such substituents could include alkyl groups; the less polar the Csp²-X bond is, the smaller the likelihood for zirconium insertion in the bond would be.

To put this developed technology in the context of application, aminoalcohols obtained *via* the hydroaminoalkylation reaction were subsequently subjected to a cyclization reaction to afford α -arylated amines. Conditions for this cyclization require further optimization for the successful generation of the target amines.

The experimental for Chapter 3 starts on page 127.

Chapter 4: *N*-alkyl- and *N*-arylamines as substrates in zirconium catalyzed hydroaminoaminoalkylation to access secondary α -arylated amines

4.1 Introduction

Inspired by the development of the zirconium catalyzed hydroaminoalkylation of alkenes with *N*-TMS-amines, we investigated the expansion of the method development toward the synthesis of secondary *N*-alkyl- and *N*-arylamines. In Chapter 4, the generic structure of the target α -arylated amines will be of the type of **4.1** (Figure 4.1); secondary α -arylated amines. Secondary and tertiary α -arylated amines are more frequently met in both pharmaceuticals and natural products as compared to their primary counterparts. As shown in Figure 4.1, nicotine derivatives and synthetic drugs bear the motif of an α -arylated *N*-heterocycle.

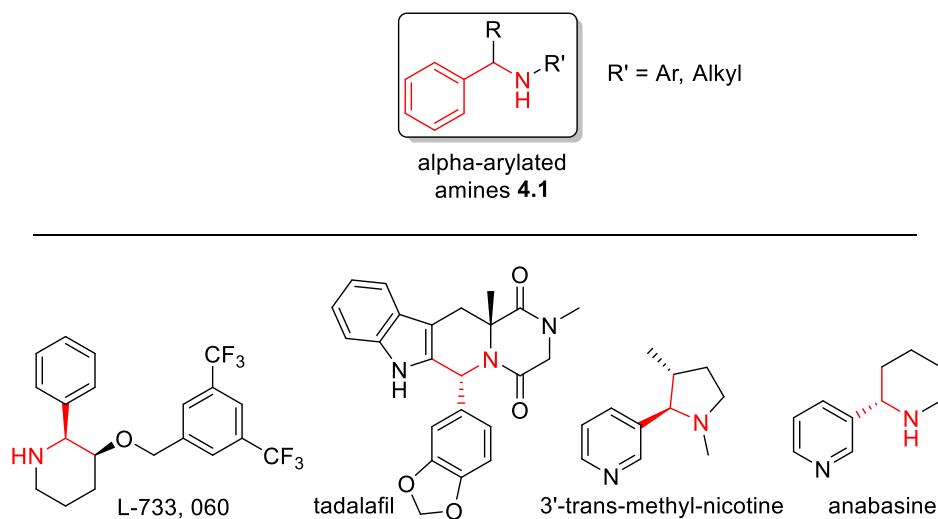
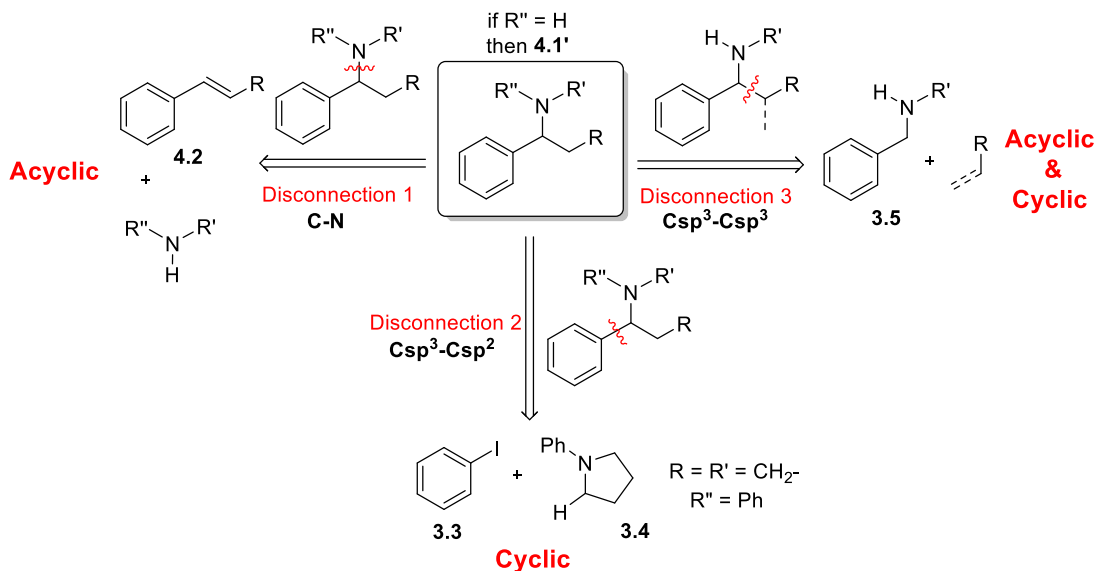


Figure 4.1 Secondary α -arylated amine motif present in pharmaceuticals/natural products

4.2 Overview of α -arylated amine synthesis

Following the same flow as in Chapter 3 (Scheme 3.1), there are three logical disconnections to access secondary α -arylated amines (Scheme 4.1). For disconnection 1 which represents the transform for the C-N bond formation, stoichiometric examples include the Petasis reaction (a

borono-Mannich type reaction) and the Eschweiler-Clarke reaction. These two reactions use secondary amines as substrates and, thus, they are used primarily for the preparation of tertiary amines. More recently, a catalytic example includes the copper catalyzed hydroamination of styrenes of type **4.2** (Scheme 4.1).¹⁸⁸ Metal-free catalytic reactions have also been reported, including the acid catalyzed hydroamination of styrenes with aromatic amines.¹⁸⁹ Disconnection 2 pertains to the Csp³-Csp² bond scission and the catalytic examples were thoroughly discussed in Chapter 3. One of the limitations of this cross-coupling synthetic approach is the use of precious metals for these catalytic transformations. For non-catalytic transformations, such as the addition of a phenyl lithium onto the electrophilic carbon of an imine,^{190, 191} the use of stoichiometric reagents and, thus, the generation of byproducts poses a limitation for considering the transformation as a preferred route to access our target structures.



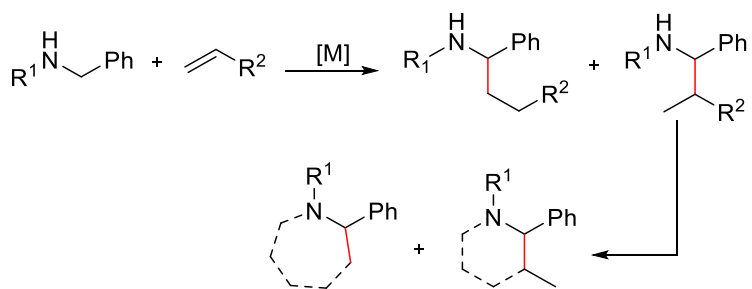
Scheme 4.1 Possible disconnections to access secondary and tertiary α -arylated amines using catalysts

The synthons for disconnection 3 are an *N*-substituted benzylamine **3.5** and the incoming substituent R. The stoichiometric matching reactions can be a nucleophilic addition of an alkyl-

lithium onto an imine¹³⁹ or a catalytic variant is the hydroaminoalkylation of alkenes with secondary amines. This is a Csp³-Csp³ bond forming approach and is the focus of this chapter.

4.3 Early transition metal catalyzed hydroaminoalkylation: a conscious choice for secondary α -arylated amines

As illustrated in Scheme 4.2 the asset of disconnection 3 is the flexibility offered to access acyclic amines that can be further reacted to give *N*-heterocycles. In the case of the catalytic variants, the cost factor of the metal catalysts sets limitations for considering their use in transformations.

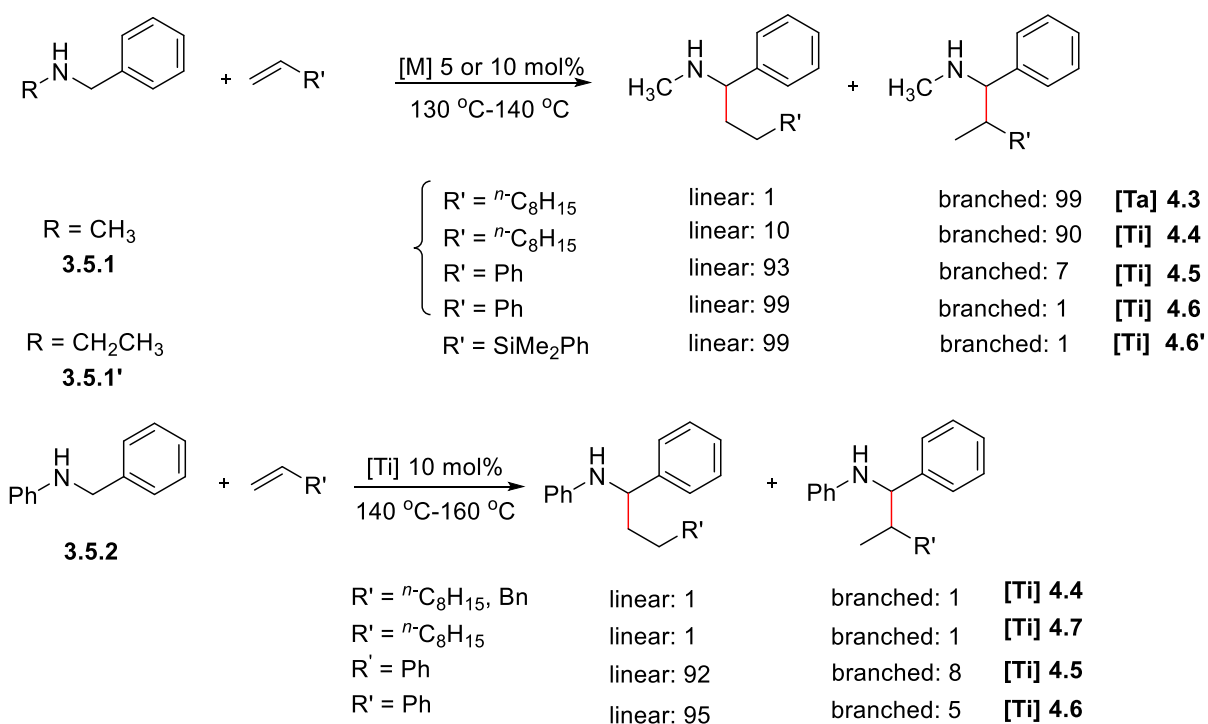
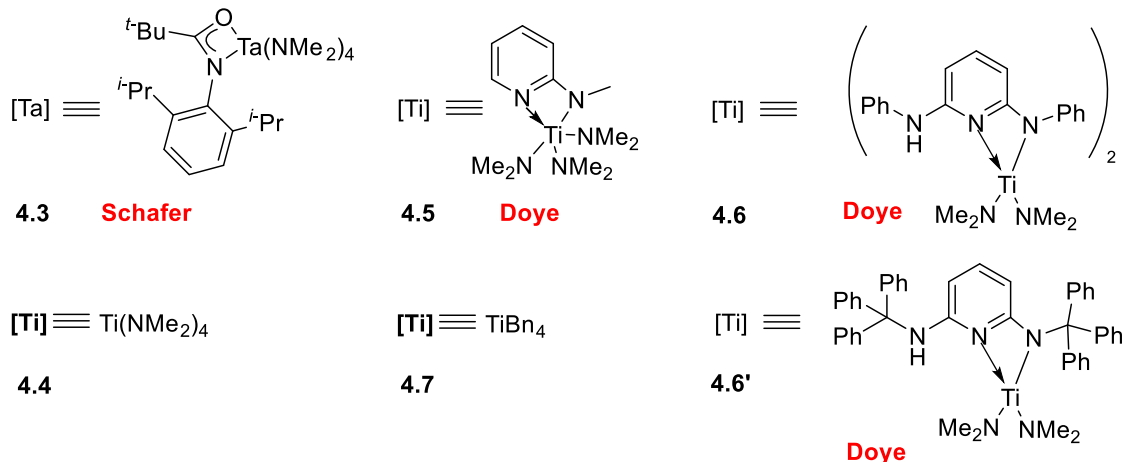


Scheme 4.2 Hydroaminoalkylation: flexibility to access both cyclic and acyclic amines

There are only six reported complexes to have catalyzed the installation of an α -arylated amine using a benzylated amine starting material (Scheme 4.3). The Schafer group reported the tantalum catalyzed hydroaminoalkylation of *N*-methylbenzylamine **3.5.1** and the Doye group has presented the titanium catalyzed hydroaminoalkylation of *N*-methylbenzylamine **3.5.1**, *N*-ethylbenzylamine **3.5.1'** and *N*-phenylbenzylamine **3.5.2** with the use of five different titanium complexes (Scheme 4.3). For *N*-methylbenzylamine **3.5.1** the tantalum complex **4.3** shown in Scheme 4.3 delivered exclusively the branched product with an excellent diastereoselectivity of 20:1¹³⁶ while $Ti(NMe_2)_4$ **4.4** afforded a mixture of linear:branched products in a ratio of 10:90, respectively.¹⁴⁸ It was only when bulky ligands were introduced on titanium (titanium complexes

4.5, 4.6 and 4.6')^{137, 138, 192} and the alkene substrate was changed to styrene that a dramatic shift toward the formation of the linear product was observed (Scheme 4.3).

Schafer - Ta & Doye - Ti



Scheme 4.3 Titanium and tantalum catalyzed hydroaminoalkylation of *N*-alkyl- and *N*-phenylbenzylamines

For *N*-phenylbenzylamine **3.5.2**, titanium complexes $\text{Ti}(\text{NMe}_2)_4$ ¹⁴⁸ **4.4** and TiBn_4 ¹⁹³ **4.7** afforded a mixture of linear:branched 1:1 products with 1-octene or allylbenzene. A maximum ratio of

linear:branched 95:5 products was achieved when the bulky titanium complex **4.6** was used as the precatalyst with the use of an activated alkene such as styrene.¹³⁸ All these results show that bulky ligands on the catalyst in combination with the use of activated alkenes can alter the regioselectivity of the reaction (Scheme 4.3).

Despite the fact there are metal complexes which deliver the linear and/or the branched product for *N*-methylbenzylamine **3.5.1**, there are no reports presenting the use of sterically demanding *N*-alkylamines as substrates for this transformation. Additionally, in the work by Doye where titanium complex **4.6** delivered the linear product with excellent regioselectivity (linear:branched 99:1),¹³⁸ the authors were not successful in isolating the desired product from the unreacted starting material. Therefore, although the linear product was exclusively formed, it could not be isolated as a pure product (Scheme 4.3). For *N*-ethylbenzylamine **3.5.1'**, the linear product was successfully obtained as a sole regioisomer and free of any starting material, with the use of dimethylphenylsilane and the bulky titanium complex **4.6'**.¹⁹² For *N*-aryl- α -arylated amines, no linear products have been obtained as single regioisomers; the best regioselectivity ratio observed to date is linear:branched 95:5 (Scheme 4.3).¹³⁸

In Chapter 3, the development of the zirconium catalyzed hydroaminoalkylation of alkenes with the sterically demanding benzylated *N*-TMS amines as substrates was presented. It was also shown that in the presence of the sterically demanding vinylsilane substrate, the linear product was obtained exclusively, consistent with substrate controlled regioselectivity for the reaction.

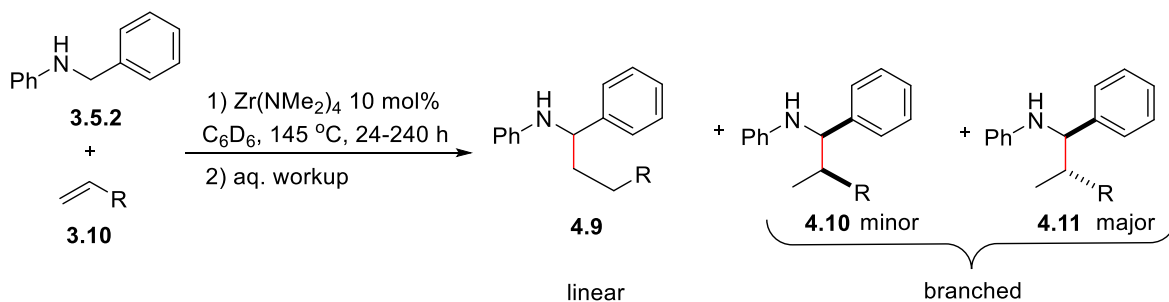
We questioned whether zirconium could be more suitable, as compared to tantalum and titanium, for the hydroaminoalkylation of the sterically demanding *N*-isopropylbenzylamine **4.8** and *N*-phenylbenzylamine **3.5.2**. This work explores enhanced substrate diversity as the former is a new substrate and the latter has been only reported for the hydroaminoalkylation of styrene and 1-

octene. This chapter will discuss the development of zirconium catalyzed hydroaminoalkylation of alkenes with *N*-isopropylbenzylamine **4.8** and *N*-phenylbenzylamine **3.5.2** as substrates. Effects of steric properties of the alkenes employed will be examined.

4.4 Zirconium catalyzed hydroaminoalkylation of alkenes with *N*-phenylbenzylamine and *N*-isopropylbenzylamine as substrates

In Scheme 4.4 the general reaction scheme of zirconium catalyzed hydroaminoalkylation is shown. Table 4.1 shows the series of alkenes used. As shown in Table 4.1, when the steric bulk of the alkene is removed from the double bond then a mixture of regioisomers is obtained, with the formation of the branched product being favored (alkenes **3.10.1**, **3.10.2** and **3.10.4**). When the silylated alcohol **3.10.3** and allylbenzene **3.10.5** were used, a shift toward the formation of the linear product was observed; however, a mixture of regioisomers was still obtained (linear:branched 1:2). A 1:1 regioselectivity ratio (RR) of linear and branched was obtained in the cases of vinylcyclohexane **3.10.6** and vinyl-4-cyclohexene **3.10.7**. The diastereoselectivity ratio (DR) of products (**4.11.6:4.10.6**) is 8:1 as opposed to the latter for which the ratio of products (**4.11.7:4.10.7**) is 1:1. This regio- and diastereoselectivity ratio of 1:1 for products **4.9.7**, **4.10.7** and **4.11.7** rendered the characterization of their mixture (Appendix A.4) challenging. Only certain signals in the benzylic area in both the ^1H and ^{13}C NMR were reported as indicative signals for their formation. As expected, the alkene possessing a bulky silyl group (alkene **3.10.10**) delivered only the linear product. Notably, when allyltrimethylsilane (alkene **3.10.12**) was used only the branched regioisomer was observed with a diastereoselectivity ratio of 4:1. Diene **3.10.13** was also tested and though reactivity was observed for the terminal alkene, as was the case with *N*-TMS amine **3.5.3**, the product isolation proved challenging.

The delivery of the linear product in the presence of the sterically bulky vinylsilanes shows the same trend observed for *N*-TMS amines in Chapter 3, reinforcing the proposed substrate controlled regioselectivity. Additionally, the tolerance of oxygen containing alkenes offers the opportunity for subsequent cyclization reactions.



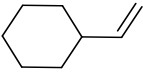
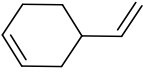
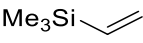
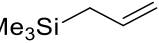
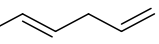
Scheme 4.4 Zirconium catalyzed hydroaminoalkylation of alkenes with *N*-phenylbenzylamine

Table 4.1 Zirconium catalyzed hydroaminoalkylation with *N*-phenylbenzylamine - alkene scope

| Alkene | Structure | Time (h) | Yield (%) ^a (4.9+4.10+4.11) | RR ^b [4.9:(4.10+4.11)] | DR ^b 4.11:4.10 |
|---------------|-----------|----------|---|--------------------------------------|------------------------------|
| 3.10.1 | | 48 | 78 | 1:5 | 6:1 |
| 3.10.2 | | 48 | 91 | 1:5 | 4:1 |
| 3.10.4 | | 72 | 84 | 1:3 | 7:1 |
| 3.10.3 | | 48 | 82 | 1:2 | 3:1 |
| 3.10.5 | | 48 | 93 | 1:2 | 4:1 |

Table 4.1 cont'd on page 85

Table 4.1 cont'd from page 84

| | | | | | |
|---------|---|-----|----|------|-----|
| 3.10.6 |  | 120 | 79 | 1:1 | 8:1 |
| 3.10.7 |  | 120 | 78 | 1:1 | 1:1 |
| 3.10.10 |  | 24 | 75 | 99:1 | - |
| 3.10.12 |  | 240 | 85 | 1:99 | 4:1 |
| 3.10.13 |  | 72 | - | - | - |

^a Isolated yields of mixtures of regio- and diastereoisomers. ^b Regio- and diastereoselectivity ratios have been calculated based on the ¹H NMR spectra of the isolated mixtures of regio- and diastereoisomers.

Notably, for both *N*-TMS- and *N*-phenylbenzylamines, the different regioisomers and diastereoisomers of the obtained products were clearly seen by the diagnostic splitting patterns of their benzylic protons in the 3.50-4.00 and 4.00-4.50 ppm, respectively; a triplet for the linear products and a doublet is present for each branched diastereomer (Figures 3.2 & 4.2).

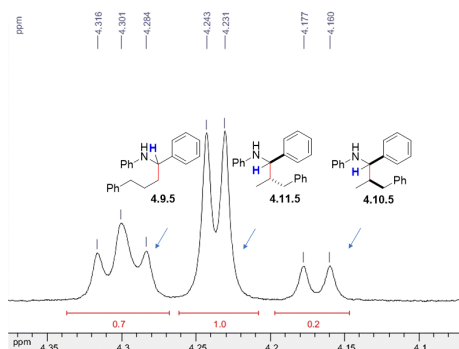
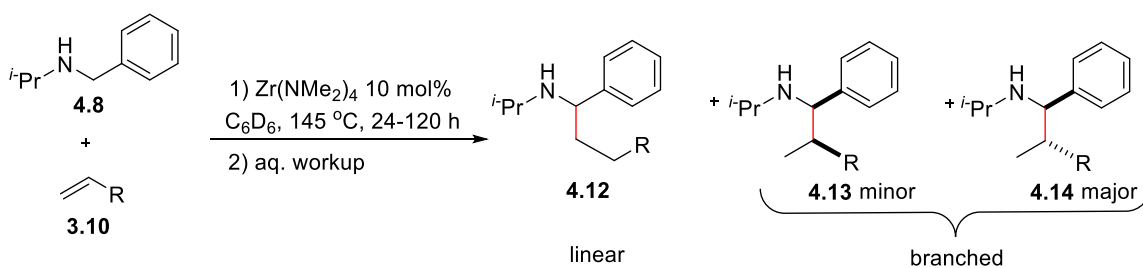


Figure 4.2 Diagnostic ¹H NMR spectrum peaks for the different isomers 4.9.5, 4.10.5 and 4.11.5

N-isopropylbenzylamine **4.8**, has not been reported as a substrate in early transition metal hydroaminoalkylation to date. It is considered to be an important substrate as it prepares the ground for the use of α -chiral amine-derived substrates. The general reaction scheme for this transformation is presented in Scheme 4.5 and the data is summarized in Table 4.2. As shown in Table 4.2, alkene **3.10.1** afforded products **4.12.1-4.14.1** with a regioselectivity ratio (RR) of 1:4 linear: branched and diastereoselectivity ratio (DR) 4:1. The different regio- and diastereomers were discernible by ^1H NMR spectroscopy; a doublet of doublets for the benzylic proton of linear regioisomer **4.12.1** and two triplets for the two branched diastereomers **4.13.1** and **4.14.1**. 4-Phenyl butene (**3.10.2**) and vinylcyclohexane (**3.10.6**) gave a mixture of linear:branched products with a ratio of 1:17 and 1:2, respectively. The shift toward the formation of the linear product for the latter alkene is attributed to the presence of steric bulk near the the reactive site of the alkene. In this case, the different regio- and diastereoisomers were discernible by ^1H NMR, however due to the overlap of the peaks corresponding to the benzylic protons, the ratios could not be calculated based on the relative integrations of the benzylic signals. Gratifyingly, all three products were present in different excess in the mixtures so this allowed for using their GCFID chromatograms as a way to provide the actual ratio of the products.



Scheme 4.5 Zirconium catalyzed hydroaminoalkylation of alkenes with *N*-isopropylbenzylamine

Table 4.2 Zirconium catalyzed hydroaminoalkylation of alkenes with *N*-isopropylbenzylamine - alkene scope

| Alkene | Structure | Time (h) | Yield (%) ^a (4.12+4.13+4.14) | RR ^{b,c} [4.12:(4.13+4.14)] | DR ^{b,c} 4.14:4.13 | [4.14:(4.13+4.12)] |
|----------------|-----------|----------|--|---|--------------------------------|--------------------|
| 3.10.1 | | 48 | 61 | 1:4 ^b | 4:1 ^b | - |
| 3.10.2 | | 48 | 75 | 1:17 ^c | 8:1 ^c | - |
| 3.10.6 | | 120 | 20 | 1:2 ^c | 17:1 ^c | - |
| 3.10.5 | | 48 | 58 | - | - | 3:1 |
| 3.10.7 | | 120 | 40 | - | - | 1:2 |
| 3.10.13 | | 48 | 62 | 1:5 ^{b,c} | 99:1 ^{b,c} | - |
| 3.10.10 | | 24 | 76 | 99:1 ^b | - | - |

^a Isolated yields of mixtures of regio- and diastereoisomers. ^b Regio- and diastereoselectivity ratios have been calculated based on the ¹H NMR spectra of the isolated mixtures of regio- and diastereoisomers. ^c Regio- and diastereoselectivity ratios have been calculated based on the GCFID chromatograms of the isolated mixtures of regio- and diastereoisomers.

In the case of products **4.12.5**, **4.13.5** and **4.14.5** the ¹H NMR spectra of the benzylic region shows the doublet for the benzylic proton for the major branched diastereomer **4.14.5** but the

overlap for the benzylic proton peaks of the minor branched diastereomer **4.13.5** and the linear **4.12.5** (Figure 4.3) does not allow to even discern their splitting patterns. For that, RR and DR could not be calculated based on ^1H NMR peak integrations. Only the ratio of the major branched diastereomer to the sum of the minor branched diastereomer and the linear regioisomer could be calculated based on the peak integration of the GC-FID chromatogram of the mixture of products. Similar was the case for products **4.12.7-4.14.7** derived from the reaction of *N*-isopropylbenzylamine and vinyl-4-cyclohexene **3.10.7**. What was unique for these products was that they were formed in isomeric ratios as revealed by the GC-FID chromatogram. Diene **3.10.13** afforded the product free of any impurities, with a regioselectivity ratio of linear:branched 1:5 and an excellent diastereoselectivity ratio of 99:1 of products **4.14.13:4.13.13**. For these products, RR and DR could be calculated either with the use of ^1H NMR spectra or GC-FID chromatograms. To reinforce the suggestion for substrate controlled regioselectivity for this third alkene scope presented in this thesis, vinylsilane **3.10.10** offered the linear product exclusively.

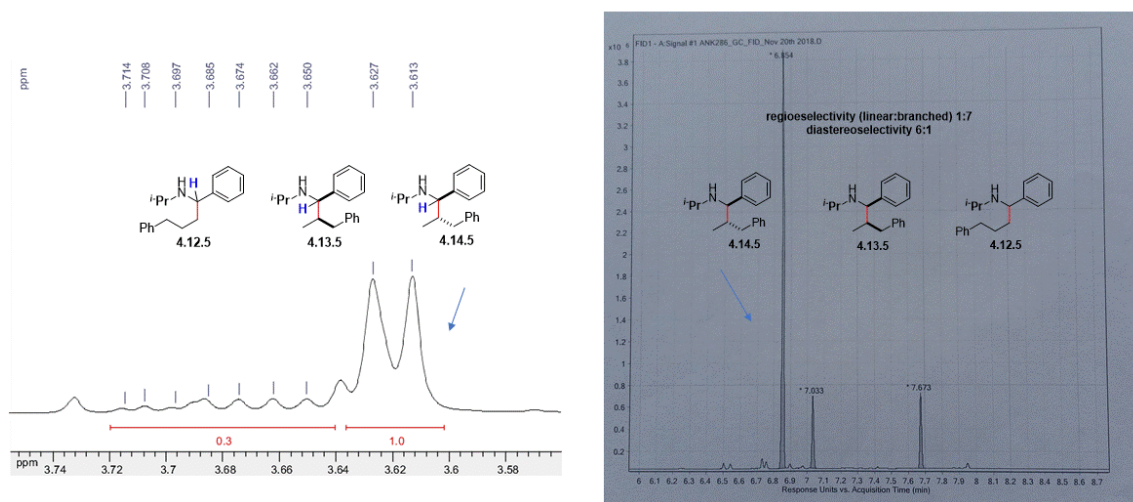


Figure 4.3 ^1H NMR spectrum (benzylic region) and GC-FID chromatogram for the different isomers **4.12.5**, **4.13.5** and **4.14.5**

A comparison among the three alkene scopes reveals the following: diene **3.10.13** successfully delivered the product free of impurities in the case of *N*-isopropylbenzylamine, however efforts to isolate the pure product from the reaction with *N*-TMS amine and *N*-phenylbenzylamine were not fruitful. Allyltrimethylsilane **3.10.12** was a successful substrate for the reaction with *N*-isopropylbenzylamine, however the isolation of the products proved to be challenging. Additionally, silylated alcohols **3.10.3** and **3.10.4** delivered the corresponding hydroaminoalkylation products **4.9.3-4.11.3** and **4.9.4-4.11.4** (Table 4.1) with the OTBS group present in the products. Likewise, the OTBS group remained intact in products **4.12.3-4.14.3** and **4.12.4-4.14.4** (Table 4.2), however the removal of the starting amine proved to be challenging in this case and thus the products are not shown in Table 4.2. With the employment of the same alkene, products **3.11.4-3.13.4** (Table 3.2) were obtained with the free unprotected alcohol. This is due to different aqueous workup which was conducted for each case.

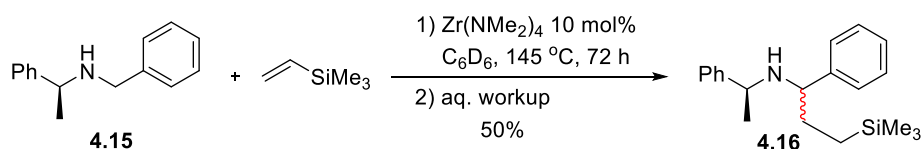
For this alkene reactivity with *N*-isopropylbenzylamine, there was unreacted starting amine in all cases that was removed upon isolation of the products, except for products **4.12.3-4.14.3** and **4.12.4-4.14.4**. On the contrary, in the cases of *N*-phenylbenzylamine **3.5.2** and *N*-TMS amine **3.5.3**, the starting amine was fully consumed as determined by ¹H NMR spectroscopy. A proposed explanation for this observation is that the different electronic and steric properties of the *N*-isopropylbenzylamine impact the rate determining step for the hydroaminoalkylation, which is the protonolysis step (Scheme 3.11, Chapter 3).¹⁶⁵ The *N*-isopropylbenzylamine is an electron rich amine, however this substrate as compared to the other two amines is sterically hindered. Thus, the protonolysis step, which is proposed to be the turnover limiting step is even more challenging with this substrate. When comparing electronic effects for *N*-phenyl and *N*-TMS amine, increased reactivity is shown for the *N*-phenylbenzylamine as shown from the

reaction times with the same alkenes. Both Buchwald¹⁴⁰ and Whitby³ suggested the lower the availability of the lone pair on the nitrogen, the higher the reactivity, perhaps due to reduced competition with the alkene binding for the alkene insertion step.

Interestingly, there is no reactivity with *N*-methyl- and *N*-ethylbenzylamine. This lack of reactivity can be attributed to the formation of robust and energetically less reactive zirconaziridines. Due to their stability, these zirconaziridines may not react with the alkene to afford the five membered metallacycle intermediate **3.36** (Scheme 3.11, Chapter 3).

4.5 Zirconium catalyzed hydroaminoalkylation of alkenes: other sterically demanding secondary amine substrates

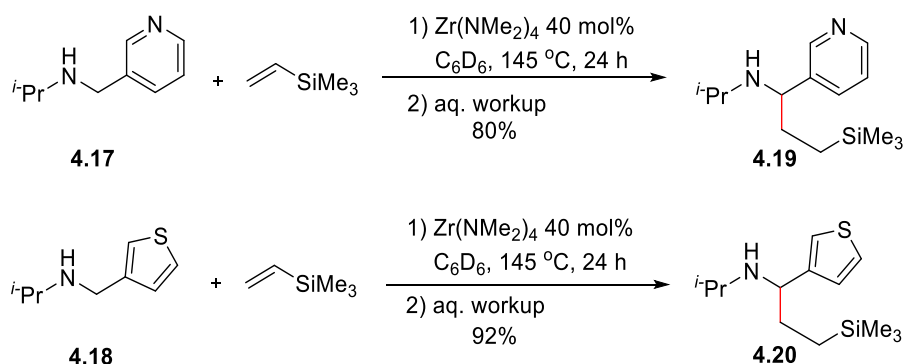
The rationale for pursuing the hydroaminoalkylation with other sterically demanding amines is that both chiral amines and unsaturated heterocycles are frequently encountered motifs in pharmaceuticals. As well as *N*-isopropylbenzylamine **4.8**, the (*S*)-*N*-benzyl-1-phenylethan-1-amine **4.15** is a sterically demanding and also a chiral amine. The question for amine **4.15** was whether it would afford a single diastereomer or a mixture of diastereomers upon the hydroaminoalkylation of vinyltrimethylsilane. Unfortunately, the isolated product **4.16** corresponds to a mixture of diastereomers in a 1:1 ratio (Scheme 4.6).



Scheme 4.6 Zirconium catalyzed hydroaminoalkylation of vinylsilane with (*S*)-*N*-benzyl-1-phenylethan-1-amine

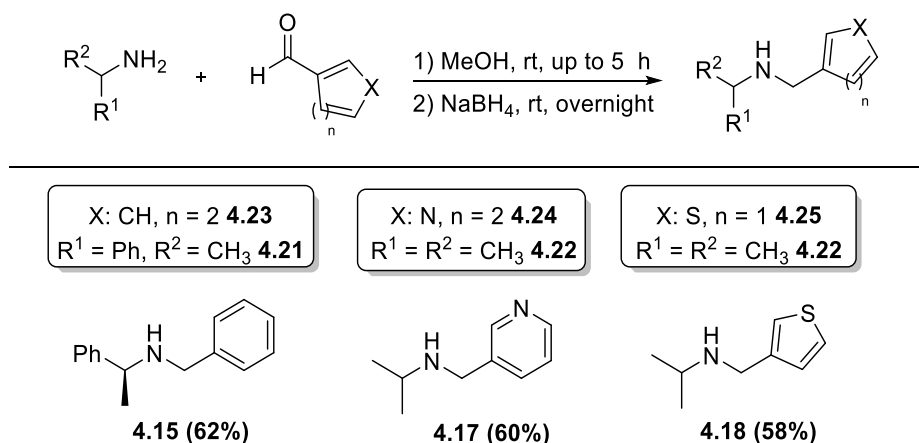
Other sterically demanding *N*-isopropylbenzylamines such as **4.17** and **4.18**, which are heteroaromatic, were subjected to the zirconium catalyzed hydroaminoalkylation of vinyltrimethylsilane **3.10.10** (Scheme 4.7). As shown in Scheme 4.7, these amines afforded

products **4.19** and **4.20**, respectively. In the case of the heteroarylated amines, the catalyst loading needed to be 40 mol% as otherwise the reaction did not reach completion (Scheme 4.7). The high demand in catalyst loading is attributable to the N or S chelation of the amines **4.17** and **4.18** to the electropositive zirconium. Although this is a high catalyst loading, this is the first example for the use of unsaturated heterocyclic amines in the early transition metal catalyzed hydroaminoalkylation.



Scheme 4.7 Zirconium catalyzed hydroaminoalkylation of vinylsilane with heteroarylated *N*-isopropylbenzylamines

The above amine substrates **4.15**, **4.17** and **4.18** were not commercially available.



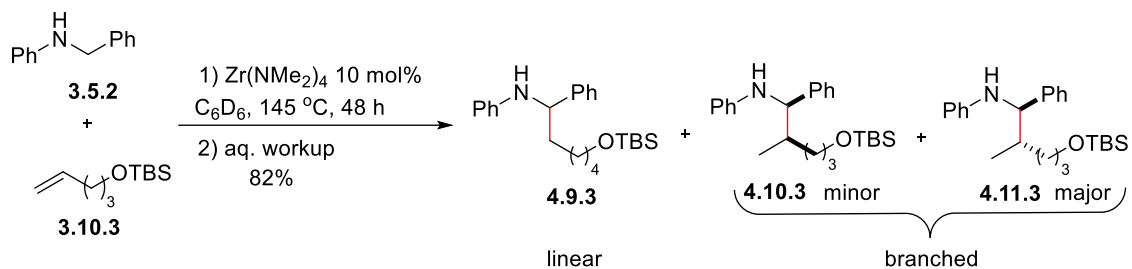
Scheme 4.8 Reductive amination conditions to access additional sterically demanding benzylamines; all amine-products are reported in the literature: **4.15**,¹⁹⁴ **4.17**,¹⁹⁵ **4.18**¹⁹⁶

As such, they were synthesized according to the above general reaction scheme (Scheme 4.8), via the reductive amination between an amine (**4.21**, **4.22**, **4.22**) and an aldehyde (**4.23**, **4.24**, **4.25**), respectively (Scheme 4.8).¹⁹⁷

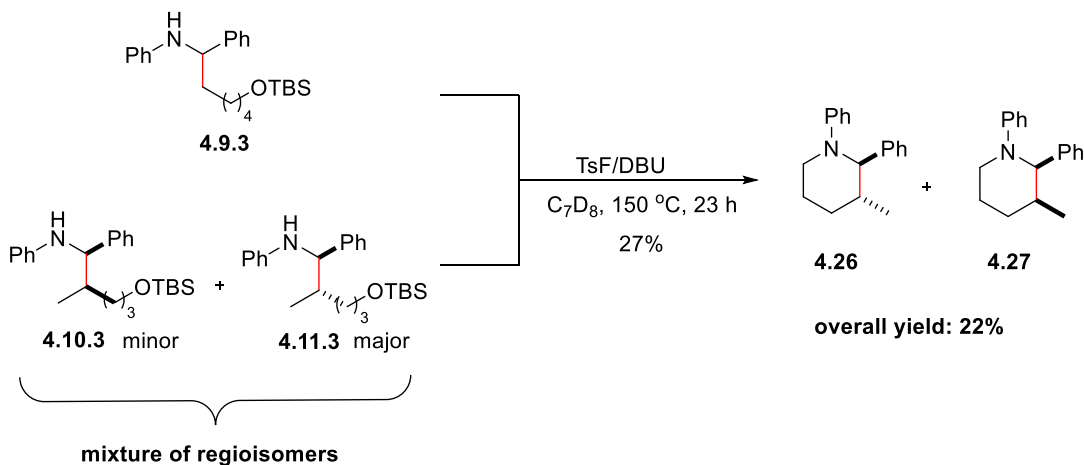
4.6 Application of the zirconium catalyzed hydroaminoalkylation toward the formation of saturated *N*-heterocycles

A route to obtain heterocyclic amines is to use hydroaminoalkylation products in a subsequent cyclization reaction. As presented in Tables 4.1 and 4.2, alkenes with oxygen containing functional groups, such as the homoallylic silylated alcohol (alkenes **3.10.3**, Tables 4.1 and 4.2) and its next homolog (alkenes **3.10.4**, Tables 4.1 and 4.2), can be used as substrates. The Schafer group disclosed in 2013 a method for the cyclization of amines and silylated alcohols using TsF.¹⁹⁸ Alkene **3.10.3** (Table 4.1) was chosen for hydroaminoalkylation and the mixture of products **4.9.3**, **4.10.3** and **4.11.3** was subjected to the intramolecular cyclization. Upon isolation only the branched products **4.26** and **4.27** were obtained with a diastereoisomeric ratio of syn:anti 3:1 (**4.27**:**4.26** 3:1) (Scheme 4.9). This example opens the door for a series of heterocyclic amines which could resemble nicotine and nicotine analogs (3'-trans-methyl nicotine and anabasine, Figure 4.1). Notably, 3'-trans-methyl nicotine, which is a candidate molecule to be obtained *via* this methodology, has previously been synthesized *via* traditional stoichiometric reactions in a seven- and five-step synthetic routes 1 & 2 (Schemes 4.10 & 4.11), respectively.¹⁹⁹⁻²⁰¹ For the installation of the branch at the 3' position steps involving stoichiometric enolate chemistry (route 1) and reductive amination (route 2) are required. Moreover, this is a powerful example of how this developed method has the potential to replace existing stoichiometric reactions to access pharmaceutically relevant products containing α -arylated amines.

Hydroaminoalkylation reaction

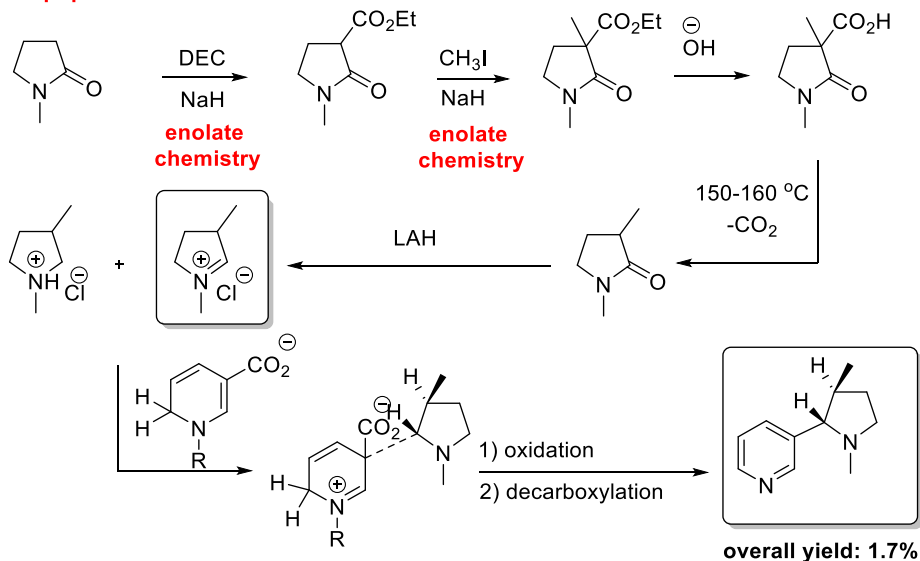


Cyclization reaction

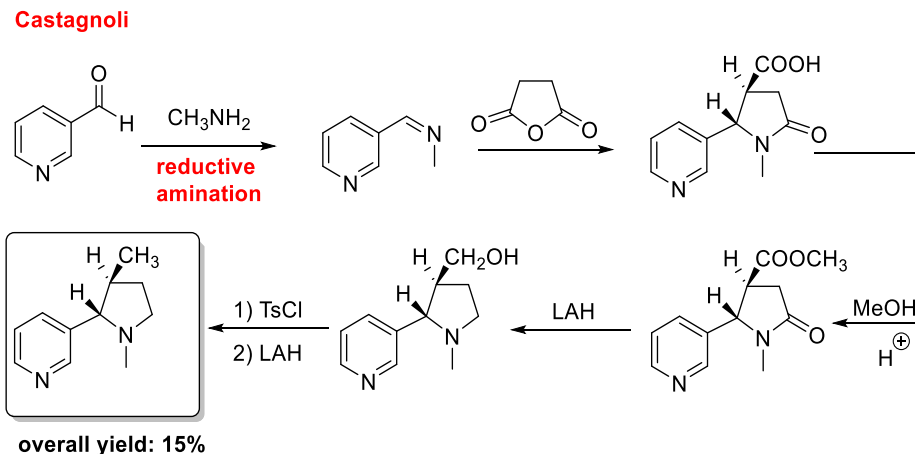


Scheme 4.9 Intramolecular cyclization of hydroaminoalkylation products to access heterocyclic amines

Rapoport



Scheme 4.10 Previously reported route for the synthesis of 3'-trans methyl nicotine (route 1)



Scheme 4.11 Previously reported route for the synthesis of 3'-*trans* methyl nicotine (route 2)

A comparison of yields between the two previously reported multi-step synthetic routes (Schemes 4.10 and 4.11) and our two-step synthetic approach (Scheme 4.9) shows the superiority in both the obtained yield and brevity of steps. Unoptimized results show promise for the pyridine containing analogs to have been obtained with a yield of 16%.

For nicotine and nicotine analogs (2-substituted pyrrolidines) which lack the methyl group at the 3' position, efficient syntheses have been reported by the groups of Stepanenko²⁰² and Short,²⁰³ using enolate chemistry.

4.7 Conclusions

Following the development of the zirconium catalyzed hydroaminoalkylation of alkenes with *N*-TMS amines in Chapter 3, Chapter 4 aimed to expand the method to non-silylated secondary amines which possess a sterically bulky substituent appended to the nitrogen. *N*-Isopropylbenzylamine and *N*-phenylbenzylamine were used as substrates in the transformation to examine the alkene scope of the reaction; it was shown in the presence of sterically bulky vinylsilanes the linear product was obtained exclusively. A mixture of regioisomers was obtained

when the steric bulk of the alkene was moved away from the reactive site. The regio- and diastereoselectivity trends were similar for both *N*-phenyl- and *N*-isopropylbenzylamine.

Other sterically demanding secondary benzylamines, chiral or heteroaromatic, were also tested in the transformation with vinyltrimethylsilane as the alkene. This allowed for the engagement of unsaturated heteroaromatic amines, substrates which are not known for early transition metal catalyzed hydroaminoalkylation. Successful application of the developed method toward the formation of tertiary saturated heterocyclic amines was reported. These two last reactions open the door to access valuable motifs in pharmaceuticals with alternative routes which utilize earth abundant metals and more affordable starting materials. These assets offer low cost options that generate minimal waste in large scale synthesis of medicinal products.

The experimental for Chapter 4 starts on page 150.

Chapter 5: Summary and future work

5.1 Summary

This thesis presented the use of *N*-silylated amines as substrates in stoichiometric and catalytic transformations; C-N and C-C bond formation in Chapters 2 and 3, respectively. Chapter 4 was an expansion of Chapter 3, and presented the exploitation of *N*-alkyl- and *N*-arylamines as substrates in the catalytic hydroaminoalkylation reaction developed in Chapter 3.

In Chapter 2 the *N*-silylated amines proved to be valuable synthons as they served as precursors to negatively charged nitrogen, a species necessary for nucleophilic attack with electron deficient amines for the amidation reaction. As well as engaging electron poor heteroarylamines in the amidation reaction, the use of a bench stable electrophile (thioester) and the facile isolation of the derived diheteroarylamides *via* filtration rendered the protocol amenable to parallel synthesis, which has the power to generate libraries of molecules in a short period of time.

In Chapter 3, the silicon protected primary α -arylated amines served as a mask which allowed *N*-silylated amines to undergo the zirconium catalyzed hydroaminoalkylation and deliver primary amines with a branch at position α to nitrogen. Chapter 4 was a continuation of Chapter 3 and presented secondary amines as substrates for the zirconium catalyzed hydroaminoalkylation reaction, including both *N*-aryl- and *N*-alkylamines. α -Arylated secondary amines were successfully obtained. One attractive feature in all three cases was the isolation of the linear product, as a single regioisomer, when using bulky vinylsilanes due to substrate controlled regioselectivity.

The real power of a methodology lies in its synthetic applications toward medicinally relevant molecules. For our amidation protocol, a series of 19 diheteroarylamides were synthesized which were structural analogs of **2.2** (Chapter 2), a compound which has shown promise as an antiviral

agent against HIV. For the methodologies developed in Chapter 3 and 4, efforts and accomplishments toward the formation of heterocyclic amines were discussed. As shown in Figures 3.1 and 4.1, primary, secondary and tertiary heterocyclic amines are often incorporated in pharmaceuticals.

5.2 Future work

5.2.1 Methods refinement

5.2.1.1 Amidation protocol

Due to the facility of product isolation (*via* simple vacuum filtration) the amidation protocol which was discussed in Chapter 2 possesses features which render it green, such as minimum waste generation and recycling of the byproducts. Additional improvement could include the replacement of existing solvents (such as MeCN, THF and diethylether) with greener solvents such as 2-Me-THF. Moreover, the *N*-silylation of amines can be pursued with the use of catalytic methods which were thoroughly discussed in Chapter 1, therefore replacing the super- or stoichiometric use of TMSCN. The tolerance of a wider range of (heteroaryl)amines which deliver amides with the same physicochemical properties, resulting in their precipitation out of the reaction mixture, would further strengthen the robustness of the protocol.

As shown in Chapter 2 the protocol is amenable to parallel synthesis at a manual level. A next level test would be to automate the parallel synthesis where robotic arms could perform the amidation reaction as described herein.

5.2.1.2 Hydroaminoalkylation protocol

In Chapters 3 and 4, the hydroaminoalkylation of alkenes with *N*-TMS-, *N*-phenyl- and *N*-alkylamines was discussed. In all three cases a mixture of regio- and diastereomers were obtained, unless the alkene employed possessed a sterically bulky group such as vinylsilane to

achieve substrate controlled regioselectivity. Different silicon substituents on the nitrogen were examined for their ability to tune the regioselectivity of the reaction. Results showed that the regioselectivity can be altered but not completely shifted to only either the branched or linear products.

Catalyst controlled regioselectivity would be attractive but was not explored in this work. Here only $\text{Zr}(\text{NMe}_2)_4$ was extensively investigated. Future work could explore other ligands, including *N,O*-chelated complexes.

5.2.2 Applications

5.2.2.1 Amidation protocol

The amidation protocol has already been applied toward the synthesis of 19 diheteroarylamides which are structural analogs of the antiviral **2.2** (Chapter 2.1). Structural information for the target is lacking. Thus, the ongoing synthesis of diheteroarylamides would provide libraries of molecules to test the hypothesis for interactions between the target and the potential agonists/antagonists.

5.2.2.2 Hydroaminoalkylation protocol

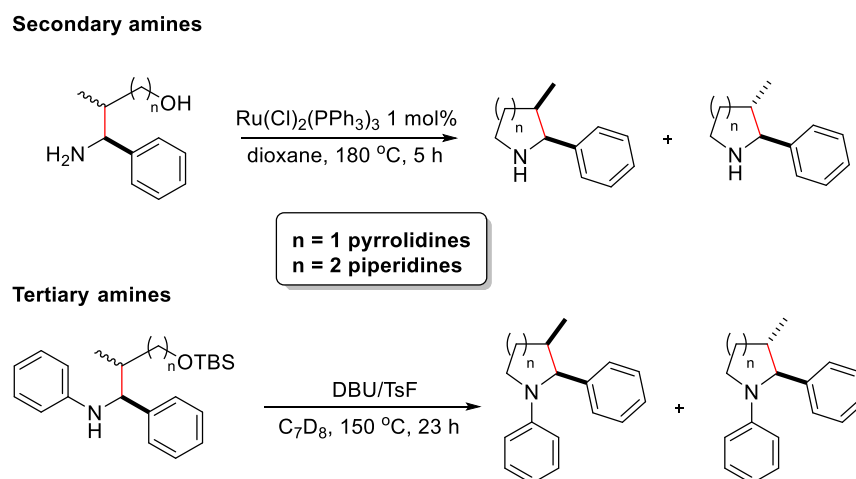
The developed hydroaminoalkylation can be directed toward heterocycle and *de novo* aminoacid syntheses. Both heterocycles and amino acids are essential building blocks in pharmaceuticals, as proven below by the literature that highlights their importance.

5.2.2.2.1 Heterocycle syntheses

○ Piperidines and pyrrolidines

Two examples for the formation of heterocycles reported in Chapters 3 and 4 include the synthesis of secondary and tertiary piperidines, respectively. Pyrrolidines can be formed under the same reaction conditions if the previous alkene homolog (silylated homoallylic alcohol) is

used in the hydroaminoalkylation reaction (Scheme 5.1). The products obtained from the hydroaminoalkylation reaction undergo the intramolecular cyclization reactions to furnish secondary and tertiary amines. Secondary amines are isolated *via* basic aqueous extraction while the primary amines undergo acidic and basic aqueous extraction. Due to the different isolation conditions, the -OTBS group remains intact for secondary amines while for primary amines the product with the free alcohol is obtained.

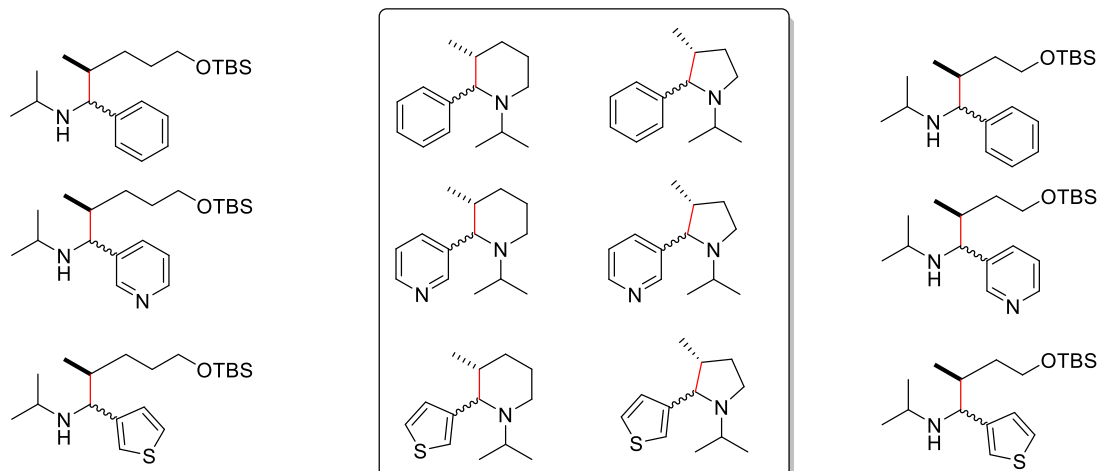


Scheme 5.1 Two different cyclization routes for the formation of piperidines and pyrrolidines^{185, 186, 198}

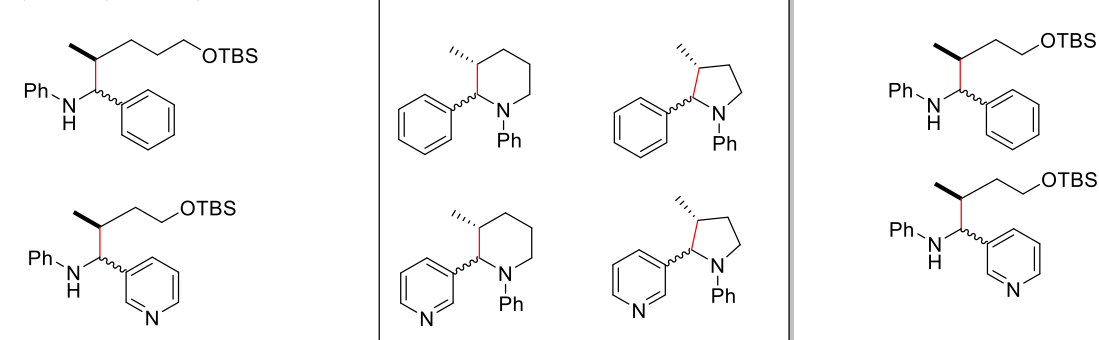
With this intramolecular cyclization, heterocyclic amines are obtained and if nitrogen is present as a heteroatom in the aryl substituent α to nitrogen, then structures resembling nicotine are obtained. Even in the absence of the pyridine nitrogen, the molecules remain of interest. In Figure 5.1 a series of suggested piperidine and pyrrolidine analogs, which can be obtained *via* the intramolecular cyclization routes from the hydroaminoalkylation products shown in Scheme 5.1, is presented. For nicotine, other than the two observed hydrogen bonds for both the pyridine and pyrrolidine nitrogens, there is an additional π -cationic interaction of the charged pyrrolidine nitrogen with the aromatic ring of a tryptophan, an amino acid which is part of the nicotinic receptor. This additional interaction is observed only with the nicotinic receptors in the brain and

not with the nicotinic receptors in the neuromuscular junction, and explains the higher affinity of nicotine for the former receptors.²⁰⁴

1) *N*-isopropyl heterocyclic amines



2) *N*-phenyl heterocyclic amines



3) Heterocyclic amines

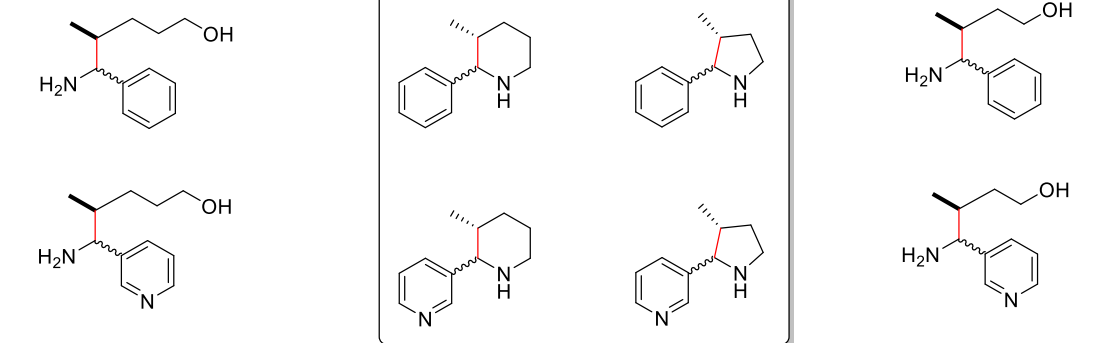


Figure 5.1 Nicotine derivatives to be obtained from the intramolecular cyclization of the hydroaminoalkylation products

With the molecules possessing an aryl ring on the piperidine or pyrrolidine nitrogen, we open the door to a new class of nicotinic derivatives, which lack the pyridine nitrogen and are expected to demonstrate only π -stacking interactions and one less hydrogen bond. As such we are envisioning a class of highly selective nicotinic derivatives (Figure 5.1).

Nicotine is also associated with neurological disorders, such as Alzheimer's and Parkinson's diseases, and there is pronounced need for the identification of ion-channel modulators.²⁰⁵ The developed method has the potential to deliver analogs which can be evaluated as ion-channel agents.

o **Tetrahydroquinolines**

Both tetrahydroquinolines and indolines are prominent motifs in pharmaceuticals and natural products.²⁰⁶ Their synthesis is achieved *via* sequence (domino, tandem or cascade) reactions and examples include intramolecular reduction/reductive amination,²⁰⁷ reduction/Michael addition,^{208, 209} reductive amination/ S_NAR ,^{210, 211} S_NAR /Michael addition,²¹² metal catalyzed oxidative cyclizations of aminoalcohols¹⁸² and photochemical syntheses.²¹³ In Figure 5.2, representative bioactive molecules possessing tetrahydroquinolines substituted at the 2nd position are presented.

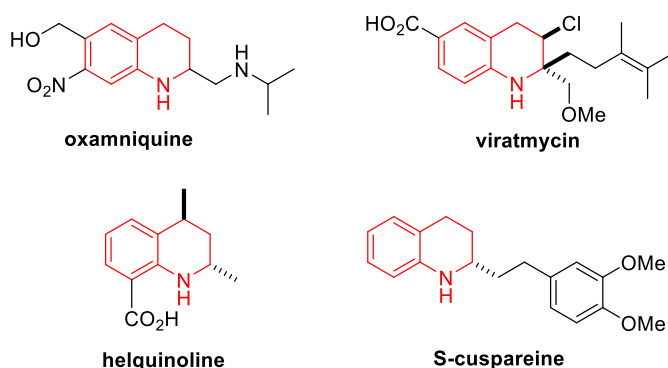
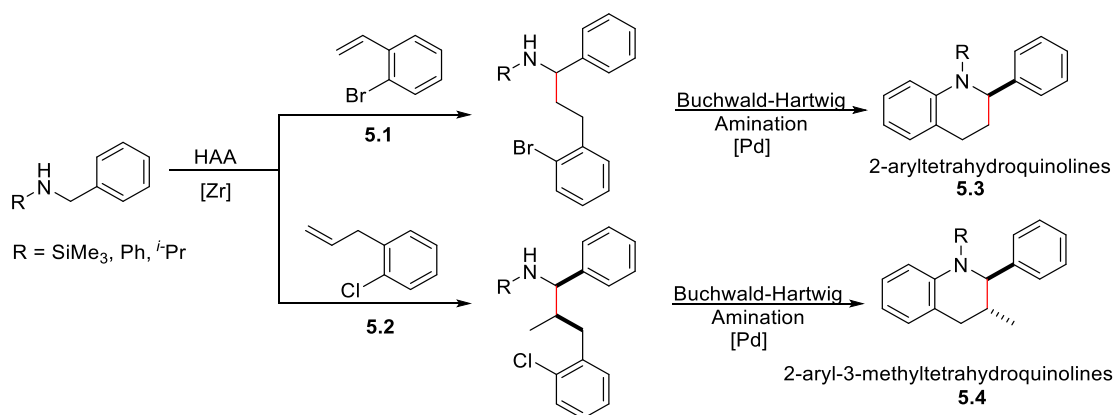


Figure 5.2 Tetrahydroquinoline containing pharmaceuticals and natural products

With the developed technology in Chapters 3 and 4 to obtain the hydroaminoalkylation products, there are possibilities for further reactions to obtain tetrahydroquinolines. If aryl halides are engaged in the hydroaminoalkylation reaction, then *via* an intramolecular Buchwald-Hartwig amination the above motif can be obtained. As shown in Scheme 5.2 the reaction of 2-bromostyrene **5.1** and 2-chlorobenzene **5.2** can lead to products which can serve as substrates in the Buchwald-Hartwig amination to obtain 2-aryltetrahydroquinolines **5.3** and 2-aryl-3-methyltetrahydroquinolines **5.4**, respectively. Notably, due to the higher regioselectivity observed with styrenes, there is greater synthetic utility toward the former heterocyclic motif.



Scheme 5.2 Tetrahydroquinolines to be obtained from the intramolecular Buchwald-Hartwig amination of the hydroaminoalkylation products

○ Azetidines

Azetidines have received attention in the recent years as a target for exploration in both drug discovery and methods development, as presented by the number of arising azetidine containing pharmaceuticals in the recent years (Figure 5.3). The Baran²¹⁴ and Schindler²¹⁵ groups have disclosed two distinct methodologies, including release strain amination and visible-light cycloaddition to achieve azetidine syntheses, respectively. Other photochemical cycloaddition pathways have been presented recently by the groups of Maruoka²¹⁶ and Sivaguru.²¹⁷

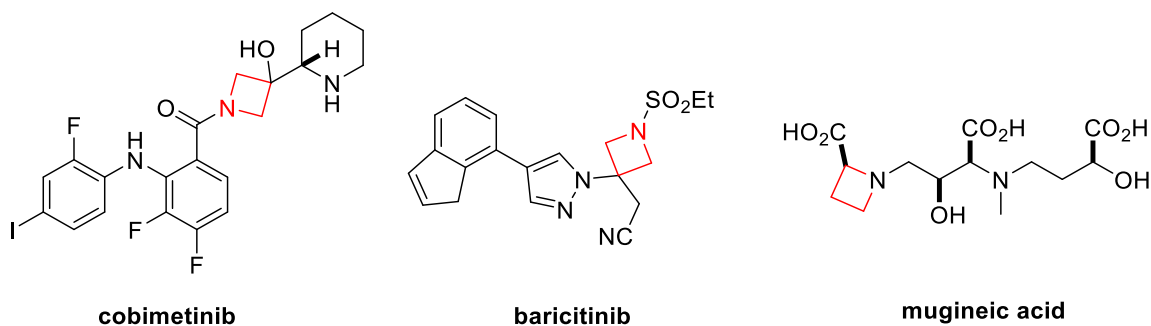
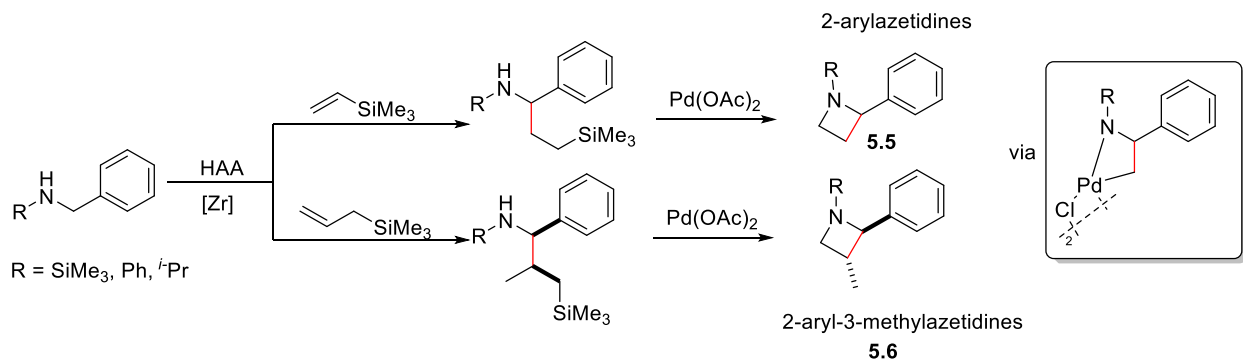


Figure 5.3 Azetidine containing pharmaceuticals and natural products

Hydroaminoalkylation would be useful for the synthesis of azetidines as it can provide substrates for intramolecular cyclization *via* the cleavage of carbon-silicon bond of aminosilanes which are obtained as single regioisomers from the hydroaminoalkylation (Scheme 5.3). The carbon-silicon bond cleavage is known for Csp^2 -Si and activated Csp^3 -Si (such as benzylic carbons),²¹⁸ however it is not known for unactivated Csp^3 -Si bonds. For future work, we envision to form the 2-arylazetidines **5.5** and 2-aryl-3-methylazetidines **5.6** *via* this activation (Scheme 5.3).



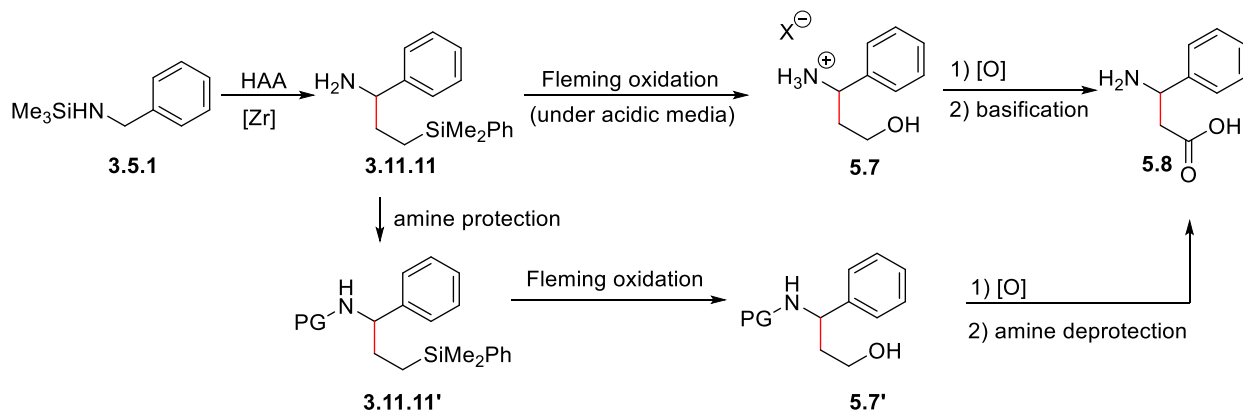
Scheme 5.3 Proposed route to obtain 2-aryl- and 2-aryl-3-methylazetidines *via* Csp^3 -Si activation

5.2.2.2.2 Unnatural amino acid synthesis

Unnatural amino acids are non-proteinogenic amino acids which occur naturally or can be chemically synthesized. They serve as chiral building blocks, conformational constraints, medicinal scaffolds and pharmacologically active compounds. This functional versatility is due to their structural diversity. Their incorporation is useful in medicinal chemistry scaffolds and

allows for increased activity, selectivity and plasma stability in drug discovery due to their proteolytic resistance.^{219, 220} They have served as excellent tools in the identification of leads in peptidic and non-peptidic compounds.

Our developed methodology can offer the option to access unnatural amino acids or as otherwise called peptidomimetics, structural analogs of amino acids. As shown in Scheme 5.4, the proposed route includes the *N*-TMS amine **3.5.1** which can deliver amino silane **3.11.11** via hydroaminoalkylation and the derived amine can undergo the Fleming oxidation, which is a functionalization of unactivated Csp³-Si bonds, to afford alcohol **5.7** which upon oxidation can lead to carboxylic acid **5.8**. To avoid any amine oxidation, it is shown that the medium needs to be acidic so that the lone pair of the amine remains unavailable, or the amine needs to be protected (as **3.11.11'**) before performing the Fleming oxidation.



Scheme 5.4 Proposed route for the synthesis of peptidomimetics

5.3 Conclusions

Two methods have been developed with the use of *N*-silylated amines as substrates: an amidation and a Csp³-Csp³ bond formation protocol. For the amidation protocol, both the synthesis and reactivity of amines was achieved and examined, respectively, *via* stoichiometric reactions. For the Csp³-Csp³ bond formation, the *N*-silylated amines were synthesized stoichiometrically while

their reactivity was examined in hydroaminoalkylation reaction which is a catalytic transformation. With catalysis being the ninth principle of Green Chemistry, a possibility to upgrade both methodologies to a greener level includes the catalytic synthesis of amines prior to their engagement in catalytic transformations. In Chapter 2, several catalytic amide bond methods were discussed and this provides insight for considering a catalytic amidation protocol with electron deficient amines, questioning even the necessity for the silyl protecting group. For the hydroaminoalkylation reaction it was shown that the silyl group is necessary for it to occur. Catalysis allows for the incorporation of all starting materials to the final products, and consequently higher atom economy is achieved. Both catalysis and atom economy are principles of Green Chemistry, and offer a qualitative assessment of the greenness of a process. Sequential reactions are important for achieving even higher atom economy, thus catalytic Si-N dehydrocoupling followed by the Csp^3-Csp^3 bond formation with the same or a second metal complex is an approach to consider for the method improvement.

For reaction efficiency, not only atom economy must be considered but also selectivity. Although not the exclusive products of the reaction, due to their polarity the amide products precipitate out from the reaction mixture and can be selectively isolated by facile vacuum filtration from the byproducts of the reaction. The zirconium catalyzed hydroaminoalkylation reaction delivered exclusively the linear product only when bulky vinylsilanes were used as alkenes achieving, in this way, substrate controlled regioselectivity. Catalyst regio- and diastereoselectivity remain unexplored. Nature's demanding sensitivity to chiral molecules is an impetus for even pursuing enantioselectivity in the hydroaminoalkylation reaction. The introduction of bulky ligands on titanium has been shown to shift the regioselectivity toward the linear product (Doye group). Ligands which increase the electrophilicity on tantalum have been

shown to selectively deliver the branched product (Schafer group). The appendage of chiral ligands to niobium has allowed for the generation of complexes competent to realize asymmetric hydroaminoalkylation (Hultzch group). All these tactics can be considered and followed in the zirconium catalyzed hydroaminoalkylation to achieve the desired regio-, diastereo- and enantioselectivity.

Chapter 6: Experimental

6.1 General considerations and materials

All chemicals were purchased from Sigma Aldrich, Oakwood Chemicals, Combi-blocks and they were used without purification unless mentioned. In the Faculty of Pharmaceutical Sciences, all solvents were dried and kept under N₂. At the Chemistry Department, all air and moisture sensitive reactions were performed using a MBraun LABmaster glovebox filled with a N₂ atmosphere. All pieces of glassware, Teflon coated magnetic stirring bars and canulas were dried for at least overnight in a 180 °C oven before being transferred into the glovebox or used in the Schlenk line. Ether was passed over activated alumina columns into Teflon sealed Straus flasks and stored therein until use. C₆D₆ was dried over molecular sieves 3Å, degassed, and stored in Teflon sealed Schlenk flasks prior to use. Zr(NMe₂)₄ (Sigma-Aldrich) was used as received. All amines and alkenes were purchased from commercial sources (Sigma-Aldrich, Oakwood, Combi-blocks), dried over CaH₂ and distilled before use. ⁿBuli 1.6 M in hexanes was purchased from Sigma-Aldrich. TMSCl was purchased from Sigma-Aldrich, dried over CaH₂, distilled and stored in Teflon sealed Straus flasks. *N*-Silylation of the amines was conducted with the use of the Schlenk line. *N*-Phenylbenzylamine was sublimed and *N*-isopropylamine was distilled prior to being transferred in the glovebox for catalysis.

The hydroaminoalkylation reaction were conducted on NMR tube scale and performed in J-Young NMR tubes (8" x 5 mm) sealed with screw-type Teflon caps.

¹H, ¹³C and ¹⁹F NMR spectra were recorded at 400, 100, and 376 MHz, respectively, on a Bruker AC 400 Ultrashield 10 spectrophotometer in the Faculty of Pharmaceutical Sciences. Chemical shifts are expressed in ppm, (δ scale). When peak multiplicities are reported, the following abbreviations are used: s (singlet), d (doublet), m (multiplet), t (triplet), dd (doublet of doublet),

td (triplet of doublet), tdd (triplet of doublet of doublet), td (triplet of doublet), ddd (doublet of doublet of doublet). Coupling constants are reported in Hertz (Hz). In the Faculty of Pharmaceutical Sciences, all low and high resolution mass spectra were recorded on a AB Sciex UHPLC/MS/MS System and a Thermo Scientific Q Exactive Orbitrap High Resolution Mass Spectrometer, respectively. At the Chemistry Department, mass spectra were recorded on a Kratos MS-50 spectrometer using an electron impact (70 eV) source or a Bruker Esquire LC spectrometer using electrospray ionization source with the fragment signals being reported in mass to charge number (m/z). Column chromatography was carried out using silica gel (Silicycle, Silicaflash® F60, 40-63 μ m, 230-400 mesh), or on a Biotage Isolera purification system, (PartnerTech Åtvidaberg AB) using pre-packed silica gel columns (Biotage, part no. FSKO-1107-0010, FSKO-1107-0025, or FSKO-1107-0050). A Biotage Initiator 2.5 apparatus was used for experiments using microwave heating. IR spectra (cm^{-1}) were recorded on an Agilent Technologies (Cary 600 series). GCFID chromatograms were obtained on an Agilent Technologies instrument, too. FT-IR spectrometer, using a PIKE MIRacle ATR accessory for sampling. All melting points were determined with open capillary tubes on a MEL-TEMP II (USA) and are uncorrected.

6.2 Experimental data for Chapter 2

General procedure for amidation reaction to access diheteroarylamides 2.2, 2.2' and 2.6

A solution of thioester **2.33** or **2.47** (0.2 mmol, 2 equiv) in MeCN (1-2 mL) was transferred to a narrow vial (diameter: 1-1.5 cm; height: 8-15 cm) containing the requisite *N*-silylated amine **2.40** (1 equiv), and the mixture was stirred at 50 °C for 10 min under nitrogen (note that for the preparation of **2.6.8** and **2.6.16** 4 equiv of thioester **2.33/2.47** was used, and 1 equiv was employed to prepare amide **2.2**). Then, TBAF 1 M in THF (1 equiv) was added and heating at 50

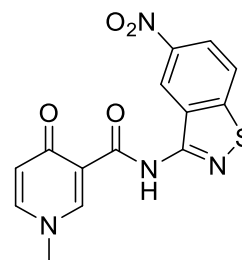
°C (or rt for **2.2**) was continued overnight (16 h) under a slight stream of nitrogen. After heating the precipitated product was collected by suction filtration and washed with cold MeCN (cold acetone wash for amide product **2.2**). Note, for compound **2.6.4** ether was added to the reaction mixture at the end of the heating period to induce product precipitation, and the product isolated by suction filtration was washed with cold ether. To isolate the thioester **2.47** used in excess, the filtrates for a series of reactions of **2.47** with TMS-amines **2.40** were concentrated, dissolved in minimal MeCN and extracted with heptane to remove the liberated thiol (isolated after heptane removal as its disulphide **2.48**). The MeCN layer was then concentrated and the residue was triturated multiple times with ether. Concentration of the combined ether washes allowed recovery of thioester **2.47** (30-40% of expected amount).

***N*-(5-nitrobenzo[*d*]thiazol-3-yl)-1-methyl-4-oxo-1,4-dihydropyridine-3-carboxamide (2.2)** (Table 2.1, Entry 11) and **3-(3-imino-5-nitro-2,3-dihydrobenzo[*d*]isothiazole-2-carbonyl)-1-methylpyridin-4(1*H*)-one (2.2')**

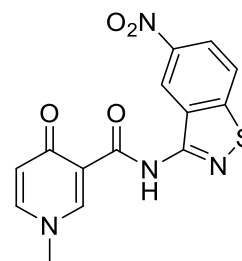
Using 1 equiv of thioester **2.33/2.47**, compound **2.2** was obtained as a brownish solid, m.p. >300 °C. Yield with **2.33/2.47** (33%/25%). ¹H NMR (400 MHz, DMSO-*d*₆): δ = 3.92 (s, 3 H, NCH₃), 6.75 (d, *J* = 7.9 Hz, 1 H, Hpyr), 7.78 (d, *J* = 9.3 Hz, 1 H, Hpyr), 8.03 (dd, *J* = 5.4 Hz, 1 H, ArH), 8.17 (d, *J* = 9.5 Hz, 1 H, Hpyr), 8.76 (s, 1 H, ArH), 8.85 (d, 1 H, ArH), 15.58 (s, 1 H, NH).

¹H NMR data match with the data reported.⁵⁹

Using 2 equiv of thioester **2.33/2.47**, a 1:1 mixture of **2.2** and **2.2'** was obtained as a brownish solid. The solid material was washed with DMSO-*d*₆ (2 x 1 ml). The remaining solid material, which solubilized when taken up in



suggested structure for 2.2

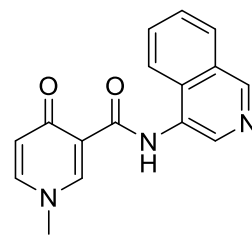


suggested structure for 2.2'

further DMSO-*d*₆ (1 mL) corresponded to pure compound **2.2'**. ¹H NMR (400 MHz, DMSO-*d*₆): δ = 3.87 (s, 3 H, NCH₃), 6.63 (d, *J* = 7.2 Hz, 1 H, Hpyr), 7.92–7.95 (dd, *J* = 7.4 Hz, *J* = 2.2 Hz, 1 H, Hpyr), 8.52–8.55 (dd, *J* = 9.4 Hz, *J* = 2.9 Hz, 1 H, ArH), 8.72 (d, *J* = 2.3 Hz, 1 H, Hpyr), 8.75 (d, *J* = 2.7 Hz, 1 H, ArH), 8.82 (d, *J* = 9.4 Hz, 1 H, ArH), 14.26 (s, 1 H, NH). ¹³C NMR (100 MHz, DMSO-*d*₆): δ = 44.2, 102.1, 116.4, 117.4, 120.1, 121.1, 129.5, 129.6, 143.4, 146.9, 147.2, 163.8, 176.5. MS (Turbo Spray) *m/z*: 329.0 (MH⁺).

***N*-(isoquinolin-4-yl)-1-methyl-4-oxo-1,4-dihydropyridine-3-carboxamide (2.6.1) (Table 2.1, Entry 1)**

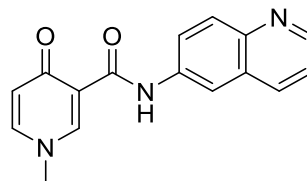
White solid, m.p. >300 °C. Yield with **2.33/2.47** (15%/11%). ¹H NMR (400 MHz, DMSO-*d*₆): δ = 3.89 (s, 3 H, NCH₃), 6.65 (d, *J* = 7.0 Hz, 1 H, Hpyr), 7.77 (s, *J* = 7.5 Hz, 1 H, ArH), 7.95 (s, 2 H, Hpyr), 8.19–8.26 (dd, *J* = 8.2 Hz, *J* = 3.0 Hz, 2 H, ArH), 8.75 (s, 1 H, Hpyr), 9.11 (s, 1 H, ArH), 9.51 (s,



1 H, ArH), 13.69 (s, 1 H, NH). ¹³C NMR (100 MHz, DMSO-*d*₆): δ = 44.8, 118.2, 120.4, 120.5, 128.1, 128.6, 129.0, 129.8, 132.0, 134.6, 143.8, 147.0, 148.5, 166.1, 177.3. IR (ATR): ν = 1660, 1774, 3435 cm⁻¹. HRMS (HESI) *m/z* calcd for C₁₆H₁₃N₃O₂H⁺ [M + H⁺], 280.1081; Found 280.1079.

1-methyl-4-oxo-*N*-(quinolin-6-yl)-1,4-dihydropyridine-3-carboxamide (2.6.2) (Table 2.1, Entry 2)

White solid, m.p. 225–226 °C. Yield with **2.33/2.47** (16%/20%). ¹H NMR (400 MHz, DMSO-*d*₆): δ = 3.86 (s, 3 H, NCH₃), 6.58 (d, *J* = 6.7 Hz, 1 H, Hpyr), 7.49–7.51 (m, 1 H, ArH), 7.89–7.92 (m, 2 H, Hpyr),



8.00 (d, *J* = 8.3 Hz, 1 H, ArH), 8.32 (d, *J* = 7.5 Hz, 1 H, ArH), 8.42 (s, 1 H, ArH), 8.66 (s, 1 H, Hpyr), 8.80 (s, 1 H, ArH), 13.19 (s, 1 H, NH). ¹³C NMR (100 MHz, DMSO-*d*₆): δ = 44.0, 115.6,

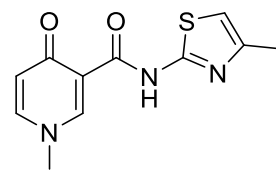
117.7, 119.9, 121.9, 123.8, 128.5, 129.9, 135.5, 136.5, 142.8, 144.9, 146.1, 149.2, 162.6, 176.5.

IR (ATR): ν bar = 1635, 1678, 3026, 3416 cm^{-1} . HRMS (HESI) m/z calcd for $\text{C}_{16}\text{H}_{13}\text{N}_3\text{O}_2\text{H}^+$ [$\text{M} + \text{H}^+$], 280.1081; Found 280.1079.

1-methyl-*N*-(4-methylthiazol-2-yl)-4-oxo-1,4-dihydropyridine-3-carboxamide (2.6.3) (Table 2.1, Entry 3)

Off-white solid, m.p. 272-274 °C. Yield with **2.33/2.47** (14%/25%). ^1H

NMR (400 MHz, $\text{DMSO-}d_6$): δ = 2.27 (s, 3 H, ArCH₃), 3.85 (s, 3 H, NCH₃), 6.60 (d, J = 7.2 Hz, 1 H, Hpyr), 6.81 (s, 1 H, ArH), 7.90–7.93



(dd, J = 7.4 Hz, J = 2.1 Hz, 1 H, Hpyr), 8.68 (d, J = 2.1 Hz, 1 H, Hpyr), 14.04 (s, 1 H, NH). ^{13}C

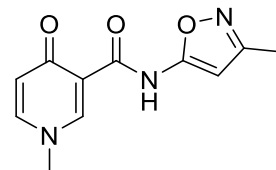
NMR (100 MHz, $\text{DMSO-}d_6$): δ = 17.0, 44.1, 108.5, 115.7, 120.0, 143.2, 146.6, 147.2, 156.3,

161.8, 176.3. IR (ATR): ν bar = 1636, 1678, 3010, 3068, 3270, 3439 cm^{-1} . HRMS (HESI) m/z

calcd for $\text{C}_{11}\text{H}_{11}\text{N}_3\text{O}_2\text{SNa}^+$ [$\text{M} + \text{Na}^+$], 272.0464; Found 272.0464.

1-methyl-*N*-(3-methylisoxazol-5-yl)-4-oxo-1,4-dihydropyridine-3-carboxamide (2.6.4) (Table 2.1, Entry 4)

Note, after stirring overnight, ether was added to the reaction mixture to facilitate the precipitation of the amide product. The amide product was obtained by filtration and the precipitate was washed with $\text{Et}_2\text{O}/\text{MeCN}$.



Off-white solid, m.p. 235-236 °C. Yield with **2.33/2.47** (24%/17%). ^1H NMR (400 MHz,

$\text{DMSO-}d_6$): δ = 2.21 (s, 3 H, ArCH₃), 3.86 (s, 3 H, NCH₃), 6.25 (s, 1 H, ArH), 6.62 (d, J = 7.2 Hz, 1 H, Hpyr), 7.92–7.94 (dd, J = 7.2 Hz, J = 2.2 Hz, 1 H, Hpyr), 8.69 (d, J = 2 Hz, 1 H, Hpyr),

14.04 (s, 1 H, NH). ^{13}C NMR (100 MHz, $\text{DMSO-}d_6$): δ = 11.4, 44.1, 89.3, 115.9, 120.0, 143.4,

146.7, 160.3, 160.6, 161.0, 176.4. IR (ATR): ν bar = 1650, 1693, 3066 cm^{-1} . HRMS (HESI) m/z

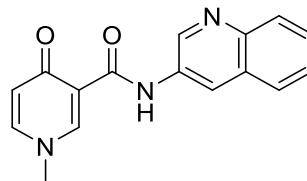
calcd for $\text{C}_{11}\text{H}_{11}\text{N}_3\text{O}_3\text{Na}^+$ [$\text{M} + \text{Na}^+$], 256.0693; Found 256.0693.

1-methyl-4-oxo-*N*-(quinolin-3-yl)-1,4-dihydropyridine-3-carboxamide (2.6.5) (Table 2.1, Entry 5)

White solid, m.p. 244-245 °C. Yield with **2.33/2.47** (17%/15%). ¹H

NMR (400 MHz, DMSO-*d*₆): δ = 3.87 (s, 3 H, NCH₃), 6.59 (d, *J* = 7.3

Hz, 1 H, Hpyr), 7.59 (t, *J* = 7.4 Hz, 1 H, ArH), 7.66 (t, *J* = 7.4 Hz, 1 H,



ArH), 7.91 (d, *J* = 7.3 Hz, 1 H, Hpyr), 7.97 (d, *J* = 7.9 Hz, 2 H, ArH), 8.67 (s, 1 H, Hpyr), 8.80

(s, 1 H, ArH), 9.00 (s, 1 H, ArH), 13.27 (s, 1 H, NH). ¹³C NMR (100 MHz, DMSO-*d*₆): δ = 44.0,

117.4, 120.0, 122.7, 127.2, 127.8, 128.0, 128.6, 132.4, 142.9, 144.4, 144.9, 146.2, 163.1, 176.4.

IR (ATR): ν bar = 1633, 1678, 2942, 3369, 3439 cm⁻¹. HRMS (HESI) *m/z* calcd for

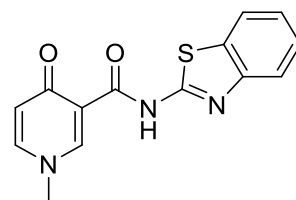
C₁₆H₁₃N₃O₂H⁺ [M + H⁺], 280.1081; Found 280.1085.

***N*-(benzo[*d*]thiazol-2-yl)-1-methyl-4-oxo-1,4-dihydropyridine-3-carboxamide (2.6.6) (Table 2.1, Entry 6)**

White solid, m.p. >300 °C. Yield with **2.33/2.47** (70%/70%). ¹H NMR

(400 MHz, DMSO-*d*₆): δ = 3.88 (s, 3 H, NCH₃), 6.65 (d, *J* = 7.3 Hz, 1

H, Hpyr), 7.32 (m, 1 H, ArH), 7.45 (m, 1 H, ArH), 7.78 (d, *J* = 8.1 Hz,



1 H, ArH), 7.95 (d, *J* = 7.3 Hz, 1 H, Hpyr), 8.01 (d, *J* = 8.3 Hz, 1 H, ArH), 8.77 (s, 1 H, Hpyr),

14.43 (s, 1 H, NH). ¹³C NMR (100 MHz, DMSO-*d*₆): δ = 44.1, 115.4, 120.2, 120.8, 121.8, 123.7,

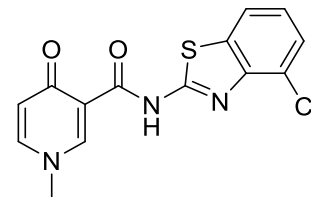
126.3, 131.9, 143.4, 147.0, 148.7, 157.0, 162.8, 176.5. IR (ATR): ν bar = 1634, 1681, 3053 cm⁻¹.

HRMS (HESI) *m/z* calcd for C₁₄H₁₁N₃O₂SNa⁺ [M + Na⁺], 308.0464; Found 308.0469.

***N*-(4-chlorobenzo[*d*]thiazol-2-yl)-1-methyl-4-oxo-1,4-dihydropyridine-3-carboxamide (2.6.7) (Table 2.1, Entry 7)**

White solid, m.p. >300 °C. Yield with **2.33/2.47** (68%/68%). ¹H NMR

(400 MHz, DMSO-*d*₆): δ = 3.88 (s, 3 H, NCH₃), 6.68 (d, *J* = 7.3 Hz, 1 H, Hpyr), 7.32 (t, *J* = 7.8 Hz, 1 H, ArH), 7.53–7.56 (dd, *J* = 8.0 Hz, *J* =

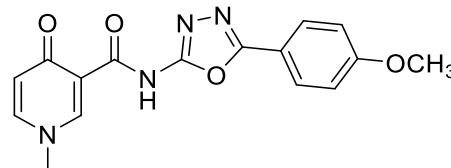


1.0 Hz, 1 H, ArH), 7.94–7.97 (dd, *J* = 7.3 Hz, *J* = 2 Hz, 1 H, Hpyr), 7.98–8.00 (dd, *J* = 8.0 Hz, *J* = 1 Hz, 1 H, ArH), 8.78 (d, *J* = 2 Hz, 1 H, Hpyr), 14.57 (s, 1 H, NH). ¹³C NMR (100 MHz, DMSO-*d*₆): δ = 44.2, 115.2, 120.3, 121.0, 124.6 (2xC), 126.4, 133.5, 143.5, 145.6, 147.1, 158.0, 163.1, 176.5. IR (ATR): ν bar = 1637, 1686, 3054 cm⁻¹. HRMS (HESI) *m/z* calcd for C₁₄H₁₀ClN₃O₂SNa⁺ [M + Na⁺], 342.0075; Found 342.0074.

***N*-(5-(4-methoxyphenyl)-1,3,4-oxadiazol-2-yl)-1-methyl-4-oxo-1,4-dihydropyridine-3-carboxamide (2.6.8) (Table 2.1, Entry 8)**

White solid, m.p. 276-277 °C. Yield with **2.33/2.47**

(88%/88%). ¹H NMR (400 MHz, DMSO-*d*₆): δ = 3.85 (s, 3 H, NCH₃), 3.88 (s, 3 H, OCH₃), 6.67 (d, *J* = 7.2 Hz, 1 H,

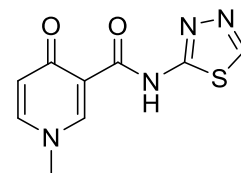


Hpyr), 7.15 (d, AA'BB', *J*_{AB} = 8.2 Hz, 2 H, ArH), 7.90 (d, AA'BB', *J*_{A'B'} = 8.2 Hz, 2 H, ArH), 7.97 (d, *J* = 6.6 Hz, 1 H, Hpyr), 8.72 (s, 1 H, Hpyr), 14.36, (s, 1 H, NH). ¹³C NMR (100 MHz, DMSO-*d*₆): δ = 44.2, 55.5, 114.9, 115.8, 115.9, 120.0, 127.9, 143.6, 147.0, 156.5, 160.6, 161.1, 161.8, 176.4 IR (ATR): ν bar = 1656, 1704, 2916, 2958, 3066, 3082 cm⁻¹. HRMS (HESI) *m/z* calcd for C₁₆H₁₄N₄O₄Na⁺ [M + Na⁺], 349.0913; Found 349.0908.

1-methyl-4-oxo-*N*-(1,3,4-thiadiazol-2-yl)-1,4-dihydropyridine-3-carboxamide (2.6.9) (Table 2.1, Entry 9)

White solid, m.p. >300 °C. Yield with **2.33/2.47** (92%/96%). ¹H NMR (400

MHz, DMSO-*d*₆): δ = 3.87 (s, 3 H, NCH₃), 6.66 (d, *J* = 7.6 Hz, 1 H, Hpyr),



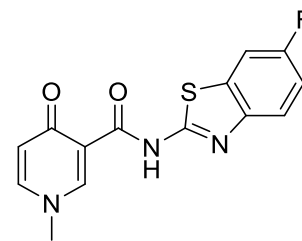
7.95–7.97 (dd, $J = 7.3$ Hz, $J = 1.6$ Hz, 1 H, Hpyr), 8.78 (d, $J = 1.7$ Hz, 1 H, Hpyr), 9.21 (s, 1 H, ArH), 14.61 (s, 1 H, NH). ^{13}C NMR (400 MHz, DMSO- d_6): $\delta = 44.1, 115.0, 120.1, 143.4, 147.0, 149.2, 157.7, 162.3, 176.5$. IR (ATR): $\nu_{\text{bar}} = 1637, 1678, 3058, 3079$ cm^{-1} . HRMS (HESI) m/z calcd for $\text{C}_9\text{H}_8\text{N}_4\text{O}_2\text{SNa}^+$ [$\text{M} + \text{Na}^+$], 259.0260; Found 259.0265.

***N*-(6-fluorobenzo[*d*]thiazol-2-yl)-1-methyl-4-oxo-1,4-dihydropyridine-3-carboxamide**

(2.6.10) (Table 2.1, Entry 10)

White solid, m.p. >300 °C (dec). Yield with **2.33/2.47** (68%/68%). ^1H

NMR (400 MHz, DMSO- d_6): $\delta = 3.88$ (s, 3 H, NCH₃), 6.65 (d, $J = 7.4$ Hz, 1 H, Hpyr), 7.28–7.33 (ddd, $J = 9.3$ Hz, $J = 8.8$ Hz, $J = 2.6$ Hz, 1 H, ArH), 7.77–7.81 (m, 1 H, ArH), 7.91–7.94 (dd, $J = 8.8$ Hz, $J = 2.6$ Hz,



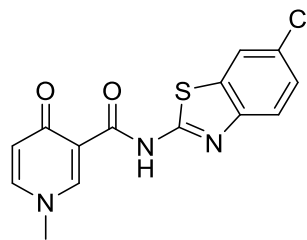
1 H, ArH), 7.95–7.97 (dd, $J = 7.5$ Hz, $J = 2.4$ Hz, 1 H, Hpyr), 8.78 (d, $J = 2.3$ Hz, 1 H, Hpyr), 14.46 (s, 1 H, NH). ^{13}C NMR (100 MHz, DMSO- d_6): $\delta = 44.1, 108.3$ (d, $^2J_{\text{CF}} = 26.9$ Hz), 114.4 (d, $^2J_{\text{CF}} = 24.7$ Hz), 115.2, 120.2, 121.8 (d, $^3J_{\text{CF}} = 9.4$ Hz), 133.1 (d, $^2J_{\text{CF}} = 11.1$ Hz), 143.4, 145.4, 147.0, 157.0 (d, $^4J_{\text{CF}} = 2.9$ Hz), 158.7 (d, $^1J_{\text{CF}} = 240.0$ Hz), 162.9, 176.5. IR (ATR): $\nu_{\text{bar}} = 1632, 1672, 3061$ cm^{-1} . HRMS (HESI) m/z calcd for $\text{C}_{14}\text{H}_{10}\text{FN}_3\text{O}_2\text{SNa}^+$ [$\text{M} + \text{Na}^+$], 326.0370; Found 326.0372.

***N*-(6-chlorobenzo[*d*]thiazol-2-yl)-1-methyl-4-oxo-1,4-dihydropyridine-3-carboxamide**

(2.6.12) (Table 2.1, Entry 12)

White solid m.p. >300 °C. Yield with **2.33/2.47** (85%/84%). ^1H NMR

(400 MHz, DMSO- d_6): $\delta = 3.88$ (s, 3 H, NCH₃), 6.66 (d, $J = 7.1$ Hz, 1 H, Hpyr), 7.46–7.49 (dd, $J = 8.1$ Hz, $J = 1.6$ Hz, 1 H, ArH), 7.78 (d, $J = 8.5$ Hz, 1 H, ArH), 7.94–7.96 (dd, $J = 7.4$ Hz, $J = 1.9$ Hz, 1 H,



Hpyr), 8.16 (s, 1 H, ArH), 8.77 (s, 1 H, Hpyr), 14.52 (s, 1 H, NH). ^{13}C NMR (100 MHz, DMSO-

d_6): $\delta = 44.2, 115.2, 120.2, 121.6, 122.0, 126.7, 127.8, 133.6, 143.5, 147.1, 147.6, 157.8, 163.0, 176.5$. IR (ATR): $\nu_{\text{bar}} = 1638, 1686, 2917, 3057 \text{ cm}^{-1}$. HRMS (HESI) m/z calcd for $\text{C}_{14}\text{H}_{10}\text{ClN}_3\text{O}_2\text{SNa}^+ [\text{M} + \text{Na}^+]$, 342.0075; Found 342.0075.

***N*-(6-bromobenzo[*d*]thiazol-2-yl)-1-methyl-4-oxo-1,4-dihydropyridine-3-carboxamide**

(2.6.13) (Table 2.1, Entry 13)

White solid, m.p. $>300 \text{ }^\circ\text{C}$. Yield with **2.33/2.47** (82%/86%). ^1H NMR

(400 MHz, $\text{DMSO-}d_6$): $\delta = 3.88$ (s, 3 H, NCH_3), 6.66 (d, $J = 6.9 \text{ Hz}$, 1

H, Hpyr), 7.59 (d, $J = 8.2 \text{ Hz}$, 1 H, ArH), 7.72 (d, $J = 8.2 \text{ Hz}$, 1 H,

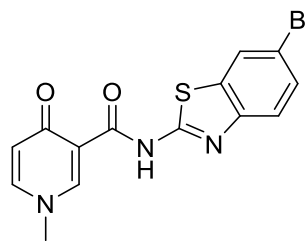
ArH), 7.95 (d, $J = 7.4 \text{ Hz}$, 1 H, Hpyr), 8.28 (s, 1 H, ArH), 8.77 (s, 1 H,

Hpyr), 14.53 (s, 1 H, NH). ^{13}C NMR (100 MHz, $\text{DMSO-}d_6$): $\delta = 44.1, 115.2, 115.7, 120.2, 122.4,$

124.4, 129.3, 134.1, 143.5, 147.0, 147.9, 157.8, 163.0, 176.5. IR (ATR): $\nu_{\text{bar}} = 1687, 3056,$

3084 cm^{-1} . HRMS (HESI) m/z calcd for $\text{C}_{14}\text{H}_{10}\text{BrN}_3\text{O}_2\text{SH}^+ [\text{M} + \text{H}^+]$, 363.9750; Found

363.9749.



***N*-(5-(2-chlorophenyl)-1,3,4-oxadiazol-2-yl)-1-methyl-4-oxo-1,4-dihydropyridine-3-**

carboxamide (2.6.14) (Table 2.1, Entry 14)

White solid, m.p. $220\text{--}222 \text{ }^\circ\text{C}$. Yield with **2.33/2.47** (66%/65%).

^1H NMR (400 MHz, $\text{DMSO-}d_6$): $\delta = 3.88$ (s, 3 H, NCH_3), 6.68 (d, J

$= 7.3 \text{ Hz}$, 1 H, Hpyr), 7.56–7.59 (td, $J = 7.5 \text{ Hz}$, $J = 1.2 \text{ Hz}$, 1 H,

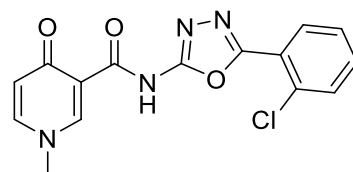
ArH), 7.62–7.66 (td, $J = 7.6 \text{ Hz}$, $J = 1.4 \text{ Hz}$, 1 H, ArH), 7.71 (d, $J = 7.9 \text{ Hz}$, 1 H, ArH), 7.95–7.98

(m, 2 H, ArH, Hpyr), 8.74 (d, $J = 2 \text{ Hz}$, 1 H, Hpyr), 14.55 (s, 1 H, NH). ^{13}C NMR (100 MHz,

$\text{DMSO-}d_6$): $\delta = 44.2, 115.8, 120.0, 122.6, 127.9, 131.1$ (2xC), 131.6, 133.0, 143.7, 147.1, 157.3,

158.5, 161.0, 176.4. IR (ATR): $\nu_{\text{bar}} = 1602, 1645, 3052 \text{ cm}^{-1}$. HRMS (HESI) m/z calcd for

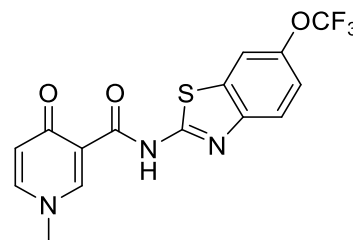
$\text{C}_{15}\text{H}_{11}\text{ClN}_4\text{O}_3\text{Na}^+ [\text{M} + \text{Na}^+]$, 353.0412; Found 353.0418.



1-methyl-4-oxo-N-(6-(trifluoromethoxy)benzo[d]thiazol-2-yl)-1,4-dihydropyridine-3-carboxamide (2.6.15) (Table 2.1, Entry 15)

White solid, m.p. >300 °C (dec). Yield with **2.33/2.47** (67%/67%).

¹H NMR (400 MHz, DMSO-*d*₆): δ = 3.88 (s, 3 H, NCH₃), 6.67 (d, *J* = 7.0 Hz, 1 H, Hpyr), 7.43–7.46 (dd, *J* = 8.8 Hz, *J* = 2.0 Hz, 1 H, ArH), 7.86 (d, *J* = 8.6 Hz, 1 H, ArH), 7.95–7.98 (dd, *J* = 7.2 Hz, *J*

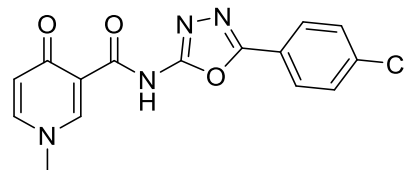


= 2 Hz, 1 H, Hpyr), 8.16 (d, *J* = 2 Hz, 1 H, ArH), 8.78 (d, *J* = 2 Hz, 1 H, Hpyr), 14.56 (s, 1 H, NH). ¹³C NMR (100 MHz, DMSO-*d*₆): δ = 44.1, 120.2, 120.2 (q, ¹*J*_{CF} = 255.6 Hz), 121.8, 124.0, 133.1, 143.5, 144.2 (2xC), 143.5, 147.1, 147.8, 158.5, 163.0, 176.5. ¹⁹F NMR (376 MHz, DMSO-*d*₆): δ = -59.98. IR (ATR): ν bar = 1637, 1681, 3063 cm⁻¹. HRMS (HESI) *m/z* calcd for C₁₅H₁₀F₃N₃O₃SH⁺ [M + H⁺], 370.0465; Found 370.0463.

N-(5-(4-chlorophenyl)-1,3,4-oxadiazol-2-yl)-1-methyl-4-oxo-1,4-dihydropyridine-3-carboxamide (2.6.16) (Table 2.1, Entry 16)

White solid, m.p. 225-226 °C. Yield with **2.33/2.47**

(83%/82%). ¹H NMR (400 MHz, DMSO-*d*₆): δ = 3.88 (s, 3 H, NCH₃), 6.68 (d, *J* = 7.5 Hz, 1 H, Hpyr), 7.68 (d, AA'BB', *J*_{AB} =



8.3 Hz, 2 H, ArH), 7.96 (d, AA'BB', *J*_{A'B'} = 8.3 Hz, 2 H, ArH), 7.96 (d, *J* = 8 Hz, 1 H, Hpyr), 8.72 (s, 1 H, Hpyr), 14.52 (s, 1 H, NH). ¹³C NMR (100 MHz, DMSO-*d*₆): δ = 44.2, 115.8, 120.0, 122.4, 127.8, 129.6, 136.3, 143.7, 147.0, 157.1, 159.7, 161.0, 176.4. IR (ATR): ν bar = 1650, 1703, 3061, 3403 cm⁻¹. HRMS (HESI) *m/z* calcd for C₁₅H₁₁ClN₄O₃Na⁺ [M + Na⁺], 353.0412; Found 353.0410.

1-methyl-4-oxo-*N*-(6-(trifluoromethyl)benzo[*d*]thiazol-2-yl)-1,4-dihydropyridine-3-carboxamide (2.6.17) (Table 2.1, Entry 17)

White solid, m.p. >300 °C. Yield with **2.33/2.47** (69%/63%). ¹H

NMR (400 MHz, DMSO-*d*₆): δ = 3.89 (s, 3H, NCH₃), 6.67 (d, 1 H,

J = 7.0 Hz, 1 H, Hpyr), 7.76 (d, *J* = 7.5 Hz, 1 H, ArH), 7.90 (d, *J* =

8.7 Hz, 1 H, ArH), 7.97 (d, *J* = 7.0 Hz, 1 H, Hpyr), 8.53 (s, 1 H,

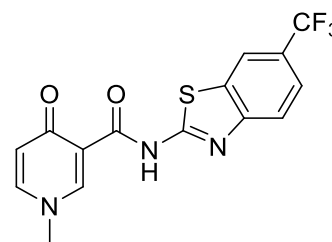
ArH), 8.79 (s, 1 H, Hpyr), 14.66 (s, 1 H, NH). ¹³C NMR (100 MHz, DMSO-*d*₆): δ = 44.1, 115.0,

120.0, 120.0 (q, ³*J*_{CF} = 4.3 Hz), 121.1, 123.0 (q, ³*J*_{CF} = 4.3 Hz), 123.7 (q, ²*J*_{CF} = 31.2 Hz), 124.5

(q, ¹*J*_{CF} = 274.0 Hz), 132.4, 143.5, 147.1, 151.5, 160.2, 163.2, 176.5. ¹⁹F NMR (376 MHz,

DMSO-*d*₆): δ = -59.43. IR (ATR): ν bar = 1638, 1682, 3060 cm⁻¹. HRMS (HESI) *m/z* calcd for

C₁₅H₁₀F₃N₃O₂SH⁺ [M + H⁺], 354.0519; Found 354.0516.



1-methyl-4-oxo-*N*-(6-((trifluoromethyl)thio)benzo[*d*]thiazol-2-yl)-1,4-dihydropyridine-3-carboxamide (2.6.18) (Table 2.1, Entry 18)

White solid, m.p. >300 °C (dec). Yield with **2.33/2.47** (53%/53%).

¹H NMR (400 MHz, DMSO-*d*₆): δ = 3.88 (s, 3 H, NCH₃), 6.67 (d, *J*

= 7.6 Hz, 1 H, Hpyr), 7.73–7.75 (dd, *J* = 7.8 Hz, *J* = 1.9 Hz, 1 H,

ArH), 7.89 (d, *J* = 8.3 Hz, 1 H, ArH), 7.96–7.98 (dd, *J* = 7.2 Hz, *J*

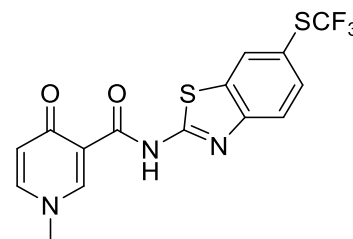
= 1.9 Hz, 1 H, Hpyr), 8.50 (d, *J* = 2 Hz, 1 H, ArH), 8.78 (d, *J* = 1.8 Hz, 1 H, Hpyr), 14.65 (s, 1 H,

NH). ¹³C NMR (100 MHz, DMSO-*d*₆): δ = 44.1, 115.1, 116.8, 120.2, 121.7, 130.7, 132.8 (q, *J* =

306.3 Hz), 133.2, 134.2, 143.5, 147.1, 151.0, 159.9, 163.1, 176.5. ¹⁹F NMR (376 MHz, DMSO-

*d*₆): δ = -59.98. IR (ATR): ν bar = 1637, 1682, 1758, 3059 cm⁻¹. HRMS (HESI) *m/z* calcd for

C₁₅H₁₀F₃N₃O₂S₂H⁺ [M + H⁺], 386.0239; Found 386.0243.



N-(5-bromobenzo[*d*]thiazol-2-yl)-1-methyl-4-oxo-1,4-dihydropyridine-3-carboxamide

(2.6.19) (Table 2.11, Entry 19)

White solid, m.p. >300 °C. Yield with **2.33/2.47** (80%/81%). ¹H

NMR (400 MHz, DMSO-*d*₆): δ = 3.88 (s, 3 H, NCH₃), 6.66 (d, *J* =

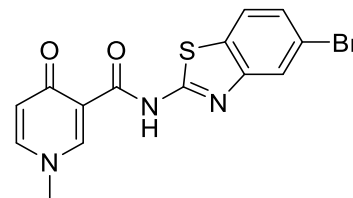
7.2 Hz, 1 H, Hpyr), 7.48 (d, *J* = 8.2 Hz, 1 H, ArH), 7.96 (d, *J* = 6.7

Hz, 1 H, Hpyr), 7.98 (s, 1 H, ArH), 7.99 (s, 1 H, ArH), 8.78 (s, 1 H, Hpyr), 14.55 (s, 1 H, NH).

¹³C NMR (100 MHz, DMSO-*d*₆): δ = 44.1, 115.2, 119.0, 120.2, 123.1, 123.7, 126.4, 131.2,

143.5, 147.1, 150.3, 158.7, 163.0, 176.5. IR (ATR): ν_{bar} = 1644, 1679, 2850, 3047, 3417 cm⁻¹.

HRMS (HESI) *m/z* calcd for C₁₄H₁₀BrN₃O₂SH⁺ [M + H⁺], 363.9750; Found 363.9748.



S-Benzyl 1-methyl-4-oxo-1,4-dihydropyridine-3-carbothioate (**2.33**)

Benzyl mercaptan **2.39** (0.46 mL, 3.9 mmol, 1.2 equiv) was added to a

suspension of carboxylic acid **2.37** (500 mg, 3.26 mmol, 1 equiv),

TFFH (861 mg, 3.26 mmol, 1 equiv) and DIEA (2.8 mL, 16.3 mmol, 5

equiv) in MeCN (10 mL), and the mixture was stirred under N₂ overnight at r.t. The mixture was

subsequently concentrated, and the residue was taken-up in sat'd aqueous NaHCO₃ and extracted

with DCM. The combined organic layers were washed with HCl 0.5 N, sat'd aqueous NaHCO₃

and brine, then dried over Na₂SO₄ and concentrated. The solid residue was washed with ether to

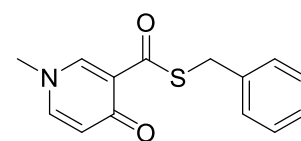
remove impurities and dried under vacuum. Thioester **2.33** was obtained as yellow crystalline

solid (845 mg, 95%). M.p.: 163-164 °C. ¹H NMR (400 MHz, CD₃CN): δ = 3.67 (s, 3 H, NCH₃),

4.14 (s, 2 H, CH₂), 6.36 (d, *J* = 7.5 Hz, 1 H, Hpyr), 7.21-7.24 (m, 1 H, ArH), 7.28-7.32 (m, 2 H,

ArH), 7.35-7.37 (m, 2 H, ArH), 7.46-7.49 (dd, *J* = 7.4 Hz, *J* = 2.2 Hz, 1 H, Hpyr), 8.27 (d, *J* =

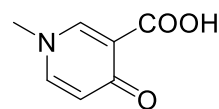
2.4 Hz, 1 H, Hpyr). ¹³C NMR (100 MHz, CD₃CN): δ = 34.1, 45.1, 123.2, 124.2, 128.2, 129.8,



130.3, 140.3, 142.5, 146.4, 176.5, 190.0. IR (ATR): ν bar = 1566, 1650, 3056 cm^{-1} . HRMS (HESI) m/z calcd for $\text{C}_{14}\text{H}_{13}\text{NO}_2\text{SNa}^+$ [$\text{M} + \text{Na}^+$], 282.0559; Found 282.0561.

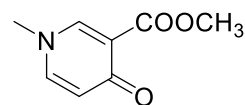
1-methyl-4-oxo-1,4-dihydropyridine-3-carboxylic acid (2.37)

Ester **2.36** (8 g, 47.80 mmol) is dissolved in a mixture of MeOH/THF/ H_2O 2:2:1 (325 ml in total). To this solution LiOH (3.44 g, 143.60 mmol, 3 equiv) and the resulting suspension is stirred overnight at room temperature. The solvents are evaporated and water is added to the residue, followed by the dropwise addition of HCl 6 N under ice. The resulting precipitate is left overnight in the fridge and then filtered and washed with water to afford an off-white solid which corresponds to carboxylic acid **2.37** (5.43 g, 73%). M.p.: 235-237 °C. ^1H NMR ($\text{DMSO}-d_6$): δ = 3.88 (s, 3 H, NCH_3), 6.75 (d, J = 7.4 Hz, 1 H, Hpyr), 8.06-8.09 (dd, J = 7.4 Hz, J = 2.2 Hz, 1 H, Hpyr), 8.70 (s, J = 2.3 Hz, 1 H, Hpyr). ^1H NMR data match with the data reported.⁵⁹



1-methyl-4-oxo-1,4-dihydropyridine-3-carboxylate (2.36)

Methylester **2.35** (2 g, 12 mmol) was dissolved in MeCN (16 ml) and to this solution a substoichiometric amount of methyl iodide (0.2 ml, 3.00 mmol, 0.25 equiv) was added. The mixture was transferred to a microwave vial and put to stir at 120 °C under microwave conditions for 1 h. The solvent was then removed and an oily residue was obtained. Yield (2 g, >98%). ^1H NMR (CDCl_3): δ = 3.69 (s, 3 H, NCH_3), 3.83 (s, 3 H, OCH_3), 6.44 (d, J = 7.5 Hz, 1 H, Hpyr), 7.21–7.24 (dd, J = 7.7 Hz, J = 2.5 Hz, 1 H, Hpyr), 8.12 (s, 1 H, Hpyr). ^{13}C NMR (CDCl_3): δ = 44.9, 51.9, 118.1, 122.7, 139.8, 146.6, 165.3, 174.8. IR (ATR): ν bar = 1186, 1645, 1717, 2950, 3013, 3053, 3094 cm^{-1} . HRMS (HESI) m/z calcd for $\text{C}_8\text{H}_9\text{NO}_3\text{H}^+$ [$\text{M} + \text{H}^+$], 168.0655; Found 168.0657.

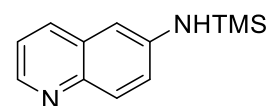


General procedure for the N-silylation reaction of amines 2.40

The *N*-silylation of amines was adapted from reference.¹⁰ *N*-silylated amines **2.40.1-2.40.19** were prepared by reaction of the requisite heteroaromatic amine precursor in neat TMSCN (1 mL of TMSCN per mmol of the amine) with stirring under nitrogen at 70 °C. The *N*-silylation times for each amine are also shown in Table 1. The excess TMSCN was removed under high vacuum and the derived *N*-silylated amine was used without purification in the amidation reaction. The percent conversion of each amine to its *N*-silylated derivative was determined by ¹H NMR spectroscopy (CD₃CN); passed through a basic alumina column prior to use). The ¹H NMR data for compounds **2.40.1**, **2.40.3**, **2.40.4**, **2.40.6**, **2.40.7**, **2.40.9**, **2.40.11** and **2.40.14** were identical to that described in literature.^{12, 120}

***N*-(trimethylsilyl)quinolin-6-amine (2.40.2) (Table 2.1, Entry 2)**

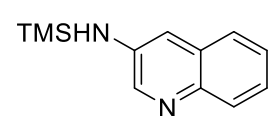
Yellow-brown solid; 95% silylation based on ¹H NMR; ¹H NMR (400 MHz, CD₃CN): δ = 0.31 (s, 3 H), 4.53 (s, 1 H), 6.93 (d, *J* = 2.8 Hz, 1 H),



7.20 – 7.23 (dd, *J* = 9 Hz, *J* = 2.7 Hz, 1 H), 7.25 – 7.29 (dd, *J* = 8.3 Hz, *J* = 4.1 Hz, 1 H), 7.77 (d, *J* = 8.9 Hz, 1 H), 7.96 – 7.98 (dd, *J* = 8.4 Hz, *J* = 1.5 Hz, 1 H), 8.53-8.55 (m, 1 H).

***N*-(trimethylsilyl)quinolin-3-amine (2.40.5) (Table 2.1, Entry 5)**

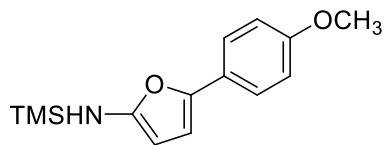
Off-white solid (100% silylation based on ¹H NMR). ¹H NMR (400 MHz, CD₃CN): δ = 0.32 (s, 3 H, 3xCH₃), 4.56 (s, 1 H, NH), 7.26 (d, *J* = 2.8 Hz,



1 H, ArH), 7.36–7.43 (m, 2 H, ArH), 7.65–7.68 (m, 1 H, ArH), 7.83–7.85 (m, 1 H, ArH), 8.48 (d, *J* = 2.9 Hz, 1 H, ArH).

5-(4-methoxyphenyl)-*N*-(trimethylsilyl)-1,3,4-oxadiazol-2-amine (2.40.8) (Table 2.1, Entry 8)

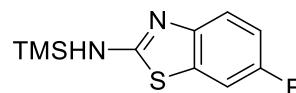
Off-white solid (90% silylation based on ¹H NMR). ¹H NMR



(400 MHz, CD₃CN): δ = 0.32 (s, 9 H, 3xCH₃), 3.84 (s, 3H, OCH₃), 5.51 (s, 1 H, NH), 7.02 (d, AA'BB', J_{AB} = 8.6 Hz, 2 H, ArH), 7.79 (d, AA'BB', $J_{A'B'}$ = 8.6 Hz, 2 H, ArH).

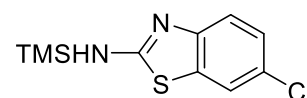
6-fluoro-*N*-(trimethylsilyl)benzo[*d*]thiazol-2-amine (2.40.10) (Table 2.1, Entry 10)

White solid (95% silylation based on ¹H NMR). ¹H NMR (400 MHz, CD₃CN): δ = 0.32 (s, 3 H, 3xCH₃), 5.84 (s, 1 H, NH), 7.00–7.05 (ddd, J = 9.4 Hz, J = 8.9 Hz, J = 2.6 Hz, 1 H, ArH), 7.36–7.41 (m, 2 H).



6-chloro-*N*-(trimethylsilyl)benzo[*d*]thiazol-2-amine (2.40.12) (Table 2.1, Entry 12)

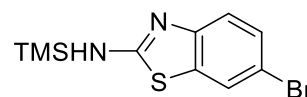
Off-white solid (100% silylation based on ¹H NMR). ¹H NMR (400 MHz, CD₃CN): δ = 0.32 (s, 3 H, 3xCH₃), 5.94 (s, 1 H, NH), 7.21–7.24



(dd, J = 8.4 Hz, J = 2.1 Hz, 1 H, ArH), 7.36 (d, J = 8.5 Hz, 1 H, ArH), 7.62 (d, J = 2.2 Hz, 1 H, ArH).

6-bromo-*N*-(trimethylsilyl)benzo[*d*]thiazol-2-amine (2.40.13) (Table 2.1, Entry 13)

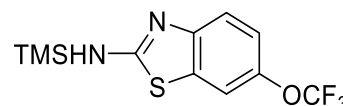
White solid (95% silylation based on ¹H NMR). ¹H NMR (400 MHz, CD₃CN): δ = 0.32 (s, 3 H, 3xCH₃), 5.95 (s, 1 H, NH), 7.30 (d, J = 8.5



Hz, 1 H, ArH), 7.35–7.38 (dd, J = 8.3 Hz, J = 2.0 Hz, 1 H, ArH), 7.75 (d, J = 2.0 Hz, 1 H, ArH).

6-(trifluoromethoxy)-*N*-(trimethylsilyl)benzo[*d*]thiazol-2-amine (2.40.15) (Table 2.1, Entry 15)

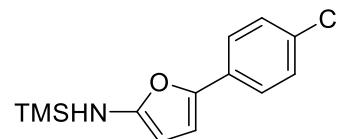
Brown-oil (95% silylation based on ¹H NMR). ¹H NMR (400 MHz, CD₃CN): δ = 0.33 (s, 3 H, 3xCH₃), 5.97 (s, 1 H, NH), 7.16–7.19 (dd,



J = 8.6 Hz, J = 2.4 Hz, 1 H, ArH), 7.43 (d, J = 8.8 Hz, 1 H, ArH), 7.59 (d, J = 2.2 Hz, 1 H, ArH).

5-(4-chlorophenyl)-*N*-(trimethylsilyl)-1,3,4-oxadiazol-2-amine

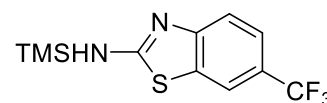
(2.40.16) (Table 2.1, Entry 16) Off-white solid (80% silylation



based on ^1H NMR). ^1H NMR (400 MHz, CD_3CN): δ = 0.33 (s, 9 H, $3\times\text{CH}_3$), 5.57 (s, 1 H, NH), 7.51 (d, AA'BB', J_{AB} = 8.5 Hz, 2 H, ArH), 7.83 (d, AA'BB', $J_{A'B'}$ = 8.5 Hz, 2 H, ArH).

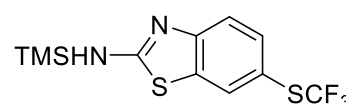
6-(trifluoromethyl)-*N*-(trimethylsilyl)benzo[*d*]thiazol-2-amine (2.40.17) (Table 2.1, Entry 17)

Brown oil (100% silylation based on ^1H NMR). ^1H NMR (400 MHz, $\text{CD}_3\text{CN}-d_3$): δ = 0.34 (s, 3 H, $3\times\text{CH}_3$), 6.15 (s, 1 H, NH), 7.50–7.55 (m, 2 H, ArH), 7.96 (s, 1 H, ArH).



6-((trifluoromethyl)thio)-*N*-(trimethylsilyl)benzo[*d*]thiazol-2-amine (2.40.18) (Table 2.1, Entry 18)

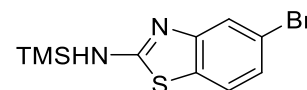
Brown-oil (100% silylation based on ^1H NMR). ^1H NMR (400 MHz, CD_3CN): δ = 0.34 (s, 3 H, $3\times\text{CH}_3$), 6.13 (s, 1 H, NH), 7.47 (d,



J = 8.2 Hz, 1 H, ArH), 7.54–7.56 (dd, J = 8.5 Hz, J = 1.8 Hz, 1 H, ArH), 7.96 (d, J = 1.8 Hz, 1 H, ArH).

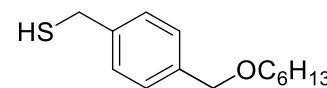
5-bromo-*N*-(trimethylsilyl)benzo[*d*]thiazol-2-amine (2.40.19) (Table 2.1, Entry 19)

White solid (95% silylation based on ^1H NMR). ^1H NMR (400 MHz, CD_3CN): δ = 0.32 (s, 3 H, $3\times\text{CH}_3$), 6.03 (s, 1 H, NH), 7.18–7.21 (dd, J = 8.3 Hz, J = 2.0 Hz, 1 H, ArH), 7.52 (d, J = 8.4 Hz, 1 H, ArH), 7.58 (d, J = 2.0 Hz, 1 H, ArH).



(4-((hexyloxy)methyl)phenyl)methanethiol (2.41)

From thioester 2.46. To a solution of thioester **2.46** (280 mg, 1 mmol, 1 equiv) in MeOH (3 mL) was added K_2CO_3 (152 mg, 1.1



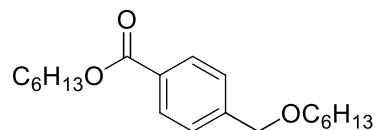
mmol, 1.1 equiv), and the mixture was stirred at rt under N_2 for 0.5 h. The reaction mixture was then acidified with HCl (aq.) 1N to pH 3-4 and concentrated under vacuum. The residue was dissolved in heptane and the resulting solution was washed with water, dried over Na_2SO_4 and

concentrated to afford benzyl mercaptan **2.41** as a yellowish liquid (185 mg, 78%). ¹H NMR (400 MHz, CDCl₃): δ = 0.89 (t, *J* = 7.0 Hz, 3 H, CH₃), 1.26–1.40 (m, 6 H, 3xCH₂), 1.57–1.64 (m, 2 H, CH₂), 1.74 (t, *J* = 7.2 Hz, 1 H, SH), 3.46 (t, *J* = 6.5 Hz, 2 H, CH₂O), 3.74 (d, *J* = 7.5 Hz, 2 H, ArCH₂S), 4.48 (s, 2 H, ArCH₂O), 7.30 (s, 4 H, ArH). ¹³C NMR (100 MHz, CDCl₃): δ = 14.3, 22.8, 26.1, 28.9, 29.9, 31.9, 70.8, 72.7, 128.2, 128.2, 137.8, 140.6. HRMS (HESI) *m/z* calcd for C₁₄H₂₂OSNa⁺ [*M* + Na⁺], 261.1289; Found 261.1281.

From disulfide 2.48 Adapting a literature procedure,¹¹⁹ disulfide **2.48** (360 mg, 0.76 mmol, 1 equiv) was added dropwise over 15 min to a stirred suspension of lithium aluminum hydride (115 mg, 3.04 mmol, 4 equiv) in dry Et₂O (10 mL), which was maintained under nitrogen at 0 °C. The mixture was refluxed for 20 min, then cooled to 0 °C prior to the addition of water to quench the reaction. The biphasic mixture was acidified with H₂SO₄ (aq.) 15% and the ether layer was separated and washed with water. The combined aqueous layers were saturated with sodium chloride and extracted with ether. The combined ether layers were washed with water and brine, dried over anhydrous Na₂SO₄, and concentrated, affording benzyl mercaptan **2.41** in essentially quantitative yield.

Hexyl 4-((hexyloxy)methyl) benzoate (**2.43**)

Sodium (2.5 g, 109 mmol, 10 equiv) was added to anhydrous hexanol (30 mL) and the mixture was stirred under nitrogen for

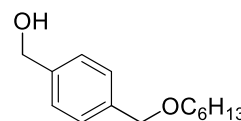


48 h at 90 °C. To this reaction, methyl 4-(bromo)methyl benzoate (**2.42**) (2.5 g, 10.9 mmol, 1 equiv) was subsequently added, and the resulting mixture was stirred for 4 h at 40 °C. The cooled reaction was then diluted with toluene (30 mL) and quenched by addition of HCl (aq.) 6 N. The organic-aqueous layers were separated and the acidic aqueous layer was extracted with toluene. The combined organic layers were dried over Na₂SO₄ and concentrated. The residue was

silica flash column chromatographed (Heptane/EtOAc 97:3), affording ester **2.43** as a yellow-orange liquid (2.625 g, 75%). ^1H NMR (400 MHz, CDCl_3): δ = 0.89 (t, J = 7 Hz, 6 H, $2\times\text{CH}_3$), 1.30–1.46 (m, 12 H, $2\times 3\times\text{CH}_2$), 1.59–1.66 (m, 2 H, $2\times\text{CH}_2$), 1.73–1.79 (m, 2 H, $2\times\text{CH}_2$), 3.48 (t, J = 6.8 Hz, 2 H, CH_2O), 4.31 (t, J = 6.6 Hz, 2 H, ArCH_2O), 4.55 (s, 2 H, CH_2OCO), 7.40 (d, AA'BB', J_{AB} = 8.1 Hz, 2 H, ArH), 8.01 (d, AA'BB', $J_{A'B'}$ = 8.1 Hz, 2 H, ArH). ^{13}C NMR (100 MHz, CDCl_3): δ = 14.2, 14.3, 22.8, 22.8, 25.9, 26.1, 28.9, 29.9, 31.7, 31.9, 65.3, 71.1, 72.5, 127.3, 129.8, 144.2, 166.8. IR (ATR): ν bar = 1718, 2858, 2929 cm^{-1} . HRMS (HESI) m/z calcd for $\text{C}_{20}\text{H}_{32}\text{O}_3\text{H}^+$ [$\text{M} + \text{H}^+$], 321.2424; Found 321.2419.

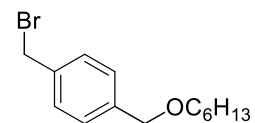
4-((hexyloxy)methyl)phenyl)methanol (2.44)

A solution of ester **2.43** (640 mg, 2 mmol, 1 equiv) in 2-Me-THF (5 mL) was added to a suspension of LiAlH_4 (305 mg, 8 mmol, 4 equiv) in THF (10 mL), and the mixture was stirred for 4 h at room temperature under N_2 . The reaction was quenched by the addition of H_2O (0.3 mL), aqueous NaOH (aq.) 15% (0.3 mL) and H_2O (0.9 mL) and the solid materials formed were removed by suction filtration. The filtrate was washed with brine, dried over Na_2SO_4 and evaporated under high vacuum to afford alcohol **2.44** as a colourless liquid (342 mg, 77%). ^1H NMR (400 MHz, CDCl_3): δ = 0.89 (t, J = 7.0 Hz, 3 H, CH_3), 1.26–1.40 (m, 6 H, $3\times\text{CH}_2$), 1.57–1.64 (m, 2 H, CH_2), 1.94 (s, 1 H, OH), 3.45 (t, J = 6.6 Hz, 2 H, CH_2O), 4.49 (s, 2 H, ArCH_2O), 4.66 (s, 2 H, ArCH_2OH), 7.33 (s, 4 H, ArH). ^{13}C NMR (100 MHz, CDCl_3): δ = 14.3, 22.8, 26.1, 29.9, 31.9, 65.3, 70.7, 72.8, 127.2, 128.0, 138.3, 140.4. IR (ATR): ν bar = 2856, 2930, 3343 cm^{-1} . HRMS (HESI) m/z calcd for $\text{C}_{14}\text{H}_{22}\text{O}_2\text{Na}^+$ [$\text{M} + \text{Na}^+$], 245.1512; Found 245.1512.



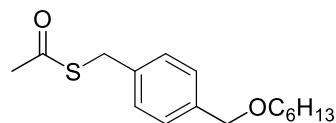
1-(bromomethyl)-4-((hexyloxy)methyl)phenyl)-benzene (2.45)

Synthesized according to reference.¹¹⁶ A solution of thionylbromide (0.77 mL, 9.9 mmol, 1.1 equiv) in DCM (11 mL) was added to a solution of alcohol **2.44** (2 g, 9 mmol, 1 equiv) in DCM (190 mL) under nitrogen at room temperature. The mixture was stirred overnight under nitrogen at room temperature, and then concentrated. The residue was dissolved in heptane and washed three times with water and once with sat'd NaHCO₃ (aq.). The heptane layer was dried over Na₂SO₄ and concentrated to give **2.45** as a yellowish liquid which crystallizes in the fridge (2.7 g, > 98%). ¹H NMR (400 MHz, CDCl₃): δ = 0.89 (t, J = 7.1 Hz, 3 H, CH₃), 1.30–1.40 (m, 6 H, 3xCH₂), 1.60–1.63 (m, 2 H, CH₂), 3.47 (t, J = 6.5 Hz, 2 H, CH₂O), 4.48 (s, 4 H, ArCH₂O), 7.31 (d, AA'BB', J_{AB} = 8.0 Hz, 2 H, ArH), 7.37 (d, AA'BB', $J_{A'B'}$ = 8.0 Hz, 2 H, ArH). ¹³C NMR (100 MHz, CDCl₃): δ = 14.3, 22.8, 26.1, 29.9, 31.9, 33.6, 70.9, 72.6, 128.1, 129.3, 137.1, 139.4. MS (Turbo Spray) m/z : 302.3 and 304.3 (1:1) (MNH₄⁺).



S-(4-((hexyloxy)methyl)benzyl) ethanethioate (2.46)

Synthesized according to reference.¹¹⁷ To a solution of bromide **2.45** (6.2 g, 22 mmol, 1 equiv) in 2-Me-THF (70 mL) was added thioacetic acid (1.70 ml, 24 mmol, 1.1 equiv) and K₂CO₃ (3.6 g, 26 mmol, 1.2 equiv). The reaction was stirred under N₂ for up to 6 h at room temperature and then acidified using HCl (aq.) 6 N and diluted by addition of water (40 mL). The organic-aqueous layers were separated and the aqueous layer was extracted with 2-Me-THF. The combined organic layers was washed with water, dried over Na₂SO₄ and concentrated. The residue was silica flash column chromatographed (Heptane/EtOAc 95:5), affording **2.46** as a yellow-brown liquid (3.9 g, 64%). ¹H NMR (400 MHz, CDCl₃): δ = 0.90 (t, J = 7.0 Hz, 3 H, CH₃), 1.28–1.41 (m, 6 H, 3xCH₂), 1.58–1.65 (m, 2 H, CH₂), 2.36 (s, 3 H, COCH₃), 3.47 (t, J = 6.5 Hz, 2 H, CH₂O), 4.13 (s, 2 H,

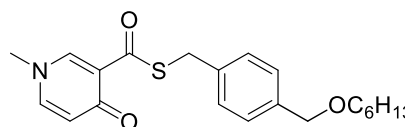


ArCH₂S), 4.48 (s, 2 H, ArCH₂O), 7.28 (s, 4 H, ArH). ¹³C NMR (100 MHz, CDCl₃): δ = 14.3, 22.8, 26.1, 29.9, 30.5, 31.9, 33.4, 70.8, 72.7, 128.1, 129.0, 137.0, 138.0, 195.3. IR (ATR): ν bar = 1690, 2928 cm⁻¹. HRMS (HESI) *m/z* calcd for C₁₆H₂₄O₂SNa⁺ [M + Na⁺], 303.1395; Found 303.1387.

S-(4-((hexyloxy)methyl)benzyl)-1-methyl-4-oxo-1,4-dihydropyridine-3-carbothioate (2.47)

Synthesized according to reference.¹¹⁷ Benzyl mercaptan **2.41**

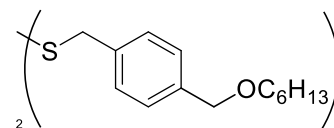
(474 mg, 1.99 mmol, 1.2 equiv) was added to a suspension of



carboxylic acid **2.37** (254 mg, 1.66 mmol, 1 equiv) and TFFH (438 mg, 1.66 mmol, 1 equiv) in MeCN (5 mL) containing DIEA (1.45 ml, 8.3 mmol, 5 equiv) and the mixture was stirred under N₂ at r.t for 16 h. The solvent was then removed and the residue was taken up in sat'd NaHCO₃ (aq.) and extracted with EtOAc. The combined organic layers were washed with HCl (aq.) 0.5 N, sat'd NaHCO₃ (aq.) and brine, then dried over Na₂SO₄ and concentrated. The residue was taken up in Et₂O and precipitation of thioester **2.47** was induced by addition of 4-5 drops of water. The ethereal layer is decanted and the precipitate was washed with a minimal volume of Et₂O (2-3 mL). Compound **2.47** was obtained as an off-white solid (312 mg, 50%). M.p.: 68-70 °C. ¹H NMR (400 MHz, CD₃CN-*d*₃): δ = 0.88 (t, *J* = 6.8 Hz, 3 H, CH₃), 1.26–1.36 (m, 6 H, 3xCH₂), 1.53–1.57 (m, 2 H, CH₂), 3.42 (t, *J* = 6.6 Hz, 2 H, CH₂O), 3.67 (s, 3 H, NCH₃), 4.12 (s, 2 H, ArCH₂S), 4.42 (s, 2 H, ArCH₂O), 6.37 (d, *J* = 7.6 Hz, 1 H, Hpyr), 7.24 (d, AA'BB', *J*_{AB} = 8.1 Hz, 2 H, ArH), 7.32 (d, AA'BB', *J*_{A'B'} = 8.1 Hz, 2 H, ArH), 7.39–7.42 (dd, *J* = 7.6 Hz, *J* = 2.4 Hz, 1 H, Hpyr), 8.22 (d, *J* = 2.4 Hz, 1 H, Hpyr). ¹³C NMR (100 MHz, CD₃CN-*d*₃): δ = 14.7, 23.7, 27.0, 30.8, 32.8, 33.8, 45.1, 71.4, 73.3, 123.1, 124.1, 129.0, 139.1, 139.3, 142.5, 146.4, 176.4, 189.9. IR (ATR): ν bar = 1101, 1270, 1718, 2858, 2929 cm⁻¹. HRMS (HESI) *m/z* calcd for C₂₁H₂₇NO₃SH⁺ [M + H⁺], 374.1784; Found 374.1781.

1,2-bis(4-((hexyloxy)methyl)benzyl)disulfane (2.48)

Yellowish orange liquid. ^1H NMR (400 MHz, CDCl_3): δ = 0.85 (t, J = 6.9 Hz, 6 H, $2\times\text{CH}_3$), 1.18–1.35 (m, 12 H, $2\times 3\times\text{CH}_2$), 1.53–1.60 (m, 4 H, $2\times\text{CH}_2$), 3.41 (t, J = 6.7 Hz, 4 H, $2\times\text{CH}_2\text{O}$), 3.57 (s, 4 H, $2\times\text{ArCH}_2\text{S}$), 4.45 (s, 4 H, $2\times\text{ArCH}_2\text{O}$), 7.18 (d, AA'BB', J_{AB} = 8.2 Hz, 4 H, ArH), 7.26 ppm (d, AA'BB', $J_{A'B'}$ = 8.2 Hz, 4 H, ArH). ^{13}C NMR (100 MHz, CDCl_3): δ = 14.2, 22.8, 26.0, 29.9, 31.9, 43.2, 70.7, 72.7, 128.0, 129.6, 136.7, 138.2. IR (ATR): ν bar = 1095, 2360, 2854, 2927 cm^{-1} . MS (Turbo Spray): m/z 497.4 [MNa^+].



6.3 Experimental data for Chapter 3

General Procedure for the Hydroaminoalkylation Reaction

To a solution of $\text{Zr}(\text{NMe}_2)_4$ (0.1 equiv, 0.05 mmol, 13.37 mg) in 200-300 μL C_6D_6 , the amine **3.5.3** (1 equiv, 0.50 mmol, 89.67 mg) was added followed by the addition of the alkene **3.10** (1.8 equiv, 0.90 mmol). The solution was then transferred quantitatively into a J-Young tube via an additional 200-300 μL C_6D_6 and placed in an oil bath at 145 $^\circ\text{C}$. The reaction times for each product are presented below. Upon the reaction completion, the J-Young seal was broken and DCM and MeOH were added to the existing solution. The quenched solution was then passed through a celite pipet and 2-3 droplets of NaOH 3M were added to the filtrate. The solvents were evaporated and ether was added to the residue. The amine was extracted in the form of its hydrochloric salt (4x10 mL) with HCl 1M and the combined aqueous layers were basified with NaOH 3M. The amine was back-extracted with ether (3x20 mL). The ethereal layers were dried over anhydrous Na_2SO_4 and evaporated to afford the product as a single or mixture of regioisomers.

Linear: 1-phenylnonan-1-amine (3.11.1)

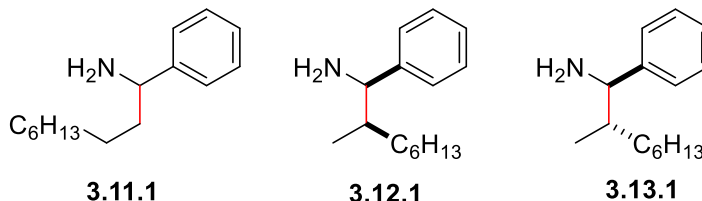
Branched: 2-methyl-1-phenyloctan-1-amine (3.12.1 and 3.13.1)

Catalyst Loading (0.1 equiv); Reaction

time: 72 h. Physical state: Yellow oil.

^1H NMR RR (**linear:branched** 1:2). ^1H

NMR DR (**3.13.1:3.12.1** 3:1). Yield



(55%). **The major branched diastereomer 3.13.1:** ^1H NMR (400 MHz, CDCl₃): δ = 0.84-0.89 (m, 6 H, CH₃CH, CH₃CH₂), 1.00-1.33 (m, 10 H, 5xCH₂), 1.62-1.72 (m, 1 H, CHCH₃), 3.78 (d, J = 6.2 Hz, 1 H, CHNH₂), 7.22-7.25 (m, 1 H, ArH), 7.28-7.33 (m, 4 H, ArH); **Clearly separated diagnostic peaks of the minor branched diastereomer 3.12.1:** ^1H NMR (400 MHz, CDCl₃): δ = 0.74 (d, J = 7.1 Hz, 3 H, CH₃CH), 0.84-0.89 (m, 3 H, CH₃CH₂), 3.69 (d, J = 7.4 Hz, 1 H, CHNH₂); **Clearly separated diagnostic peaks of the linear regioisomer 3.11.1:** ^1H NMR (400 MHz, CDCl₃): δ = 0.84-0.89 (m, 3H, CH₃), 3.86 (t, J = 7.0 Hz, 1 H, CHNH₂). **Clearly separated diagnostic peaks of the major branched diastereomer 3.13.1:** ^{13}C NMR (100 MHz, CDCl₃): δ = 14.3 (CH₃CH), 22.8 (CH₂), 27.4 (CH₂), 22.8 (CH₂), 29.7 (CH₂), 32.1 (CH₂), 40.5 (CH₃CH), 60.6 (CHNH₂), 145.9 (CCHNH₂); **Clearly separated diagnostic peaks of the minor branched diastereomer 3.12.1:** ^{13}C NMR (100 MHz, CDCl₃): δ = 16.5 (CH₃CH), 22.9 (CH₂), 27.2 (CH₂), 29.7 (CH₂), 29.9 (CH₂), 32.1 (CH₂), 40.5 (CH₃CH), 61.4 (CHNH₂), 145.6 (CCHNH₂); **Clearly separated diagnostic peaks of the linear regioisomer 3.11.1:** ^{13}C NMR (100 MHz, CDCl₃): δ = 14.3 (CH₃CH), 22.9 (CH₂), 26.8 (CH₂), 29.5 (2xCH₂), 33.0 (CH₂), 34.0 (CH₂), 39.9 (CH₂CHNH₂), 56.5 (CHNH₂), 147.1 (CCHNH₂); **Aromatic peaks (all three products):** ^{13}C NMR (100 MHz, CDCl₃): δ = 126.5, 126.8, 126.9, 127.0, 127.1, 127.3, 128.3, 128.6. HRMS (HESI) m/z calcd for C₁₅H₂₅NH⁺ [M + H⁺], 220.2065: Found 220.2057.

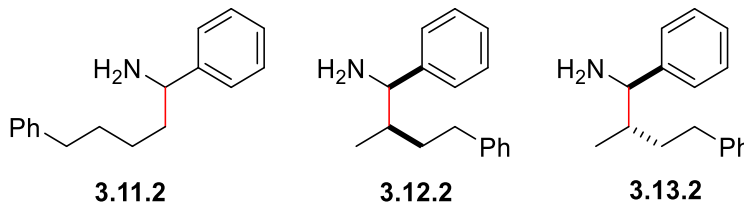
Linear: 1,5-diphenylpentan-1-amine (3.11.2)

Branched: 2-methyl-1,4-diphenylbutan-1-amine (3.12.2 and 3.13.2)

Catalyst Loading (0.1 equiv);

Reaction time: 48 h. Physical state:

Yellow oil. ^1H NMR RR



(linear:branched 1:3). ^1H NMR

DR (3.13.2:3.12.2 3:1). Yield (78%). **The major branched diastereomer 3.13.2:** ^1H NMR (400 MHz, CDCl_3): δ = 0.99 (d, J = 6.4 Hz, 3 H, CH_3CH), 1.60-1.81 (m, 5 H, $\text{CH}_2\text{CH}_2\text{Ph}$, CH_3CH), 2.49-2.61 (m, 1 H, CH_2Ph), 2.66-2.79 (m, 1 H, CH_2Ph), 3.83 (d, J = 6.7 Hz, 1 H, CHNH_2), 7.10-7.20 (m, 2 H, ArH), 7.24-7.34 (m, 8 H, ArH); **Clearly separated diagnostic peaks of the minor branched diastereomer 3.12.2:** ^1H NMR (400 MHz, CDCl_3): δ = 0.86 (d, J = 6.8 Hz, 3 H, CH_3CH), 1.89-1.98 (m, 1 H, CH_3CH), 3.76 (d, J = 6.7 Hz, 1 H, CHNH_2); **Clearly separated diagnostic peaks of the linear regioisomer 3.12.1:** ^1H NMR (400 MHz, CDCl_3): δ = 3.88 (t, J = 6.7 Hz, 1 H, CHNH_2). **Clearly separated diagnostic peaks of the major branched diastereomer 3.13.2:** ^{13}C NMR (100 MHz, CDCl_3): δ = 15.2 (CH_3CH), 33.7 ($\text{CH}_2\text{CH}_2\text{Ph}$), 35.6 ($\text{CH}_2\text{CH}_2\text{Ph}$), 40.0 (CH_3CH), 60.6 (CHNH_2), 142.7 (CCH_2), 145.6 (CCHNH_2); **Clearly separated diagnostic peaks of the minor branched diastereomer 3.12.2:** ^{13}C NMR (100 MHz, CDCl_3): δ = 16.4 (CH_3CH), 33.6 ($\text{CH}_2\text{CH}_2\text{Ph}$), 34.9 ($\text{CH}_2\text{CH}_2\text{Ph}$), 40.2 (CH_3CH), 61.2 (CHNH_2), 142.9 (CCH_2), 145.3 (CCHNH_2); **Clearly separated diagnostic peaks of the linear regioisomer 3.11.2:** ^{13}C NMR (100 MHz, CDCl_3): δ = 26.5 ($\text{CH}_2\text{CH}_2\text{CH}_2\text{Ph}$), 31.7 ($\text{CH}_2\text{CH}_2\text{Ph}$), 36.0, 39.7 ($\text{CH}_2\text{CH}_2\text{Ph}$), 56.4 (CHNH_2), 142.8 (CCH_2), 146.9 (CCHNH_2); **Aromatic peaks (all three products):** ^{13}C NMR (100 MHz, CDCl_3): δ = 125.8, 125.9, 126.5, 126.9, 127.0, 127.1 (2xC), 127.3, 128.4 (3xC), 128.5 (2xC), 128.6 (2xC). HRMS (HESI) m/z calcd for $\text{C}_{17}\text{H}_{21}\text{NH}^+$ [$\text{M} + \text{H}^+$], 240.1752: Found 240.1753.

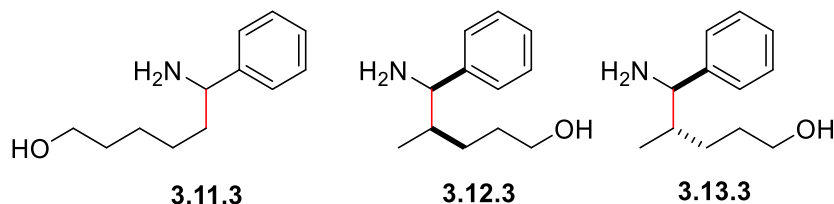
Linear: 5-amino-5-phenylpentan-1-ol (3.11.3)

Branched: 4-amino-3-methyl-4-phenylbutan-1-ol (3.12.3 and 3.13.3)

Catalyst Loading (0.1 equiv);

Reaction time: 48 h. Physical

state: Yellow oil. ^1H NMR



RR (**linear:branched** 1:2). ^1H NMR DR (**3.13.3:3.12.3** 3:1). Yield (74%). **The major branched**

diastereomer 3.13.3: ^1H NMR (400 MHz, CD_3OD): $\delta = 1.00$ (d, $J = 6.8$ Hz, 3 H, CH_3CH), 1.04-

1.68 (m, 5 H, $\text{CH}_2\text{CH}_2\text{CH}_2\text{OH}$), 1.69-1.84 (m, 1 H, CH_3CH), 3.54 (t, $J = 6.1$ Hz, 2 H, CH_2OH),

3.72 (d, $J = 7.0$ Hz, 1 H, CHNH_2), 7.26-7.29 (m, 1 H, ArH), 7.33-7.36 (m, 4 H, ArH); **Clearly**

separated diagnostic peaks of the minor branched diastereomer 3.12.3: ^1H NMR (400 MHz,

CD_3OD): $\delta = 0.78$ (d, $J = 6.8$ Hz, 3 H, CH_3CH), 3.58-3.61 (m, 2 H, CH_2OH), 3.68 (d, $J = 6.7$ Hz,

1 H, CHNH_2); **Clearly separated diagnostic peaks of the linear regioisomer 3.11.3:** ^1H NMR

(400 MHz, CD_3OD): $\delta = 3.45$ -3.50 (m, 2 H, CH_2OH), 3.83-3.86 (dd, $J = 7.8$ Hz, $J = 6.4$ Hz, 1 H,

CHNH_2). **Clearly separated diagnostic peaks of the major branched diastereomer 3.13.3:**

^{13}C NMR (100 MHz, CD_3OD): $\delta = 15.8$ (CH_3CH), 31.1, 31.5, 41.5 (CH_3CH), 62.1 (CHNH_2),

63.4 (CH_2OH), 146.1 (CCHNH_2); **Clearly separated diagnostic peaks of the minor branched**

diastereomer 3.12.3: ^{13}C NMR (100 MHz, CD_3OD): $\delta = 16.7$ (CH_3CH), 30.5, 31.2, 41.4

(CH_3CH), 62.3 (CHNH_2), 63.4 (CH_2OH), 145.7 (CCHNH_2); **Clearly separated diagnostic**

peaks of the linear regioisomer 3.11.3: ^{13}C NMR (100 MHz, CD_3OD): $\delta = 27.0$, 27.5, 33.7,

40.3 (CHCH_2), 57.5 (CHNH_2), 63.0 (CH_2OH), 147.0 (CCHNH_2); **Aromatic peaks (all three**

products): ^{13}C NMR (100 MHz, CD_3OD): $\delta = 127.8$, 128.1, 128.2 (2xC), 128.3, 128.6, 129.4,

129.5, 129.7. HRMS (HESI) m/z calcd for $\text{C}_{12}\text{H}_{19}\text{NOH}^+$ [$\text{M} + \text{H}^+$], 194.1545: Found 194.1548.

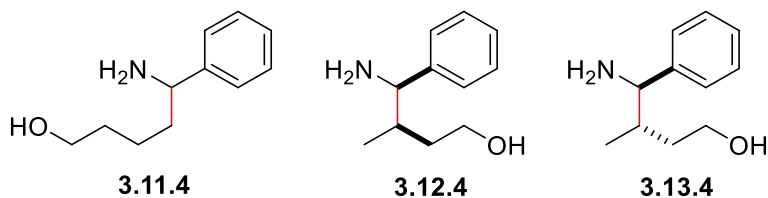
Linear: 4-amino-4-phenylbutan-1-ol (3.11.4)

Branched: 3-amino-2-methyl-3-phenylpropan-1-ol (3.12.4 and 3.13.4)

Catalyst Loading (0.1 equiv);

Reaction time: 72 h. Physical state:

Yellow oil. ^1H NMR RR



(linear:branched 1:3). ^1H NMR DR (3.13.4:3.12.4 3:1). Yield (51%). **The major branched**

diastereomer 3.13.4: ^1H NMR (400 MHz, CDCl_3): δ = 0.87 (d, J = 6.8 Hz, 3 H, CH_3CH), 1.43-1.59 (m, 1 H, $\text{CH}_2\text{CH}_2\text{OH}$), 1.63-1.71 (m, 1 H, $\text{CH}_2\text{CH}_2\text{OH}$), 1.95-1.99 (m, 1 H, CH_3CH), 3.61 (t, J = 6.4 Hz, 2 H, CH_2OH), 3.99 (d, J = 4.2 Hz, 1 H, CHNH_2), 7.24-7.27 (m, 1 H, ArH), 7.30-7.36 (m, 4 H, ArH); **Clearly separated diagnostic peaks of the minor branched diastereomer**

3.12.4: ^1H NMR (400 MHz, CDCl_3): δ = 0.78 (d, J = 6.8 Hz, 3 H, CH_3CH); **Clearly separated diagnostic peaks of the linear regioisomer 3.11.4:** ^1H NMR (400 MHz, CDCl_3): δ = 3.88 (t, J = 6.8, 1 H, CHNH_2). **Clearly separated diagnostic peaks of the major branched diastereomer**

3.13.4: ^{13}C NMR (100 MHz, CDCl_3): δ = 15.4 (CH_3CH), 37.1 ($\text{CH}_2\text{CH}_2\text{OH}$), 39.4 (CH_3CH), 59.8 (CHNH_2), 60.7 (CH_2OH), 143.9 (CCHNH_2); **Clearly separated diagnostic peaks of the**

minor branched diastereomer 3.12.4: ^{13}C NMR (100 MHz, CDCl_3): δ = 19.4 (CH_3CH), 38.1 ($\text{CH}_2\text{CH}_2\text{OH}$), 40.0 (CH_3CH), 60.5 (CH_2OH), 61.5 (CHNH_2), 146.0 (CCHNH_2); **Clearly separated diagnostic peaks of the linear regioisomer 3.11.4:** ^{13}C NMR (100 MHz, CDCl_3): δ =

22.9, 32.8, 39.4 (CHCH_2), 56.4 (CHNH_2), 62.8 (CH_2OH), 146.7 (CCHNH_2); **Aromatic peaks (all three products):** ^{13}C NMR (100 MHz, CDCl_3): δ = 126.5, 126.7, 127.2, 127.3 (2xC), 128.4,

128.7, 128.8. HRMS (HESI) m/z calcd for $\text{C}_{11}\text{H}_{17}\text{NOH}^+$ [$\text{M} + \text{H}^+$], 180.1388: Found 180.1381.

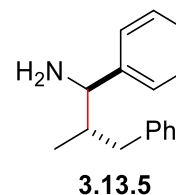
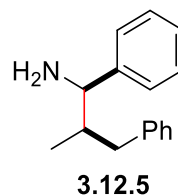
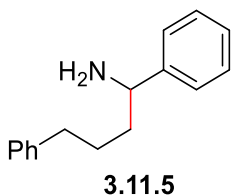
Linear: 1,4-diphenylbutan-1-amine (3.11.5)

Branched: 2-methyl-1,3-diphenylpropan-1-amine (3.12.5 and 3.13.5)

Catalyst Loading (0.1 equiv); Reaction

time: 72 h. Physical state: Yellow oil.

^1H NMR RR (**linear:branched** 1:2). ^1H



NMR DR (**3.13.5:3.12.5** 3:1). Yield (82%). **The major branched diastereomer 3.13.5:** ^1H

NMR (400 MHz, CDCl_3): δ = 0.86 (d, J = 6.8 Hz, 3 H, CH_3CH), 2.01-2.08 (m, 2 H, CH_2Ph),

2.72-2.76 (dd, J = 13.2 Hz, J = 5.1 Hz, 1 H, CHCH_3), 3.83 (d, J = 6.2 Hz, 1 H, CHNH_2), 7.12-

7.19 (m, 3 H, ArH), 7.24-7.35 (m, 7 H, ArH); **Clearly separated diagnostic peaks of the minor**

branched diastereomer 3.12.5: ^1H NMR (400 MHz, CDCl_3): δ = 0.69 (d, J = 6.8 Hz, 3 H,

CH_3CH), 2.01-2.08 (m, 2 H, CH_2Ph), 2.99-3.03 (dd, J = 13.2 Hz, J = 5.1 Hz, 1 H, CHCH_3), 3.81

(d, J = 6.2 Hz, 1 H, CHNH_2); **Clearly separated diagnostic peaks of the linear regioisomer**

3.11.5: ^1H NMR (400 MHz, CDCl_3): δ = 1.63-1.75 (m, 2 H, $\text{CH}_2\text{CH}_2\text{Ph}$), 2.24-2.31 (m, 2 H,

$\text{CH}_2\text{CH}_2\text{CH}_2\text{Ph}$), 2.61 (t, J = 7.4 Hz, 2 H, CH_2Ph), 3.90 (t, J = 6.6 Hz, 1 H, CHNH_2). **Clearly**

separated diagnostic peaks of the major branched diastereomer 3.13.5: ^{13}C NMR (100 MHz,

CDCl_3): δ = 14.7 (CH_3CH), 40.5 ($\text{CH}_2\text{CH}_2\text{Ph}$), 42.8 (CH_3CH), 60.2 (CHNH_2), 141.4 (CCH_2),

145.6 (CCHNH_2); **Clearly separated diagnostic peaks of the minor branched diastereomer**

3.12.5: ^{13}C NMR (100 MHz, CDCl_3): δ = 16.3 (CH_3CH), 39.5 ($\text{CH}_2\text{CH}_2\text{Ph}$), 42.7 (CH_3CH), 61.2

(CHNH_2), 142.5 (CCH_2), 146.7 (CCHNH_2); **Clearly separated diagnostic peaks of the linear**

regioisomer 3.11.5: ^{13}C NMR (100 MHz, CDCl_3): δ = 28.6 ($\text{CH}_2\text{CH}_2\text{CH}_2\text{Ph}$), 36.0 ($\text{CH}_2\text{CH}_2\text{Ph}$),

39.9 ($\text{CH}_2\text{CH}_2\text{Ph}$), 56.4 (CHNH_2), 141.3 (CCH_2), 145.2 (CCHNH_2); **Aromatic peaks (all three**

products): ^{13}C NMR (100 MHz, CDCl_3): δ = 25.9, 126.0, 126.5, 127.0, 127.1, 127.1, 127.3,

128.4, 128.6, 128.7, 129.2, 129.3, 129.4. HRMS (HESI) m/z calcd for $\text{C}_{16}\text{H}_{19}\text{NH}^+$ [$\text{M} + \text{H}^+$],

226.1596; Found 226.1593.

Linear: 3-cyclohexyl-1-phenylpropan-1-amine (3.11.6)

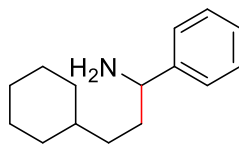
Branched: 2-cyclohexyl-1-phenylpropan-1-amine (3.12.6 and 3.13.6)

Catalyst Loading (0.1 equiv); Reaction

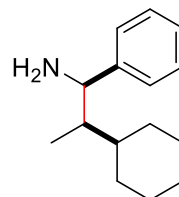
time: 72 h. Physical state: Yellow oil.

^1H NMR RR (**linear:branched** 3:1).

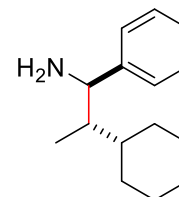
^1H NMR DR (**3.13.6:3.12.6** 3:1).



3.11.6



3.12.6



3.13.6

Yield (66%). **The linear regioisomer 3.11.6:** ^1H NMR (400 MHz, CDCl_3): δ = 0.75-0.85 (m, 2 H, CH_2), 1.00-1.24 (m, 5 H, CH_{cyc} , $2\times\text{CH}_2$), 1.55-1.65 (m, 8 H, $4\times\text{CH}_2$), 3.78 (t, J = 6.9 Hz, 1 H, CHNH_2), 7.15-7.23 (m, 1 H, ArH), 7.24-7.30 (m, 4 H, ArH); **Clearly separated diagnostic peaks of the major branched diastereomer 3.13.6:** ^1H NMR (400 MHz, CDCl_3): δ = 0.82 (d, J = 6.9 Hz, 1 H, CH_3), 3.92 (d, J = 6.7 Hz, 1 H, CHNH_2); **Clearly separated diagnostic peaks of the minor branched diastereomer 3.12.6:** ^1H NMR (400 MHz, CDCl_3): δ = 0.49 (d, J = 7.1 Hz, 1 H, CH_3), 3.65 (d, J = 6.7 Hz, 1 H, CHNH_2). **Clearly separated diagnostic peaks of the linear regioisomer 3.11.6:** ^{13}C NMR (100 MHz, CDCl_3): δ = 26.7, 29.9, 33.5, 33.6, 34.5, 37.2, 37.9 (CH_2CHCH_2), 38.3, 56.9 (CHNH_2), 147.0 (CCHNH_2); **Clearly separated diagnostic peaks of the major branched diastereomer 3.13.6:** ^{13}C NMR (100 MHz, CDCl_3): δ = 11.0 (CH_3), 26.7, 26.9, 28.8, 32.1, 39.7, 45.9 (CH_2CHCH_2), 57.7 (CHNH_2), 146.6 (CCHNH_2); **Clearly separated diagnostic peaks of the minor branched diastereomer 3.12.6:** ^{13}C NMR (100 MHz, CDCl_3): δ = 12.2 (CH_3), 32.7, 38.3, 45.6 (CH_2CHCH_2), 59.0 (CHNH_2), 146.4 (CCHNH_2); **Aromatic peaks (all three products):** ^{13}C NMR (100 MHz, CDCl_3): δ = 126.5, 126.7, 126.9, 127.0, 127.4, 128.4, 128.5, 128.6. HRMS (HESI) m/z calcd for $\text{C}_{15}\text{H}_{23}\text{NH}^+$ [$\text{M} + \text{H}^+$], 218.1909: Found 218.1909.

Linear: 3-(cyclohex-3-en-1-yl)-1-phenylpropan-1-amine (3.11.7 and 3.11.7')

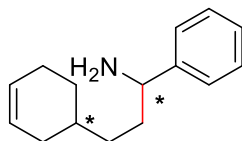
Branched: 2-(cyclohex-3-en-1-yl)-1-phenylpropan-1-amine (3.12.7 and 3.13.7)

Catalyst Loading (0.1 equiv);

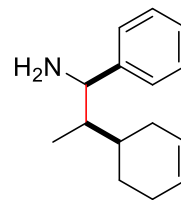
Reaction time: 72 h. Physical state:

Yellow oil. ^1H NMR RR

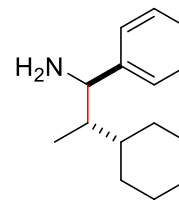
(linear:branched 3:1). ^1H NMR ^1H



3.11.7



3.12.7



3.13.7

NMR DR (3.13.7:3.12.7 1:1). Yield (64%). **Clearly separated peaks of the linear regioisomer**

3.11.7: ^1H NMR (400 MHz, CD_3OD): $\delta = 3.81$ (t, $J = 6.8$ Hz, 1 H, CHNH_2); **Clearly separated**

diagnostic peaks of the branched diastereomers 3.12.7 and 3.13.7: ^1H NMR (400 MHz,

CD_3OD): $\delta = 3.85$ (t, $J = 7.6$ Hz, 1 H, CHNH_2), 3.90 (t, $J = 7.6$ Hz, 1 H, CHNH_2). **Clearly**

separated peaks of the linear regioisomer 3.11.7: ^{13}C NMR (100 MHz, CD_3OD): $\delta = 57.8$

(CHNH_2); **The branched diastereomers 3.12.7 and 3.13.7:** ^{13}C NMR (100 MHz, CD_3OD): $\delta =$

59.6 (CHNH_2), 59.7 (CHNH_2). HRMS (HESI) m/z calcd for $\text{C}_{15}\text{H}_{21}\text{NH}^+$ [$\text{M} + \text{H}^+$], 216.1752:

Found 216.1747.

Linear: 1-phenyl-3-(o-tolyl)propan-1-amine (3.11.8)

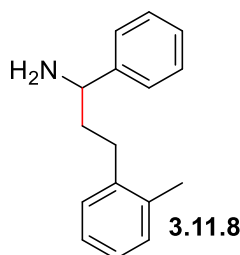
Branched: 1-phenyl-2-(o-tolyl)propan-1-amine (3.12.8 and 3.13.8)

Catalyst Loading (0.1 equiv); Reaction

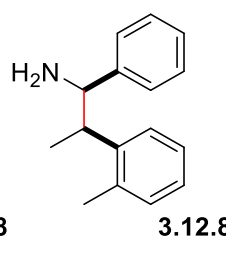
time: 48 h. Physical state: Yellow oil.

^1H NMR RR (linear:branched 17:1).

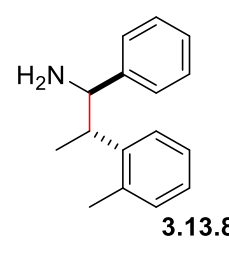
^1H NMR DR (3.13.8:3.12.8 7:1). Yield



3.11.8



3.12.8



3.13.8

(56%). **The linear regioisomer 3.11.8:** ^1H NMR (400 MHz, CD_3OD): $\delta = 1.85$ -2.04 (m, 2 H,

CH_2CH), 2.16 (s, 3 H, ArCH_3), 2.36-2.44 (m, 1 H, CH_2Ar), 2.52-2.59 (m, 1 H, CH_2Ar), 3.85-

3.89 (dd, $J = 8.1$ Hz, $J = 6.0$ Hz, 1 H, CHNH_2), 7.01-7.08 (m, 4 H, ArH), 7.24-7.29 (m, 1 H,

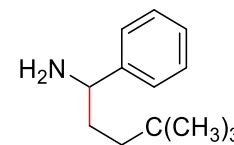
ArH), 7.33-7.37 (m, 4 H, ArH); **Clearly separated diagnostic peaks of the major branched**

diastereomer 3.13.8: ^1H NMR (400 MHz, CD_3OD): $\delta = 1.32$ (d, $J = 7.1$ Hz, 3 H, CH_3CH), 4.00

(d, $J = 8.8$ Hz, 1 H, $CHNH_2$); **Clearly separated diagnostic peaks of the minor branched diastereomer 3.12.8:** 1H NMR (400 MHz, CD_3OD): $\delta = 1.12$ (d, $J = 6.4$ Hz, 3 H, CH_3CH), 4.07 (d, $J = 9.5$ Hz, 1 H, $CHNH_2$). **The linear regioisomer 3.11.8:** ^{13}C NMR (100 MHz, CD_3OD): $\delta = 19.4$ (Ar CH_3), 31.4 (2x CH_2Ar), 40.8 (CH_2CH_2Ar), 57.5 ($CHNH_2$), 127.1 (ArC), 127.9 (ArC), 128.4 (ArC), 129.8 (ArC), 129.9 (ArC), 131.3 (ArC), 136.9 (ArC), 141.5 (ArC), 146.6 (C $CHNH_2$); **Clearly separated diagnostic peaks of the major branched diastereomer 3.13.8:** ^{13}C NMR (100 MHz, CD_3OD): $\delta = 18.3$ (Ar CH_3), 43.7 (CH_3CHAr), 62.6 ($CHNH_2$), 127.0 (2xArC), 127.8 (ArC), 128.2 (ArC), 129.0 (ArC), 131.2 (ArC), 136.7 (ArC), 144.4 (ArC), 145.5 (C $CHNH_2$). HRMS (HESI) m/z calcd for $C_{16}H_{19}NH^+$ [$M + H^+$], 226.1596: Found 226.1598.

4,4-dimethyl-1-phenylpentan-1-amine (3.11.9)

Catalyst Loading (0.1 equiv); Reaction time: 240 h. Physical state: Yellow oil. Yield (47%). 1H NMR (400 MHz, CD_3OD): $\delta = 0.85$ (s, 9 H, $C(CH_3)_3$), 0.92-0.99 (m, 1 H, $CH_2C(CH_3)_3$), 1.19-1.26 (m, 1 H, $CH_2C(CH_3)_3$), 1.61-1.79 (m, 2 H, $CH_2CH_2C(CH_3)_3$), 3.73 (t, $J = 6.8$ Hz, 1 H, $CHNH_2$), 7.22-7.25 (m, 1 H, ArH), 7.30-7.34 (m, 4 H, ArH). ^{13}C NMR (100 MHz, CD_3OD): $\delta = 29.9$ (CH_3), 31.0 ($C(CH_3)_3$), 35.2 ($CH_2CH_2(CH_3)_3$), 41.9 ($CH_2CH_2(CH_3)_3$), 58.3 (CH_2NH_2), 127.9 (2xArC), 128.3 (Ar C_4), 129.7 (2xArC), 146.9 (C $CHNH_2$). HRMS (HESI) m/z calcd for $C_{13}H_{21}NH^+$ [$M + H^+$], 192.1752: Found 192.1748.



1-phenyl-3-(trimethylsilyl)propan-1-amine (3.11.10)

Catalyst Loading (0.1 equiv); Reaction time: 24 h. Physical state: Yellow oil. Yield (52%). 1H NMR (400 MHz, $CDCl_3$): $\delta = -0.07$ (s, 9 H, $Si(CH_3)_3$), 0.26-0.34 (m, 1 H, CH_2Si), 0.48-0.56 (m, 1 H, CH_2Si), 1.58-1.64 (m, 2 H, CH_2CH_2Si), 3.76 (t, $J = 6.7$ Hz, 1 H, $CHNH_2$), 7.21-7.30 (m, 5 H, ArH). ^{13}C NMR (100 MHz,

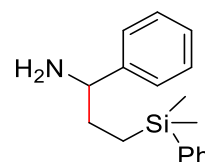


CDCl₃): δ = -1.6 (CH₃), 13.5 (CH₂Si), 34.1 (CH₂CH₂Si), 59.2 (CH₂NH₂), 126.7 (2xArC), 127.1 (ArC₄), 128.6 (2xArC), 146.6 (CCHNH₂). HRMS (HESI) m/z calcd for C₁₂H₂₁NSiH⁺ [M + H⁺], 208.1522: Found 208.1522.

3-(dimethyl(phenyl)silyl)-1-phenylpropan-1-amine (3.11.11)

Catalyst Loading (0.1 equiv); Reaction time: 24 h. Physical state: Yellow oil.

Yield (58%). ¹H NMR (400 MHz, CDCl₃): δ = 0.2 (s, 6 H, Si(CH₃)₂Ph), 0.55-0.63 (m, 1 H, CH₂Si), 0.76-0.84 (m, 1 H, CH₂Si), 1.63-1.68 (m, 2 H,

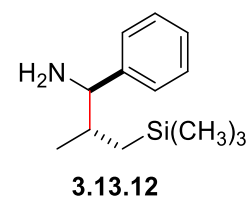


CH₂CH₂Si), 3.79 (t, J = 6.8 Hz, 1 H, CHNH₂), 7.24-7.34 (m, 8 H, ArH), 7.45-7.47 (m, 2 H, ArH). ¹³C NMR (100 MHz, CDCl₃): δ = -3.0 (CH₃), -2.9 (CH₃), 12.6 (CH₂Si), 34.0 (CH₂CH₂Si), 59.1 (CH₂NH₂), 126.7 (2xArC), 127.1 (ArC₄), 128.0 (2xArC), 128.6 (2xArC), 129.1 (ArC), 133.8 (2xArC), 139.3 (C_{ar}Si), 146.6 (CCHNH₂). HRMS (HESI) m/z calcd for C₁₇H₂₃NSiH⁺ [M + H⁺], 270.1678: Found 270.1678.

Linear: 1-phenyl-4-(trimethylsilyl)butan-1-amine (3.11.12)

Branched: 2-methyl-1-phenyl-3-(trimethylsilyl)propan-1-amine (3.12.12 and 3.13.13)

Catalyst Loading (0.1 equiv); Reaction time: 240 h. Physical state:



Yellow oil. ¹H NMR RR

(linear:branched 1:7). ¹H NMR DR (3.13.12:3.12.12 3:1). Yield (68%). **The major branched diastereomer 3.13.12:** ¹H NMR (400 MHz, CDCl₃): δ = -0.03 (s, 9 H, Si(CH₃)₃), 0.26-0.36 (m, 1 H, CH₂Si), 0.60-0.64 (dd, J = 14.2 Hz, J = 3.2 Hz, 1 H, CH₂Si), 0.90 (d, J = 6.6 Hz, 3 H, CH₃CH), 1.83-1.92 (m, 1 H, CHCH₃), 3.72 (d, J = 6.2 Hz, 1 H, CHNH₂), 7.20-7.25 (m, 1 H, ArH), 7.27-7.34 (m, 4 H, ArH); **Clearly separated diagnostic peaks of the minor branched**

diastereomer 3.12.12: ^1H NMR (400 MHz, CDCl_3): $\delta = -0.02$ (s, 9 H, $\text{Si}(\text{CH}_3)_3$), 0.82 (d, $J = 6.6$ Hz, 3 H, CH_3CH), 3.64 (d, $J = 6.2$ Hz, 1 H, CHNH_2); **Clearly separated diagnostic peaks of the linear regioisomer 3.11.12:** ^1H NMR (400 MHz, CDCl_3): $\delta = -0.05$ (s, 9 H, $\text{Si}(\text{CH}_3)_3$), 0.48-0.52 (m, 2 H, CH_2Si), 0.82 (d, $J = 6.6$ Hz, 3 H, CH_3CH), 1.65-1.71 (m, 2 H, CHCH_2), 3.89 (d, $J = 7.1$ Hz, 1 H, CHNH_2). **Clearly separated diagnostic peaks of the major branched diastereomer 3.13.12:** ^{13}C NMR (100 MHz, CDCl_3): $\delta = -0.5$ ($\text{Si}(\text{CH}_3)_3$), 18.0 (CH_3CH), 21.6 (CH_2Si), 37.0 (CH_3CH), 63.3 (CHNH_2), 145.5 (CCHNH_2); **Clearly separated diagnostic peaks of the minor branched diastereomer 3.12.12:** ^{13}C NMR (100 MHz, CDCl_3): $\delta = -0.5$ ($\text{Si}(\text{CH}_3)_3$), 19.7 (CH_3CH), 21.2 (CH_2Si), 37.4 (CH_3CH), 63.5 (CHNH_2), 145.6 (CCHNH_2); **Clearly separated diagnostic peaks of the linear regioisomer 3.11.12:** ^{13}C NMR (100 MHz, CDCl_3): $\delta = -1.4$ ($\text{Si}(\text{CH}_3)_3$), 16.8 (CH_2Si), 21.2 ($\text{CH}_2\text{CH}_2\text{Si}$), 43.8 (CHCH_2), 56.2 (CHNH_2), 147.1 (CCHNH_2); **Aromatic peaks (all three products):** ^{13}C NMR (100 MHz, CDCl_3): $\delta = 126.5, 126.9, 127.0, 127.3, 127.3, 128.3, 128.6$. HRMS (HESI) m/z calcd for $\text{C}_{13}\text{H}_{23}\text{NSiH}^+$ [$\text{M} + \text{H}^+$], 222.1678; Found 222.1681.

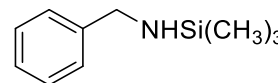
General Procedure for Trimethylsilanamines

The *N*-silylation of amines was adapted from reference.¹⁶⁸ $n\text{-BuLi}$ 1.6 M in hexanes (1 equiv) was added to a solution of amine (1 equiv) in ether at 0 °C or -78 °C (see below for each amine) and left to stir at this temperature for 5-10 min. TMSCl (1.2 equiv) was added to the formed lithium-amide at 0 °C and then a white precipitate - corresponding to LiCl - started to form. The suspension was left to reach room temperature and stirred overnight or over two nights (see below for each amine). Then the amine was canula-filtered to another Schlenk flask. Ether was evaporated at 0 °C and the residue corresponding to the amine was canula-transferred to a 25 ml Schlenk flask containing CaH_2 . After overnight stirring over CaH_2 at room temperature, the

amines were distilled and brought into the glove box where they were stored. Specific conditions for the *N*-silylation of the amines are presented below.

***N*-benzyl-1,1,1-trimethylsilanamine (3.5.3)¹⁶⁸**

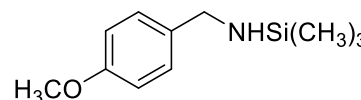
Prepared according to the general procedure. Lithiation temperature: 0 °C, *N*-silylation temperature 0 °C. Stirred overnight after the addition of



TMSCl. Yield (5.6 g, 67%). Colorless liquid. NMR data match with the reported data.

***N*-(4-methoxybenzyl)-1,1,1-trimethylsilanamine (3.14)¹⁶⁹**

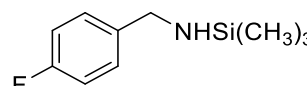
Prepared according to the general procedure. Lithiation temperature: 0 °C, *N*-silylation temperature 0 °C. Stirred overnight



after the addition of TMSCl. Yield (2.38 g, 39%). Colorless liquid. ¹H NMR (400 MHz, C₆D₆): δ = 0.01 (s, 9 H, Si(CH₃)₃), 0.39 (broad s, 1 H, NH), 3.31 (s, 3 H, OCH₃), 3.70 (d, *J* = 8.1 Hz, 2 H, CH₂), 6.76 (d, *J* = 8.5 Hz, 2 H, ArH), 7.09 (d, *J* = 8.8 Hz, 2 H, ArH). NMR data match with the reported data.¹⁶⁹

***N*-(4-fluorobenzyl)-1,1,1-trimethylsilanamine (3.15)⁸**

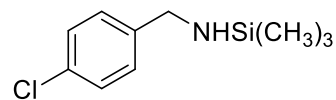
Prepared according to the general procedure. Lithiation temperature: 0 °C, *N*-silylation temperature 0 °C. Stirred overnight after the addition



of TMSCl. Yield (2.45 g, 39%). Colorless liquid. ¹H NMR (400 MHz, C₆D₆): δ = 0.03 (s, 9 H, Si(CH₃)₃), 0.32 (broad s, 1 H, NH), 3.62 (d, *J* = 8.4 Hz, 2 H, CH₂), 6.86 (t, ³*J*_{HF} = 8.6 Hz, 2 H, ArH_{3,5}), 7.09 (dd, ³*J*_{HH} = 8.5 Hz, ⁴*J*_{HF} = 5.6 Hz, 2 H, ArH_{2,6}). ¹³C NMR (100 MHz, C₆D₆): δ = 0.4 (q, *J* = 11.7 Hz, 3xCH₃), 45.7 (CH₂NHSi), 115.5 (d, ²*J*_{CF} = 21.2 Hz, 2xArC_{3,5}), 129.0 (d, ³*J*_{CF} = 8.1 Hz, 2xArC_{2,6}), 140.7 (d, ⁴*J*_{CF} = 3.1 Hz, CCH₂NHSi), 162.5 (d, ¹*J*_{CF} = 243.2 Hz, CF). ¹⁹F NMR (376 MHz, C₆D₆): -116.65.

***N*-(4-chlorobenzyl)-1,1,1-trimethylsilanamine (3.16)**

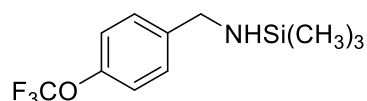
Prepared according to the general procedure. Lithiation temperature:



0 °C, *N*-silylation temperature 0 °C. Stirred overnight after the addition of TMSCl. Yield (1.85 g, 31%). Colorless liquid. ¹H NMR (400 MHz, C₆D₆): δ = 0.01 (s, 9 H, Si(CH₃)₃), 0.30 (broad s, 1 H, NH), 3.58 (d, *J* = 8.1 Hz, 2 H, CH₂), 6.94 (d, *J* = 8.4 Hz, 2 H, ArH), 7.15 (d, *J* = 8.4 Hz, 2 H, ArH). ¹³C NMR (100 MHz, C₆D₆): δ = 0.5 (3xCH₃), 45.7(CH₂NHSi), 128.9 (ArC), 132.6 (CCH₂NHSi), 143.5 (ArC₄). MS (EI) *m/z*: 213.

1,1,1-trimethyl-*N*-(4-(trifluoromethoxy)benzyl)silanamine (3.17)

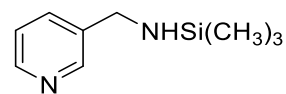
Prepared according to the general procedure. Lithiation



temperature: 0 °C, *N*-silylation temperature 0 °C. Stirred overnight after the addition of TMSCl. Yield (4.20 g, 51%). Colorless liquid. ¹H NMR (400 MHz, C₆D₆): δ = 0.02 (s, 9 H, Si(CH₃)₃), 0.30 (broad s, 1 H, NH), 3.60 (d, *J* = 8.0 Hz, 2 H, CH₂), 6.98 (d, *J* = 2.7 Hz, 4 H, ArH). ¹³C NMR (100 MHz, C₆D₆): δ = 0.3 (3xCH₃), 45.7 (CH₂NHSi), 121.4 (2xArC), 121.7 (q, ¹*J*_{CF3} = 255.5 Hz, CF₃), 128.7 (2xArC), 143.9 (CCH₂NHSi), 148.5 (ArC₄). ¹⁹F NMR (376 MHz, C₆D₆): δ = -57.98. MS (EI) *m/z*: 263.

1,1,1-trimethyl-*N*-(pyridin-3-ylmethyl)silanamine (3.18)

Prepared according to the general procedure. Lithiation temperature: -78

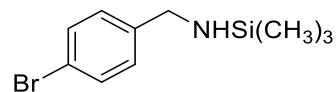


°C, *N*-silylation temperature 0 °C. Stirred over two nights after the addition of TMSCl. Yield (1.79 g, 34%). Colorless liquid. ¹H NMR (400 MHz, C₆D₆): δ = -0.01 (s, 9 H, Si(CH₃)₃), 0.32 (broad s, 1 H, NH), 3.55 (d, *J* = 8.2 Hz, 2 H, CH₂), 6.78-6.81 (dd, *J* = 7.7 Hz, *J* = 4.6 Hz, 1 H, ArH₄), 7.22-7.26 (d, 1 H, ArH₅), 8.50 (d, *J* = 4.5 Hz, ArH₆), 8.62 (d, *J* = 1.3 Hz, ArH₂). ¹³C NMR (100 MHz, C₆D₆): δ = 0.4 (3xCH₃), 43.9 (CH₂NHSi), 123.5 (ArC₅), 134.5 (ArC₄), 139.7 (CCH₂NHSi), 148.8 (ArC₂), 149.9 (ArC₆). MS (EI) *m/z*: 180.

N-(4-bromobenzyl)-1,1,1-trimethylsilanamine (3.19)

Prepared according to the general procedure. Lithiation temperature:

0 °C, *N*-silylation temperature 0 °C. Stirred overnight after the

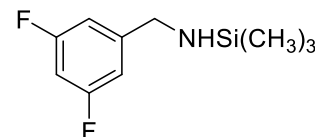


addition of TMSCl. Yield (4.5 g, 40%). Colorless liquid. ¹H NMR (400 MHz, C₆D₆): δ = 0.01 (s, 9 H, Si(CH₃)₃), 0.27 (broad s, 1 H, NH), 3.55 (d, *J* = 8.2 Hz, 2 H, CH₂), 6.87 (d, *J* = 8.2 Hz, 2 H, ArH), 7.30 (d, *J* = 8.4 Hz, 2 H, ArH). ¹³C NMR (100 MHz, C₆D₆): δ = 0.4 (q, *J* = 12.3 Hz, 3xCH₃), 45.7 (CH₂NHSi), 120.7 (2xArC), 129.3 (2xArC), 131.8 (CCH₂NHSi), 144.0 (ArC₄). MS (EI) *m/z*: 258.

***N*-(3,5-difluorobenzyl)-1,1,1-trimethylsilanamine (3.20)**

Prepared according to the general procedure. Lithiation temperature: 0

°C, *N*-silylation temperature 0 °C. Stirred overnight after the addition



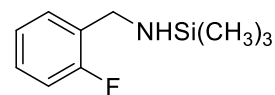
of TMSCl. Yield (4.9 g, 70%). Colorless liquid. ¹H NMR (400 MHz,

C₆D₆): δ = -0.04 (s, 9 H, Si(CH₃)₃), 0.20 (broad s, 1 H, NH), 3.45 (d, *J* = 8.2 Hz, 2 H, CH₂), 6.44-6.50 (d, 1 H, ArH₄), 6.67 (d, *J* = 6.5 Hz, 2 H, ArH_{2,6}). ¹³C NMR (100 MHz, C₆D₆): δ = 0.3 (q, *J*_{CSi} = 12.6 Hz, 3xCH₃), 45.6 (CH₂NHSi), 102.1 (t, ²*J*_{CF} = 25.6 Hz, ArC), 109.7-110.0 (dd, ²*J*_{CF} = 18.6 Hz, ⁴*J*_{CF} = 6.6 Hz, 2xArC), 149.9 (t, ³*J*_{CF} = 7.9 Hz, ArC), 162.6-165.2 (dd, ¹*J*_{CF} = 247.1 Hz, ³*J*_{CF} = 12.4 Hz, 2xArC). ¹⁹F NMR (376 MHz, C₆D₆): δ = -110.25. MS (EI) *m/z*: 215.

***N*-(2-fluorobenzyl)-1,1,1-trimethylsilanamine (3.21)**

Prepared according to the general procedure. Lithiation temperature: 0 °C,

N-silylation temperature 0 °C. Stirred overnight after the addition of



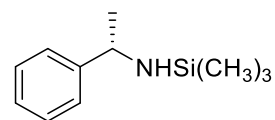
TMSCl. Yield (6.4 g, 67%). Colorless liquid. ¹H NMR (400 MHz, C₆D₆): δ = 0.02 (s, 9 H, Si(CH₃)₃), 0.38 (broad s, 1 H, NH), 3.89 (d, *J* = 8.3 Hz, 2 H, CH₂), 6.81-6.86 (m, 1 H, ArH₃), 6.87-6.91 (m, 2 H, ArH_{4,5}), 7.22-7.26 (m, 1 H, ArH₆). ¹³C NMR (100 MHz, C₆D₆): δ = 0.4 (q, *J* = 11.9 Hz, 3xCH₃), 40.0 (CH₂NHSi), 115.5 (d, ²*J*_{CF} = 21.3 Hz, ArC₃), 124.5 (d, ³*J*_{CF} = 3.6 Hz,

ArC₄), 128.5 (ArC₅), 129.6 (d, ³J_{CF} = 5.2 Hz, ArC₆), 132.0 (d, ²J_{CF} = 14.6 Hz, CCH₂NHSi), 161.5 (d, ¹J_{CF} = 244.6 Hz, CF). ¹⁹F NMR (376 MHz, C₆D₆): -120.00. MS (EI) *m/z*: 197.

(S)-1,1,1-trimethyl-N-(1-phenylethyl)silanamine (3.22)

Prepared according to the general procedure. Lithiation temperature: 0

°C, *N*-silylation temperature 0 °C. Stirred overnight after the addition of

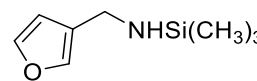


TMSCl. Yield (3.23 g, 40%). Colorless liquid. ¹H NMR (400 MHz, C₆D₆): δ = 0.02 (s, 9 H, Si(CH₃)₃), 0.57 (broad s, 1 H, NH), 1.24 (d, *J* = 6.6 Hz, 3 H, CHCH₃), 3.92-4.00 (dq, *J* = 9.4 Hz, *J* = 6.7 Hz, 1 H, CHCH₃), 7.07-7.11 (m, 1 H, ArH₄), 7.17-7.22 (m, 4 H, ArH). ¹³C NMR (100 MHz, C₆D₆): δ = 0.9 (q, *J* = 12.4 Hz, 3xCH₃), 28.6 (CHCH₃) 52.2 (CH₂NHSi), 126.5 (2xArC), 126.9 (ArC₄), 128.8 (2xArC), 149.9 (ArC₁). MS (EI) *m/z*: 193.

N-(furan-3-ylmethyl)-1,1,1-trimethylsilanamine (3.23)

Prepared according to the general procedure. Lithiation temperature: 0 °C,

N-silylation temperature 0 °C. Stirred overnight after the addition of



TMSCl. Yield (5.2 g, 60%). Colorless liquid. ¹H NMR (400 MHz, C₆D₆): δ = 0.02 (s, 9 H, Si(CH₃)₃), 0.48 (broad s, 1 H, NH), 3.75 (d, *J* = 8.1 Hz, 2 H, CH₂), 5.95-5.96 (dd, *J* = 3.2 Hz, 1 H, ArH₅), 6.11-6.12 (dd, *J* = 3.1 Hz, *J* = 1.9 Hz, 1 H, ArH₄), 7.12 (d, *J* = 1.9 Hz, 1 H, ArH₂). ¹³C NMR (100 MHz, C₆D₆): δ = 0.3 (s, 3xCH₃), 39.7 (CH₂NHSi), 105.4 (ArC₅), 110.7 (ArC₄), 141.7 (ArC₂), 158.5 (CCH₂NHSi). MS (EI) *m/z*: 169.

General Procedure for the Hydroaminoalkylation Reaction

Note: For non-heterocyclic N-silylated amines, the catalyst loading was 10 mol%. For 1,1,1-trimethyl-N-(pyridin-3-ylmethyl)silanamine (3.18), the catalyst loading was 20 mol%.

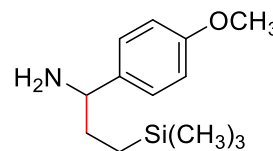
To a solution of Zr(NMe₂)₄ (0.1 or 0.2 equiv, 0.05 or 0.1 mmol, 13.37 or 26.74 mg) in 200-300 μL C₆D₆, the amine **3.14-3.23** (Scheme 3.10) (1 equiv, 0.50 mmol) was added followed by the

addition of vinyltrimethylsilane **3.10.10** (1.8 equiv, 0.90 mmol). The solution was then transferred quantitatively into a J-Young tube via an additional 200-300 μL C_6D_6 and placed in an oil bath at 145 $^\circ\text{C}$ for 24 h. Upon the reaction completion, the J-Young seal was broken and DCM and MeOH were added to the existing solution. The quenched solution was then passed through a celite pipet and 2-3 droplets of NaOH 3M were added to the filtrate. The solvents were evaporated and ether was added to the residue. The amine was extracted in the form of its hydrochloric salt (4x10 mL) with HCl 1M and the combined aqueous layers were basified with NaOH 3M. The amine was back-extracted with ether (3x20 mL). The ethereal layers were dried over anhydrous Na_2SO_4 and evaporated to afford the product as a single regioisomer.

1-(4-methoxyphenyl)-3-(trimethylsilyl)propan-1-amine (3.24)

Catalyst Loading (0.1 equiv); Reaction time: 24 h. Physical state: Yellow

oil. Yield (69%). ^1H NMR (400 MHz, CDCl_3): $\delta = -0.05$ (s, 9 H, $\text{Si}(\text{CH}_3)_3$), 0.27-0.35 (m, 1 H, CH_2Si), 0.48-0.56 (m, 1 H, CH_2Si), 1.55-



1.66 (m, 2 H, $\text{CH}_2\text{CH}_2\text{Si}$), 3.75 (t, $J = 6.6$ Hz, 1 H, CHNH_2), 3.80 (s, 3 H, OCH_3), 6.87 (d, $J = 8.5$ Hz, 2 H, ArH), 7.22 (d, $J = 8.5$ Hz, 2 H, ArH). ^{13}C NMR (100 MHz, CDCl_3): $\delta = -1.6$ (q, $J_{\text{CSi}} = 12.2$ Hz, CH_3), 13.6 (CH_2Si), 34.2 ($\text{CH}_2\text{CH}_2\text{Si}$), 55.4 (OCH_3), 58.6 (CH_2NH_2), 113.9 (ArC), 127.6 (ArC), 138.8 (ArC₁), 158.6 (COCH_3). HRMS (HESI) m/z calcd for $\text{C}_{13}\text{H}_{23}\text{NOSiH}^+$ [$\text{M} + \text{H}^+$], 238.1627: Found 238.1620.

1-(4-fluorophenyl)-3-(trimethylsilyl)propan-1-amine (3.25)

Catalyst Loading (0.1 equiv); Reaction time: 24 h. Physical state: Yellow

oil. Yield (55%). ^1H NMR (400 MHz, CDCl_3): $\delta = -0.06$ (s, 9 H, $\text{Si}(\text{CH}_3)_3$), 0.24-0.32 (m, 1 H, CH_2Si), 0.47-0.55 (m, 1 H, CH_2Si), 1.55-1.60 (m, 2 H,



$\text{CH}_2\text{CH}_2\text{Si}$), 3.78 (t, $J = 6.6$ Hz, 1 H, CHNH_2), 7.00 (t, $J = 8.7$ Hz, 2 H, ArH_{3,5}), 7.25 (t, $J = 8.1$

Hz, 2 H, ArH_{2,6}). ¹³C NMR (100 MHz, CDCl₃): δ = -1.6 (q, *J*_{CSi} = 12.1 Hz, CH₃), 13.5 (CH₂Si), 34.3 (CH₂CH₂Si), 58.5 (CH₂NH₂), 115.3 (d, ²*J*_{CF} = 21.6 Hz, 2xArC_{3,5}), 128.1 (d, ³*J*_{CF} = 7.4 Hz, 2xArC_{2,6}), 142.3 (d, ⁴*J*_{CF} = 3.3 Hz, CCHNH₂), 161.94 (d, ¹*J*_{CF} = 245.5 Hz, ArC₄). ¹⁹F NMR (376 MHz, CDCl₃): -116.12. HRMS (HESI) *m/z* calcd for C₁₂H₂₀FNSiH⁺ [M + H⁺], 226.1427: Found 226.1424.

1-(4-chlorophenyl)-3-(trimethylsilyl)propan-1-amine (3.26)

Catalyst Loading (0.1 equiv); Reaction time: 24 h. Physical state: Yellow

oil. Yield (41%). ¹H NMR (400 MHz, CDCl₃): δ = -0.05 (s, 9 H, Si(CH₃)₃), 0.25-0.33 (m, 1 H, CH₂Si), 0.47-0.55 (m, 1 H, CH₂Si), 1.56-1.62 (m, 2 H,



CH₂CH₂Si), 3.79 (t, *J* = 6.7 Hz, 1 H, CHNH₂), 7.24 (d, *J* = 8.6 Hz, 2 H, ArH), 7.30 (d, *J* = 8.6 Hz, 2 H, ArH). ¹³C NMR (100 MHz, CDCl₃): δ = -1.6 (q, *J*_{CSi} = 12.1 Hz, CH₃), 13.4 (CH₂Si), 34.2 (CH₂CH₂Si), 58.6 (CH₂NH₂), 128.1 (2xArC), 128.7 (2xArC), 132.6 (ArC₄), 145.0 (CCHNH₂). HRMS (HESI) *m/z* calcd for C₁₂H₂₀FNSiH⁺ [M + H⁺], 242.1132: Found 242.1122.

1-(4-(trifluoromethoxy)phenyl)-3-(trimethylsilyl)propan-1-amine (3.27)

Catalyst Loading (0.1 equiv); Reaction time: 24 h. Physical state: Yellow

oil. Yield 7%). ¹H NMR (400 MHz, CD₃OD): δ = -0.03 (s, 9 H, Si(CH₃)₃), 0.24-0.31 (m, 1 H, CH₂Si), 0.47-0.55 (m, 1 H, CH₂Si), 1.59-



1.78 (m, 2 H, CH₂CH₂Si), 3.78 (t, *J* = 6.6 Hz, 1 H, CHNH₂), 3.80 (s, 3 H), 7.23 (d, *J* = 8.2 Hz, 2 H, ArH), 7.42 (d, *J* = 8.5 Hz, 2 H, ArH). ¹³C NMR (100 MHz, CD₃OD): δ = -1.7 (q, *J*_{CSi} = 12.4 Hz), 14.1, 34.6, 59.6, 122.1 (q, ¹*J*_{CF3} = 257.2 Hz), 122.2 (2xArC), 129.6 (2xArC), 146.1 (ArC₄), 149.6 (CCHNH₂). ¹⁹F NMR (376 MHz, CD₃OD): -59.55. HRMS (HESI) *m/z* calcd for C₁₃H₂₀F₃NOSiH⁺ [M + H⁺], 292.1345: Found 292.1334.

1-(pyridin-3-yl)-3-(trimethylsilyl)propan-1-amine (3.28)

Catalyst Loading (0.2 equiv); Reaction time: 24 h. Physical state: Yellow oil.

Yield (63%). ^1H NMR (400 MHz, CDCl_3): $\delta = -0.05$ (s, 9 H, $\text{Si}(\text{CH}_3)_3$), 0.26-

0.34 (m, 1 H, CH_2Si), 0.49-0.57 (m, 1 H, CH_2Si), 1.56-1.66 (m, 2 H,

$\text{CH}_2\text{CH}_2\text{Si}$), 3.85 (t, $J = 6.7$ Hz, 1 H, CHNH_2), 7.24-7.27 (dd, $J = 7.2$ Hz, $J = 5.1$ Hz, 1 H,

ArH_5), 7.64-7.67 (dt, $J = 7.8$ Hz, $J = 2.1$ Hz, 1 H, ArH_4), 8.48-8.50 (dd, $J = 4.7$ Hz, $J = 1.7$ Hz,

1 H, ArH_6), 8.54 (d, $J = 2.3$ Hz, 1 H, ArH_2). ^{13}C NMR (100 MHz, CDCl_3): $\delta = -1.6$ (q, $J_{\text{CSi}} = 12.0$

Hz, CH_3), 13.3 (CH_2Si), 34.2 ($\text{CH}_2\text{CH}_2\text{Si}$), 56.8 (CH_2NH_2), 123.7 (ArC_5), 134.1 (ArC_4), 141.6

(CCHNH_2), 148.7 (ArC_6), 149.0 (ArC_2). HRMS (HESI) m/z calcd for $\text{C}_{11}\text{H}_{20}\text{N}_2\text{SiH}^+$ [$\text{M} + \text{H}^+$],

209.1474; Found 209.1481.



1-(4-bromophenyl)-3-(trimethylsilyl)propan-1-amine (3.29)

Catalyst Loading (0.1 equiv); Reaction time: 24 h. Physical state: Yellow

oil. Yield (25%). ^1H NMR (400 MHz, CDCl_3): $\delta = -0.05$ (s, 9 H, $\text{Si}(\text{CH}_3)_3$),

0.25-0.33 (m, 1 H, CH_2Si), 0.47-0.55 (m, 1 H, CH_2Si), 1.54-1.66 (m, 2 H,

$\text{CH}_2\text{CH}_2\text{Si}$), 3.76 (t, $J = 6.6$ Hz, 1 H, CHNH_2), 7.19 (d, $J = 8.4$ Hz, 2 H, ArH), 7.44 (d, $J = 8.4$

Hz, 2 H, ArH). ^{13}C NMR (100 MHz, CDCl_3): $\delta = -1.6$ (q, $J_{\text{CSi}} = 12.3$ Hz, CH_3), 13.4 (CH_2Si),

34.2 ($\text{CH}_2\text{CH}_2\text{Si}$), 58.6 (CHNH_2), 120.6 (2x ArC) 128.5 (2x ArC), 131.6 (ArC_4), 145.6

(CCHNH_2). HRMS (HESI) m/z calcd for $\text{C}_{12}\text{H}_{20}\text{BrNSiH}^+$ [$\text{M} + \text{H}^+$], 286.0627; Found 286.0621.



1-(3,5-difluorophenyl)-3-(trimethylsilyl)propan-1-amine (3.30)

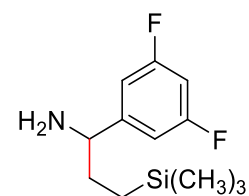
Catalyst Loading (0.1 equiv); Reaction time: 24 h. Physical state: Yellow

oil. Yield (33%). ^1H NMR (400 MHz, CDCl_3): $\delta = -0.04$ (s, 9 H, $\text{Si}(\text{CH}_3)_3$),

0.22-0.36 (m, 1 H, CH_2Si), 0.48-0.56 (m, 1 H, CH_2Si), 1.55-1.61 (m, 2 H,

$\text{CH}_2\text{CH}_2\text{Si}$), 3.80 (t, $J = 6.7$ Hz, 1 H, CHNH_2), 6.64-6.70 (tt, $J = 8.9$ Hz, $J = 2.4$ Hz, 1 H, ArH_4),

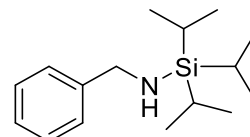
6.82-6.87 (dd, $J = 7.6$ Hz, $J = 2.2$ Hz, 2 H, $\text{ArH}_{2,6}$). ^{13}C NMR (100 MHz, CDCl_3): $\delta = -1.6$ (q, J_{CSi}



= 12.5 Hz, CH₃), 13.2 (CH₂Si), 34.1 (CH₂CH₂Si), 58.6 (CHNH₂), 102.3 (t, ²J_{CF} = 25.5 Hz, ArC₄), 109.3-109.6 (dd, ²J_{CF} = 18.5 Hz, ⁴J_{CF} = 6.6 Hz, 2xArC_{2,6}), 150.9 (t, ³J_{CF} = 8.2 Hz, CCHNH₂), 163.2 (dd, ¹J_{CF} = 247.7 Hz, ³J_{CF} = 11.9 Hz, 2xArC_{3,5}). ¹⁹F NMR (376 MHz, CDCl₃): -110.01. HRMS (HESI) *m/z* calcd for C₁₂H₁₉F₂NSiH⁺ [M + H⁺], 244.1333; Found 244.1340.

***N*-benzyl-1,1,1-triisopropylsilanamine (3.38)**

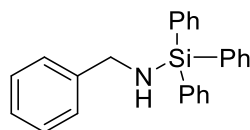
n-Buli 1.6 M in hexanes (1 equiv, 46.7 mmol, 29 mL) was added to a solution of amine **3.5.3** (1 equiv, 46.7 mmol, 5 g) in 50-60 mL ether at 0 °C and left to stir at this temperature for 5-10 min. TIPSCl (1 equiv, 46.7 mmol, 9 g) was dissolved in 20-30 mL anhydrous ether and added to the formed lithium-amide at 0 °C and then a white precipitate - corresponding to LiCl - started to form. The suspension was left to reach room temperature and stirred overnight. Then the amine was canula-filtered to another Schlenk flask. Ether was evaporated at 0 °C and the residue corresponding to the amine was canula-transferred to a 25 ml Schlenk flask containing CaH₂. After overnight stay over CaH₂, the amine was distilled and brought into the glovebox.



Yield (8.94 g, 72%). Colorless liquid. ¹H NMR (400 MHz, C₆D₆): δ = 0.36 (broad s, 1 H, NH), 0.97-1.04 (m, 3 H, 3xSiCH), 1.05-1.10 (m, 18 H, 3xCH(CH₃)₂), 3.92 (d, *J* = 7.9 Hz, 2 H, CH₂), 7.12 (t, *J* = 7.5 Hz, 1 H, ArH₄), 7.33 (t, *J* = 7.5 Hz, 2 H, ArH), 7.33 (d, *J* = 7.5 Hz, 2 H, ArH). ¹³C NMR (100 MHz, C₆D₆): δ = 12.5 (3xSiCH), 19.0 (3xCH(CH₃)₂), 47.4 (CH₂NHSi), 127.1 (ArC₁), 127.4 (2xArC), 128.9 (2xArC), 145.0 (ArC₄). MS (EI) *m/z*: 263.

***N*-benzyl-1,1,1-triphenylsilanamine (3.39)**

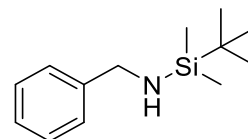
n-Buli 1.6 M in hexanes (1 equiv, 46.7 mmol, 29 mL) was added to a solution of amine **3.5.3** (1 equiv, 46.7 mmol, 5 g) in 50-60 mL ether at 0 °C



and left to stir at this temperature for 5-10 min. TPSCl (1 equiv, 46.7 mmol 13.8 g) was dissolved in 100 mL anhydrous ether and added to the formed lithium-amide at 0 °C and then a white precipitate - corresponding to LiCl - started to form. The suspension was left to reach room temperature and stirred overnight. Then the amine was canula-transferred to another Schlenk flask. The flask was cooled to 0 °C and the formed *N*-TPS amine crushed out from the solution. Ether was evaporated at 0 °C and the white solid corresponding to the amine was brought into the glovebox, and washed further with ether prior to use in catalysis. Yield (12.5 g, 74%). White solid. ¹H NMR (400 MHz, C₆D₆): δ = 1.29 (broad s, 1 H, NH), 4.01 (d, *J* = 7.7 Hz, 2 H, CH₂), 7.06-7.10 (m, 1 H, ArH₄), 7.14-7.24 (m, 14 H, ArH), 7.69-7.72 (m, 5 H, ArH). ¹³C NMR (100 MHz, C₆D₆): δ = 47.3 (CH₂NHSi), 127.2 (ArC), 127.8 (ArC), 128.6 (ArC), 128.9 (ArC), 130.3 (ArC), 136.4 (ArC), 136.4 (ArC), 144.2 (ArC). MS (EI) *m/z*: 365.

***N*-benzyl-1-(tert-butyl)-1,1-dimethylsilanamine (3.40)**

n-Buli 1.6 M in hexanes (1 equiv, 46.7 mmol, 29 mL) was added to a solution of amine **3.5.3** (1 equiv, 46.7 mmol, 5 g) in 50-60 mL ether at 0 °C and left to stir at this temperature for 5-10 min. TBSCl (1 equiv, 46.7



mmol, 7 g) was dissolved in 20 mL anhydrous ether and added to the formed lithium-amide at 0 °C and then a white precipitate - corresponding to LiCl - started to form. The suspension was left to reach room temperature and stirred overnight. Then the amine was canula-filtered to another Schlenk flask. Ether was evaporated at 0 °C and the residue corresponding to the *N*-silylated amine was canula-transferred to a 25 mL Schlenk flask containing CaH₂. After overnight stay over CaH₂, the amine was distilled and brought into the glovebox. Yield (5.9 g, 57%). Colorless liquid. ¹H NMR (400 MHz, C₆D₆): δ = 0.01 (s, 6 H, Si(CH₃)₂), 0.39 (broad s, 1 H, NH), 0.92 (s, 9 H, C(CH₃)₃), 3.83 (d, *J* = 8.0 Hz, 2 H, CH₂), 7.09-7.13 (m, 1 H, ArH), 7.19-7.26 (m, 4 H, ArH).

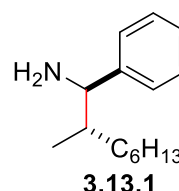
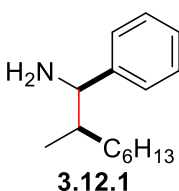
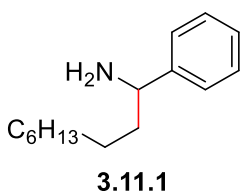
^{13}C NMR (100 MHz, C_6D_6): $\delta = -4.5$ (q, $J_{\text{CSi}} = 12.7$ Hz, $\text{Si}(\text{CH}_3)_2$), 19.1 ($\text{C}(\text{CH}_3)_3$), 27.0 ($\text{C}(\text{CH}_3)_3$), 47.2 (CH_2NHSi), 127.1 (ArC_1), 127.5 ($2\times\text{ArC}$), 128.9 ($2\times\text{ArC}$), 145.2 (ArC_4). MS (EI) m/z : 221.

Linear: 1-phenylnonan-1-amine (3.11.1)

Branched: 2-methyl-1-phenyloctan-1-amine (3.12.1 and 3.13.1)

N-TPS amine

3.39 (1 equiv,
0.50 mmol, 183



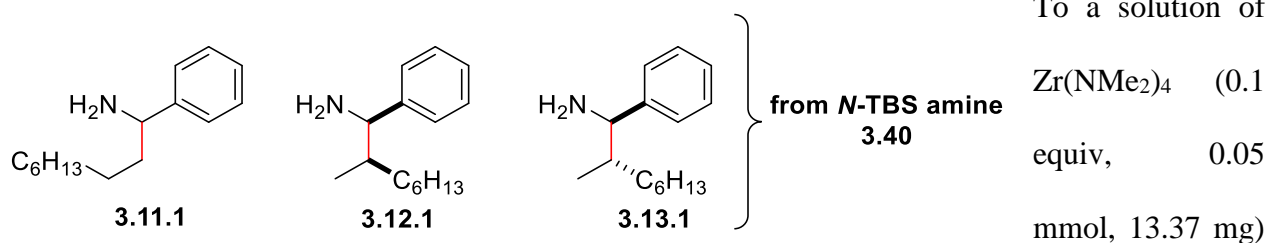
} from *N*-TPS amine
3.39

mg) was added via 200 μL C_6D_6 to a vial containing $\text{Zr}(\text{NMe}_2)_4$ (0.1 equiv, 0.05 mmol, 13.37 mg). An additional 200 μL C_6D_6 was used for the quantitative transfer of the starting amine in the second vial. 1-octene (1.8 equiv, 0.90 mmol, 112 mg). The solution was then transferred quantitatively into a J-Young tube via an additional 200 μL C_6D_6 and placed in an oil bath at 145 $^\circ\text{C}$ for 120 h. The J-Young seal was broken and DCM and MeOH were added to the existing solution. The quenched solution was then passed through a celite pipet and 2-3 droplets of NaOH 3M were added to the filtrate. **Workup 1 (via formation of the hydrochloric salt)**: The solvents were evaporated and ether was added to the residue. The amine was extracted with HCl 1M (4x10 mL) and the combined aqueous layers were basified. The amine was back extracted with ether (3x15 mL) and the combined ethereal layers were dried over anhydrous Na_2SO_4 . Ether was evaporated and the residue corresponded to the mixture of regioisomers **3.11.1**, **3.12.1** and **3.13.1**, and silanol (byproduct). ^1H NMR RR (**linear:branched** 1:1). ^1H NMR DR (**3.13.1:3.12.1** 2:1). **Workup 2 (via formation of the oxalic salt)**: The solvents were evaporated and NaOH 3M was added to the residue. The amine was extracted with ether (3x20 mL) and the ethereal layers were dried over anhydrous Na_2SO_4 . Ether was evaporated and the residue was uptaken in 1 mL

ether prior to the addition of excess of oxalic acid. The salt was left to form over a period of 72 h prior to the ether decantation. The oxalic salt was basified with NaOH 3M and the liberated amine was extracted with ether (3x10 mL). The ethereal layers were dried over anhydrous Na₂SO₄ and evaporated. The residue was purified by column chromatography (DCM: MeOH:Et₃N 95:5:0.1) to afford 35 mg of free base. Physical state: yellow oil. ¹H NMR RR (**linear:branched** 1:1). ¹H NMR DR (**3.13.1:3.12.1** 2:1). Yield: 32%. **The linear regioisomer 3.11.1:** ¹H NMR (300 MHz, CDCl₃): δ = 0.73-0.82 (m, 3 H, CH₃CH₂), 1.14-1.34 (m, 10 H, 5xCH₂), 1.62-1.73 (m, 2 H, CHCH₂), 3.86 (d, *J* = 7.0 Hz, 1 H, CHNH₂), 7.20-7.25 (m, 1 H, ArH), 7.27-7.33 (m, 4 H, ArH); **Clearly separated diagnostic peaks of the major branched diastereomer 3.13.1:** ¹H NMR (400 MHz, CDCl₃): δ = 3.77 (d, *J* = 6.2 Hz, 1H, CHNH₂); **Clearly separated diagnostic peaks of the minor branched diastereomer 3.12.1:** ¹H NMR (400 MHz, CDCl₃): δ = 0.74 (d, *J* = 6.7 Hz, 3 H, CH₃), 3.69 (t, *J* = 7.0 Hz, 1 H, CHNH₂). MS (CI) *m/z*: 203.1 [M-16].

Linear: 1-phenylnonan-1-amine (3.11.1)

Branched: 2-methyl-1-phenyloctan-1-amine (3.12.1 and 3.13.1)



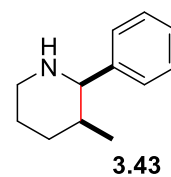
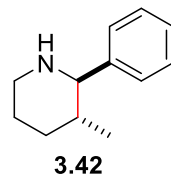
in 200 μL C₆D₆ *N*-TBS amine **3.40** (1 equiv, 0.50 mmol, 110.71 mg) was added. 1-octene (1.8 equiv, 0.90 mmol, 112 mg) was then added and the resulting solution was then transferred quantitatively into a J-Young tube via an additional 200-300 μL C₆D₆ and placed in an oil bath at 145 °C for 72 h. The J-Young seal was broken and DCM and MeOH were added to the existing

solution. The quenched solution was then passed through a celite pipet and 2-3 droplets of NaOH 3M were added to the filtrate. **Workup 1 (via formation of the hydrochloric salt):** The solvents were evaporated and ether was added to the residue. The amine was extracted with HCl 1M (4x10 mL) and the combined aqueous layers were basified. The amine was back extracted with ether (3x15 mL) and the combined ethereal layers were dried over anhydrous Na₂SO₄. Ether was evaporated and the residue corresponded to the mixture of regioisomers **3.11.1**, **3.12.1** and **3.13.1**. ¹H NMR RR (**linear:branched** 1:1). ¹H NMR DR (**3.13.1:3.12.1** 2:1). Yield 19%.

Workup 2 (via formation of the oxalic salt): The solvents were evaporated and NaOH 3M was added to the residue. The amine was extracted with ether (3x20 mL) and the ethereal layers were dried over anhydrous Na₂SO₄. Ether was evaporated and the residue was uptaken in 1 mL ether prior to the addition of excess of oxalic acid. The salt was left to form overnight prior to the ether decantation. The oxalic salt was basified with NaOH 3M and the liberated amine was extracted with ether. The ethereal layers were dried over anhydrous Na₂SO₄ and evaporated to afford 40 mg of free base. Physical state: yellow oil. ¹H NMR RR (**linear:branched** 2:1). ¹H NMR DR (**3.13.1:3.12.1** 1.5:1). Yield: 37%. **The linear regioisomer 3.11.1:** ¹H NMR (300 MHz, CDCl₃): δ = 0.84-0.92 (m, 3 H, CH₃CH₂), 1.15-1.36 (m, 10 H, 5xCH₂), 1.63-1.70 (m, 2 H, CHCH₂), 3.86 (d, J = 7.0 Hz, 1 H, CHNH₂), 7.20-7.25 (m, 1 H, ArH), 7.28-7.35 (m, 4 H, ArH); **Clearly separated diagnostic peaks of the major branched diastereomer 3.13.1:** ¹H NMR (400 MHz, CDCl₃): δ = 3.78 (d, J = 6.5 Hz, 1 H, CHNH₂); **Clearly separated diagnostic peaks of the minor branched diastereomer 3.12.1:** ¹H NMR (400 MHz, CDCl₃): δ = 0.74 (d, J = 6.8 Hz, 3 H, CH₃), 3.70 (t, J = 7.0 Hz, 1 H, CHNH₂). MS (CI) m/z : 203.1 [M-16].

3-methyl-2-phenylpiperidine (3.42 and 3.43)¹⁸⁷

Synthesized according to reference.¹⁸⁶ The mixture of regioisomers **3.11.3**, **3.12.3** and **3.13.3** (0.41 mmol, 80 mg) was transferred into a bomb with a stirring bar and dried



under high vacuum overnight. 0.2 mL anhydrous dioxane were added to the bomb and to the resulting solution $\text{RuCl}_2(\text{PPh}_3)_3$ (0.0041 mmol, 4 mg). Then the bomb was sealed and placed in an oil bath at 180 °C and stirred for 5 h. The reaction was monitored by LRMS. Upon the reaction completion, DCM and MeOH were added to the reaction mixture and the suspension was converted into a clear solution. The solvents were evaporated and ether was added to the residue. The amine was extracted with HCl 1M in the form of its hydrochloric salt (4x10 mL) and the combined aqueous layers were basified with NaOH 3M. The liberated base was back extracted with ether (3x15 mL) and the ethereal layers were dried over anhydrous Na_2SO_4 . Ether was evaporated to afford 30 mg of a brownish oil. The obtained product corresponded to the branched regioisomer and was a mixture of diastereomers. Yield 42%. The ^1H NMR data of the obtained product match with the reported data, however the purity is below 95%. **The *syn* branched diastereomer 3.43:** ^1H NMR (400 MHz, CD_3OD): δ = 0.75 (d, J = 7.0 Hz, 3 H, CH_3CH), 1.33-1.50 (m, 1 H), 1.65-1.85 (m, 3 H), 1.89-2.08 (m, 1 H), 2.72-2.81 (m, 1 H), 3.13-3.24 (m, 1 H), 3.95 (d, J = 3.0 Hz, 1 H, CH_2N), 7.20-7.36 (m, 5 H, ArH); **Clearly separated diagnostic peaks of the minor *anti* branched diastereomer 3.42:** ^1H NMR (400 MHz, CD_3OD): δ = 0.64 (d, J = 7.0 Hz, 3 H, CH_3CH), 3.33-3.35 (m, 1 H). MS (ESI) m/z : 176.4 [$\text{M} + \text{H}^+$]. ^1H NMR data match with the data presented in the literature.¹⁸⁷

6.4 Experimental data for Chapter 4

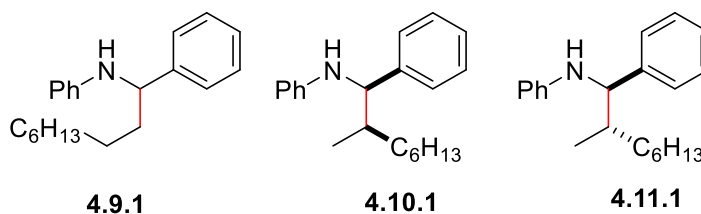
General Procedure for the Hydroaminoalkylation Reaction

A solution of *N*-phenylbenzylamine **3.5.2** (1 equiv, 0.50 mmol, 91.65 mg) in 200 μ L C_6D_6 was added to a solution of $Zr(NMe_2)_4$ (0.1 equiv, 0.05 mmol, 13.37 mg) in 200 μ L C_6D_6 , and 200 μ L C_6D_6 were used for the quantitative transfer of the starting amine into the resulting solution. The alkene (1.8 equiv, 0.90 mmol) was then added to the above solution. The solution was then transferred quantitatively into a J-Young tube via an additional 200 μ L C_6D_6 and placed in an oil bath at 145 $^\circ$ C. The reaction times for each product are presented below. Upon the reaction completion, the J-Young seal was broken and DCM and MeOH were added to the existing solution. The quenched solution was then passed through a celite pipet and the solvents were evaporated and NaOH 3M was added to the residue. The amine was extracted with ether (3x20 mL). The ethereal layers were dried over anhydrous Na_2SO_4 and evaporated to afford the product as a single or mixture of regioisomers.

Linear: *N*-(1-phenylnonyl)aniline (4.9.1)

Branched: *N*-(2-methyl-1-phenyloctyl)aniline (4.10.1 and 4.11.1)

Catalyst Loading (0.1 equiv); Reaction time: 48 h. Physical state: Yellow oil. 1H NMR RR (**linear:branched** 1:5). 1H NMR DR (**4.11.1:4.10.1** 6:1). Yield



(78%). **The major branched diastereomer 4.11.1:** 1H NMR (400 MHz, CD_3OD): δ = 0.81-0.88 (m, 3 H, CH_3CH_2), 0.95 (d, J = 6.7 Hz, CH_3CH), 1.18-1.43 (m, 10 H, $5 \times CH_2$), 1.83-1.89 (m, 1 H, $CHCH_3$), 4.21 (d, J = 5.5 Hz, 1 H, CHN), 6.47 (t, J = 7.2 Hz, 2 H, ArH), 6.51 (d, J = 8.7 Hz, 1 H, ArH), 6.92-6.98 (m, 2 H, ArH), 7.14-7.17 (m, 1 H, ArH), 7.24-7.34 (m, 4 H, ArH); **Clearly separated diagnostic peaks of the minor branched diastereomer 4.10.1:** 1H NMR (400 MHz, CD_3OD): δ = 4.14 (d, J = 6.5 Hz, 1 H, CHN); **Clearly separated diagnostic peaks of the linear**

regioisomer 4.9.1: ^1H NMR (400 MHz, CD_3OD): $\delta = 0.81\text{-}0.84$ (m, 3 H, CH_3), 4.26 (t, $J = 7.0$ Hz, 1 H, CHN). **Clearly separated diagnostic peaks of the major branched diastereomer 4.11.1:** ^{13}C NMR (100 MHz, CD_3OD): $\delta = 14.6$ (CH_3CH_2), 15.9 (CH_3CH), 23.8 (CH_2), 28.5 (CH_2), 30.7(CH_2), 33.1 (CH_2), 35.2 (CH_2), 41.2 (CH_3CH), 63.3 (CHN), 145.2 (CCHNPh), 149.9 (C_{PhN}); **Clearly separated diagnostic peaks of the branched diastereomer 4.10.1:** ^{13}C NMR (100 MHz, CD_3OD): $\delta = 14.6$ (CH_3CH_2), 17.3 (CH_3CH), 40.9 (CH_3CH), 64.1 (CHN), 144.6 (CCHNPh), 149.9 (C_{PhN}); **Clearly separated diagnostic peaks of the linear regioisomer 4.9.1:** ^{13}C NMR (100 MHz, CD_3OD): $\delta = 40.0$ (CH_2CHN), 59.4 (CHN), 146.5 (CCHNPh), 149.7 (C_{PhN}); **Aliphatic peaks (methylene protons of minor branched diastereomer 4.10.1 and linear regioisomer 4.9.1):** ^{13}C NMR (100 MHz, CD_3OD): $\delta = 23.9, 27.7, 28.4, 30.6, 30.8, 30.9, 33.2$ (2xC), 34.2 **Aromatic peaks (all three products):** ^{13}C NMR (100 MHz, CD_3OD): $\delta = 114.4$ (2xC), 114.6, 117.4, 117.6, 127.6, 127.7, 127.8 (2xC), 128.5, 128.8, 129.1, 129.2, 129.5, 129.9. HRMS (HESI) m/z calcd for $\text{C}_{21}\text{H}_{29}\text{NH}^+$ [$\text{M} + \text{H}^+$], 296.2378: Found 296.2371.

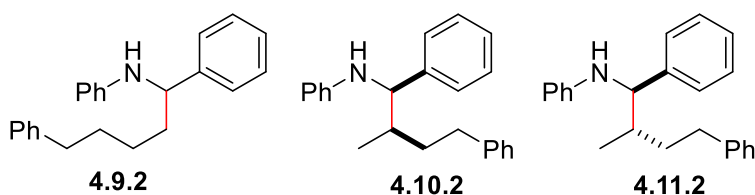
Linear: *N*-(1,5-diphenylpentyl)aniline (4.9.2)

Branched: *N*-(2-methyl-1,4-diphenylbutyl)aniline (4.10.2 and 4.11.2)

Catalyst Loading (0.1 equiv);

Reaction time: 48 h. Physical state:

Yellow oil. ^1H NMR RR



(linear:branched 1:5). ^1H NMR DR (4.11.2:4.10.2 4:1). Yield (91%). **The branched major**

diastereomer 4.11.2: ^1H NMR (400 MHz, CD_3OD): $\delta = 1.01$ (d, $J = 6.9$ Hz, 3 H, CH_3CH), 1.44-1.54 (m, 1 H, $\text{CH}_2\text{CH}_2\text{Ph}$), 1.74-1.81 (m, 1 H, $\text{CH}_2\text{CH}_2\text{Ph}$), 1.87-1.96 (m, 1 H, CHCH_3), 2.51-2.58 (m, 1 H, CH_2Ph), 2.64-2.72 (m, 1 H, CH_2Ph), 4.29 (d, $J = 5.9$ Hz, 1 H, CHN), 6.49-6.55 (m, 3 H, ArH), 6.94-6.99 (m, 2 H, ArH), 7.08-7.14 (m, 3 H, ArH), 7.16-7.31 (m, 7 H, ArH); **Clearly**

separated diagnostic peaks of the minor branched diastereomer **4.10.2**: ^1H NMR (400 MHz, CD_3OD): $\delta = 0.91$ (d, $J = 6.8$ Hz, 3 H, CH_3CH), 4.20 (d, $J = 6.6$ Hz, 1 H, CHN); **Clearly separated diagnostic peaks of the linear regioisomer 4.9.2**: ^1H NMR (400 MHz, CD_3OD): $\delta = 4.26$ (t, $J = 6.9$ Hz, 1 H, CHN). **Clearly separated diagnostic peaks of the branched diastereomer 4.11.2**: ^{13}C NMR (100 MHz, CD_3OD): $\delta = 15.9$ (CH_3CH), 34.6 ($\text{CH}_2\text{CH}_2\text{Ph}$), 37.1 ($\text{CH}_2\text{CH}_2\text{Ph}$), 40.6 (CH_3CH), 63.0 (CHN), 143.9 ($\text{C}_{\text{Ph}}\text{CH}_2$), 145.0 (CCHN), 149.9 ($\text{C}_{\text{Ph}}\text{N}$); **Clearly separated diagnostic peaks of the minor branched diastereomer 4.10.2**: ^{13}C NMR (100 MHz, CD_3OD): $\delta = 17.3$ (CH_3CH), 34.6 ($\text{CH}_2\text{CH}_2\text{Ph}$), 37.1 ($\text{CH}_2\text{CH}_2\text{Ph}$), 40.4 (CH_3CH), 63.9 (CHN), 143.9 ($\text{C}_{\text{Ph}}\text{CH}_2$), 144.5 (CCHN), 149.8 ($\text{C}_{\text{Ph}}\text{N}$); **Clearly separated diagnostic peaks of the linear regioisomer 4.9.2**: ^{13}C NMR (100 MHz, CD_3OD): $\delta = 27.3$ ($\text{CH}_2\text{CH}_2\text{CH}_2\text{CH}_2\text{Ph}$), 32.8 ($\text{CH}_2\text{CH}_2\text{CH}_2\text{CH}_2\text{Ph}$), 36.3 ($\text{CH}_2\text{CH}_2\text{CH}_2\text{CH}_2\text{Ph}$), 39.7 ($\text{CH}_2\text{CH}_2\text{CH}_2\text{CH}_2\text{Ph}$), 59.3 (CHN), 144.1 ($\text{C}_{\text{Ph}}\text{CH}_2$), 146.4 (CCHN), 149.6 ($\text{C}_{\text{Ph}}\text{N}$); **Aromatic peaks (all three products)**: ^{13}C NMR (100 MHz, CD_3OD): $\delta = 114.4$, 114.5, 114.6, 117.4, 117.6, 126.8 (2xC), 127.7, 127.8 (2xC), 128.5, 128.8, 129.2 (2xC), 129.4 (2xC), 129.5 (3xC), 129.9 (2xC). HRMS (HESI) m/z calcd for $\text{C}_{23}\text{H}_{25}\text{NH}^+ [\text{M} + \text{H}^+]$, 316.2065; Found 316.2066.

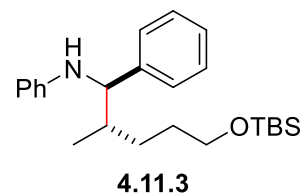
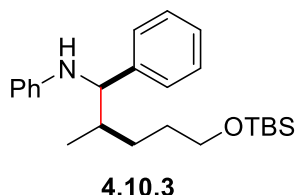
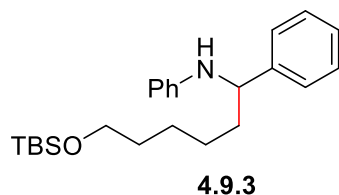
Linear: *N*-(6-((tert-butyldimethylsilyl)oxy)-1-phenylhexyl)aniline (4.9.3)

Branched: *N*-(5-((tert-butyldimethylsilyl)oxy)-2-methyl-1-phenylpentyl)aniline (4.10.3 and 4.11.3)

Catalyst Loading

(0.1 equiv);

Reaction time: 48



h. Physical state: Yellow oil. ^1H NMR RR (**linear:branched 1:2**). ^1H NMR DR (**4.11.3:4.10.3 3:1**). Yield (82%). **The major branched diastereomer 4.11.3**: ^1H NMR (400 MHz, CD_3OD): δ

= 0.02 (s, 6 H, Si(CH₃)₂), 0.87 (s, 9 H, C(CH₃)₃), 1.01 (d, *J* = 6.7 Hz, 3 H, CH₃CH), 1.17-1.66 (m, 4 H, CH₂CH₂CH₂OTBS), 1.82-1.93 (m, 1 H, CHCH₃), 3.57-3.62 (m, 2 H, CH₂OTBS), 4.22 (d, *J* = 6.1 Hz, 1 H, CHN), 6.49 (t, *J* = 6.9 Hz, 2 H, ArH), 6.53 (d, *J* = 8.3 Hz, 1 H, ArH), 6.95-6.99 (m, 2 H, ArH), 7.17 (t, *J* = 7.1 Hz, 1 H, ArH), 7.25-7.26 (m, 2 H, ArH), 7.31-7.35 (m, 2 H, ArH); **Clearly separated diagnostic peaks of the minor branched diastereomer 4.10.3:** ¹H NMR (400 MHz, CD₃OD): δ = 0.08 (s, 6 H, Si(CH₃)₂), 0.99 (d, *J* = 6.9 Hz, 3 H, CH₃CH), 4.16 (d, *J* = 6.5 Hz, 1 H, CHN); **Clearly separated diagnostic peaks of the linear regioisomer 4.9.3:** ¹H NMR (400 MHz, CD₃OD): δ = 0.04 (s, 6 H, Si(CH₃)₂), 4.29 (t, *J* = 6.9 Hz, 1 H, CHN). **Clearly separated diagnostic peaks of the major branched diastereomer 4.11.3:** ¹³C NMR (100 MHz, CD₃OD): δ = -4.99 (q, *J*_{CSi} = 12.0 Hz, Si(CH₃)₂), 16.1 (CH₃CH), 19.3 (C(CH₃)₃), 26.6 (C(CH₃)₃), 31.4 (CH₂), 31.9 (CH₂), 41.1 (CH₃CH), 63.4 (CHN), 64.6 (CH₂OTBS), 145.0 (CCHN), 149.9 (C_{Ph}N); **Clearly separated diagnostic peaks of the minor branched diastereomer 4.10.3:** ¹³C NMR (100 MHz, CD₃OD): δ = -4.99 (q, *J*_{CSi} = 12.0 Hz, Si(CH₃)₂), 17.3 (CH₃CH), 19.3 (C(CH₃)₃), 26.6 (C(CH₃)₃), 30.6 (CH₂), 31.7 (CH₂), 40.7 (CH₃CH), 64.1 (CHN), 64.8 (CH₂OTBS), 144.5 (CCHN), 149.8 (C_{Ph}N); **Clearly separated diagnostic peaks of the linear regioisomer 4.9.3:** ¹³C NMR (100 MHz, CD₃OD): δ = -4.99 (q, *J*_{CSi} = 12.0 Hz, Si(CH₃)₂), 19.3 (C(CH₃)₃), 26.6 (C(CH₃)₃), 26.9 (CH₂), 27.4 (CH₂), 33.9 (CH₂), 39.9 (CH₂CH), 59.3 (CHN), 64.3 (CH₂OTBS), 146.4 (CCHN), 149.6 (C_{Ph}N); **Aromatic peaks (all three products):** ¹³C NMR (100 MHz, CD₃OD): δ = 114.4, 114.5, 114.7, 117.4, 117.6, 127.7, 127.8, 127.9, 128.6, 128.8, 129.2, 129.3, 129.5, 129.8, 129.9. HRMS (HESI) *m/z* calcd for C₂₄H₃₇NH⁺ [M + H⁺], 384.2723: Found 384.2724.

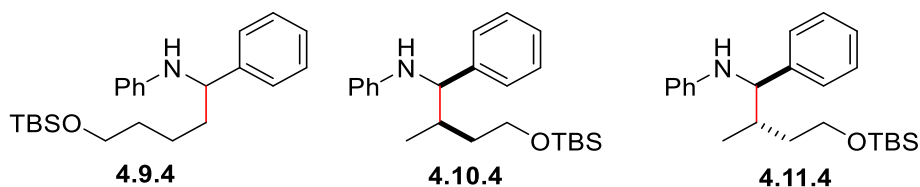
Linear: *N*-(5-((tert-butyldimethylsilyloxy)-1-phenylpentyl)aniline (4.9.4)

Branched: *N*-(4-((tert-butyldimethylsilyl)oxy)-2-methyl-1-phenylbutyl)aniline (4.10.4 and 4.11.4)

Catalyst Loading (0.1

equiv); Reaction time:

72 h. Physical state:



Yellow oil. ^1H NMR RR (**linear:branched** 1:3). ^1H NMR DR (**4.11.4:4.10.4** 7:1). Yield (84%).

The major branched diastereomer 4.11.4: ^1H NMR (400 MHz, CD_3OD): δ = 0.03 (s, 6 H, $\text{Si}(\text{CH}_3)_2$), 0.90 (s, 9 H, $\text{C}(\text{CH}_3)_3$), 0.97 (d, J = 7.0 Hz, 3 H, CH_3CH), 1.36-1.45 (m, 1 H, $\text{CHCH}_2\text{CH}_2\text{OTBS}$), 1.65-1.77 (m, 1 H, $\text{CHCH}_2\text{CH}_2\text{OTBS}$), 2.07-2.16 (m, 1 H, CHCH_3), 3.60-3.74 (m, 2 H, CH_2OTBS), 4.28 (d, J = 5.7 Hz, 1 H, CHN), 6.49 (t, J = 7.3 Hz, 2 H, ArH), 6.53 (d, J = 8.0 Hz, 1 H, ArH), 6.97 (t, J = 7.0 Hz, 2 H, ArH), 7.15-7.19 (m, 1 H, ArH), 7.27 (t, J = 7.2 Hz, 2 H, ArH), 7.31-7.35 (m, 2 H, ArH); **Clearly separated diagnostic peaks of the minor branched diastereomer 4.10.4:** ^1H NMR (400 MHz, CD_3OD): δ = 4.19 (d, J = 6.4 Hz, 1 H, CHN); **Clearly separated diagnostic peaks of the linear regioisomer 4.9.4:** ^1H NMR (400 MHz, CD_3OD): δ = 1.47-1.50 (m, 2 H, $\text{CH}_2\text{CH}_2\text{CH}_2\text{CH}_2\text{OTBS}$ or $\text{CH}_2\text{CH}_2\text{CH}_2\text{CH}_2\text{OTBS}$), 1.80-1.90 (m, 1 H, $\text{CH}_2\text{CH}_2\text{CH}_2\text{CH}_2\text{OTBS}$), 4.28 (t, J = 6.5 Hz, 1 H, CHN). **Clearly separated diagnostic peaks of the major branched diastereomer 4.11.4:** ^{13}C NMR (100 MHz, CD_3OD): δ = -5.00 (m, $\text{Si}(\text{CH}_3)_2$), 15.8 (CH_3CH), 19.3 ($\text{C}(\text{CH}_3)_3$), 26.6 ($\text{C}(\text{CH}_3)_3$), 37.6 (CH_3CH), 38.1 (CHCH_2), 41.1 (CH_3CH), 62.5 (CH_2OTBS), 63.0 (CHN), 144.5 (CCHN), 149.8 (C_{PhN}); **Clearly separated diagnostic peaks of the minor branched diastereomer 4.10.4:** ^{13}C NMR (100 MHz, CD_3OD): -5.00 (m, $\text{Si}(\text{CH}_3)_2$), 17.7 (CH_3CH), 19.3 ($\text{C}(\text{CH}_3)_3$), 26.6 ($\text{C}(\text{CH}_3)_3$), 37.1 (CHCH_2), 37.7 (CH_3CH), 62.2 (CH_2OTBS), 64.2 (CHN), 144.5 (CCHN); **Clearly separated diagnostic peaks of the linear regioisomer 4.9.4:** ^{13}C NMR (100 MHz, CD_3OD): δ = -5.00 (m, $\text{Si}(\text{CH}_3)_2$),

19.3 (C(CH₃)₃), 24.1 (CH₂), 26.6 (C(CH₃)₃), 33.9 (CH₂), 39.6 (CH₂CH), 59.4 (CHN), 64.3 (CH₂OTBS), 146.3 (CCHN), 149.6 (C_{Ph}N); **Aromatic peaks (all three products):** ¹³C NMR (100 MHz, CD₃OD): δ = 114.4 (2xC), 114.6, 117.4, 117.5, 117.6, 127.7, 127.8, 127.9, 128.5, 128.8, 129.2, 129.3, 129.5, 129.9. HRMS (HESI) *m/z* calcd for C₂₃H₃₅NOSiH⁺ [M + H⁺], 370.2566: Found 370.2560.

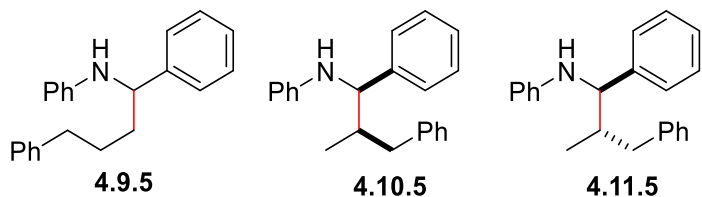
Linear: *N*-(1,4-diphenylbutyl)aniline (4.9.5)

Branched: *N*-(2-methyl-1,3-diphenylpropyl)aniline (4.10.5 and 4.11.5)

Catalyst Loading (0.1 equiv); Reaction

time: 48 h. Physical state: Yellow oil.

¹H NMR RR (**linear:branched** 1:2). ¹H



NMR DR (**4.11.5:4.10.5** 4:1). Yield (93%). **The major branched diastereomer 4.11.5:** ¹H

NMR (400 MHz, CD₃OD): δ = 0.90 (d, *J* = 6.5 Hz, 3 H, CH₃CH), 2.14-2.22 (m, 2 H, CH₃CH), 2.41-2.53 (m, 1 H, CH₂Ph), 2.76-2.82 (m, 1 H, CH₂Ph), 4.24 (d, *J* = 5.0 Hz, 1 H, CHN), 6.46-

6.54 (m, 3 H, ArH), 6.94-6.98 (m, 2 H, ArH), 7.11-7.32 (m, 10 H, ArH); **Clearly separated**

diagnostic peaks of the minor branched diastereomer 4.10.5: ¹H NMR (400 MHz, CD₃OD): δ

= 0.70 (d, *J* = 6.6 Hz, 3 H, CH₃CH), 4.17 (d, *J* = 7.1 Hz, 1 H, CHN); **Clearly separated**

diagnostic peaks of the linear regioisomer 4.9.5: ¹H NMR (400 MHz, CD₃OD): δ = 1.60-1.89

(m, 4 H, 2xCH₂), 2.61 (t, *J* = 6.7 Hz, 2 H, CH₂Ph), 4.30 (t, *J* = 6.7 Hz, 1 H, CHN). **Clearly**

separated diagnostic peaks of the major branched diastereomer 4.11.5: ¹³C NMR (100 MHz,

CD₃OD): δ = 15.1 (CH₃CH), 41.7 (CHCH₂Ph), 44.0 (CH₃CH), 61.8 (CHN), 142.6 (C_{Ph}CH₂),

145.0 (CCHN), 149.8 (C_{Ph}N); **Clearly separated diagnostic peaks of the minor branched**

diastereomer 4.10.5: ¹³C NMR (100 MHz, CD₃OD): δ = 16.9 (CH₃CH), 40.7 (CHCH₂Ph), 42.9

(CH₃CH), 63.8 (CHN), 142.3 (C_{Ph}CH₂), 143.2 (CCHN), 144.6 (C_{Ph}N); **Clearly separated**

diagnostic peaks of the linear regioisomer 4.9.5: ^{13}C NMR (100 MHz, CD_3OD): $\delta = 29.7, 36.8$ ($\text{CH}_2\text{CH}_2\text{Ph}$), 39.4, 59.2 (CHN), 143.7 ($\text{C}_{\text{Ph}}\text{CH}_2$), 146.4 (CCHN), 149.6 ($\text{C}_{\text{Ph}}\text{N}$); **Aromatic peaks (all three products):** ^{13}C NMR (100 MHz, CD_3OD): $\delta = 114.5$ (2xC), 114.7, 117.5, 117.6, 126.9 (2xC), 127.0 (2xC), 127.1, 127.7, 127.8, 127.9, 128.1, 128.4, 128.9, 129.3 (3xC), 129.4 (2xC), 129.5, 129.6 (2xC), 129.9, 130.3 (2xC), 130.6. HRMS (HESI) m/z calcd for $\text{C}_{22}\text{H}_{23}\text{NH}^+ [\text{M} + \text{H}^+]$, 302.1909; Found 302.1906.

Linear: *N*-(3-cyclohexyl-1-phenylpropyl)aniline (4.9.6)

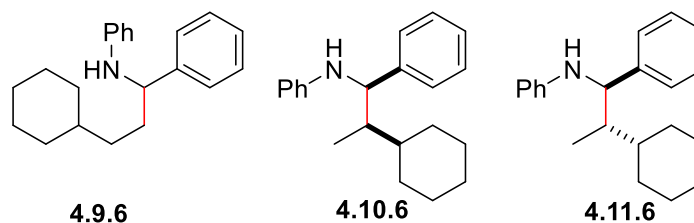
Branched: *N*-(2-cyclohexyl-1-phenylpropyl)aniline (4.10.6 and 4.11.6)

Catalyst Loading (0.1 equiv); Reaction

time: 120 h. Physical state: Yellow oil.

^1H NMR RR (**linear:branched** 1:1).

^1H NMR DR (**4.11.5:4.10.5** 8:1). Yield



(79%). **The linear regioisomer 4.9.6:** ^1H NMR (400 MHz, CD_3OD): $\delta = 0.84\text{-}1.87$ (m, 15 H, CH_{cyc} , 7x CH_2), 4.22 (t, $J = 6.9$ Hz, 1 H, CHN), 6.45-6.53 (m, 3 H, ArH), 6.96 (t, $J = 8.2$ Hz, 2 H, ArH), 7.13-7.17 (td, $J = 7.0$ Hz, $J = 1.8$ Hz, 1 H, ArH), 7.23-7.33 (m, 4 H, ArH); **Clearly separated diagnostic peaks of the major branched diastereomer 4.11.6:** ^1H NMR (400 MHz, CD_3OD): $\delta = 0.90$ (d, $J = 7.0$ Hz, 1 H, CH_3), 4.42 (d, $J = 5.9$ Hz, 1 H, CHN). **Clearly separated diagnostic peaks of the minor branched diastereomer 4.10.6:** ^1H NMR (400 MHz, CD_3OD): $\delta = 0.57$ (d, $J = 7.1$ Hz, 1 H, CH_3), 4.15 (d, $J = 9.5$ Hz, 1 H, CHN). **Clearly separated diagnostic peaks of the linear regioisomer 4.9.6:** ^{13}C NMR (100 MHz, CD_3OD): $\delta = 56.7$ (CHN); **Clearly separated diagnostic peaks of the major branched diastereomer 4.11.6:** ^{13}C NMR (100 MHz, CD_3OD): $\delta = 11.8$ (CH_3), 60.4 (CHN); **Clearly separated diagnostic peaks of the minor branched diastereomer 4.10.6:** ^{13}C NMR (100 MHz, CD_3OD): $\delta = 13.0$ (CH_3), 61.4 (CHN);

Aliphatic peaks (methylene and methyne peaks of linear and major branched diastereomer): ^{13}C NMR (100 MHz, CD_3OD): $\delta = 27.6$ (CH_2), 27.7 (CH_2), 27.8 (CH_2), 27.9 (CH_2 , 2xC), 28.0 (CH_2), 30.8 (CH_2), 32.8 (CH_2), 34.7 (CH_2 , 2xC), 37.3 (CH_2), 39.1 (CH), 41.1 (CH), 49.9 (CH); **Aromatic peaks (linear 4.9.6 and major branched diastereomer 4.11.6):** ^{13}C NMR (100 MHz, CD_3OD): 114.2, 114.6, 117.3, 117.6, 127.5, 127.8, 127.9, 128.4, 129.3, 129.4, 129.9 (2xC), 145.7, 146.5, 149.6, 149.8. HRMS (HESI) m/z calcd for $\text{C}_{21}\text{H}_{27}\text{NH}^+$ [$\text{M} + \text{H}^+$], 294.2221: Found 294.2221.

Linear: *N*-(3-(cyclohex-3-en-1-yl)-1-phenylpropyl)aniline (4.9.7)

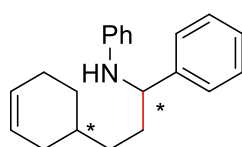
Branched: *N*-(2-(cyclohex-3-en-1-yl)-1-phenylpropyl)aniline (4.10.7 and 4.11.7)

Catalyst Loading (0.1 equiv); Reaction

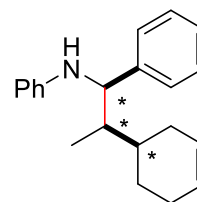
time: 120 h. Physical state: Yellow oil.

^1H NMR RR (**linear:branched** 1:1).

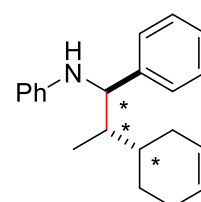
^1H NMR DR (**4.11.7:4.10.7** 1:1). Yield



4.9.7



4.10.7



4.11.7

(78%). **Clearly separated diagnostic benzylic peaks of the linear regioisomer 4.9.7:** ^1H NMR (400 MHz, CD_3OD): $\delta = 4.25$ (t, $J = 6.9$ Hz, 1 H, CHN); **Clearly separated diagnostic benzylic peaks of the branched diastereomers 4.10.7 and 4.11.7:** ^1H NMR (400 MHz, CD_3OD): $\delta = 4.46$ (t, $J = 5.6$ Hz, 1 H, CHN), 4.49 (t, $J = 5.6$ Hz, 1 H, CHN). **Clearly separated diagnostic benzylic peaks of the linear regioisomer 4.9.7:** ^{13}C NMR (100 MHz, CD_3OD): $\delta = 59.6$ (CHN), 59.7 (CHN); **Clearly separated peaks of the branched diastereomers 4.10.7 and 4.11.7:** ^{13}C NMR (100 MHz, CD_3OD): $\delta = 60.3$ (CHN), 60.4 (CHN). HRMS (HESI) m/z calcd for $\text{C}_{15}\text{H}_{21}\text{NH}^+$ [$\text{M} + \text{H}^+$], 216.1752: Found 216.1747.

***N*-(1-phenyl-3-(trimethylsilyl)propyl)aniline (4.9.10)**

Catalyst Loading (0.1 equiv); Reaction time: 24 h. Physical state: Yellow

oil. Yield (75%). ^1H NMR (400 MHz, CDCl_3): $\delta = -0.02$ (d, $J = 1.4$ Hz, 9 H, $\text{Si}(\text{CH}_3)_3$), 0.44-0.52 (m, 1 H, CH_2Si), 0.61-0.69 (m, 1 H, CH_2Si), 1.73-



1.83 (m, 2 H, $\text{CH}_2\text{CH}_2\text{Si}$), 4.07 (broad s, 1 H, NH), 4.22 (t, $J = 6.7$ Hz, 1 H, CHN), 6.53 (d, $J = 7.7$ Hz, 2 H, ArH), 6.64 (t, $J = 7.1$ Hz, 1 H, ArH), 7.09 (t, $J = 8.5$ Hz, 2 H, ArH), 7.22-7.25 (m, 1 H, ArH), 7.31-7.37 (m, 4 H, ArH). ^{13}C NMR (100 MHz, CDCl_3): $\delta = -1.6$ (CH_3), 13.4 (CH_2Si), 33.4 ($\text{CH}_2\text{CH}_2\text{Si}$), 61.1 (CH_2N), 113.5 (2xArC), 117.3 (ArC), 126.7 (2xArC), 127.1 (ArC), 128.7 (2xArC), 129.3 (2xArC), 144.3 (CCHNHPh), 147.8 (C_{PhN}). HRMS (HESI) m/z calcd for $\text{C}_{18}\text{H}_{25}\text{NSiH}^+ [\text{M} + \text{H}^+]$, 284.1835; Found 284.1832.

***N*-(2-methyl-1-phenyl-3-(trimethylsilyl)propyl)aniline (4.10.12 and 4.11.12)**

Catalyst Loading (0.1 equiv); Reaction time: 240 h.

Physical state: Yellow oil. ^1H NMR RR (linear:branched 1:99). ^1H NMR DR



4.10.12



4.11.12

(4.11.12:4.10.12 4:1). Yield (85%). **The major**

branched diastereomer 4.11.12: ^1H NMR (400 MHz, CD_3OD): $\delta = 0.02$ (s, 9 H, $\text{Si}(\text{CH}_3)_3$), 0.49-0.55 (dd, $J = 14.6$ Hz, $J = 9.9$ Hz, 1 H, CH_2Si), 0.77-0.82 (dd, $J = 14.2$ Hz, $J = 4.3$ Hz, 1 H, CH_2Si), 1.02 (d, $J = 6.8$ Hz, 3 H, CH_3CH), 2.07-2.14 (m, 1 H, CHCH_3), 4.17 (d, $J = 5.7$ Hz, 1 H, CHN), 6.52 (t, $J = 7.4$ Hz, 1 H, ArH), 6.56 (d, $J = 8.1$ Hz, 2 H, ArH), 7.00 (t, $J = 8.7$ Hz, 1 H, ArH), 7.18-7.22 (m, 2 H, ArH), 7.20-7.25 (m, 1 H, ArH), 7.28-7.35 (m, 4 H, ArH); **Clearly separated diagnostic peaks of the minor branched diastereomer 4.10.12:** ^1H NMR (400 MHz, CD_3OD): $\delta = -0.00$ (s, 9 H, $\text{Si}(\text{CH}_3)_3$), 0.99 (d, $J = 6.8$ Hz, 3 H, CH_3CH). **Clearly separated diagnostic peaks of the major branched diastereomer 4.11.12:** ^{13}C NMR (100 MHz, CD_3OD): $\delta = -0.5$ (q, $J_{\text{CSi}} = 12.6$ Hz, $\text{Si}(\text{CH}_3)_3$), 19.0 (CH_3CH), 22.9 (CH_2Si), 37.8

(CH₃CH), 66.0 (CHN), 114.5 (2xArC), 117.4 (ArC), 127.7 (ArC), 128.7 (2xArC), 129.2 (2xArC), 129.8 (2xArC), 145.0 (CCHNHPH), 149.9 (C_{Ph}N); **Clearly separated diagnostic peaks of the minor branched diastereomer 4.10.12:** ¹³C NMR (100 MHz, CD₃OD): δ = -0.5 (Si(CH₃)₃), 20.7 (CH₃CH), 37.4 (CH₃CH), 66.3 (CHN), 128.7 (2xArC), 129.1 (2xArC), 144.7 (CCHNHPH). HRMS (HESI) *m/z* calcd for C₁₉H₂₈NSiH⁺ [M + H⁺], 298.1991: Found 298.2002.

General Procedure for the Hydroaminoalkylation Reaction

To a solution of Zr(NMe₂)₄ (0.1 equiv, 0.05 mmol, 13.37 mg) in 200-300 μL C₆D₆, the amine **4.8** (1 equiv, 0.50 mmol, 74.62 mg) was added followed by the addition of the alkene **3.10** (1.8 equiv, 0.90 mmol). The solution was then transferred quantitatively into a J-Young tube via an additional 200-300 μL C₆D₆ and placed in an oil bath at 145 °C. The reaction times for each product are presented below. Upon the reaction completion, the J-Young seal was broken and DCM and MeOH were added to the existing solution. The quenched solution was then passed through a celite pipet and the solvents were evaporated and NaOH 3M was added to the residue. The amine was extracted with ether (3x20 mL). The ethereal layers were dried over anhydrous Na₂SO₄ and evaporated to afford the product as a single or mixture of regioisomers.

Linear: *N*-isopropyl-1-phenylnonan-1-amine (4.12.1)

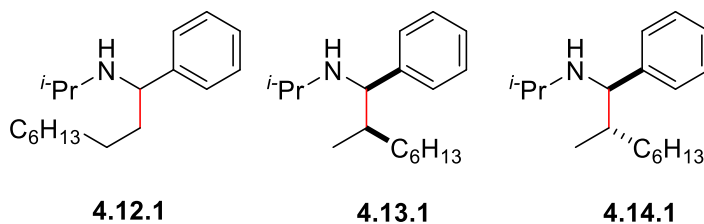
Branched: *N*-isopropyl-2-methyl-1-phenyloctan-1-amine (4.13.1 and 4.14.1)

Catalyst Loading (0.1 equiv); Reaction

time: 48 h. Physical state: Yellow oil.

¹H NMR RR (**linear:branched** 1:4).

¹H NMR DR (**4.14.1:4.13.1** 4:1). Yield



(61%). **The major branched diastereomer 4.14.1:** ¹H NMR (400 MHz, CD₃OD): δ = 0.83-0.99 (m, 12 H), 1.14-1.32 (m, 10 H), 1.57-1.82 (m, 1 H, CHCH₃), 2.46-2.53 (m, 1 H, NHCH(CH₃)₂),

3.52 (d, $J = 6.8$ Hz, 1 H, CHN), 7.19-7.31 (m, 5 H, ArH); **Clearly separated diagnostic peaks of 4.13.1:** ^1H NMR (400 MHz, CD_3OD): $\delta = 3.58$ (d, $J = 6.2$ Hz, 1 H, CHN); **Clearly separated diagnostic peaks of the linear regioisomer 4.12.1:** ^1H NMR (400 MHz, CD_3OD): $\delta = 3.62$ -3.66 (dd, $J = 9.5$ Hz, $J = 4.9$ Hz, 1 H, CHN). **Clearly separated diagnostic peaks of 4.14.1:** ^{13}C NMR (100 MHz, CD_3OD): $\delta = 14.6, 17.1, 21.8, 23.8, 24.1, 28.3, 30.7, 33.1, 34.2, 40.6$ (CH_3CH), 46.9 ($\text{CH}(\text{CH}_3)_2$), 66.7 (CHN), 128.0 (ArC), 129.3 (2xArC), 144.1 (CCHN); **Clearly separated diagnostic peaks of 4.13.1:** ^{13}C NMR (100 MHz, CD_3OD): $\delta = 40.1$ (CH_3CH), 46.8 ($\text{CH}(\text{CH}_3)_2$), 65.9 (CHN); **Clearly separated diagnostic peaks of the linear regioisomer 4.12.1:** ^{13}C NMR (100 MHz, CD_3OD): $\delta = 38.7$ (CH_3CH), 46.3 ($\text{CH}(\text{CH}_3)_2$), 61.5 (CHN). GCFID rt: **4.14.1:** 8.239, **4.13.1:** 8.265 or 8.566, **4.12.1:** 8.265 or 8.566. HRMS (HESI) m/z calcd for $\text{C}_{18}\text{H}_{31}\text{NH}^+$ [$\text{M} + \text{H}^+$], 262.2535: Found 262.2534.

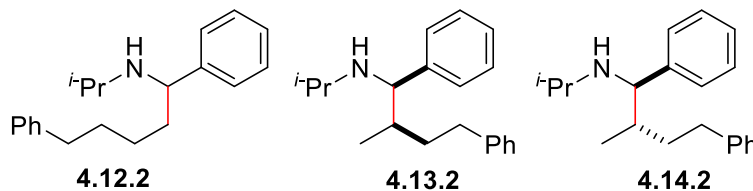
Linear: *N*-isopropyl-1,5-diphenylpentan-1-amine (4.12.2)

Branched: *N*-isopropyl-2-methyl-1,4-diphenylbutan-1-amine (4.13.2 and 4.14.2)

Catalyst Loading (0.1 equiv);

Reaction time: 48 h. Physical state:

Yellow oil. GCFID RR



(linear:branched 1:17). GCFID DR (**4.14.2:4.13.2** 8:1). Yield (75%). **The major branched diastereomer 4.14.2:** ^1H NMR (400 MHz, CD_3OD): $\delta = 0.99$ -1.02 (dd, $J = 8.5$ Hz, $J = 6.3$ Hz, 6 H, $\text{CH}(\text{CH}_3)_2$), 1.04 (d, $J = 6.5$ Hz, 3 H, CH_3CH), 1.20-1.30 (m, 1 H, $\text{CH}_2\text{CH}_2\text{Ph}$), 1.64-1.73 (m, 1 H, $\text{CH}_2\text{CH}_2\text{Ph}$), 1.75-1.82 (m, 1 H, CHCH_3), 2.42-2.51 (m, 1 H, CH_2Ph), 2.47-2.56 (NHCH(CH_3) $_2$), 2.63-2.70 (m, 1 H, CH_2Ph), 3.60 (d, $J = 6.8$ Hz, 1 H, CHN), 7.05-7.33 (m, 10 H, ArH); **Clearly separated diagnostic peaks of the minor branched diastereomer 4.13.2:** ^1H NMR (400 MHz, CD_3OD): $\delta = 0.83$ (d, $J = 6.6$ Hz, 3 H, CH_3CH), 3.65 (d, $J = 6.0$ Hz, 1 H,

CHN); **Clearly separated diagnostic peaks of the linear regioisomer 4.12.2:** ^1H NMR (400 MHz, CD_3OD): $\delta = 3.65\text{-}3.69$ (m, 1 H, *CHN*). **Clearly separated diagnostic peaks of the major branched diastereomer 4.14.2:** ^{13}C NMR (100 MHz, CD_3OD): $\delta = 17.0$ (CH_3CH), 21.9 ($\text{CH}(\text{CH}_3)_2$), 24.0 ($\text{CH}(\text{CH}_3)_2$), 34.6 ($\text{CH}_2\text{CH}_2\text{Ph}$), 36.4 ($\text{CH}_2\text{CH}_2\text{Ph}$), 40.0 (CH_3CH), 46.9 ($\text{CH}(\text{CH}_3)_2$), 66.5 (*CHN*), 126.8 (ArC), 128.0 (ArC), 129.3 (2xArC), 129.4 (ArC), 129.6 (ArC), 144.0 (*CCHN*, $C_{\text{Ph}}\text{CH}_2$); **Clearly separated diagnostic peaks of the minor branched diastereomer 4.13.2:** ^{13}C NMR (100 MHz, CD_3OD): $\delta = 16.1$ (CH_3CH), 21.8 ($\text{CH}(\text{CH}_3)_2$), 24.0 ($\text{CH}(\text{CH}_3)_2$), 46.8 ($\text{CH}(\text{CH}_3)_2$), 65.8 (*CHN*); **Clearly separated diagnostic peaks of the linear regioisomer 4.12.2:** ^{13}C NMR (100 MHz, CD_3OD): $\delta = 21.8$ ($\text{CH}(\text{CH}_3)_2$), 23.8 ($\text{CH}(\text{CH}_3)_2$), 46.3 ($\text{CH}(\text{CH}_3)_2$), 61.5 (*CHN*). GCFID rt: **4.14.2:** 7.144, **4.13.2:** 7.375, **4.12.2:** 8.388. HRMS (HESI) m/z calcd for $\text{C}_{20}\text{H}_{27}\text{NH}^+$ [$\text{M} + \text{H}^+$], 282.2222; Found 282.2218.

Linear: *N*-isopropyl-1,4-diphenylbutan-1-amine (4.12.5)

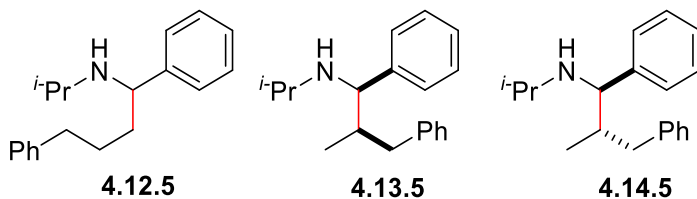
Branched: *N*-isopropyl-2-methyl-1,3-diphenylpropan-1-amine (4.13.5 and 4.14.5)

Catalyst Loading (0.1 equiv); Reaction

time: 48 h. Physical state: Yellow oil.

GCFID ratio [**4.14.5:(4.13.5+4.12.5)**

3:1]. Yield (58%). **The major**



branched diastereomer 4.14.5: ^1H NMR (400 MHz, CD_3OD): $\delta = 0.86$ (d, $J = 6.3$ Hz, 3 H, CH_3CH), 0.98-1.04 (m, 6 H, $\text{CH}(\text{CH}_3)_2$), 2.02-2.08 (CH_3CH), 2.09-2.15 (m, 1 H, CH_2Ph), 2.52-2.63 (m, 1 H, $\text{NHCH}(\text{CH}_3)_2$), 2.73-2.77 (dd, $J = 11.4$ Hz, $J = 3.4$ Hz, 1 H, CH_2Ph), 3.66 (d, $J = 5.6$ Hz, 1 H, *CHN*), 7.09-7.39 (m, 10 H, ArH); **Clearly separated diagnostic peaks of the minor branched diastereomer 4.13.5:** ^1H NMR (400 MHz, CD_3OD): $\delta = 0.66$ (d, $J = 6.4$ Hz, 3 H, CH_3CH), 2.97-3.02 (dd, $J = 13.1$ Hz, $J = 4.8$ Hz, 1 H, CH_2Ph), 3.67 (d, $J = 5$ Hz, 1 H, *CHN*);

Clearly separated diagnostic peaks of the linear regioisomer 4.12.5: ^1H NMR (400 MHz, CD_3OD): $\delta = 3.69\text{-}3.75$ (m, 1 H, *CHN*). **Clearly separated diagnostic peaks of the major branched diastereomer 4.14.5:** ^{13}C NMR (100 MHz, CD_3OD): $\delta = 16.4$ (CH_3CH), 21.9 ($\text{CH}(\text{CH}_3)_2$), 24.1 ($\text{CH}(\text{CH}_3)_2$), 40.8 (CHCH_2Ph), 43.2 (CH_3CH), 47.0 ($\text{CH}(\text{CH}_3)_2$), 66.1 (*CHN*), 126.9 (ArC), 128.1 (ArC), 129.3 (2xArC), 129.4 (ArC), 130.3 (ArC), 142.8 ($\text{C}_{\text{Ph}}\text{CH}_2$), 144.0 (*CCHN*); **Clearly separated diagnostic peaks of the minor branched diastereomer 4.13.5:** ^{13}C NMR (100 MHz, CD_3OD): $\delta = 16.1$ (CH_3CH), 66.0 (*CHN*), **Clearly separated diagnostic peaks of the linear regioisomer 4.12.5:** ^{13}C NMR (100 MHz, CD_3OD): $\delta = 61.4$ (*CHN*); GCFID rt: **4.14.5:** 6.854, **4.13.5:** 7.033 or 7.673, **4.12.5:** 7.033 or 7.673. HRMS (HESI) m/z calcd for $\text{C}_{19}\text{H}_{25}\text{NH}^+ [\text{M} + \text{H}^+]$, 268.2065: Found 268.2066.

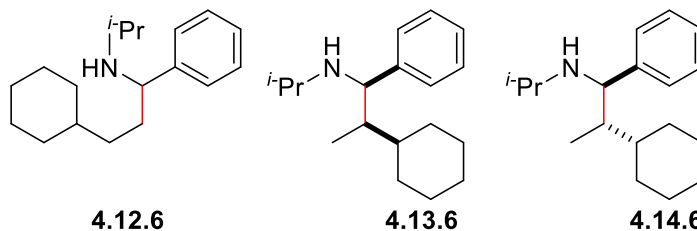
Linear: 3-cyclohexyl-*N*-isopropyl-1-phenylpropan-1-amine (4.12.6)

Branched: 2-cyclohexyl-*N*-isopropyl-1-phenylpropan-1-amine (4.13.6 and 4.14.6)

Catalyst Loading (0.1 equiv); Reaction time: 120 h. Physical state: Yellow oil.

GCFID RR [4.12.6:(4.13.6+4.14.6)]

1:2. GCFID DR [4.14.6:4.13.6] 17:1.



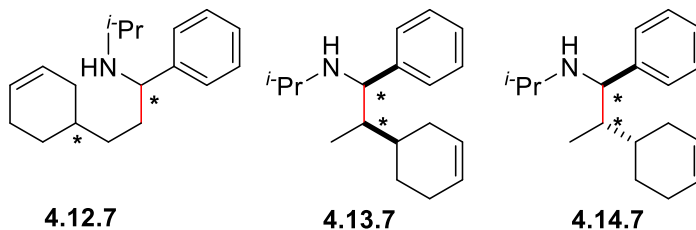
(Yield (20%)). **The major branched diastereomer 4.14.6:** ^1H NMR (400 MHz, CD_3OD): $\delta = 0.92\text{-}1.00$ (m, 9 H, CH_3CH , $\text{CH}(\text{CH}_3)_2$), 1.03-1.67 (m, 12 H, 5x CH_2 , CH_{cyc} , CH_3CH), 2.42-2.49 (m, 1 H, $\text{CH}(\text{CH}_3)_2$), 3.65 (d, $J = 8$ Hz, 1 H, *CHN*), 7.21-7.33 (m, 5 H, ArH); **Clearly separated diagnostic peaks of the minor branched diastereomer 4.13.6:** ^1H NMR (400 MHz, CD_3OD): $\delta = 0.52$ (d, $J = 6.5$ Hz, 3 H, CH_3CH); **Clearly separated diagnostic peaks of the linear diastereomer 4.12.6:** ^1H NMR (400 MHz, CD_3OD): $\delta = 2.49\text{-}2.55$ (m, 1 H, $\text{CH}(\text{CH}_3)_2$), 3.60-3.63 (dd, $J = 9.4$ Hz, $J = 4.7$ Hz, 1 H, *CHN*). **The major branched diastereomer 4.14.6:** ^{13}C

NMR (100 MHz, CD₃OD): δ = 12.4 (CH₃CH), 21.8 (CH(CH₃)₂), 24.2 (CH(CH₃)₂), 27.8, 28.0, 28.1, 28.6, 33.5, 40.5 (CH_{cyc}), 47.1 (CH(CH₃)₂), 64.5 (CHN), 129.0 (2xArC), 129.4 (2xArC), 129.7 (ArC), 145.0 (CCHN); **Clearly separated diagnostic peaks of the minor branched diastereomer 4.13.6:** ¹³C NMR (100 MHz, CD₃OD): δ = 24.0 (CH₃); **Clearly separated diagnostic peaks of the linear regioisomer 4.12.6:** ¹³C NMR (100 MHz, CD₃OD): δ = 21.3 (CH(CH₃)₂), 23.7 (CH(CH₃)₂), 27.6, 34.4, 34.8, 35.4, 36.0 (NHCHCH₂), 39.2 (CH_{cyc}), 46.3 (CH(CH₃)₂), 61.9 (CHN), 128.0 (2xArC), 128.3 (ArC), 128.7 (2xArC), 144.5 (CCHN). GCFID rt: **4.14.6:** 6.415, **4.13.6:** 6.440, **4.12.6:** 6.633. HRMS (HESI) *m/z* calcd for C₁₈H₂₉NH⁺ [M + H⁺], 260.2378; Found 260.2379.

Linear: 3-(cyclohex-3-en-1-yl)-*N*-isopropyl-1-phenylpropan-1-amine (4.12.7)

Branched: 2-(cyclohex-3-en-1-yl)-*N*-isopropyl-1-phenylpropan-1-amine (4.13.7 and 4.14.7)

Catalyst Loading (0.1 equiv); Reaction time: 120 h. Physical state: Yellow oil. GCFID [**4.14.7:(4.13.7+4.12.7)**] 1:2 or Yield (40%). As all three products are



in almost isomeric ratio and the clearly diagnostic peaks are not discernible, the ¹H NMR spectra are examined by region and no number of protons is provided for each group of signals.

It is shown on the ¹H NMR spectrum the branched product 4.14.7 is in slight excess as compared to the other two products 4.13.7 and 4.12.7. The presence of two CH₃CH carbons in the ¹³C NMR spectrum provides evidence for two branched diastereomeric products present. By elimination the third GCFID chromatogram peak belongs to the linear product 4.12.7. Aliphatic

region (all products): ¹H NMR (400 MHz, CD₃OD): δ = 0.96-1.02 (m, 2xCH₃CH_{branched}, CH(CH₃)₂), 1.03-2.05 (m, 5xCH₂(linear), 3xCH₂(branched), CH_{cyc}branched, CH_{cyc}linear, CH₃CH_{branched}),

2.43-2.46 (m, $CH(CH_3)_2$), 7.21-7.33 (m, 5 H, ArH); **Benzylic region (all products):** 1H NMR (400 MHz, CD_3OD): $\delta = 3.66-3.77$ (m, CHN); **Vinylic region (all products):** 1H NMR (400 MHz, CD_3OD): $\delta = 5.51-5.65$ (m, $2 \times CH=$); **Aromatic region (all products):** 1H NMR (400 MHz, CD_3OD): $\delta = 7.21-7.33$ (m, 5 H, ArH). **Aliphatic region (all products):** ^{13}C NMR (100 MHz, CD_3OD): $\delta = 11.8$ (CH_3CH), 12.3 (CH_3CH), 21.2 ($CH(CH_3)_2$), 21.8 ($CH(CH_3)_2$), 23.6 ($CH(CH_3)_2$), 24.1 ($CH(CH_3)_2$), 25.0, 26.3, 27.1, 27.3, 29.5, 29.9, 30.4, 31.9, 32.9, 33.2, 34.5, 34.7, 35.0, 35.8, 35.9, 36.3, 36.4, 45.2 ($CH(CH_3)_2$), 45.9, ($CH(CH_3)_2$) 46.5 ($CH(CH_3)_2$), 47.1 ($CH(CH_3)_2$), 145.0 ($CCHN$); **Benzylic region (all products):** ^{13}C NMR (100 MHz, CD_3OD): $\delta = 61.8$ (CHN), 63.4 (CHN), 63.6 (CHN), 64.2 (CHN), 64.5 (CHN); **Aromatic and vinylic region (all products):** ^{13}C NMR (100 MHz, CD_3OD): $\delta = 127.5, 127.7, 127.8, 128.0, 128.1$ ($2 \times C$), 128.5, 128.7, 129.0 ($2 \times C$), 129.4 ($2 \times C$), 129.5, 129.7, 144.2 ($CCHN$), 144.7 ($CCHN$), 144.8 ($CCHN$). GCFID rt: **4.14.7:** 6.524, **4.13.7:** 6.507 or 6.694, **4.12.7:** 6.507 or 6.694. HRMS (HESI) m/z calcd for $C_{18}H_{27}NH^+$ [$M + H^+$], 258.2222: Found 258.2217.

***N*-isopropyl-1-phenyl-3-(trimethylsilyl)propan-1-amine (4.12.10)**

Catalyst Loading (0.1 equiv); Reaction time: 24 h. Physical state: Yellow

oil. Yield (76%). 1H NMR (400 MHz, $CDCl_3$): $\delta = -0.03$ (s, $Si(CH_3)_3$),



0.24-0.32 (ddd, $J = 14.2$ Hz, $J = 13.1$ Hz, $J = 4.4$ Hz, 1 H, CH_2Si), 0.24-

0.47-0.55 (ddd, $J = 14.1$ Hz, $J = 13.1$ Hz, $J = 4.6$ Hz, 1 H, CH_2Si), 1.01 (d, $J = 6.3$ Hz,

$CH(CH_3)_3$), 1.05 (d, $J = 6.3$ Hz, $CH(CH_3)_3$), 1.55-1.64 (m, 1 H, CH_2CH_2Si), 1.68-1.77 (m, 1 H,

CH_2CH_2Si), 2.59-2.65 (m, 1 H, $CH(CH_3)_3$), 3.61-3.65 (dd, $J = 7.8$ Hz, $J = 6.0$ Hz, 1 H, CHN),

7.27-7.30 (m, 3 H, ArH), 7.35-7.39 (m, 2 H, ArH). ^{13}C NMR (100 MHz, $CDCl_3$): $\delta = -1.6$ ($J_{CSi} =$

12.3 Hz, CH_3), 13.5 (CH_2Si), 22.2 ($CH(CH_3)_3$), 24.5 ($CH(CH_3)_3$), 33.2 (CH_2CH_2Si), 45.7

(CH(CH₃)₃), 63.4 (CH₂N), 126.9 (ArC₄), 127.5 (2xArC), 128.4 (2xArC), 144.9 (CCHN). HRMS (HESI) *m/z* calcd for C₁₅H₂₇NSiH⁺ [M + H⁺], 250.1991: Found 250.1996.

Linear: *N*-isopropyl-1-phenylhept-5-en-1-amine (4.12.13)

Branched: *N*-isopropyl-2-methyl-1-phenylhex-4-en-1-amine (4.13.13 and 4.14.14)

Catalyst Loading (0.1 equiv); Reaction time: 48 h. Physical state: Yellow oil. ¹H NMR RR

(**linear:branched** 1:5). ¹H NMR

DR (**4.14.1:4.13.1** 99:1). Yield

(62%). **Diastereomer 4.14.13:**

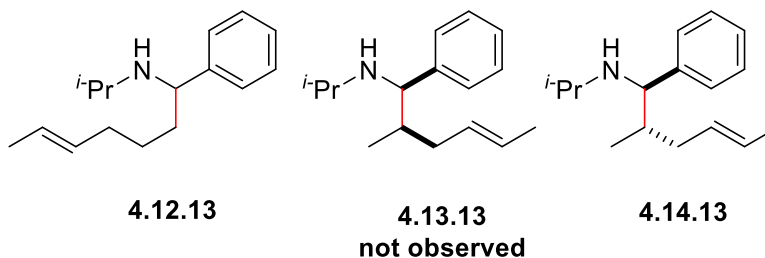
¹H NMR (400 MHz, CD₃OD): δ

= 0.90 (d, *J* = 6.6 Hz, 3 H, CH₃CH-), 0.97 (d, *J* = 6.4 Hz, 6 H, CH(CH₃)₂), 1.54-1.66 (m, 5 H, CH₂, CH₃CH=), 1.72-1.82 (m, 1 H, CHCH₃), 2.45-2.54 (NHCH(CH₃)₂), 3.52 (d, *J* = 6.2 Hz, 1 H, CHN), 5.32-5.34 (m, 2 H, CH=), 7.22-7.32 (m, 5 H, ArH); **Clearly separated diagnostic peaks**

of the linear regioisomer 4.12.13: ¹H NMR (400 MHz, CD₃OD): δ = 0.66 (d, *J* = 6.6 Hz, 3 H, CH₃CH-), 3.62-3.66 (dd, *J* = 9.7 Hz, *J* = 4.7 Hz, 1 H, CHN), 5.43-5.46 (m, 2 H, CH=). **Clearly separated diagnostic peaks of 4.14.13 (some peaks are accompanied by a neighbour ill-**

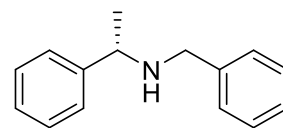
defined peak reported in parenthesis): ¹³C NMR (100 MHz, CD₃OD): δ = 16.9 (CH₃CH), 18.3 (18.4) (CH₃CH=), 21.7 (CH(CH₃)₂), 24.0 (CH(CH₃)₂), 37.6 (38.1) (CH₂), 40.9 (40.3) (CH₃CH), 49.9 (46.8) (CH(CH₃)₂), 66.1 (65.5) (CHN), 127.6 (126.2) (CH=), 128.1 (ArC), 129.3 (2xArC), 131.0 (132.3) (CH=), 143.8 (CCHN); **Clearly separated diagnostic peaks of the linear**

regioisomer 4.12.13: ¹³C NMR (100 MHz, CD₃OD): δ = 16.4 (CH₃CH), 18.2 (CH₃CH=), 21.3 (CH(CH₃)₂), 23.7 (CH(CH₃)₂), 33.6 (CH₂), 38.6 (CH₂), 46.4 (CH(CH₃)₂), 61.4 (CHN), 127.8 (126.2) (CH=), 130.8 (CH=). HRMS (HESI) *m/z* calcd for C₁₆H₂₅NH⁺ [M + H⁺], 232.2065: Found 232.2067.



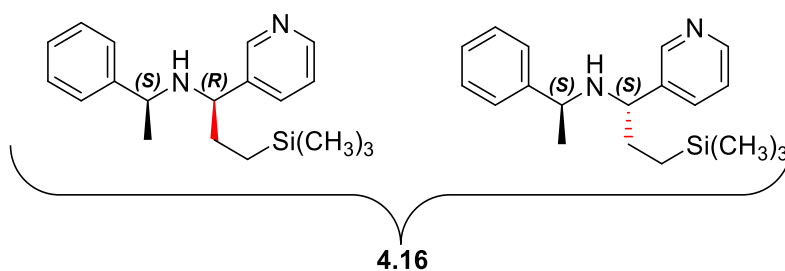
(S)-N-benzyl-1-phenylethan-1-amine¹⁹⁴ (4.15)

Synthesized according to reference.¹⁹⁷ Benzaldehyde (**4.23**) (41.26 mmol, 4.38 g, 4.2 mL) was dissolved in 100 mL MeOH followed by the addition of *S*-1-phenylethanamine (**4.21**) (41.26 mmol, 5.0 g, 5.32 mL). The resulting solution was stirred for 5 hours and was monitored with GC-MC prior to the addition of NaBH₄ (124 mmol, 4.68 g) in small portions at 0 °C, and the resulting suspension was stirred overnight at room temperature. 100 mL of water were added to the suspension to quench NaBH₄ and MeOH was evaporated. The aqueous layer was extracted with DCM and the combined DCM layers were dried over anhydrous Na₂SO₄. After the evaporation of DCM, the amine was placed over CaH₂ and distilled to afford 5.41 g of **4.15** (distillation temperature 145 °C/0.61 mbar). Yield 62%. The ¹H NMR data of the distilled amine match with the reported data.¹⁹⁴ ¹H NMR (400 MHz, CDCl₃): δ = 1.27 (d, *J* = 6.6 Hz, 3 H, CHCH₃), 1.46 (broad s, 1 H, NH), 3.49 (d, *J*_{AB} = 13.3 Hz, 2 H, CH₂), 3.56 (d, *J*_{AB} = 13.3 Hz, 2 H, CH₂), 3.71 (q, *J* = 6.6 Hz, 1 H, CHCH₃), 7.12-7.26 (m, 10 H, ArH).



***N*-((S)-1-phenylethyl)-1-(pyridin-3-yl)-3-(trimethylsilyl)propan-1-amine (4.16)**

A solution of (*S*)-*N*-benzyl-1-phenylethan-1-amine (**4.15**) (1 equiv, 0.50 mmol, 105.66 mg) in 200 μL C₆D₆ was added



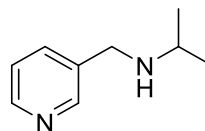
Zr(NMe₂)₄ (0.1 equiv, 0.05 mmol, 13.37 mg), and 200 μL C₆D₆ were used for the quantitative transfer of the starting amine into the resulting solution. Vinyltrimethylsilane **3.10.10** (1.8 equiv, 0.9 mmol, 210 mg) was added to the above solution. The solution was then transferred quantitatively into a J-Young tube via an additional 200-300 μL C₆D₆ and placed in an oil bath at

145 °C. Upon the reaction completion (72 h), the J-Young seal was broken and DCM and MeOH were added to the existing solution. The quenched solution was then passed through a celite pipet and the solvents were evaporated and NaOH 3M was added to the residue. The amine was extracted with ether (3x20 mL). The ethereal layers were dried over anhydrous Na₂SO₄ and evaporated and the residue was purified by column chromatography (hexane:ethyl acetate 90:10) to afford both the separated diastereomers and a mixture of them. Physical state: Yellow oil. ¹H NMR DR (1:1). Yield of the mixture of diastereomers **4.16** (72 mg, 50%). **Diastereomer 1 (not assigned):** ¹H NMR (400 MHz, CDCl₃): δ = -0.11 (s, 9 H, Si(CH₃)₃), 0.11-0.28 (m, 1 H, CH₂Si), 0.36-0.51 (m, 1 H, CH₂Si), 1.26 (d, *J* = 6.7 Hz, 3 H, CHCH₃), 1.46-1.60 (m, 2 H, CH₂CH₂Si), 3.19 (t, *J* = 7.0 Hz, 1 H, CHN), 3.47 (q, *J* = 6.7 Hz, 1 H, CHCH₃), 7.15-7.34 (m, 10 H, ArH); **Diastereomer 2 (not assigned):** ¹H NMR (400 MHz, CDCl₃): δ = -0.08 (s, 9 H, Si(CH₃)₃), 0.11-0.28 (m, 1 H, CH₂Si), 0.36-0.50 (m, 1 H, CH₂Si), 1.33 (d, *J* = 6.7 Hz, 3 H, CHCH₃), 1.70-1.80 (m, 2 H, CH₂CH₂Si), 3.55-3.58 (dd, *J* = 7.9 Hz, *J* = 5.5 Hz, 1 H, CHN), 3.68 (q, *J* = 6.5 Hz, 1 H, CHCH₃), 7.15-7.34 (m, 10 H, ArH). **Diastereomer 1 (not assigned):** ¹³C NMR (100 MHz, CDCl₃): δ = -1.6 (*J*_{CSi} = 12.7 Hz, Si(CH₃)₃), 13.3 (CH₂Si), 25.3 (CHCH₃), 33.2 (CH₂CH₂Si), 55.1 (CHCH₃), 63.0 (CH₂N), 126.8 (ArC), 126.9 (ArC), 127.6 (ArC), 128.5 (ArC), 128.6 (ArC), 144.9, 146.0; **Diastereomer 2 (not assigned):** ¹³C NMR (100 MHz, CDCl₃): δ = -1.6 (*J*_{CSi} = 12.7 Hz, Si(CH₃)₃), 13.1 (CH₂Si), 22.6 (CHCH₃), 31.8 (CH₂CH₂Si), 54.9 (CHCH₃), 63.2 (CH₂N), 126.8 (ArC), 127.0 (ArC), 127.6 (ArC), 128.5 (ArC), 128.6 (ArC), 144.5, 146.3. HRMS (HESI) *m/z* calcd for C₁₉H₂₈N₂SiH⁺ [M + H⁺], 313.2100: Found 313.2257.

***N*-(pyridin-3-ylmethyl)propan-2-amine¹⁹⁵ (4.17)**

Synthesized according to reference¹⁹⁷ 3-pyridine-carboxaldehyde (**4.24**) (40

mmol, 4.28 g, 3.75 mL) was dissolved in 100 mL MeOH followed by the



addition of isopropylamine **4.22** (40 mmol, 2.36 g, 3.27 mL). The resulting solution was stirred for 5 hours and was monitored with GC-MC prior to the addition of NaBH₄ (120 mmol, 4.53 g) in small portions at 0 °C, and the resulting suspension was stirred overnight at room temperature.

100 mL of water were added to the suspension to quench NaBH₄ and MeOH was evaporated.

The aqueous layer was extracted with DCM and the combined DCM layers were dried over anhydrous Na₂SO₄. After the evaporation of DCM, the amine was placed over CaH₂ and distilled

to afford 3.59 g of product **4.17**. Yield 60%. The ¹H NMR data of the distilled amine match with the reported data.¹⁹⁵ ¹H NMR (300 MHz, C₆D₆): δ = 0.52 (broad s, 1 H, NH), 0.87 (d, J = 6.3

Hz, 6 H, CH(CH₃)₂), 2.48-2.56 (m, 1 H, CH(CH₃)₂), 3.36 (s, 2 H, CH₂), 6.76-6.80 (dd, J = 7.7

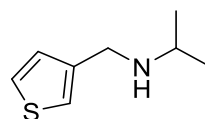
Hz, J = 5.0 Hz, 1 H, ArH₄), 7.33-7.37 (dt, J = 7.8 Hz, J = 1.8 Hz, 1 H, ArH₅), 8.51-8.53 (dd, J =

4.7 Hz, J = 1.7 Hz, ArH₆), 8.67 (d, J = 1.8 Hz, ArH₂).

***N*-(thiophen-3-ylmethyl)propan-2-amine¹⁹⁶ (**4.18**)**

Synthesized according to reference.¹⁹⁷ 3-thiophene-carboxaldehyde (**4.25**) (89

mmol, 9.98 g, 7.8 mL) was dissolved in 20 mL MeOH followed by the



addition of isopropylamine **4.22** (89 mmol, 5.26 g, 7.3 mL) and diluted with an additional 60 mL

of MeOH. The resulting solution was stirred for 5 hours and was monitored with GC-MC prior

to the addition of NaBH₄ (26.7 mmol, 10.1 g) in small portions at 0 °C, and the resulting

suspension was stirred for 3 h at room temperature. 50 mL of water were added to the suspension

to quench NaBH₄ and MeOH was evaporated. The aqueous layer was extracted with DCM and

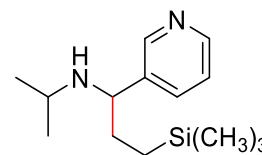
the combined DCM layers were dried over anhydrous Na₂SO₄. After the evaporation of DCM of

pure amine were obtained. The amine was placed over CaH₂ and distilled to afford 8.0 g of

product **4.18** prior to its transfer into the glovebox. Yield 58%. The ^1H NMR data of the distilled amine match with the reported data.¹⁹⁶ ^1H NMR (400 MHz, C_6D_6): δ = 0.65 (broad s, 1 H, NH), 0.92 (d, J = 6.2 Hz, 6 H, $\text{CH}(\text{CH}_3)_2$), 2.58-2.65 (m, 1 H, $\text{CH}(\text{CH}_3)_2$), 3.57 (s, 2 H, CH_2), 6.87-6.89 (m, 1 H, ArH₄), 6.94 (d, J = 1.0 Hz, 1 H, ArH₅), 6.94 (s, 1 H, ArH₂).

***N*-isopropyl-1-(pyridin-3-yl)-3-(trimethylsilyl)propan-1-amine (4.19)**

A solution of *N*-(pyridin-3-ylmethyl)propan-2-amine **4.17** (1 equiv, 0.50 mmol, 75.11 mg) in 200 μL C_6D_6 was added $\text{Zr}(\text{NMe}_2)_4$ (0.4 equiv, 0.20 mmol, 53.48 mg), and 300 μL C_6D_6 were used for the quantitative transfer

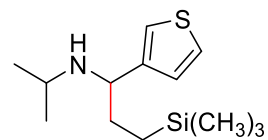


of the starting amine into the resulting solution. Vinyltrimethylsilane **3.10.10** (4.2 equiv, 2.1 mmol, 210 mg) was added to the above solution. The solution was then transferred quantitatively into a J-Young tube via an additional 200-300 μL C_6D_6 and placed in an oil bath at 145 $^\circ\text{C}$. Upon the reaction completion, the J-Young seal was broken and DCM and MeOH were added to the existing solution. The quenched solution was then passed through a celite pipet and the solvents were evaporated and NaOH 3M was added to the residue. The amine was extracted with ether (3x20 mL). The ethereal layers were dried over anhydrous Na_2SO_4 and evaporated to afford the product as a single regioisomer. Reaction time: 24 h. Physical state: Brownish oil. Yield (100 mg, 80%). ^1H NMR (400 MHz, CDCl_3): δ = -0.07 (s, 9 H, $\text{Si}(\text{CH}_3)_3$), 0.19-0.26 (ddd, J = 14.2 Hz, J = 13.1 Hz, J = 4.4 Hz, 1 H, CH_2Si), 0.42-0.50 (ddd, J = 13.9 Hz, J = 13.1 Hz, J = 4.8 Hz, 1 H, CH_2Si), 0.96 (d, J = 6.1 Hz, 3 H, $\text{CH}(\text{CH}_3)_2$), 1.01 (d, J = 6.1 Hz, 3 H, $\text{CH}(\text{CH}_3)_2$), 1.50-1.59 (m, 1 H, $\text{CH}_2\text{CH}_2\text{Si}$), 1.62-1.71 (m, 1 H, $\text{CH}_2\text{CH}_2\text{Si}$), 2.52-2.58 (m, 1 H, $\text{CH}(\text{CH}_3)_2$), 3.63 (t, J = 7.0 Hz, 1 H, CHN), 7.24-7.27 (m, 1 H, ArH), 7.60-7.63 (dt, J = 7.7 Hz, J = 1.8 Hz, 1 H, ArH), 8.47 (d, 1 H, J = 1.9 Hz, ArH), 8.49 (s, 1 H, ArH). ^{13}C NMR (100 MHz, CDCl_3): δ = -1.6 (J_{CSi} = 11.4 Hz, $\text{Si}(\text{CH}_3)_3$), 13.3 (CH_2Si), 23.3 ($\text{CH}(\text{CH}_3)_2$), 24.5 ($\text{CH}(\text{CH}_3)_2$), 34.2 ($\text{CH}_2\text{CH}_2\text{Si}$), 46.0

(CH(CH₃)₂), 61.1 (CH₂N), 123.7 (ArC), 134.8 (ArC), 140.3 (C_{Ph}CHN), 148.6 (ArC), 149.7 (ArC). HRMS (HESI) *m/z* calcd for C₁₄H₂₆N₂SiH⁺ [M + H⁺], 251.1944: Found 251.1940.

***N*-isopropyl-1-(thiophen-3-yl)-3-(trimethylsilyl)propan-1-amine (4.20)**

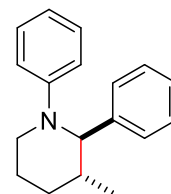
A solution of *N*-(thiophen-3-ylmethyl)propan-2-amine (**4.18**) (1 equiv, 0.50 mmol, 77.23 mg) in 200 μL C₆D₆ was added Zr(NMe₂)₄ (0.4 equiv, 0.20 mmol, 53.48 mg), and 300 μL C₆D₆ were used for the quantitative



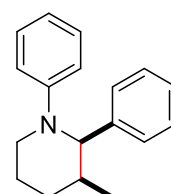
transfer of the starting amine into the resulting solution. Vinyltrimethylsilane **3.10.10** (4.2 equiv, 2.1 mmol, 210 mg) was added to the above solution. The solution was then transferred quantitatively into a J-Young tube via an additional 200-300 μL C₆D₆ and placed in an oil bath at 145 °C. Upon the reaction completion, the J-Young seal was broken and DCM and MeOH were added to the existing solution. The quenched solution was then passed through a celite pipet and the solvents were evaporated and NaOH 3M was added to the residue. The amine was extracted with ether (3x20 mL). The ethereal layers were dried over anhydrous Na₂SO₄ and evaporated to afford the product as a single regioisomer. Reaction time: 24 h. Physical state: Brownish oil. Yield (115 mg, 92%). ¹H NMR (400 MHz, CDCl₃): δ = -0.06 (s, 9 H, Si(CH₃)₃), 0.24-0.32 (ddd, *J* = 14.3 Hz, *J* = 13.0 Hz, *J* = 4.4 Hz, 1 H, CH₂Si), 0.40-0.50 (m, 1 H, CH₂Si), 0.98 (d, *J* = 6.1 Hz, 3 H, CH(CH₃)₂), 1.02 (d, *J* = 6.1 Hz, 3 H, CH(CH₃)₂), 1.46-1.72 (m, 2 H, CH₂CH₂Si), 2.58-2.67 (m, 1 H, CH(CH₃)₂), 3.70-3.74 (dd, *J* = 7.9 Hz, *J* = 5.7 Hz, 1 H, CHN), 6.99 (d, *J* = 4.9 Hz, 1 H, ArH₅), 7.04 (d, *J* = 3.0 Hz, 1 H, ArH₂), 7.26-7.28 (dd, *J* = 4.8 Hz, *J* = 2.7 Hz, 1 H, ArH₄). ¹³C NMR (100 MHz, CDCl₃): δ = -1.6 (*J*_{C_{Si}} = 12.6 Hz, Si(CH₃)₃), 13.3 (CH₂Si), 22.4 (CH(CH₃)₂), 24.4 (CH(CH₃)₂), 32.4 (CH₂CH₂Si), 45.8 (CH(CH₃)₂), 58.9 (CH₂N), 121.1 (ArC₅), 125.7 (ArC₄), 126.2 (ArC₂), 146.3 (CCHNH₂). HRMS (HESI) *m/z* calcd for C₁₃H₂₅NSSiH⁺ [M + H⁺], 256.1555: Found 256.1559.

3-methyl-1,2-diphenylpiperidine (4.26 and 4.27)

The mixture of regioisomers **4.9.3**, **4.10.3** and **4.11.3** (0.34 mmol, 130 mg) was transferred into a bomb via 1 mL toluene. TsF (1.02 mmol, 1.77 mg) and DBU (1.02 mmol, 155 mg, 0.15 mL) were added to the above solution. The bomb was sealed, placed in an oil bath at 150 °C and stirred for 23 h. The amine was extracted from



4.26



4.27

toluene with HCl 1M in the form of its hydrochloric salt (4x10 mL) and the combined aqueous layers were basified with NaOH 3M. The liberated base was back extracted with ether (3x15 mL) and the ethereal layers were dried over anhydrous Na₂SO₄. Ether was evaporated to afford 23 mg of a brownish oil. The obtained product corresponded to the branched regioisomer and was a mixture of diastereomers. ¹H NMR DR (**4.27:4.26** 3:1). Yield 27%. **The major syn branched diastereomer 4.27:** ¹H NMR (400 MHz, CD₃OD): δ = 0.80 (d, *J* = 7.0 Hz, 3 H, CH₃CH), 1.64-1.69 (m, 2 H), 1.72-1.83 (m, 1 H), 2.09-2.14 (m, 1 H), 2.18-2.23 (m, 1 H, CHCH₃), 3.15-3.21 (ddd, *J* = 12.0 Hz, *J* = 7.1 Hz, *J* = 4.5 Hz, 1 H, CH₂N), 3.46-3.52 (ddd, *J* = 12.3 Hz, *J* = 7.9 Hz, *J* = 4.3 Hz, 1 H, CH₂N), 4.65 (d, *J* = 7.8 Hz, 1 H, CHN), 6.67 (t, *J* = 7.2 Hz, 1 H, ArH), 6.88 (d, *J* = 8.6 Hz, 2 H, ArH), 6.97-7.23 (m, 7 H, ArH); **Clearly separated diagnostic peaks of the minor anti branched diastereomer 4.26:** ¹H NMR (400 MHz, CD₃OD): δ = 0.71 (d, *J* = 7.0 Hz, 3 H, CH₃CH), 1.29-1.36 (m, 1 H), 1.72-1.97 (m, 4 H), 2.87-2.93 (td, *J* = 11.6, *J* = 2.9 Hz, 1 H), 3.33-3.35 (m, 1 H), 3.60 (d, *J* = 8.8 Hz, 1 H, CHN), 6.79 (t, *J* = 7.2 Hz, 1 H, ArH). **Clearly separated diagnostic peaks of the major syn branched diastereomer 4.27:** ¹³C NMR (100 MHz, CD₃OD): δ = 18.0 (CH₃CH), 25.0, 29.6, 36.5 (CH₃CH), 50.9 (CH₂N), 62.1 (CHN), 142.9 (CCHN), 153.3 (C_{Ph}N); **Clearly separated diagnostic peaks of the minor anti branched diastereomer 4.26:** ¹³C NMR (100 MHz,

CD₃OD): δ = 19.9 (CH₃CH), 27.1, 34.4, 39.9 (CH₃CH), 58.5 (CH₂N), 73.5 (CHN), 144.1 (C_qCHN), 154.6 (C_qN); **Aromatic peaks (both diastereomers):** ¹³C NMR (100 MHz, CD₃OD): δ = 120.1, 120.8, 124.1, 125.6, 127.5, 127.6, 128.7, 128.9, 129.5, 129.7, 130.0, 130.5. HRMS (HESI) m/z calcd for C₁₈H₂₁NH⁺ [M + H⁺], 252.1752: Found 252.1748.

Bibliography

1. E. J. Corey, *Pure Appl. Chem.*, 1967, **14**, 19-38.
2. E. J. Corey, *Chem. Soc. Rev.*, 1988, **17**, 111-133.
3. N. Coles, M. C. J. Harris, R. J. Whitby and J. Blagg, *Organometallics*, 1994, **13**, 190-199.
4. S. A. Cummings, J. A. Tunge and J. R. Norton, *Topics Organomet. Chem.*, 2005, **10**, 1-39.
5. A. B. Burg and E. S. Kuljian, *J. Am. Chem. Soc.*, 1950, **72**, 3103-3107.
6. S. Sujishi and S. Witz, *J. Am. Chem. Soc.*, 1954, **76**, 4631-4636.
7. R. Fessenden and J. S. Fessenden, *Chem. Rev.*, 1961, **61**, 361-388.
8. A. V. Lebedev, A. B. Lebedeva, V. D. Sheludyakov, S. N. Ovcharuk, E. A. Kovaleva and O. L. Ustinova, *Russ. J. Gen. Chem.*, 2006, **76**, 469-477.
9. D. B. Ushakov, K. Gilmore and P. H. Seeberger, *Chem. Commun.*, 2014, **50**, 12649-12651.
10. K. Mai and G. Patil, *J. Org. Chem.*, 1986, **51**, 3545-3548.
11. S. Rajeswari, R. J. Jones and M. P. Cava, *Tetrahedron Lett.*, 1987, **28**, 5099-5102.
12. M. Zamiri and D. S. Grierson, *Synthesis*, 2017, **49**, 571-578.
13. Y. Oishi, M. Kakimoto and Y. Imai, *Macromolecules*, 1987, **20**, 703-704.
14. M. Chandrasekhar, G. Sekar and V. K. Singh, *Tetrahedron Lett.*, 2000, **41**, 10079-10083.
15. S. Bresciani and D. O'Hagan, *Tetrahedron Lett.*, 2010, **51**, 5795-5797.
16. R. L. Melen, *Chem. Soc. Rev.*, 2016, **45**, 775-788.
17. R. Waterman, *Chem. Soc. Rev.*, 2013, **42**, 5629-5641.
18. M. Oestreich, J. Hermeke and J. Mohr, *Chem. Soc. Rev.*, 2015, **44**, 2202-2220.
19. B. Marciniec, S. Kostera, B. Wyrzykiewicz and P. Pawluć, *Dalton Trans.*, 2015, **44**, 782-786.
20. S. Anga, Y. Sarazin, J.-F. Carpentier and T. K. Panda, *ChemCatChem*, 2016, **8**, 1373-1378.
21. J. F. Dunne, S. R. Neal, J. Engelkemier, A. Ellern and A. D. Sadow, *J. Am. Chem. Soc.*, 2011, **133**, 16782-16785.
22. M. S. Hill, D. J. Liptrot, D. J. MacDougall, M. F. Mahon and T. P. Robinson, *Chem. Sci.*, 2013, **4**, 4212-4222.
23. C. Bellini, V. Dorcet, J.-F. Carpentier, S. Tobisch and Y. Sarazin, *Chem. Eur. J.*, 2016, **22**, 4564-4583.
24. C. Bellini, T. Roisnel, J.-F. Carpentier, S. Tobisch and Y. Sarazin, *Chem. Eur. J.*, 2016, **22**, 15733-15743.
25. F. Buch and S. Harder, *Organometallics*, 2007, **26**, 5132-5135.
26. S. Rendler and M. Oestreich, *Angew. Chem. Int. Ed.*, 2008, **47**, 5997-6000.
27. D. T. Hog and M. Oestreich, *Eur. J. Org. Chem.*, 2009, **2009**, 5047-5056.
28. M. Mewald and M. Oestreich, *Chem. Eur. J.*, 2012, **18**, 14079-14084.
29. J. Hermeke, M. Mewald and M. Oestreich, *J. Am. Chem. Soc.*, 2013, **135**, 17537-17546.
30. L. Greb, S. Tamke and J. Paradies, *Chem. Commun.*, 2014, **50**, 2318-2320.

31. L. K. Allen, R. García-Rodríguez and D. S. Wright, *Dalton Trans.*, 2015, **44**, 12112-12118.
32. H. Q. Liu and J. F. Harrod, *Organometallics*, 1992, **11**, 822-827.
33. H. Liu and J. Harrod, *Can. J. Chem.*, 1992, **70**, 107-110.
34. E. Matarasso-Tchiroukhine, *J. Chem. Soc., Chem. Commun.*, 1990, 681-682.
35. C. K. Toh, H. T. Poh, C. S. Lim and W. Y. Fan, *J. Organomet. Chem.*, 2012, **717**, 9-13.
36. C. D. F. Königs, M. F. Müller, N. Aiguabella, H. F. Klare and M. Oestreich, *Chem. Commun.*, 2013, **49**, 1506-1508.
37. J. Hermeke, H. F. T. Klare and M. Oestreich, *Chem. Eur. J.*, 2014, **20**, 9250-9254.
38. S. Itagaki, K. Kamata, K. Yamaguchi and N. Mizuno, *Chem. Commun.*, 2012, **48**, 9269-9271.
39. T. Tsuchimoto, Y. Iketani and M. Sekine, *Chem. Eur. J.*, 2012, **18**, 9500-9504.
40. L. H. Sommer and J. D. Citron, *J. Org. Chem.*, 1967, **32**, 2470-2472.
41. K. Takaki, T. Kamata, Y. Miura, T. Shishido and K. Takehira, *J. Org. Chem.*, 1999, **64**, 3891-3895.
42. K. Takaki, K. Komeyama and K. Takehira, *Tetrahedron*, 2003, **59**, 10381-10395.
43. W. Xie, H. Hu and C. Cui, *Angew. Chem. Int. Ed.*, 2012, **51**, 11141-11144.
44. A. Pindwal, A. Ellern and A. D. Sadow, *Organometallics*, 2016, **35**, 1674-1683.
45. J. X. Wang, A. K. Dash, J. C. Berthet, M. Ephritikhine and M. S. Eisen, *J. Organomet. Chem.*, 2000, **610**, 49-57.
46. D. M. Makley and J. N. Johnston, *Org. Lett.*, 2014, **16**, 3146-3149.
47. S. P. Bew, S. A. Fairhurst, D. L. Hughes, L. Legentil, J. Liddle, P. Pesce, S. Nigudkar and M. A. Wilson, *Org. Lett.*, 2009, **11**, 4552-4555.
48. F. Gosselin, P. D. O'Shea, S. Roy, R. A. Reamer, C.-y. Chen and R. P. Volante, *Org. Lett.*, 2005, **7**, 355-358.
49. C. P. Lenges, P. S. White and M. Brookhart, *J. Am. Chem. Soc.*, 1999, **121**, 4385-4396.
50. E. K. J. Lui, J. W. Brandt and L. L. Schafer, *J. Am. Chem. Soc.*, 2018, **140**, 4973-4976.
51. E. K. J. Lui, D. Hergesell and L. L. Schafer, *Org. Lett.*, 2018, **20**, 6663-6667.
52. K. Hong and J. P. Morken, *J. Am. Chem. Soc.*, 2013, **135**, 9252-9254.
53. D. W. Robbins, T. A. Boebel and J. F. Hartwig, *J. Am. Chem. Soc.*, 2010, **132**, 4068-4069.
54. Y. Tsuji, M. Kobayashi, F. Okuda and Y. Watanabe, *J. Chem. Soc., Chem. Commun.*, 1989, 1253-1254.
55. Y. Watanabe, K. Nishiyama, F. Okuda and T. Kondo, *J. Mol. Catal.*, 1992, **71**, 15-23.
56. R. M. Lanigan and T. D. Sheppard, *Eur. J. Org. Chem.*, 2013, **2013**, 7453-7465.
57. J. Tazi, N. Bakkour, V. Marchand, L. Ayadi, A. Aboufirassi and C. Branlant, *FEBS J.*, 2010, **277**, 867-876.
58. N. Bakkour, Y.-L. Lin, S. Maire, L. Ayadi, F. Mahuteau-Betzer, C. H. Nguyen, C. Mettling, P. Portales, D. Grierson, B. Chabot, P. Jeanteur, C. Branlant, P. Corbeau and J. Tazi, *PLoS Path.*, 2007, **3**, 1530-1539.
59. P. K. Cheung, D. Horhant, L. E. Bandy, M. Zamiri, S. M. Rabea, S. K. Karagiosov, M. Matloobi, S. McArthur, P. R. Harrigan, B. Chabot and D. S. Grierson, *J. Med. Chem.*, 2016, **59**, 1869-1879.

60. L. Shkreta, M. Blanchette, J. Toutant, E. Wilhelm, B. Bell, B. A. Story, A. Balachandran, A. Cochrane, P. K. Cheung, P. R. Harrigan, D. S. Grierson and B. Chabot, *Nucleic Acids Res.*, 2017, **45**, 4051-4067.
61. Z. S. Qureshi, S. A. Revankar, M. V. Khedkar and B. M. Bhanage, *Catal. Today*, 2012, **198**, 148-153.
62. J. R. Martinelli, T. P. Clark, D. A. Watson, R. H. Munday and S. L. Buchwald, *Angew. Chem. Int. Ed.*, 2007, **46**, 8460-8463.
63. K. Kumar, A. Zapf, D. Michalik, A. Tillack, T. Heinrich, H. Böttcher, M. Arlt and M. Beller, *Org. Lett.*, 2004, **6**, 7-10.
64. P. J. Tambade, Y. P. Patil, M. J. Bhanushali and B. M. Bhanage, *Synthesis*, 2008, **2008**, 2347-2352.
65. Y. Ben-David, M. Portnoy and D. Milstein, *J. Am. Chem. Soc.*, 1989, **111**, 8742-8744.
66. J. Yin and S. L. Buchwald, *Org. Lett.*, 2000, **2**, 1101-1104.
67. A. Klapars, J. C. Antilla, X. Huang and S. L. Buchwald, *J. Am. Chem. Soc.*, 2001, **123**, 7727-7729.
68. C. L. Allen and J. M. J. Williams, *Chem. Soc. Rev.*, 2011, **40**, 3405-3415.
69. R. M. de Figueiredo, J.-S. Suppo and J.-M. Campagne, *Chem. Rev.*, 2016, **116**, 12029-12122.
70. V. R. Pattabiraman and J. W. Bode, *Nature*, 2011, **480**, 471.
71. A. Ojeda-Porras and D. Gamba-Sánchez, *J. Org. Chem.*, 2016, **81**, 11548-11555.
72. L. J. Gooßen, D. M. Ohlmann and P. P. Lange, *Synthesis*, 2009, **2009**, 160-164.
73. L. A. Carpino and A. El-Faham, *J. Am. Chem. Soc.*, 1995, **117**, 5401-5402.
74. L. A. Carpino, D. Sadat-Aalae, H. G. Chao and R. H. DeSelms, *J. Am. Chem. Soc.*, 1990, **112**, 9651-9652.
75. G. S. Lal, G. P. Pez, R. J. Pesaresi, F. M. Prozonc and H. Cheng, *J. Org. Chem.*, 1999, **64**, 7048-7054.
76. T. Ohshima, Y. Hayashi, K. Agura, Y. Fujii, A. Yoshiyama and K. Mashima, *Chem. Commun.*, 2012, **48**, 5434-5436.
77. C. A. G. N. Montalbetti and V. Falque, *Tetrahedron*, 2005, **61**, 10827-10852.
78. E. Valeur and M. Bradley, *Chem. Soc. Rev.*, 2009, **38**, 606-631.
79. H. Lundberg, F. Tinnis, N. Selander and H. Adolfsson, *Chem. Soc. Rev.*, 2014, **43**, 2714-2742.
80. A. Leggio, J. Bagalà, E. L. Belsito, A. Comandè, M. Greco and A. Liguori, *Chem. Cent. J.*, 2017, **11**, 87-98.
81. H. Lundberg, F. Tinnis and H. Adolfsson, *Synlett*, 2012, **23**, 2201-2204.
82. J. D. Wilson and H. Weingarten, *Can. J. Chem.*, 1970, **48**, 983-986.
83. C. L. Allen, A. R. Chhatwal and J. M. J. Williams, *Chem. Commun.*, 2012, **48**, 666-668.
84. H. Lundberg, F. Tinnis and H. Adolfsson, *Chem. Eur. J.*, 2012, **18**, 3822-3826.
85. D. C. Lenstra, D. T. Nguyen and J. Mecerovič, *Tetrahedron*, 2015, **71**, 5547-5553.
86. H. Lundberg and H. Adolfsson, *ACS Catal.*, 2015, **5**, 3271-3277.
87. M. A. Ali, S. M. A. H. Siddiki, K. Kon and K.-i. Shimizu, *ChemCatChem*, 2015, **7**, 2705-2710.
88. D. T. Nguyen, D. C. Lenstra and J. Mecerovič, *RSC Adv.*, 2015, **5**, 77658-77661.
89. K. Ishihara, S. Ohara and H. Yamamoto, *J. Org. Chem.*, 1996, **61**, 4196-4197.
90. K. Ishihara, S. Ohara and H. Yamamoto, *Macromolecules*, 2000, **33**, 3511-3513.

91. R. M. Lanigan, P. Starkov and T. D. Sheppard, *J. Org. Chem.*, 2013, **78**, 4512-4523.
92. S. Liu, Y. Yang, X. Liu, F. K. Ferdousi, A. S. Batsanov and A. Whiting, *Eur. J. Org. Chem.*, 2013, **2013**, 5692-5700.
93. M. T. Sabatini, L. T. Boulton and T. D. Sheppard, *Sci. Adv.*, 2017, **3**.
94. M. T. Sabatini, V. Karaluka, R. M. Lanigan, L. T. Boulton, M. Badland and T. D. Sheppard, *Chem. Eur. J.*, 2018, **24**, 7033-7043.
95. T. Ben Halima, J. Masson-Makdissi and S. G. Newman, *Angew. Chem. Int. Ed.*, 2018, **57**, 12925-12929.
96. T. Ben Halima, J. K. Vandavasi, M. Shkoor and S. G. Newman, *ACS Catal.*, 2017, **7**, 2176-2180.
97. B. Gnanaprakasam and D. Milstein, *J. Am. Chem. Soc.*, 2011, **133**, 1682-1685.
98. Z. Liu, J. Zhang, S. Chen, E. Shi, Y. Xu and X. Wan, *Angew. Chem. Int. Ed.*, 2012, **51**, 3231-3235.
99. M. E. Due-Hansen, S. K. Pandey, E. Christiansen, R. Andersen, S. V. F. Hansen and T. Ulven, *Org. Biomol. Chem*, 2016, **14**, 430-433.
100. H.-O. Kim, B. Gardner and M. Kahn, *Tetrahedron Lett.*, 1995, **36**, 6013-6016.
101. J. R. Bowser, P. J. Williams and K. Kurz, *J. Org. Chem.*, 1983, **48**, 4111-4113.
102. C. S. Schindler, P. M. Forster and E. M. Carreira, *Org. Lett.*, 2010, **12**, 4102-4105.
103. G. A. Olah and S. J. Kuhn, *J. Org. Chem.*, 1961, **26**, 225-227.
104. J. S. Oliver and A. Oyelere, *J. Org. Chem.*, 1996, **61**, 4168-4171.
105. J.-N. Bertho, A. Loffet, C. Pinel, F. Reuther and G. Sennyey, *Tetrahedron Lett.*, 1991, **32**, 1303-1306.
106. J. W. Lippert, *ARKIVOC*, 2005, **2005**, 87-95.
107. F. Beaulieu, L.-P. Beauregard, G. Courchesne, M. Couturier, F. LaFlamme and A. L'Heureux, *Org. Lett.*, 2009, **11**, 5050-5053.
108. T. Scattolin, K. Deckers and F. Schoenebeck, *Org. Lett.*, 2017, **19**, 5740-5743.
109. N. Stuhr-Hansen, N. Bork and K. Strømgaard, *Org. Biomol. Chem*, 2014, **12**, 5745-5751.
110. W. Yang and D. G. Drueckhammer, *J. Am. Chem. Soc.*, 2001, **123**, 11004-11009.
111. E. A. Castro, *Chem. Rev.*, 1999, **99**, 3505-3524.
112. R. Lang, A. Wahl, T. Skurk, E. F. Yagar, L. Schmiech, R. Eggers, H. Hauner and T. Hofmann, *Anal. Chem.*, 2010, **82**, 1486-1497.
113. B. A. de Marco, B. S. Rechelo, E. G. Tócoli, A. C. Kogawa and H. R. N. Salgado, *Saudi Pharm. J.*, 2018, DOI: <https://doi.org/10.1016/j.jsps.2018.07.011>.
114. M. Matoba, T. Kajimoto and M. Node, *Synlett*, 2007, **2007**, 1930-1934.
115. J.-y. Hasegawa, M. Hamada, T. Miyamoto, K. Nishide, T. Kajimoto, J.-i. Uenishi and M. Node, *Carbohydr. Res.*, 2005, **340**, 2360-2368.
116. T. Nagata, Y. Kikuzawa and A. Osuka, *Inorg. Chim. Acta*, 2003, **342**, 139-144.
117. C.-C. Han and R. Balakumar, *Tetrahedron Lett.*, 2006, **47**, 8255-8258.
118. B. Trost, *Science*, 1991, **254**, 1471-1477.
119. R. C. Arnold, A. P. Lien and R. M. Alm, *J. Am. Chem. Soc.*, 1950, **72**, 731-733.
120. H. R. Kricheldorf, *Justus Liebigs Ann. Chem.*, 1971, **745**, 81-86.
121. H. Böshagen and W. Geiger, *Chem. Ber.*, 1976, **109**, 659-668.
122. W. Geiger, H. Böshagen and H. Medenwald, *Chem. Ber.*, 1969, **102**, 1961-1975.
123. <https://njardarson.lab.arizona.edu/content/top-pharmaceutical-poster>.

124. X. Tan, S. Gao, W. Zeng, S. Xin, Q. Yin and X. Zhang, *J. Am. Chem. Soc.*, 2018, **140**, 2024-2027.
125. W. Chen, L. Ma, A. Paul and D. Seidel, *Nat. Chem.*, 2017, **10**, 165-169.
126. D. Seidel, *Acc. Chem. Res.*, 2015, **48**, 317-328.
127. Z. Zuo, D. T. Ahneman, L. Chu, J. A. Terrett, A. G. Doyle and D. W. C. MacMillan, *Science*, 2014, **345**, 437-440.
128. D. T. Ahneman and A. G. Doyle, *Chem. Sci.*, 2016, **7**, 7002-7006.
129. A. McNally, C. K. Prier and D. W. C. MacMillan, *Science*, 2011, **334**, 1114-1117.
130. N. Hussain, B.-S. Kim and P. J. Walsh, *Chem. Eur. J.*, 2015, **21**, 11010-11013.
131. P. Jain, P. Verma, G. Xia and J.-Q. Yu, *Nat. Chem.*, 2016, **9**, 140-144.
132. J. E. Spangler, Y. Kobayashi, P. Verma, D.-H. Wang and J.-Q. Yu, *J. Am. Chem. Soc.*, 2015, **137**, 11876-11879.
133. K. R. Campos, A. Klapars, J. H. Waldman, P. G. Dormer and C.-y. Chen, *J. Am. Chem. Soc.*, 2006, **128**, 3538-3539.
134. S. J. Pastine, D. V. Gribkov and D. Sames, *J. Am. Chem. Soc.*, 2006, **128**, 14220-14221.
135. Z. Li and C.-J. Li, *J. Am. Chem. Soc.*, 2004, **126**, 11810-11811.
136. P. Eisenberger, R. O. Ayinla, J. M. P. Lauzon and L. L. Schafer, *Angew. Chem. Int. Ed.*, 2009, **48**, 8361-8365.
137. J. Dörfler and S. Doye, *Angew. Chem. Int. Ed.*, 2013, **52**, 1806-1809.
138. J. Dörfler, T. Preuß, A. Schischko, M. Schmidtmann and S. Doye, *Angew. Chem. Int. Ed.*, 2014, **53**, 7918-7922.
139. K. Tomioka, I. Inoue, M. Shindo and K. Koga, *Tetrahedron Lett.*, 1990, **31**, 6681-6684.
140. S. L. Buchwald, B. T. Watson, M. W. Wannamaker and J. C. Dewan, *J. Am. Chem. Soc.*, 1989, **111**, 4486-4494.
141. M. G. Clerici and F. Maspero, *Synthesis*, 1980, **1980**, 305-306.
142. W. A. Nugent, D. W. Ovenall and S. J. Holmes, *Organometallics*, 1983, **2**, 161-162.
143. S. B. Herzon and J. F. Hartwig, *J. Am. Chem. Soc.*, 2007, **129**, 6690-6691.
144. S. B. Herzon and J. F. Hartwig, *J. Am. Chem. Soc.*, 2008, **130**, 14940-14941.
145. F. Liu, G. Luo, Z. Hou and Y. Luo, *Organometallics*, 2017, **36**, 1557-1565.
146. A. E. Nako, J. Oyamada, M. Nishiura and Z. Hou, *Chem. Sci.*, 2016, **7**, 6429-6434.
147. J. A. Bexrud, P. Eisenberger, D. C. Leitch, P. R. Payne and L. L. Schafer, *J. Am. Chem. Soc.*, 2009, **131**, 2116-2118.
148. R. Kubiak, I. Prochnow and S. Doye, *Angew. Chem. Int. Ed.*, 2009, **48**, 1153-1156.
149. R. Kubiak, I. Prochnow and S. Doye, *Angew. Chem. Int. Ed.*, 2010, **49**, 2626-2629.
150. T. Preuß, W. Saak and S. Doye, *Chem. Eur. J.*, 2013, **19**, 3833-3837.
151. I. Prochnow, R. Kubiak, O. N. Frey, R. Beckhaus and S. Doye, *ChemCatChem*, 2009, **1**, 162-172.
152. I. Prochnow, P. Zark, T. Müller and S. Doye, *Angew. Chem. Int. Ed.*, 2011, **50**, 6401-6405.
153. G. Zi, F. Zhang and H. Song, *Chem. Commun.*, 2010, **46**, 6296-6298.
154. F. Zhang, H. Song and G. Zi, *Dalton Trans.*, 2011, **40**, 1547-1566.
155. A. L. Reznichenko, T. J. Emge, S. Audörsch, E. G. Klauber, K. C. Hultsch and B. Schmidt, *Organometallics*, 2011, **30**, 921-924.
156. A. L. Reznichenko and K. C. Hultsch, *J. Am. Chem. Soc.*, 2012, **134**, 3300-3311.

157. N. Chatani, T. Asaumi, S. Yorimitsu, T. Ikeda, F. Kakiuchi and S. Murai, *J. Am. Chem. Soc.*, 2001, **123**, 10935-10941.
158. C.-H. Jun, *Chem. Commun.*, 1998, **0**, 1405-1406.
159. S. Pan, K. Endo and T. Shibata, *Org. Lett.*, 2011, **13**, 4692-4695.
160. K. Tsuchikama, M. Kasagawa, K. Endo and T. Shibata, *Org. Lett.*, 2009, **11**, 1821-1823.
161. S. M. Thullen and T. Rovis, *J. Am. Chem. Soc.*, 2017, **139**, 15504-15508.
162. E. Chong and L. L. Schafer, *Org. Lett.*, 2013, **15**, 6002-6005.
163. P. W. Roesky, *Angew. Chem. Int. Ed.*, 2009, **48**, 4892-4894.
164. R. C. DiPucchio, S.-C. Roşca and L. L. Schafer, *Angew. Chem.*, 2018, **130**, 3527-3530.
165. D. J. Gilmour, J. M. P. Lauzon, E. Clot and L. L. Schafer, *Organometallics*, 2018, **37**, 4387-4394.
166. D. Becker, P. W. Atkins and L. Jones, W.H. Freeman, New York, 2000.
167. S. G. Wierschke, J. Chandrasekhar and W. L. Jorgensen, *J. Am. Chem. Soc.*, 1985, **107**, 1496-1500.
168. D. A. Gaul, O. Just and W. S. Rees, *Inorg. Chem.*, 2000, **39**, 5648-5654.
169. R. M. Archer, M. Hutchby, C. L. Winn, J. S. Fossey and S. D. Bull, *Tetrahedron*, 2015, **71**, 8838-8847.
170. M. Fujiwara, J. Ichikawa, T. Okauchi and T. Minami, *Tetrahedron Lett.*, 1999, **40**, 7261-7265.
171. T. Fujita, K. Fuchibe and J. Ichikawa, *Angew. Chem. Int. Ed.*, 2019, **58**, 390-402.
172. K. Nienkemper, G. Kehr, S. Kehr, R. Fröhlich and G. Erker, *J. Organomet. Chem.*, 2008, **693**, 1572-1589.
173. P. M. Edwards and L. L. Schafer, *Org. Lett.*, 2017, **19**, 5720-5723.
174. J. P. Hardy and W. D. Cumming, *J. Am. Chem. Soc.*, 1971, **93**, 928-932.
175. H. J. Schneider and V. Hoppen, *J. Org. Chem.*, 1978, **43**, 3866-3873.
176. E. L. Eliel and H. Satici, *J. Org. Chem.*, 1994, **59**, 688-689.
177. C. H. Marzabadi, J. E. Anderson, J. Gonzalez-Outeirino, P. R. J. Gaffney, C. G. H. White, D. A. Tocher and L. J. Todaro, *J. Am. Chem. Soc.*, 2003, **125**, 15163-15173.
178. S. Bähn, S. Imm, L. Neubert, M. Zhang, H. Neumann and M. Beller, *ChemCatChem*, 2011, **3**, 1853-1864.
179. Y. Zhang, X. Qi, X. Cui, F. Shi and Y. Deng, *Tetrahedron Lett.*, 2011, **52**, 1334-1338.
180. E. Zhang, H. Tian, S. Xu, X. Yu and Q. Xu, *Org. Lett.*, 2013, **15**, 2704-2707.
181. T. Yan, B. L. Feringa and K. Barta, *Nat. Commun.*, 2014, **5**, 5602.
182. K.-i. Fujita, K. Yamamoto and R. Yamaguchi, *Org. Lett.*, 2002, **4**, 2691-2694.
183. S. Rösler, M. Ertl, T. Irrgang and R. Kempe, *Angew. Chem. Int. Ed.*, 2015, **54**, 15046-15050.
184. S. Elangovan, J. Neumann, J.-B. Sortais, K. Junge, C. Darcel and M. Beller, *Nat. Commun.*, 2016, **7**, 12641.
185. Y. Tsuji, K. T. Huh, Y. Ohsugi and Y. Watanabe, *J. Org. Chem.*, 1985, **50**, 1365-1370.
186. K. Felföldi, M. S. Klyavlin and M. Bartók, *J. Organomet. Chem.*, 1989, **362**, 193-195.
187. S. P. France, S. Hussain, A. M. Hill, L. J. Hepworth, R. M. Howard, K. R. Mulholland, S. L. Flitsch and N. J. Turner, *ACS Catal.*, 2016, **6**, 3753-3759.
188. Y. Miki, K. Hirano, T. Satoh and M. Miura, *Angew. Chem. Int. Ed.*, 2013, **52**, 10830-10834.

189. L. L. Anderson, J. Arnold and R. G. Bergman, *J. Am. Chem. Soc.*, 2005, **127**, 14542-14543.
190. J. G. Rodríguez and A. Urrutia, *Tetrahedron*, 1998, **54**, 15613-15618.
191. N. Cabello, J.-C. Kizirian, S. Gille, A. Alexakis, G. Bernardinelli, L. Pinchard and J.-C. Caille, *Eur. J. Org. Chem.*, 2005, **2005**, 4835-4842.
192. L. H. Lühning, M. Rosien and S. Doye, *Synlett*, 2017, **28**, 2489-2494.
193. I. Prochnow, R. Kubiak, O. N. Frey, R. Beckhaus and S. Doye, *ChemCatChem*, 2009, **1**, 162-172.
194. C. Guérin, V. Bellosta, G. Guillaumot and J. Cossy, *Org. Lett.*, 2011, **13**, 3534-3537.
195. D. Kim, B. Kang and S. H. Hong, *Org. Chem. Front.*, 2016, **3**, 475-479.
196. S. Agarwal, S. Sasane, P. Deshmukh, B. Rami, D. Bandyopadhyay, P. Giri, S. Giri, M. Jain and R. C. Desai, *ACS Med. Chem. Lett.*, 2016, **7**, 1134-1138.
197. S. Mo and J. Xu, *ChemCatChem*, 2014, **6**, 1679-1683.
198. P. R. Payne, P. Garcia, P. Eisenberger, J. C. H. Yim and L. L. Schafer, *Org. Lett.*, 2013, **15**, 2182-2185.
199. M. Cushman and N. Castagnoli, *J. Org. Chem.*, 1972, **37**, 1268-1271.
200. M. L. Rueppel and H. Rapoport, *J. Am. Chem. Soc.*, 1971, **93**, 7021-7028.
201. M. L. Rueppel and H. Rapoport, *J. Am. Chem. Soc.*, 1970, **92**, 5528-5530.
202. K. Huang, M. Ortiz-Marciales, M. De Jesús and V. Stepanenko, *J. Heterocycl. Chem.*, 2009, **46**, 1252-1258.
203. J. H. Burckhalter and J. H. Short, *J. Org. Chem.*, 1958, **23**, 1281-1286.
204. X. Xiu, N. L. Puskar, J. A. P. Shanata, H. A. Lester and D. A. Dougherty, *Nature*, 2009, **458**, 534.
205. D. Lemoine, R. Jiang, A. Taly, T. Chataigneau, A. Specht and T. Grutter, *Chem. Rev.*, 2012, **112**, 6285-6318.
206. B. Nammalwar and R. Bunce, *Molecules*, 2014, **19**, 204-232.
207. R. A. Bunce, D. M. Herron, L. B. Johnson and S. V. Kotturi, *J. Org. Chem.*, 2001, **66**, 2822-2827.
208. R. A. Bunce, B. Nammalwar and L. M. Slaughter, *J. Heterocycl. Chem.*, 2009, **46**, 854-860.
209. R. A. H. Bunce, Derrick M.; Ackerman, Matthew L., *J. Org. Chem.*, 2000, **65**, 2847-2850.
210. R. A. Bunce and T. Nago, *J. Heterocycl. Chem.*, 2008, **45**, 1155-1160.
211. R. A. Bunce and J. E. Schammerhorn, *Org. Prep. Proced. Int.*, 2010, **42**, 71-82.
212. R. A. Bunce and E. J. Lee, *J. Heterocycl. Chem.*, 2010, **47**, 1176-1182.
213. K. H. Park, H. S. Joo, K. I. Ahn and K. Jun, *Tetrahedron Lett.*, 1995, **36**, 5943-5946.
214. R. Gianatassio, J. M. Lopchuk, J. Wang, C.-M. Pan, L. R. Malins, L. Prieto, T. A. Brandt, M. R. Collins, G. M. Gallego, N. W. Sach, J. E. Spangler, H. Zhu, J. Zhu and P. S. Baran, *Science*, 2016, **351**, 241-246.
215. M. R. Becker, A. D. Richardson and C. S. Schindler, *ChemRxiv*, 2018, DOI: <https://doi.org/10.26434/chemrxiv.7218272.v1>.
216. R. Sakamoto, T. Inada, S. Sakurai and K. Maruoka, *Org. Lett.*, 2016, **18**, 6252-6255.
217. E. Kumarasamy, S. K. Kandappa, R. Raghunathan, S. Jockusch and J. Sivaguru, *Angew. Chem. Int. Ed.*, 2017, **56**, 7056-7061.
218. J.-M. Valk, J. Boersma and G. van Koten, *J. Organomet. Chem.*, 1994, **483**, 213-216.

219. K. Lang and J. W. Chin, *Chem. Rev.*, 2014, **114**, 4764-4806.
220. C. H. Kim, J. Y. Axup and P. G. Schultz, *Curr. Opin. Chem. Biol.*, 2013, **17**, 412-419.

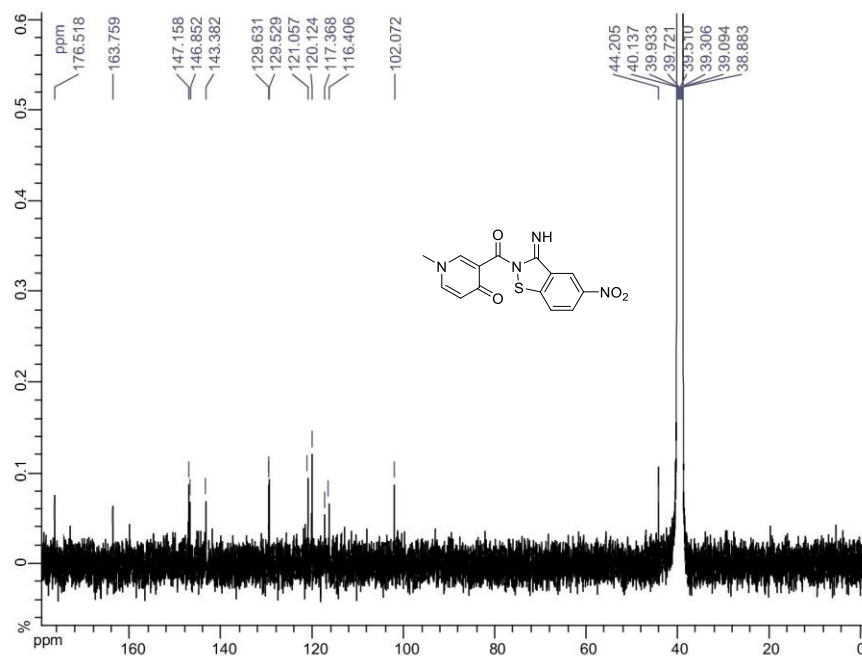
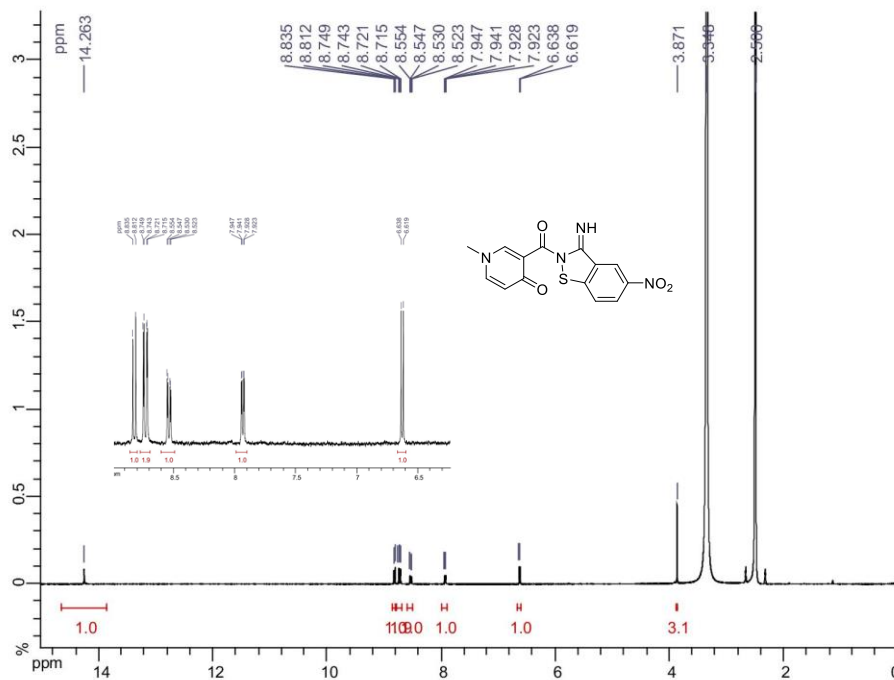
Appendix A NMR spectra

A.1 General considerations

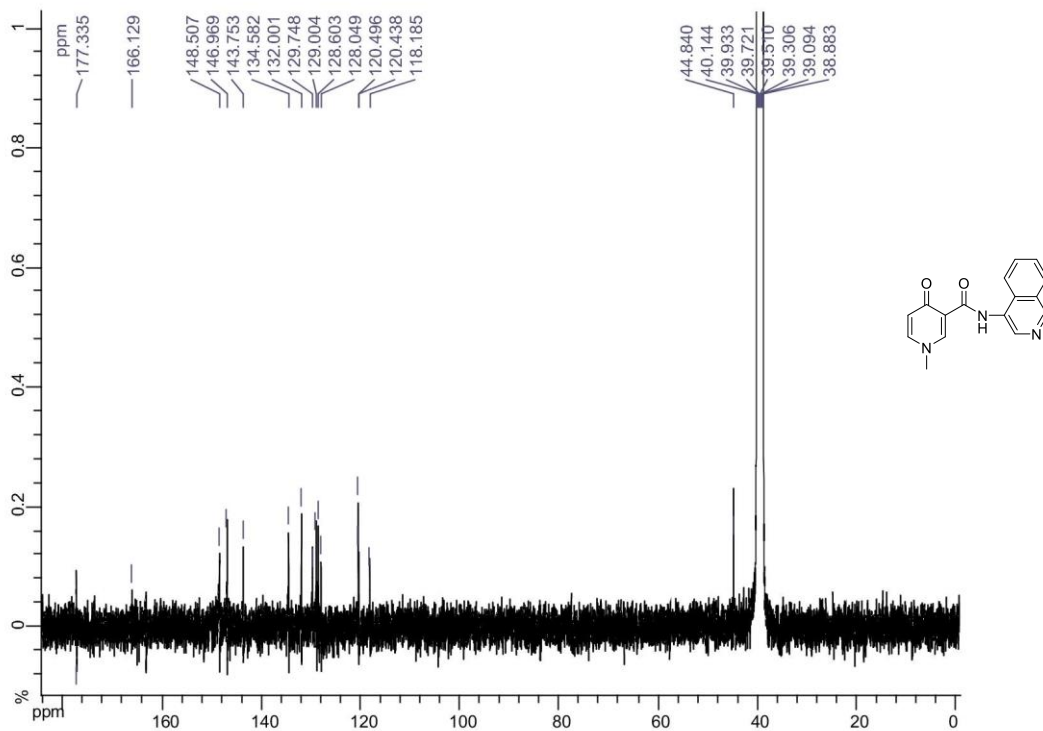
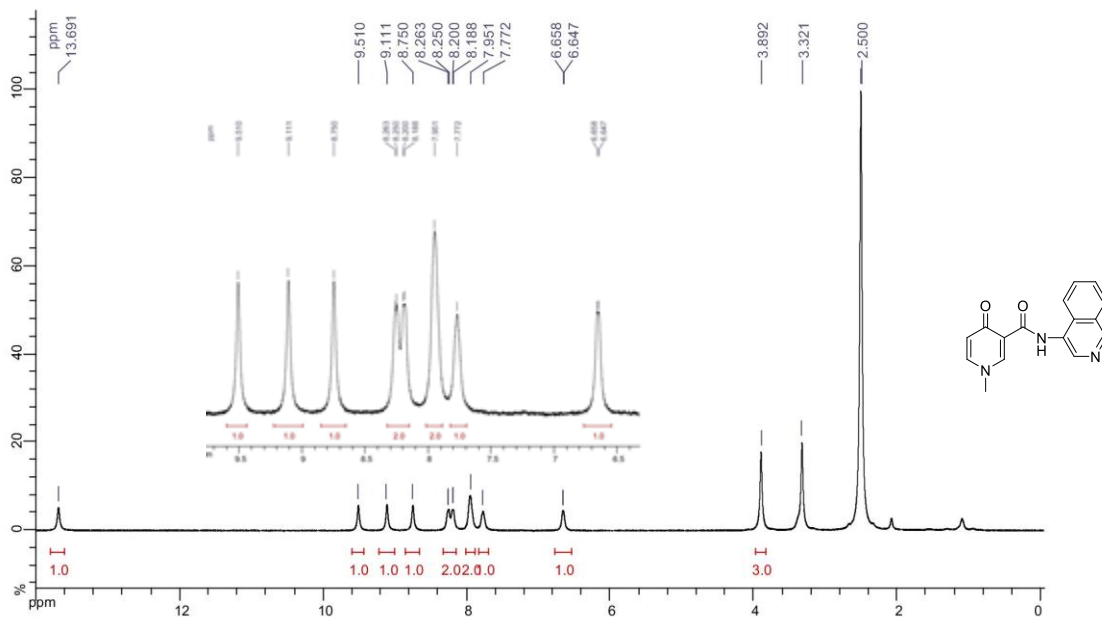
^1H , ^{13}C and ^{19}F spectra were processed with software NMR Notebook.

A.2 ^1H , ^{13}C and ^{19}F NMR spectra of compounds in Chapter 2

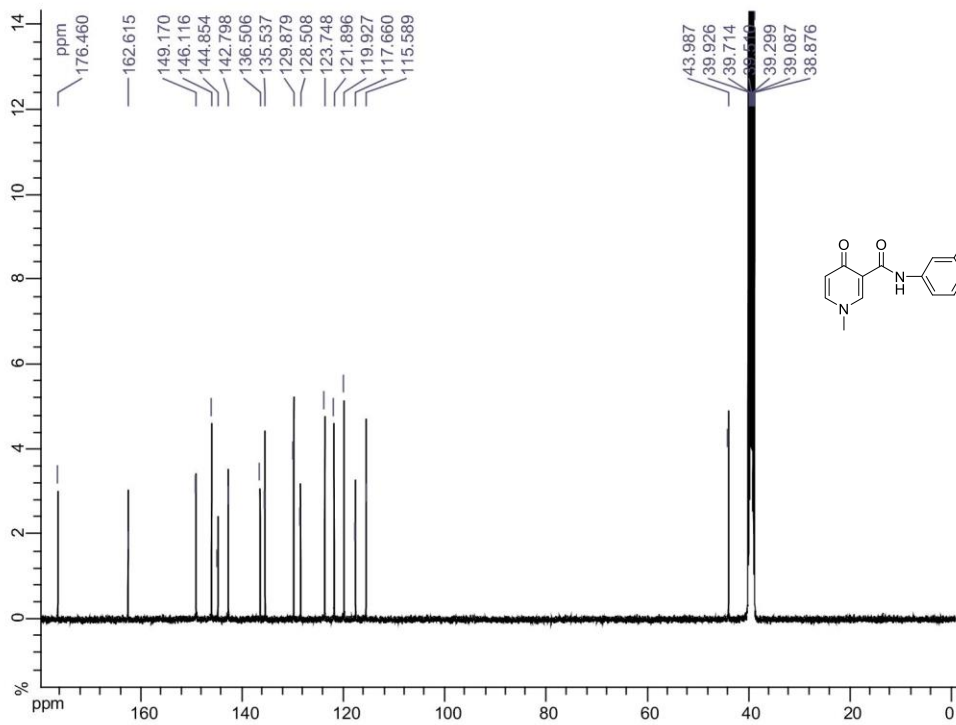
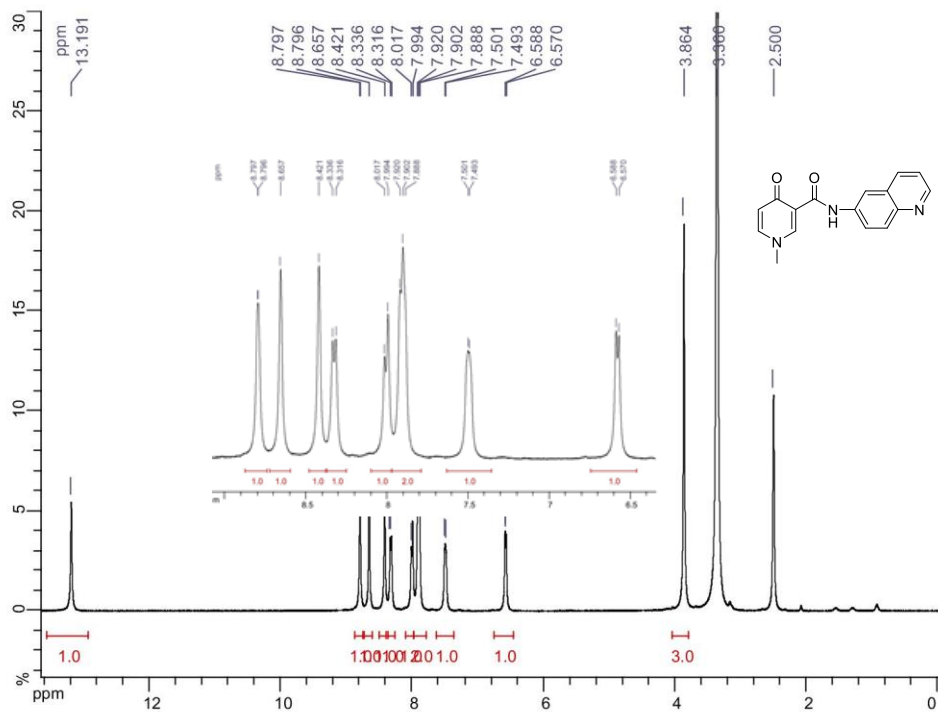
Presumed structure: 3-(3-Imino-5-nitro-2,3-dihydrobenzo[*d*]isothiazole-2-carbonyl)-1-methylpyridin-4(1*H*)-one
(2.2')



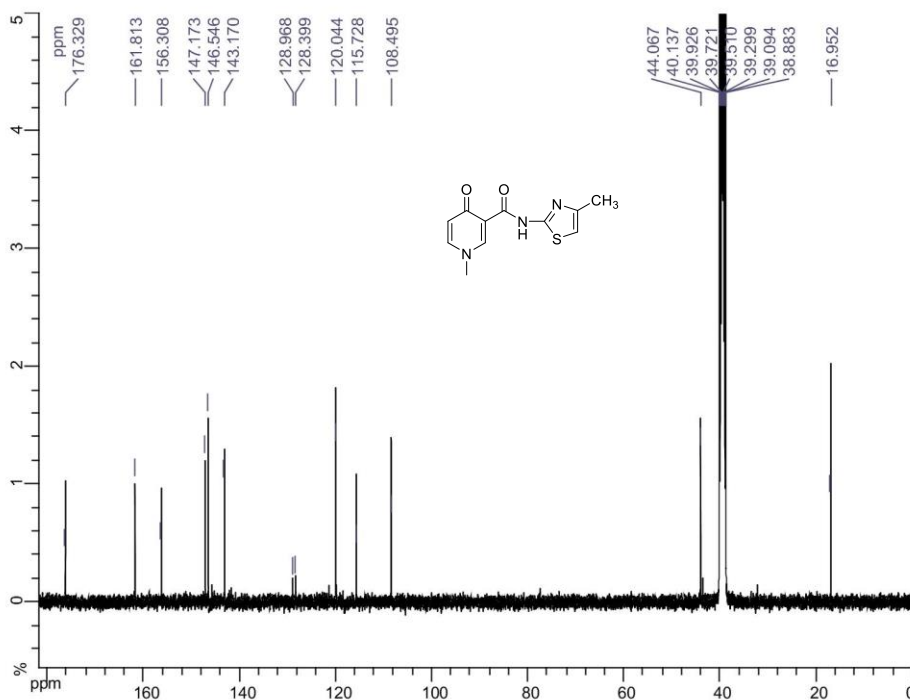
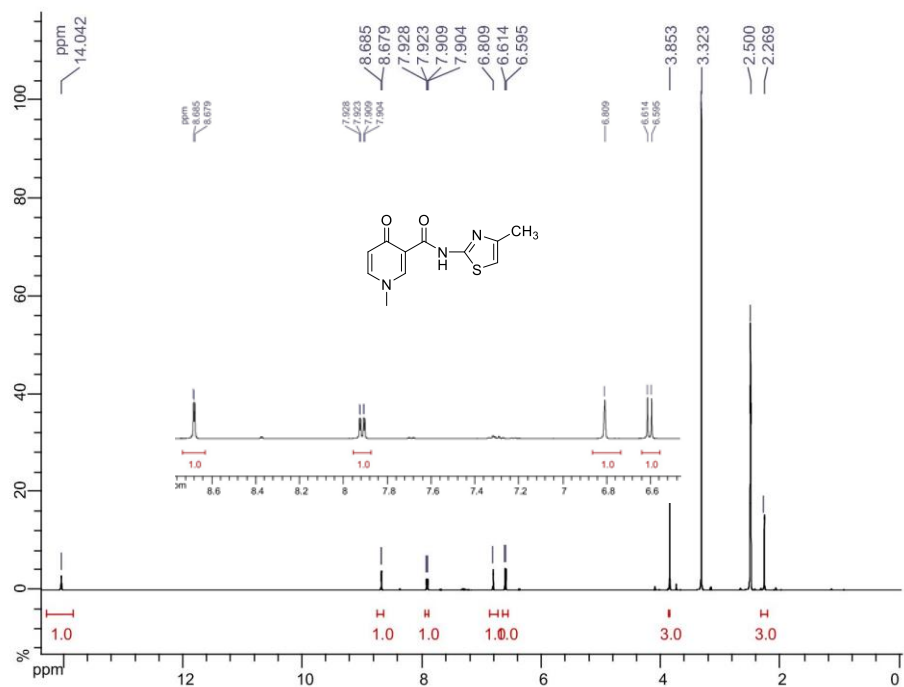
***N*-(Isoquinolin-4-yl)-1-methyl-4-oxo-1,4-dihydropyridine-3-carboxamide (2.6.1)**



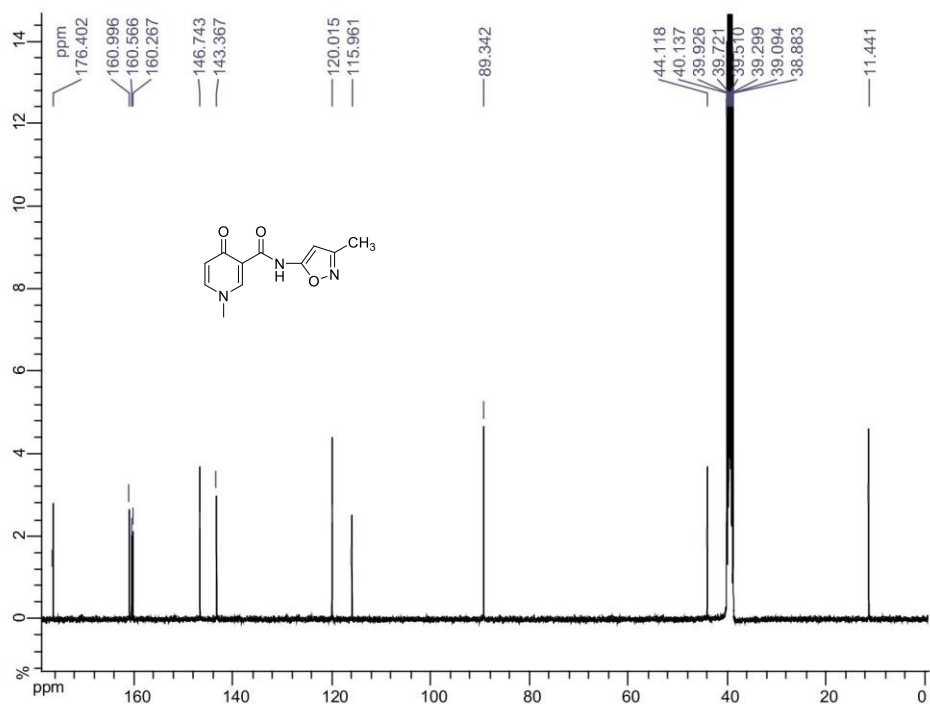
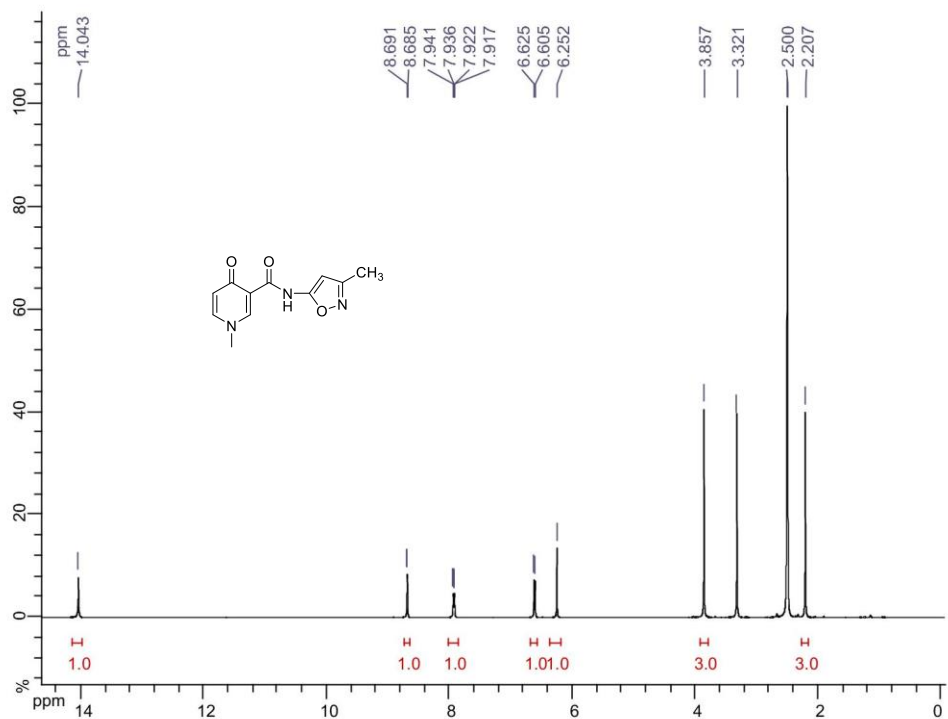
1-Methyl-4-oxo-N-(quinolin-6-yl)-1,4-dihydropyridine-3-carboxamide (2.6.2)



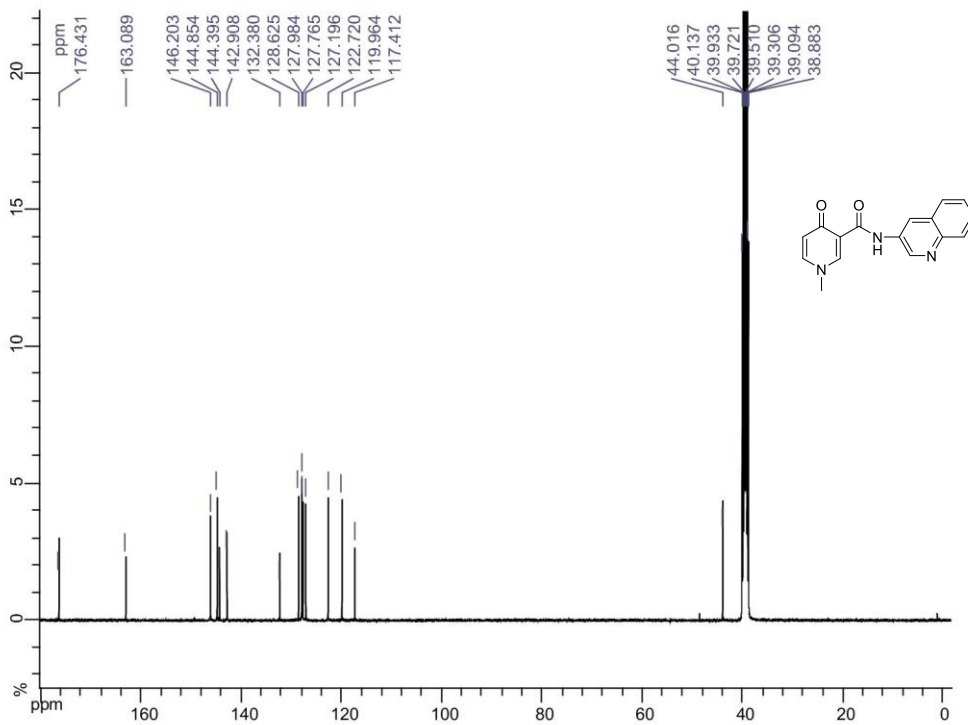
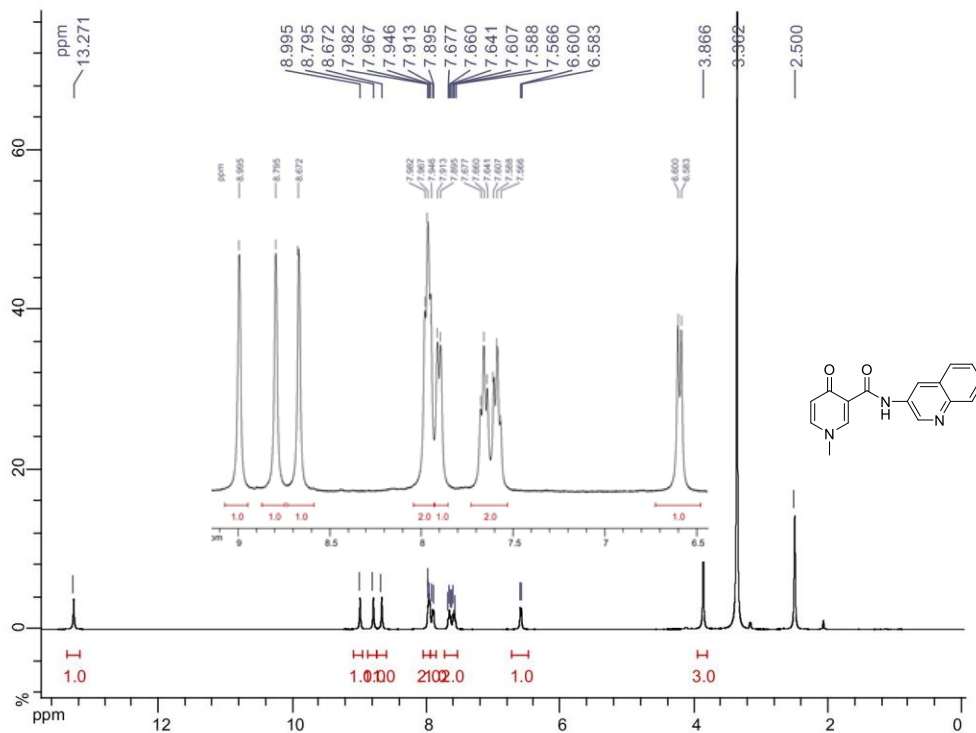
1-Methyl-*N*-(4-methylthiazol-2-yl)-4-oxo-1,4-dihydropyridine-3-carboxamide (2.6.3)



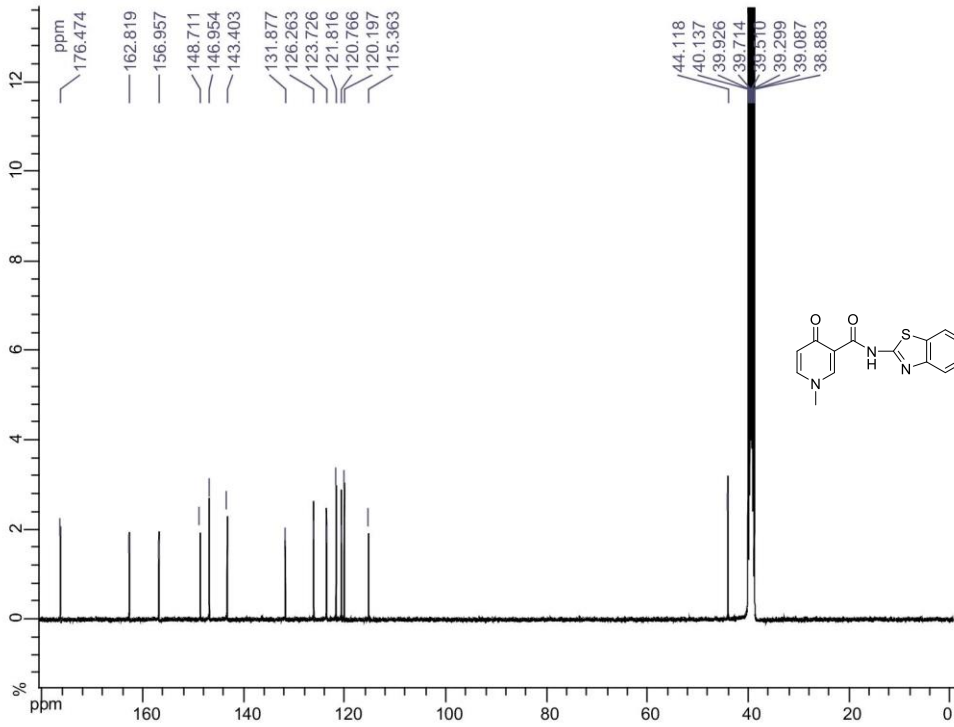
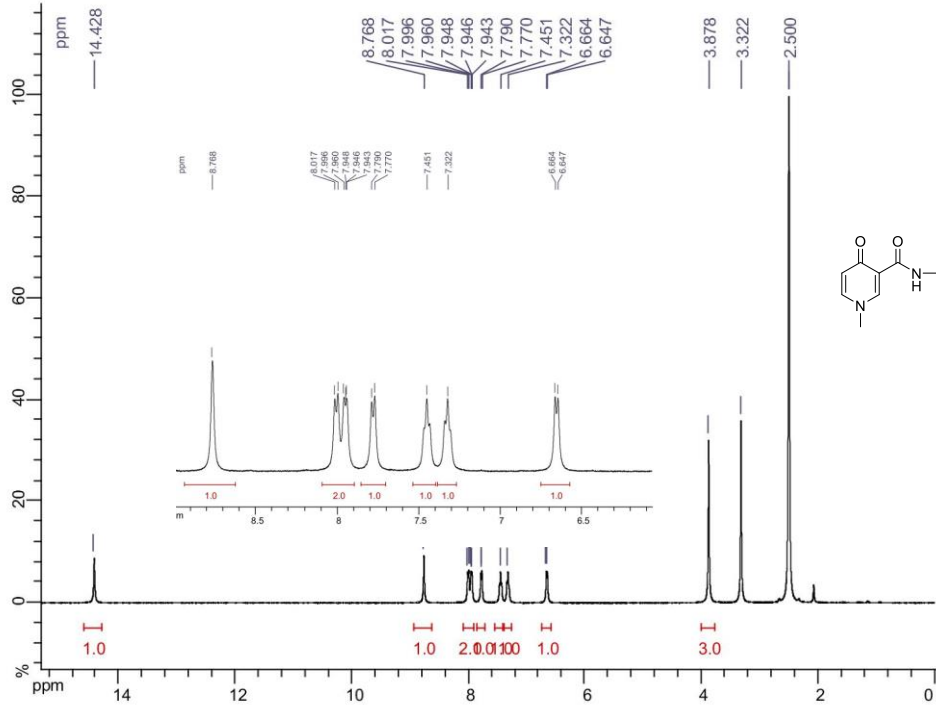
1-Methyl-N-(3-methylisoxazol-5-yl)-4-oxo-1,4-dihydropyridine-3-carboxamide (2.6.4)



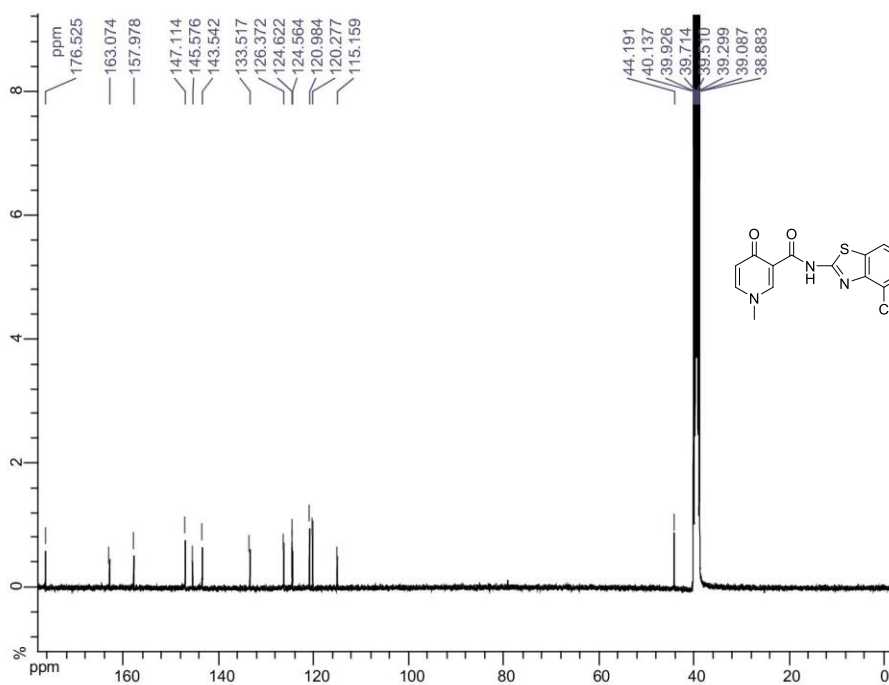
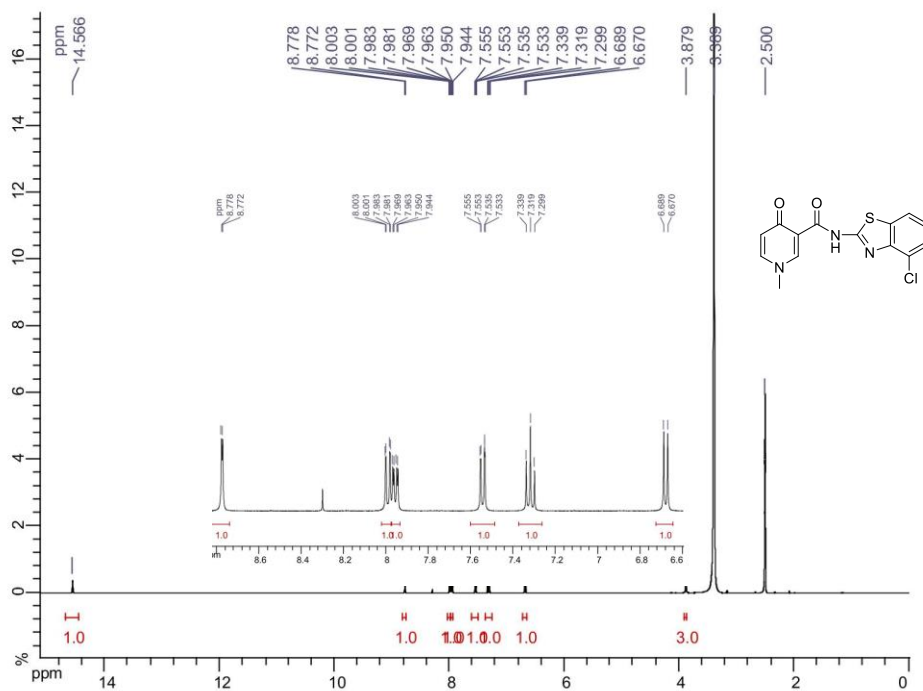
1-Methyl-4-oxo-N-(quinolin-3-yl)-1,4-dihydropyridine-3-carboxamide (2.6.5)



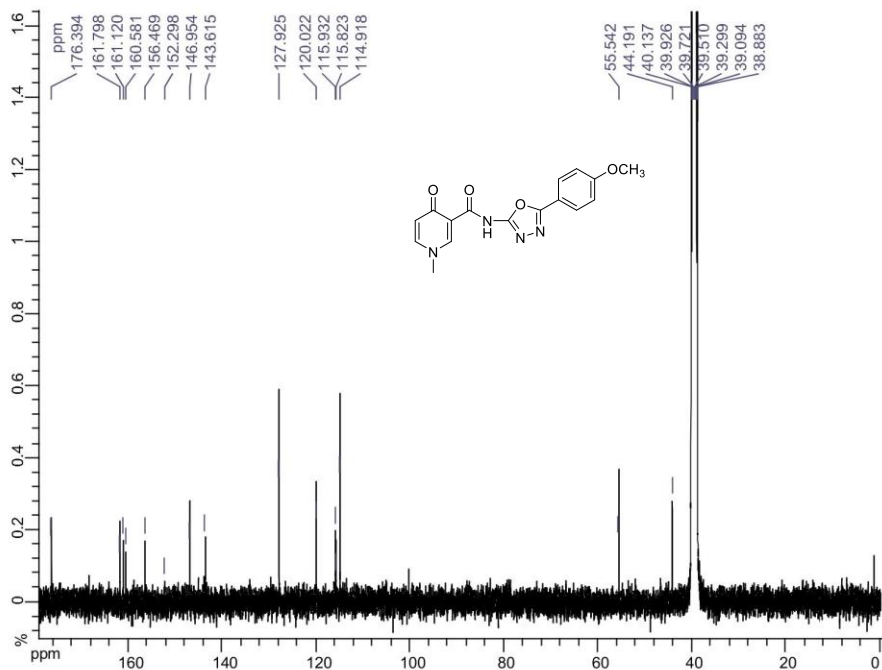
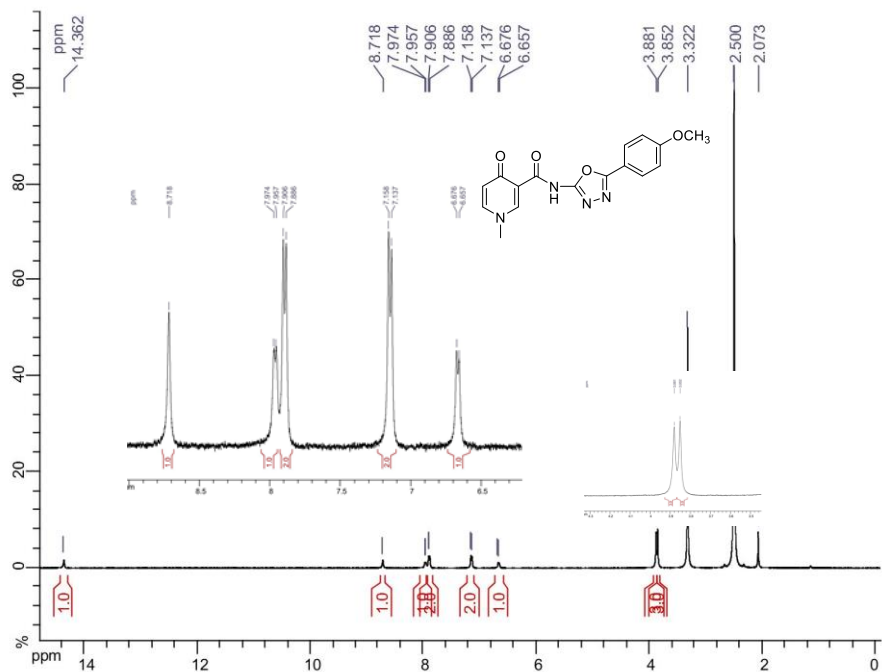
***N*-(Benzo[*d*]thiazol-2-yl)-1-methyl-4-oxo-1,4-dihydropyridine-3-carboxamide (2.6.6)**



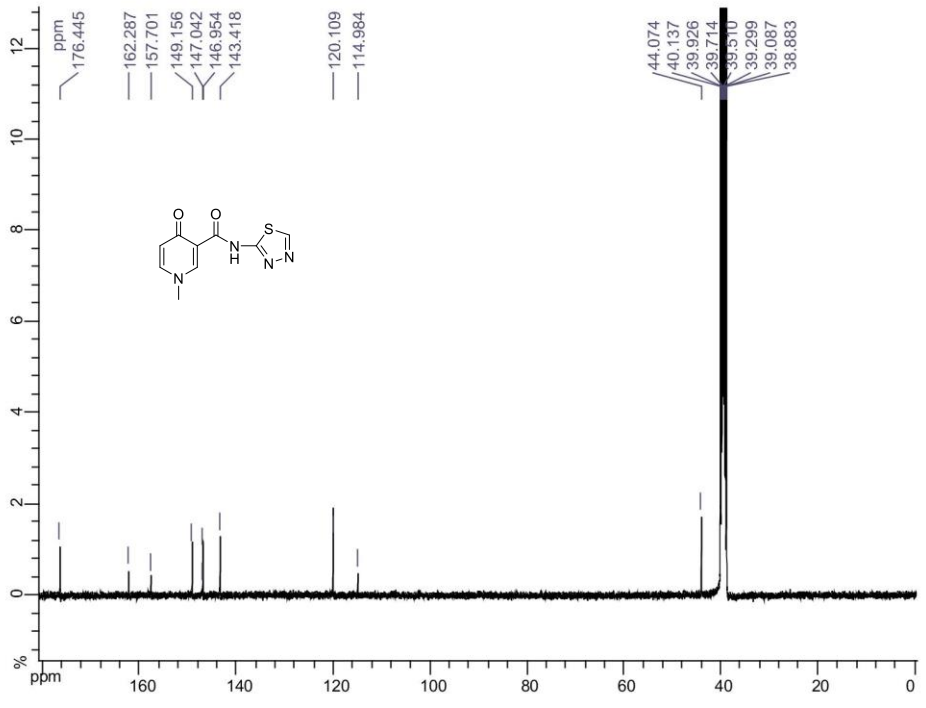
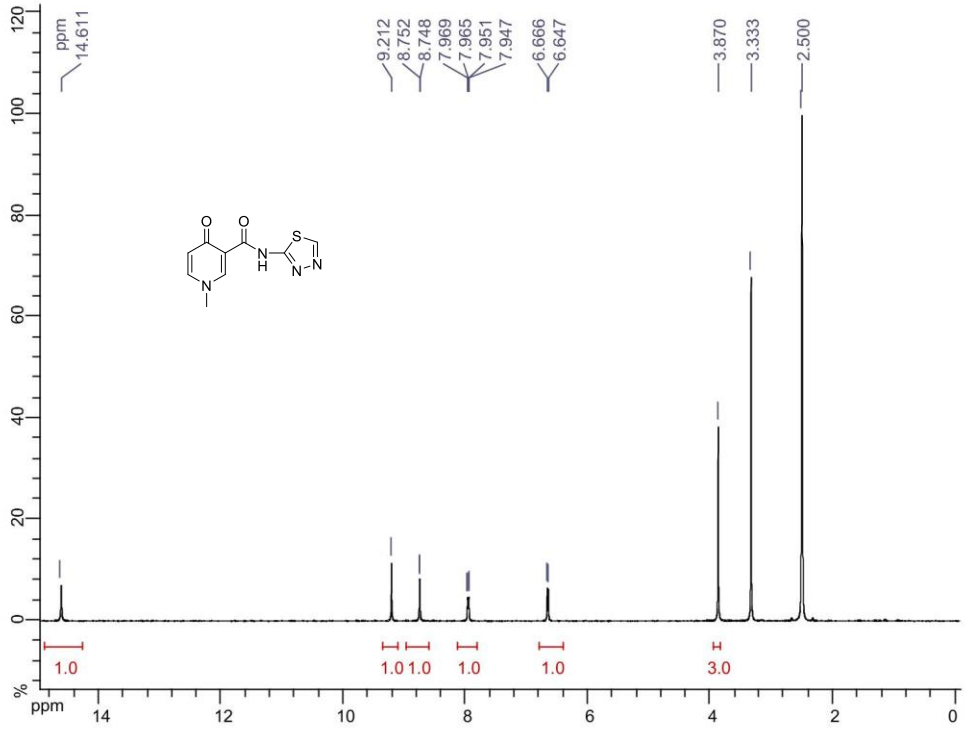
***N*-(4-Chlorobenzo[d]thiazol-2-yl)-1-methyl-4-oxo-1,4-dihydropyridine-3-carboxamide (2.6.7)**



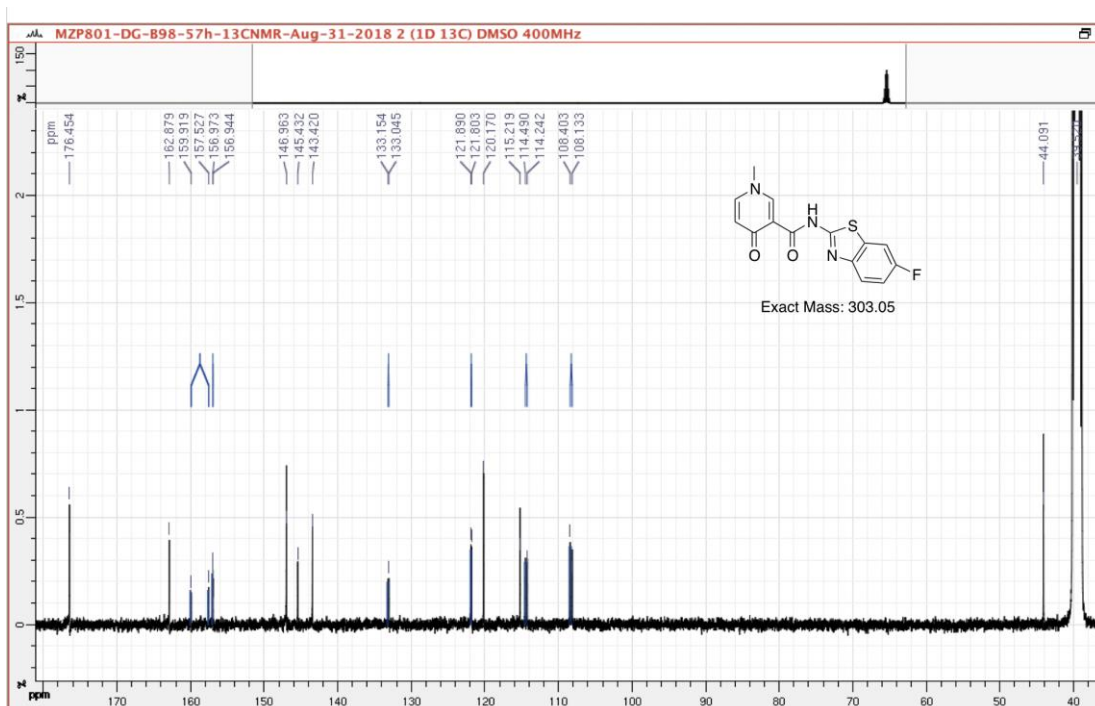
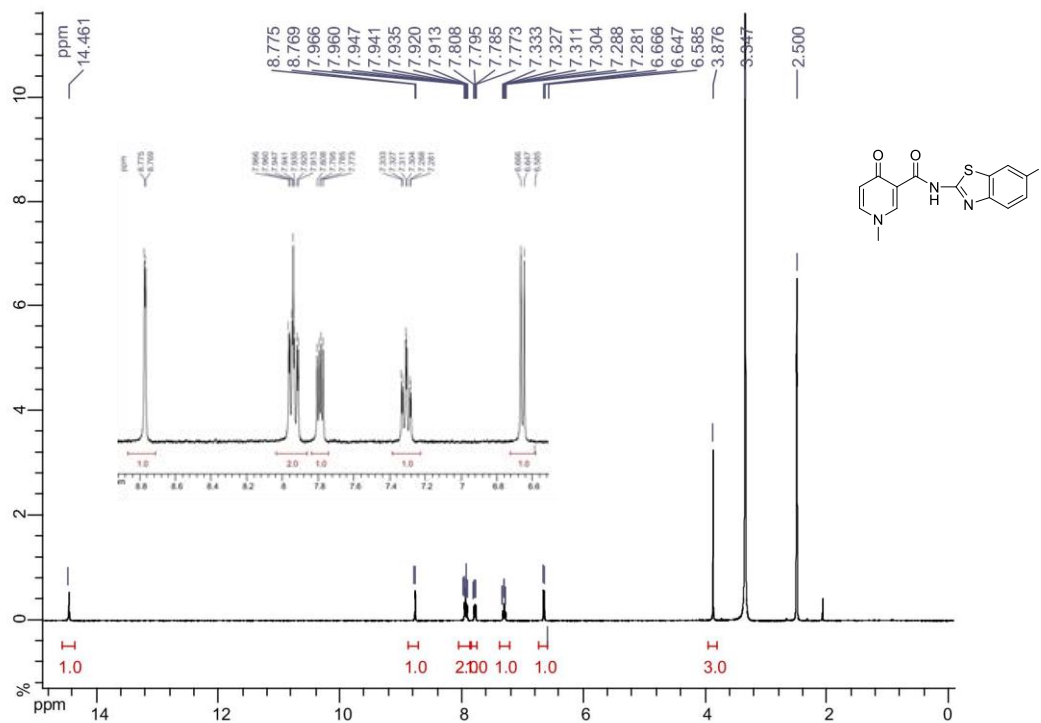
***N*-(5-(4-Methoxyphenyl)-1,3,4-oxadiazol-2-yl)-1-methyl-4-oxo-1,4-dihydropyridine-3-carboxamide (2.6.8)**



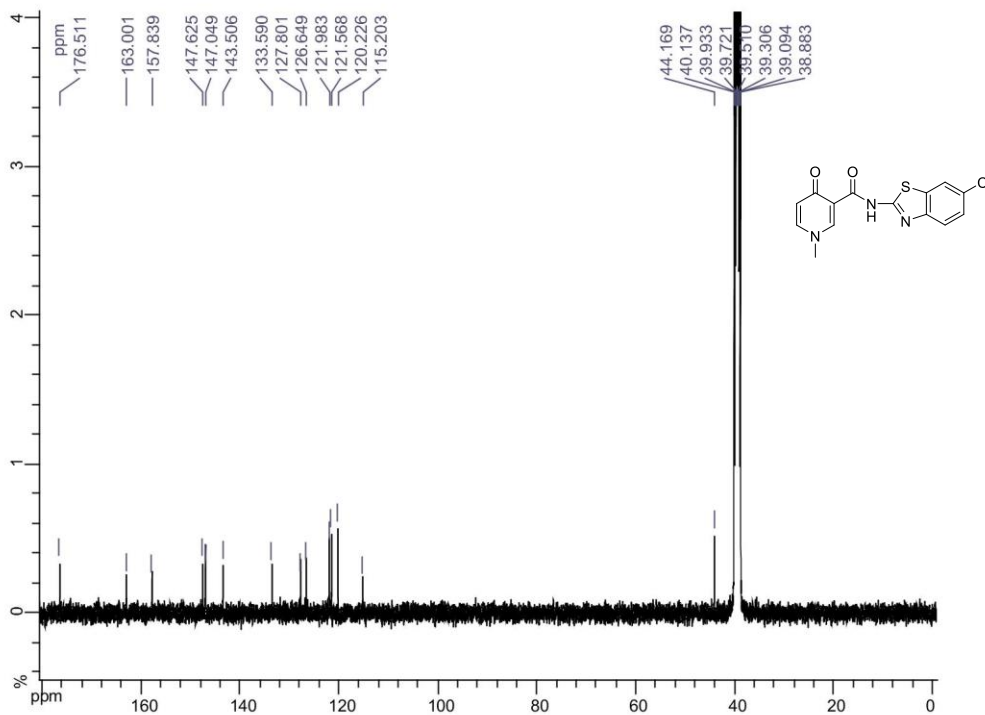
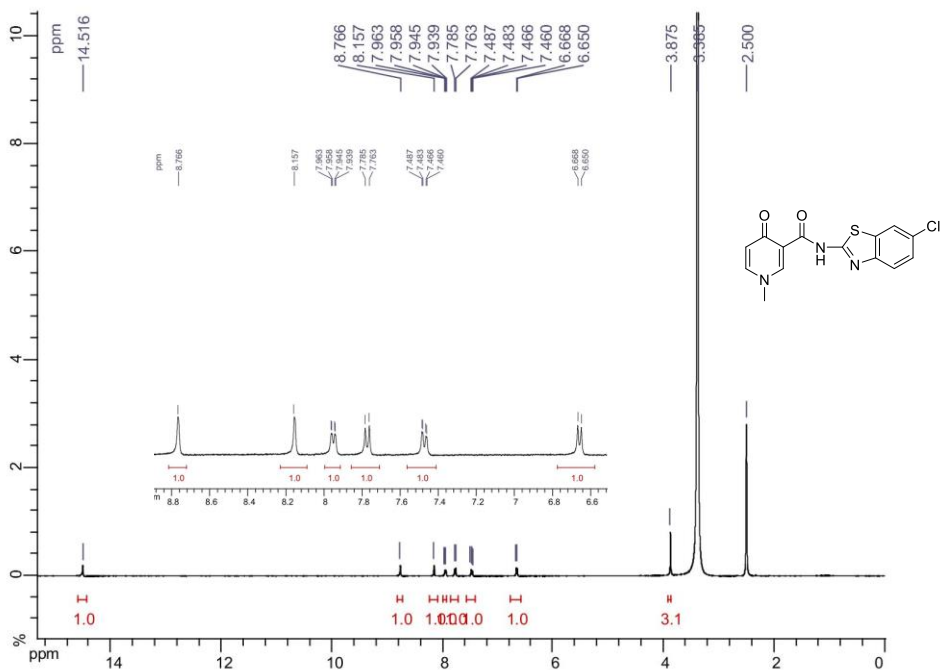
1-Methyl-4-oxo-N-(1,3,4-thiadiazol-2-yl)-1,4-dihydropyridine-3-carboxamide (2.6.9)



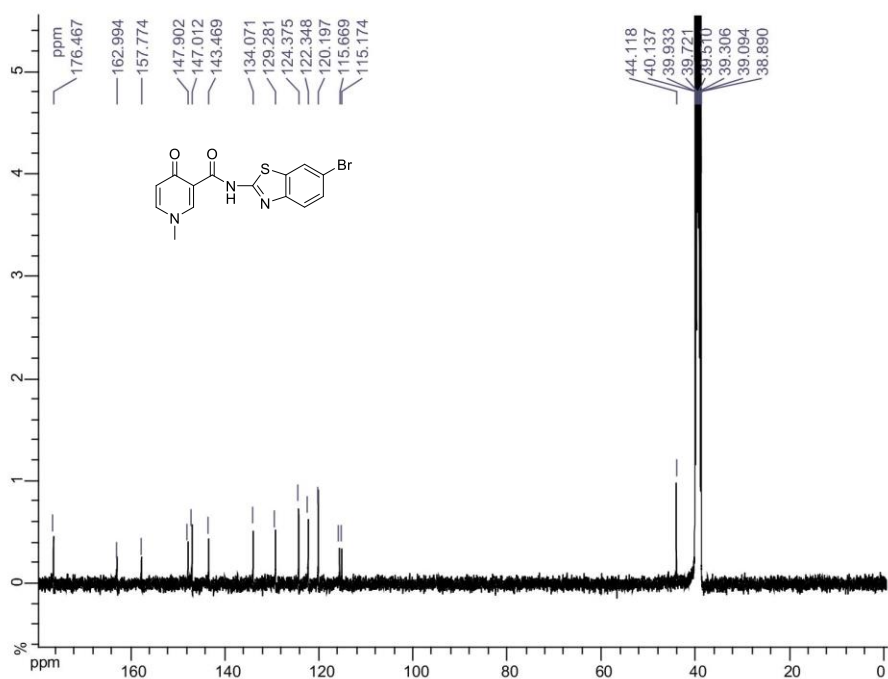
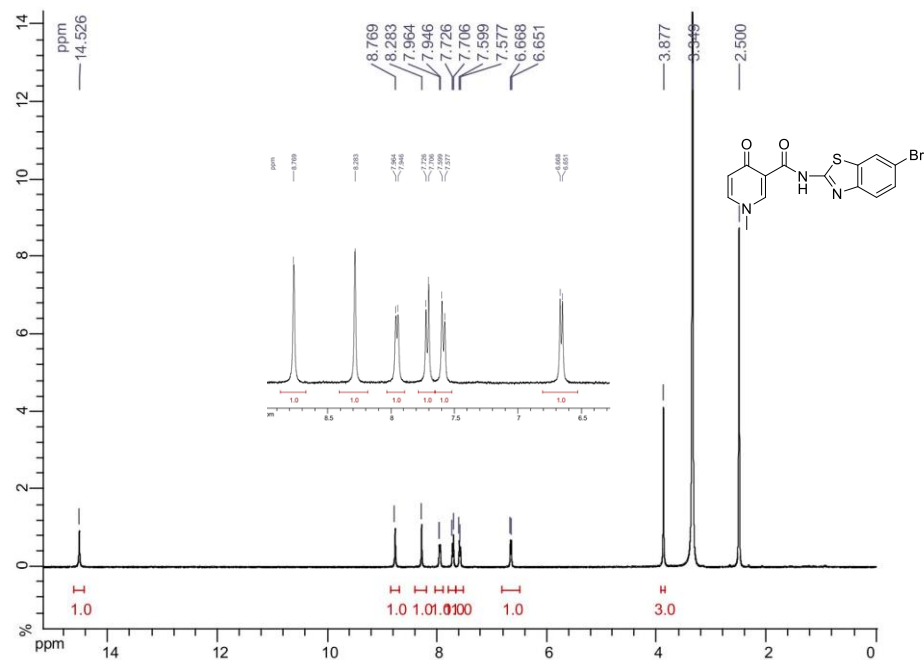
***N*-(6-Fluorobenzo[*d*]thiazol-2-yl)-1-methyl-4-oxo-1,4-dihydropyridine-3-carboxamide (2.6.10)**



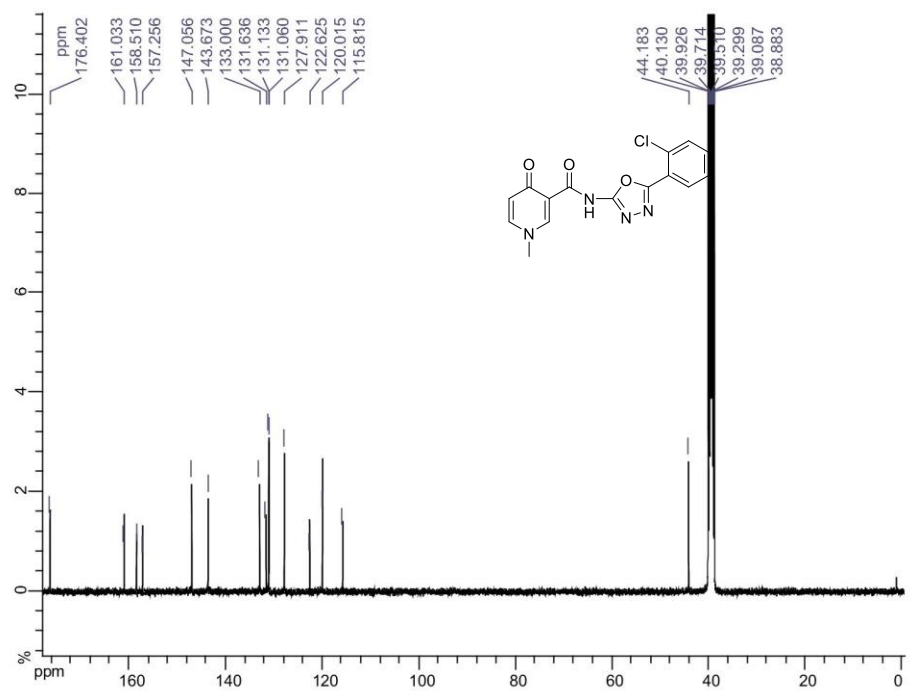
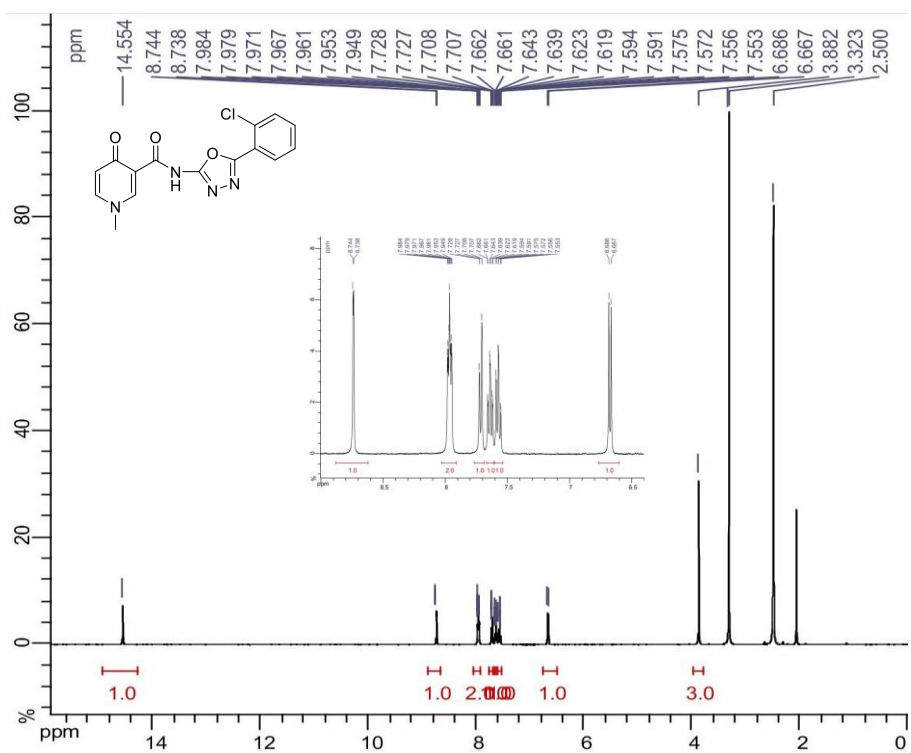
***N*-(6-Chlorobenzo[*d*]thiazol-2-yl)-1-methyl-4-oxo-1,4-dihydropyridine-3-carboxamide (2.6.12)**



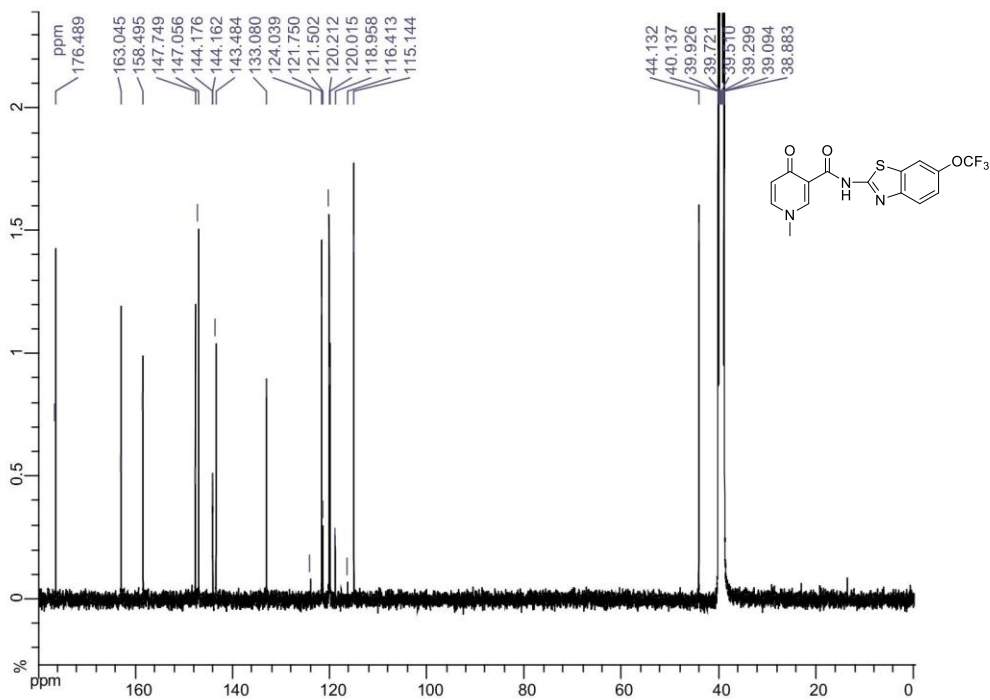
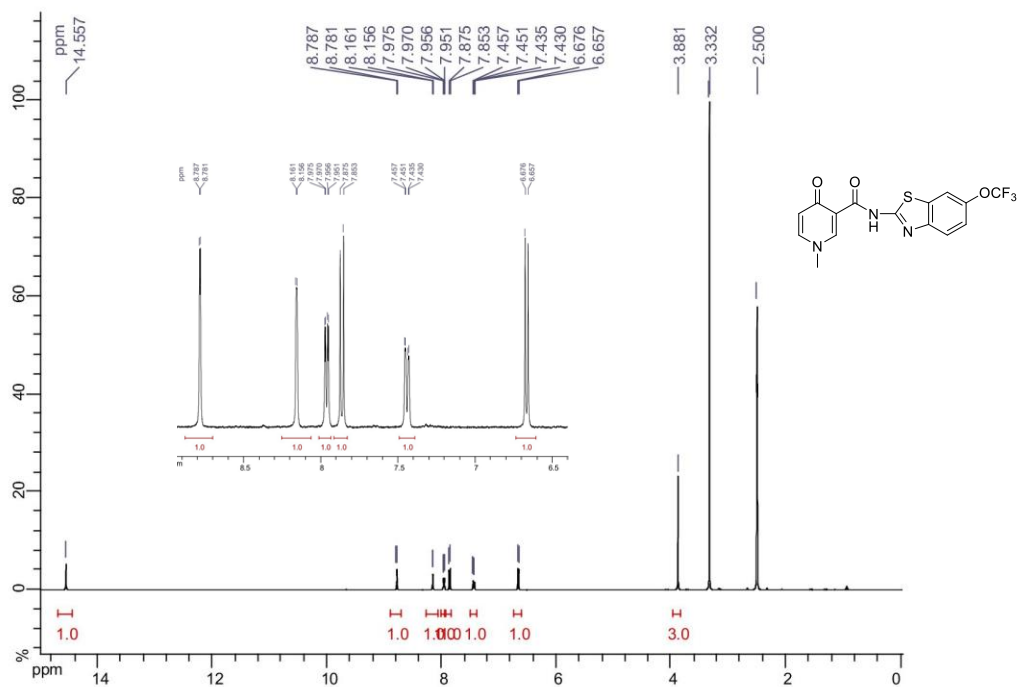
***N*-(6-Bromobenzo[d]thiazol-2-yl)-1-methyl-4-oxo-1,4-dihydropyridine-3-carboxamide (2.6.13)**

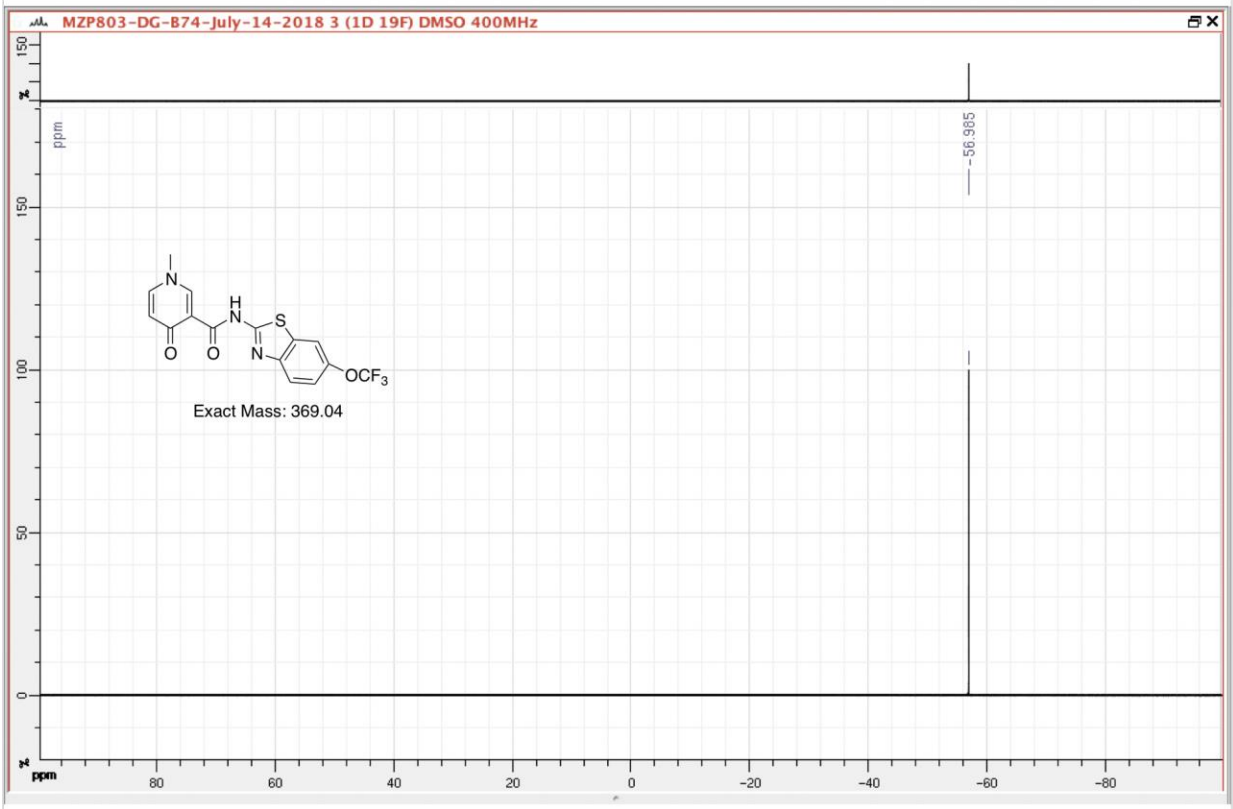


***N*-(5-(2-Chlorophenyl)-1,3,4-oxadiazol-2-yl)-1-methyl-4-oxo-1,4-dihydropyridine-3-carboxamide (2.6.14)**

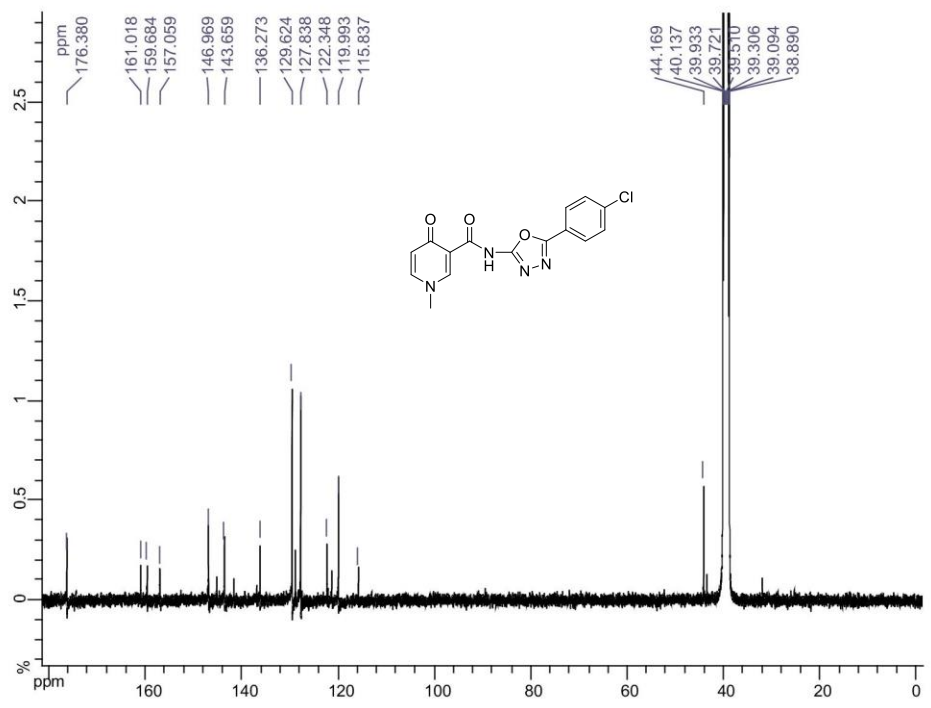
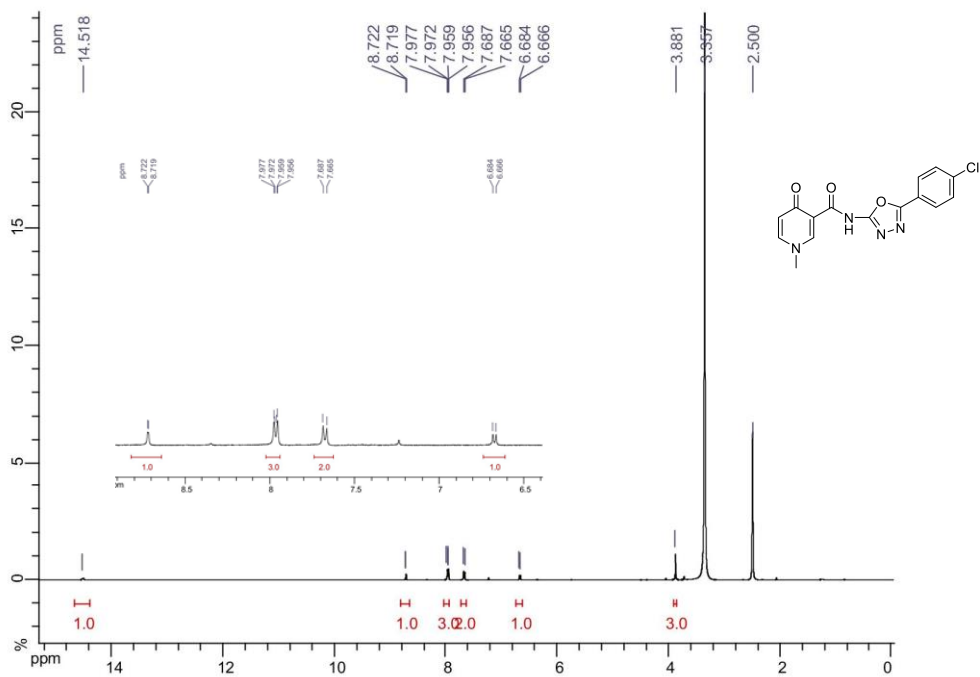


1-Methyl-4-oxo-N-(6-(trifluoromethoxy)benzo[d]thiazol-2-yl)-1,4-dihydropyridine-3-carboxamide (2.6.15)

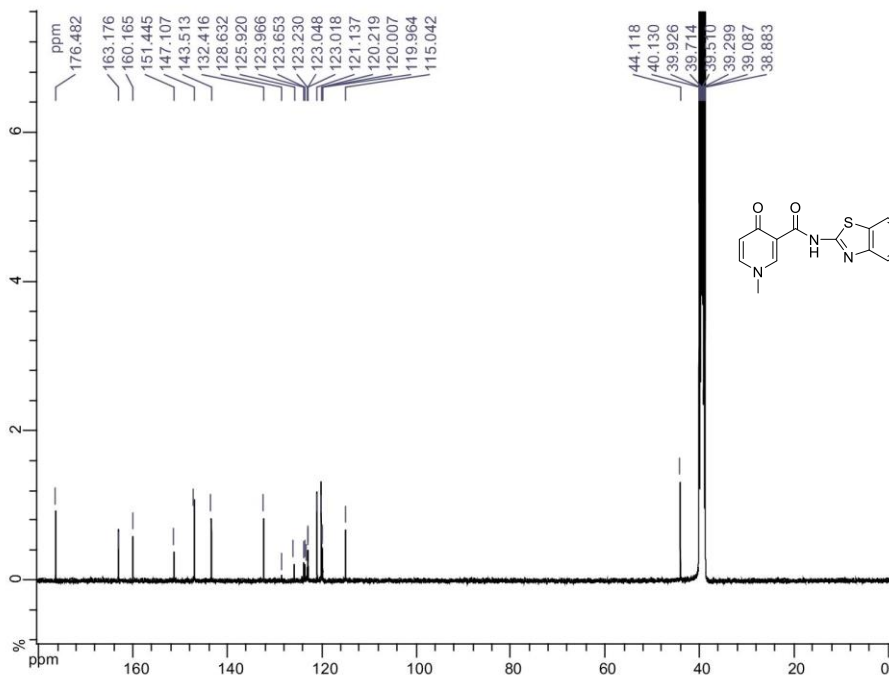
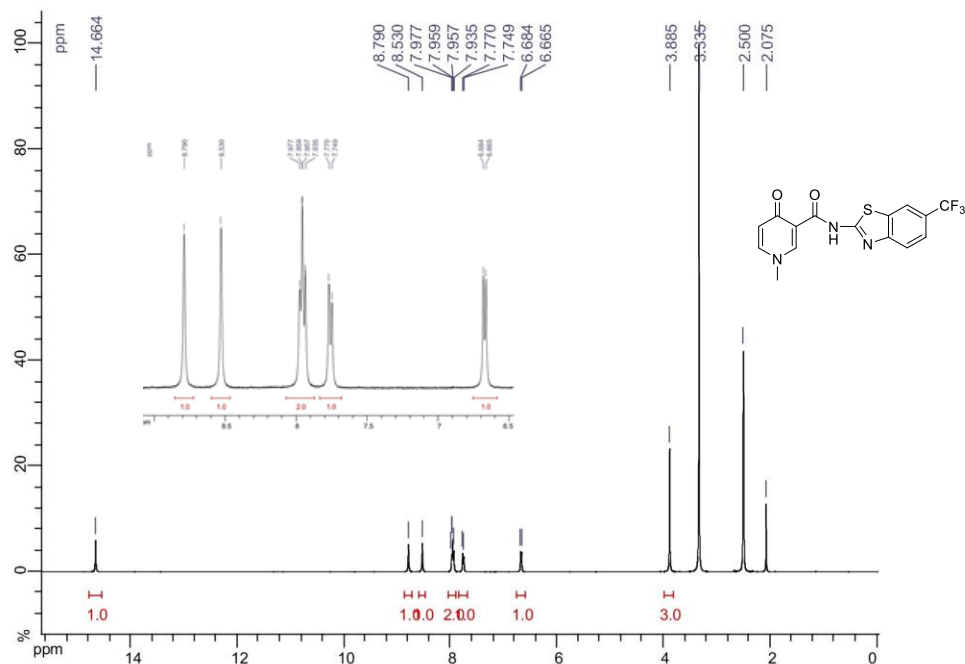


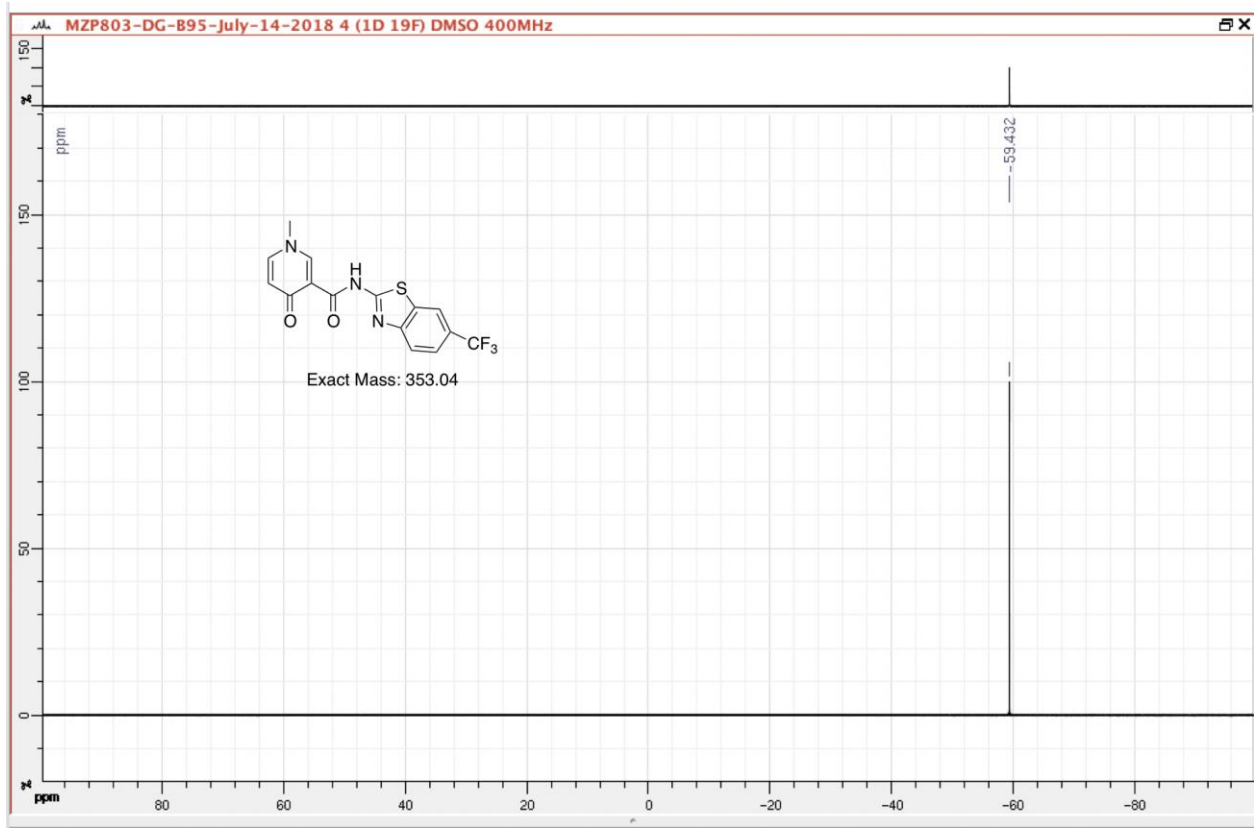


N-(5-(4-Chlorophenyl)-1,3,4-oxadiazol-2-yl)-1-methyl-4-oxo-1,4-dihydropyridine-3-carboxamide (2.6.16)

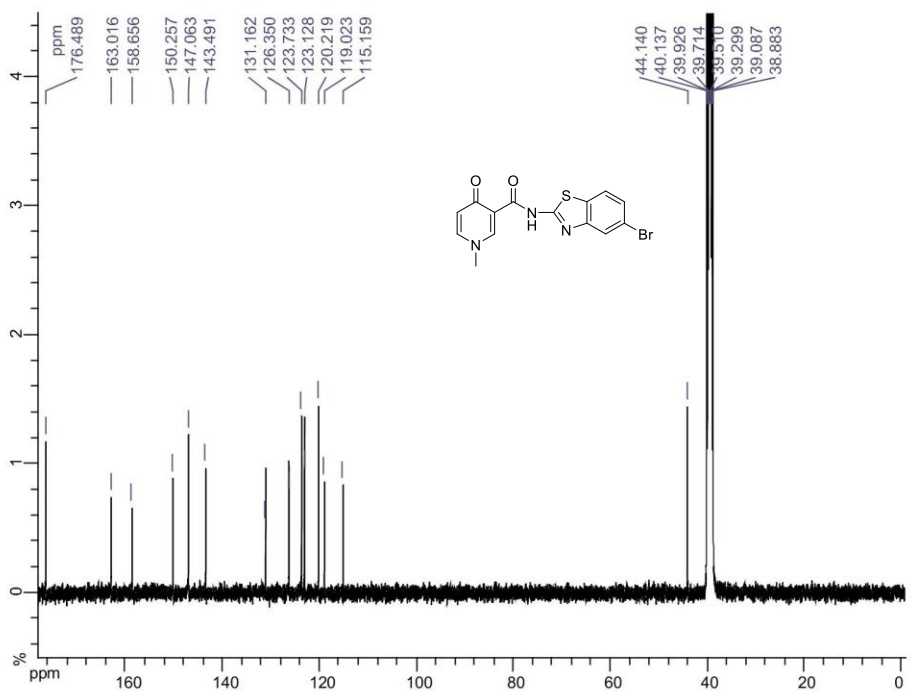
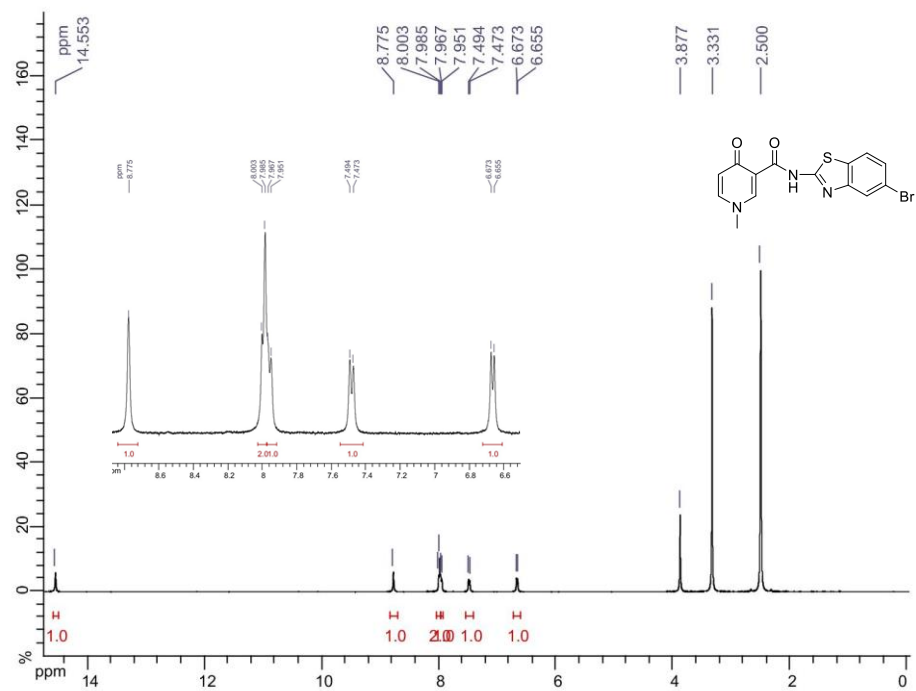


1-Methyl-4-oxo-N-(6-(trifluoromethyl)benzo[d]thiazol-2-yl)-1,4-dihydropyridine-3-carboxamide (2.6.17)

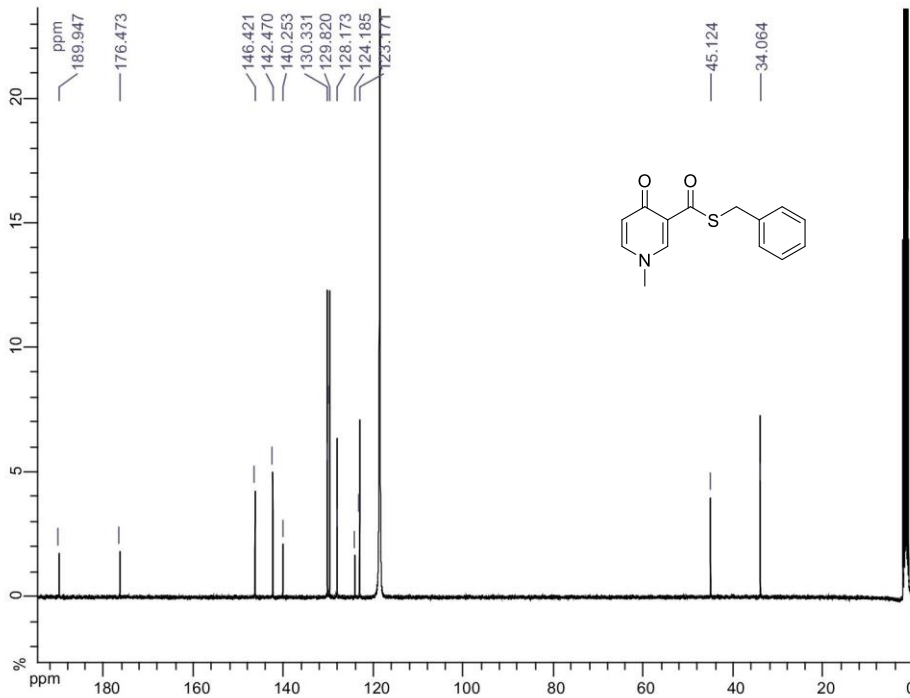
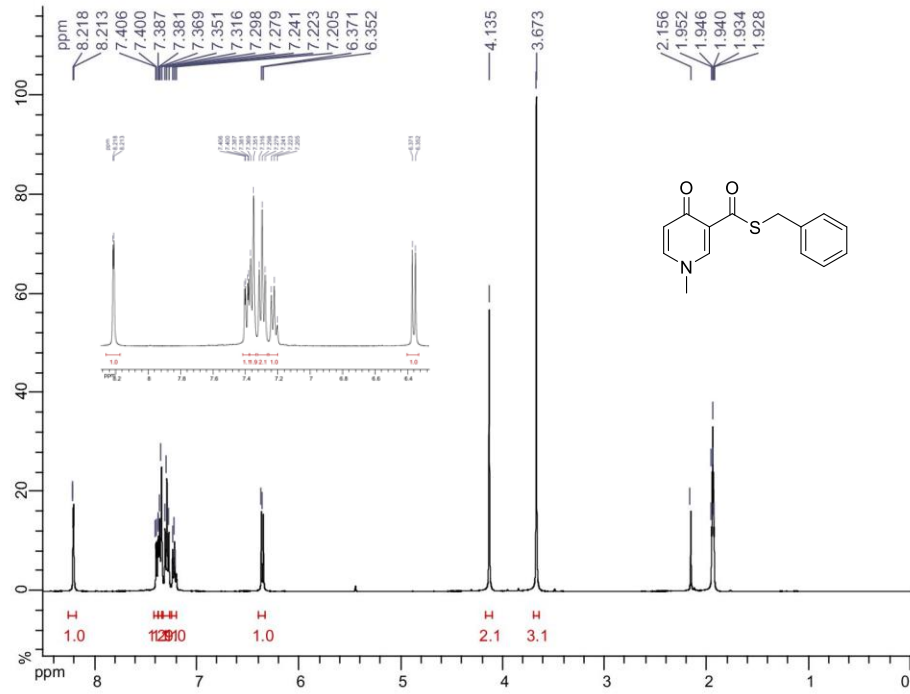




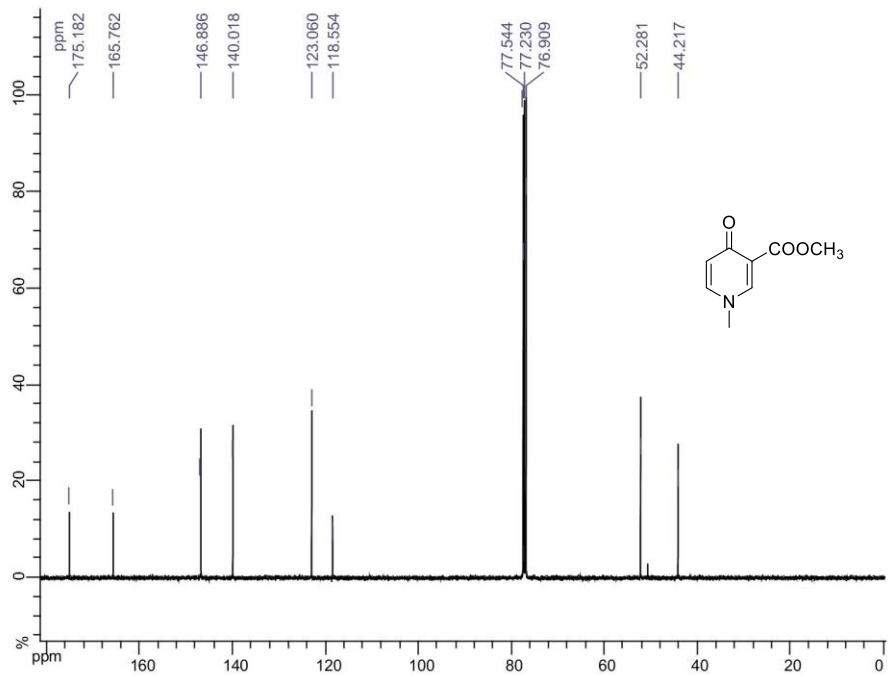
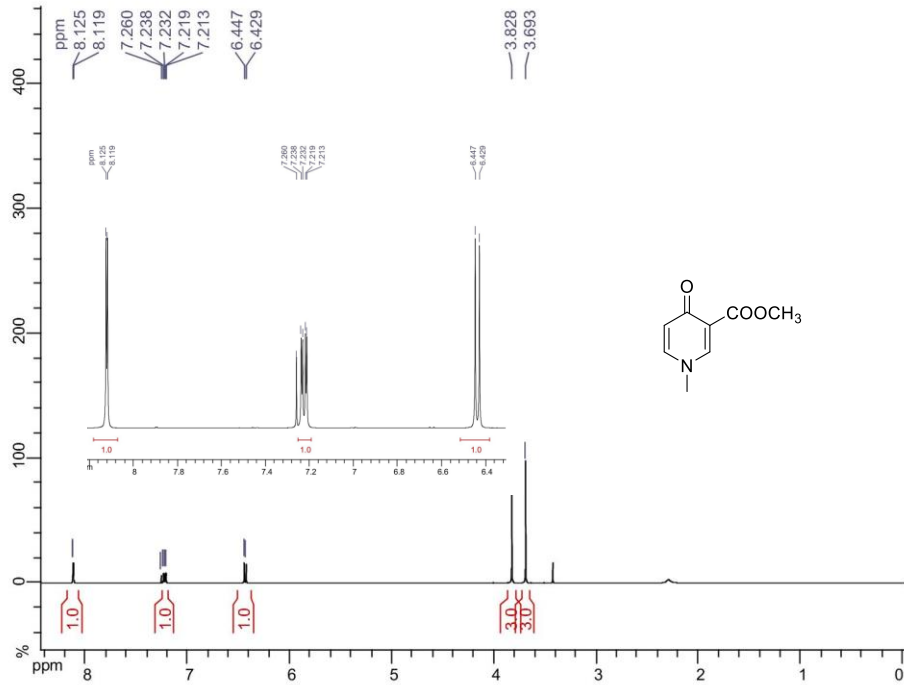
***N*-(5-Bromobenzo[d]thiazol-2-yl)-1-methyl-4-oxo-1,4-dihydropyridine-3-carboxamide (2.6.19)**



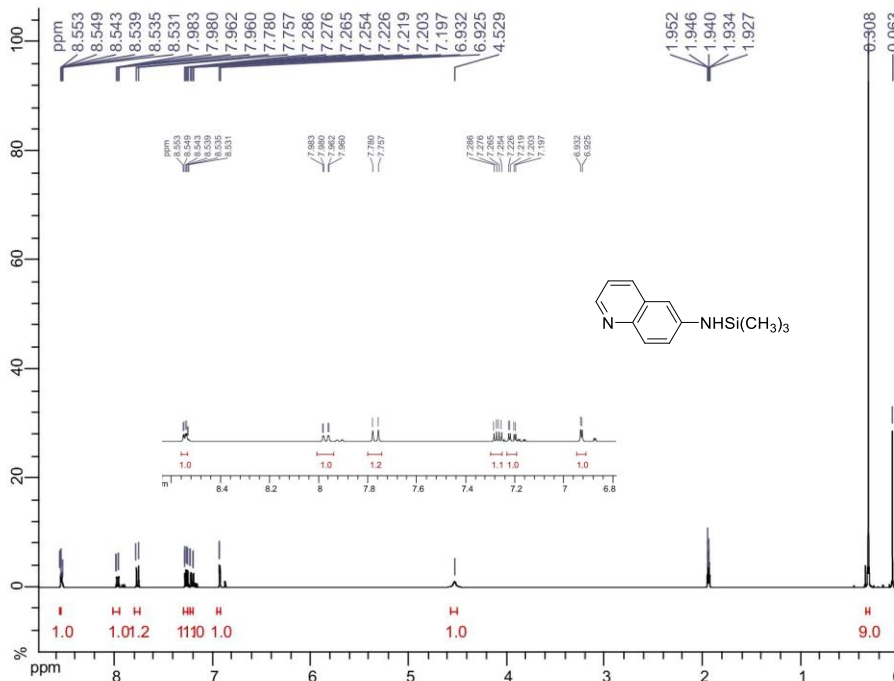
S-Benzyl-1-methyl-4-oxo-1,4-dihydropyridine (2.33)



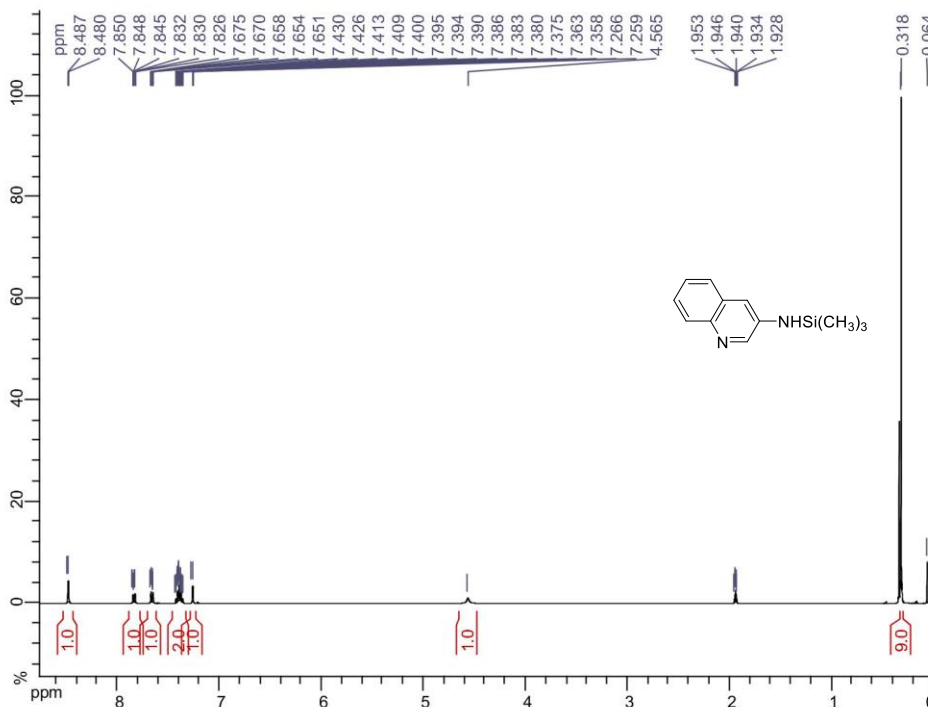
Methyl 1-methyl-4-oxo-1,4-dihydropyridine-3-carboxylate (2.36)



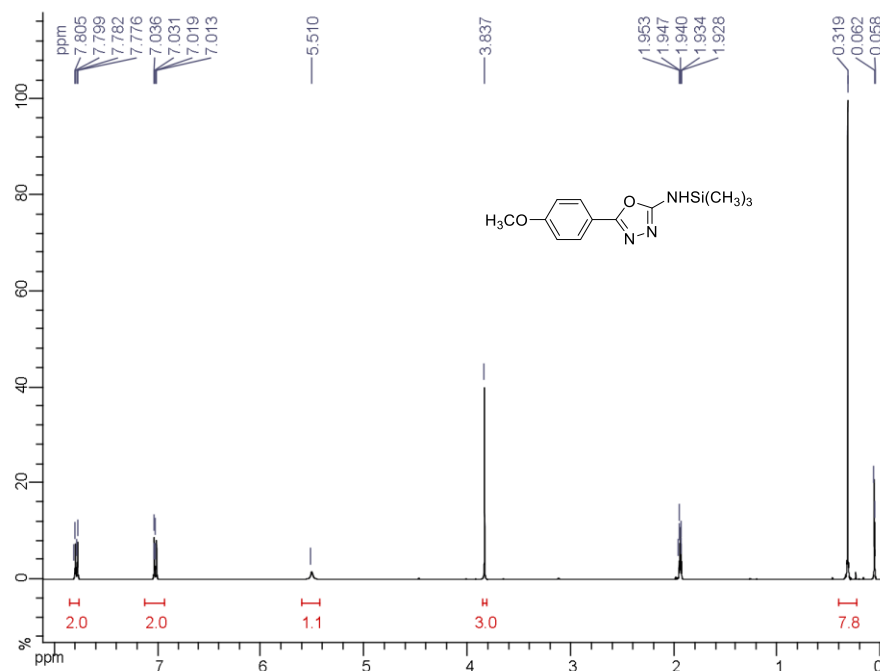
N-(Trimethylsilyl)quinolin-6-amine (2.40.2)



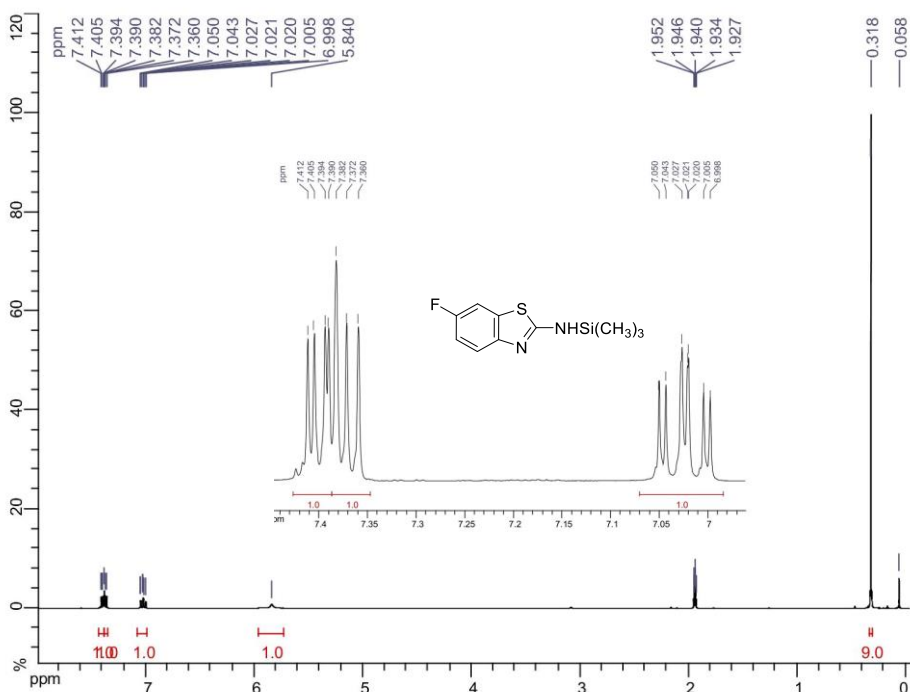
N-(Trimethylsilyl)quinolin-3-amine (2.40.5)



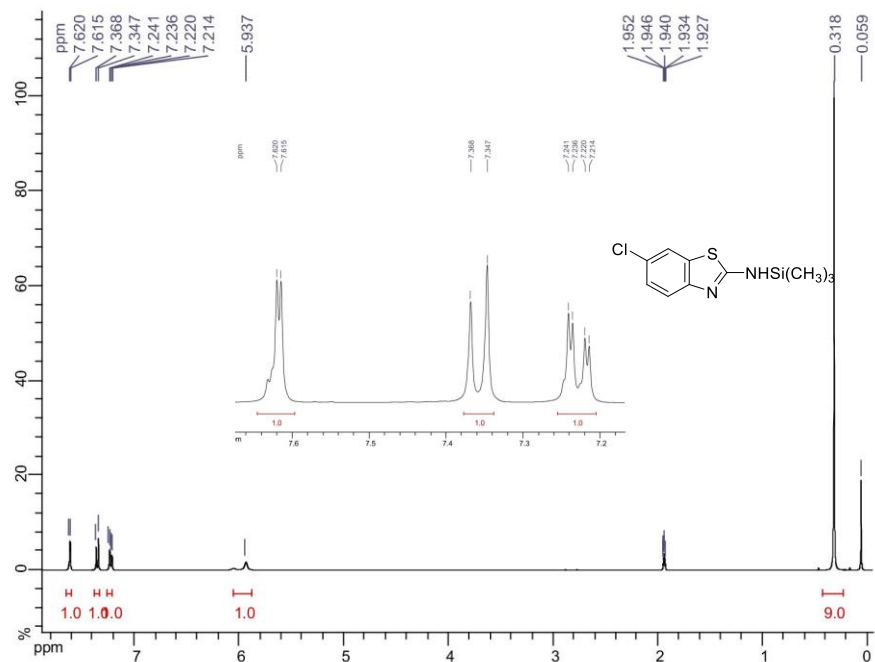
5-(4-Methoxyphenyl)-*N*-(trimethylsilyl)-1,3,4-oxadiazol-2-amine (2.40.8)



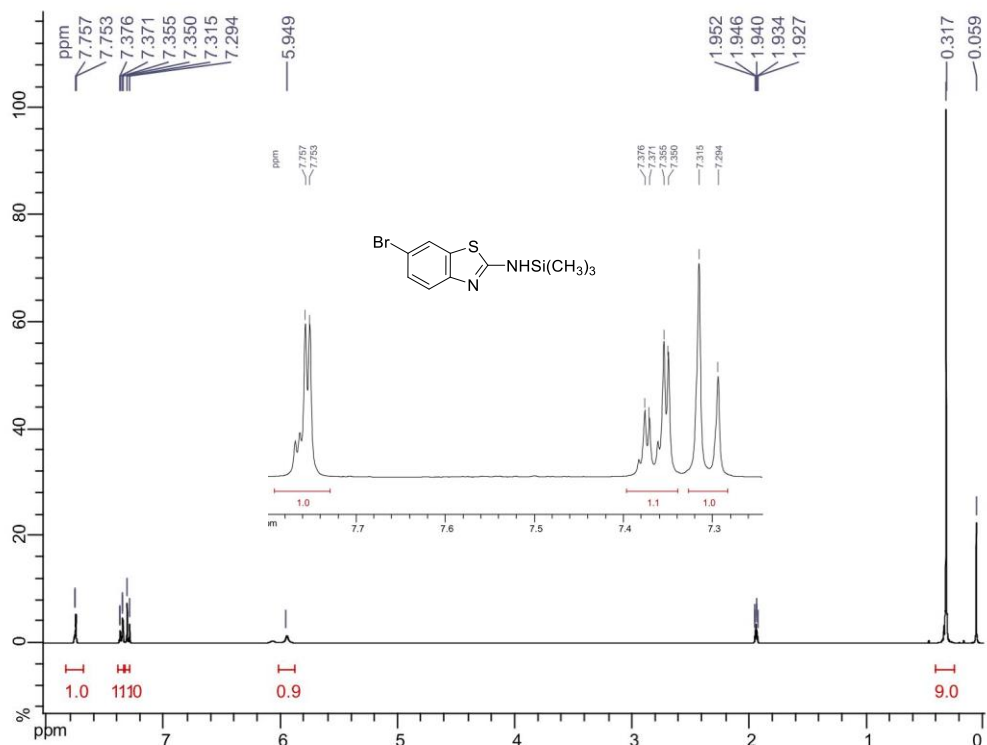
6-Fluoro-*N*-(trimethylsilyl)benzo[*d*]thiazol-2-amine (2.40.10)



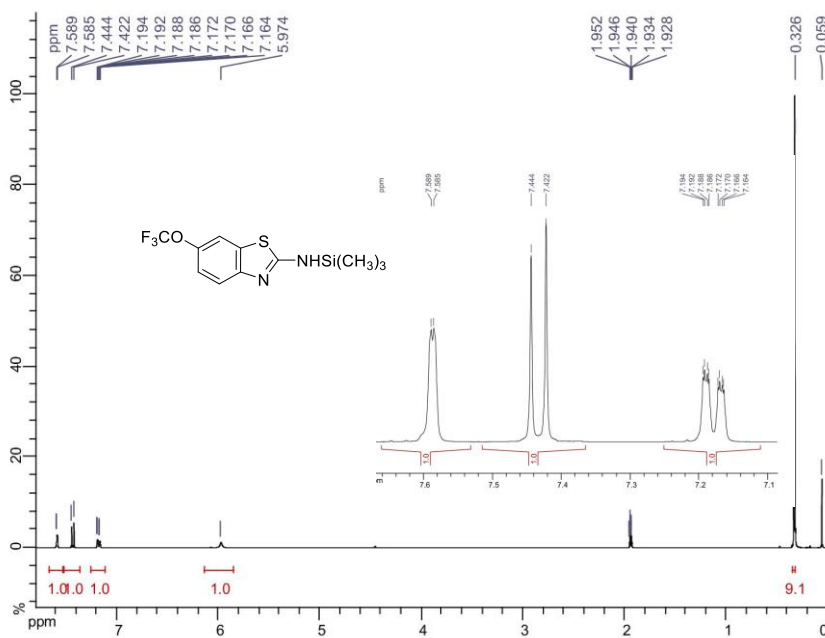
6-Chloro-*N*-(trimethylsilyl)benzo[*d*]thiazol-2-amine (2.40.12)



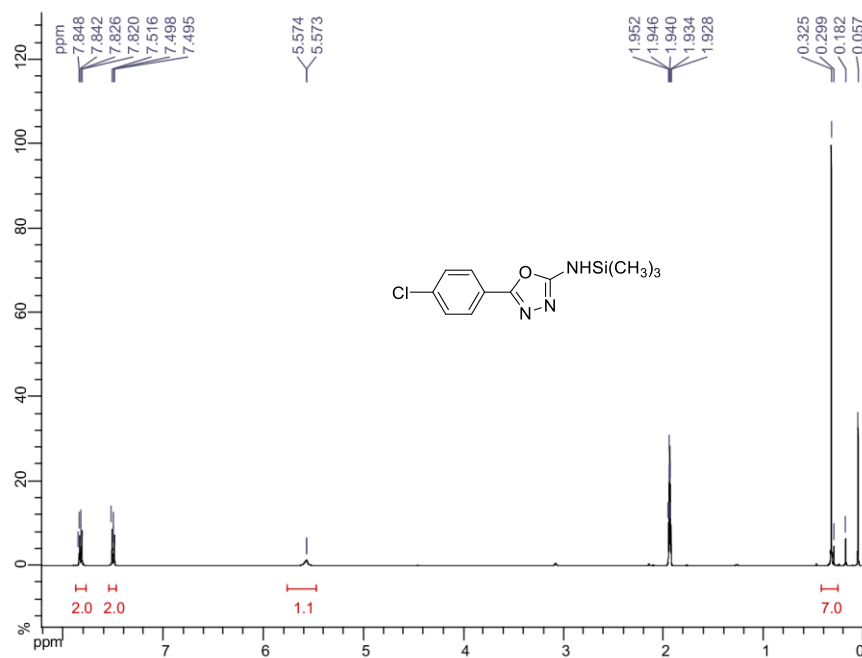
6-Bromo-*N*-(trimethylsilyl)benzo[*d*]thiazol-2-amine (2.40.13)



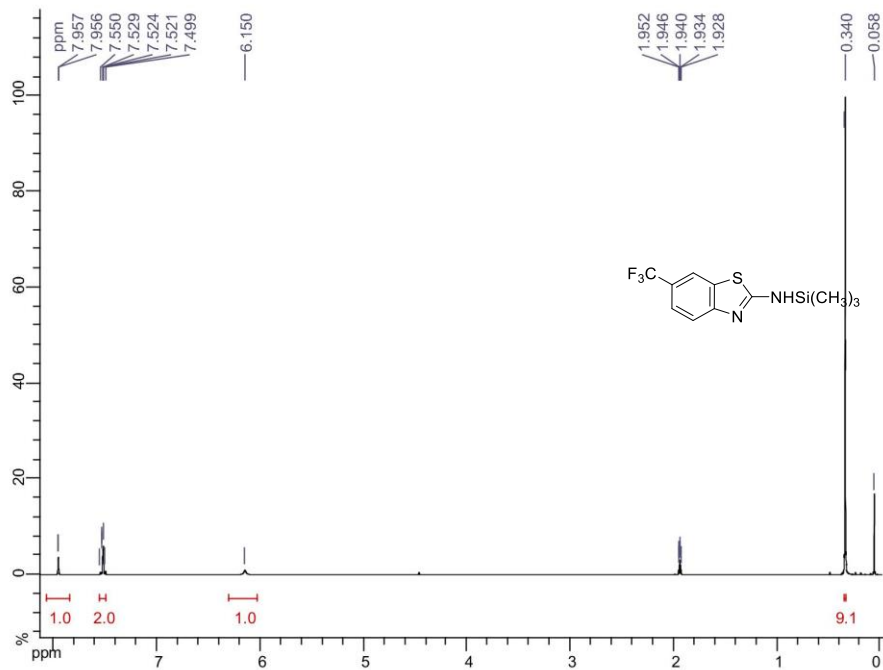
6-(Trifluoromethoxy)-*N*-(trimethylsilyl)benzo[*d*]thiazol-2-amine (2.40.15)



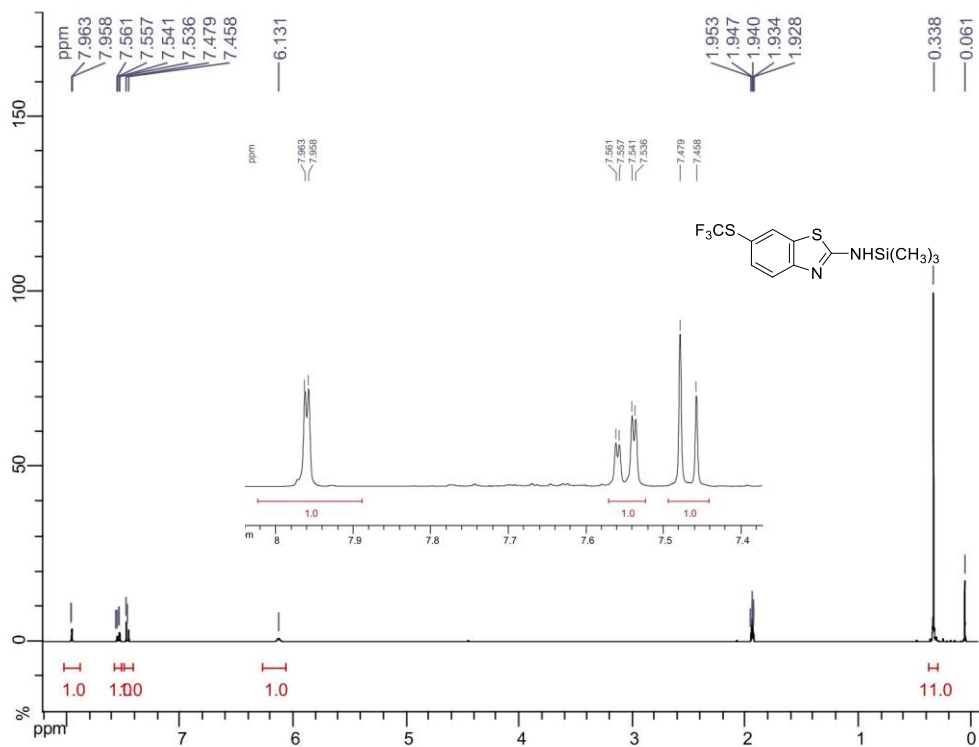
5-(4-Chlorophenyl)-*N*-(trimethylsilyl)-1,3,4-oxadiazol-2-amine (2.40.16)



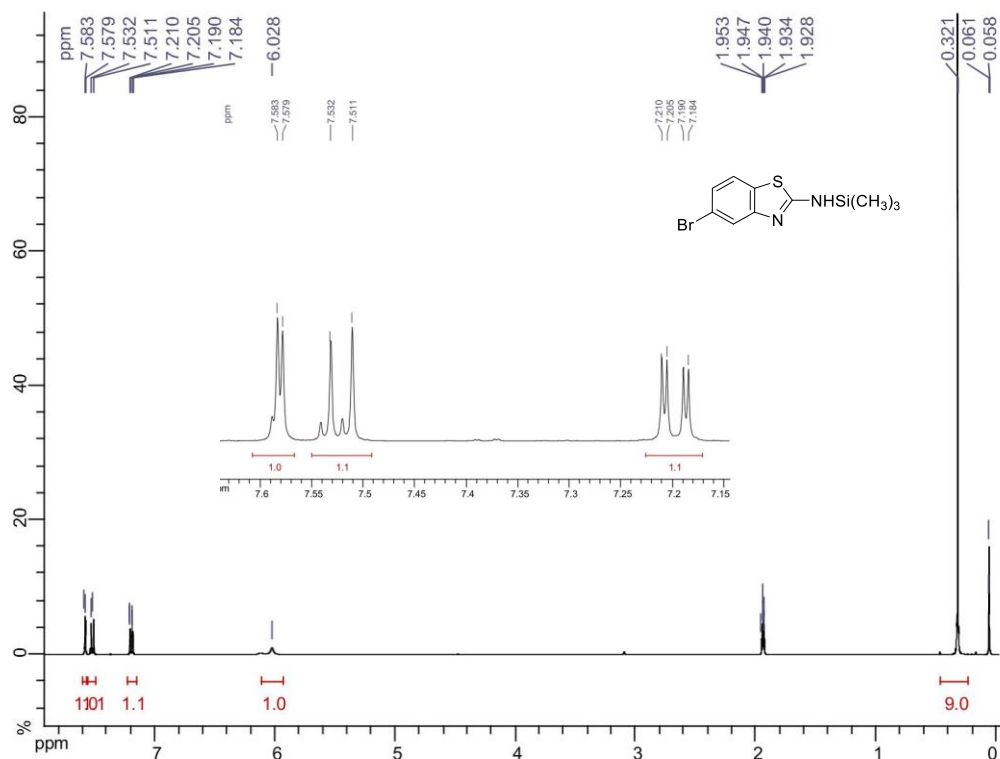
6-(Trifluoromethyl)-*N*-(trimethylsilyl)benzo[*d*]thiazol-2-amine (2.40.17)



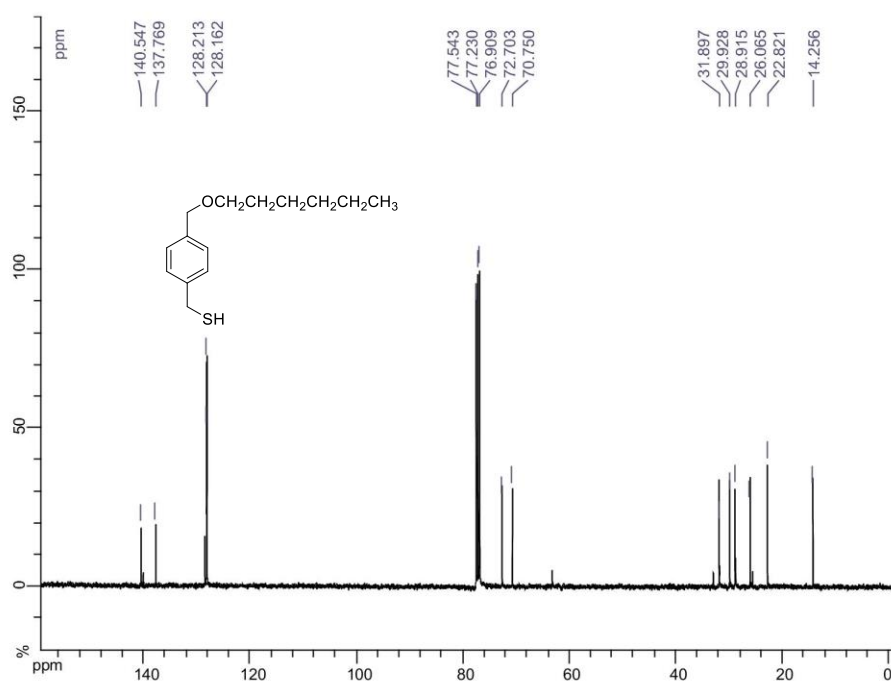
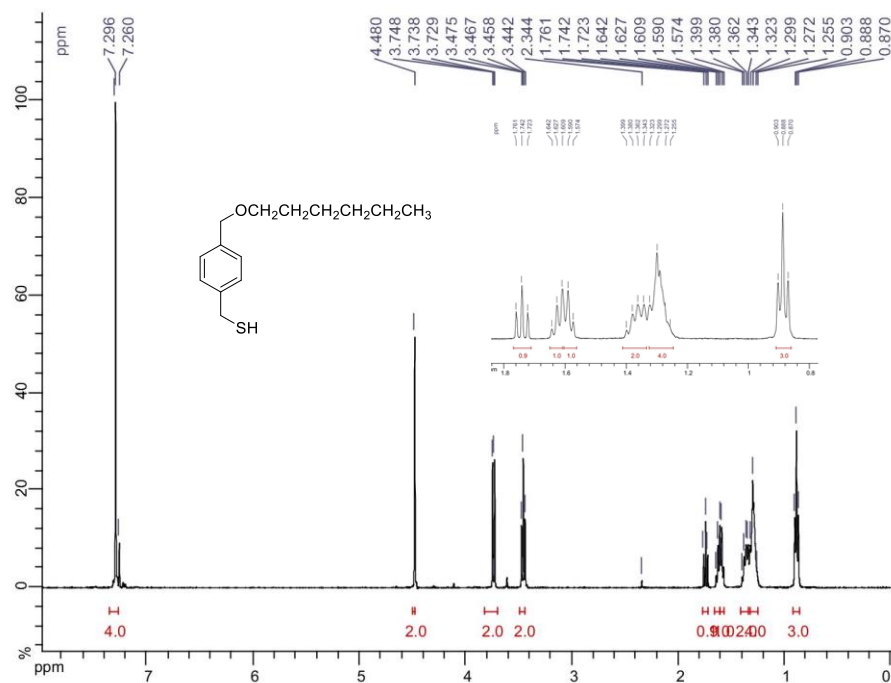
6-((Trifluoromethyl)thio)-*N*-(trimethylsilyl)benzo[*d*]thiazol-2-amine (2.40.18)



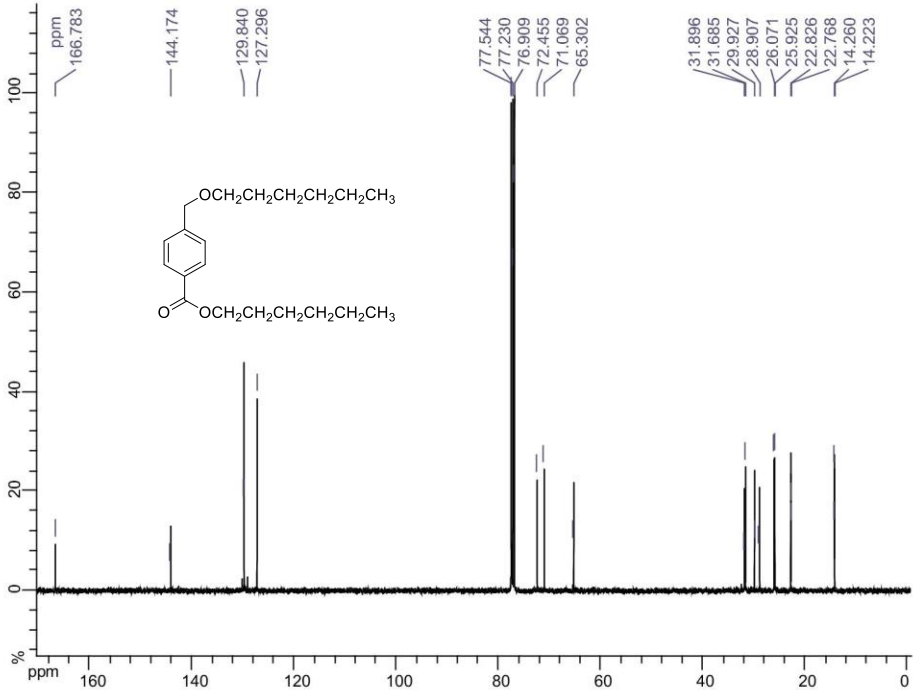
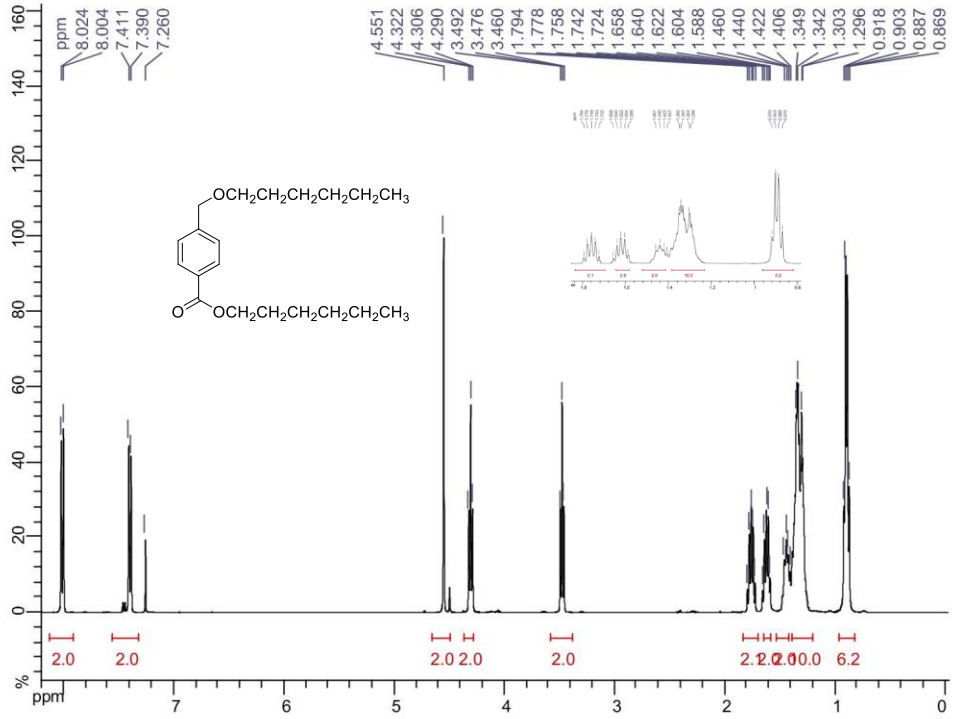
5-Bromo-N-(trimethylsilyl)benzo[d]thiazol-2-amine (2.40.19)



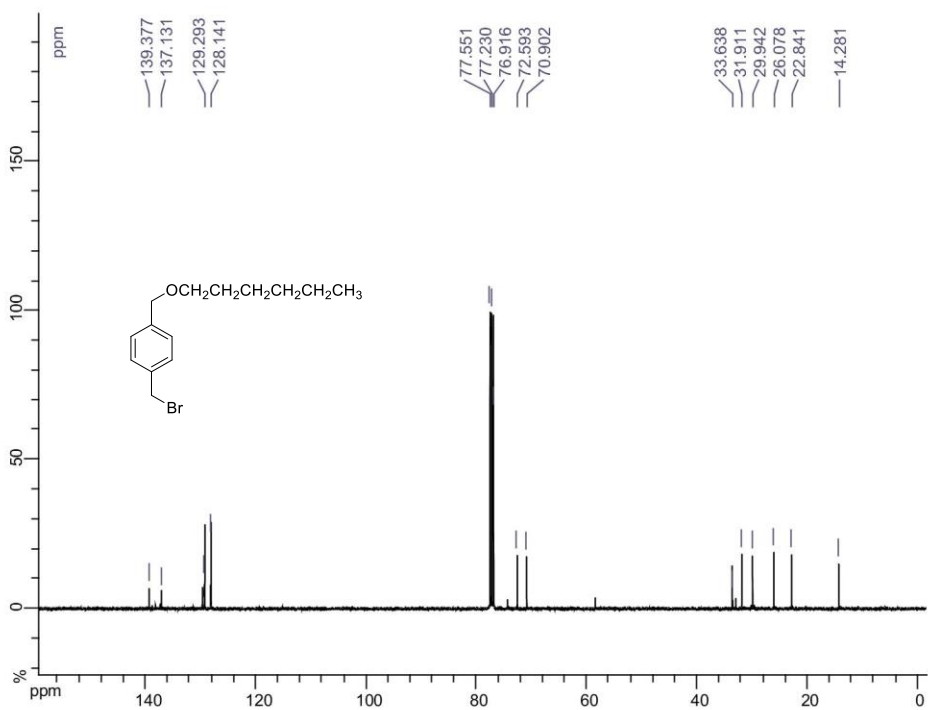
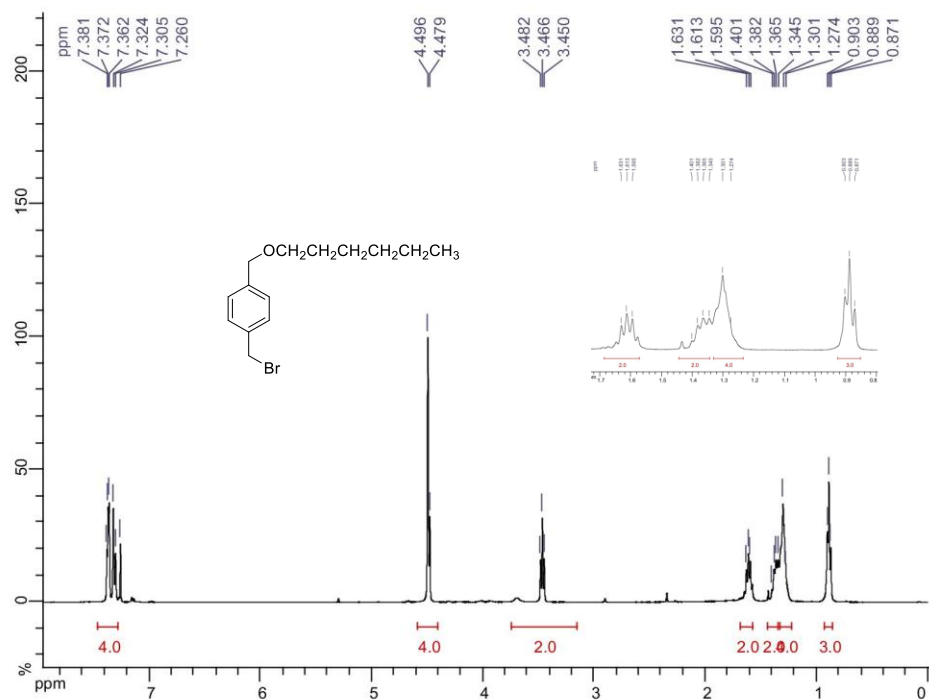
(4-((Hexyloxy)methyl)phenyl)methanethiol (2.41)



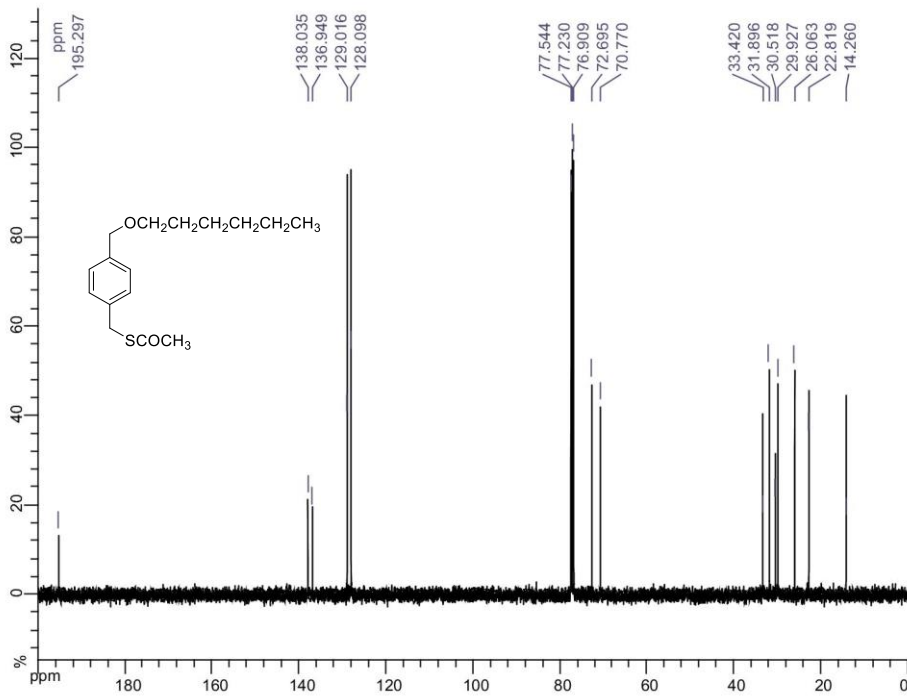
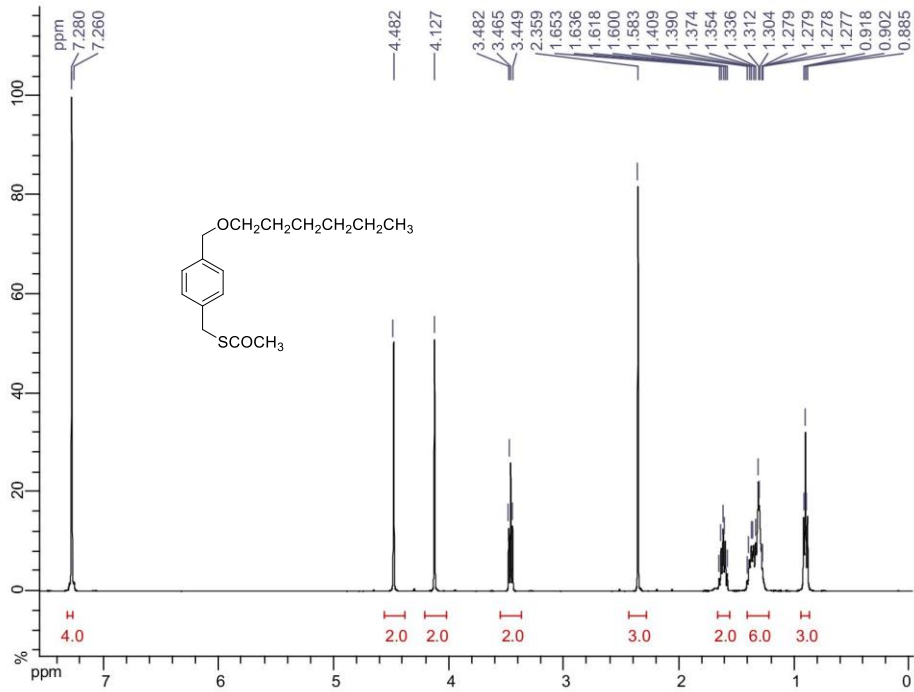
Hexyl 4-((hexyloxy)methyl) benzoate (2.43)



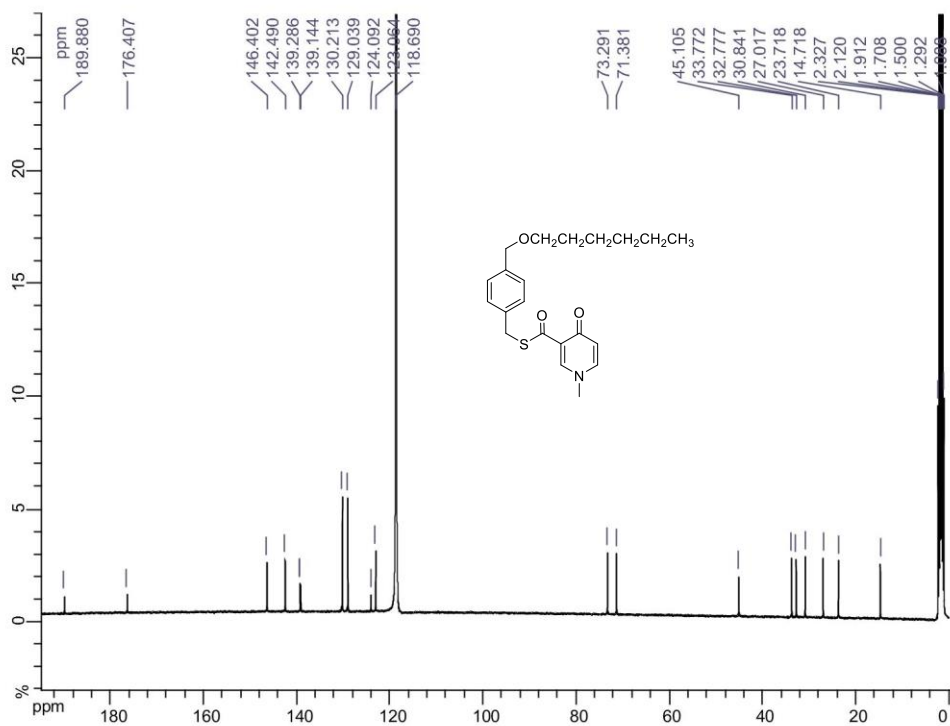
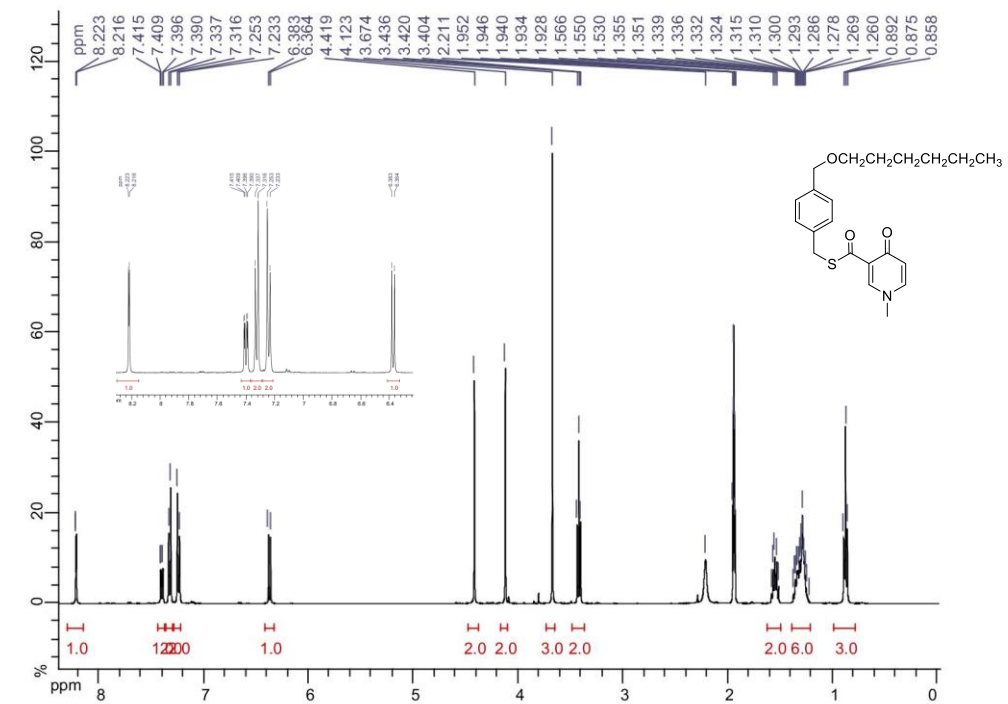
1-(Bromomethyl)-4-((hexyloxy)methyl)phenyl)benzene (2.45)



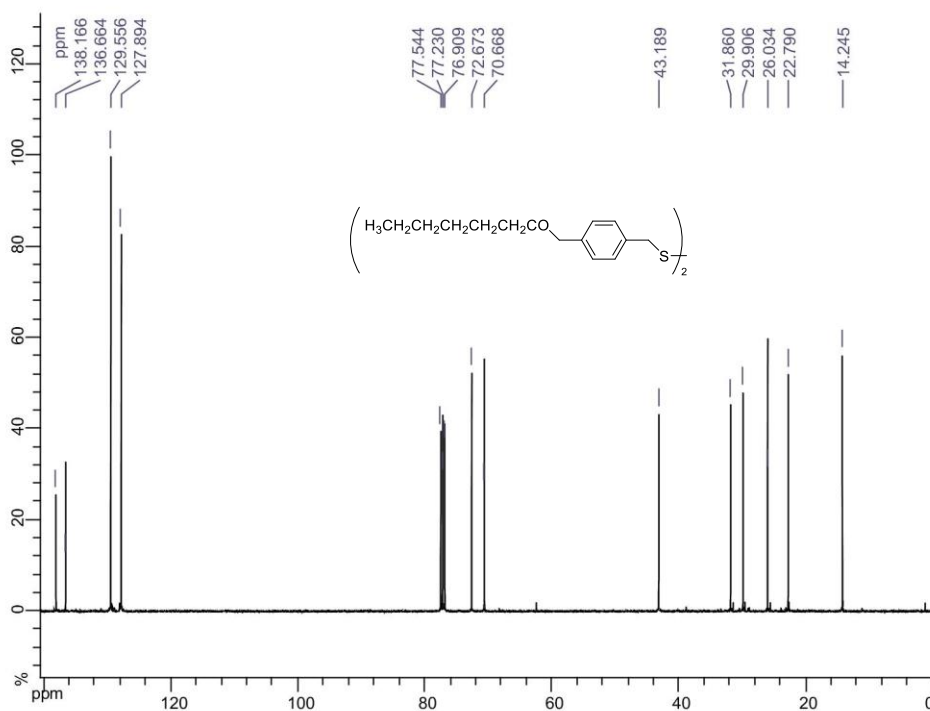
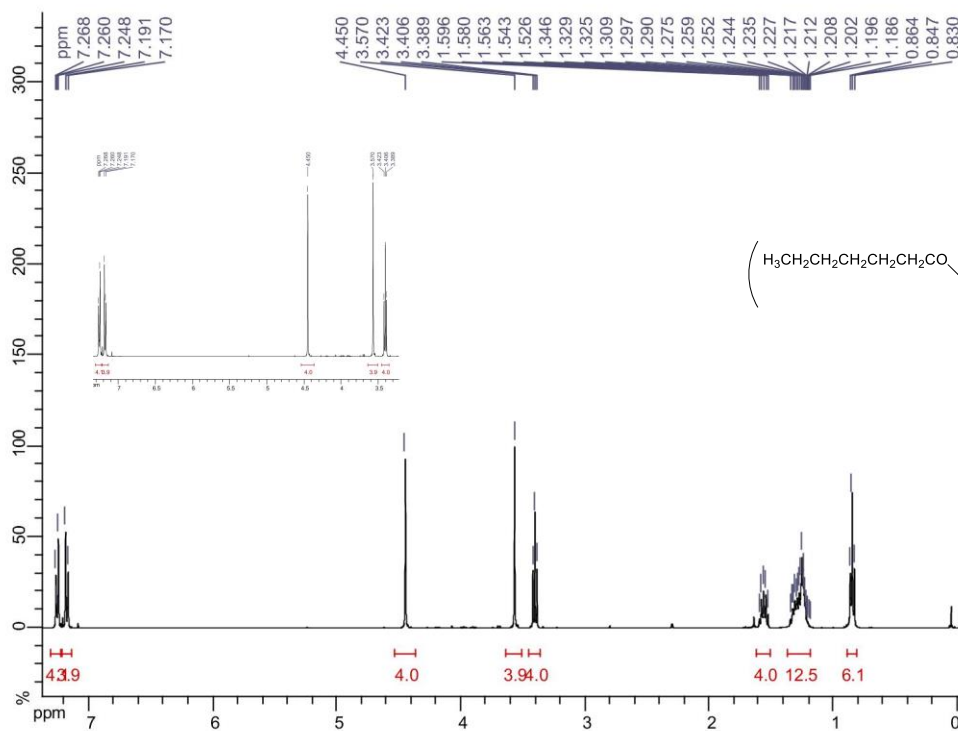
S-(4-((Hexyloxy)methyl)benzyl) ethanethioate (2.46)



S-(4-((Hexyloxy)methyl)benzyl)-1-methyl-4-oxo-1,4-dihydropyridine-3-carbothioate (2.47)



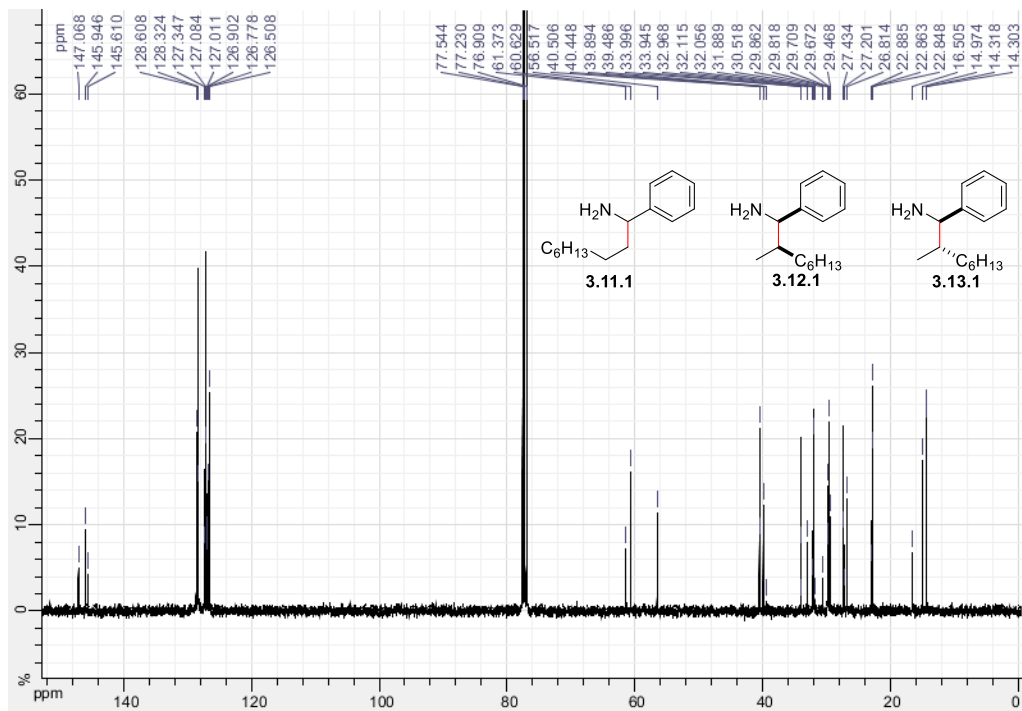
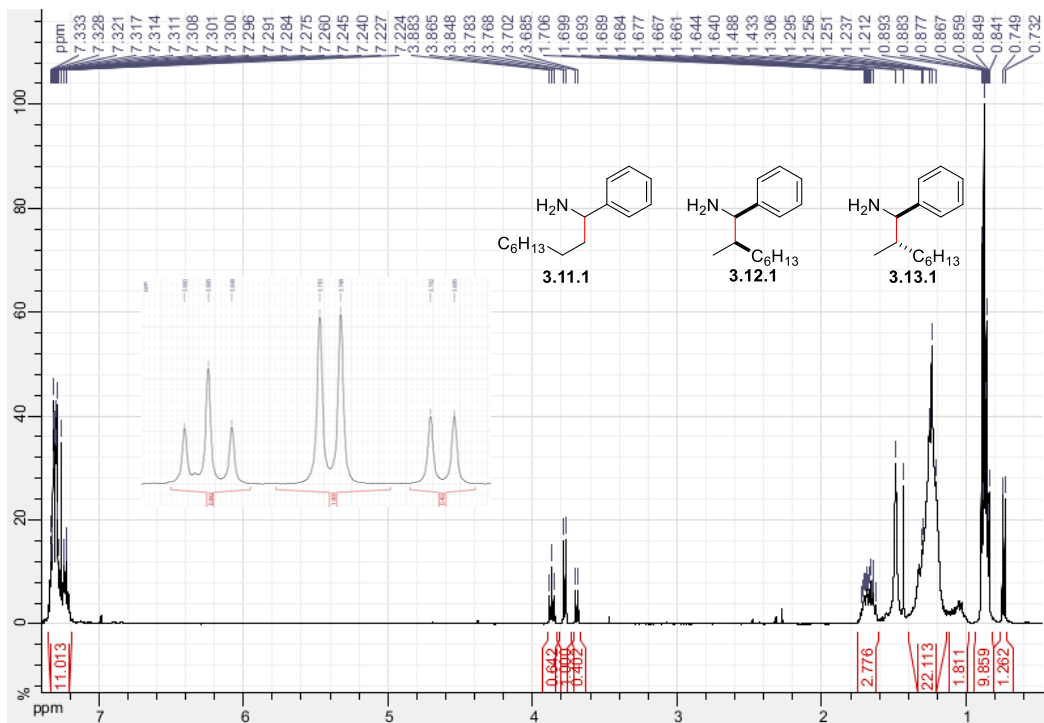
1,2-bis(4-((hexyloxy)methyl)benzyl)disulfane (2.48)



A.3 ^1H , ^{13}C and ^{19}F NMR spectra of compounds in Chapter 3

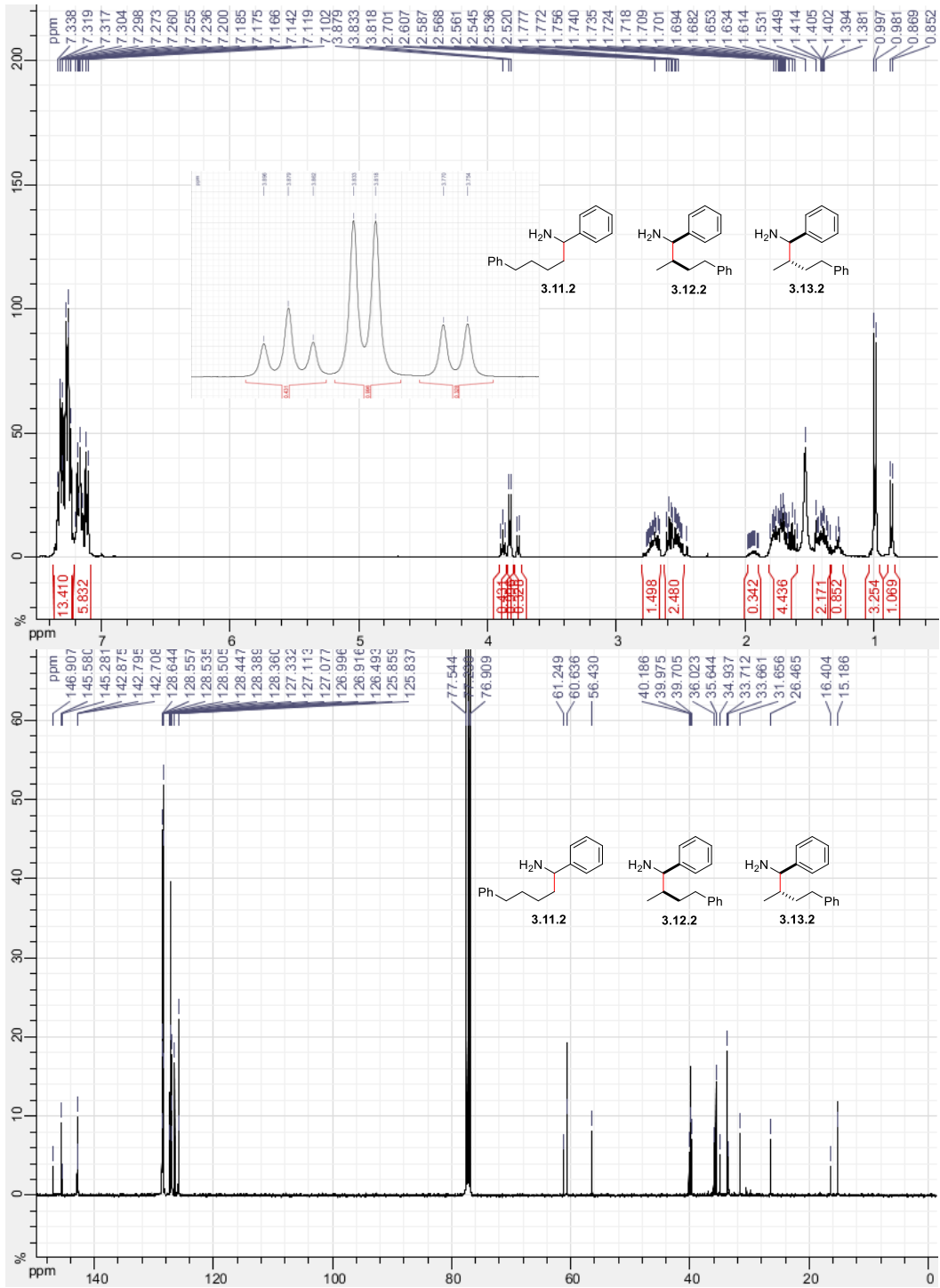
Linear: 1-phenylnonan-1-amine (3.11.1)

Branched: 2-methyl-1-phenyloctan-1-amine (3.12.1 and 3.13.1)



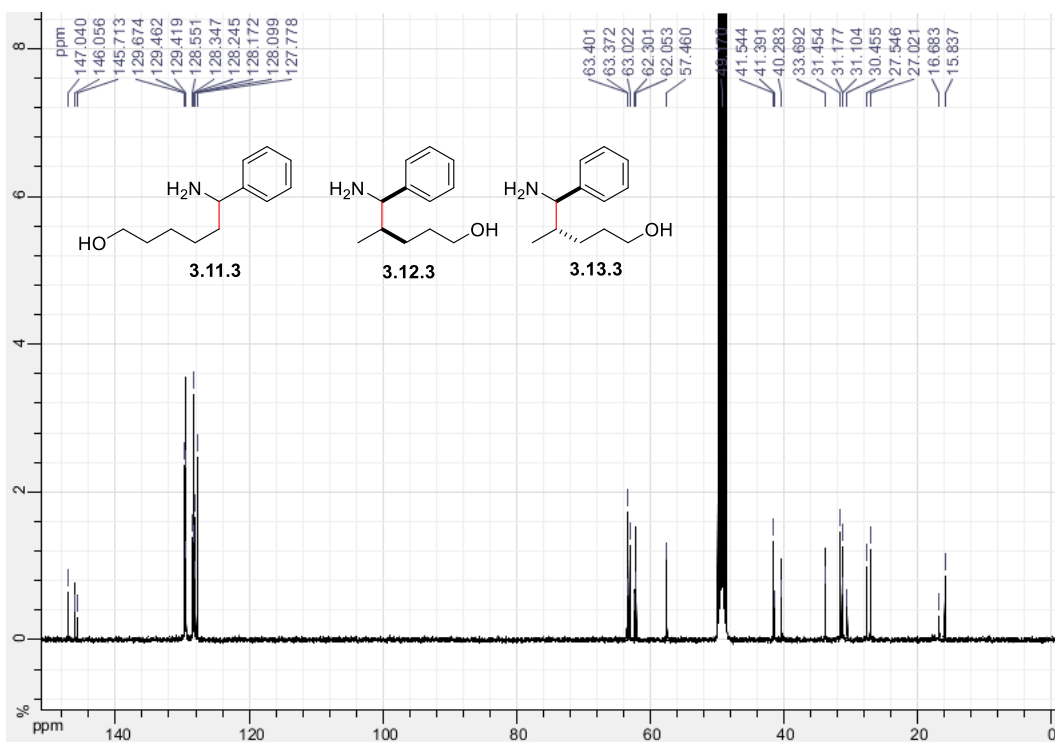
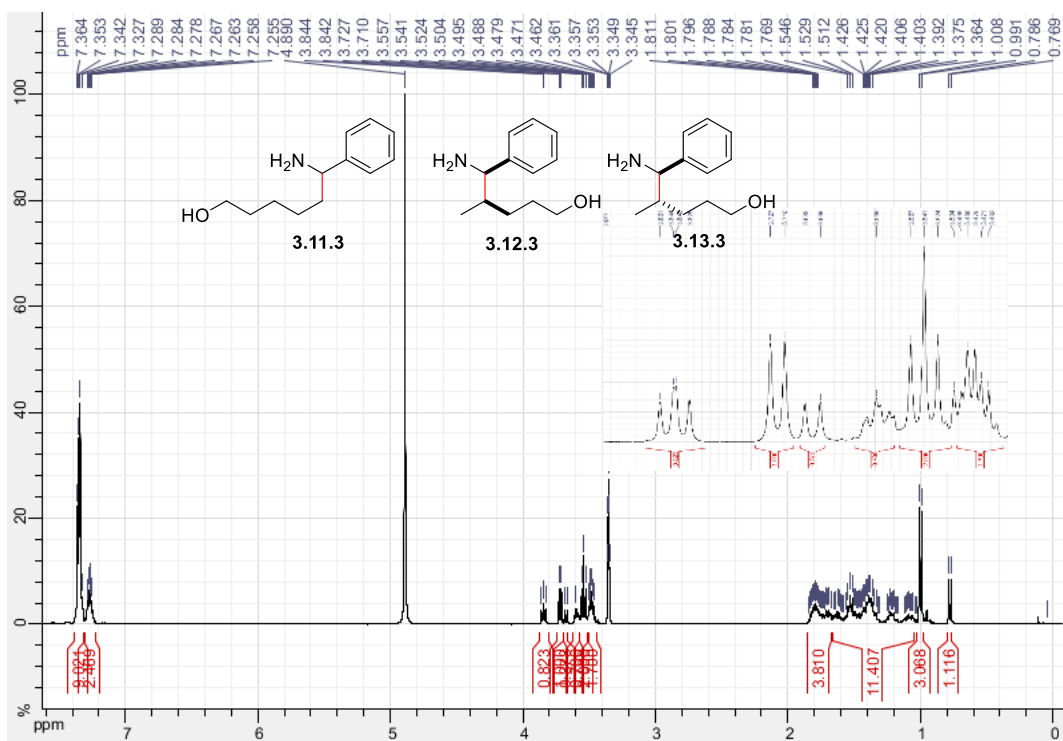
Linear: 1,5-diphenylpentan-1-amine (3.11.2)

Branched: 2-methyl-1,4-diphenylbutan-1-amine (3.12.2 and 3.13.2)



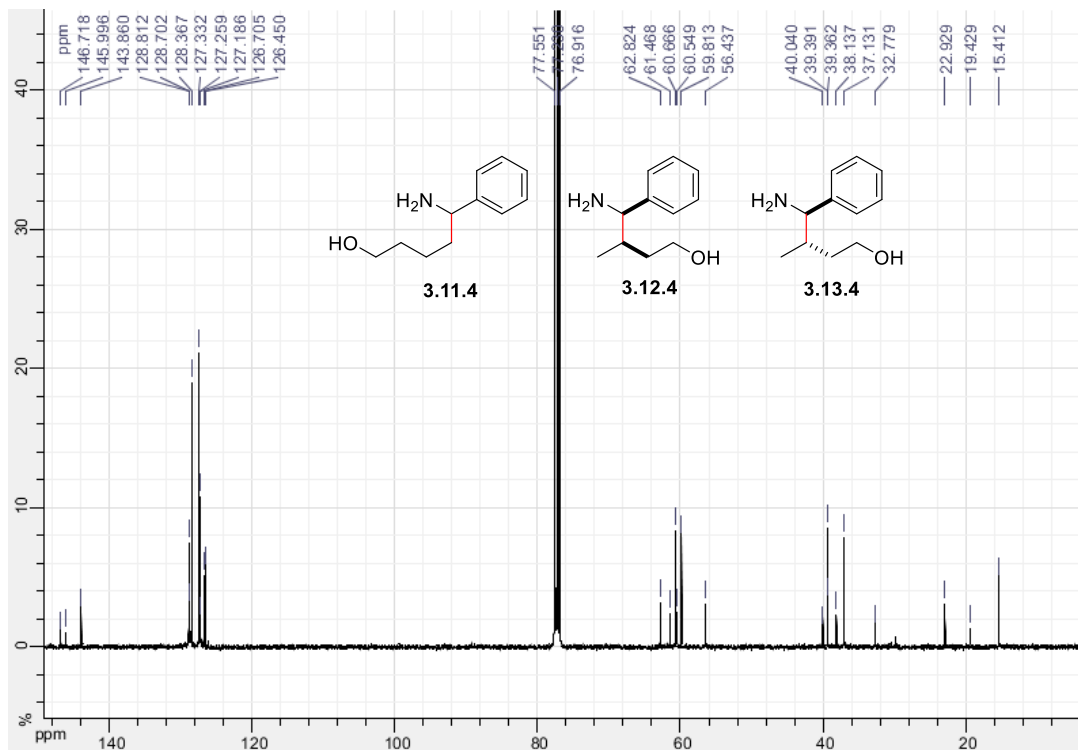
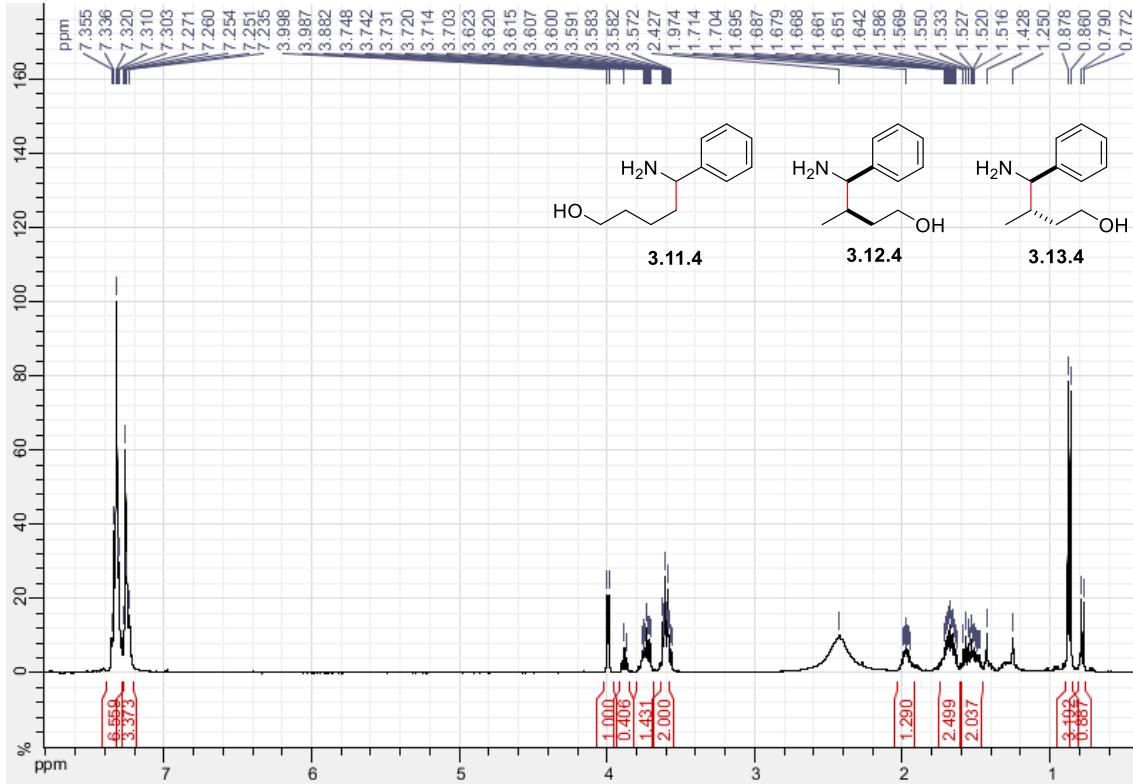
Linear: 5-amino-5-phenylpentan-1-ol (3.11.3)

Branched: 4-amino-3-methyl-4-phenylbutan-1-ol (3.12.3 and 3.13.3)



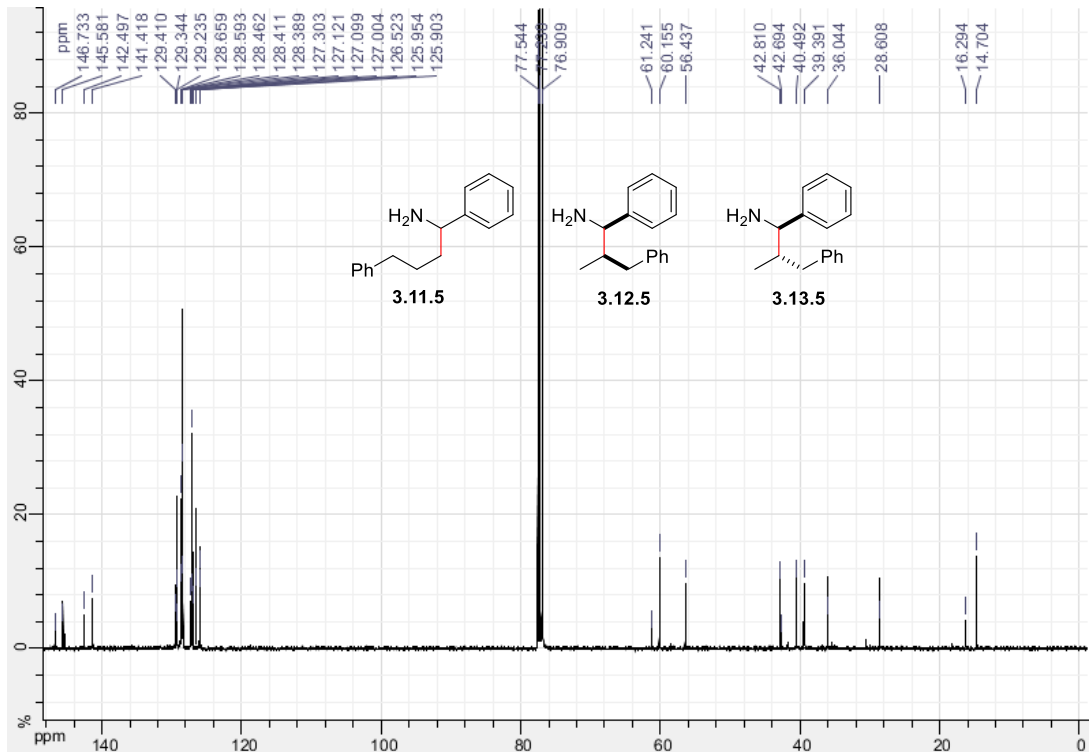
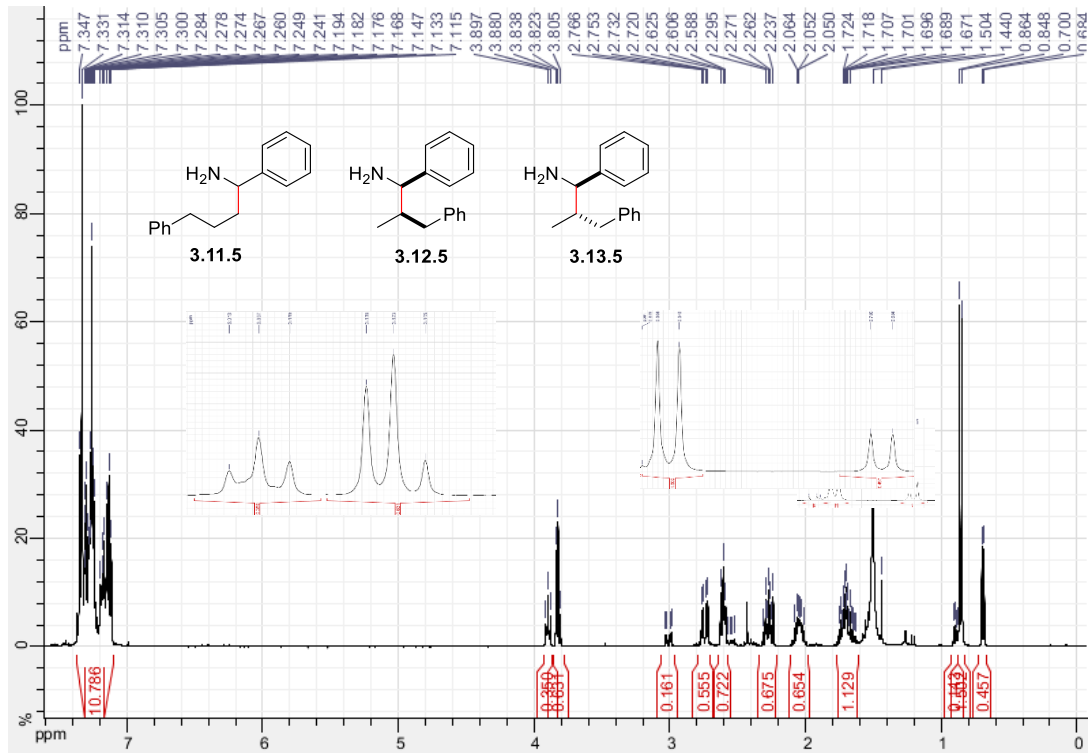
Linear: 4-amino-4-phenylbutan-1-ol (3.11.4)

Branched: 3-amino-2-methyl-3-phenylpropan-1-ol (3.12.4 and 3.13.4)



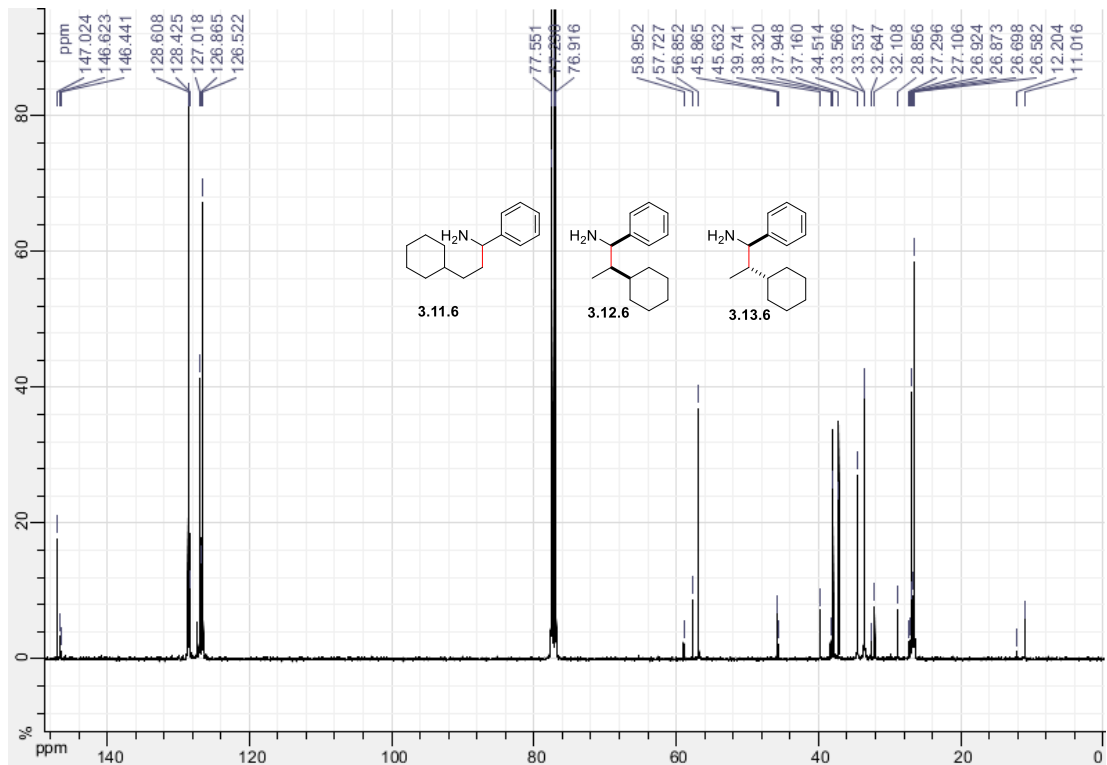
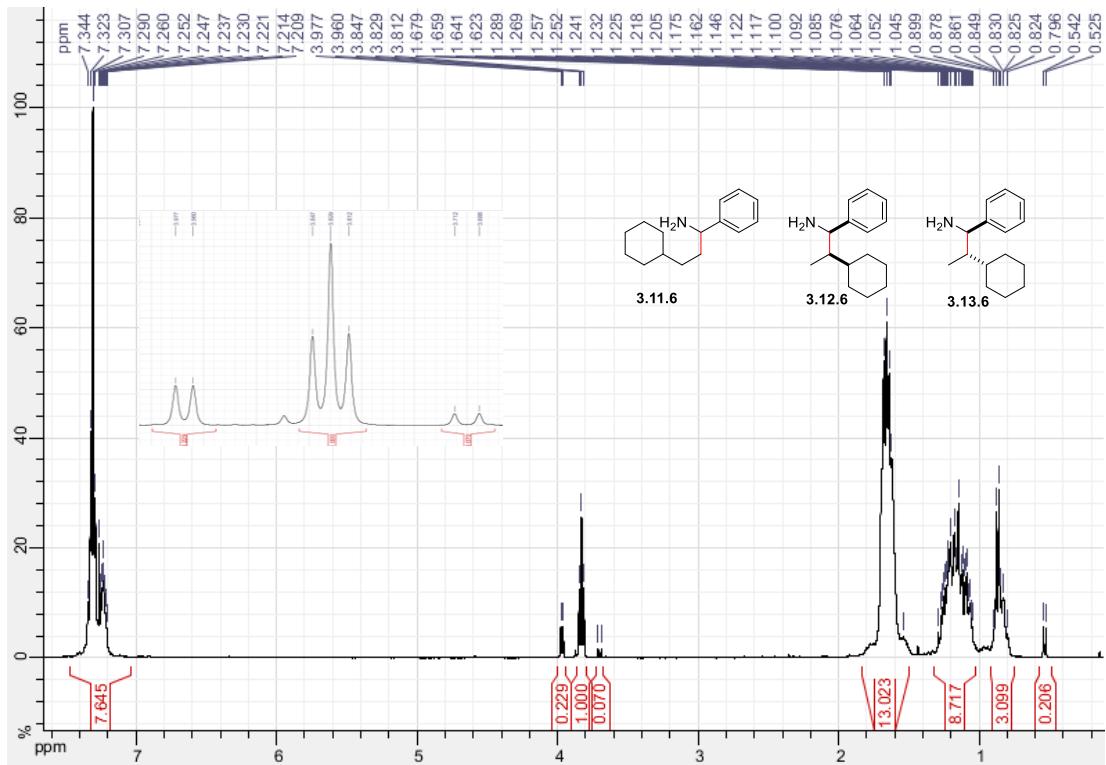
Linear: 1,4-diphenylbutan-1-amine (3.11.5)

Branched: 2-methyl-1,3-diphenylpropan-1-amine (3.12.5 and 3.13.5)



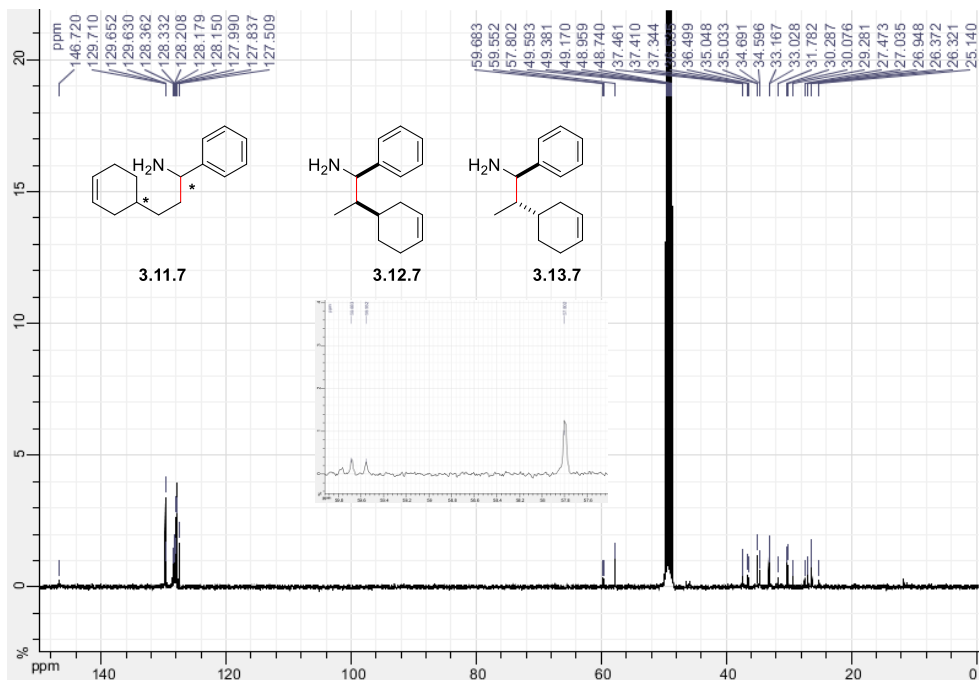
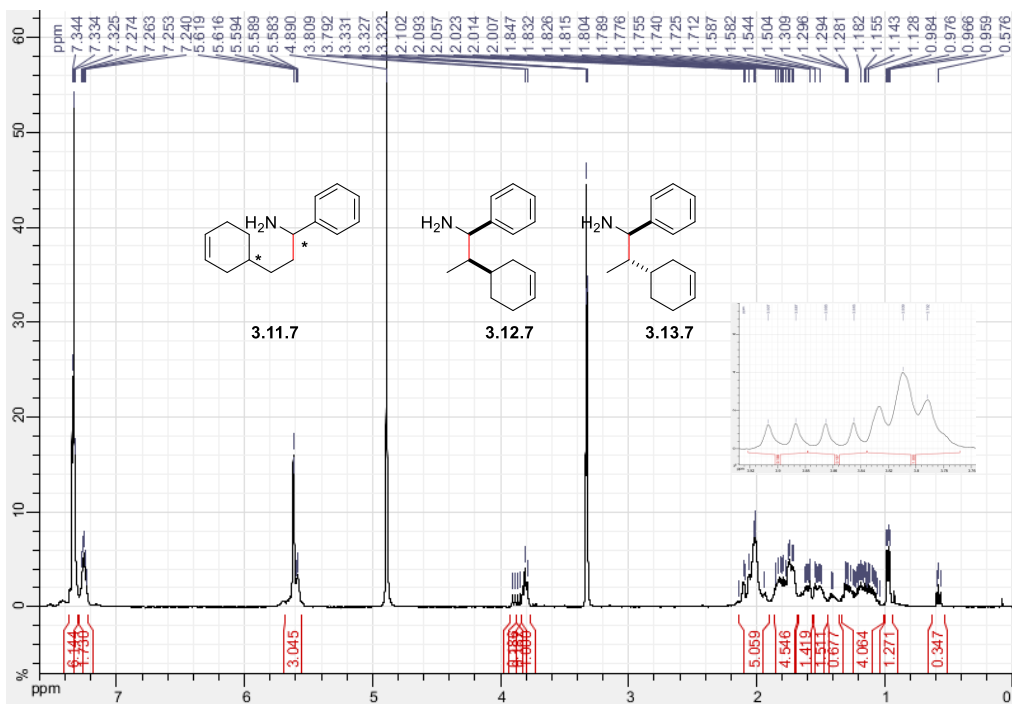
Linear: 3-cyclohexyl-1-phenylpropan-1-amine (3.11.6)

Branched: 2-cyclohexyl-1-phenylpropan-1-amine (3.12.6 and 3.13.6)



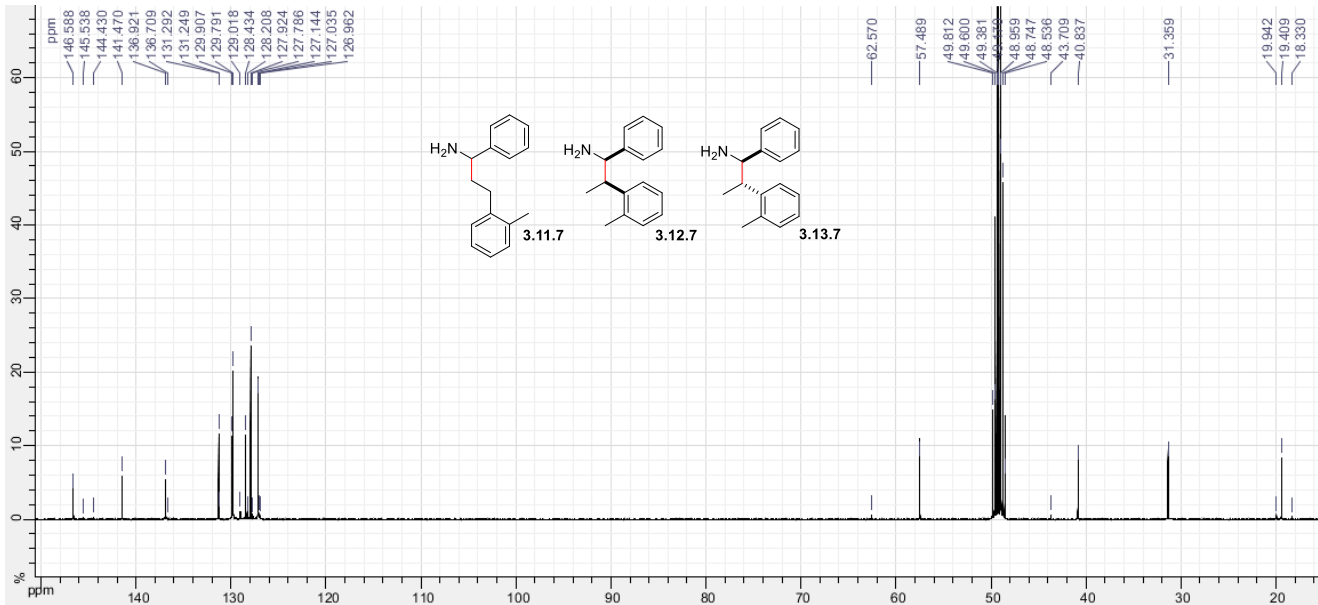
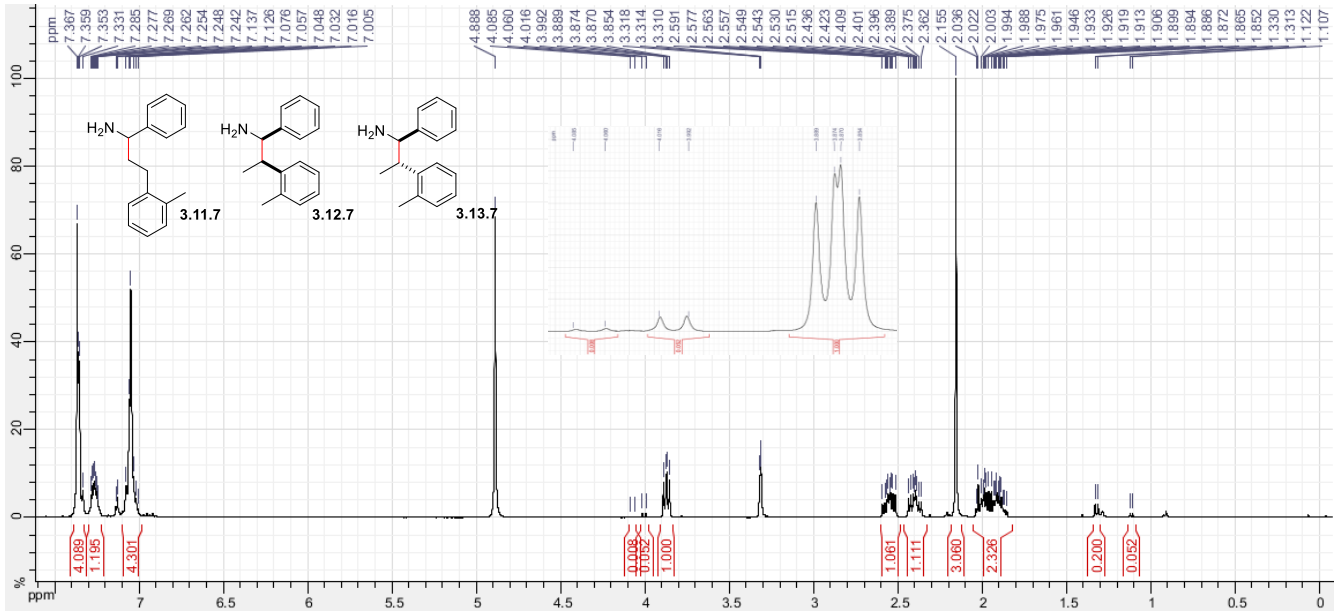
Linear: 3-(cyclohex-3-en-1-yl)-1-phenylpropan-1-amine (3.11.7 and 3.11.7')

Branched: 2-(cyclohex-3-en-1-yl)-1-phenylpropan-1-amine (3.12.7 and 3.13.7)

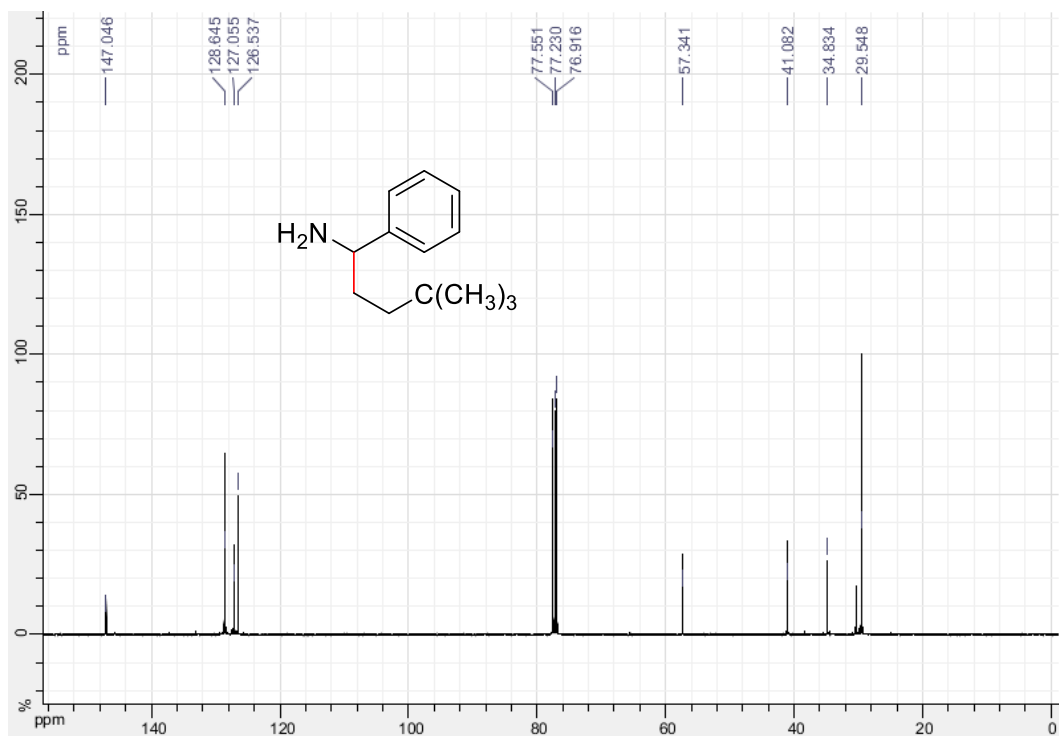
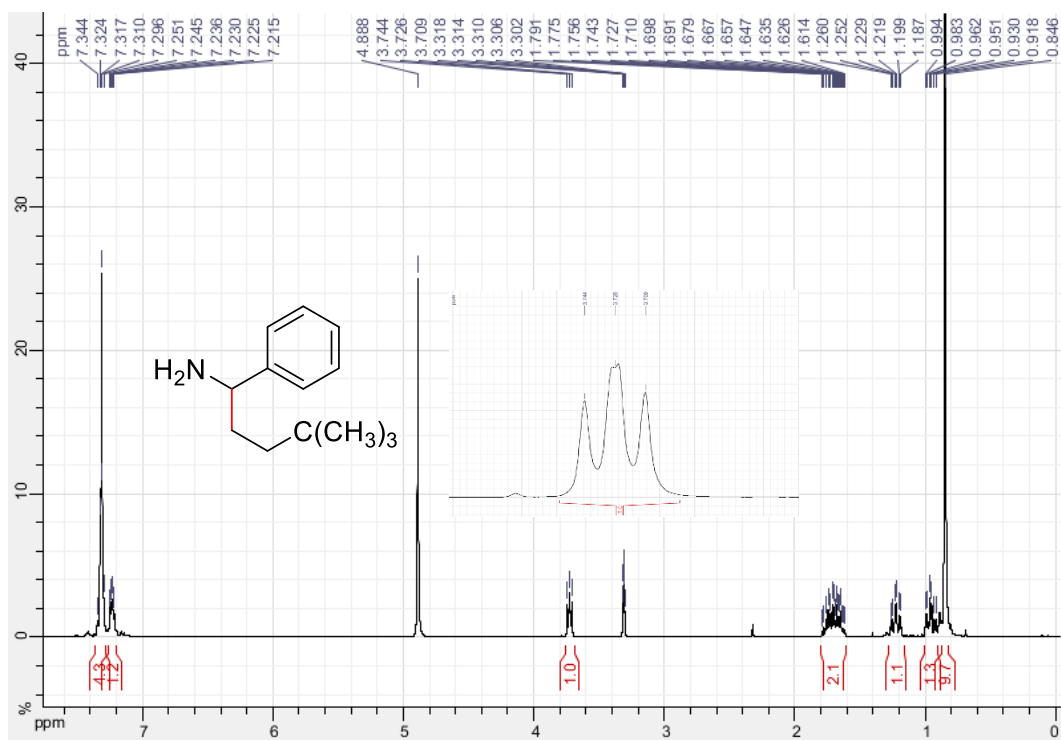


Linear: 1-phenyl-3-(o-tolyl)propan-1-amine (3.11.8)

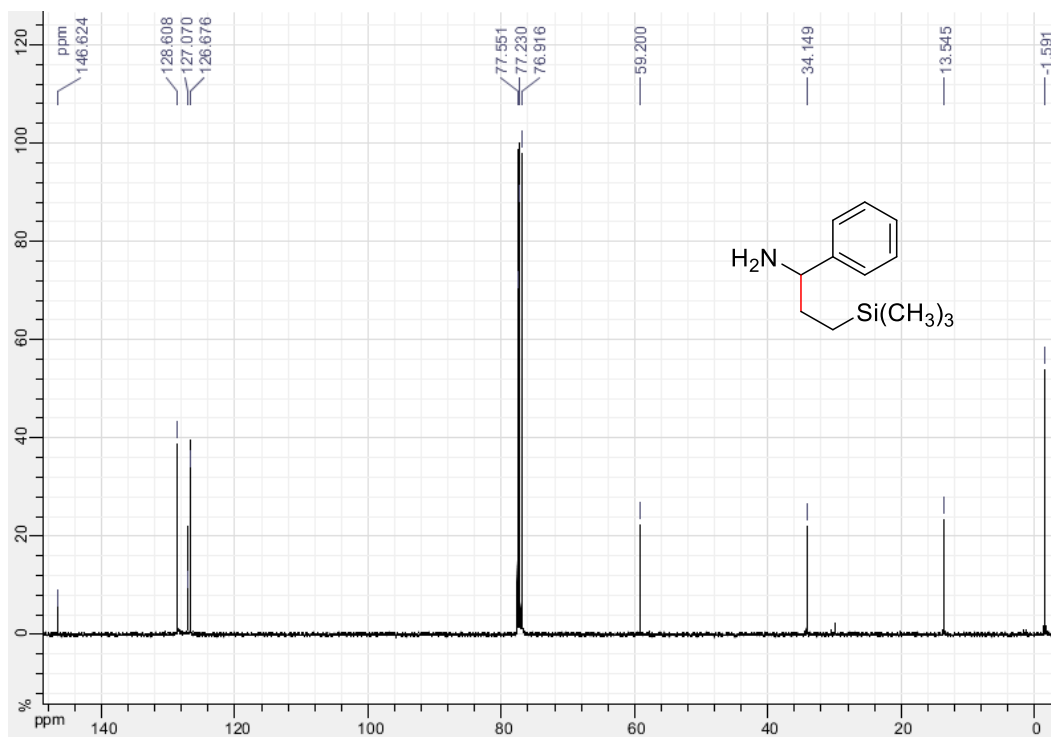
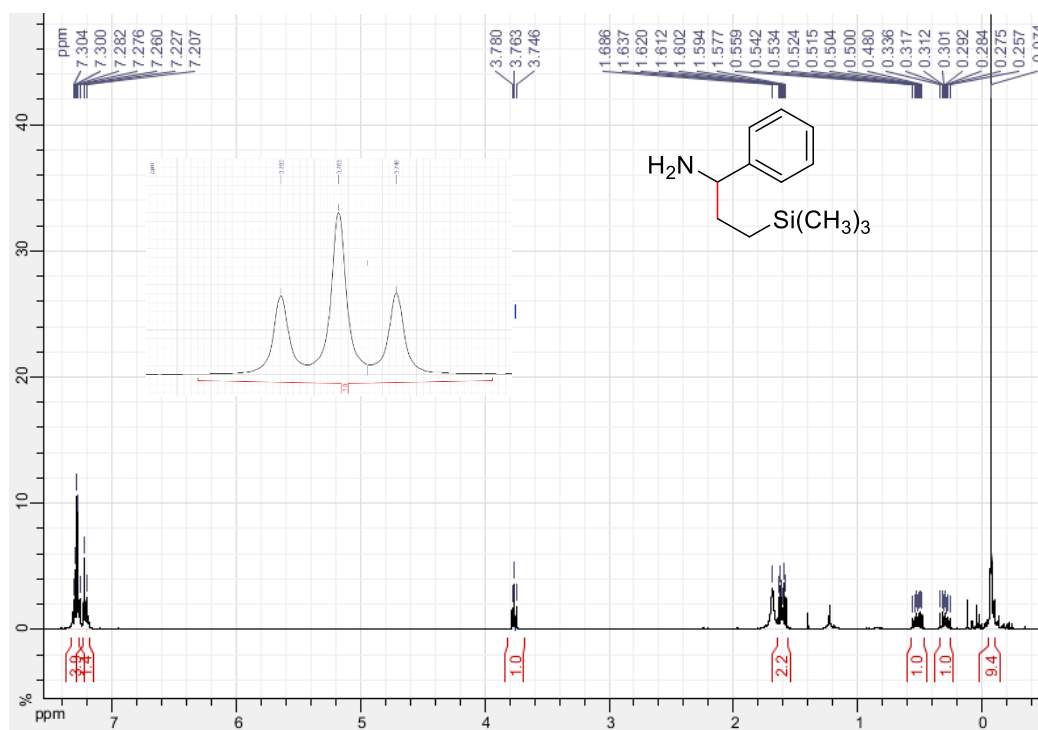
Branched: 1-phenyl-2-(o-tolyl)propan-1-amine (3.12.8 and 3.13.8)



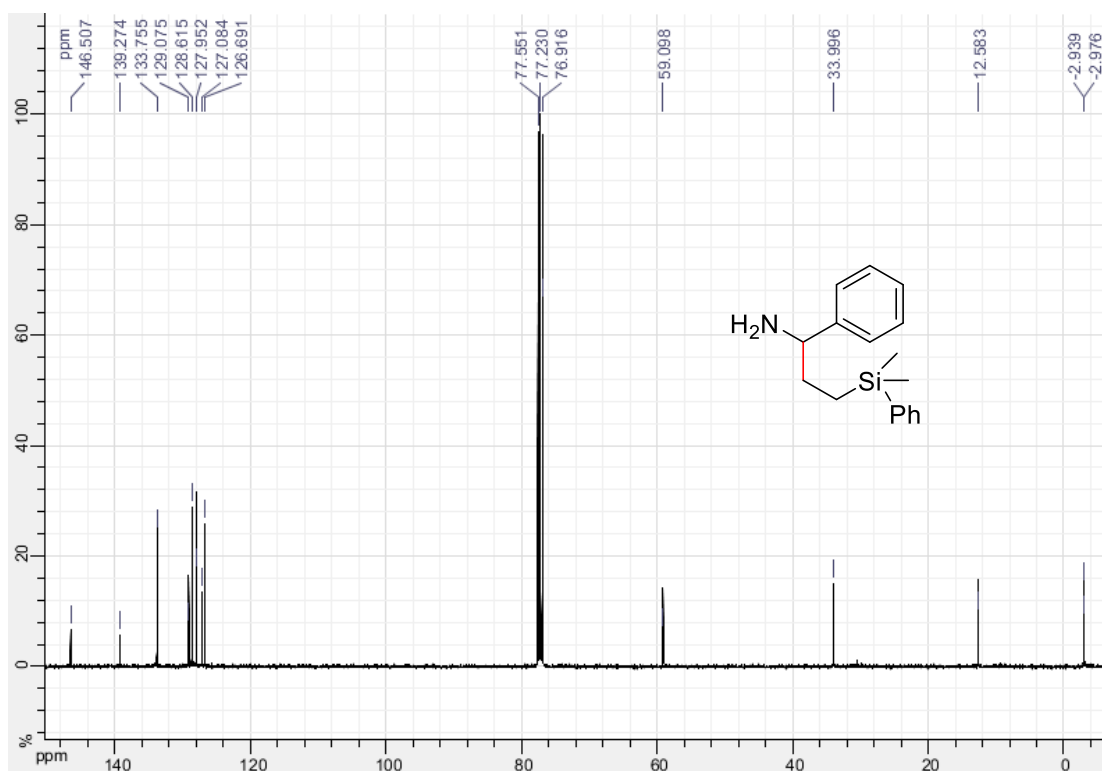
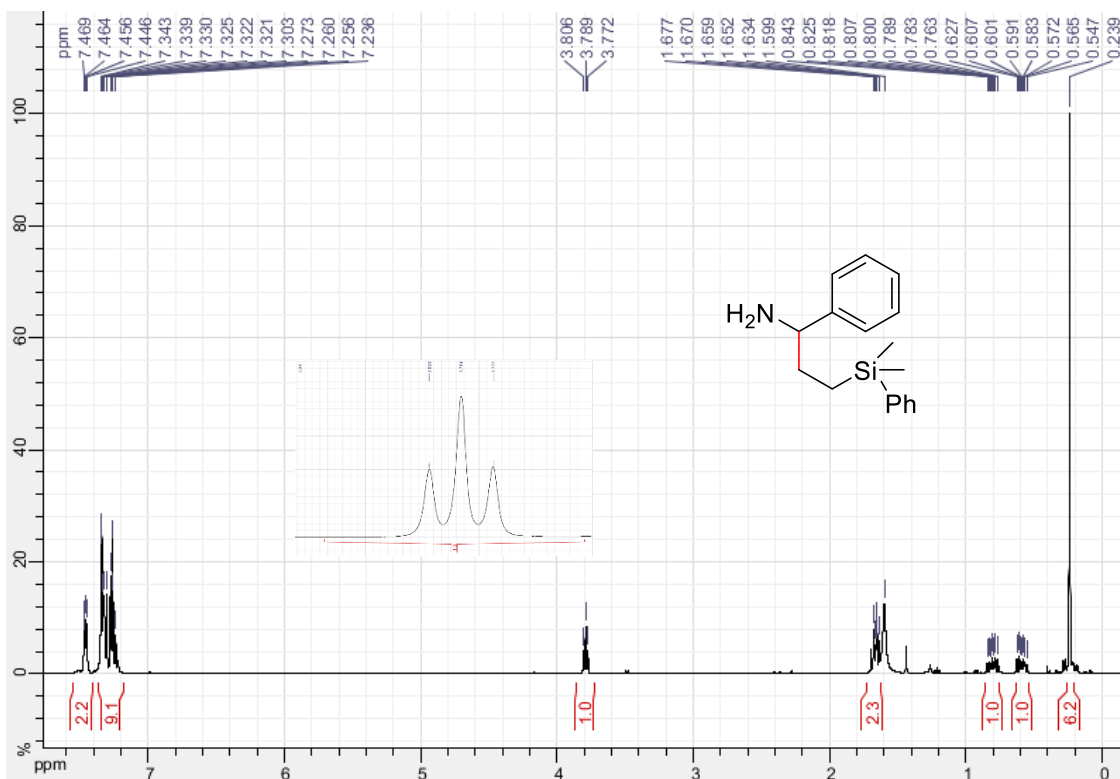
1,4-dimethyl-1-phenylpentan-1-amine (3.11.9)



1-phenyl-3-(trimethylsilyl)propan-1-amine (3.11.10)

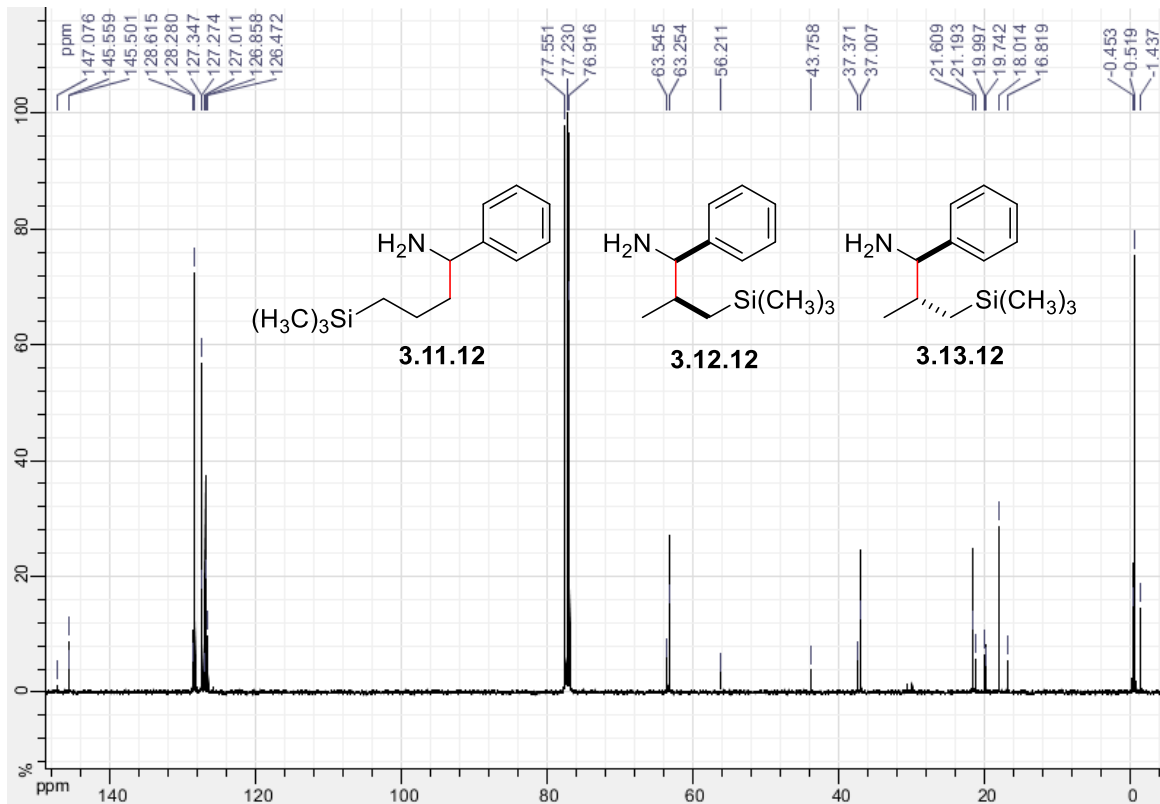
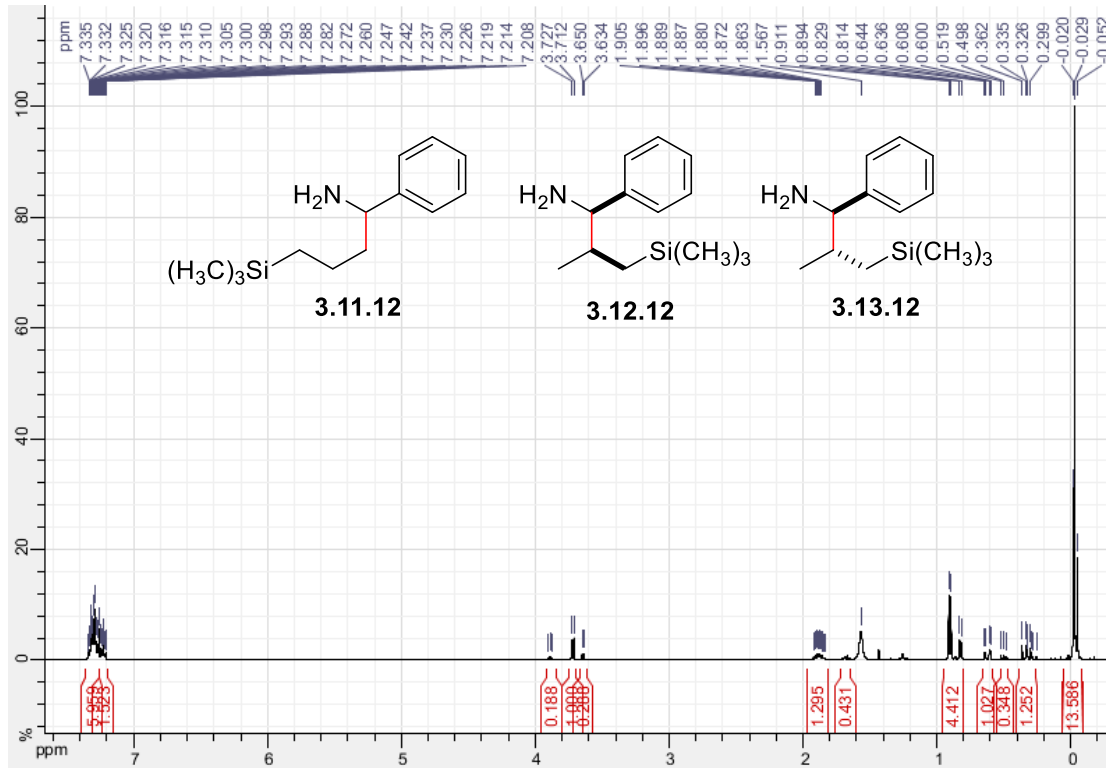


3-(dimethyl(phenyl)silyl)-1-phenylpropan-1-amine (3.11.11)

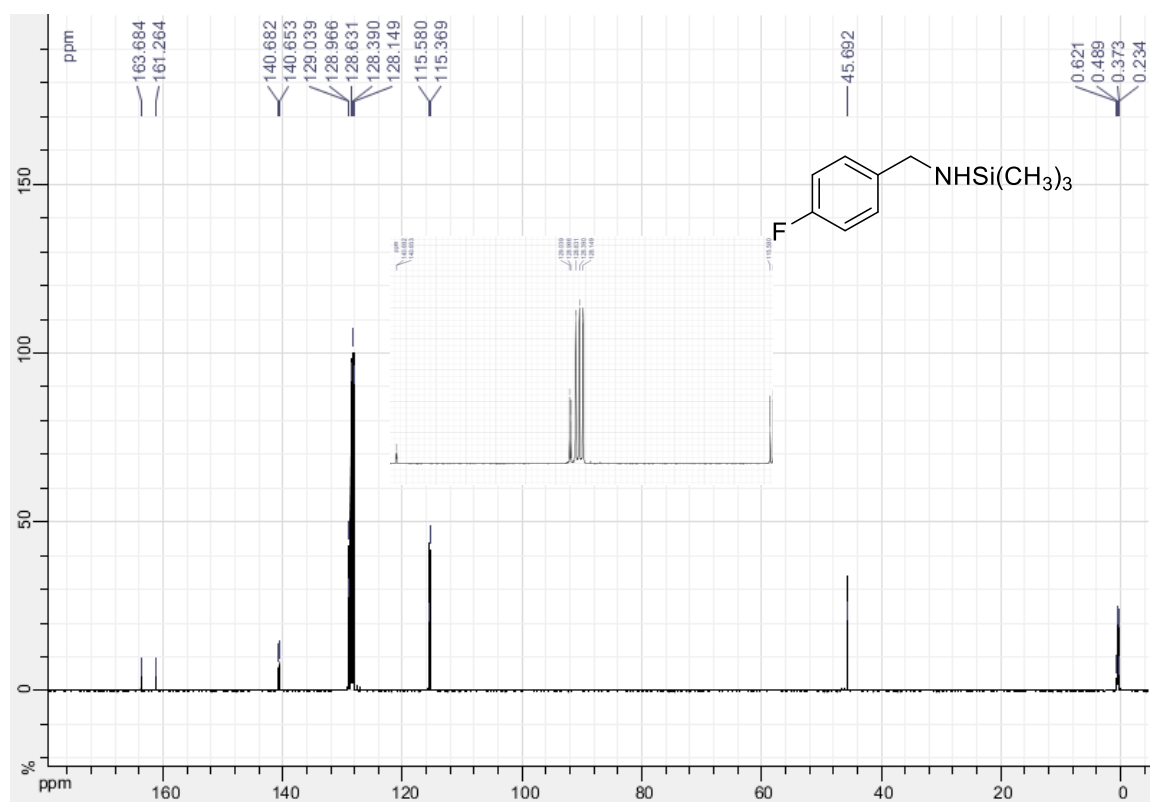
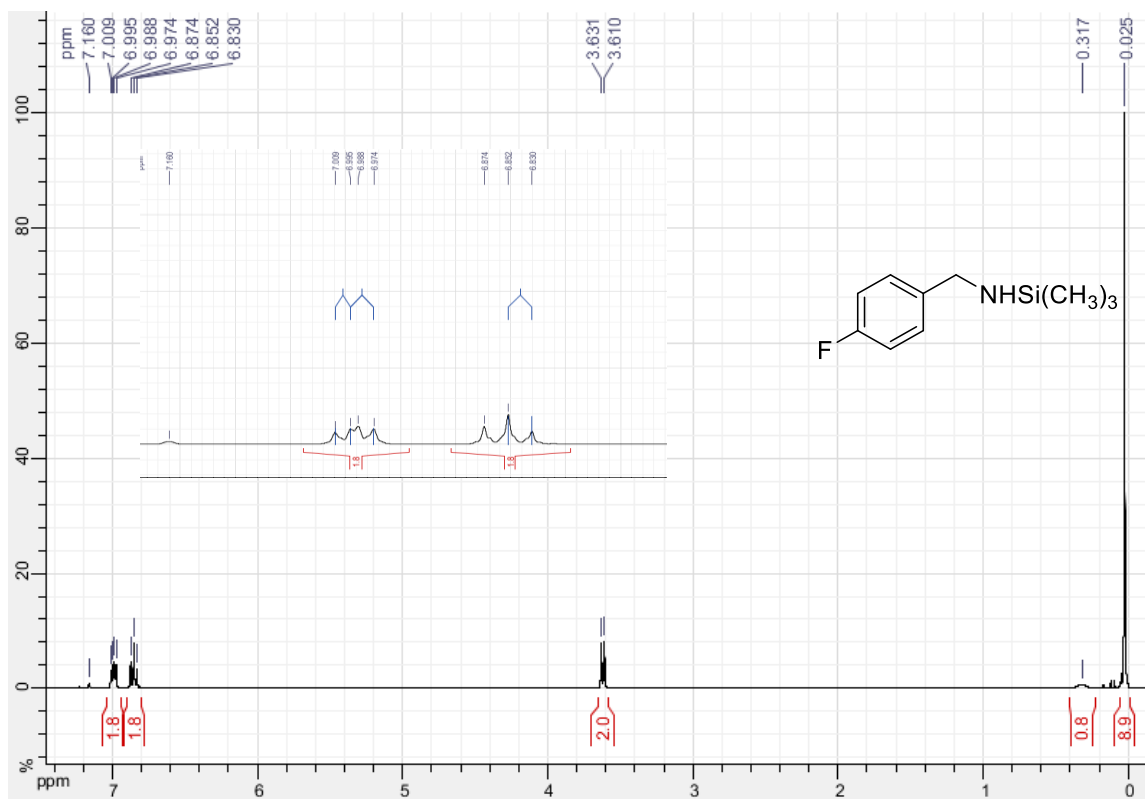


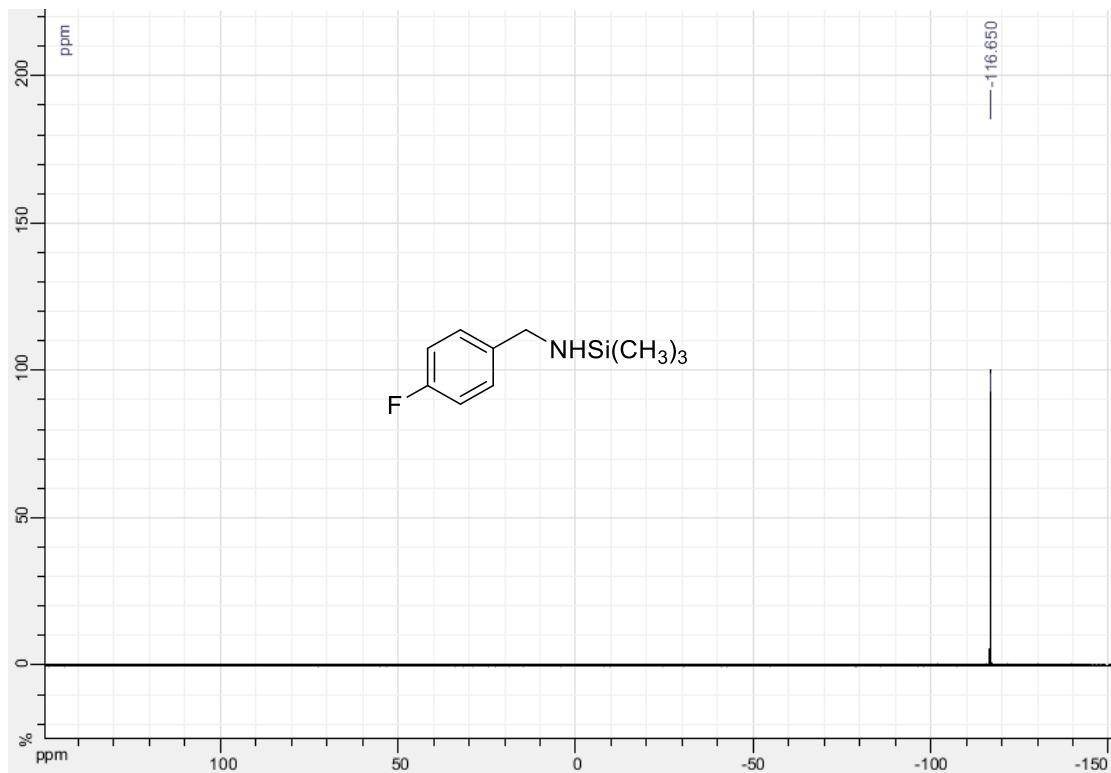
Linear: 1-phenyl-4-(trimethylsilyl)butan-1-amine (3.11.12)

Branched: 2-methyl-1-phenyl-3-(trimethylsilyl)propan-1-amine (3.12.12 and 3.13.12)

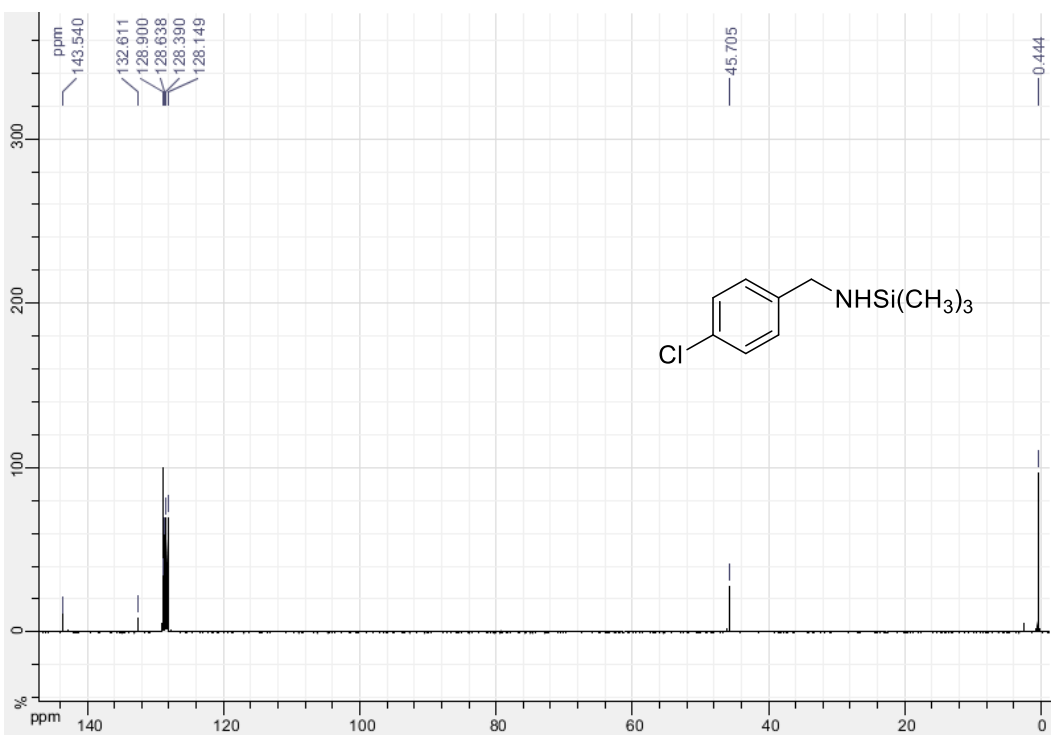
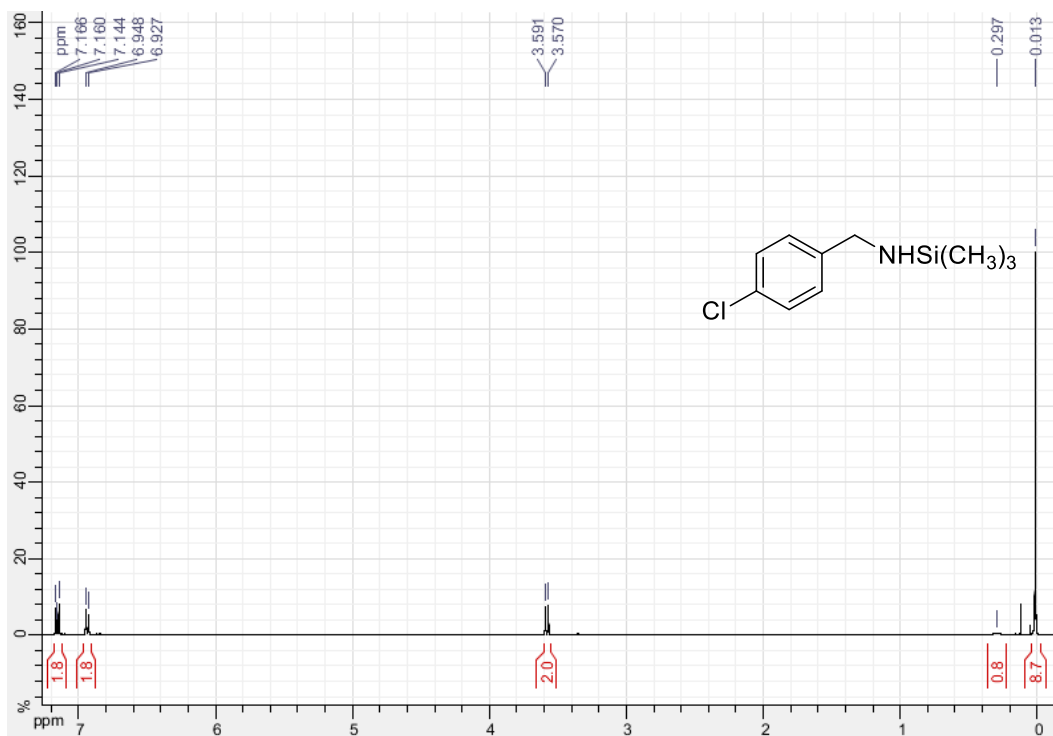


***N*-(4-fluorobenzyl)-1,1,1-trimethylsilanamine (3.15)**

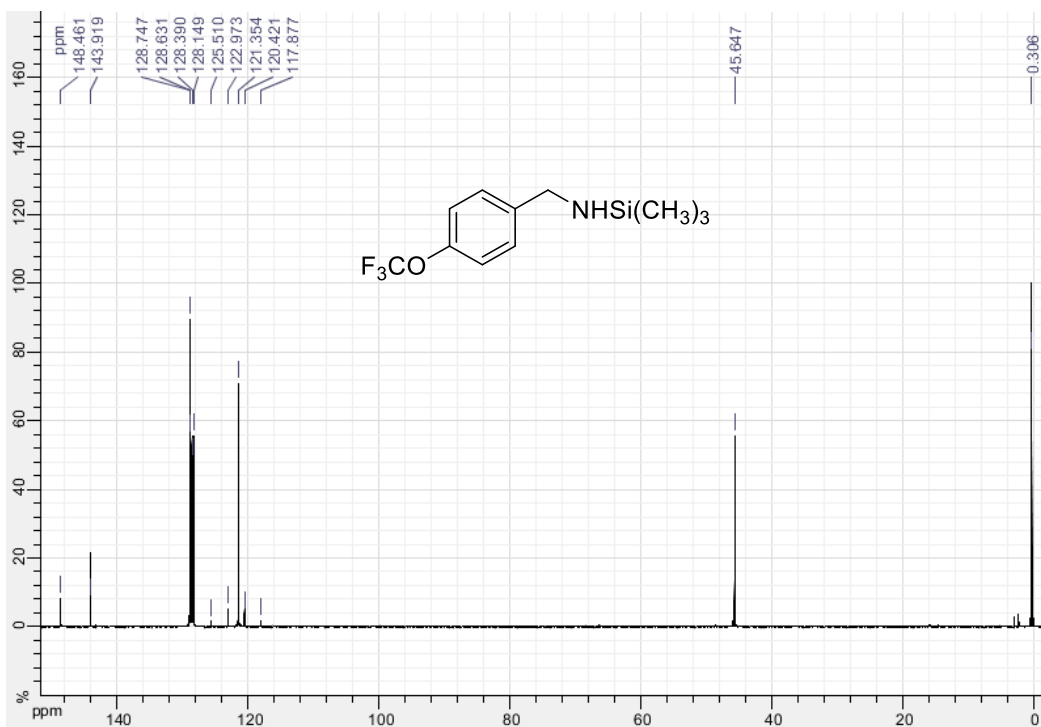
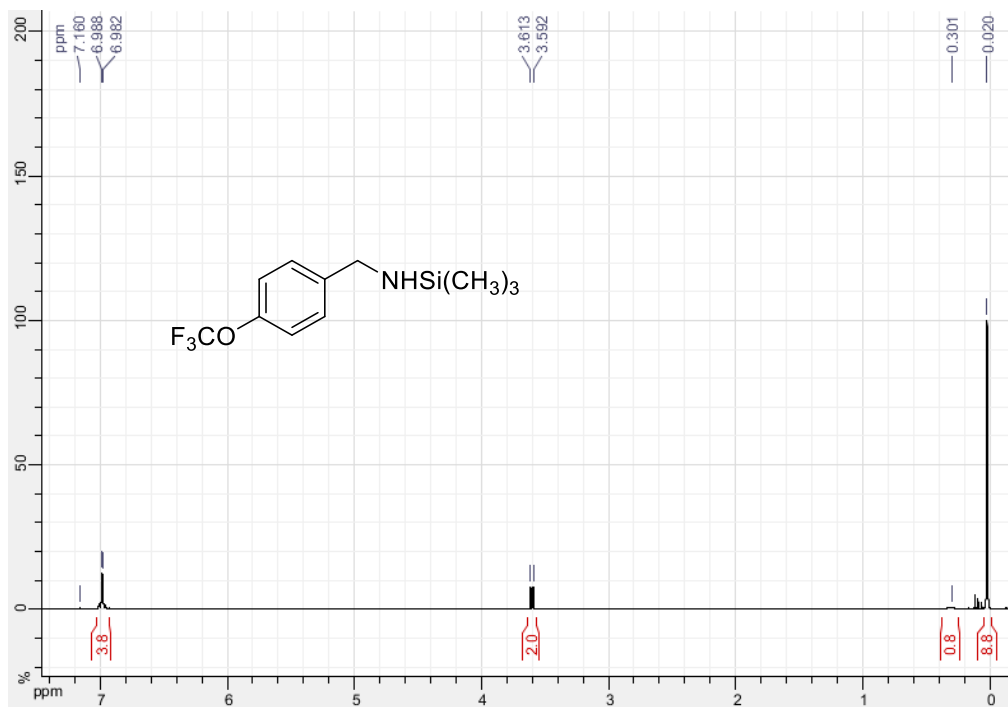


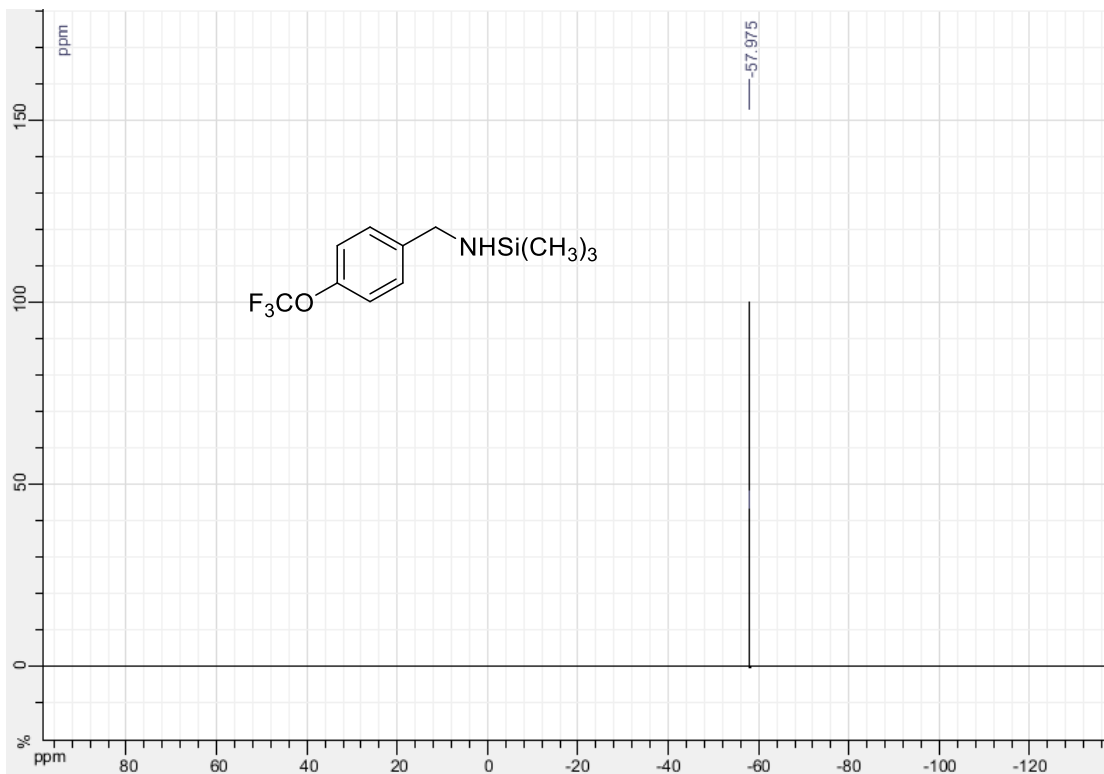


***N*-(4-chlorobenzyl)-1,1,1-trimethylsilanamine (3.16)**

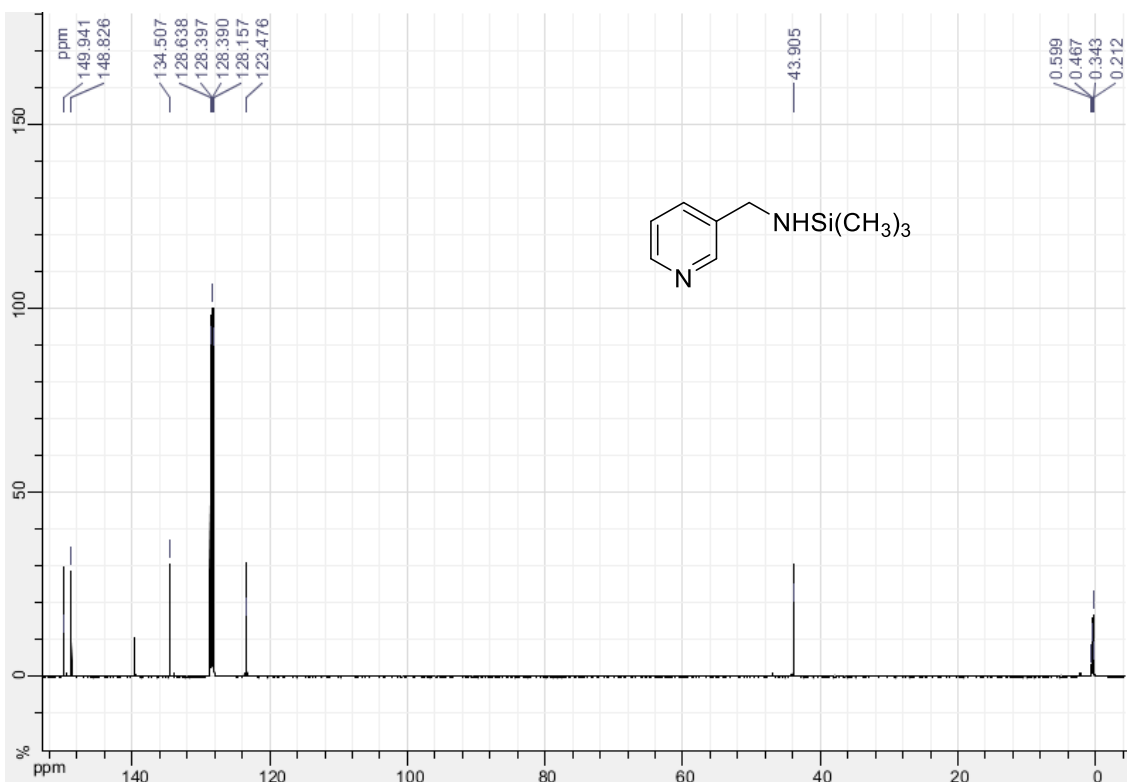
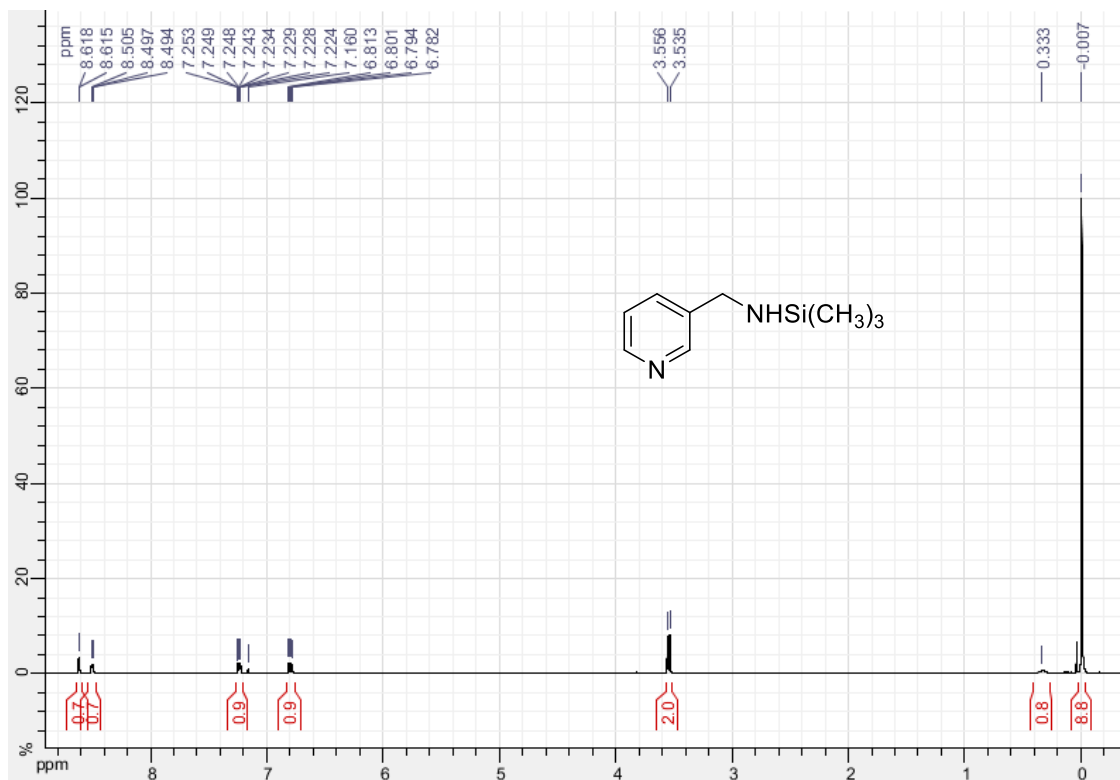


1,1,1-trimethyl-N-(4-(trifluoromethoxy)benzyl)silanamine (3.17)

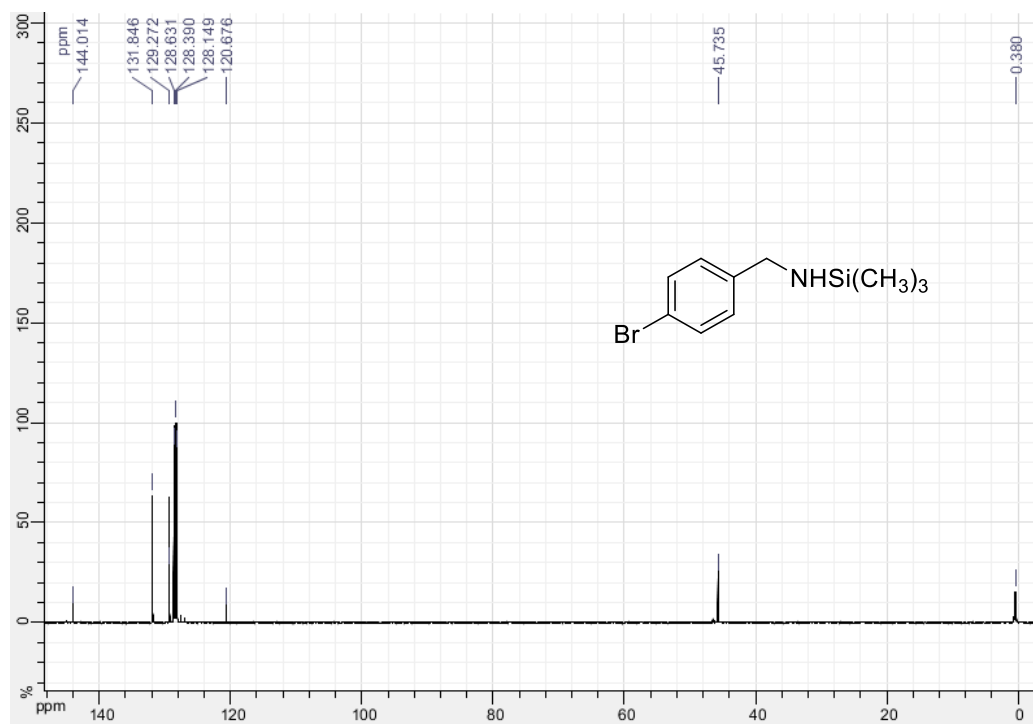
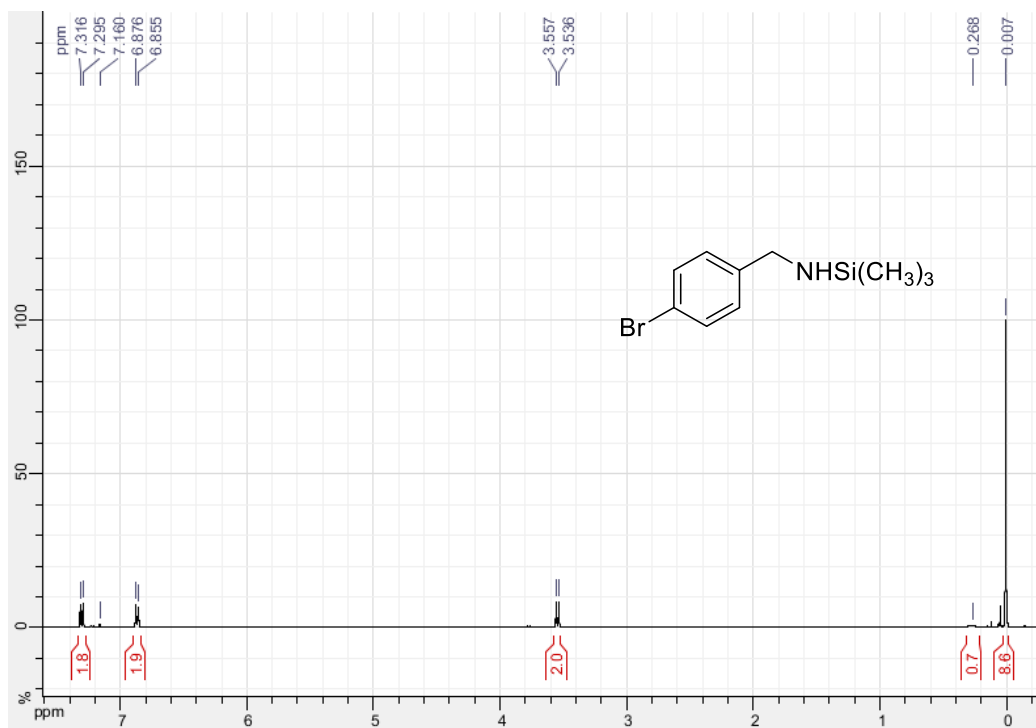




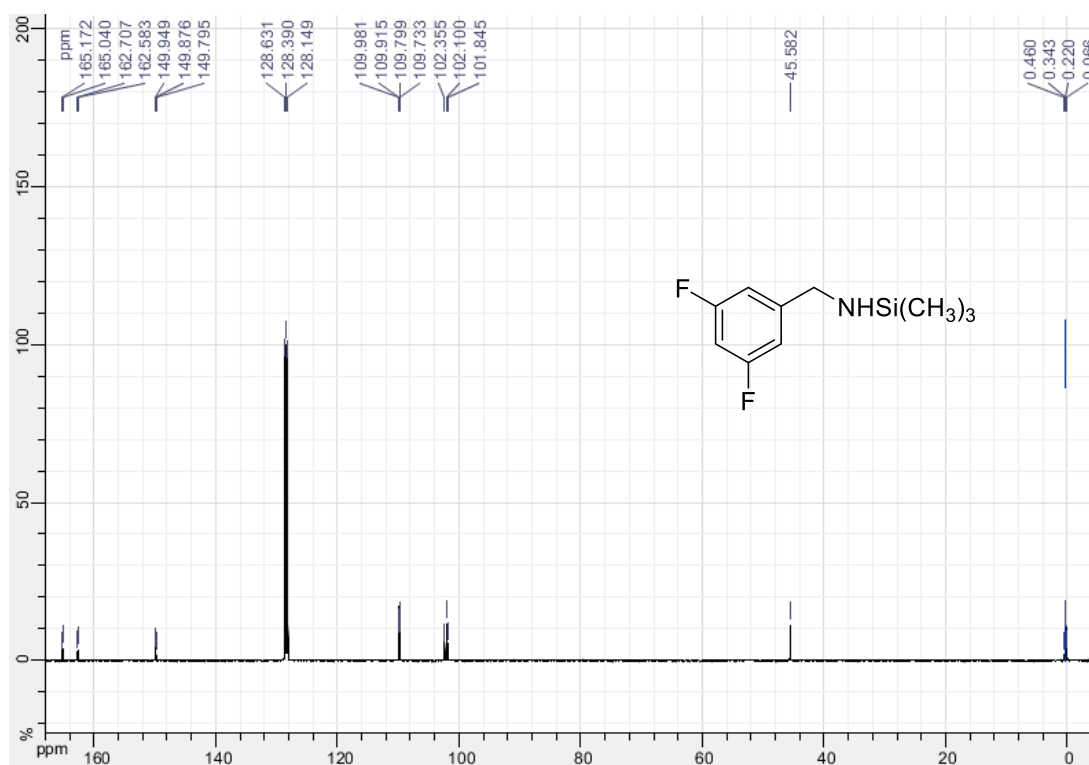
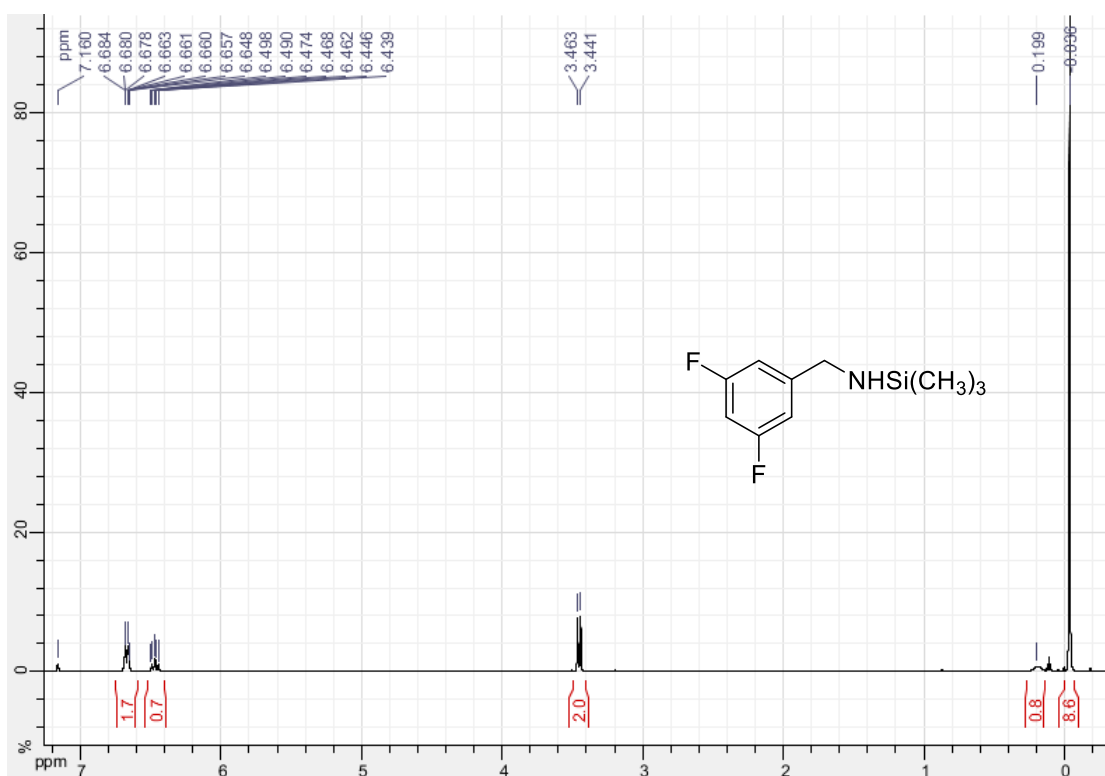
1,1,1-trimethyl-N-(pyridin-3-ylmethyl)silanamine (3.18)

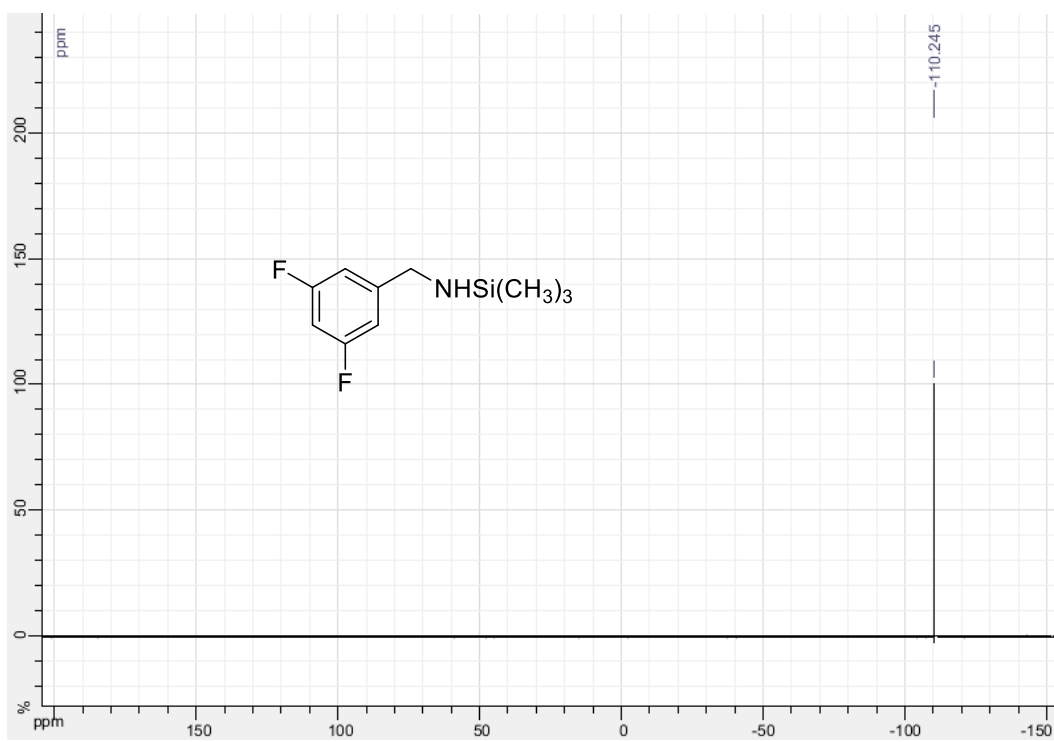


***N*-(4-bromobenzyl)-1,1,1-trimethylsilanamine (3.19)**

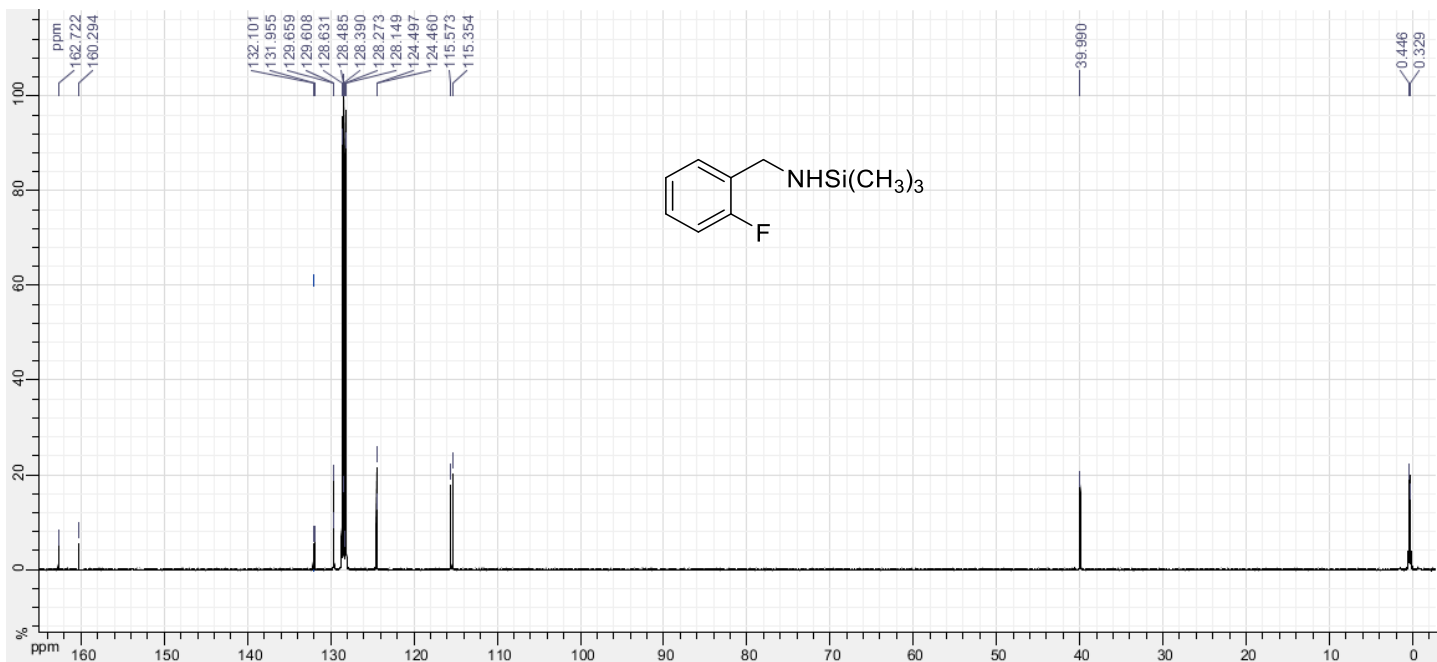
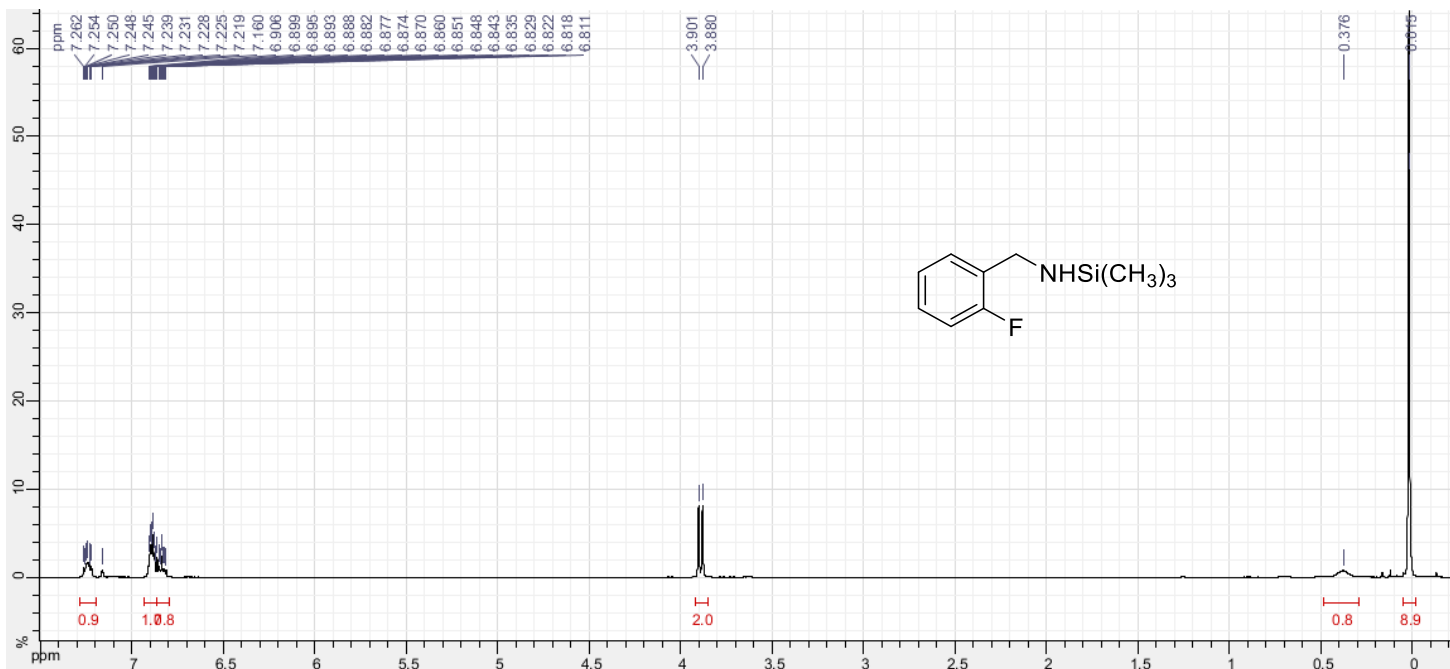


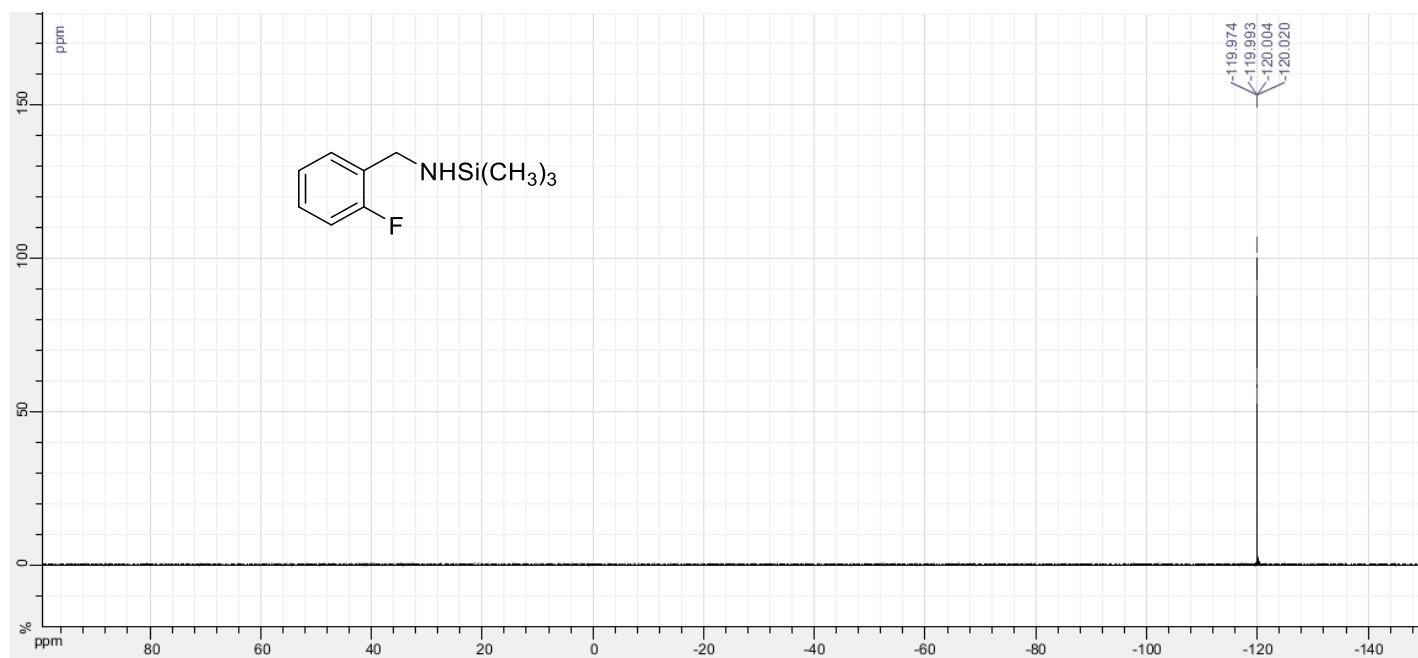
***N*-(3,5-difluorobenzyl)-1,1,1-trimethylsilanamine (3.20)**



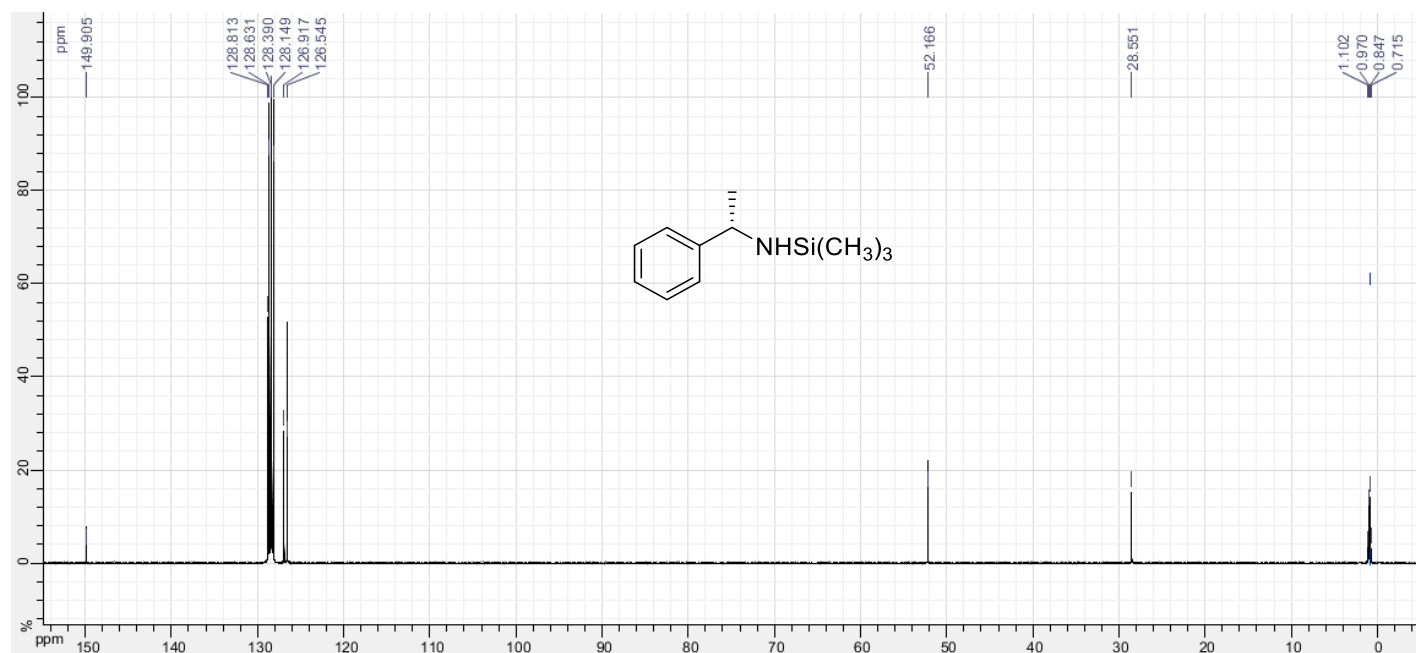
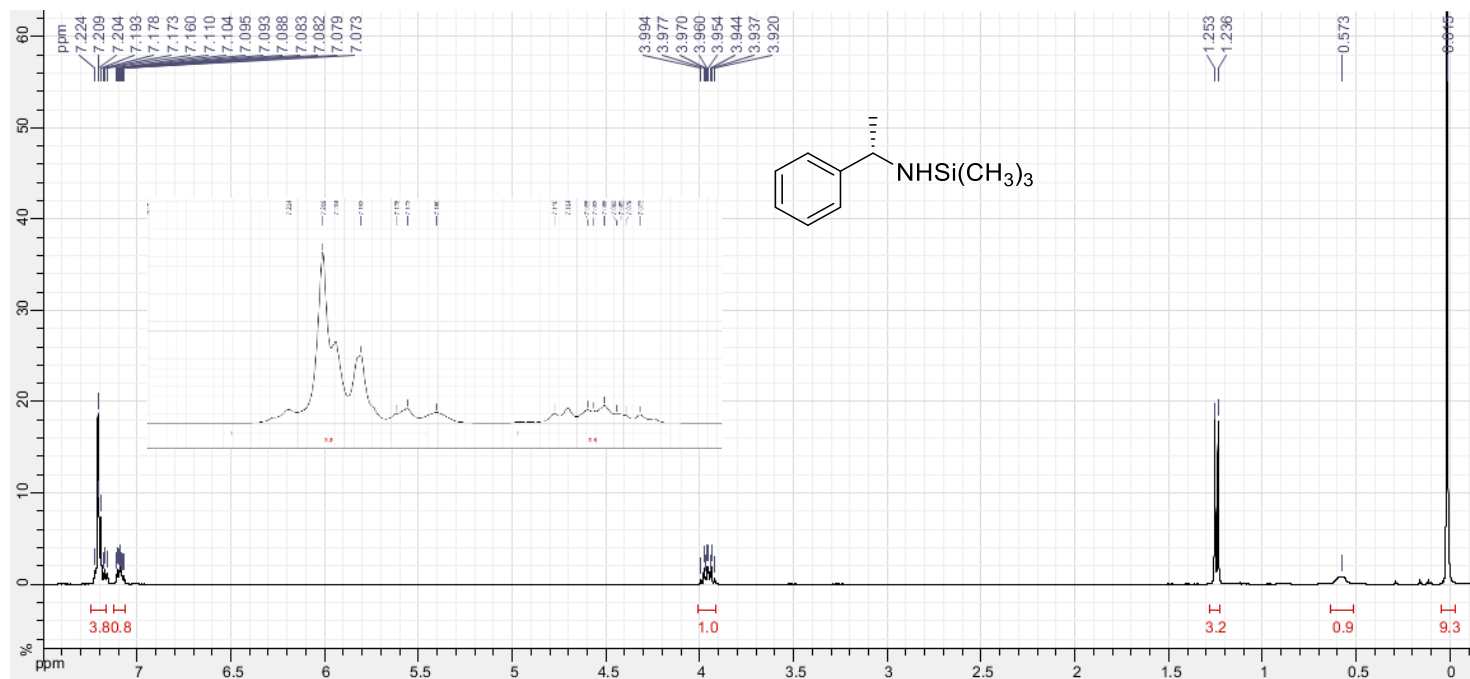


***N*-(2-fluorobenzyl)-1,1,1-trimethylsilanamine (3.21)**

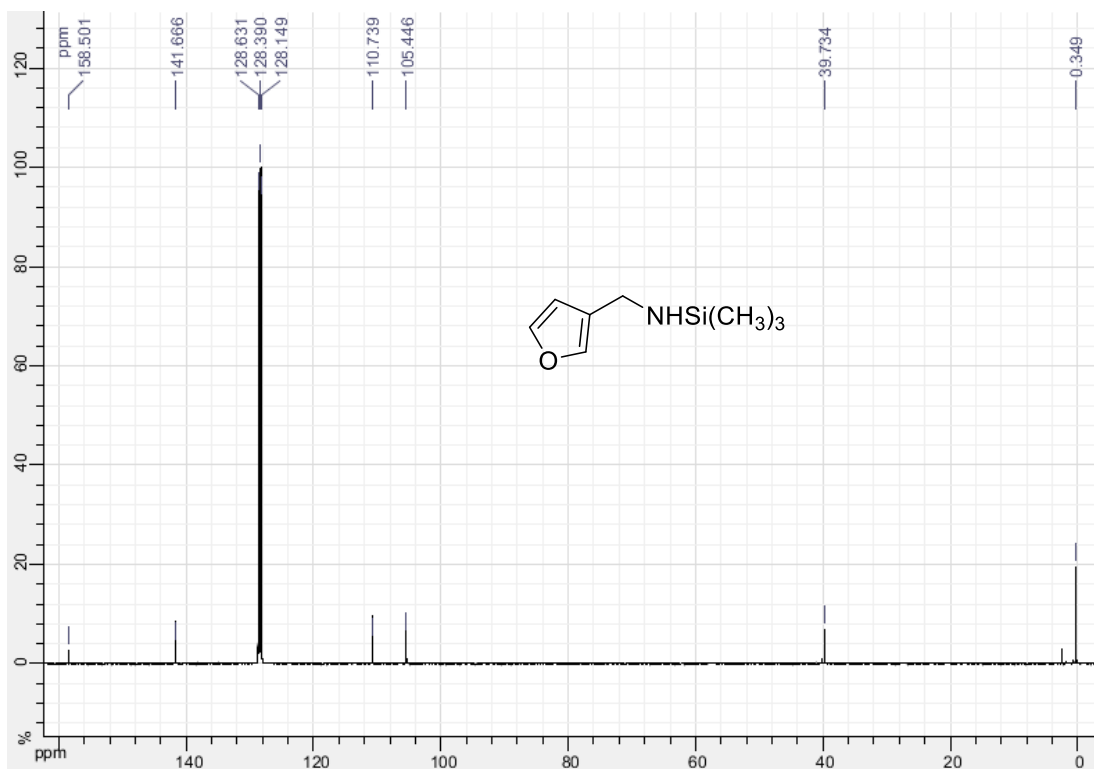
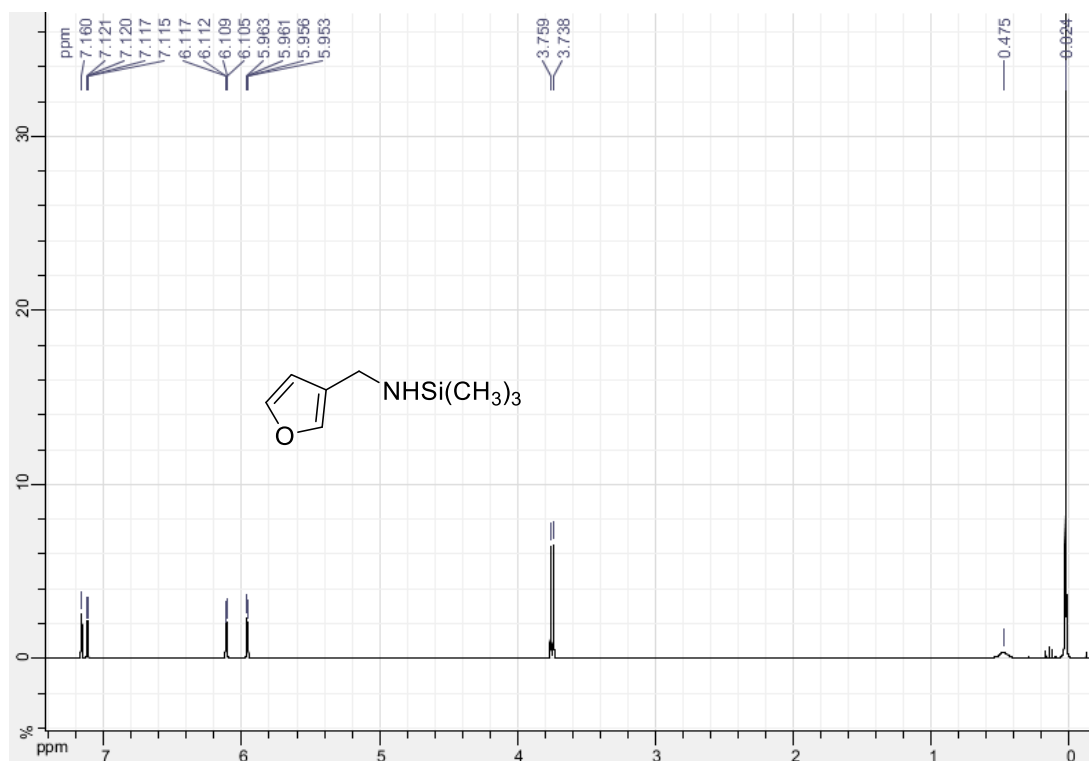




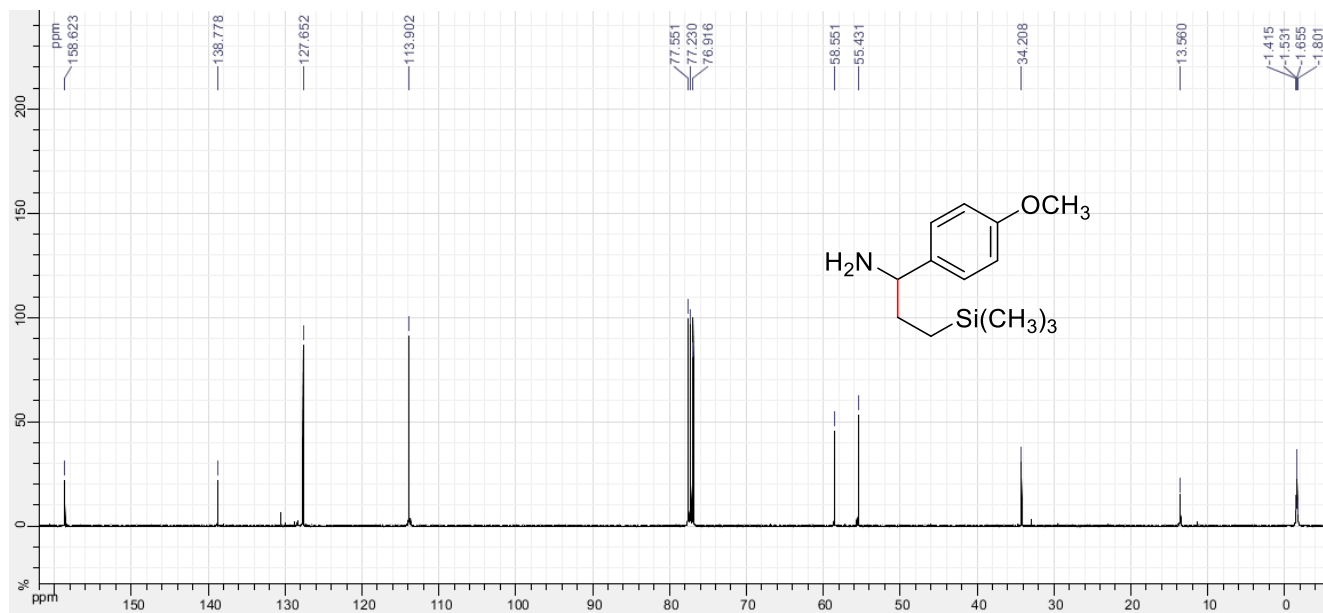
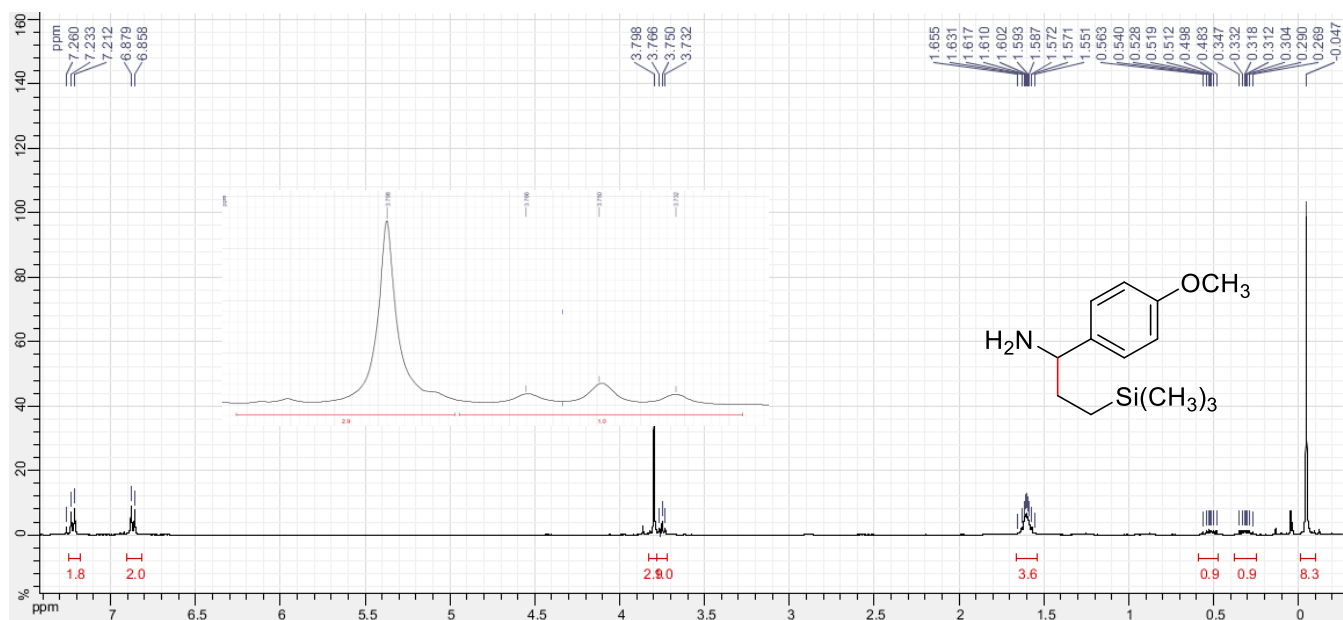
(S)-1,1,1-trimethyl-N-(1-phenylethyl)silanamine (3.22)



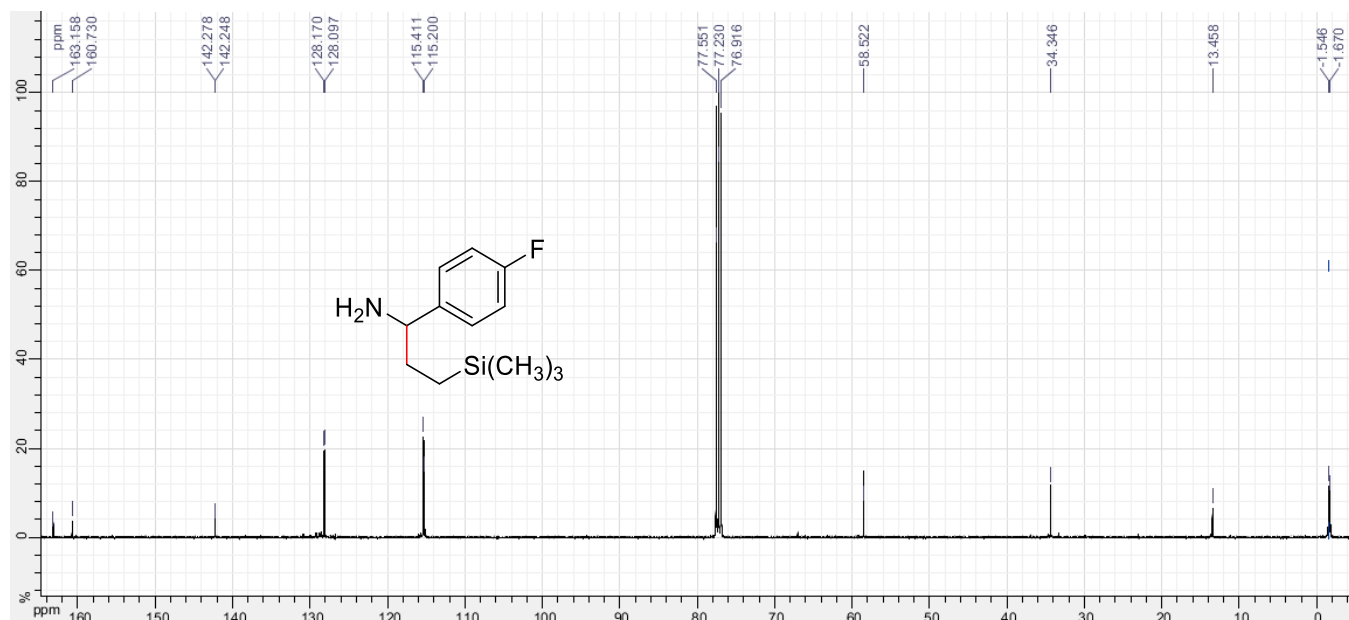
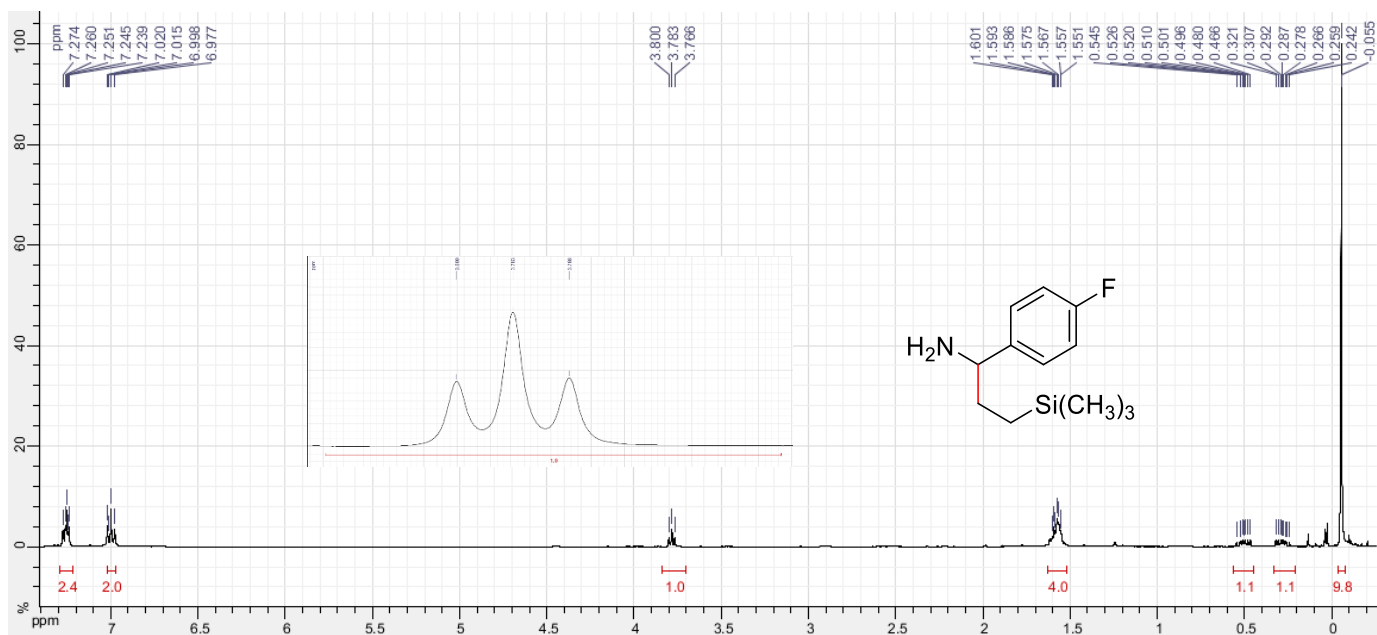
N-(furan-3-ylmethyl)-1,1,1-trimethylsilanamine (3.23)

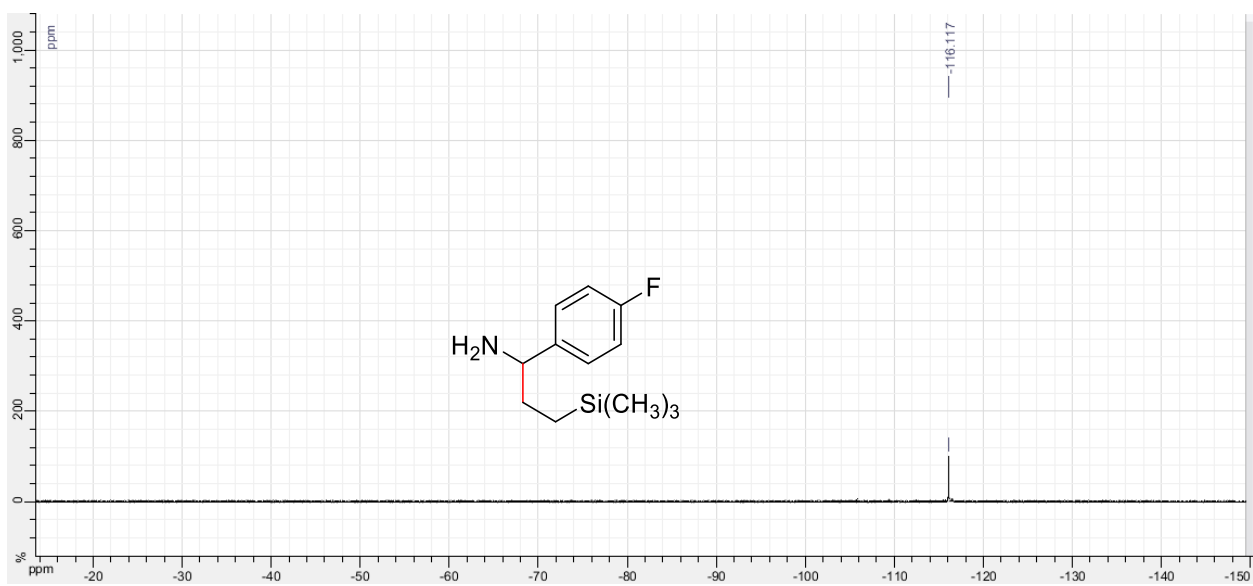


1-(4-methoxyphenyl)-3-(trimethylsilyl)propan-1-amine (3.24)

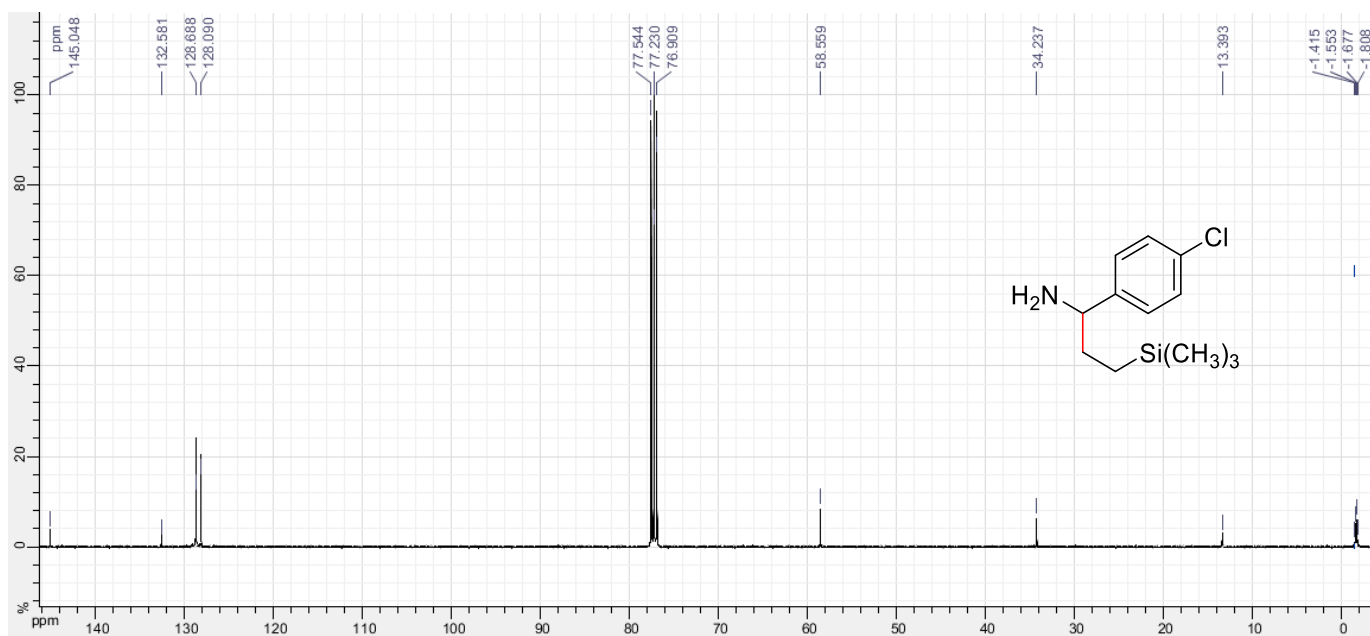
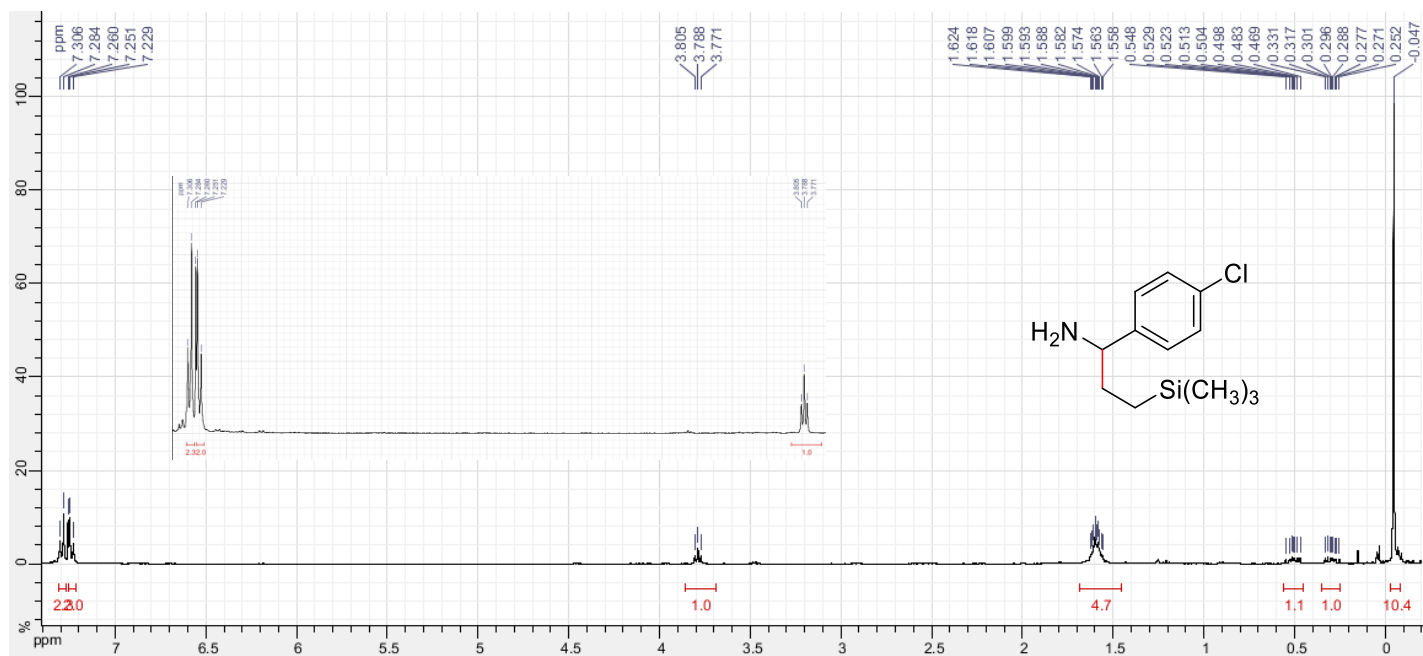


1-(4-fluorophenyl)-3-(trimethylsilyl)propan-1-amine (3.25)

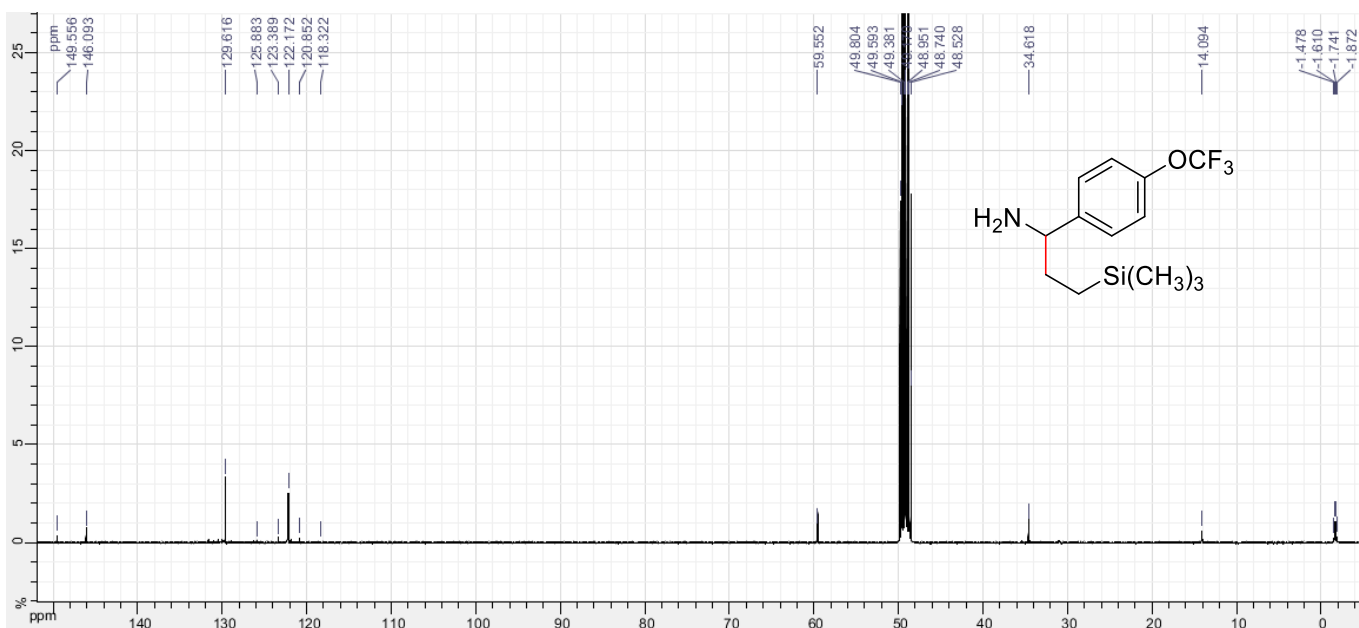
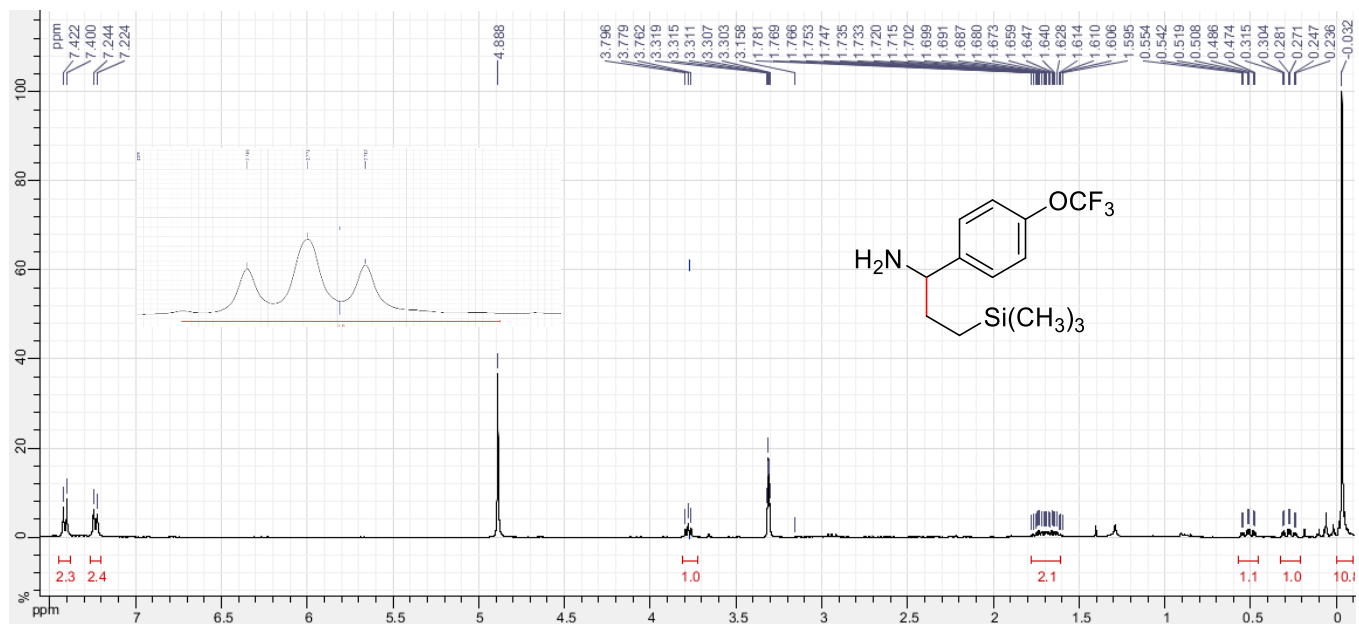


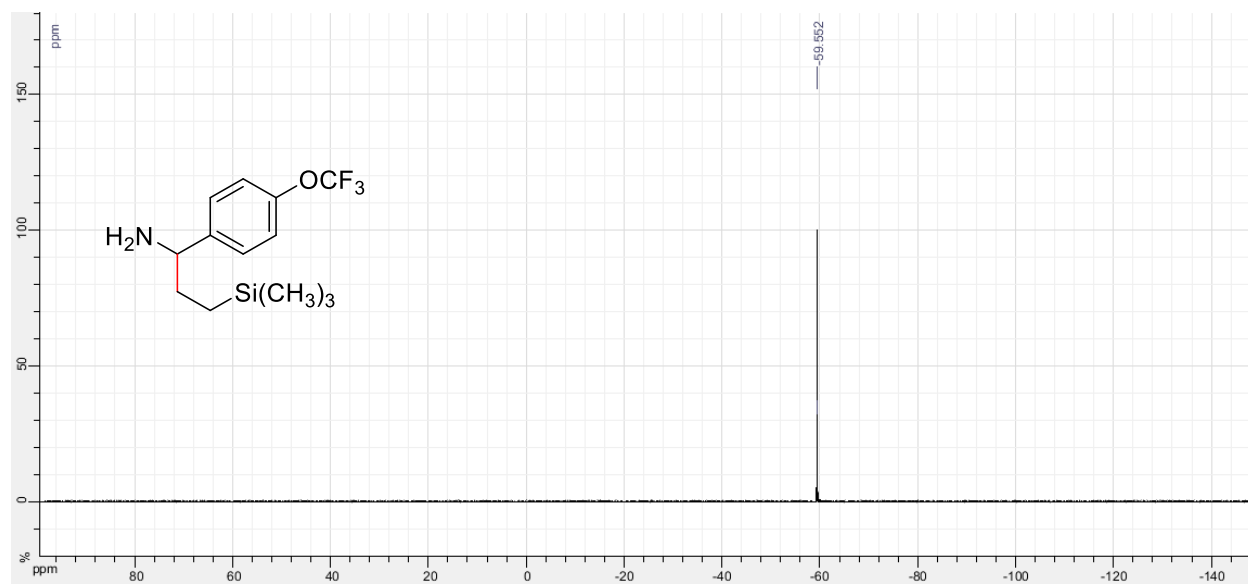


1-(4-chlorophenyl)-3-(trimethylsilyl)propan-1-amine (3.26)

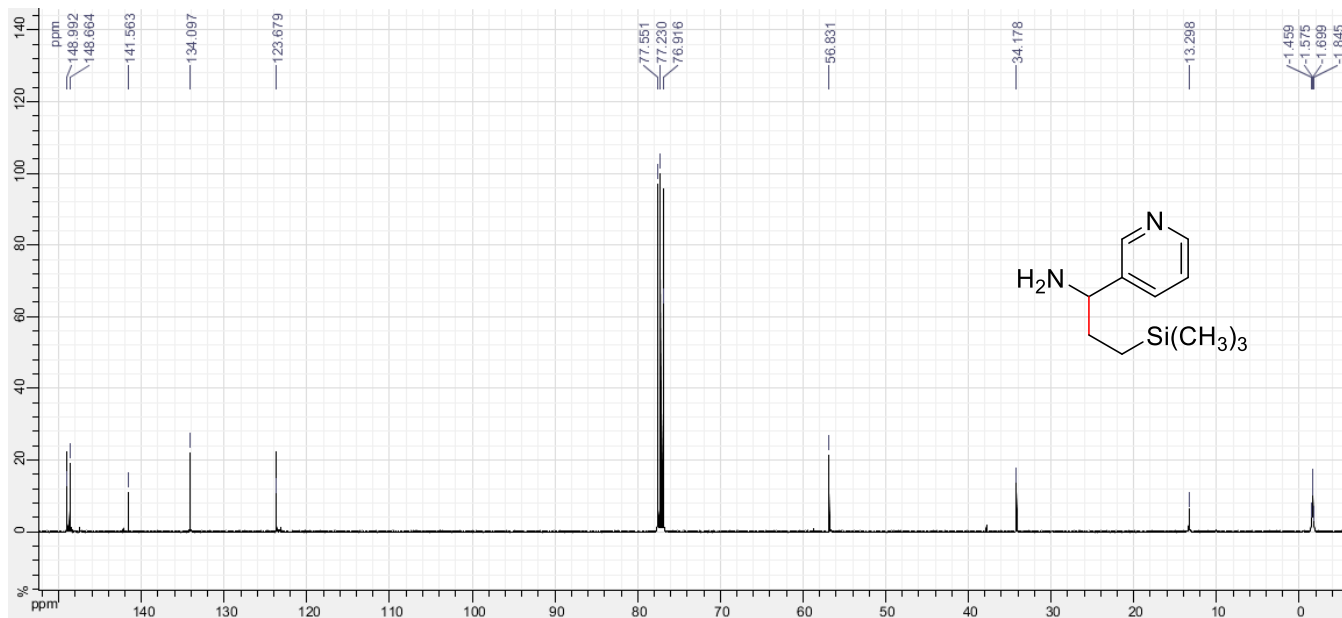
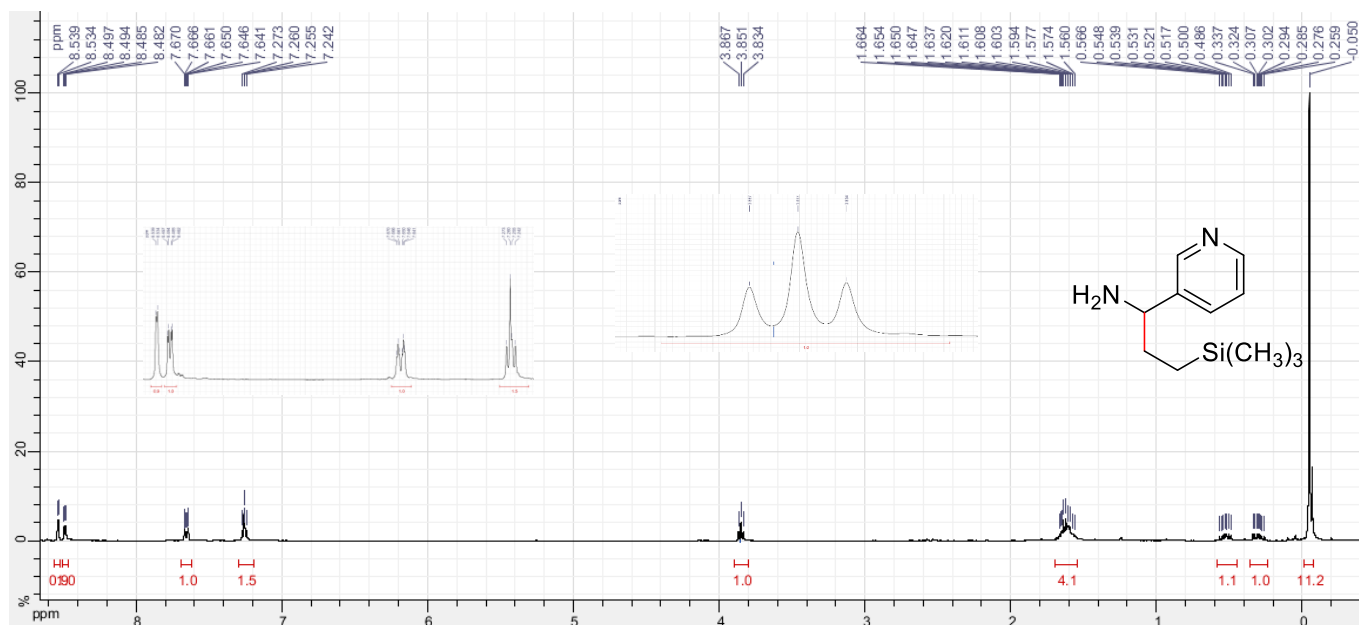


1-(4-(trifluoromethoxy)phenyl)-3-(trimethylsilyl)propan-1-amine (3.27)

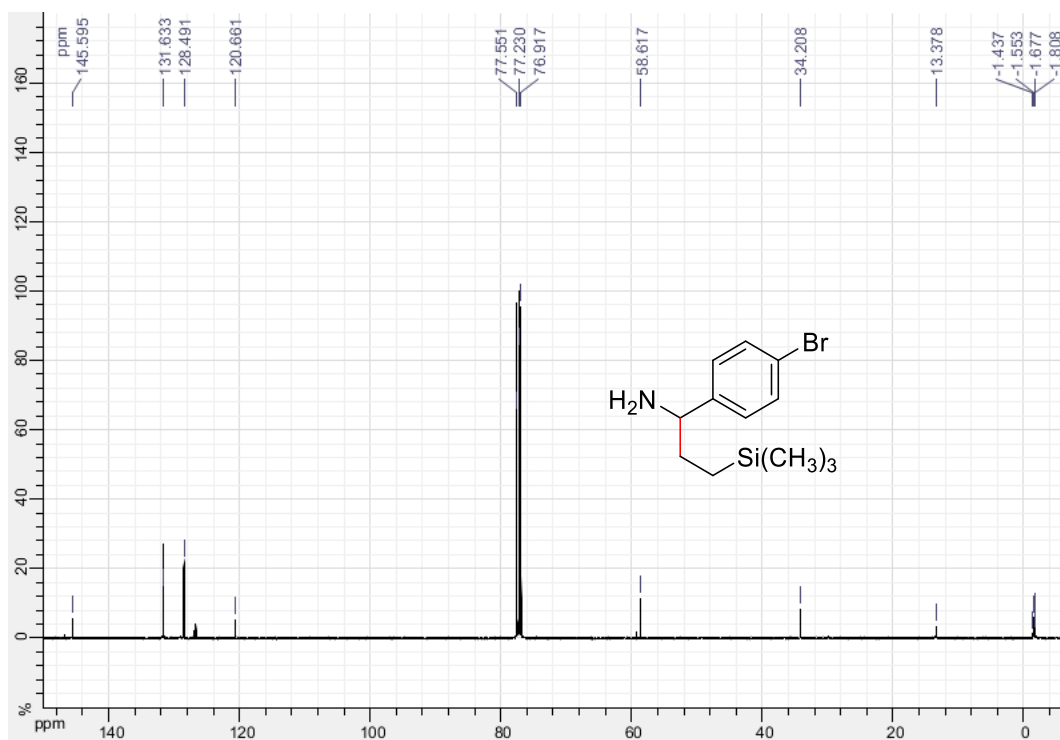
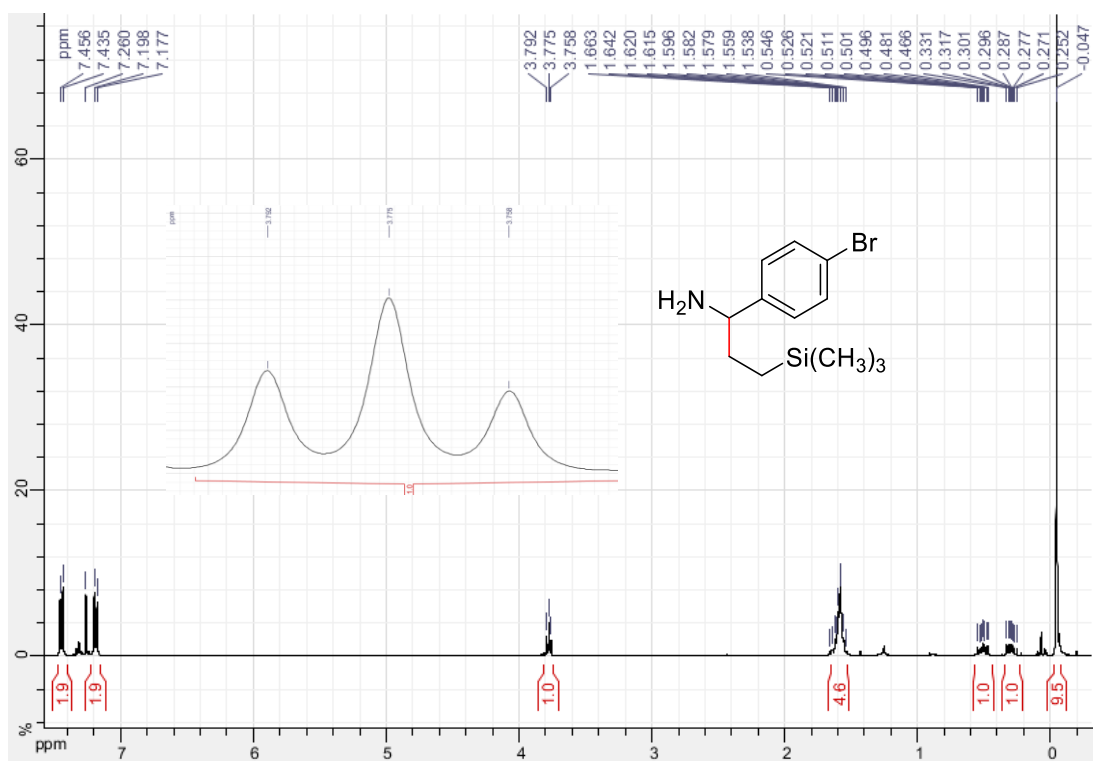




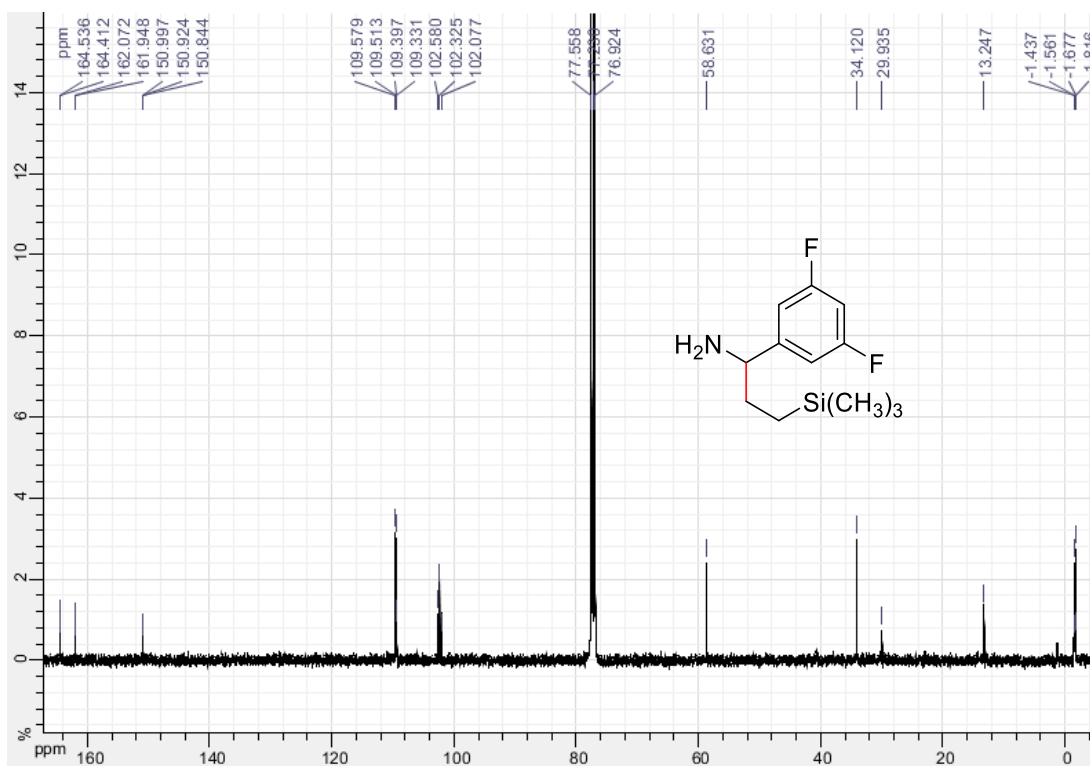
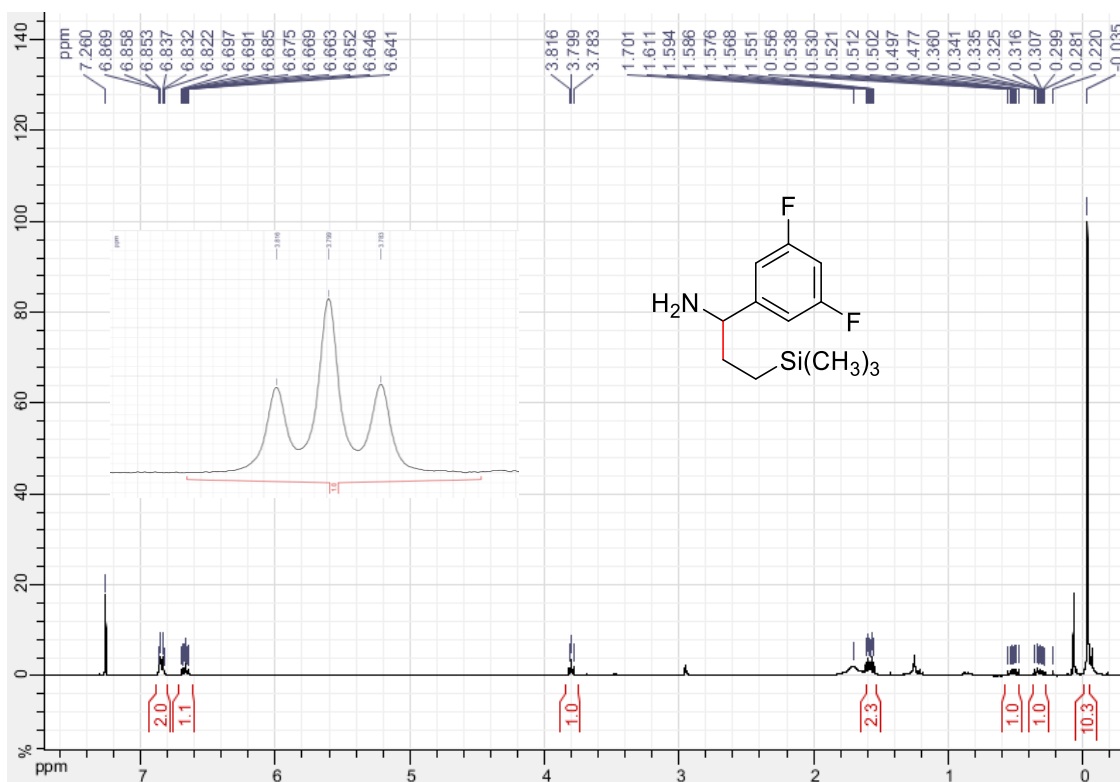
1-(pyridin-3-yl)-3-(trimethylsilyl)propan-1-amine (3.28)

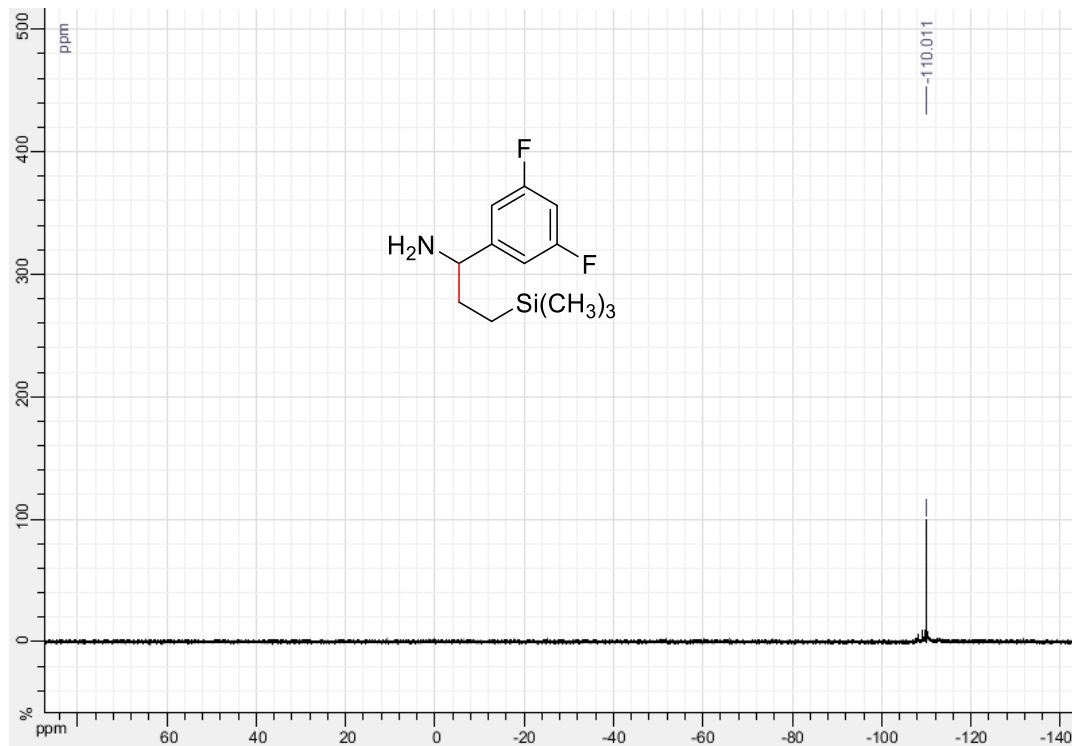


1-(4-bromophenyl)-3-(trimethylsilyl)propan-1-amine (3.29)

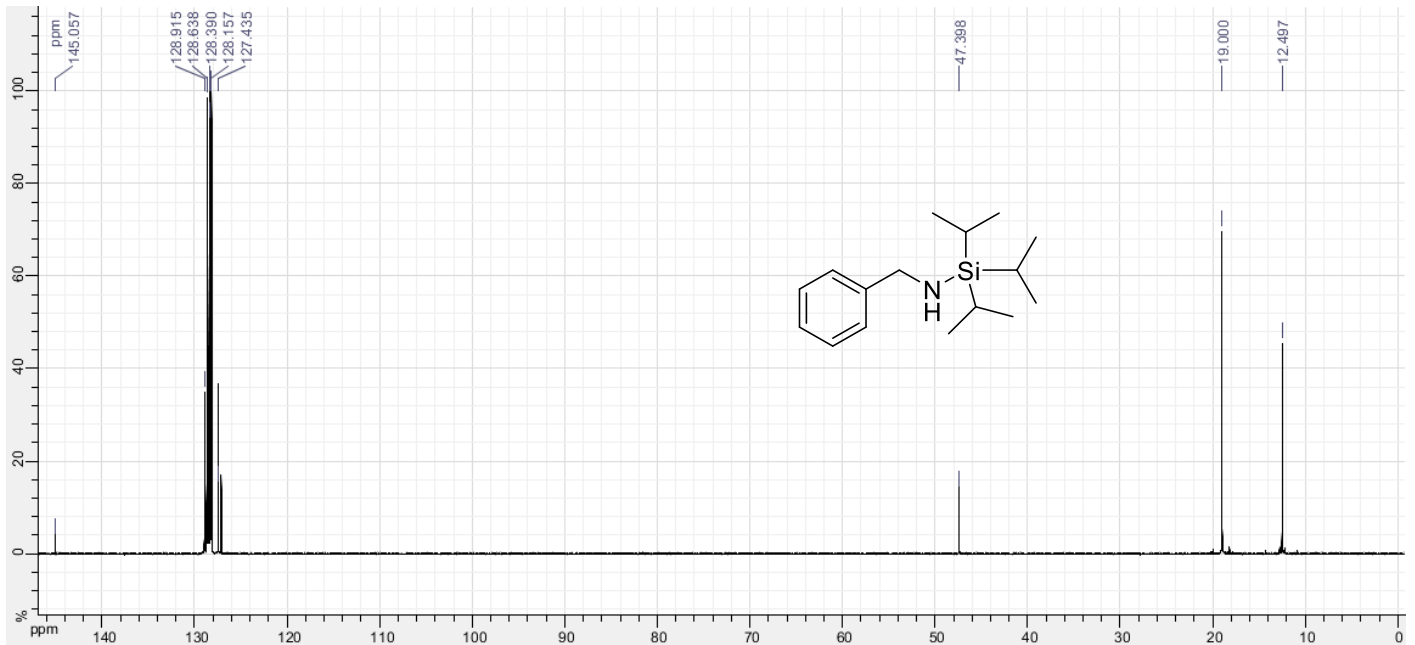
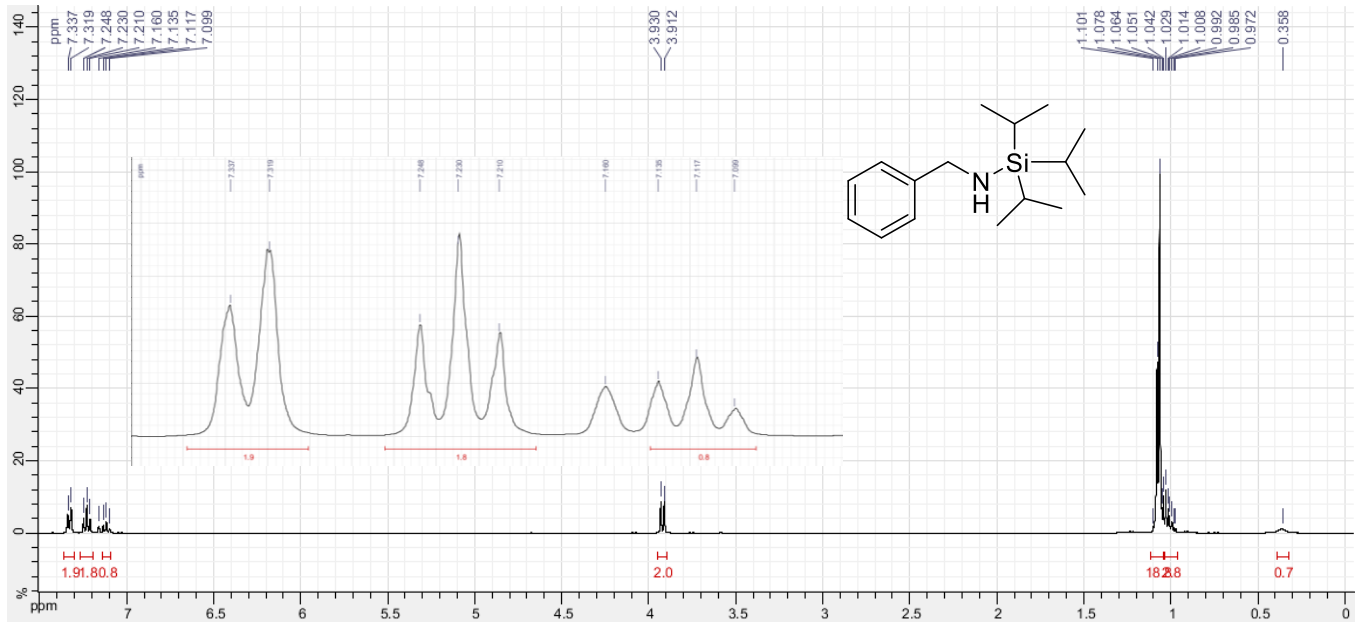


1-(3,5-difluorophenyl)-3-(trimethylsilyl)propan-1-amine (3.30)

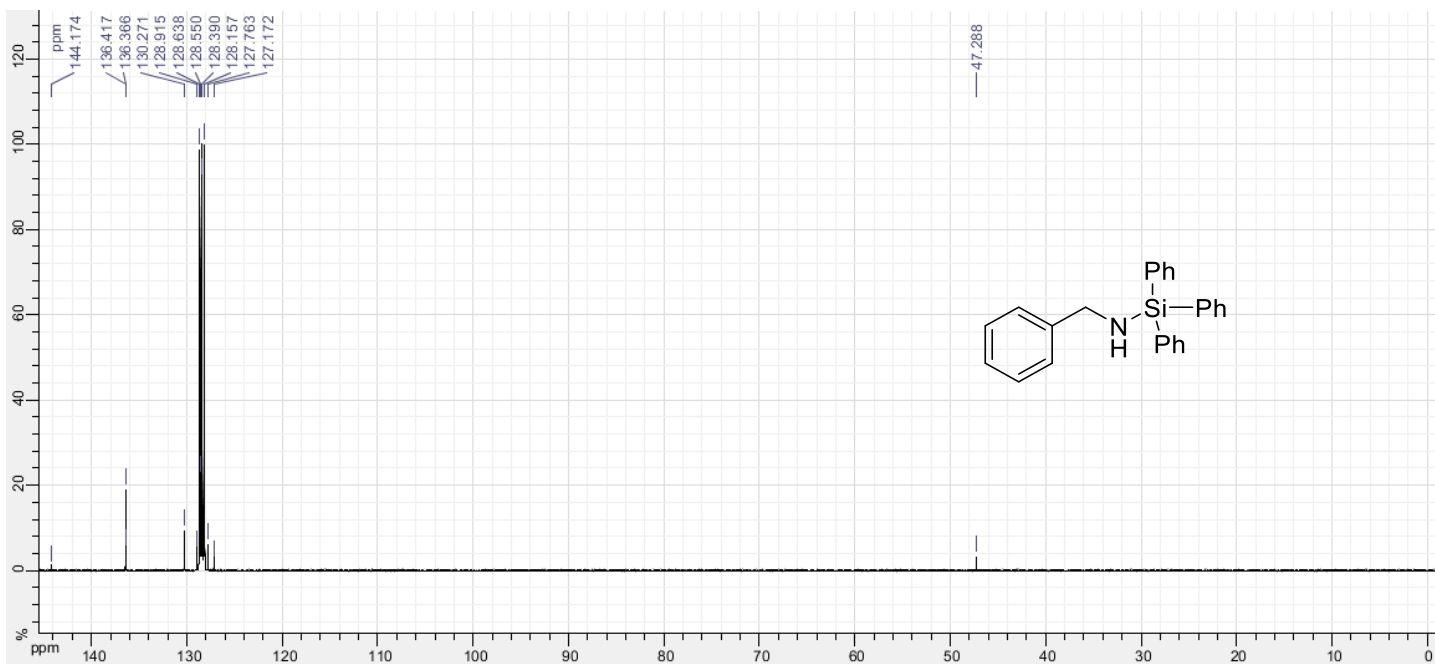
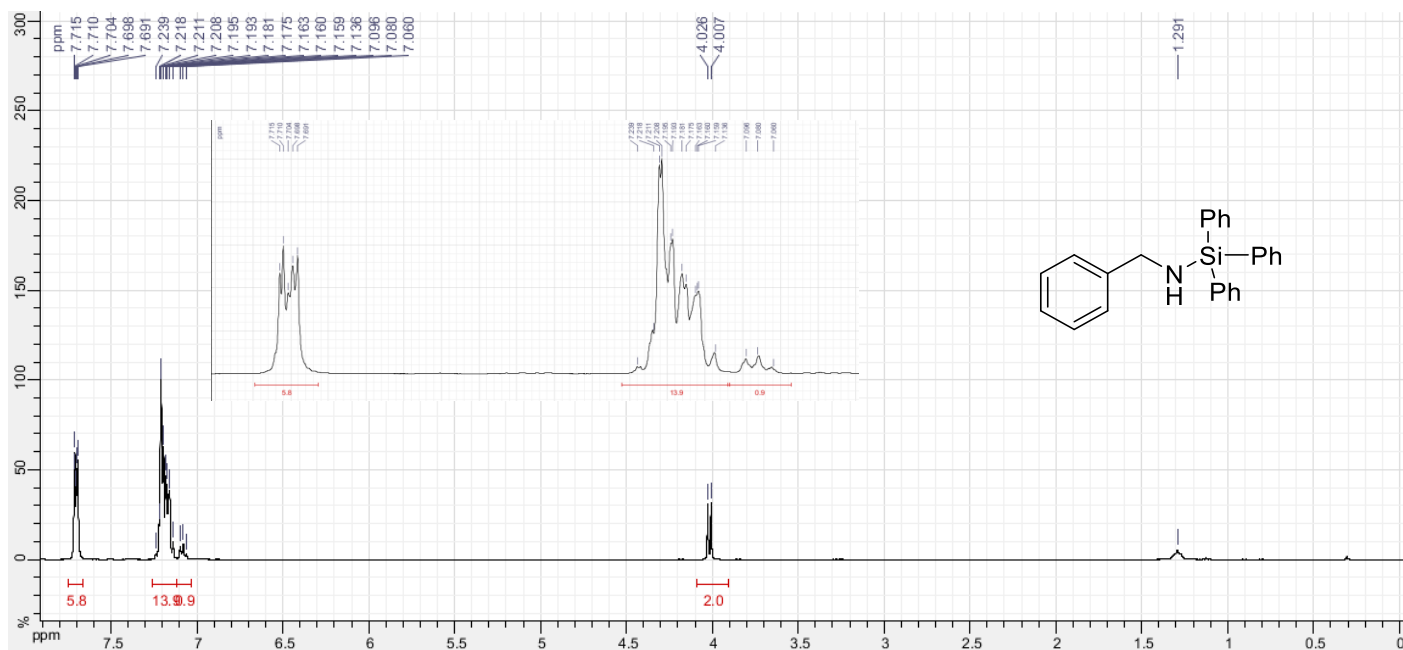




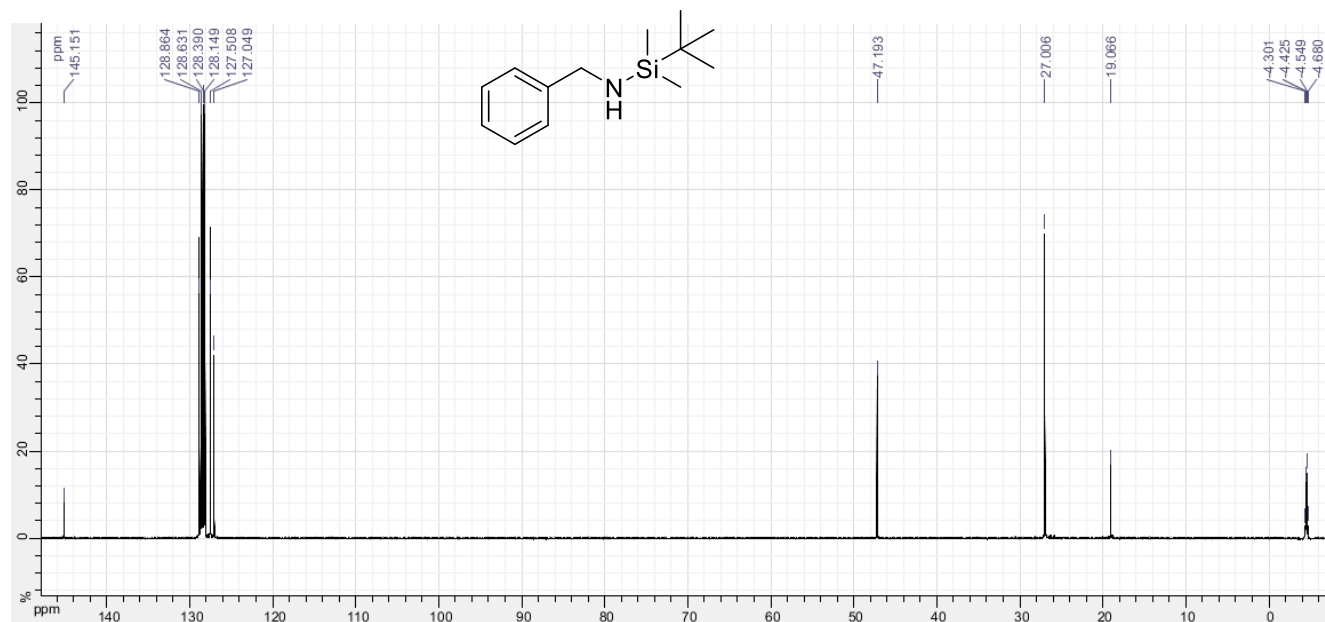
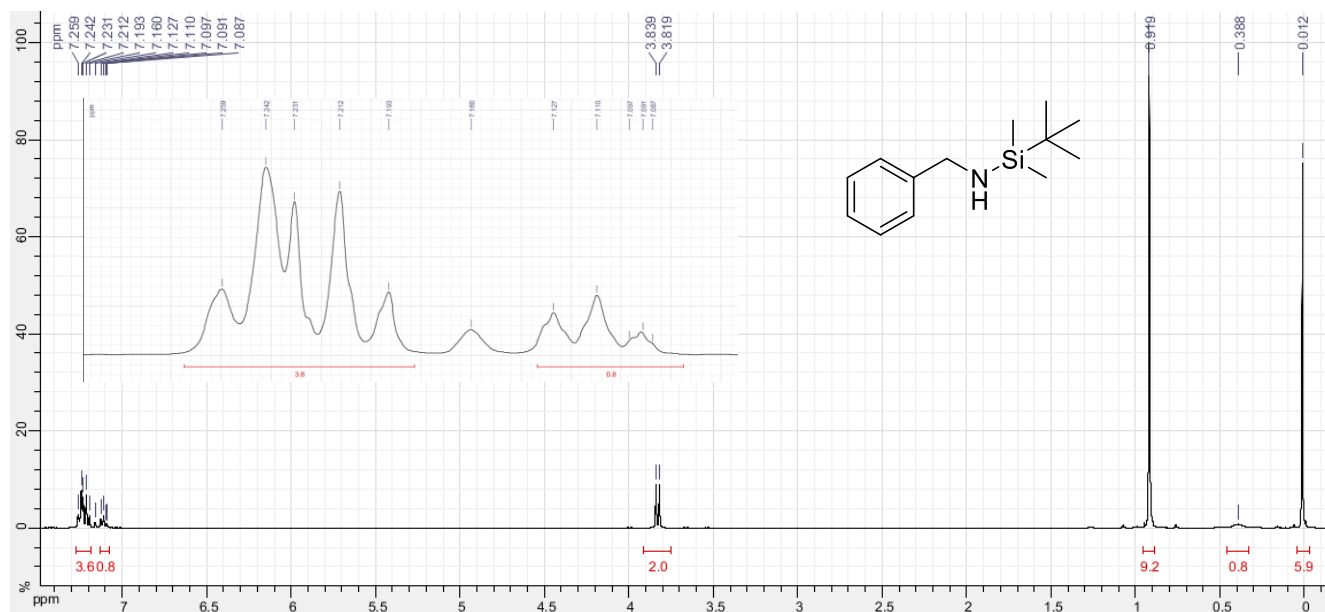
N-benzyl-1,1,1-triisopropylsilanamine (3.38)



***N*-benzyl-1,1,1-triphenylsilanamine (3.39)**

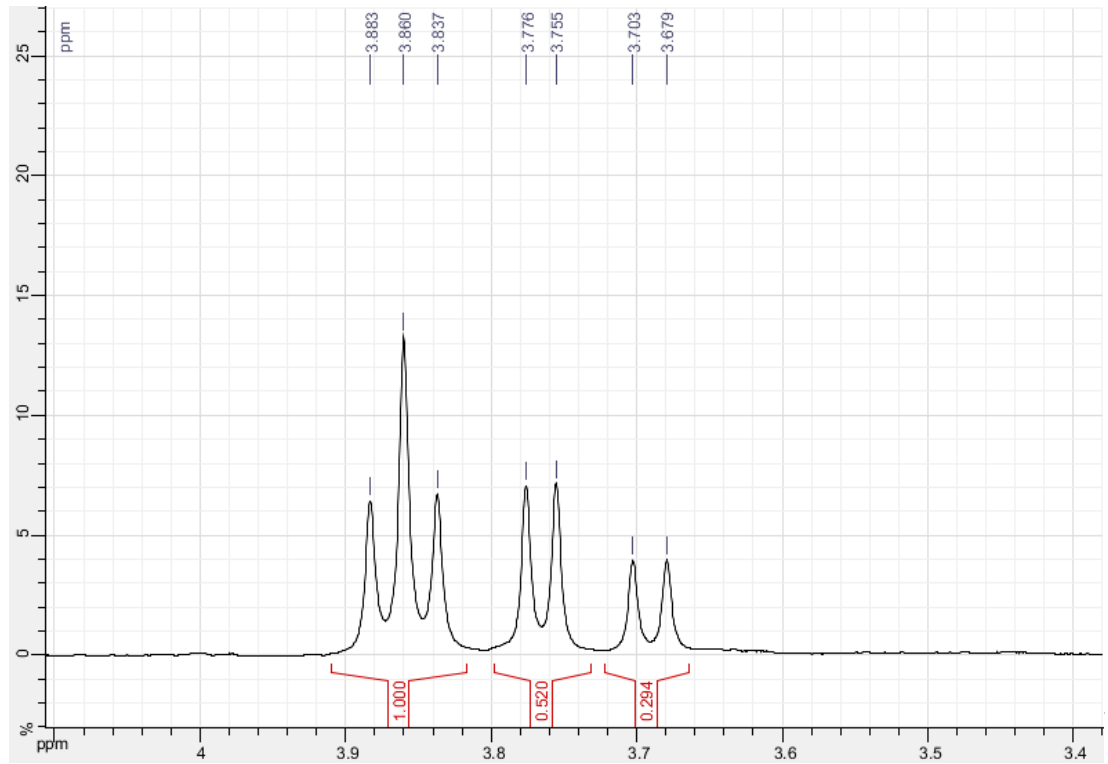
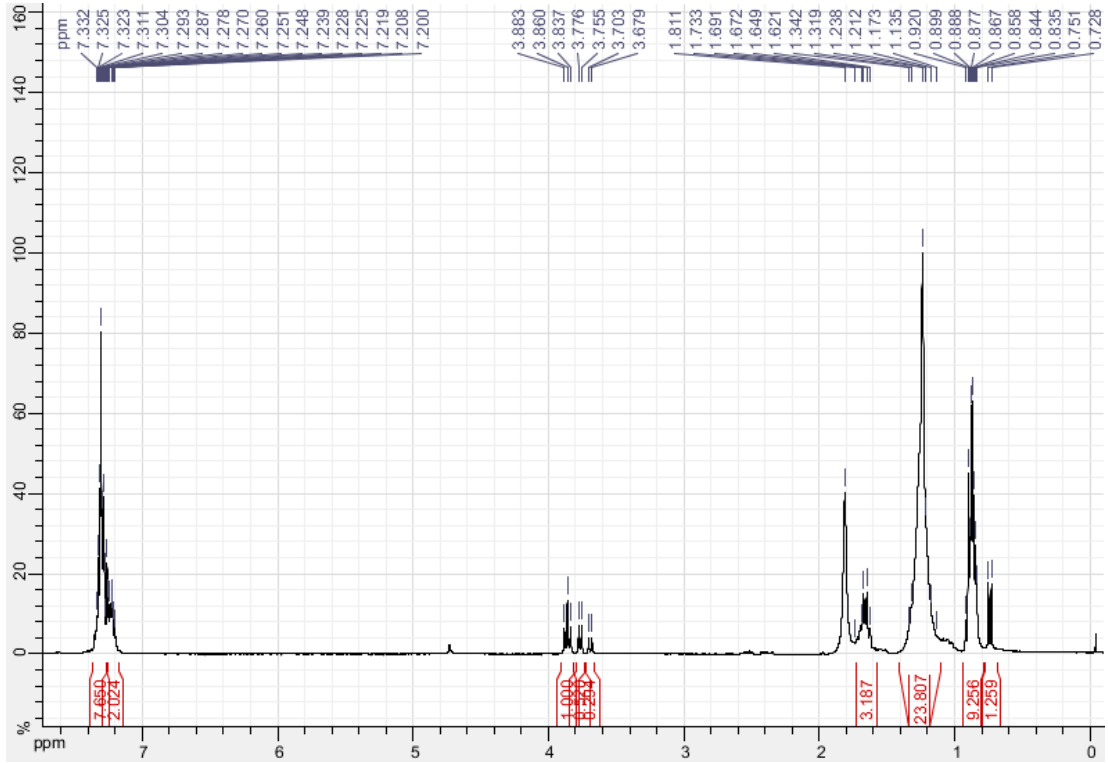


N-benzyl-1-(tert-butyl)-1,1-dimethylsilanamine (3.40)



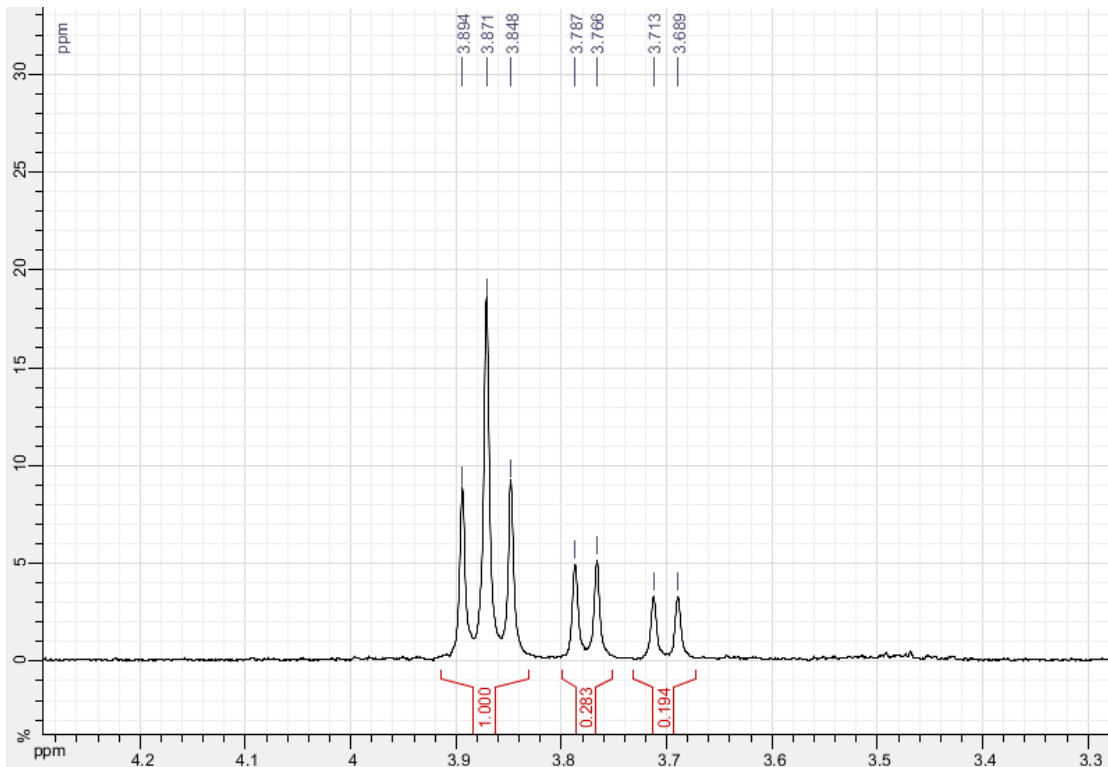
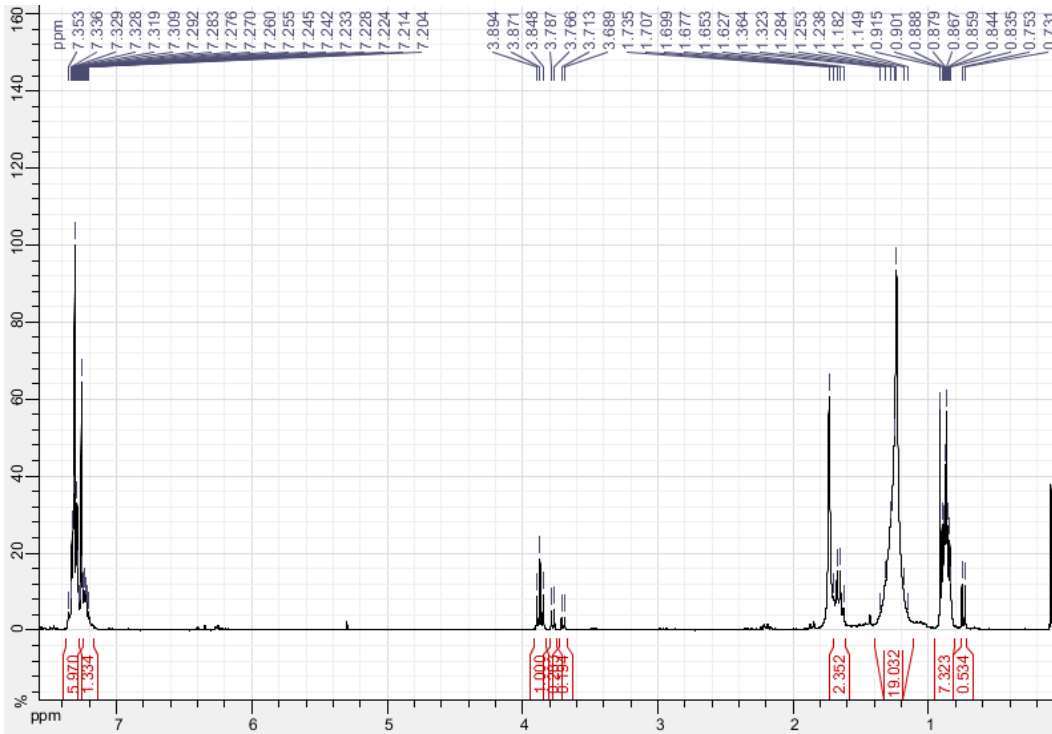
Linear: 1-phenylnonan-1-amine (3.11.1)

Branched: 2-methyl-1-phenyloctan-1-amine (3.12.1 and 3.13.1)

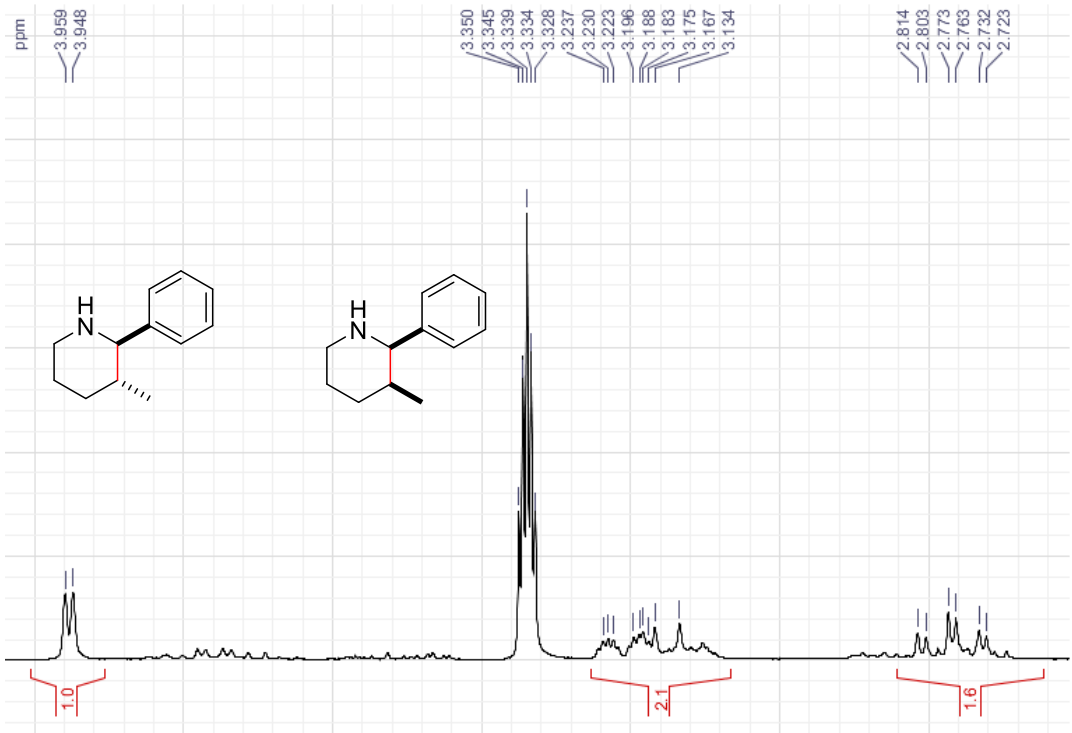
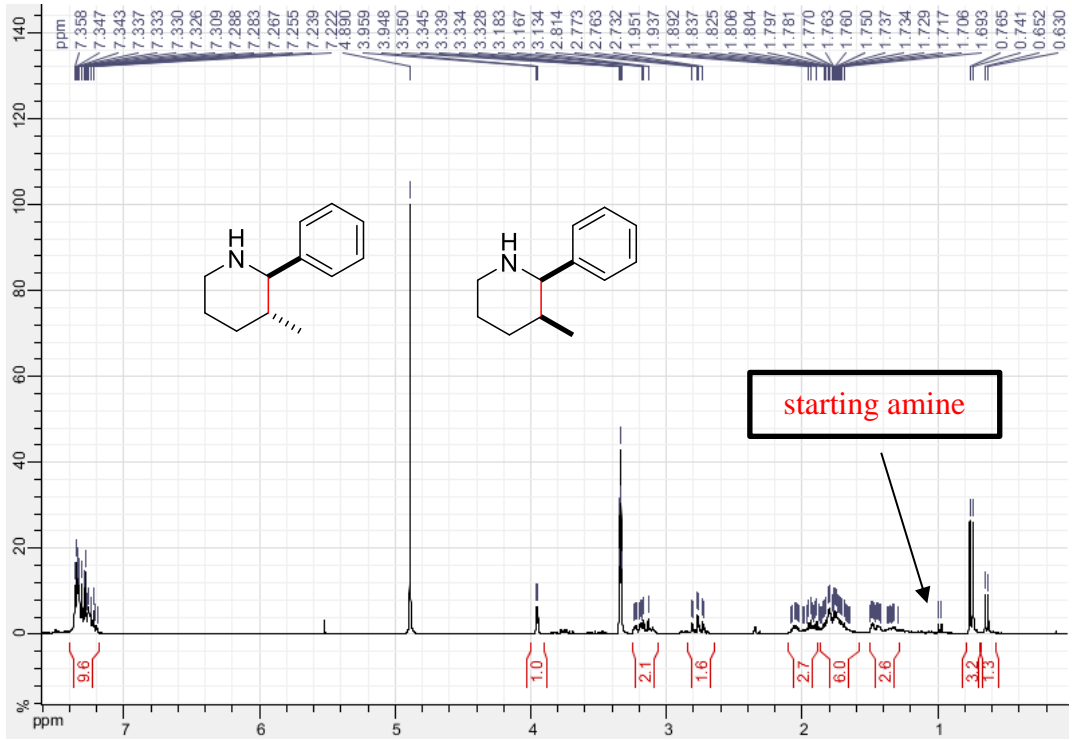


Linear: 1-phenylnonan-1-amine (3.11.1)

Branched: 2-methyl-1-phenyloctan-1-amine (3.12.1 and 3.13.1)



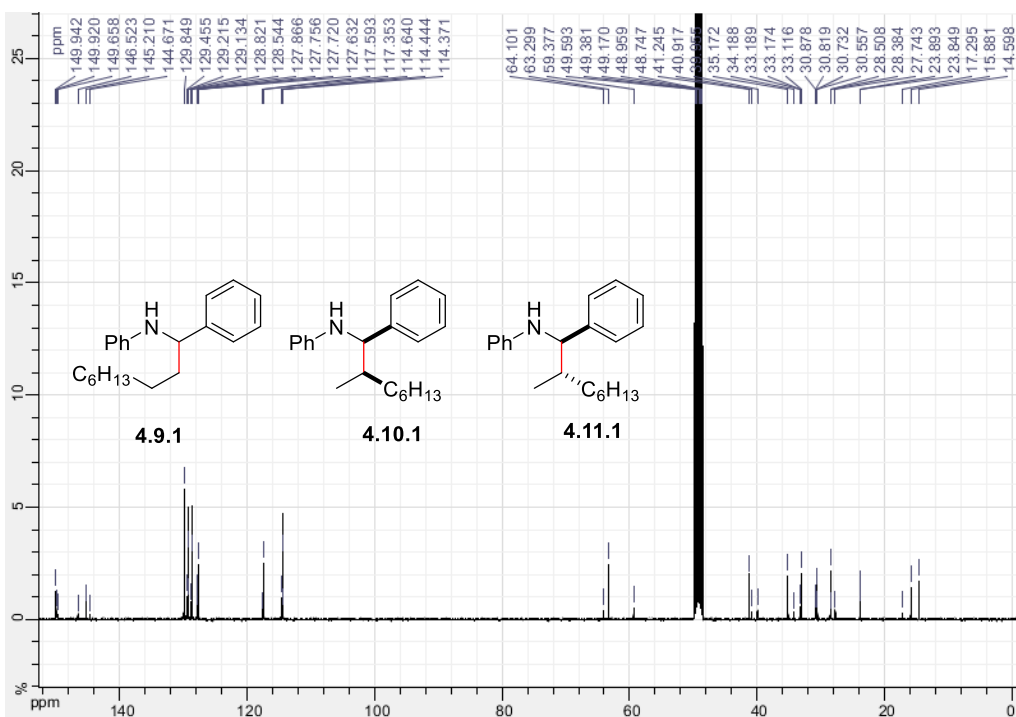
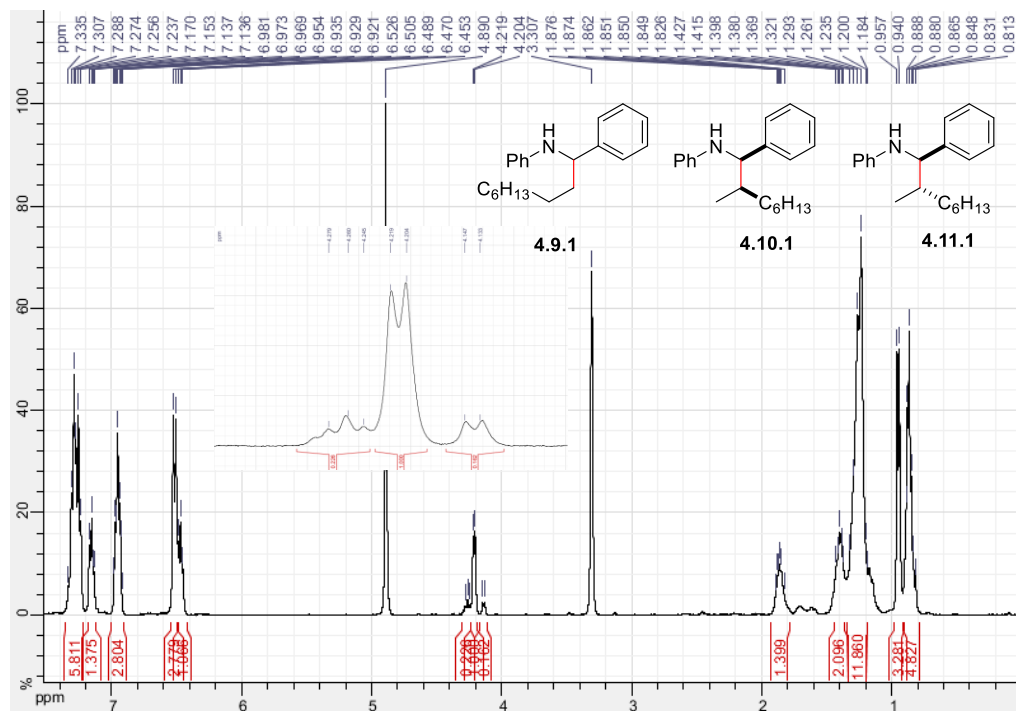
3-methyl-2-phenylpiperidine (3.42 & 3.43)



A.4 ^1H and ^{13}C spectra and GCFID chromatograms of compounds in Chapter 4

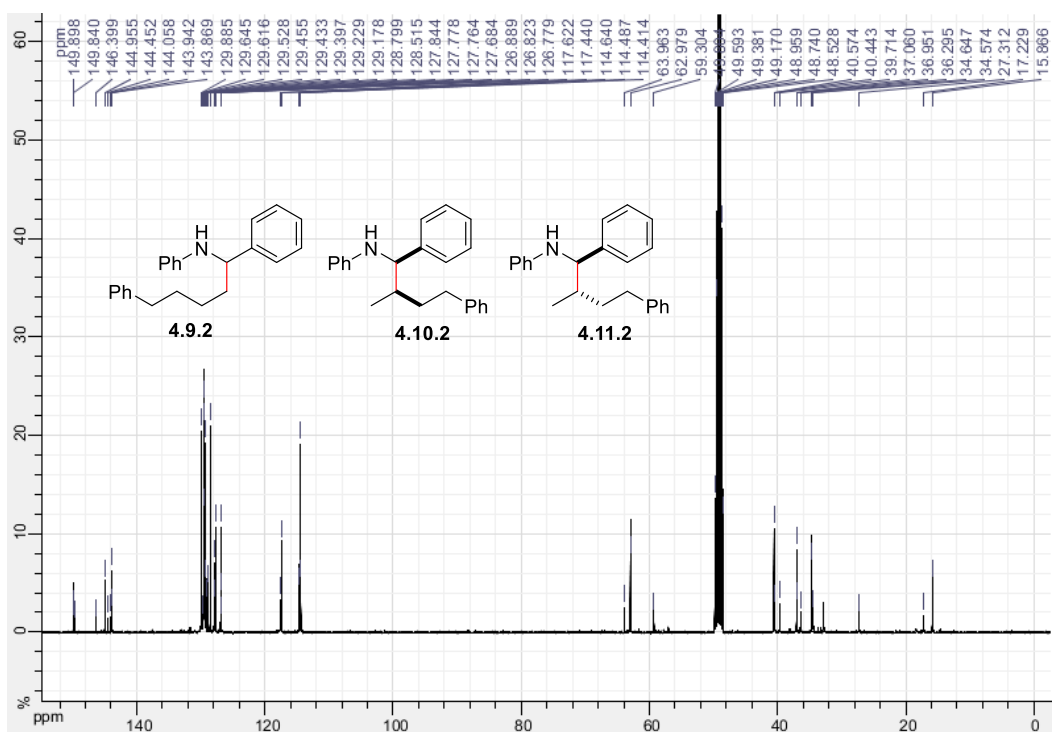
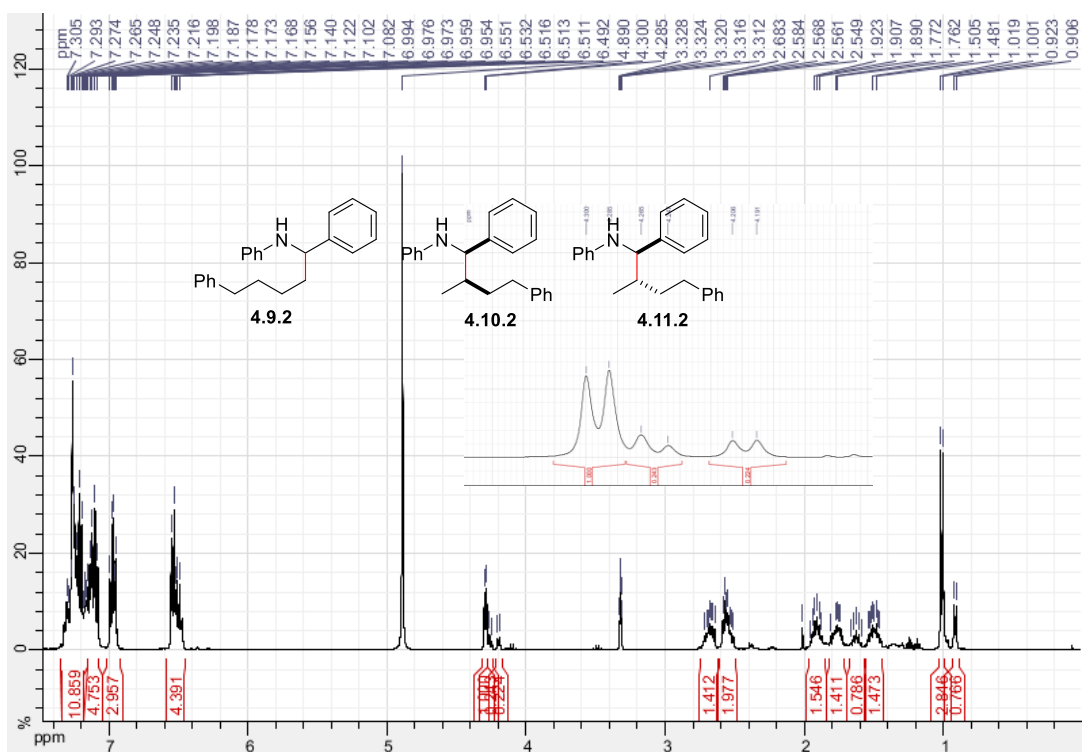
Linear: *N*-(1-phenylonyl)aniline (4.9.1)

Branched: *N*-(2-methyl-1-phenyloctyl)aniline (4.10.1 and 4.11.1)



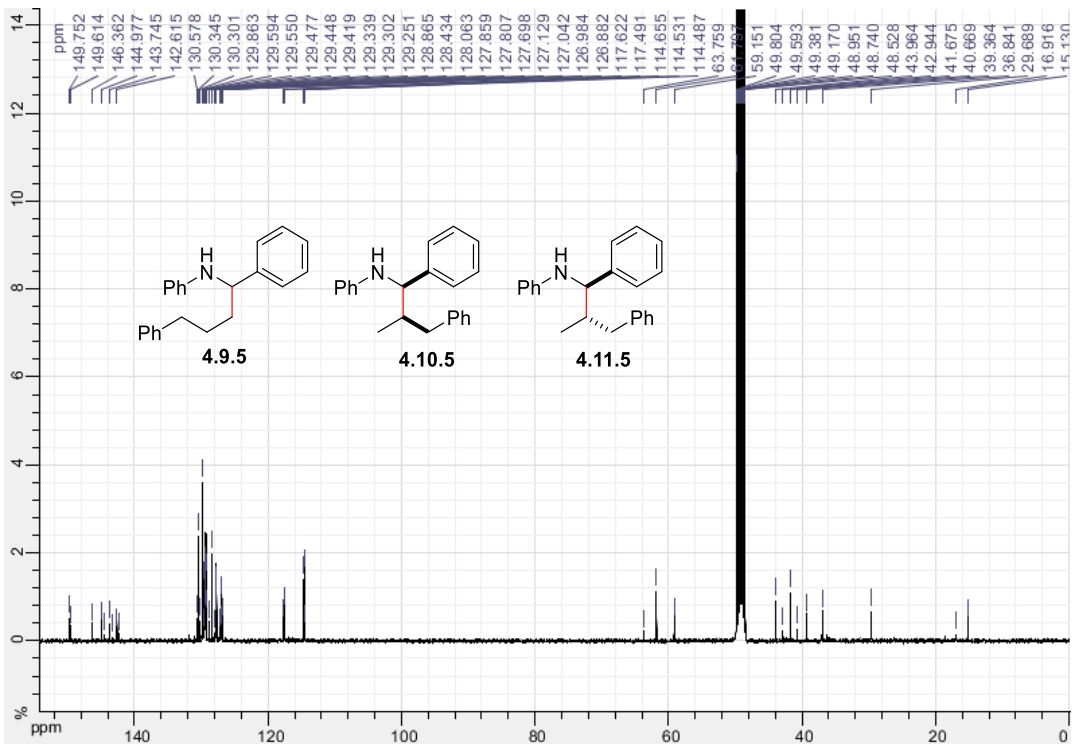
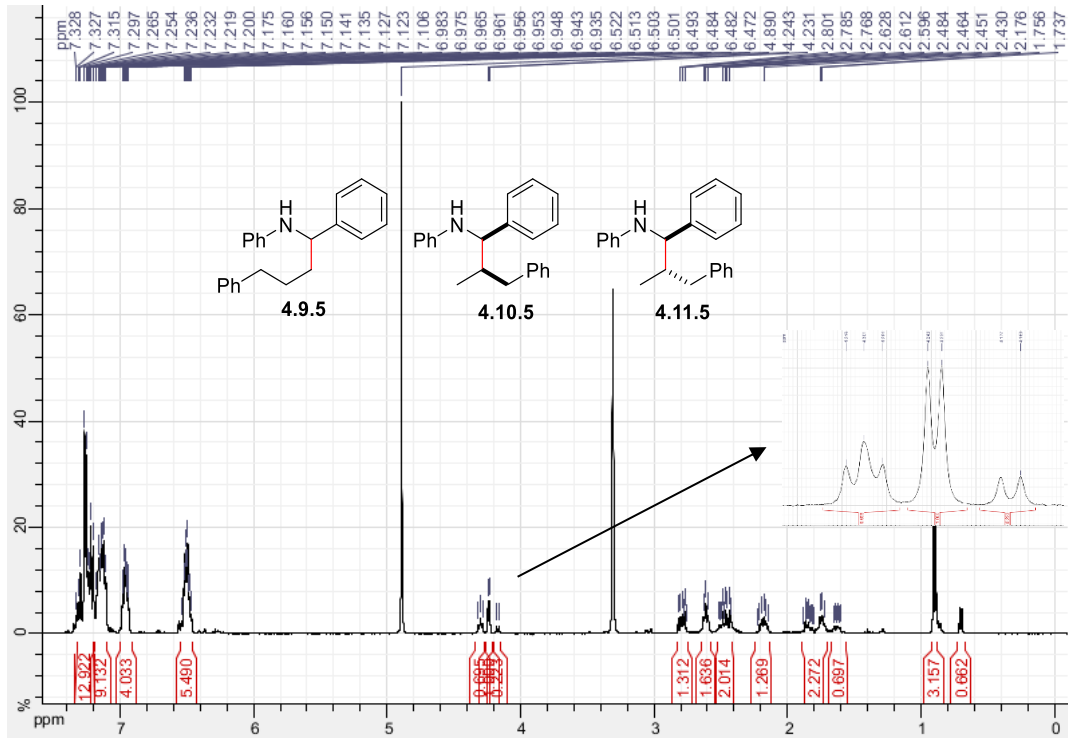
Linear: *N*-(1,5-diphenylpentyl)aniline (4.9.2)

Branched: *N*-(2-methyl-1,4-diphenylbutyl)aniline (4.10.2 and 4.11.2)



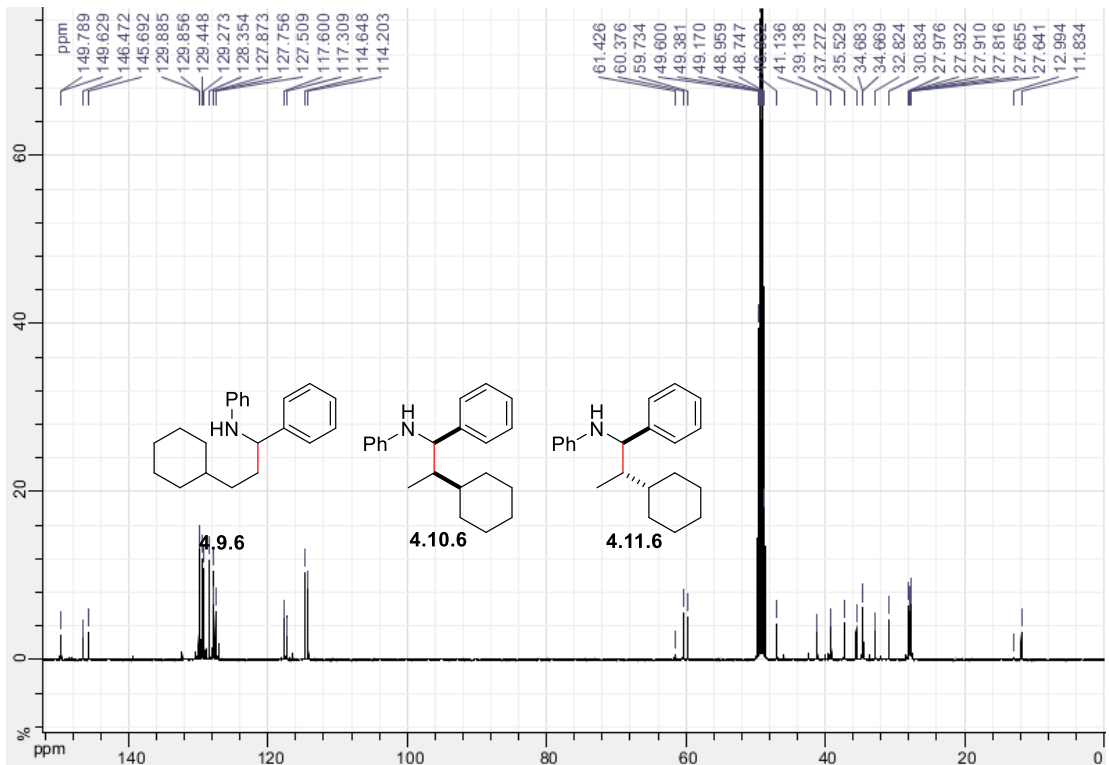
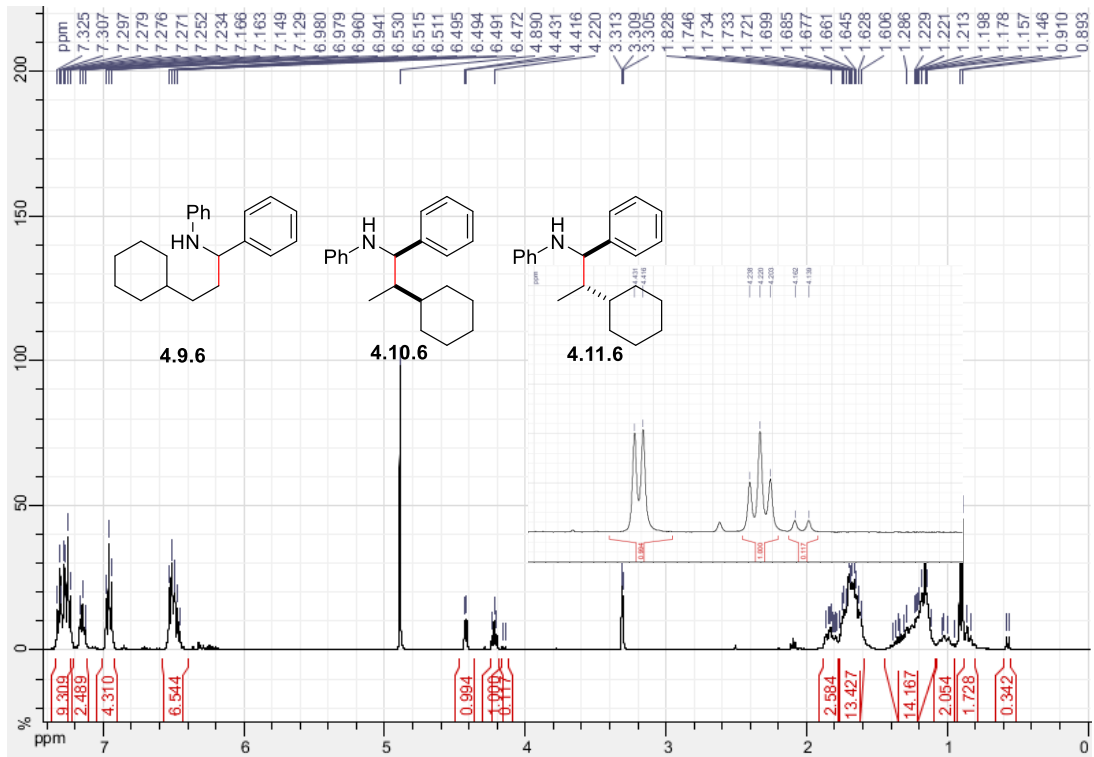
Linear: *N*-(1,4-diphenylbutyl)aniline (4.9.5)

Branched: *N*-(2-methyl-1,3-diphenylpropyl)aniline (4.10.5 and 4.11.5)



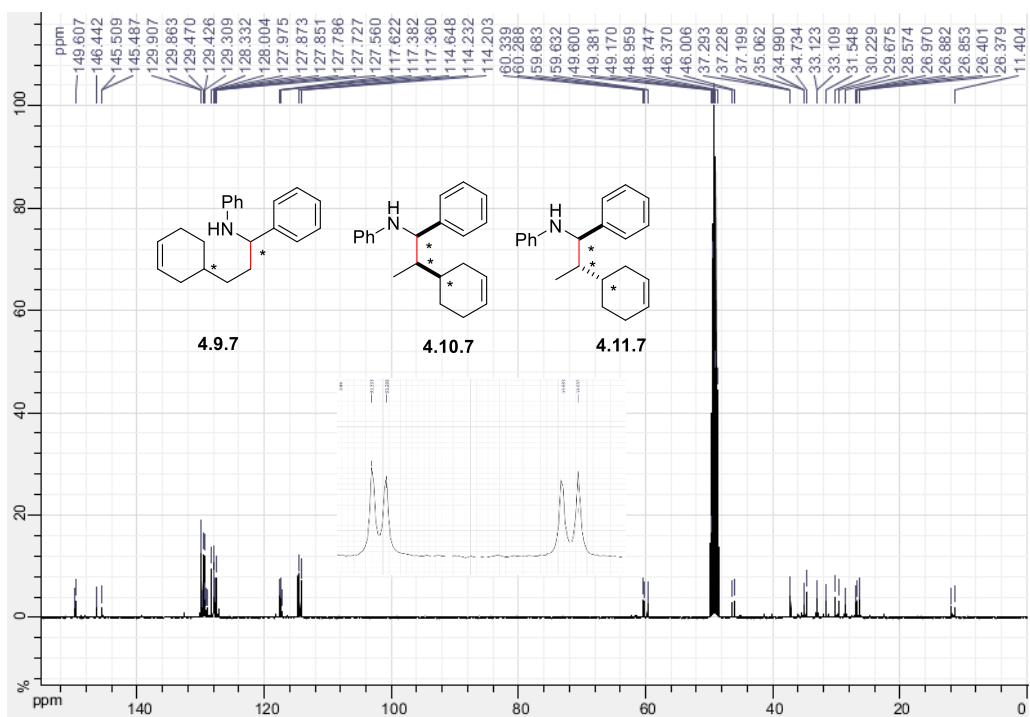
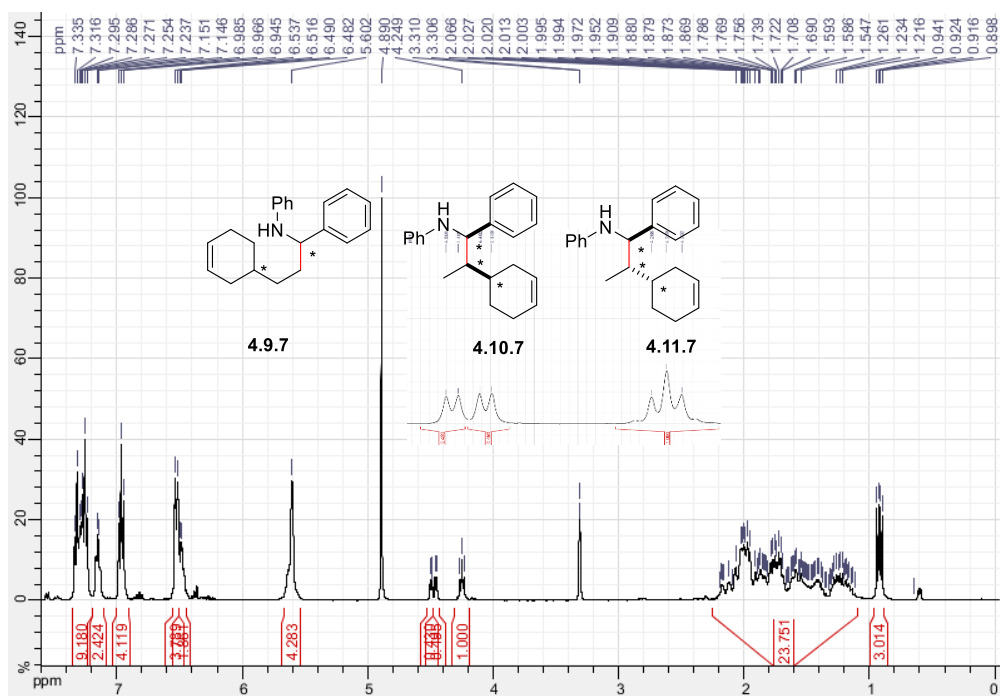
Linear: *N*-(3-cyclohexyl-1-phenylpropyl)aniline (4.9.6)

Branched: *N*-(2-cyclohexyl-1-phenylpropyl)aniline (4.10.6 and 4.11.6)

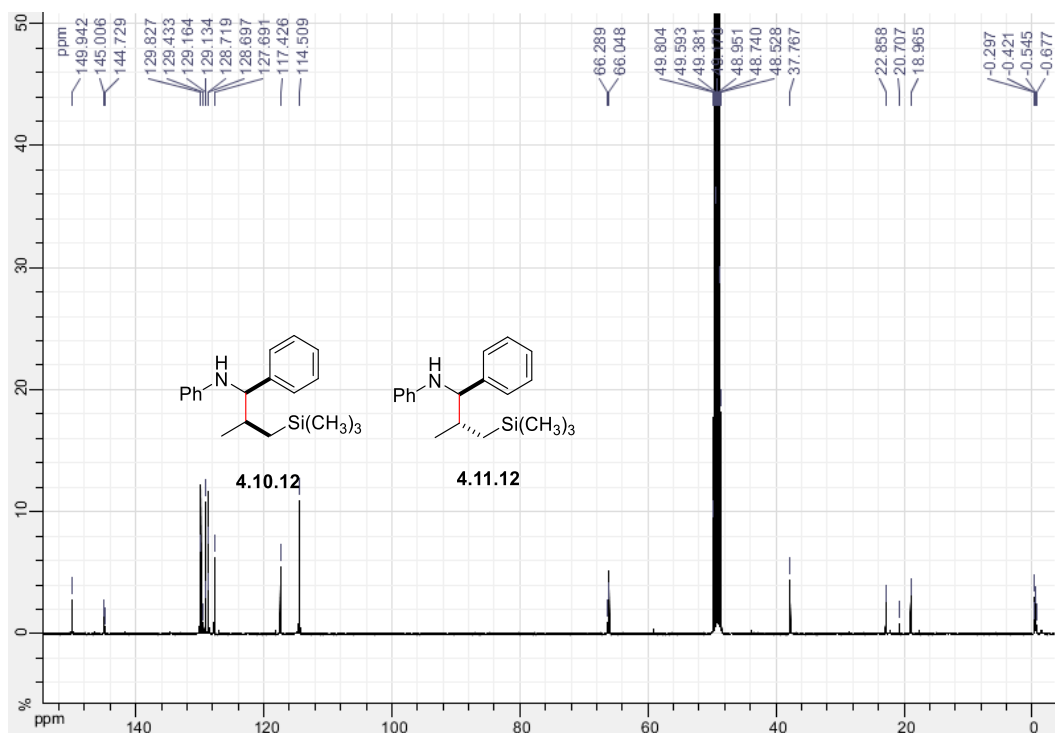
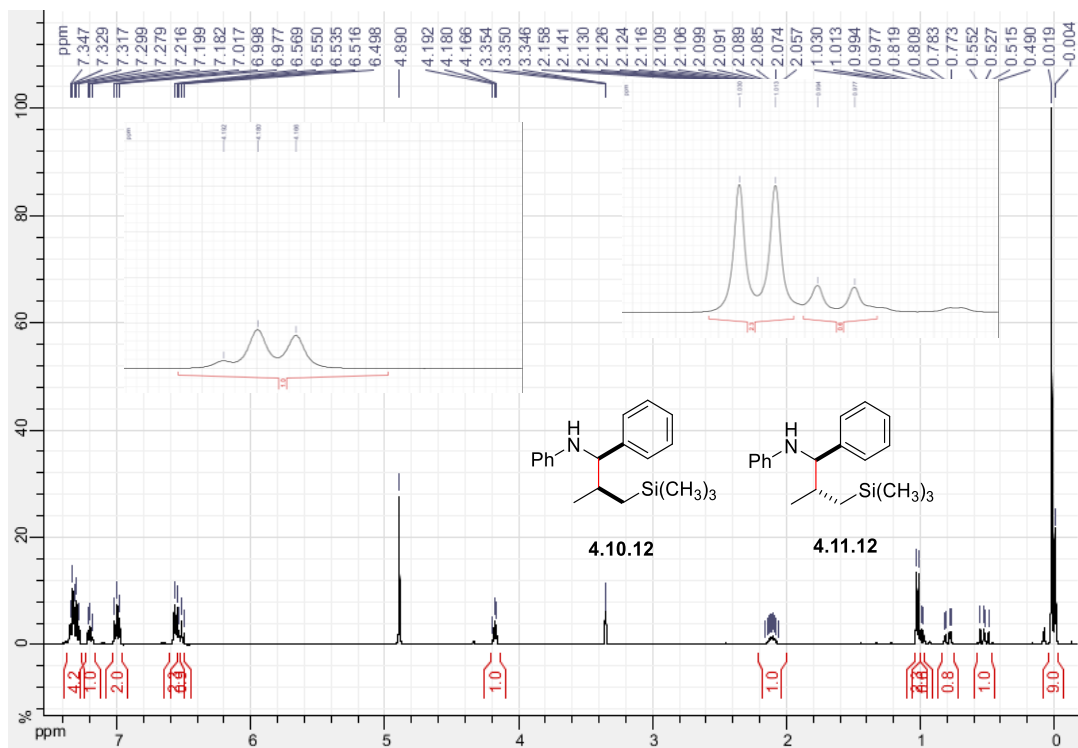


Linear: *N*-(3-(cyclohex-3-en-1-yl)-1-phenylpropyl)aniline (4.9.7)

Branched: *N*-(2-(cyclohex-3-en-1-yl)-1-phenylpropyl)aniline (4.10.7 and 4.11.7)

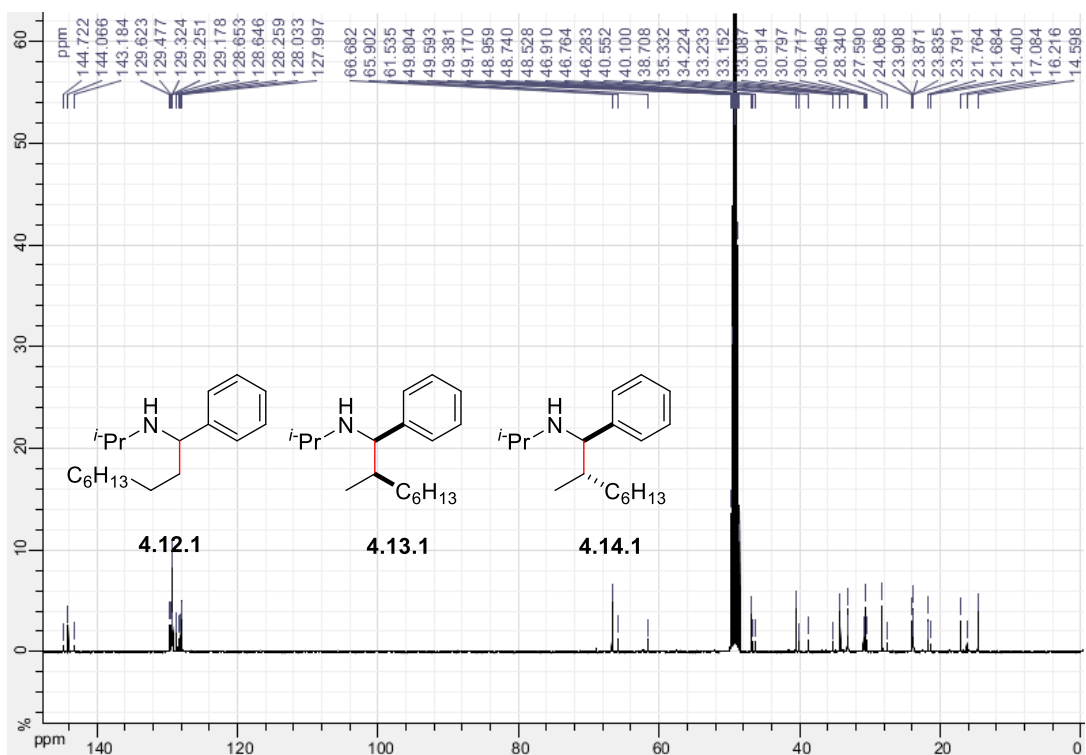
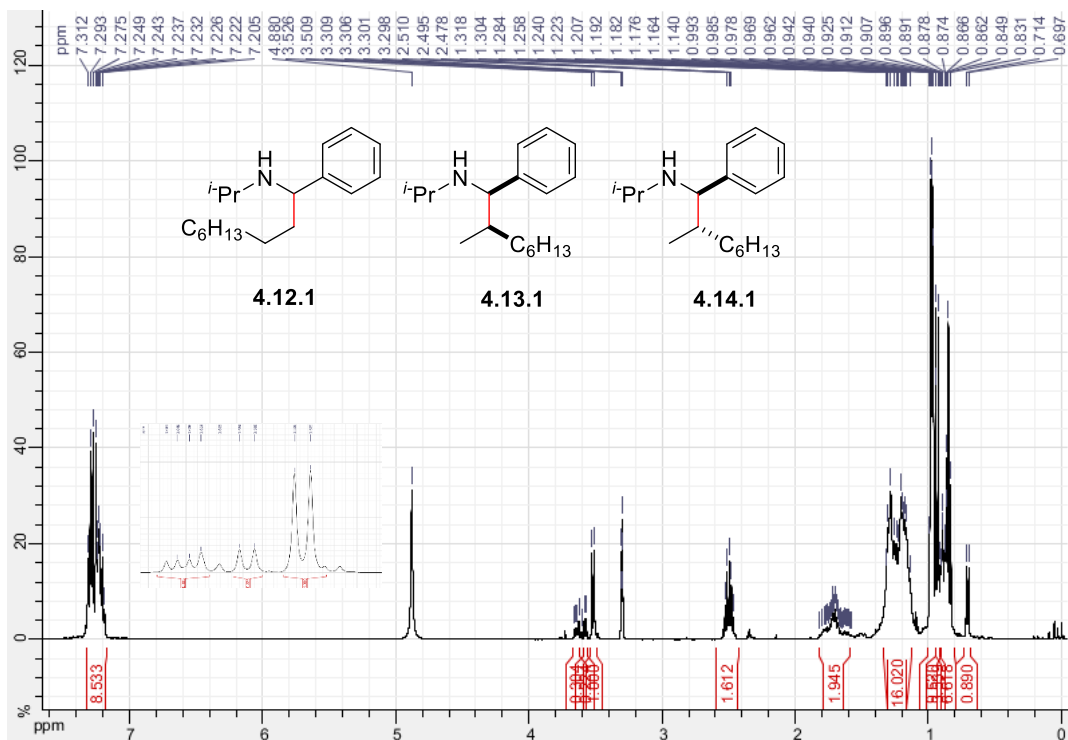


N-(2-methyl-1-phenyl-3-(trimethylsilyl)propyl)aniline (4.10.12 and 4.11.12)



Linear: *N*-isopropyl-1-phenylnonan-1-amine (4.12.1)

Branched: *N*-isopropyl-2-methyl-1-phenyloctan-1-amine (4.13.1 and 4.14.1)



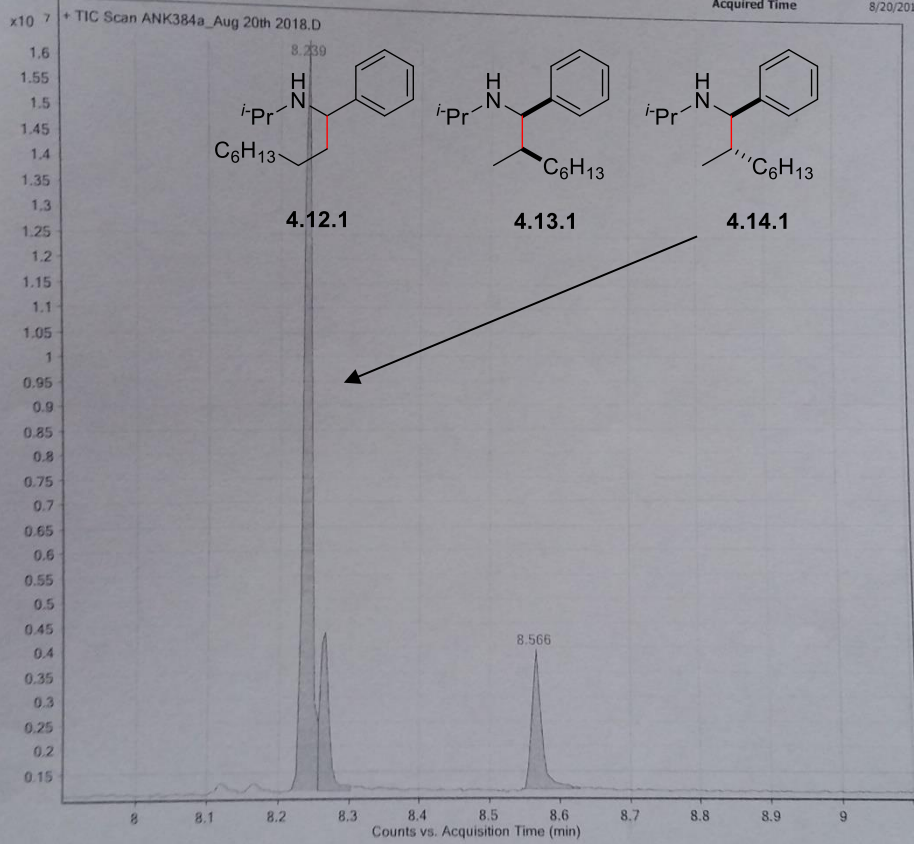
ANK384a_Aug 20th 2018

Schafer

SCHAFER.M

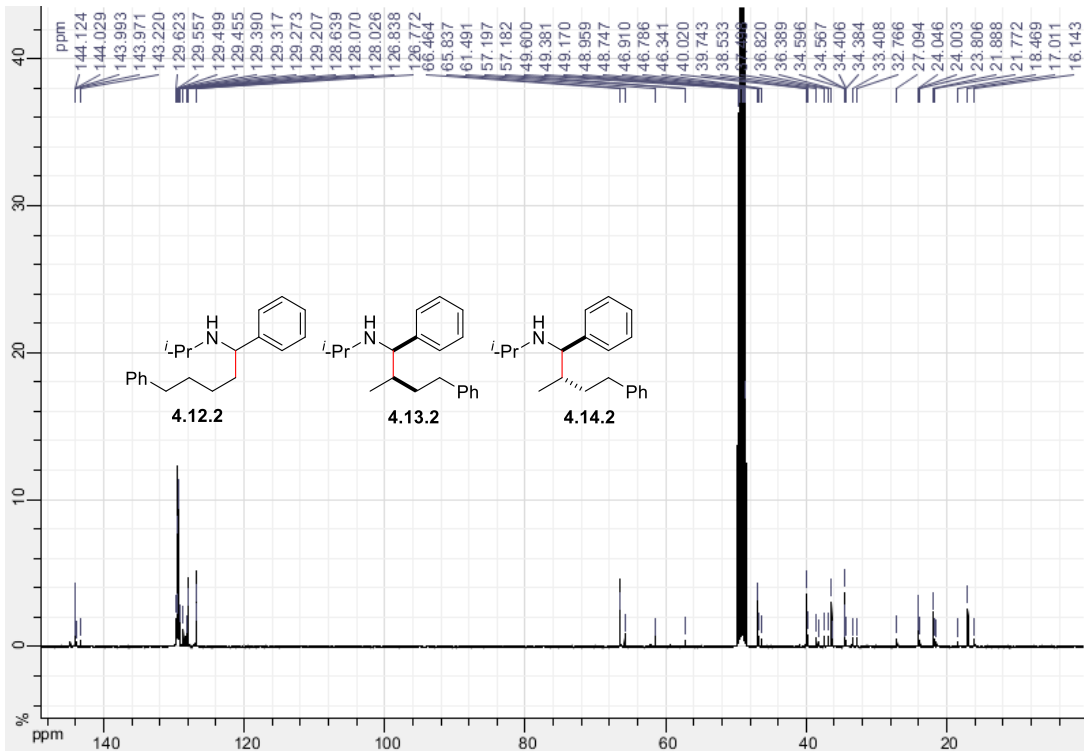
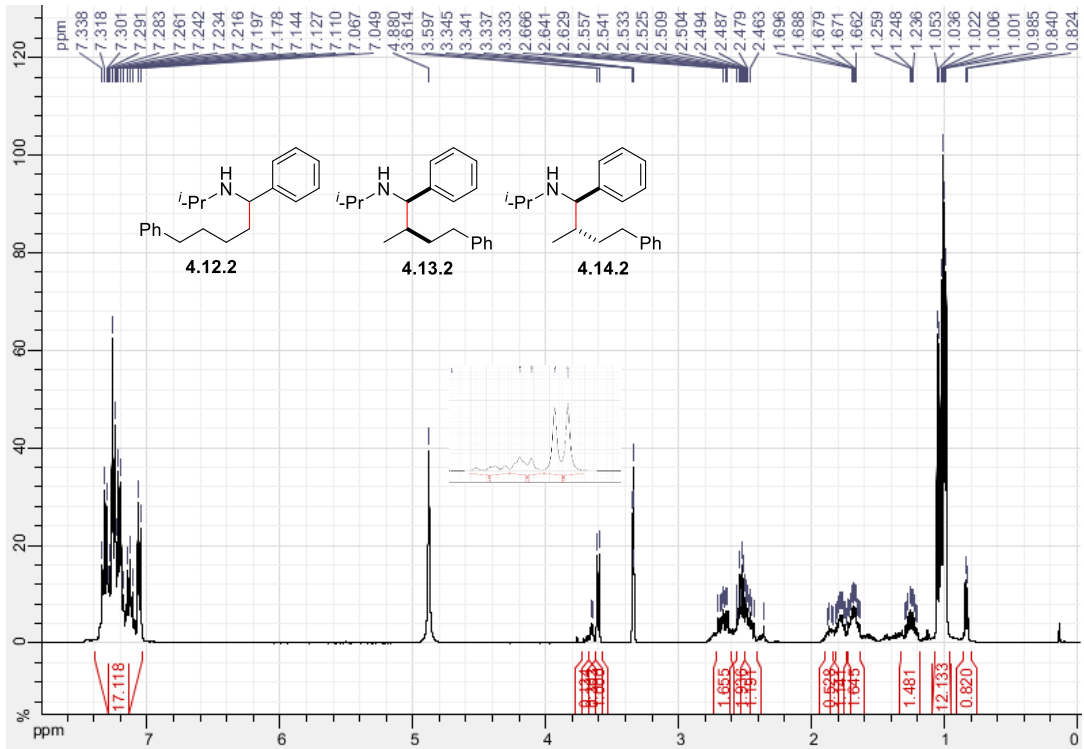
Position 51
Inj Vol 1
IRM Calibration Status Not Applicable
Comment

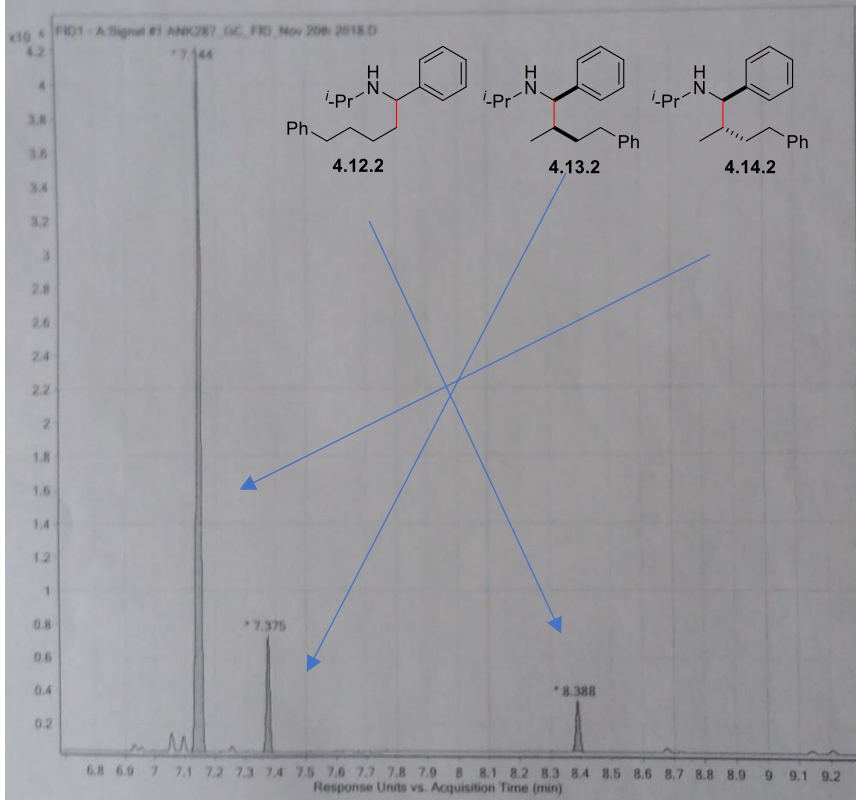
Instrument Name GCMS
InjPosition
Data Filename ANK384a_4
Acquired Time 8/20/2018



Linear: *N*-isopropyl-1,5-diphenylpentan-1-amine (4.12.2)

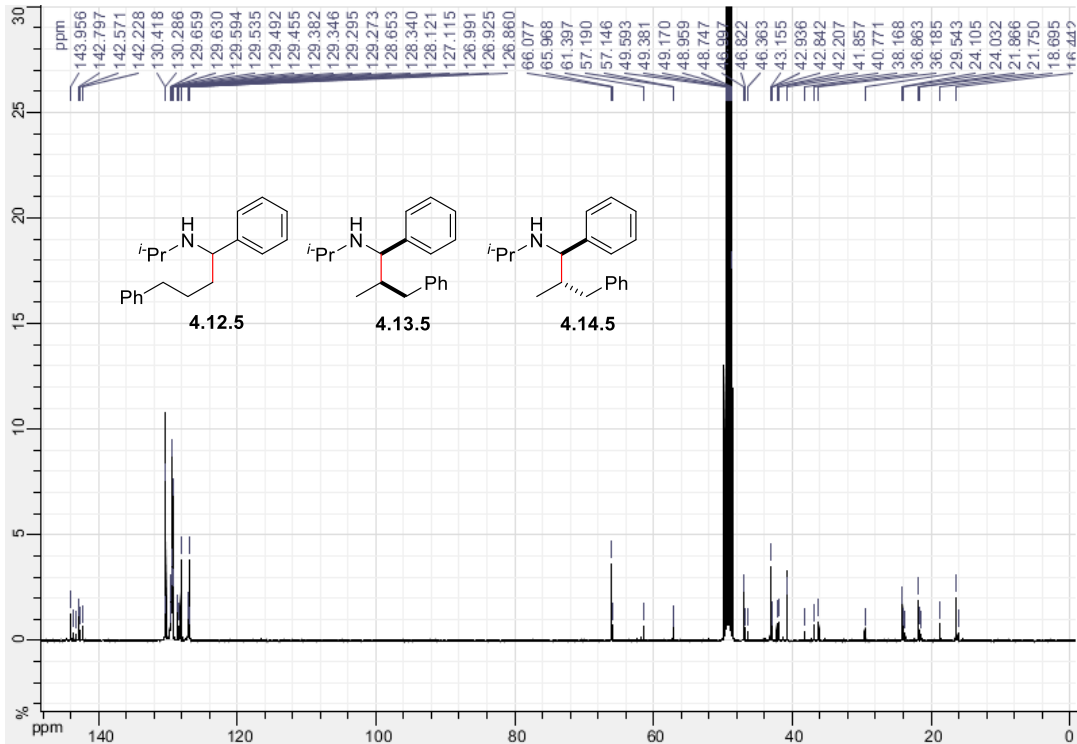
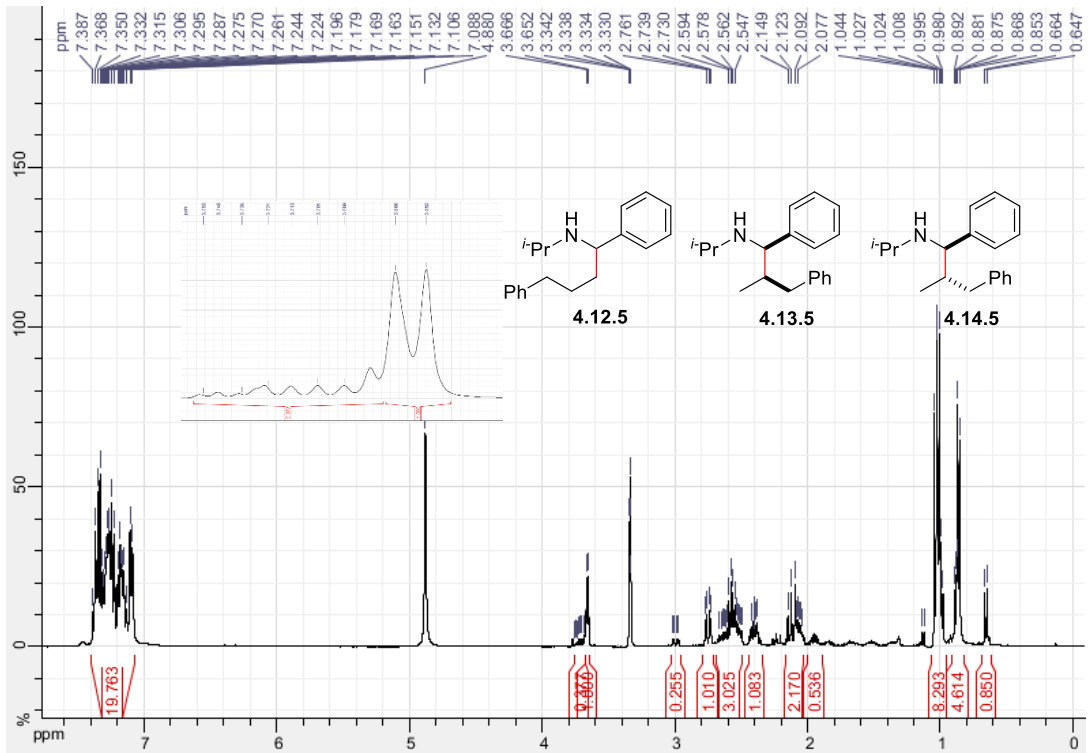
Branched: *N*-isopropyl-2-methyl-1,4-diphenylbutan-1-amine (4.13.2 and 4.14.2)

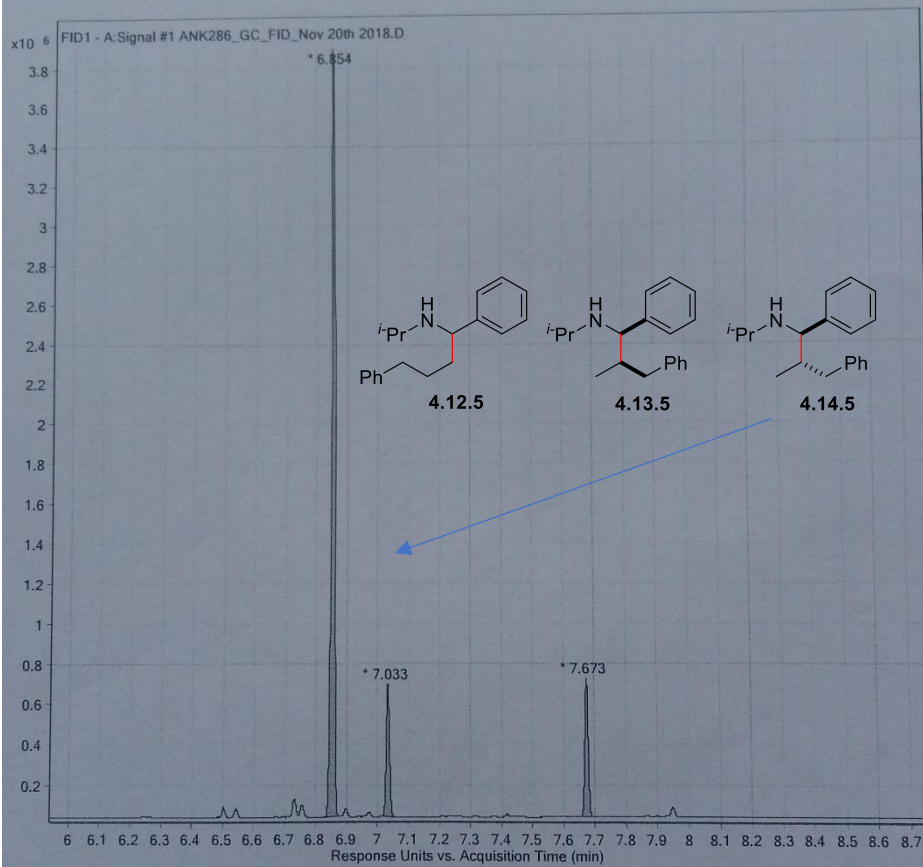




Linear: *N*-isopropyl-1,4-diphenylbutan-1-amine (4.12.5)

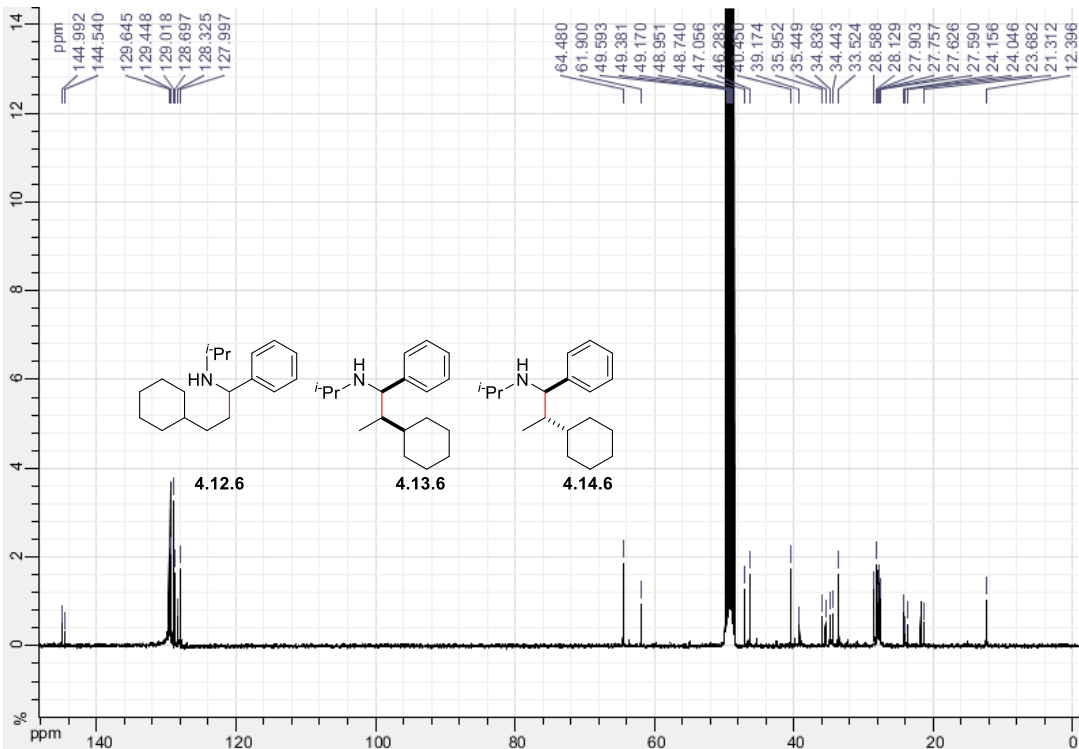
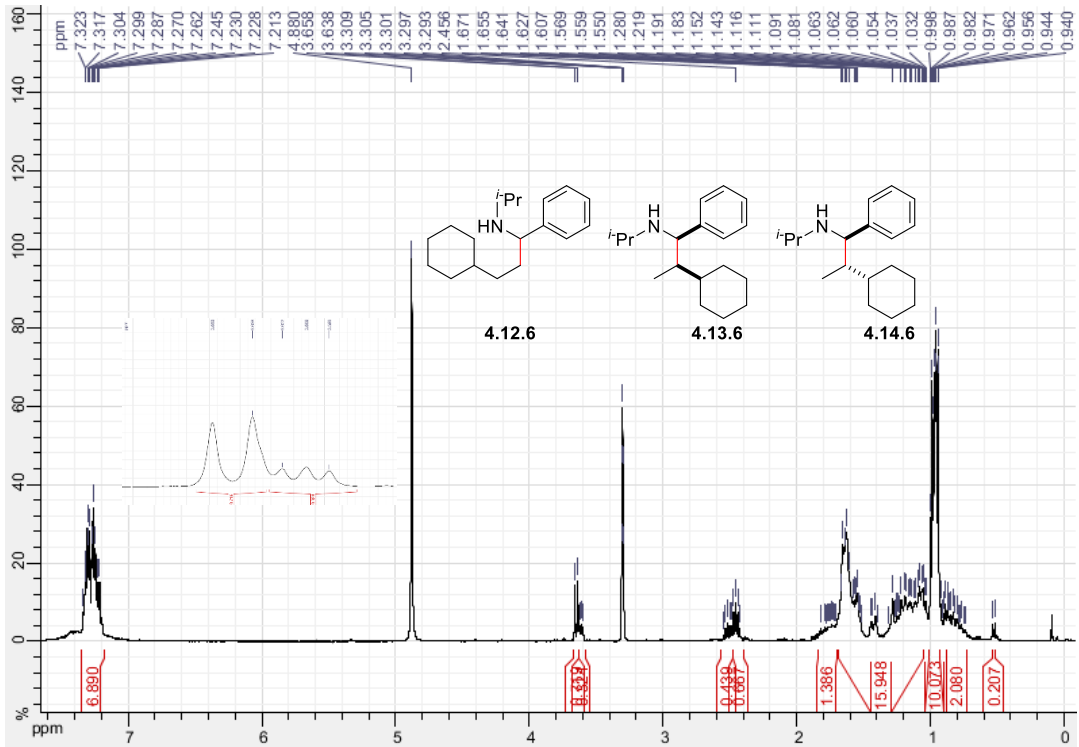
Branched: *N*-isopropyl-2-methyl-1,3-diphenylpropan-1-amine (4.13.5 and 4.14.5)





Linear: 3-cyclohexyl-N-isopropyl-1-phenylpropan-1-amine (4.12.6)

Branched: 2-cyclohexyl-N-isopropyl-1-phenylpropan-1-amine (4.13.6 and 4.14.6)

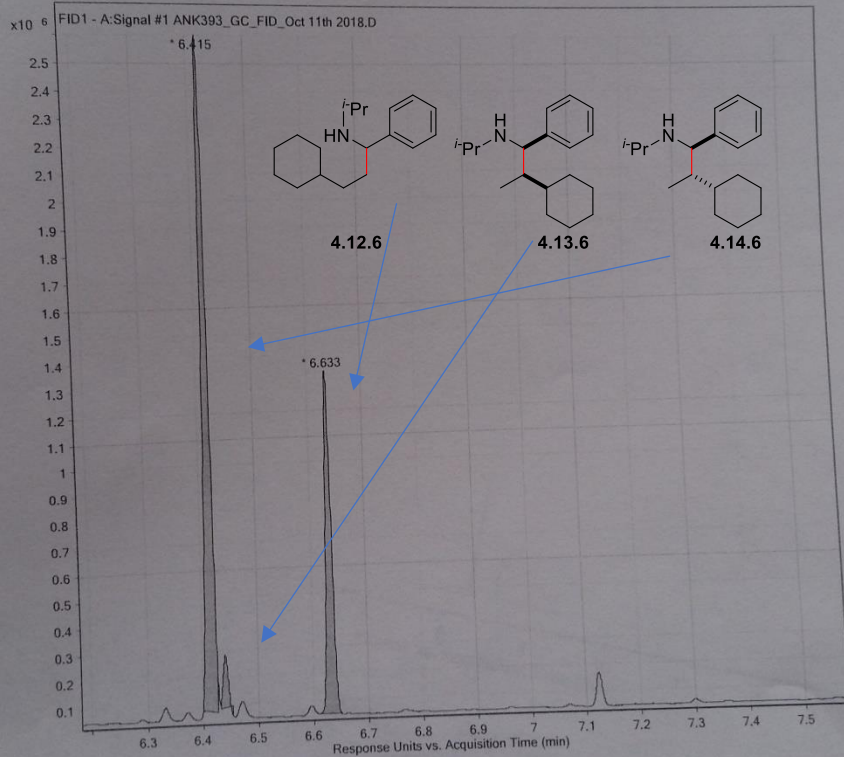


ANK393_GC_FID_Oct 11th 2018

Position 51
Inj Vol 0.2
IRM Calibration Status Not Applicable
Comment

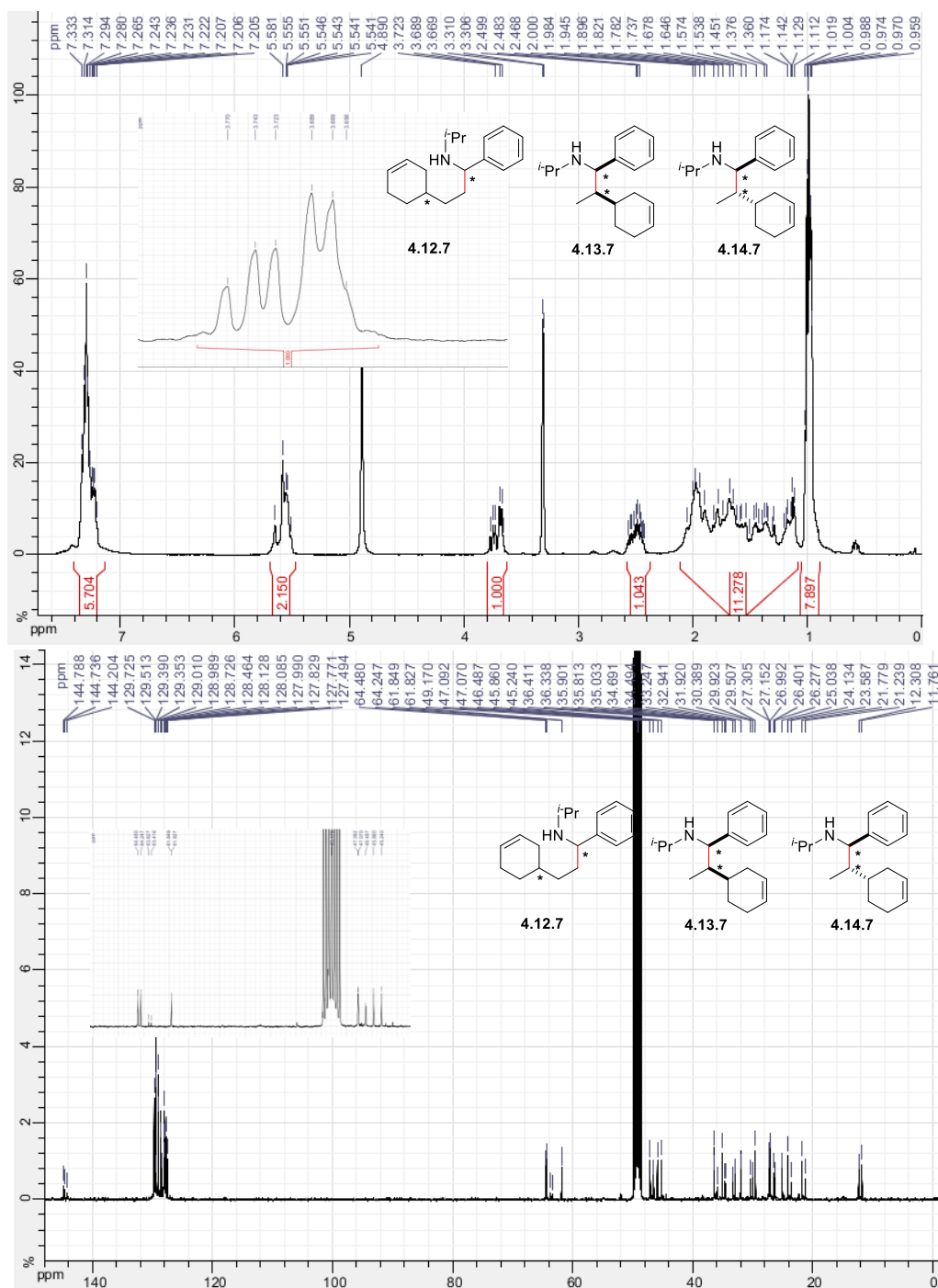
Instrument Name GCMS
InjPosition
Data Filename ANK393_GC_FID_Oct 11th 2018
Acquired Time 10/11/2018 5:59:05 PM

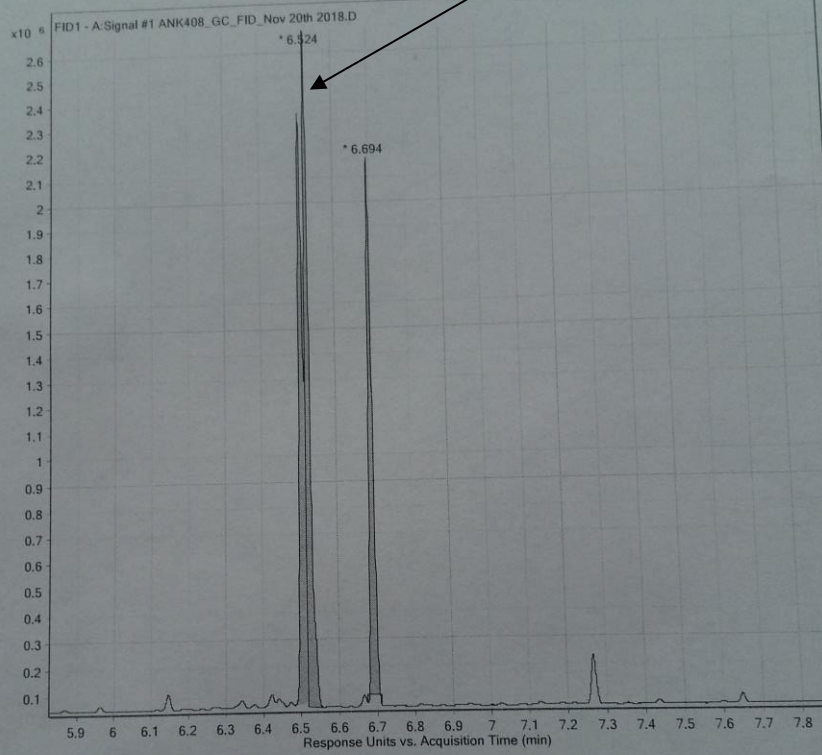
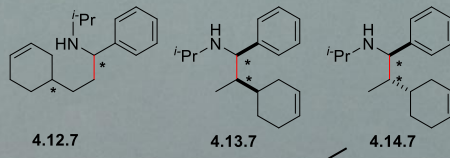
FID DGII.M



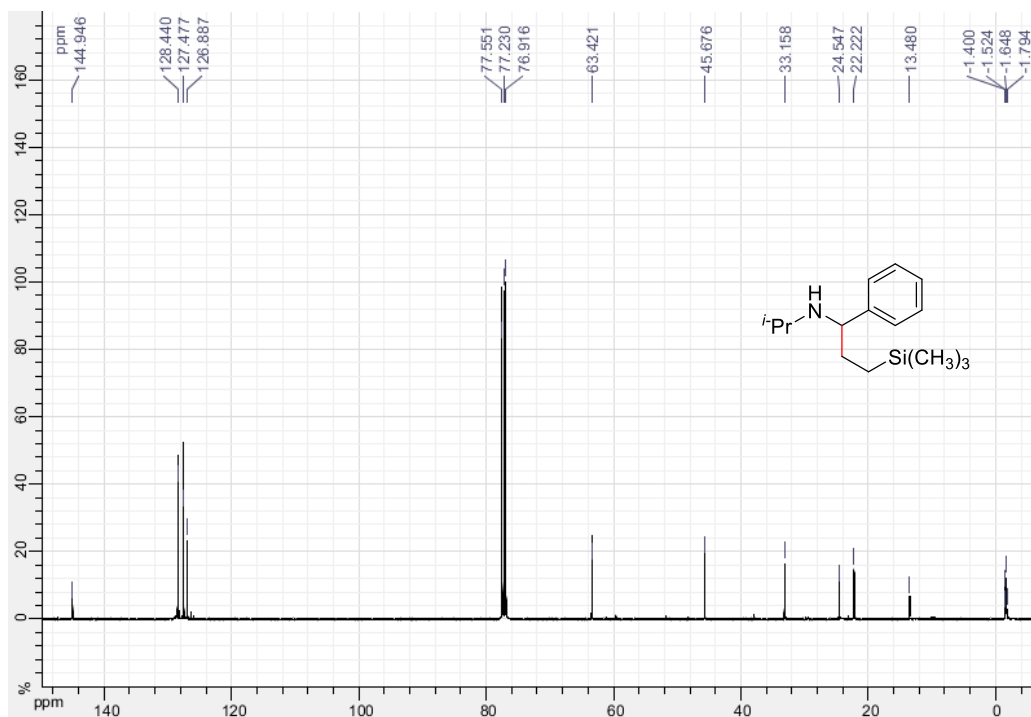
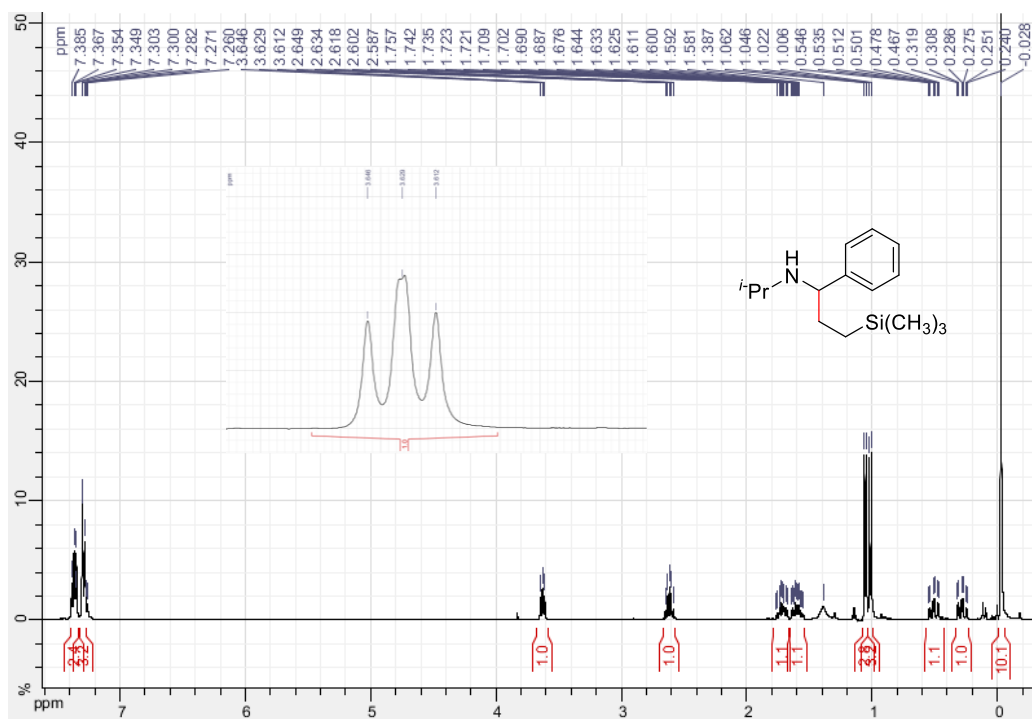
Linear: 3-(cyclohex-3-en-1-yl)-*N*-isopropyl-1-phenylpropan-1-amine (4.12.7)

Branched: 2-(cyclohex-3-en-1-yl)-*N*-isopropyl-1-phenylpropan-1-amine (4.13.7 and 4.14.7)



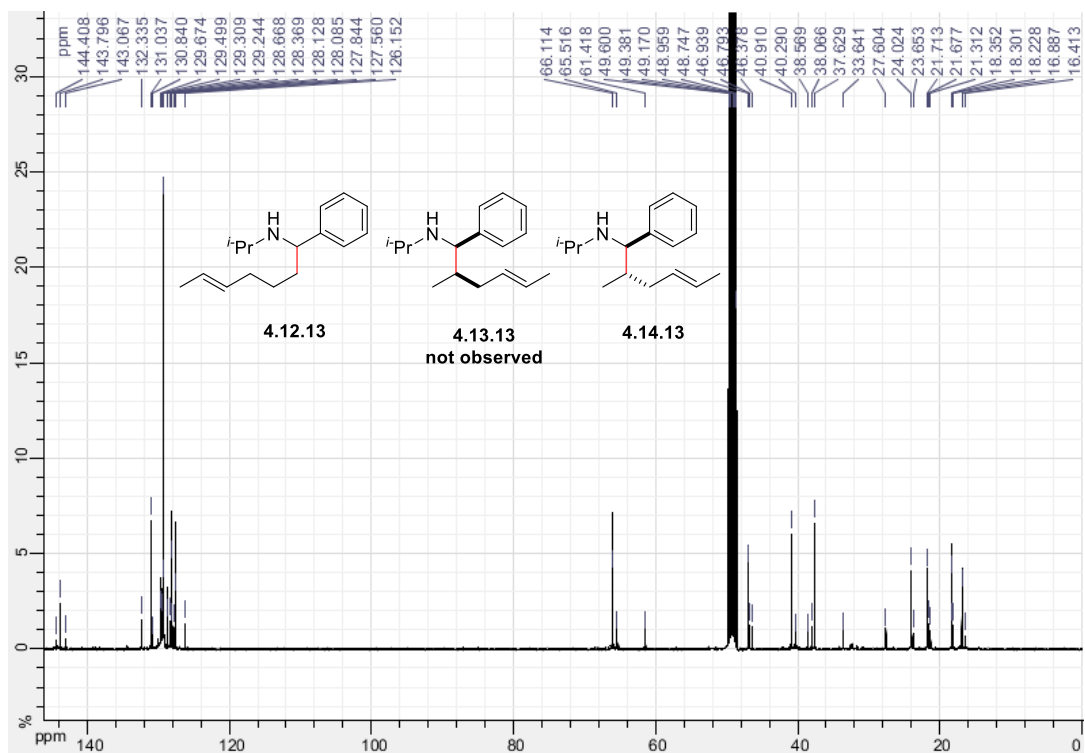
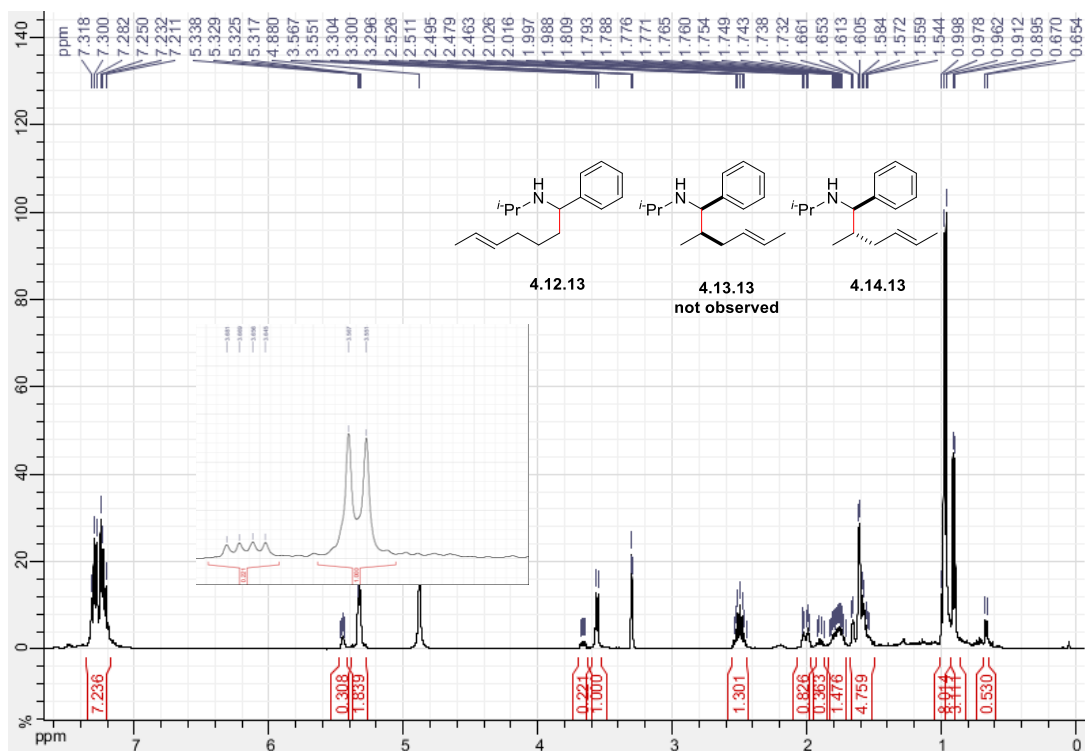


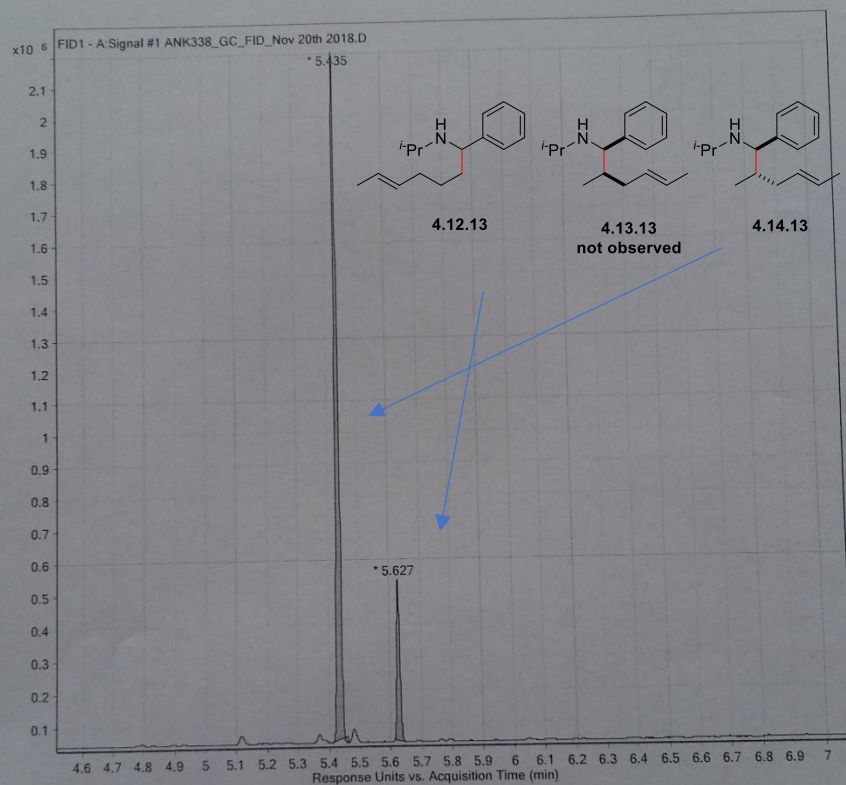
N-isopropyl-1-phenyl-3-(trimethylsilyl)propan-1-amine (4.12.10)



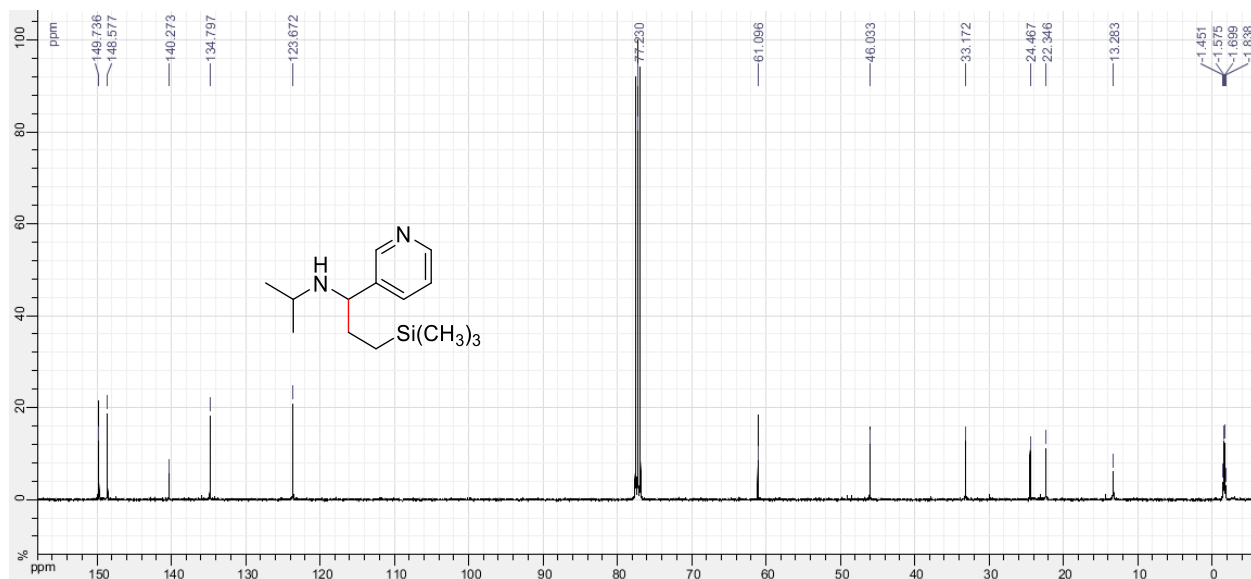
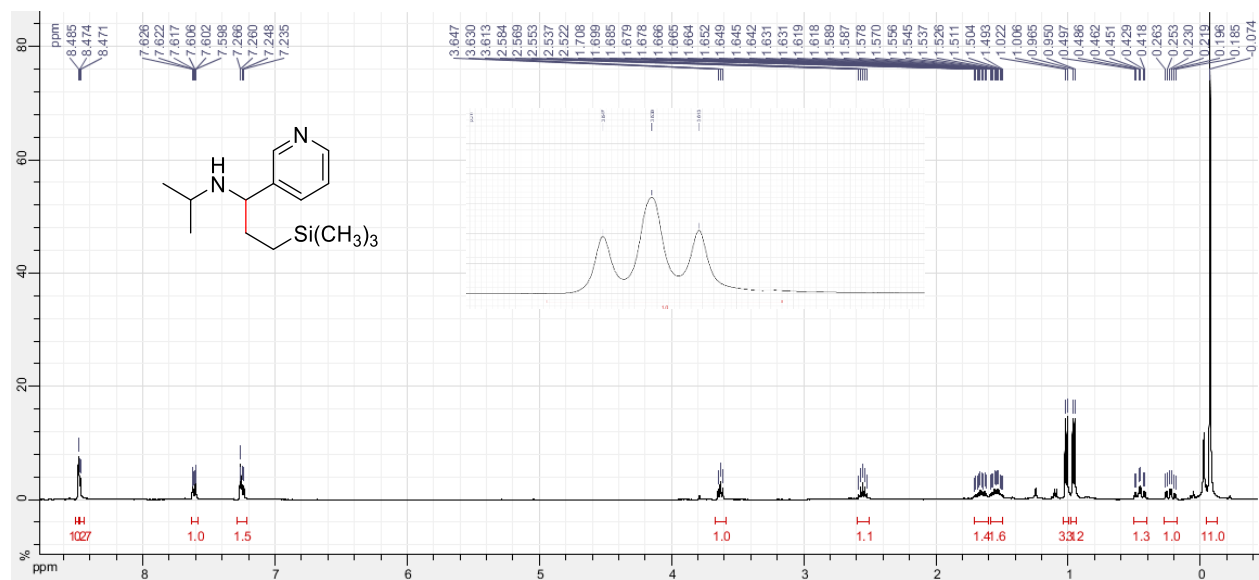
Linear: *N*-isopropyl-1-phenylhept-5-en-1-amine (4.12.13)

Branched: *N*-isopropyl-2-methyl-1-phenylhex-4-en-1-amine (4.13.13 and 4.14.13)

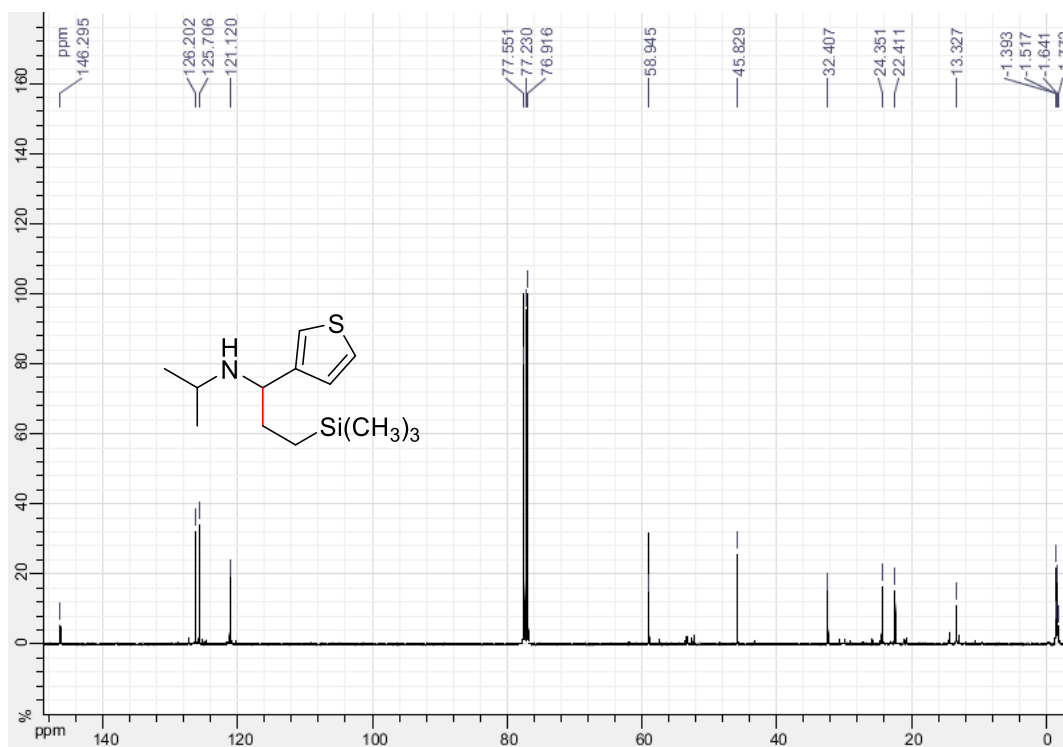
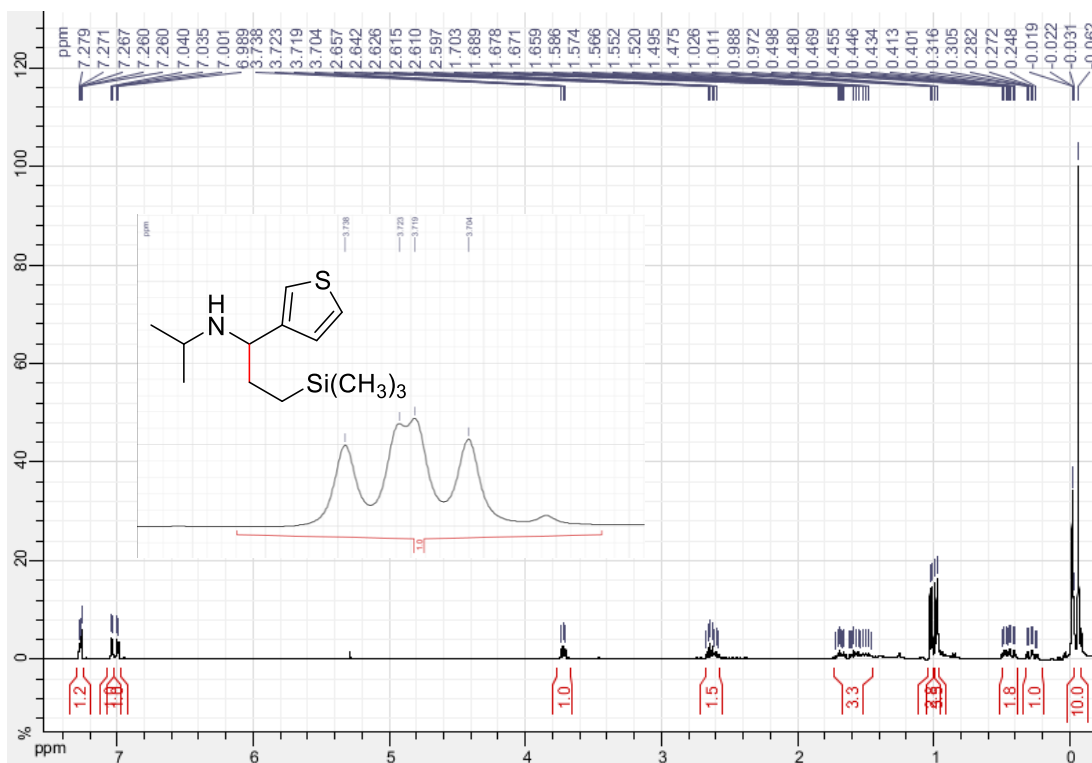




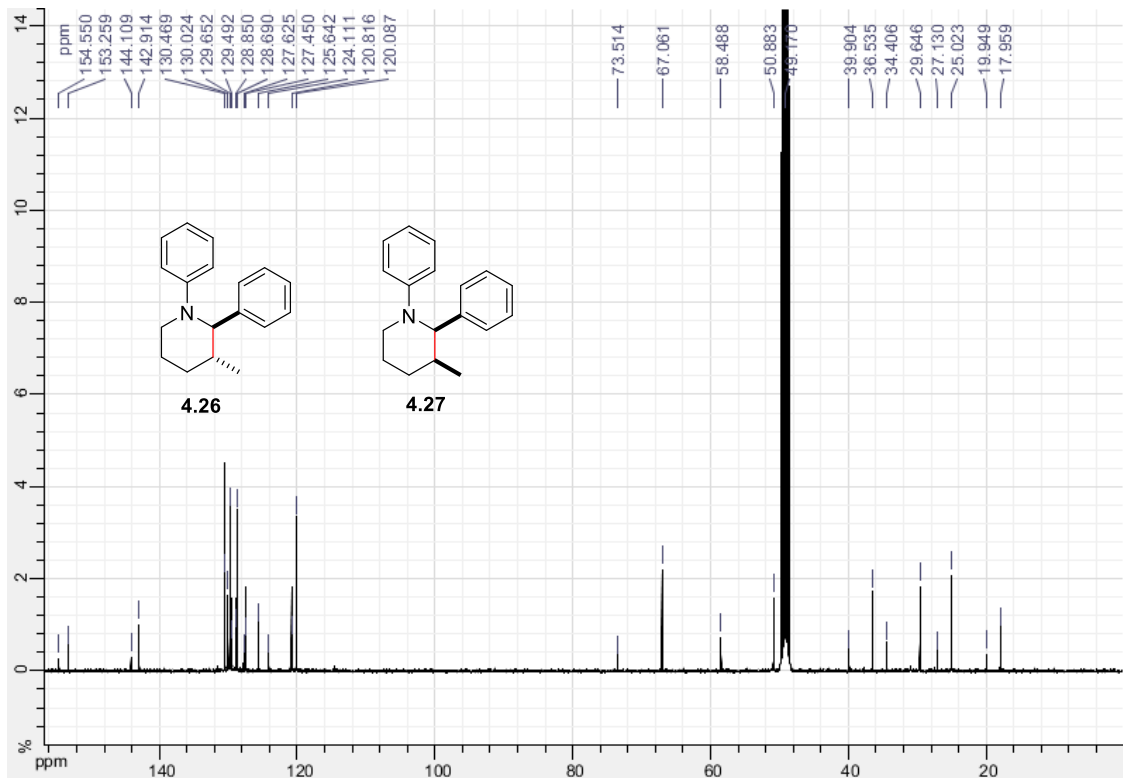
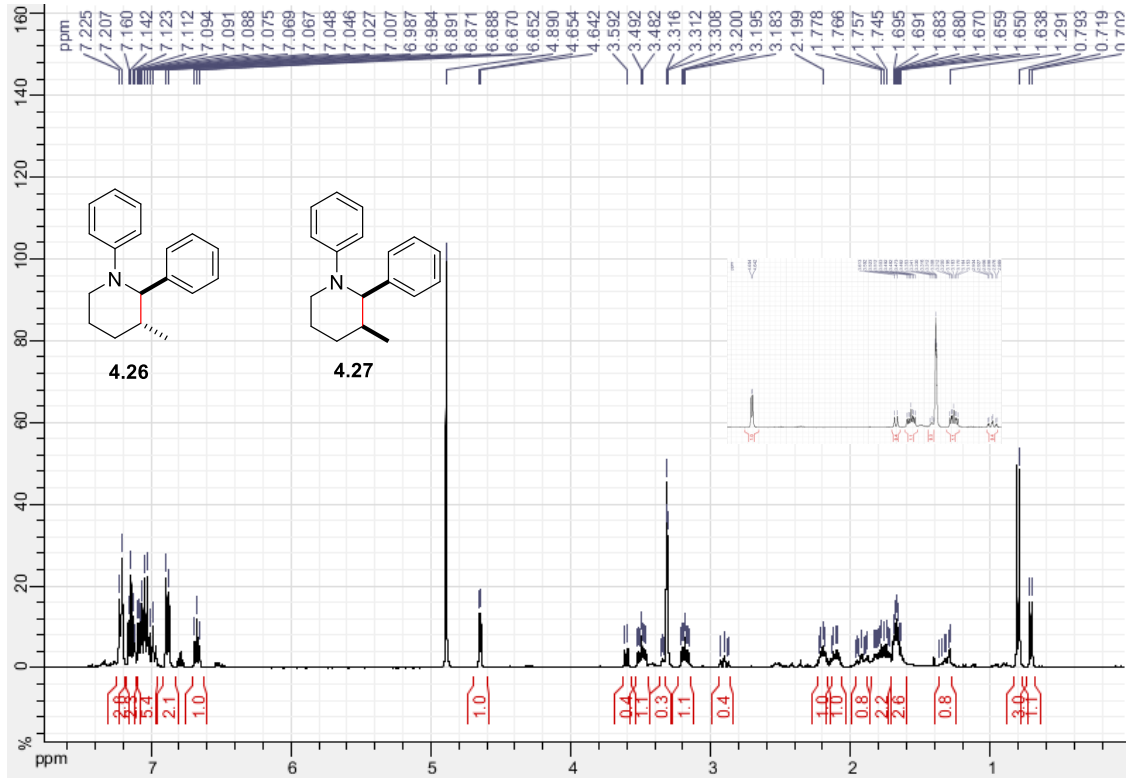
***N*-isopropyl-1-(pyridin-3-yl)-3-(trimethylsilyl)propan-1-amine (4.19)**



N-isopropyl-1-(thiophen-3-yl)-3-(trimethylsilyl)propan-1-amine (4.20)



3-methyl-1,2-diphenylpiperidine (4.26 and 4.27)



Appendix B Microreview

A. Koperniku, H. Liu and P.B. Hurley

Mono- and Difluorination of Benzylic Carbon Atoms, *Eur. J. Org. Chem.*, 2016, **5**, 871-886

